

SANDIA REPORT

SAND99-1043

Unlimited Release

Printed October 1999

Brine and Gas Flow Patterns Between Excavated Areas and Disturbed Rock Zone in the 1996 Performance Assessment for the Waste Isolation Pilot Plant for a Single Drilling Intrusion that Penetrates Repository and Castile Brine Reservoir

RECEIVED
NOV 29 1999
OSTI

Kathleen M. Economy, Jon C. Helton, Palmer Vaughn

Prepared by
Sandia National Laboratories
Albuquerque, New Mexico 87185 and Livermore, California 94550

Sandia is a multiprogram laboratory operated by Sandia Corporation,
a Lockheed Martin Company, for the United States Department of
Energy under Contract DE-AC04-94AL85000.

Approved for public release; further dissemination unlimited.



Sandia National Laboratories

Issued by Sandia National Laboratories, operated for the United States Department of Energy by Sandia Corporation.

NOTICE: This report was prepared as an account of work sponsored by an agency of the United States Government. Neither the United States Government, nor any agency thereof, nor any of their employees, nor any of their contractors, subcontractors, or their employees, make any warranty, express or implied, or assume any legal liability or responsibility for the accuracy, completeness, or usefulness of any information, apparatus, product, or process disclosed, or represent that its use would not infringe privately owned rights. Reference herein to any specific commercial product, process, or service by trade name, trademark, manufacturer, or otherwise, does not necessarily constitute or imply its endorsement, recommendation, or favoring by the United States Government, any agency thereof, or any of their contractors or subcontractors. The views and opinions expressed herein do not necessarily state or reflect those of the United States Government, any agency thereof, or any of their contractors.

Printed in the United States of America. This report has been reproduced directly from the best available copy.

Available to DOE and DOE contractors from
Office of Scientific and Technical Information
P.O. Box 62
Oak Ridge, TN 37831

Prices available from (703) 605-6000
Web site: <http://www.ntis.gov/ordering.htm>

Available to the public from
National Technical Information Service
U.S. Department of Commerce
5285 Port Royal Rd
Springfield, VA 22161

NTIS price codes
Printed copy: A02
Microfiche copy: A01

DISCLAIMER

**Portions of this document may be illegible
in electronic image products. Images are
produced from the best available original
document.**

**Brine and Gas Flow Patterns Between
Excavated Areas and Disturbed Rock Zone
in the 1996 Performance Assessment for the
Waste Isolation Pilot Plant
for a Single Drilling Intrusion that Penetrates
Repository and Castile Brine Reservoir**

Kathleen M. Economy
Applied Physics
Albuquerque, NM 87106

Jon C. Helton
Department of Mathematics
Arizona State University
Tempe, AZ 85287

Palmer Vaughn
WIPP Performance Assessment Department
Sandia National Laboratories
P.O. Box 5800
Albuquerque, New Mexico 87185

ABSTRACT

The Waste Isolation Pilot Plant (WIPP), which is located in southeastern New Mexico, is being developed for the geologic disposal of transuranic (TRU) waste by the U.S. Department of Energy (DOE). Waste disposal will take place in panels excavated in a bedded salt formation approximately 2000 ft (610 m) below the land surface. The BRAGFLO computer program, which solves a system of nonlinear partial differential equations for two-phase flow, was used to investigate brine and gas flow patterns in the vicinity of the repository for the 1996 WIPP performance assessment (PA). The present study examines the implications of modeling assumptions used in conjunction with BRAGFLO in the 1996 WIPP PA that affect brine and gas flow patterns involving two waste regions in the repository (i.e., a single waste panel and the remaining nine waste panels), a disturbed rock zone (DRZ) that lies just above and below these two regions, and a borehole that penetrates the single waste panel and a brine pocket below this panel. The two waste regions are separated by a panel closure. The following insights were obtained from this study. First, the impediment to flow between the two waste regions provided by the panel closure model is reduced due to the permeable and areally extensive nature of the DRZ adopted in the 1996 WIPP PA, which results in the DRZ becoming an effective pathway for

gas and brine movement around the panel closures and thus between the two waste regions. Brine and gas flow between the two waste regions via the DRZ causes pressures between the two to equilibrate rapidly, with the result that processes in the intruded waste panel are not isolated from the rest of the repository. Second, the connection between intruded and unintruded waste panels provided by the DRZ increases the time required for repository pressures to equilibrate with the overlying and/or underlying units subsequent to a drilling intrusion. Third, the large and areally extensive DRZ void volumes is a significant source of brine to the repository, which is consumed in the corrosion of iron and thus contributes to increased repository pressures. Fourth, the DRZ itself lowers repository pressures by providing storage for gas and access to additional gas storage in areas of the repository. Fifth, given the pathway that the DRZ provides for gas and brine to flow around the panel closures, isolation of the waste panels by the panel closures was not essential to compliance with the U.S. Environment Protection Agency's regulations in the 1996 WIPP PA.

Contents

Executive Summary	ES-1
1. Introduction	1-1
1.1 Rationale for this Study.....	1-1
1.2 Organization of this Report.....	1-9
1.3 Method of Analysis	1-10
1.4 Sampled Variables Used in the BRAGFLO Model	1-11
2. Mathematical Model of Disturbed Rock Zone.....	2-1
2.1 Numerical Implementation of the DRZ Pore Volumes.....	2-3
2.2 Derivation of Effective Brine and Gas Permeabilities for Disturbed Rock Zone, Panel Closures, and Waste Disposal Area	2-12
2.2.1 How Fluid Saturation Impacts Effective Permeability.....	2-12
2.2.2 DRZ and the Waste Panel Effective Permeabilities	2-14
2.3 Mathematical Model Used to Derive Effective Permeability	2-17
3. Gas Saturation in the Waste Disposal Areas and Adjoining DRZ.....	3-1
3.1 Comparison of Gas Saturation Between the Waste Disposal Areas and Adjoining DRZ.....	3-2
3.1.1 Summary of Gas Saturation in the Lower (WAS_SATG) and Upper (REP_SATG) Waste Panels	3-7
3.1.2 Summary of Gas Saturation in the DRZ	3-8
3.2 Effects of Gas Saturation On Fluid Flow Between Waste Regions	3-11
3.3 Variables Affecting Gas Saturation in the Waste Panels and Adjoining DRZ.....	3-12
3.3.1 Variables Influencing Lower (WAS_SATG) and Upper (REP_SATG) Waste Panel Gas Saturation Levels	3-12
3.3.2 Variables Influencing DRZ Gas Saturation Levels	3-14
4. Brine and Gas Flow in the UDRZ.....	4-1
4.1 Variables Used to Define Flow	4-3
4.1.1 Vertical Flow Between UDRZ Waste Disposal Area and the Panel Closures	4-3
4.1.2 Lateral Gas and Brine Flow in UDRZ Above the Panel Closures	4-9
4.2 Overview of Brine and Gas Flow in the UDRZ.....	4-19
4.2.1 Flow Prior to Time of Intrusion	4-19
4.2.2 Flow After Time of Intrusion	4-20
4.2.3 Scatterplots	4-24
4.2.4 Overlay Plots	4-39
4.3 Parameters Affecting Brine and Gas Flow in the UDRZ.....	4-42

Contents (Continued)

4.3.1	Brine Flow.....	4-42
4.3.2	Gas Flow	4-50
5.	Brine and Gas Flow between the Upper and Lower Panels via Panel Closures	5-1
5.1	Variables Used to Define Flow	5-2
5.2	General Summary of Lateral Flow Across the Panel Closures	5-8
5.2.1	Brine Flow.....	5-8
5.2.2	Gas Flow	5-12
5.3	Parameters Affecting Lateral Flow Across the Panel Closures.....	5-18
5.3.1	Brine Flow.....	5-18
5.3.2	Gas Flow	5-21
6	Brine and Gas Flow in Lower Disturbed Rock Zone	6-1
6.1	Variables Used to Define Flow	6-3
6.1.1	Vertical Flow.....	6-3
6.1.2	Lateral Flow	6-9
6.2	Summary of Brine Flow in LDRZ.....	6-18
6.2.1	Flow Prior to Time of Intrusion	6-18
6.2.2	Flow After Intrusion.....	6-23
6.3	Parameters Affecting Vertical and Lateral Flow in the LDRZ.....	6-32
6.3.1	Vertical Flow Between LDRZ and Lower Waste Panel Floor	6-32
6.3.2	Vertical Flow Between Panel Closures and LDRZ.....	6-37
6.3.3	Vertical Flow Between Upper Waste Panels and LDRZ	6-40
6.3.4	Lateral Flow Within the LDRZ	6-43
7.	Discussion of Overlay Plots for Brine and Gas Flow Within Borehole, UDRZ, and LDRZ.....	7-1
7.1	Realization 50 - Overlay Plot Summary.....	7-8
7.1.1	Overlay Plots for Pressures in Lower (WAS_PRES) and Upper (REP_PRES) Waste Panels; Gas Saturation in the Lower (WAS_SATG) and Upper (REP_SATG) Waste Panels; Fraction of Uncorroded Iron in Lower (FEREM_W) and Upper (FEREM_R) Waste Panels	7-8
7.1.2	Overlay Plots for Flow in Borehole.....	7-11
7.1.3	Overlay Plots for Castile Brine Reservoir Pressures (B_P_PRES) with Respect to Brine Flow Up (BRNBHUPP) and Down (BRNBHDNC) the Borehole	7-13
7.1.4	Overlay Plots for Brine Flow through the Panel Closures to the Upper and Lower Waste Panels	7-13
7.1.5	Overlay Plots for Lateral Brine Flow in DRZ Above and Below Panel Closures.....	7-17

Contents (Continued)

7.1.6	Overlay Plots for Lateral Gas Flow in the DRZ Above and Below the Panel Closures	7-18
7.1.7	Overlay Plots for Brine and Gas Flow In/Out the Ceiling and Floor of Upper Waste Panel	7-19
7.1.8	Gas Saturation Contour Plots	7-22
7.2	Realization 20 - Overlay Plot Summary	7-25
7.2.1	Overlay Plots for Pressures in Lower (WAS_PRES) and Upper (REP_PRES) Waste Panels; Gas Saturation in the Lower (WAS_SATG) and Upper (REP_SATG) Waste Panels; Fraction of Uncorroded Iron in Lower (FEREM_W) and Upper (FEREM_R) Waste Panels	7-25
7.2.2	Overlay Plots for Flow in Borehole	7-29
7.2.3	Overlay Plots for Castile Brine Reservoir Pressure (B_P_PRES) with Respect to Brine Flow Up (BRNBHUPP) and Down (BRNBHDNC) the Borehole	7-30
7.2.4	Overlay Plots for Brine Flow through the Panel Closures to the Upper and Lower Waste Panels	7-32
7.2.5	Overlay Plots for Lateral Brine Flow in DRZ Above and Below Panel Closures	7-35
7.2.6	Overlay Plots for Lateral Gas Flow in the DRZ Above and Below the Panel Closures	7-36
7.2.7	Overlay Plots for Brine and Gas Flow In/Out the Ceiling and Floor of Upper Waste Panel	7-37
7.2.8	Gas Saturation Contour Plots	7-40
7.3	Realization 27 - Overlay Plot Summary	7-42
7.3.1	Overlay Plots for Pressure in Lower (WAS_PRES) and Upper (REP_PRES) Waste Panels; Gas Saturation in the Lower (WAS_SATG) and Upper (REP_SATG) Waste Panels; Fraction of Uncorroded Iron in the Lower (FEREM_W) and Upper (FEREM_R) Waste Panels	7-42
7.3.2	Overlay Plots for Flow in Borehole	7-46
7.3.3	Overlay Plots for Castile Brine Reservoir Pressure (B_P_PRES) with Respect to Brine Flow Up (BRNBHUPP) and Down (BRNBHDNC) the Borehole	7-47
7.3.4	Overlay Plots for Brine Flow through the Panel Closures to the Upper and Lower Waste Panels	7-49
7.3.5	Overlay Plots for Lateral Brine Flow in DRZ Above and Below Panel Closures	7-49
7.3.6	Overlay Plots for Lateral Gas Flow in the DRZ Above and Below the Panel Closures	7-53
7.3.7	Overlay Plots for Brine and Gas Flow In/Out the Ceiling and Floor of Upper Waste Panel	7-53
7.3.8	Gas Saturation Contour Plots	7-57

Contents (Continued)

7.4	Realization 4 - Overlay Plot Summary.....	7-59
7.4.1	Overlay Plots for Pressures in Lower (WAS_PRES) and Upper (REP_PRES) Waste Panels; Gas Saturation in the Lower (WAS_SATG) and Upper (REP_SATG) Waste Panels; Fraction of Uncorroded Iron in Lower (FEREM_W) and Upper (FEREM_R) Waste Panels	7-59
7.4.2	Overlay Plots for Flow in Borehole.....	7-63
7.4.3	Overlay Plots for Castile Brine Reservoir Pressures (B_P_PRES) with Respect to Brine Flow Up (BRNBHUPP) and Down (BRNBHDNC) the Borehole.....	7-64
7.4.4	Overlay Plots for Brine Flow through the Panel Closures to the Upper and Lower Waste Panels	7-65
7.4.5	Overlay Plots for Lateral Brine Flow in DRZ Above and Below Panel Closures	7-68
7.4.6	Overlay Plots for Lateral Gas Flow in the DRZ Above and Below the Panel Closures	7-69
7.4.7	Overlay Plots for Brine and Gas Flow In/Out Ceiling and Floor of Upper Waste Panel	7-70
7.4.8	Gas Saturation Contour Plots	7-74
7.5	Realization 47 - Overlay Plot Summary.....	7-77
7.5.1	Overlay Plots For Pressures in Lower (WAS_PRES) and Upper (REP_PRES) Waste Panels; Gas Saturation in the Lower (WAS_SATG) and Upper Waste Panels (REP_SATG); Fraction of Uncorroded Iron in Lower (FEREM_W) and Upper (FEREM_R) Waste Panels	7-77
7.5.2	Overlay Plots for Flow in Borehole.....	7-80
7.5.3	Overlay Plots for Castile Brine Reservoir Pressure (B_P_PRES) with Respect to Brine Flow Up (BRNBHUPP) and Down (BRNBHDNC) the Borehole	7-81
7.5.4	Overlay Plots for Brine Flow through the Panel Closures to the Upper and Lower Waste Panels	7-82
7.5.5	Overlay Plots for Lateral Brine Flow in DRZ Above and Below Panel Closures	7-85
7.5.6	Overlay Plots for Lateral Gas Flow in DRZ Above and Below the Panel Closures	7-87
7.5.7	Overlay Plots for Brine and Gas Flow In/Out the Ceiling and Floor of Upper Waste Panel	7-88
7.5.8	Gas Saturation Contour Plots	7-91
	References	8-1

Figures

1.1	Brine flow in borehole measured at (a) the top of the UDRZ and (b) the top of the lower waste panel vs. time-for all realizations in Replicate 1, Scenario 3	1-4
1.2	Overlay plots for gas and brine flow within the borehole, pressure profiles for lower and upper waste panels, and metal corrosion rates	1-5
1.3	Areas under study within context of entire computational grid.....	1-7
1.4	Logical diagram of BRAGFLO computational grid and material regions used to simulate the E1 event.....	1-8
2.1	Void Volumes of the DRZ as a function of time for an E1 intrusion (individual curves represent different realizations of problem parameters).....	2-5
2.2	Boxplots for changes in waste panel (left column) and DRZ void volume (right column) at 999, 1500, and 10,000 years	2-6
2.3	Scatterplots for (a) DRZ void volumes below the south side of the lower waste panel versus DRZ void volumes below the north side of the lower waste panel at 999; (b) DRZ void volumes above north side of lower waste panel with respect to DRZ void volume above upper waste panel at 999 years; and (c) DRZ void volumes above the north side of the lower waste panel with respect to DRZ void volumes above the upper waste panel at 10,000 years	2-8
2.4	Volume of Lower versus upper waste panels (PORVOL_W vs PORVOL_R) (a) at 999 and (b) 10,000 years.....	2-9
2.5	UDRZ With Respect to upper waste panel void volumes (PVL_UOR and PORVOL_R, respectively) at (a) 999 and (b) 10,000 years (top two plots).....	2-9
2.6	DRZ Void Volumes (m^3) Above the upper waste panel (PVL_UOR) at (a) 999 and (b) 10,000 years with respect to halite porosity (HALPOR)	2-11
2.7	SRRC results showing HALPOR is the most influential LHS parameter affecting UDRZ void volumes above the upper waste panel (PVL_UOR)	2-11
2.8	Bounding Values for Effective brine saturations assigned to the waste disposal area.....	2-13
2.9	Bounding Effective Brine and gas permeabilities assigned to the waste disposal area using the functional relationship between effective permeability and residual brine and gas saturations.....	2-15
2.10	<i>Ranked</i> Effective Brine Permeabilities for the upper waste panel at absolute brine saturations of ~0.20 to 0.30.	2-17
3.1.1	Regions of Disposal System for which gas saturations were evaluated	3-2
3.1.2	Boxplots for Gas Saturation levels (unitless) taken at 999 and 1500 years in the DRZ (top row) and within the lower and upper waste panels (bottom row)	3-4
3.1.3	Boxplots for Gas Saturation levels (unitless) taken at 5500 and 10,000 years in the DRZ (top row) and within the lower and upper waste panels (bottom row)	3-5
3.1.4	Gas Saturation Hairplots for (a) lower and (b) upper waste panels	3-7
3.1.5	UDRZ Gas Saturation Levels above the (a) south and (b) north side of the lower waste panel, and (c) above the upper waste panel. LDRZ gas saturations levels below the (d) south and (e) north side of the lower waste panel, and (f) below the upper waste panel.....	3-9

Figures (Continued)

3.3.1	Standardized Rank Regression Coefficient (SRRC) results showing most influential independent variables for gas saturations in (a) lower and (b) upper waste panels	3-13
3.3.2	Standardized Rank Regression Coefficient (SRRC) results showing most influential independent variables for gas saturations above lower waste panel for area (a) south of borehole, (b) north of borehole, and (c) above the upper waste panel.....	3-15
3.3.3	Standardized Rank Regression Coefficient results showing most influential independent variables for gas saturations below the lower waste panel for area (a) south of borehole, (b) north of borehole, and (c) below the upper waste panel.....	3-16
4.1.1	Locations in UDRZ at which lateral and vertical brine and gas flow were assessed.....	4-1
4.1.2	Hairplots for cumulative vertical brine flow (m^3) between the UDRZ and the south half of the lower waste panel ceiling.....	4-4
4.1.3	Hairplots for cumulative vertical gas flow (m^3) between the UDRZ and the south half of the lower waste panel ceiling.....	4-4
4.1.4	Hairplots for cumulative vertical brine flow (m^3) between the UDRZ and the north half of the lower waste panel ceiling.....	4-5
4.1.5	Hairplots for cumulative vertical gas flow (m^3) between the UDRZ and the north half of the lower waste panel ceiling.....	4-5
4.1.6	Hairplots for cumulative vertical brine flow (m^3) between the UDRZ and the top of the panel closure.....	4-6
4.1.7	Hairplots for cumulative vertical gas flow (m^3) between the UDRZ and the top of the panel closure	4-6
4.1.8	Hairplots for cumulative vertical brine flow (m^3) crossing between ceiling of upper waste panel and UDRZ.....	4-7
4.1.9	Hairplots for cumulative vertical gas flow (m^3) crossing between ceiling of upper waste panel and UDRZ	4-8
4.1.10	Hairplots for cumulative lateral brine flow (m^3) within the UDRZ above the panel closure going in a northerly direction.....	4-11
4.1.11	Hairplots for cumulative lateral gas flow (m^3) within the UDRZ above the panel closure going in a northerly direction.....	4-11
4.1.12	Hairplots for cumulative lateral brine flow (m^3) within the UDRZ above the panel closure going in a southerly direction	4-12
4.1.13	Hairplots for cumulative lateral gas flow (m^3) within the UDRZ above the panel closure going in a southerly direction	4-12
4.1.14	Boxplots for vertical brine flow through the lower waste panel ceiling at (a) 999 years, (b) 1500 years, (c) 5500 years, and (d) 10,000 years	4-13
4.1.15	Boxplots for vertical brine flow through the top of panel closures and upper waste ceilings for (a) 999 years, (b) 1500 years, (c) 5500 years, and (d) 10,000 years	4-14

Figures (Continued)

4.1.16	Boxplots for vertical gas flow through the lower waste panel ceiling for (a) 999 years, (b) 1500 years, (c) 5500 years, and (d) 10,000 years	4-15
4.1.17	Boxplots for vertical gas flow through the top of panel closures and upper waste panel ceilings for (a) 999 years, (b) 1500 years, (c) 5500 years, and (d) 10,000 years.....	4-16
4.1.18	Boxplots for lateral brine flow in the UDRZ passing the area above the panel closures at (a) 999 years, (b) 1500 years, (c) 5500 years, and (d) 10,000 years	4-17
4.1.19	Boxplots for lateral gas flow in the UDRZ passing the area above the panel closures at (a) 999 years, (b) 1500 years, (c) 5500 years, and (d) 10,000 years	4-18
4.2.1	Scatterplots taken at 999 years, for cumulative vertical brine drainage (m^3) from the UDRZ downward through the ceiling of the upper waste panels, BRN_DRAC, with respect to halite porosity, HALPOR.....	4-25
4.2.2	Scatterplots taken at 999 years for south-flowing brine in the UDRZ passing above the closures with respect to halite porosity, HALPOR, and microbial degradation, WMICDFLG > 0.	4-26
4.2.3	Scatterplots, taken at 999 years, for gas flow out the ceiling of the north half of the lower waste panel, GSTWPNOC, with respect to north-flowing gas in the UDRZ passing above the panel closures, GSAPSNO.....	4-27
4.2.4	Scatterplots, taken at 999 years, for gas flow (m^3) out the north and south ceilings (GSTWPSOC and GSTWPNOC, respectively) of the lower waste panel with respect to gas generation processes, i.e., iron corrosion, WRGCOR, and microbial degradation, WMICDFLG > 0.....	4-28
4.2.5	Scatterplots, taken at 999 years, showing the relationship between north-flowing gas (m^3) in the UDRZ passing above the panel closures, GSAPSSIC, and gas passing from the UDRZ through the south side of the concrete shaft, GSCN3SIC, with the lower waste panel pressures (Pa).	4-29
4.2.6	Scatterplots, taken at 999 years, showing the relationship between gas flow (m^3) from the UDRZ through the south side of the concrete shaft, GSCN3SIC, with respect to flow into the UDRZ from the ceiling of the north half of the lower waste panel, GSTWPNOC, and from the ceiling of the upper lower waste panels, GAS_URAC.	4-30
4.2.7	Scatterplots, taken at 1500 years, showing the relationship between brine flow (m^3) out the north and south halves of the lower waste panel into the UDRZ (BRTPWSOC and BRTWPNOC, respectively), and north flowing brine passing above the panel closures (BRAPSSIC and BRAPSNO) with respect to brine reservoir compressibility, BPCOMP.	4-31
4.2.8	Scatterplots, taken at 1500 years and 10,000 years, showing the relationship between north-flowing brine (m^3) in UDRZ above the panel closures with respect to parameters controlling gas generation from microbial degradation (WMICDFLG > 0) and iron corrosion (WRGCOR).	4-32

Figures (Continued)

4.2.9	Scatterplots, taken at 1500 (a and b) and 10,000 (b and c) years, showing the relationship between north-flowing brine (m^3) in the UDRZ passing above the panel closures with respect to borehole permeabilities, BHPRM, and brine flow from the UDRZ down through panel closures (BRNDTPSC).....	4-33
4.2.10	Scatterplots taken at 1500 and 10,000 years (a and b) showing the relationship between brine (m^3) flow down through the top of the panel closures (BRNDTPSC) with respect to borehole permeability (BHPRM).....	4-34
4.2.11	Gas saturation contour plots taken at (a) ~1400, (b) 5400, (c) 8100, and (d) 10,000 years for realization 76 (R1S3)	4-35
4.2.12	Scatterplots, taken at 1500 years, showing the relationship between north flowing gas (m^3) in the UDRZ passing above the panel closures with respect to brine reservoir compressibilities (BPCOMP)	4-36
4.2.13	South-flowing gas (m^3) in the UDRZ (shown only as GSAPSNIC) at 1500 (left) and 10,000 (right) with respect to microbial degradation flag (WMICDFLG > 0), iron corrosion rates WGRCOR, and borehole permeability BHPRM.....	4-37
4.2.14	South-flowing gas (m^3) in the UDRZ taken at (a) 1500 and (b) 10,000 years	4-38
4.2.15	Overlay plots for Realization 27, representative of realizations assigned high BHPRM values	4-40
4.2.16	Overlay plots for Realization 4, representative of realizations assigned low BHPRM values	4-41
4.3.1	Standardized Rank Regression Coefficient (SRRC) results showing the most influential independent variables for vertical brine flow (m^3) between south portion of lower waste panel and UDRZ	4-42
4.3.2	Standardized Rank Regression Coefficient (SRRC) results showing the most influential independent variables for vertical brine flow between north portion of lower waste panel and UDRZ	4-44
4.3.3	Standardized Rank Regression Coefficient (SRRC) results showing the most influential independent variables for vertical brine flow (a) into top of waste panel closures from UDRZ and (b) out top of waste panel closures to UDRZ	4-46
4.3.4	Standardized Rank Regression Coefficient (SRRC) results showing the most influential independent variables for vertical brine flow between upper waste panel and UDRZ	4-47
4.3.5	Standardized Rank Regression Coefficient (SRRC) results showing the most influential independent variables for lateral south-flowing brine in UDRZ (a) south and (b) north of panel closures	4-48
4.3.6	Standardized Rank Regression Coefficient (SRRC) results showing the most influential independent variables for vertical brine flow (m^3) between south portion of lower waste panel and UDRZ	4-49
4.3.7	Standardized Rank Regression Coefficient (SRRC) results showing the most influential independent variables for vertical gas flow out of south portion of lower waste panel.....	4-51

Figures (Continued)

4.3.8	Standardized Rank Regression Coefficient (SRRC) results showing the most influential independent variables for vertical gas flow (a) into and (b) out of north portion of lower waste panel	4-52
4.3.9	Standardized Rank Regression Coefficient (SRRC) results showing the most influential independent variable on upward-flowing gas out of the panel closure	4-54
4.3.10	Standardized Rank Regression Coefficient (SRRC) results showing the most influential independent variables on controlling vertical gas flow (a) down to upper waste panel from DRZ and (b) up into UDRZ from upper waste panel.....	4-55
4.3.11	Standardized Rank Regression Coefficient (SRRC) results showing the most influential independent variables for lateral, north-flowing gas within UDRZ above the (a) south and (b) north side of panel closures (GSAPSSIC and GSAPSNO, respectively)	4-57
4.3.12	Standardized Rank Regression Coefficient (SRRC) results showing the most influential independent variables for controlling lateral, south-flowing gas above panel closures within the UDRZ (GSAPSSOC and GSAPSNC).....	4-58
5.1.1	Regions of disposal systems for which lateral flow across panel closures was assessed.....	5-1
5.1.2	Cumulative brine flow (m^3) across panel closures (a) out of the lower waste panel and (b) into the upper waste panel	5-4
5.1.3	Cumulative gas flow (m^3) across panel closures (a) out of the lower waste panel and (b) into the upper waste panel	5-4
5.1.4	Cumulative brine flow (m^3) across panel closures (a) into the lower waste panel and (b) out of the upper waste panel.....	5-5
5.1.5	Cumulative gas flow (m^3) across panel closures (a) into the lower waste panel and (b) out of the upper waste panel.....	5-5
5.1.6	Boxplots for brine across panel closures.	5-6
5.1.7	Boxplots of gas across panel closures.....	5-7
5.2.1	Overlay plots showing relationship between brine flow direction through panel closures with respect to borehole permeabilities and time of intrusion.....	5-11
5.2.2	Scatterplots of brine flow just prior to intrusion (999 years) (a) into lower waste panel via the south panel closure face and (b) out of the upper waste panel through the north panel closure face with respect to halite porosities for flowing brine.	5-13
5.2.3	Scatterplots of brine flow through panel closures just prior to intrusion (1000 years) with respect to residual brine saturations assigned to waste disposal area for brine flowing (a) into the upper waste panel via the south panel closure face and (b) out of the upper waste panel through the north panel closure face.	5-14
5.2.4	Scatterplots of brine flow through panel closures just prior to intrusion (1000 years) with respect to microbial degradation for brine flowing (a) into the lower waste panel via the south panel closure face and (b) out of the upper waste panel through the north panel closure face.....	5-14

Figures (Continued)

5.2.5	Scatterplots for brine entering the south face (a,b,c) of the panel closure (BRNPSOWC) and exiting the panel closure north face (d,e,f) (BRNPSIRC) with respect to BPCOMP, WMICDFLG, and WGRCOR.....	5-16
5.2.6	Scatterplots of brine flow through panel closures at 10,000 years with respect to borehole permeabilities (BHPRM) for brine flowing (a) into the lower waste panel via the south panel closure face, (b) out of the upper waste panel through the north panel closure face, (c) into the upper waste panel via the south panel closure face, and (d) out of the upper waste panel through the north panel closure face.....	5-17
5.3.1	Standardized Rank Regression Coefficient (SRRC) results showing the most influential independent variables for south-flowing brine (a) into the lower waste panel and (b) out of the upper waste panel	5-18
5.3.2	Standardized Rank Regression Coefficient (SRRC) results showing the most influential independent variables for north-flowing brine (a) out of the lower waste panel and (b) into the upper waste panel	5-19
5.3.3	Standardized Rank Regression Coefficient (SRRC) results showing the most influential independent variables for south-flowing gas (a) into the lower waste panel and (b) out of the upper waste panels.....	5-21
5.3.4	Standardized Rank Regression Coefficient (SRRC) results showing the most influential independent variable for north-flowing gas out of the lower waste panel.....	5-22
6.1.1	Locations in LDRZ at which lateral and vertical brine and gas flow were assessed.....	6-1
6.1.2	Vertical Brine Flow (m^3) (a) into and (b) out of floor of lower waste panel south of borehole	6-4
6.1.3	Vertical Gas Flow (m^3) (a) into and (b) out of floor of lower waste panel south of borehole	6-4
6.1.4	Vertical Brine Flow (m^3) (a) into and (b) out of floor of lower waste panel north of borehole.....	6-5
6.1.5	Vertical Gas Flow (m^3) (a) into and (b) out of the floor of lower waste panel north of borehole.....	6-5
6.1.6	Vertical Brine Flow (m^3) (a) into and (b) out of bottom of panel closures	6-7
6.1.7	Vertical Gas Flow (m^3) (a) into and (b) out of bottom of panel closures	6-7
6.1.8	Vertical Brine Flow (m^3) (a) into and (b) out of upper waste panel floor	6-8
6.1.9	Vertical Gas Flow (m^3) (a) into and (b) out of upper waste panel floor.....	6-8
6.1.10	Lateral North-Flowing Brine (m^3) in the LDRZ flowing in the area (a) south and (b) north of the panel closures	6-10
6.1.11	Lateral North-Flowing Gas (m^3) in the LDRZ below (a) south side of panel closures and (b) north side of panel closures.....	6-10
6.1.12	Lateral South-Flowing Brine (m^3) in the LDRZ below (a) north side of panel closures and (b) south side of panel closures.....	6-11
6.1.13	Lateral South-Flowing Gas (m^3) in the LDRZ below (a) north side of panel closures and (b) south side of panel closures.....	6-11

Figures (Continued)

6.1.14	Boxplots for Vertical Brine flow through south and north halves of lower waste panel floor (top plots); and through the bottom of the panel closures and floor of the upper waste panel. Boxplots show flow at 999 and 1500 years	6-12
6.1.15	Boxplots for Vertical Brine flow through south and north halves of lower waste panel floor (top plots); and through the bottom of the panel closures and floor of the upper waste panel. Boxplots show flow at 5500 and 10,000 years	6-13
6.1.16	Boxplots for Vertical Gas flow through the south and north halves of the lower waste panel (top plots); and through the bottom of the panel closures and floor of the upper waste panel. Boxplots show flow at 999 and 1500 years	6-14
6.1.17	Boxplots for Vertical Gas flow through the south and north halves of the lower waste panel (top plots); and through the bottom of the panel closures and floor of the upper waste panel. Boxplots show flow at 5500 and 10,000 years	6-15
6.1.18	Boxplots for Lateral Brine flow in LDRZ crossing the area under the panel closures. Boxplots show flow taken at 999, 1500, 5500, and 10,000 years	6-16
6.1.19	Boxplots for Lateral Gas flow in LDRZ crossing the area under the panel closures. Boxplots show flow taken at 999, 1500, 5500, and 10,000 years	6-17
6.2.1	Scatterplots for Brine Flow at 999 years out of MB 139 lying south of the repository to the LDRZ (BRM39SIC) and flow upward through the south floor and north floor of the lower waste panel, BRBWPSC and BRBWPNC, respectively.....	6-20
6.2.2	Scatterplots for Brine Drainage from the upper waste panel floor to the LDRZ (BRN_DRBC) at 999 years, with respect to residual brine saturation (WRBRNSAT) and halite porosity (HALPOR).	6-20
6.2.3	Scatterplots for Upward Brine flow from the LDRZ through the upper waste panel floor (BRN_URBC) with respect to upper waste panel pressure (REP_PRES) at 999 years.....	6-21
6.2.4	Scatterplots for Gas Flow downward to the LDRZ from the floor of the north half of the lower waste panel (GSBWPNC) with respect to iron corrosion rates (WGRCOR) and microbial degradation (WMICDFLG > 0); gas flow into the floor of the upper waste panels (GAS_DRBC), with respect to halite porosity (HALPOR).	6-22
6.2.5	Scatterplots Showing the Relationship between upward (BRNUPSC) and downward (BRNDBPSC) brine flow from the bottom of the panel closures to the LDRZ and borehole permeability (BHPRM); brine flow upward through the floor of the upper waste panel (BRN_URBC) with respect to flow through the bottom of the panel closures; and the relationship between upward and downward brine flow in the panel closures (BRNDBPSC versus BRNUPSC) and the floor of the upper waste panel (BRNDBPSC versus BRN_URBC).	6-24
6.2.6	Scatterplots illustrating the relationship between brine flow passing below the closures in the LDRZ in the up-dip direction (BRBPSNOC) and brine reservoir compressibilities (BPCOMP) at 1500 years (a) and 10,000 years (b).	6-25

Figures (Continued)

6.2.7	Scatterplots illustrating the relationship between south (BRBPSNIC) and north flowing brine (BRPBSNOC) passing below the panel closures and borehole permeability (BHPRM) at 1500 (plots a and b) and 10,000 (plots c and d) years.....	6-26
6.2.8	Scatterplots illustrating the relationship between brine draining from the south side of MB 139 (BRMB39SIC) and brine flow from the LDRZ up through floor of the southern and northern halves of the lower waste panels (BRBWPSIC and BRBWPNC, respectively) at 10,000 years.....	6-27
6.2.9	Scatterplots, taken at 1500 and 10,000 years, showing the relationship between brine drainage out the ‘north half’ of the lower waste panel floor (BRBWPNC), north flowing brine in the LDRZ below the panel closures (BRBPSNOC), and brine flow upward, through the floor of the upper waste panel (BRN_URBC).....	6-29
6.2.10	Overlay Plots Illustrating Changes in brine flow direction and rates representative for realizations assigned high and low borehole permeabilities.....	6-31
6.3.1	Standardized Rank Regression Coefficient (SRRC) results showing the most influential independent variables for downward, BRBWPNC (left), and upward, BRBWPNC (right), brine flow from the LDRZ to south half of the lower waste panel.....	6-33
6.3.2	Standardized Rank Regression Coefficient (SRRC) results showing the most influential independent variables for downward, BRBWPNC (left), and upward, BRBWPNC (right), brine flow from the LDRZ to lower waste panel.....	6-35
6.3.3	Standardized Rank Regression Coefficient (SRRC) results showing the most influential independent variable for downward, GSBWPSOC (left), and upward, GSBWPSIC (right), gas flow from the LDRZ to south half of the lower waste panel.....	6-36
6.3.4	Standardized Rank Regression Coefficient (SRRC) results showing the most influential independent variables for downward, GSBWPNC (left), and upward, GSBWPNC (right), gas flow from the LDRZ to north half of the lower waste panel.....	6-37
6.3.5	Standardized Rank Regression Coefficient (SRRC) results showing the most influential independent variables for downward, BRNDPSC (left), and upward, BRNUPSC (right), brine flow between the LDRZ and the panel closures	6-38
6.3.6	Standardized Rank Regression Coefficient (SRRC) results showing the most influential independent variables for downward, GASDBPSC, gas flow between the LDRZ and the panel closures	6-39
6.3.7	Standardized Rank Regression Coefficient (SRRC) results showing the most influential independent variables for downward, BRN_DRBC (left), and upward, BRN_URBC (right), brine flow from the LDRZ to upper waste panel.....	6-40
6.3.8	Standardized Rank Regression Coefficient (SRRC) results showing the most influential independent variables for downward, GAS_DRBC (left), and upward, GAS_URBC (right), gas flow from the LDRZ to upper waste panel.....	6-42

Figures (Continued)

6.3.9	Standardized Rank Regression Coefficient (SRRC) results showing the most influential independent variables for lateral south-flowing brine in the LDRZ passing under the panel closures, into the north face, BRBPSNIC (left), and out the south face, BRBPSSOC (right).....	6-43
6.3.10	Standardized Rank Regression Coefficient (SRRC) results showing the most influential independent variables for lateral south-flowing gas in the LDRZ passing under the panel closures into the north face, GSBPSNIC (left), and out the south face, GSBPSSOC (right).....	6-45
6.3.11	Standardized Rank Regression Coefficient (SRRC) results showing the most influential independent variables for lateral north-flowing brine in the LDRZ passing under the panel closures into the south face, BRBPSSIC (left), and out the north face, BRBPSNOC (right)	6-46
6.3.12	Standardized Rank Regression Coefficient (SRRC) results showing the most influential independent variables for lateral south-flowing gas in the LDRZ passing under the panel closures into the north face, GSBPSSIC (left), and out the south face, GSBPSNOC (right)	6-47
7.1	Logic diagram illustrating realizations representative of sampled parameter combinations that affect general trends in repository performance	7-2
7.2	Regions within modeled area where repository pressures, fraction of iron remaining, brine and gas saturations in lower and upper waste panels, and gas and brine borehole flow were calculated	7-3
7.3	Regions within DRZ and panel closures where lateral brine and gas flow were calculated	7-4
7.4	Regions within the DRZ/upper waste panel interface where vertical brine and gas flow were calculated	7-5
7.1.1	Overlay Plots for Realization 50 depicting pressures, fraction of iron remaining, and gas saturations for lower and upper waste panels (top plot) and cumulative brine and gas flow within borehole at intersection of borehole with the top of lower waste panel and top of the UDRZ (bottom plot).....	7-9
7.1.2	Overlay Plot for Realization 50 depicting brine reservoir pressure overlaid with brine flow up and down the borehole measured at the top and bottom of the lower waste panel.....	7-14
7.1.3	Overlay Plots for Realization 50 depicting brine flow through the panel closures overlaid with lateral brine flow within UDRZ (top plot) and LDRZ (bottom plot), crossing the area just above/below panel closures.....	7-15
7.1.4	Overlay Plots for Realization 50 depicting brine flow through the panel closures overlaid with lateral gas flow within UDRZ (top plot) and LDRZ (bottom plot), crossing the area just above/below panel closures.....	7-16
7.1.5	Overlay Plots for Realization 50 depicting vertical brine and gas flow through the ceiling of upper waste panel within the UDRZ (top plot) and LDRZ (bottom plot)....	7-20

Figures (Continued)

7.1.6	Gas Saturation Contours for realization 50. (a) 1000 years, just prior to intrusion, (b) 1212 years, (c) ~5100 years, and (d) the end of the modeled period, 10,000 years.	
	Borehole in lower waste panel is not shown; see Figure 7.4 for location of borehole	7-23
7.2.1	Overlay plots for Realization 20 depicting pressures, fraction of iron remaining, and gas saturations for lower and upper waste panels (top plot) and cumulative brine and gas flow within borehole at intersection of borehole with top of lower waste panel and top of the UDRZ (bottom plot)	7-26
7.2.2	Overlay plot for Realization 20 depicting brine reservoir pressure overlaid with brine flow up and down the borehole measured at the top and bottom of the lower waste panel.....	7-31
7.2.3	Overlay plots for Realization 20 depicting brine flow through the panel closures overlaid with lateral brine flow within UDRZ (top plot) and LDRZ (bottom plot), crossing the area just above/below panel closures.....	7-33
7.2.4	Overlay plots for Realization 20 depicting brine flow through the panel closures overlaid with lateral gas flow within UDRZ (top plot) and LDRZ (bottom plot), crossing the area just above/below panel closures.....	7-34
7.2.5	Overlay plots for Realization 20 depicting vertical brine and gas flow through the ceiling of upper waste panel within the UDRZ (top plot) and LDRZ (bottom plot)....	7-38
7.2.6	Gas saturation contours for realization 20. (a) 1000 years, just prior to intrusion, (b) ~2289 years, (c) ~6004 years, and (d) the end of the modeled period, 10,000 years.	7-41
7.3.1	Overlay plots for Realization 27 depicting pressures, fraction of iron remaining, and gas saturations for lower and upper waste panels (top plot) and cumulative brine and gas flow within borehole at intersection of borehole with top of lower waste panel and top of the UDRZ (bottom plot)	7-43
7.3.2	Overlay plot for Realization 27 depicting brine reservoir pressure overlaid with brine flow up and down the borehole measured at the top and bottom of the lower waste panel.....	7-48
7.3.3	Overlay plots for Realization 27 depicting brine flow through the panel closures overlaid with lateral brine flow within UDRZ (top plot) and LDRZ (bottom plot), crossing the area just above/below panel closures	7-50
7.3.4	Overlay plots for Realization 27 depicting brine flow through the panel closures overlaid with lateral gas flow within UDRZ (top plot) and LDRZ (bottom plot), crossing the area just above/below panel closures.....	7-51
7.3.5	Overlay plots for Realization 27 depicting vertical brine and gas flow through the ceiling of the upper waste panel within the UDRZ (top plot) and LDRZ (bottom plot)7-54	
7.3.6	Gas saturation contours for realization 27. (a) 1226 years, the time of borehole degradation, (b) ~4877 years, (c) ~6600 years, and (d) the end of the modeled period, 10,000 years.	7-58

Figures (Continued)

7.4.1	Overlay plots for Realization 4 depicting pressures, fraction of iron remaining, and gas saturations for lower and upper waste panels (top plot) and cumulative brine and gas flow within borehole at intersection of borehole with top of lower waste panel and top of the UDRZ (bottom plot).....	7-60
7.4.2	Overlay plot for Realization 4 depicting brine reservoir pressure overlaid with brine flow up and down the borehole measured at the top and bottom of the lower waste panel.....	7-65
7.4.3	Overlay plots for Realization 4 depicting brine flow through the panel closures overlaid with lateral brine flow within UDRZ (top plot) and LDRZ (bottom plot), crossing the area just above/below panel closures	7-66
7.4.4	Overlay plots for Realization 4 depicting brine flow through the panel closures overlaid with lateral gas flow within UDRZ (top plot) and LDRZ (bottom plot), crossing the area just above/below panel closures.....	7-67
7.4.5	Overlay plots for Realization 4 depicting vertical brine and gas flow through ceiling of upper waste panel within the UDRZ (top plot) and LDRZ (bottom plot).....	7-71
7.4.6	Gas saturation contours for realization 4. (a) ~1680 years, (b) ~5730 years, (c) ~6340 years, and (d) 10,000 years, the end of the modeled period.	7-74
7.5.1	Overlay plots for Realization 47 depicting pressures, fraction of iron remaining, and gas saturations for lower and upper waste panels (top plot) and cumulative brine and gas flow within borehole at intersection of borehole with top of lower waste panel and top of the UDRZ (bottom plot)	7-78
7.5.2	Overlay plot for Realization 47 depicting brine reservoir pressure overlaid with brine flow up and down the borehole measured at the top and bottom of the lower waste panel.....	7-82
7.5.3	Overlay plots for Realization 47 depicting brine flow through the panel closures overlaid with lateral brine flow within UDRZ (top plot) and LDRZ (bottom plot), crossing the area just above/below panel closures.....	7-83
7.5.4	Overlay plots for Realization 47 depicting brine flow through the panel closures overlaid with lateral gas flow within UDRZ (top plot) and LDRZ (bottom plot), crossing the area just above/below panel closures.....	7-84
7.5.5	Overlay plots for Realization 47 depicting vertical brine and gas flow through the ceiling of the upper waste panel within the UDRZ (top plot) and LDRZ (bottom plot).....	7-89
7.5.6	Gas saturation contours for Realization 47. (a) 1000 years, just prior to intrusion, (b) ~2212 years, (c) ~3986 years, and (d) the end of the modeled period, 10000 years.	7-92

Tables

1.1	LHS Variables Used in the BRAGFLO Model	1-12
2.1	Input Parameters Affecting Permeability in the DRZ, Panel Closures, and Waste Disposal Area.....	2-14
2.2	Mean, Median, Minimum, and Maximum Brine Saturations Calculated from 300 LHS Elements for the Lower and Upper Waste Panel, the DRZ Above and Below the Upper Waste Panel, and the DRZ Below the Lower Waste Panel	2-16
3-1	Dependent Variables Defining Gas Saturations in the Waste Panels and Adjoining DRZ	3-2
4.1	Dependent Variables for Vertical Brine and Gas Flow Through the Ceiling of the Lower Waste Panel South and North of Borehole (note variable names shown on boxplots are abbreviated and given in parenthesis)	4-3
4.2	Dependent Variables for Vertical Brine and Gas Flow Into and Out of Top of Panel Closures	4-3
4.3	Dependent Variables for Vertical Brine and Gas Flow Into and Out of Upper Waste Panel Closures (variable names shown on boxplots are abbreviated and given in parenthesis)	4-7
4.4	Dependent Variables for Lateral Brine and Gas Flow Within UDRZ Above South and North Panel Closures	4-10
5.1	Dependent Variables for Cumulative Brine Flow (m^3) Between the Upper and Lower Waste Panels Via Panel Closures (note variable names shown on boxplots are abbreviated and given in parenthesis.)	5-3
5.2	Dependent Variables for Cumulative Gas Flow (m^3) Between the Upper and Lower Waste Panels Via Panel Closures	5-3
6.1	Dependent Variables for Vertical Brine and Gas Flow Into/Out of Lower Waste Panel (variable names given on the boxplots in parenthesis)	6-3
6.2	Dependent Variables for Vertical Brine and Gas Flow Into/Out of Upper Waste Panel and Panel Closures (note variable names shown on boxplots are abbreviated and given in parenthesis)	6-6
6.3	Dependent Variables for Lateral Brine and Gas Flow Below Panel Closures (note variable names shown on boxplots are abbreviated and given in parenthesis).....	6-9
7.1	Representative Realizations Examined.....	7-1
7.2	Dependent Variables Described in Overlay Plots.....	7-6

Executive Summary

The Waste Isolation Pilot Plant (WIPP), located in southeastern New Mexico, is being developed for the deep geologic disposal of transuranic (TRU) waste by the U.S. Department of Energy (DOE). Waste disposal will take place in panels excavated in bedded salt approximately 2000 ft (610 m) below the land surface in the Salado Formation. In the vicinity of the repository, the bedded salt has a one degree dip, trending downward toward the south. The excavated panels follow this dip of the salt bed.

Prior to receipt of waste, the DOE was required to submit to the U.S. Environmental Protection Agency (EPA) a Compliance Certification Application (CCA) demonstrating compliance with the requirements of 40 CFR 191 and 194. The DOE submitted the application to the EPA in 1996; the EPA certified the WIPP in compliance with the requirements. One requirement of the application was for the DOE to include results from a performance assessment (PA). The PA was meant to demonstrate, in a probabilistic manner, that long-term repository performance would be within the EPA regulatory limits. The 1996 PA incorporated into the 1996 CCA was the culmination of an iterative PA development process conducted by Sandia National Laboratories (SNL) for the DOE. Some of the key elements of the process were:

- Development of conceptual models for physical processes for use in the estimation of potential radionuclide releases at the WIPP,
- Development of a probabilistic characterization of the uncertainty in the parameters employed within each conceptual model,
- Numerical implementation of these conceptual models, and
- Construction of a probabilistic characterization of different futures within a 10,000-year period.

In addition to providing support for the WIPP's certification, the 1996 PA provided a means to examine current data relevant to the WIPP's short- and long term performance, and resulted in meaningful guidance for planning future research and development.

Two types of scenarios were included in the 1996 WIPP PA calculations, based on the following assumptions:

1. The repository remains undisturbed for 10,000 years after final placement of waste and repository closure.
2. One or more drilling intrusions occur at random within the waste panels over the 10,000-year regulatory period. The time of occurrence for the individual intrusions follows a Poisson process with a rate specified by the EPA.

For the 1996 WIPP PA, several drilling intrusion 'events' were specifically modeled over a 10,000-year period. The drilling intrusion evaluated in this report was one in which a borehole penetrates both the repository and a lower pressurized brine reservoir (i.e., the Castile reservoir) at 1000 years after repository closure. This occurrence is designated an 'E1' scenario in the 1996 WIPP PA.

For the 1996 WIPP PA, many input variables were considered to have a substantial degree of subjective uncertainty (see Helton et al., 1998, Chapter 5). A distribution was developed for each of these variables to characterize its 'range of uncertainty' based on available information from current laboratory and field studies, and analyses from WIPP PAs conducted prior to the application. Variables were sampled and their resulting values were used as input parameters in several of PA's numerical models. Each sample element represented a single set of uncertain variables drawn from a larger set. One of the models, which had a high degree of uncertainty for many of its input parameter values, was the BRAGFLO numerical model. BRAGFLO is a computer program used to solve a system of nonlinear partial differential equations representing two-phase flow (gas and brine flow) within the repository and surrounding vicinity over 10,000 years.

Several simplifying assumptions with respect to model geometry were used in the application of the BRAGFLO model that are relevant to this study (Figure ES-1). These are:

- Two waste regions are numerically modeled; together, they represent the ten waste panels of the repository.
 - One waste region has the dimensions of a single waste panel. This region lies in the most down-dip portion of the excavated area and is the region through which a borehole intrusion is assumed to take place. For convenience, this region is referred to as the lower waste panel.
 - Another waste region has the dimensions of nine waste panels. This region lies up-dip from the first region and is referred to as the upper waste panels.
- The waste panels will undergo creep closure due to the visco-plastic nature of salt. Because of creep closure, the BRAGFLO model reduces the waste panel porosity down to 10–20% of its original value within the first 1000 years of the modeled period.
- In the model is a zone extending 12 meters above and 2 meters below the footprint of the repository where properties of the host rock have been altered due to the creep closure response of the salt adjacent to the excavated face. This area is designated as the disturbed rock zone (DRZ). The rationale used to extend the DRZ 12 meters above was to address the uncertainty with respect to underestimating the extent of damage above the repository which could affect performance. By adopting this model geometry, DRZ brine drainage needed for gas generation would not be underestimated, and a continuous connection is created between the repository and the three thin anhydrite interbed layers. These interbeds are the most permeable pathway to the accessible environment under undisturbed conditions.

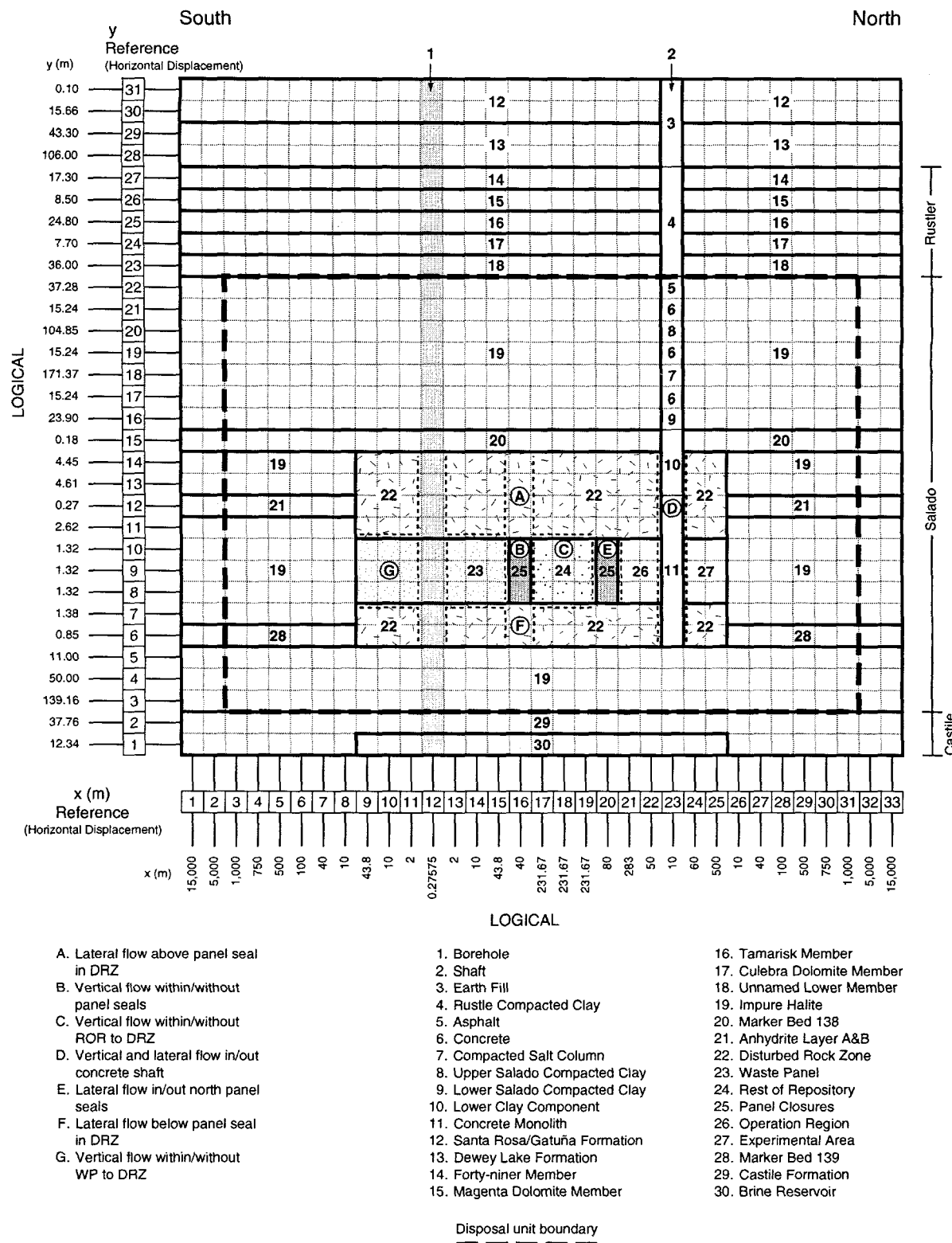


FIGURE ES-1. LOGICAL DIAGRAM OF BRAGFLO computational grid and material regions used to simulate the E1 intrusion event.

- The CCA DRZ model assumes the DRZ is a continuous, homogeneous, and highly connected porous medium (i.e., all dilated grain boundaries are interconnected). Because creep closure causes grain boundary separation, the model assumes DRZ permeability and porosity are greater than that of the host rock. In the CCA model, changes to DRZ porosity (void volumes) are modeled using (i) an exponential function dependent on the initial sampled value for halite porosity, which is increased to incorporate the effects of grain boundary separation, (ii) DRZ rock compressibility, and (iii) pressure. Consequently, as pressure within the repository increases, DRZ void volumes will also increase. DRZ permeability remains constant throughout the modeled period.

Examination of brine and gas flow patterns between the waste panels and the DRZ (detailed in this report, Sections 2 through 6) for an E1 scenario led to insights regarding how the DRZ model assumptions used in the 1996 WIPP PA (for the CCA) affect repository performance. Of particular interest was how the CCA DRZ model impacts fluid flow and pressure between the waste panels. Insights gained from this study are listed below.

1. A DRZ intrinsic permeability¹ only two orders of magnitude lower than the intrinsic permeability assigned to the waste panels, coupled with the assigned value for DRZ residual gas and brine saturation set to 0.0, can give rise to a DRZ gas and/or brine effective permeability² that is greater than that of the waste panels. This makes the DRZ a preferential flow path between the excavated areas, and results in pressures in the upper and lower waste panels differing by less than a few hundred pascals. Therefore, the effects of the processes that occur in the lower waste panel (e.g., an intrusion event) are not isolated from the rest of the repository. Also, any impediment to fluid flow between the lower and upper waste regions provided by a panel closure is reduced by the model assumptions adopted for the DRZ geometry. Pressures equilibrate between the two waste regions due to the following conditions.

¹ A measurement of the conductive properties of a porous medium that is independent of fluid properties or saturation.

² A measurement of the conductive properties of a porous medium, with respect to a specific fluid, when the medium is saturated with more than one fluid or fluid phase. Effective permeability can be several orders of magnitude lower than intrinsic permeability as fluid saturation varies.

a. Prior to Intrusion - For a few hundred years after repository closure, brine seeps from the Upper DRZ (UDRZ) downward to the waste panels. After this period of brine flow downward (and until the time of intrusion), gas is the dominant fluid within the UDRZ and flow direction is up-dip. This gas is produced from microbial degradation and iron corrosion and exits the waste panel ceilings to the UDRZ. From the UDRZ, gas moves up-dip to the northern portions of the repository where it is stored. Brine drainage from MB 139 continues long after brine drainage from Anhydrite AB and MB 138 subsides. Brine drainage from MB 139 tends to collect in the Lower DRZ (LDRZ) below the southern half of the lower waste panel. From here it moves upward through the southern portion of the lower waste panel floor where it is available for iron corrosion.

Downward flow of gas from the waste panels to the LDRZ begins within the first hundred years of repository closure for most realizations and primarily occurs in the upper waste panels, because they serve as the primary gas storage location for gas produced in both of the modeled waste panels. Gas flow downward from the upper waste panel floor prevents any LDRZ brine from flowing upward through the upper waste panel floors.

In brief, prior to intrusion, brine drains from the DRZ into the waste regions. After DRZ drainage, both the UDRZ and the LDRZ serve as a flow path for gas to access a large storage space provided by the nine upper waste panels, the experimental and operational areas, and the DRZ itself. This large gas storage space alleviates pressure buildup.

b. After intrusion and before upper borehole plug degradation, both the UDRZ and LDRZ provide a gas and brine pathway between the excavated areas and the lower borehole. If repository pressure is higher than the reservoir pressure, brine is introduced from the underlying intruded brine reservoir into the LDRZ and the lower waste panel via the borehole. A large portion of this brine flows up-dip toward the upper waste panels. As brine in the LDRZ passes below the panel closures, a portion flows upward through the closure bottom and moves up to the UDRZ or out the closure's north face to the upper waste panels. LDRZ brine that does not flow through the panel closure flows up-dip in the LDRZ toward and eventually through the floors of the upper waste panels. If repository pressure is greater than that of the brine reservoir, brine flow is down-dip,

toward the borehole from 1000 to 1200 years. After upper borehole degradation, flow patterns between the DRZ and the waste panels are dependent on borehole permeability and the dominant fluid phase residing in the two DRZ regions and the waste panels themselves.

- i. For realizations with assigned borehole permeability equal to or greater than 10^{-13} m^2 , the UDRZ provides a pathway for both brine (which tends to flow up-dip) and gas (which tends to flow down-dip) to flow between the borehole and the upper waste panels. After upper borehole degradation, gas stored in the upper waste panels and the back of the repository flows down-dip towards and into the borehole via the UDRZ. This gas is a mixture of gas produced prior to and after intrusion. Gas flow out the borehole lowers repository pressure.

When repository pressures are reduced, brine begins to flow down the borehole from upper units or drains from the south anhydrite layers into the lower waste panel.³ This brine collects in the lower waste panel. Once the lower waste panel is brine saturated, any additional brine that enters this area will flow into the UDRZ, then move up-dip towards and into the upper waste panels. Some brine passes down through the top of the panel closures to the LDRZ. Repository pressures tend to increase as this additional brine is used for gas generation. As repository pressures increase, UDRZ brine flow up-dip is replaced by gas flowing down-dip towards and out the borehole. This is gas that has been stored in the upper waste panels and the back regions of the repository. This pattern may be repeated several times depending on the extent of gas generation and the ease with which fluid flows through the borehole.

In the LDRZ after upper borehole degradation, gas flow out the bottom of the upper waste panel floor to the LDRZ ceases and is replaced by brine flow upward. This brine is primarily brine that has entered the LDRZ via the borehole, MB 139 drainage, or brine drainage from the lower waste panel floor and panel closures. This LDRZ

³ In Figure ES-1, the anhydrite units are on the left side of the repository.

brine flows up-dip towards the upper waste panel and continues from the time of upper borehole plug degradation to the end of the modeled period.

- ii. For realizations with assigned borehole permeability less than 10^{-13} m^2 , the dominant fluid in the UDRZ is gas. Gas flow direction is down-dip, from the back of the repository towards the borehole, and continues from the time of borehole degradation through the end of the modeled period. Like those realizations with higher borehole permeability, this gas is a mixture of gas produced prior to and after intrusion.

Brine in the LDRZ tends to flow down-dip until iron in the lower waste panel is corroded. Once iron is corroded in the lower waste panel, LDRZ brine flow changes direction to up-dip flow.

2. Model assumptions adopted for DRZ rock compressibility cause DRZ void volumes to increase by ~15–20% from the time of repository closure to the end of the modeled period (10,000 years). This is in contrast to model assumptions adopted for the waste panel which presume creep closure will cause waste panel void volumes to be reduced to 10-20% of their original size. Consequently, DRZ void volumes may be large with respect to waste panel void volumes, and in some realizations, DRZ void volumes are larger than waste panel volumes. Large and areally extensive DRZ void volumes may cause lower repository pressure due to the relatively large volume available to store gas or brine. Large and areally extensive DRZ void volumes result in more time being required for an intruded waste panel to equilibrate with over- and underlying units. Large and areally extensive DRZ void volumes may overestimate brine availability for gas generation.

This study generated several questions involving possible modifications with respect to DRZ geometry and flow properties for future PAs. These are:

- How would repository performance be affected if a less areally extensive DRZ model is implemented, reflective of field observations and geomechanical models that predict an ellipsoidal-shaped geometry extending only a few meters from the excavated faces?

- How would repository performance be affected if fluctuations in DRZ void volumes are estimated with a creep closure model similar to that used for the waste panels?
- How would repository performance be affected if DRZ flow properties are correlated to the response of a rock mechanics model that assumes the DRZ heals within 1000 years after repository closure?
- How would results from the anhydrite fracture formation and healing model be affected if initial DRZ volumes are less areally extensive and the DRZ is assumed to heal within 1000 years after repository closure?

Intentionally Left Blank

1. Introduction

1.1 *Rationale for this Study*

The Waste Isolation Pilot Plant (WIPP), located in southeastern New Mexico, is being developed for the deep geologic disposal of transuranic (TRU) waste by the U.S. Department of Energy (DOE). Waste disposal will take place in panels excavated in bedded salt approximately 2000 ft (610 m) below the land surface in the Salado Formation. In the vicinity of the repository, the bedded salt has a one degree dip, trending downward toward the south. The excavated panels follow this dip of the salt bed.

A series of performance assessments (PAs) have been conducted by Sandia National Laboratories to examine current data about the WIPP and to provide guidance for future research and development efforts. In the characterization of uncertainty for a WIPP PA, numerous sample sets of uncertain parameters are used as input for several deterministic models. Results of the WIPP PA are presented as a complementary cumulative distribution function (CCDF). The PA relevant to this report is the 1996 WIPP PA performed in support of the Compliance Certification Application (CCA) submitted to the U.S. Environmental Protection Agency (EPA) by the DOE (1996). The overall conceptual structure of this PA comprised three basic entities:

- Models that simulate physical processes at the WIPP that lead to estimates for radionuclide releases
- A probabilistic characterization of different futures that could occur in the next 10,000 years
- A probabilistic characterization of the uncertainty in the parameters employed within each physical model.

Two types of scenarios were considered in the 1996 WIPP PA, based on the following assumptions:

1. The repository remains undisturbed for 10,000 years after final placement of waste and repository closure.

2. One or more drilling intrusions occur at random within the WIPP land withdrawal boundary over the 10,000-year regulatory period. The time of occurrence for the individual intrusions follows a Poisson process with a rate specified by the EPA.

For the 1996 WIPP PA, five drilling intrusion events over a 10,000-year period were specifically modeled. In the modeling, three replicates of uncertain inputs (with 100 samplings per replicate) were used in the construction of a CCDF of radionuclide releases to the accessible environment. Details of the 1996 WIPP PA structure are found in Helton et al. (1998).

The drilling intrusion evaluated in this report was one in which a borehole penetrates both the repository and a lower pressurized brine reservoir (i.e., the Castile reservoir) at 1000 years after repository closure. This occurrence is designated an 'E1' scenario in the 1996 WIPP PA. Events and processes modeled that are relevant to the E1 scenario and that affect fluid flow within the repository are indicated below.

Events:

- A drilling intrusion (i.e., a borehole) penetrates the repository and the Castile reservoir at 1000 years. It is assumed the borehole is 'open' for 200 years from the repository to the Castile reservoir, thus providing connectivity between the lower Castile and the repository. A 'plug' exists within the borehole between the repository and the Salado-Rustler interface (i.e., the interface of the Salado Formation, in which the repository is located, and the Rustler Formation above it). This plug prevents flow between the repository and the overlying units for 200 years after the intrusion.
- At 1200 years, the borehole plug degrades, and the borehole is assumed to have the permeability of silty sand (see BHPRM, Table 5.1, Helton et al., 1998).
- The lower portion of the borehole in the vicinity of the Castile is assumed to have a reduced permeability by 2200 years due to creep closure. The borehole between the repository and the Castile reservoir is now given a borehole permeability one order of magnitude below that assigned to the upper borehole.

Processes:

- It is possible for brine and gas to flow between the repository and the units above and below via the borehole, given appropriate conditions (i.e., pressure gradient and permeability).
- Brine is able to drain from both the adjoining anhydrites and the disturbed rock zone (DRZ)^a above the repository (i.e., the upper DRZ or UDRZ) to the repository.
- It is possible for gas to flow from the repository through the adjoining anhydrites and the DRZ.
- Microbial degradation of cellulose, rubber, and plastics within the waste will generate gas. This gas can pressurize the repository. Brine saturation of the repository has little effect on this process.
- Iron corrosion of the waste drums will generate gas. This process requires brine coming into contact with uncorroded iron. This gas can pressurize the repository.

In the 1996 WIPP PA, the BRAGFLO program (Bean et al., 1996) was used to solve the system of nonlinear partial differential equations representing two-phase flow (gas and brine flow) in the repository and surrounding vicinity over 10,000 years. (A brief description of the sampled variables used as input for the BRAGFLO model is given in Section 1.4 of this report.) Several simplifying assumptions were adopted in the BRAGFLO program. Those with relevance to this report are listed below:

- Two waste regions are numerically modeled; together, they represent the ten waste panels of the repository.
- One panel region has the dimensions of a single waste panel. This region lies in the most down-dip portion of the excavated area, and it is in this region that the borehole intrusion is assumed to take place. For convenience, this region is referred to as the lower waste panel.

^a The DRZ is host rock whose original properties, such as porosity and permeability, have been altered because of excavation activities.

- Another region has the dimensions of nine waste panels. This region lies up-dip from the first region and is referred to as the upper waste panels.

Examination of BRAGFLO results for the E1 scenario, in which the borehole penetrates both a waste panel and a brine reservoir, revealed brine flow down the borehole measured where the borehole intersects the top of the DRZ, was greater than brine flow down the borehole measured at the top of the lower waste panel. The difference between the two was, for many simulations, 30% to 40% (Figure 1.1).

In addition, flow down the borehole measured at the top of the UDRZ continued long after downward borehole flow measured at the top of the waste panel had ceased. During examination of results representing both brine and gas flow within the borehole, it was discovered that dramatic changes in repository pressure coincided with changes in the type of fluid flowing within the borehole (depicted in Figure 1.2). Furthermore, pressure plots for both the down-dip and up-dip waste panels show that the pressure of the up-dip (unintruded) waste panel responded to the intrusion event at nearly the same time and to the same degree as that for the down-dip (intruded) waste panel. Questions began to arise regarding the role the DRZ played in the overall flow patterns within the excavated areas that could not be answered by consulting the 1996 WIPP PA Salado Flow analysis document (Bean et al., 1996).

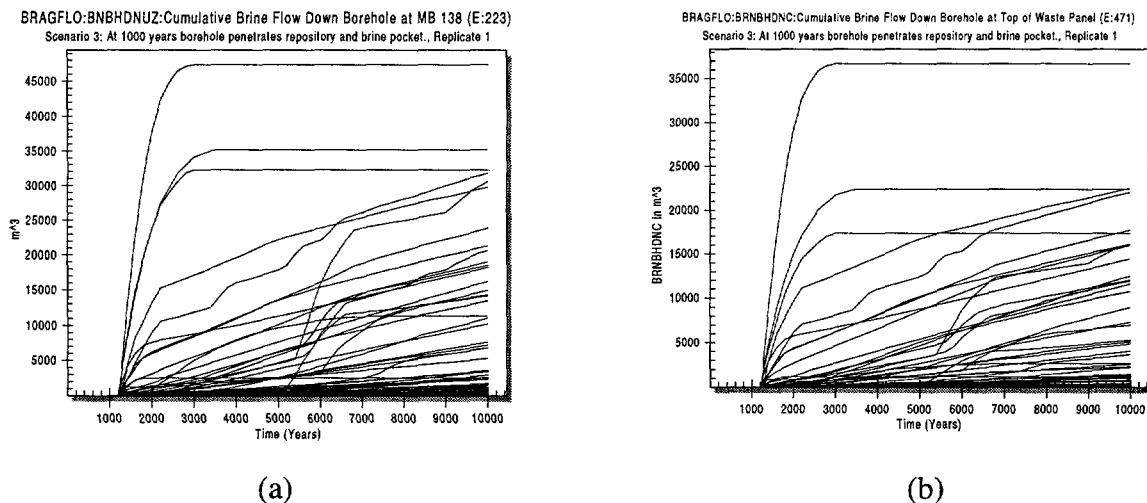


FIGURE 1.1. BRINE FLOW IN BOREHOLE MEASURED at (a) the top of the UDRZ and (b) the top of the lower waste panel vs. time-for all realizations in Replicate 1, Scenario 3

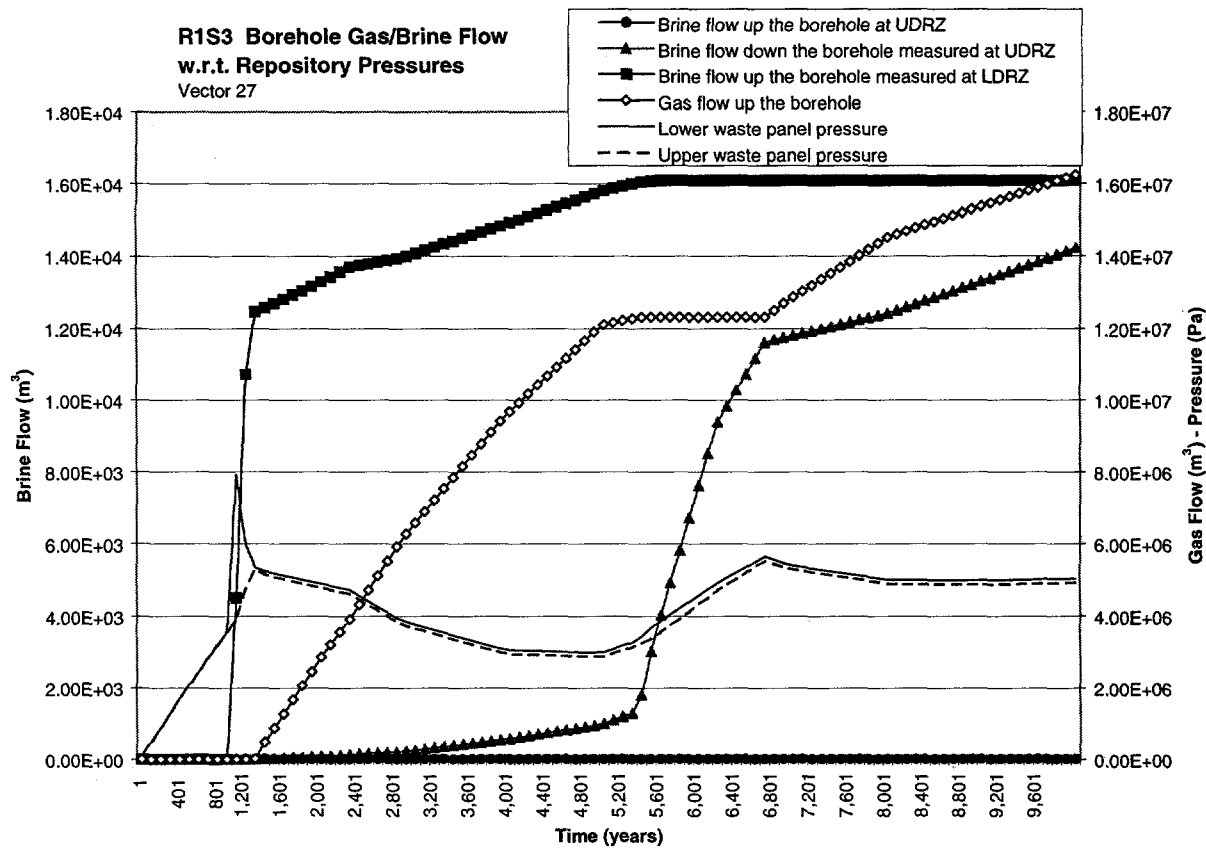


FIGURE 1.2. OVERLAY PLOTS FOR GAS and brine flow within the borehole, pressure profiles for lower and upper waste panels, and metal corrosion rates

This study addresses the following questions:

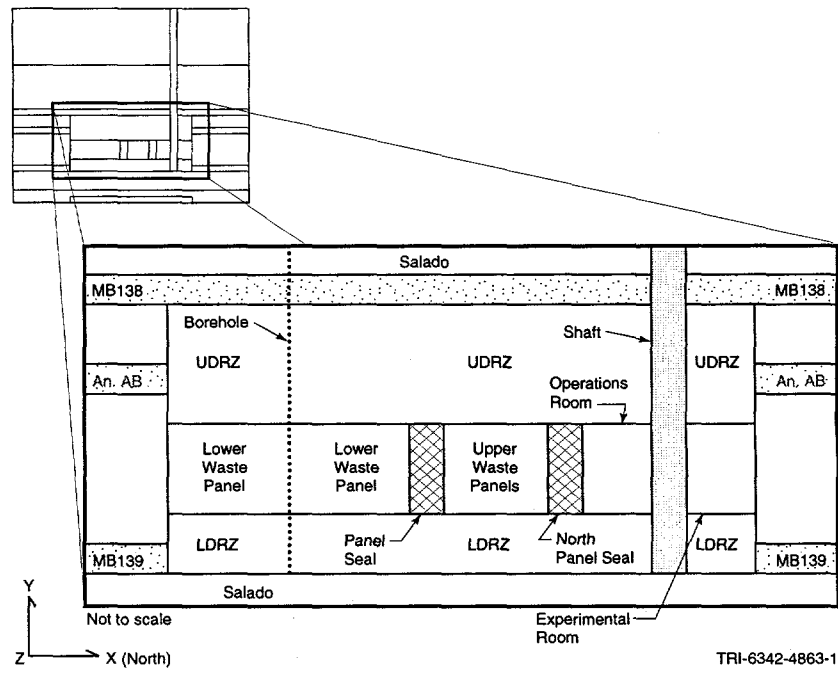
- What is the impact of the DRZ on brine and gas flow in the vicinity of the borehole and how does this affect pressures between the two modeled waste regions?
- Are there gas and brine flow patterns within the upper and lower DRZs (referenced herein as the UDRZ and LDRZ, respectively) that facilitate or impede flow between the lower and upper waste panels?

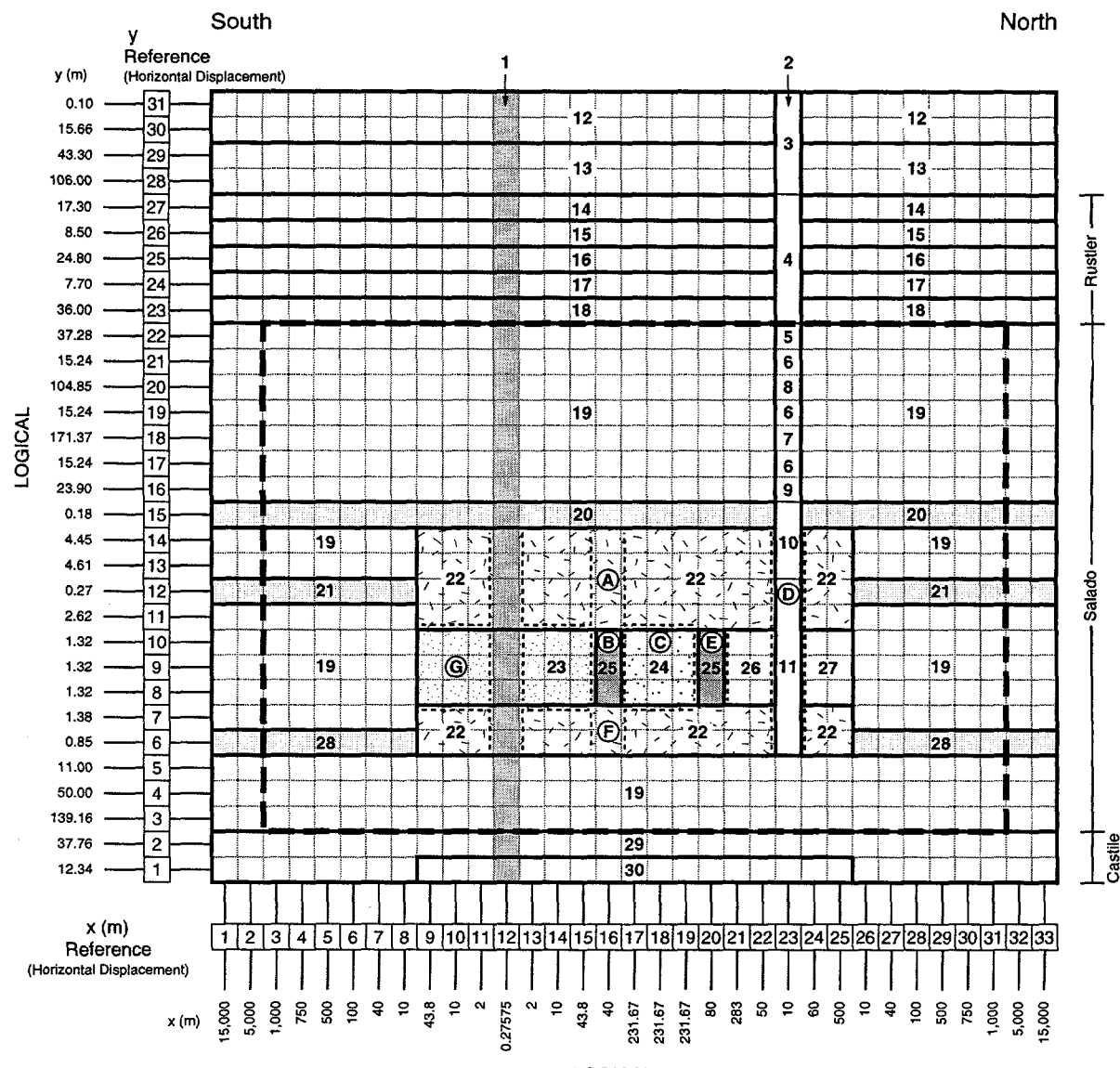
And more specifically:

- What roles do the UDRZ and LDRZ play in the flow of gas and brine between waste panels toward the borehole?
- How do the DRZ-assigned material properties affect overall flow within the repository?
- Do the DRZ volumes, with respect to the volume of the waste disposal areas, affect overall flow patterns within the repository?
- As brine saturations of the DRZ and the waste disposal regions change, so will their respective relative permeabilities. Do the changing relative permeabilities within the DRZ alter gas and brine flow patterns within the waste disposal areas and the borehole? If so, do they affect overall repository performance?

To answer these questions, BRAGFLO results for gas and brine flow within the waste disposal region (i.e., the lower waste panel and the upper waste panels), the panel closures,^b the operations region, the experimental region, the shaft, and the DRZ were examined. Figure 1.3 depicts the area of investigation for this study. Figure 1.4 depicts the BRAGFLO computational grid and highlights the area within the modeled domain (delineated by the short dotted lines) where brine and gas fluxes were assessed. The motivating factor for preparing this report was to answer the questions, which were generated by reviewers of the 1996 WIPP PA, pertaining to how, when, and where fluids might enter various portions of the waste regions via the DRZ. A synopsis of the analysis results are given in the Executive Summary. Details supporting this summary are provided in Sections 2 through 7. Because of the detailed nature of this study, the reader may wish to use this report as a reference guide to gain an understanding of the degree, extent, and sensitivity of brine and gas flow within and between the DRZ and the upper and lower waste panels.

^b Throughout this report, the term 'panel closures' is used in text; in some illustrations, the term 'panel seals' is used instead.





- A. Lateral flow above panel seal in DRZ
- B. Vertical flow within/without panel seals
- C. Vertical flow within/without ROR to DRZ
- D. Vertical and lateral flow in/out concrete shaft
- E. Lateral flow in/out north panel seals
- F. Lateral flow below panel seal in DRZ
- G. Vertical flow within/without WP to DRZ

- 1. Borehole
- 2. Shaft
- 3. Earth Fill
- 4. Rustle Compacted Clay
- 5. Asphalt
- 6. Concrete
- 7. Compacted Salt Column
- 8. Upper Salado Compacted Clay
- 9. Lower Salado Compacted Clay
- 10. Lower Clay Component
- 11. Concrete Monolith
- 12. Santa Rosa/Gatun Formation
- 13. Dewey Lake Formation
- 14. Forty-niner Member
- 15. Magenta Dolomite Member

- 16. Tamarisk Member
- 17. Culebra Dolomite Member
- 18. Unnamed Lower Member
- 19. Impure Halite
- 20. Marker Bed 138
- 21. Anhydrite Layer A&B
- 22. Disturbed Rock Zone
- 23. Waste Panel
- 24. Rest of Repository
- 25. Panel Closures
- 26. Operation Region
- 27. Experimental Area
- 28. Marker Bed 139
- 29. Castile Formation
- 30. Brine Reservoir

Disposal unit boundary

TRI-6342-4871-0

FIGURE 1.4. LOGICAL DIAGRAM OF BRAGFLO computational grid and material regions used to simulate the E1 intrusion event.

1.2 Organization of This Report

The organization of this report is as follows.

Section 2 describes the mathematical model for the DRZ, including the model assumptions, geometry, and assigned material properties. Section 3 is a brief review of those parameters that impact two-phase flow relevant to the BRAGFLO numerical model simulated for WIPP performance. Sections 4 through 6 describe two-phase flow patterns and define dependent variables describing this flow within the vicinity of the repository (i.e., gas or brine flow between the UDRZ and the ceiling of the upper waste panel) as follows:

- Section 4: Flow within the UDRZ
- Section 5: Flow through the panel closures that separate the lower waste panels from upper waste panels
- Section 6: Flow within the LDRZ

Those Latin Hypercube Sampled (LHS) independent variables that most affect flow between the DRZ and the waste panel are given at the end of each section. Detailed descriptions of flow within these regions are given relative to other dependent variables that have been reported in Helton et al. (1998) as having a direct impact on repository performance.

Section 7 presents plots of time-dependent variables affecting system performance for selected simulations. These plots are overlaid so that the reader can see the interrelationship that selected dependent variables have with respect to other dependent variables. The dependent variables are:

- pressures within the lower and upper waste panels,
- gas saturations within the lower and upper waste panels,
- the fraction of uncorroded iron remaining in the lower and upper waste panels,

- gas and brine flow exiting the repository via the borehole penetrating the UDRZ and the lower waste panel,
- vertical and horizontal gas and brine flow exiting the ceiling and floor of the upper waste panel and,
- brine crossing the panel closures between the lower waste panel and the upper waste panel.

Finally, contour plots of gas saturation within the modeled region are provided just before or after pivotal events occur. Examples of such events are:

- just after the upper borehole plug degrades and the lower borehole creep closes (1200 and 2200 years, respectively),
- when all the metal in a waste panel has corroded (the time at which this occurs varies among simulations),
- when all gas has evacuated from the southern portion of the UDRZ or the lower waste panel.

1.3 Method of Analysis

This analysis was performed to determine correlations between those dependent variables defining flow between the DRZ and waste panels, described in Sections 4 through 6, and independent sampled variables. The code PCCSRC (Iman et al., 1985) was used to determine standardized rank regression coefficient (SRRC) values. This method is frequently employed by the WIPP PA group (Helton, 1993). If the absolute value of an SRRC between variables was 0.4 or greater, it was believed the independent variable affected the behavior of the dependent variable. Sections 4 through 6 report this relationship. This program also generated plots of SRRC values for the dependent variables over the time span of the model. These SRRC plots are given in the analysis. In addition to SRRC analysis, scatterplots were generated between variables. Scatterplots provide a graphic representation of the correlation between any two variables by plotting one variable as a function of the other variable at a specified time and for all runs in a scenario (100 runs). Scatterplots are a valuable tool for sensitivity analysis because they

may indicate a correlation between variables that might not be detected when only SRRC values are assessed. Those scatterplots demonstrating significant patterns in activity between variables are given in Sections 4 through 6 as necessary. Scatterplots were generated to examine model behavior at pivotal times and/or events. These times are:

- 999 years, to represent repository processes just before intrusion,
- 1000 years, the time of intrusion,
- 1500 years, to capture repository performance affected after borehole degradation (at 1200 years),
- 5500 years, midway through the modeled period,
- 10,000 years, the end of the modeled period.

1.4 Sampled Variables Used in the BRAGFLO Model

For the 1996 WIPP PA for the CCA (see Helton et al., 1998, Chapter 5), specific values for several input variables were deemed as having a degree of subjective uncertainty. Therefore, based on available knowledge and analyses from past WIPP PAs, a distribution was developed for each variable to characterize its ‘range of uncertainty.’ These variables were sampled using the LHS method and their resulting values were used as input parameters for several of the PA models. Each realization of the PA represents a unique ‘draw’ of a single sampling from the uncertain variables. For the 1996 PA, there were 100 ‘realizations’ that were composed of a unique set of sampled input parameters. Three sampled suites (i.e., replicates) were created. A sampled suite represents a set of 100 unique realizations. Table 1.1 lists the uncertain variables that were sampled as input parameters in the BRAGFLO model and that were analyzed with respect to DRZ fluid flow. Table 1.1 is adapted from Table 5.2.1 of Helton et al. (1998), and all equations and figure numbers provided in that table correspond to that report.

Table 1.1. LHS Variables Used in the BRAGFLO Model^a

Variable	Description
<i>ANHBCEXP</i>	Brooks-Corey pore distribution parameter for anhydrite (dimensionless). Used in BRAGFLO. Defines λ in Eqs. (4.2.9) - (4.2.11) for regions 20, 21, 28 of Fig. 4.2.1 for use with Brooks-Corey model; defines λ in $m = \lambda/(1+\lambda)$ in Eqs. (4.2.18) - (4.2.20) for use with van Genuchten-Parker model in same regions. See <i>ANHBCVGP</i> . Distribution: Student's with 5 degrees of freedom. Range: 0.491 to 0.842. Mean, Median: 0.644. Database identifiers: 587 (S_MB139, PORE_DIS), 527 (S_ANH_AB, POR_DIS), 566 (S_MB138, PORE_DIS). Variable 25 in LHS. Additional information: Howarth and Christian-Frear 1997; WIPP PA 1992-1993 Vol. 3, p. 2-54.
<i>ANHBCVGP</i>	Pointer variable for selection of relative permeability model for use in anhydrite. Used in BRAGFLO. See <i>ANHBCEXP</i> . Distribution: Discrete with 60% 0, 40% 1. Value of 0 implies Brooks-Corey model defined by Eqs. (4.2.9)-(4.2.11); value of 1 implies van Genuchten-Parker model defined by Eqs. (4.2.18)-(4.2.20). Data base identifiers: 596 (S_MB139, RELP_MOD), 536 (S_ANH_AB, RELP_MOD), 575 (S_MB138, RELP_MOD). Variable 22 in LHS. Additional information: Howarth and Christian-Frear 1997; WIPP PA 1992-1993 Vol. 3, p. A-149.
<i>ANHCOMP</i>	Bulk compressibility of anhydrite (Pa^{-1}). Used in BRAGFLO. Pore compressibility β_f in Eq. (4.2.6) defined by <i>ANHCOMP</i> divided by initial porosity (i.e., ϕ_0 in Table 4.2.1) for use in regions 20, 21, 28 of Fig. 4.2.1. Distribution: Student's with 3 degrees of freedom. Range: 1.09×10^{-11} to $2.75 \times 10^{-10} \text{ Pa}^{-1}$. Mean, Median: $8.26 \times 10^{-11} \text{ Pa}^{-1}$. Correlation: -0.99 rank correlation with <i>ANHPRM</i> . Data base identifiers: 580 (S_MB139, COMP_RCK), 521 (S_ANH_AB, COMP_RCK), 560 (S_MB138, COMP_RCK). Variable 21 in LHS. Additional information: Saulnier et al. 1991, Stensrud et al. 1992.
<i>ANHPRM</i>	Logarithm of intrinsic anhydrite permeability (m^2). Used in BRAGFLO. Defines permeability tensors \mathbf{K}_g , \mathbf{K}_b in Eqs. (4.2.1), (4.2.2) for regions 20, 21, 28 in Fig. 4.2.1. Specifically, the anhydrite is assumed to be isotropic, with result that <i>ANHPRM</i> is the logarithm of the diagonal elements of \mathbf{K}_b for the indicated regions and similarly defines the diagonal elements of \mathbf{K}_g after a correction is made for the Klinkenberg effect as shown in Eq. (4.2.29). Distribution: Student's with 5 degrees of freedom. Range: -21.0 to -17.1 (i.e., permeability range is 1×10^{-21} to $1 \times 10^{-17.1} \text{ m}^2$). Mean, Median: -18.9. Correlation: -0.99 rank correlation with <i>ANHCOMP</i> . Data base identifiers: 570 (S_MB138, PRMX_LOG), 571 (S_MB138, PRMY_LOG), 572 (S_MB138, PRMZ_LOG), 531 (S_ANH_AB, PRMX_LOG), 532 (S_ANH_AB, PRMY_LOG), 533 (S_ANH_AB, PRMZ_LOG), 591 (S_MB139, PRMX_LOG), 592 (S_MB139, PRMY_LOG), 593 (S_MB139, PRMZ_LOG). Variable 20 in LHS. Additional information: Howarth and Christian-Frear 1997, Saulnier et al. 1991, Stensrud et al. 1992.

^a Adapted from Table 5.2.1, Helton et al. (1998); figure and equation numbers correspond to figures and equations in that report.

Table 1.1. LHS Variables Used in the BRAGFLO Model (Continued)^a

Variable	Description
<i>ANRBRSAT</i>	Residual brine saturation in anhydrite (dimensionless). Used in BRAGFLO. Defines S_{br} in Eqs. (4.2.13) - (4.2.14) for use in regions 20, 21, 28 of Fig. 4.2.1. Distribution: Student's with 5 degrees of freedom. Range: 7.85×10^{-3} to 1.74×10^{-1} . Mean, Median: 8.36×10^{-2} . Data base identifiers: 598 (S_MB139, SAT_RBRN), 538 (S_ANH_AB, SAT_RBRN), 577 (S_MB138, SAT_RBRN). Variable 23 in LHS. Additional information: Howarth and Christian-Frear 1997; WIPP PA 1992-1993 Vol. 3, p. 2-52.
<i>ANRGSSAT</i>	Residual gas saturation in anhydrite (dimensionless). Used in BRAGFLO. Defines S_{gr} in Eq. (4.2.14) for use in regions 20, 21, 28 of Fig. 4.2.1. Distribution: Student's with 5 degrees of freedom. Range: 1.39×10^{-2} to 1.79×10^{-1} . Mean, median: 7.71×10^{-2} . Database identifiers: 599 (S_MB139, SAT_RGAS), 539 (S_ANH_AB, SAT_RGAS), 578 (S_MB138, SAT_RGAS). Variable 24 in LHS. Additional information: Howarth and Christian-Frear 1997; WIPP PA 1992-1993 Vol. 3, p. 2-53.
<i>BHPRM^b</i>	Logarithm of intrinsic borehole permeability (m^2). Used in BRAGFLO. Defines permeability tensors \mathbf{K}_g , \mathbf{K}_b in Eqs. (4.2.1), (4.2.2) for region 1 in Fig. 4.2.1 when borehole with properties similar to silty sand is present. Specifically, the borehole is assumed to be isotropic, with result that <i>BHPRM</i> is the logarithm of the diagonal elements of \mathbf{K}_b for the indicated region and similarly defines the diagonal elements of \mathbf{K}_g after a correction is made for the Klinkenberg effect as shown in Eq. (4.2.29). Distribution: Uniform. Range: -14 to -11 (i.e., permeability range is 1×10^{-14} to $1 \times 10^{-11} m^2$). Mean, median: -12.5. Data base identifiers: 3184 (BH_SAND, PRMX_LOG), 3190 (BH_SAND, PRMY_LOG). Variable 30 in LHS. Additional information: Thompson et al. 1996.
<i>BPCOMP</i>	Logarithm of bulk compressibility of brine pocket (Pa^{-1}). Used in BRAGFLO. Pore compressibility β_f in Eq. (4.2.6) defined by 10^{BPCOMP} divided by initial porosity (i.e., ϕ_0 in Table 4.2.1) for use in region 30 of Fig. 4.2.1. Distribution: Triangular. Range: -11.3 to -8.00 (i.e., bulk compressibility range is $1 \times 10^{-11.3}$ to $1 \times 10^{-8} Pa^{-1}$). Mean, mode: -9.80, -10.0. Correlation: -0.75 rank correlation with <i>BPPRM</i> . Data base identifier: 61 (CASTILER, COMP_RCK). Variable 29 in LHS. Additional information: Freeze 1996a.
<i>BPINTPRS</i>	Initial pressure in brine pocket (Pa). Used in BRAGFLO. Defines $p_b(x, y, -5)$ in Table 4.2.4 for region 30 in Fig. 4.2.1. Distribution: Triangular. Range: 1.11×10^7 to $1.70 \times 10^7 Pa$. Mean, mode: $1.36 \times 10^7 Pa$, $1.27 \times 10^7 Pa$. Data base identifier: 66 (CASTILER, PRESSURE). Variable 27 in LHS. Additional information: Freeze and Larson 1996; WIPP PA 1992-1993 Vol. 3, Sect. 4.3.

^a Adapted from Table 5.2.1, Helton et al. (1998); figure and equation numbers correspond to figures and equations in that report.

^b Throughout this report, 'BHPRM' and 'BHPERM' are used interchangeably.

Table 1.1. LHS Variables Used in the BRAGFLO Model (Continued)^a

Variable	Description
<i>BPPRM</i>	Logarithm of intrinsic brine pocket permeability (m^2). Used in BRAGFLO. Defines permeability tensors \mathbf{K}_g , \mathbf{K}_b in Eqs. (4.2.1), (4.2.2) for region 30 in Fig. 4.2.1. Specifically, the brine pocket is assumed to be isotropic, with result that <i>BPPRM</i> is the logarithm of the diagonal elements of \mathbf{K}_b for the indicated region and similarly defines the diagonal elements of \mathbf{K}_g after a correction is made for the Klinkenberg effect as shown in Eq. (4.2.29). Distribution: Triangular. Range: -14.7 to -9.80 (i.e., permeability range is $1 \times 10^{-14.7}$ to $1 \times 10^{-9.80} \text{ m}^2$). Mean, mode: -12.1, -11.8. Correlation: -0.75 with <i>BPCOMP</i> . Data base identifiers: 67 (CASTILER, PRMX_LOG), 68 (CASTILER, PRMY_LOG). Variable 28 in LHS. Additional information: Freeze 1996b, Popielak et al. 1983.
<i>BPVOL</i>	Pointer variable for selection of brine pocket volume. Used in BRAGFLO. Distribution: Discrete, with integer values 1, 2, ..., 32 equally likely. Originally intended to select from 32 equally-likely brine pocket maps obtained by assuming five regions beneath repository, with each region either containing or not containing pressurized brine. This produces 32 (i.e., 2^5) possible brine pocket maps. This approach was abandoned when more information on brine pockets became available (Powers et al. 1996) and the only role that <i>BPVOL</i> now plays is to determine volume of brine (m^3) contained in the brine pocket. Specifically, the volumes are 32,000, 64,000, 96,000, 128,000 and 160,000 m^3 if the original maps contained 0 or 1, 2, 3, 4 or 5 brine pockets, and the corresponding probabilities are 0.1875, 0.3125, 0.3125, 0.15625 and 0.03125. The indicated volumes define V_{brn} in Eq. (4.2.16) and thus define ϕ_0 for region 30 in Fig. 4.2.1; in addition, the number of drilling intrusions nD required to deplete the pressurized brine beneath the repository is defined by $nD = 2V_{brn}/32,000$ (i.e., 2, 4, 6, 8 or 10 intrusions depending on whether the associated brine volume is 32,000, 64,000, 96,000, 128,000 or 160,000 m^3 ; see nD in Table 6.6.2 of Sect. 6.6). For the presentation of sensitivity analysis results, <i>BPVOL</i> is assigned the brine volumes that correspond to the sampled integer values. Data base identifiers: 3194 (CASTILER, GRIDFLO). Variable 31 in LHS. Additional information: Larson 1997, Swift et al. 1996, Powers et al. 1996.
<i>HALCOMP</i>	Bulk compressibility of halite (Pa^{-1}). Used in BRAGFLO. Pore compressibility β_f in Eq. (4.2.6) defined by <i>HALCOMP</i> divided by initial porosity (i.e., ϕ_0 in Table 4.2.1) for use in region 19 of Fig. 4.2.1. Distribution: Uniform. Range: 2.94×10^{-12} to $1.92 \times 10^{-10} \text{ Pa}^{-1}$. Mean, median: $9.75 \times 10^{-11} \text{ Pa}^{-1}$, $9.75 \times 10^{-11} \text{ Pa}^{-1}$. Correlation: -0.99 rank correlation with <i>HALPRM</i> . Data base identifier: 541 (S_HALITE, COMP_RCK). Variable 19 in LHS. Additional information: Christian-Frear 1996a.

^a Adapted from Table 5.2.1, Helton et al. (1998); figure and equation numbers correspond to figures and equations in that report.

Table 1.1. LHS Variables Used in the BRAGFLO Model (Continued)^a

Variable	Description
<i>HALPOR</i>	Halite porosity (dimensionless). Used in BRAGFLO. Defines ϕ_0 in Eq. (4.2.6) for region 19 in Fig. 4.2.1. Distribution: Piecewise uniform. Range: 1.0×10^{-3} to 3×10^{-2} . Mean, median: 1.28×10^{-2} , 1.00×10^{-2} . Data base identifier: 544 (S_HALITE, POROSITY). Variable 17 in LHS. Additional information: Howarth 1996; WIPP PA 1992-1993 Vol. 3, p. 2-41.
<i>HALPRM</i>	Logarithm of halite permeability (m^2). Used in BRAGFLO. Defines permeability tensors \mathbf{K}_g , \mathbf{K}_b in Eqs. (4.2.1), (4.2.2) for region 19 in Fig. 4.2.1. Specifically, the halite is assumed to be isotropic, with result that <i>HALPRM</i> is the logarithm of the diagonal elements of \mathbf{K}_b for the indicated region and similarly defines the diagonal elements of \mathbf{K}_g after a correction is made for the Klinkenberg effect as shown in Eq. (4.2.29). Distribution: Uniform. Range: -24 to -21 (i.e., permeability range is 1×10^{-24} to $1 \times 10^{-21} \text{ m}^2$). Mean, median: -22.5, -22.5. Correlation: -0.99 rank correlation with <i>HALCOMP</i> . Data base identifiers: 547 (S_HALITE, PRMX_LOG), 548 (S_HALITE, PRMY_LOG). Variable 18 in LHS. Additional information: Davies and Beauheim 1996, Domski 1996a, Christian-Frear 1996b.
<i>SALPRES</i>	Initial brine pressure, without the repository being present, at a reference point located in the center of the combined shafts at the elevation of the midpoint of MB 139 (Pa). Used in BRAGFLO. Defines p_{b0} , which is used to define $p_b(x, y, 0)$ (Table 4.2.4). With respect to computational cells in Fig. 4.2.1, defines initial brine pressure at location of cell (23,6). Distribution: Uniform. Range: 1.104×10^7 to 1.389×10^7 Pa. Mean, median: 1.247×10^7 Pa, 1.247×10^7 Pa. Data base identifier: 546 (S_HALITE, PRESSURE). Variable 26 in LHS. Additional information: Domski 1996b; WIPP PA 1992-1993 Vol. 3, p. 2-38.
<i>SHBCEXP</i>	Brooks-Corey pore distribution parameter for shaft (dimensionless). Used in BRAGFLO. Defines λ in Eqs. (4.2.9) - (4.2.11) for regions 3-11 in Fig. 4.2.1. Distribution: Piecewise uniform. Range: 0.11 to 8.10. Mean, median: 2.52, 0.94. Variable 16 in LHS. Additional information: Kelley et al. 1996a,b; Hurtado 1996.
<i>SHPRMASP</i>	Logarithm of intrinsic permeability (m^2) of asphalt component of shaft seal (m^2). Used in BRAGFLO. Permeability tensors \mathbf{K}_g , \mathbf{K}_b in Eqs. (4.2.1), (4.2.2) for region 5 in Fig. 4.2.1 are functions of asphalt permeability (i.e., $k_s = 10^x$, $x = \text{SHPRMASP}$, in Eq. (4.2.34)), halite permeability (i.e., $k_{out} = 10^x$, $x = \text{HALPRM}$, in Eq. (4.2.35)), and shaft DRZ permeability (i.e., $k_{in} = 10^x$, $x = \text{SHPRMDRZ}$, in Eq. (4.2.35)), with diagonal elements of \mathbf{K}_b defined by k_e in Eq. (4.2.34) and the diagonal elements of \mathbf{K}_g defined similarly after a correction is made for the Klinkenberg effect as shown in Eq. (4.2.29). Distribution: Triangular. Range: -21 to -18 (i.e., permeability range is 1×10^{-21} to $1 \times 10^{-18} \text{ m}^2$). Mean, mode: -19.7, -20.0. Data base identifiers: 2283 (ASPHALT, PRMX_LOG), 2284 (ASPHALT, PRMY_LOG). Variable 11 in LHS. Additional information: Kelley et al. 1996a,b; Repository Isolation Systems Department 1996.

^a Adapted from Table 5.2.1, Helton et al. (1998); figure and equation numbers correspond to figures and equations in that report.

Table 1.1. LHS Variables Used in the BRAGFLO Model (Continued)^a

Variable	Description
<i>SHPRMCLY</i>	Logarithm of intrinsic permeability (m^2) for clay components of shaft. Used in BRAGFLO. Defines permeability tensors \mathbf{K}_g , \mathbf{K}_b in Eqs. (4.2.1), (4.2.2) for regions 4, 10 in Fig. 4.2.1; specifically, the clay component is assumed to be isotropic, with result that <i>SHPRMCLY</i> is the logarithm of the diagonal elements of \mathbf{K}_b for the indicated regions and the diagonal elements of \mathbf{K}_g are defined similarly after a correction is made for Klinkenberg effect as shown in Eq. (4.2.29). Plays same role in definition of \mathbf{K}_g , \mathbf{K}_b for regions 8, 9 in Fig. 4.2.1 as <i>SHPRMASP</i> does in the definition of \mathbf{K}_g , \mathbf{K}_b for region 5 in Fig. 4.2.1, with result that \mathbf{K}_g , \mathbf{K}_b are functions of <i>SHPRMCLY</i> , <i>HALPRM</i> and <i>SHPRMDRZ</i> . Distribution: Triangular. Range: -21 to -17.3 (i.e., permeability range is 1×10^{-21} to $1 \times 10^{-17.3} \text{ m}^2$). Mean, mode: -18.9 , -18.3 . Additional information: Kelley et al. 1996a,b; Repository Isolation Systems Department 1996.
<i>SHPRMCON</i>	Same as <i>SHPRMCLY</i> (as used for regions 4, 10 in Fig. 4.2.1) but for concrete component of shaft seal (i.e., region 6 in Fig. 4.2.1) for 0 to 400 yr. Distribution: Triangular. Range: -17.0 to -14.0 (i.e., permeability range is 1×10^{-17} to $1 \times 10^{-14} \text{ m}^2$). Mean, mode: -15.3 , -15.0 . Data base identifiers: 2470 (CONC_T1, PRMX_LOG), 2471 (CONC_T1, PRMY_LOG). Variable 10 in LHS. Additional information: Kelley et al. 1996a,b; Repository Isolation Systems Department 1996.
<i>SHPRMDRZ</i>	Logarithm of intrinsic permeability (m^2) of DRZ surrounding shaft. Used in BRAGFLO. Defines k_{in} in Eq. (4.2.35). Used in definition of effective permeability for shaft in regions 5, 8, 7 and 9 of Fig. 4.2.1. See <i>SHPRMASP</i> , <i>SHPRMCLY</i> , <i>SHPRMHAL</i> . Distribution: Triangular. Range: -17.0 to -14.0 (i.e., permeability range is 1×10^{-17} to $1 \times 10^{-14} \text{ m}^2$). Mean, mode: -15.3 , -15.0 . Data base identifier: 3133 (SHFT_DRZ, PRMX_LOG). Variable 12 in LHS. Additional information: Kelley et al. 1996a,b; Knowles et al. 1996.
<i>SHPRMHAL</i>	Pointer variable (dimensionless) used to select intrinsic permeability in crushed salt component of shaft seal at different times. Used in BRAGFLO. Distribution: Uniform. Range: 0 to 1. Mean, mode: 0.5, 0.5. A distribution of permeability (m^2) in the crushed salt component of the shaft seal (i.e., region 7 in Fig. 4.2.1) is defined for each of the following time intervals: [0, 10 yr], [10, 25 yr], [25, 50 yr], [50, 100 yr], [100, 200 yr], [200, 10,000 yr] (see Table 2, Kelley et al. 1996a). <i>SHPRMHAL</i> is used to select a permeability value from the cumulative distribution function for permeability for each of the preceding time intervals with result that a rank correlation of 1 exists between the permeabilities used for the individual time intervals. Once selected, crushed salt permeabilities are used to define \mathbf{K}_g , \mathbf{K}_b in Eqs. (4.2.1), (4.2.2). For region 7 (Fig. 4.2.1) in the same manner as <i>SHPRMASP</i> is used to define \mathbf{K}_g , \mathbf{K}_b for region 5 (Fig. 4.2.1). Data base identifier: 2939 (SALT_T1, CUMPROB). Variable 13 in LHS. Additional information: Kelly et al. 1996a,b; Vaughn and McArthur 1996.

^a Adapted from Table 5.2.1, Helton et al. (1998); figure and equation numbers correspond to figures and equations in that report.

Table 1.1. LHS Variables Used in the BRAGFLO Model (Continued)^a

Variable	Description
<i>SHRBRSAT</i>	Residual brine saturation in shaft (dimensionless). Used in BRAGFLO. Defines S_{br} in Eqs. (4.2.23) - (4.2.24) for regions 3-11 in Fig. 4.2.1. Distribution: Uniform. Range: 0 to 0.4. Mean, median: 0.2, 0.2. Additional information: Kelley et al. 1996a,b.
<i>SHRGSSAT</i>	Residual gas saturation in shaft (dimensionless). Used in BRAGFLO. Defines S_{gr} in Eq. (4.2.24) for regions 3-11 in Fig. 4.2.1. Distribution: Uniform. Range: 0 to 0.4. Mean, median: 0.2, 0.2. Data base identifiers: 2529 (SALT_T1, SAT_RGAS), 2546 (SALT_T2, SAT_RGAS), 2563 (SALT_T3, SAT_RGAS), 2580 (SALT_T4, SAT_RGAS), 2597 (SALT_T5, SAT_RGAS), 2993 (SALT_T6, SAT_RGAS), 2512 (EARTH, SAT_RGAS), 3015 (CLAY_RUS, SAT_RGAS), 2543 (CL_L_T1, SAT_RGAS), 2360 (CL_L_T2, SAT_RGAS), 2377 (CL_L_T3, SAT_RGAS), 3083 (CL_L_T4, SAT_RGAS), 2394 (CL_M_T1, SAT_RGAS), 2411 (CL_M_T2, SAT_RGAS), 2428 (CL_M_T3, SAT_RGAS), 2445 (CL_M_T4, SAT_RGAS), 2462 (CL_M_T5, SAT_RGAS), 2326 (CLAY_BOT, SAT_RGAS), 2479 (CONC_T1, SAT_RGAS), 2495 (CONC_T2, SAT_RGAS), 3064 (CONC_MON, SAT_RGAS), 2292 (ASPHALT, SAT_RGAS). Variable 14 in LHS. Additional information: Kelley et al. 1996a,b; Mayer et al. 1992.
<i>WASTWICK</i>	Increase in brine saturation of waste due to capillary forces (dimensionless). Used in BRAGFLO. Defines S_{wick} in Eq. (4.2.71) for regions 23, 24 in Fig. 4.2.1. Distribution: Uniform. Range: 0 to 1. Mean, median: 0.5, 0.5. Data base identifier: 2231 (WAS_AREA, SAT_WICK), 2138 (REPOSIT, SAT_WICK). Variable 8 in LHS.
<i>WFBETCEL</i>	Scale factor used in definition of stoichiometric coefficient for microbial gas generation (dimensionless). Used in BRAGFLO. Defines β in Eq. (4.2.70) for regions 23, 24 in Fig. 4.2.1. Distribution: Uniform. Range: 0 to 1. Mean, median: 0.5, 0.5. Data base identifier: 2994 (CELLULS, FBETA). Variable 5 in LHS. Additional information: Wang and Brush 1996a,b.
<i>WGRCOR</i>	Corrosion rate for steel under inundated conditions in the absence of CO ₂ (m/s). Used in BRAGFLO. Defines R_{ci} in Eq. (4.2.49) for regions 23, 24 in Fig. 4.2.1. Distribution: Uniform. Range: 0 to 1.58×10^{-14} m/s. Mean, median: 7.94×10^{-15} m/s, 7.94×10^{-15} m/s. Data base identifier: 2907 (STEEL, CORRMCO2). Variable 1 in LHS. Additional information: Wang and Brush 1996a.
<i>WGRMICH</i>	Microbial degradation rate for cellulose under humid conditions (mol/kg•s). Used in BRAGFLO. Defines R_{mh} in Eq. (4.2.51) for regions 23, 24 in Fig. 4.2.1. Distribution: Uniform. Range: 0 to 1.27×10^{-9} mol/kg•s. Mean, median: 6.34×10^{-10} mol/kg•s, 6.34×10^{-10} mol/kg•s. Data base identifier: 656 (WAS_AREA, GRATMICH), 2127 (REPOSIT, GRATMICH). Variable 4 in LHS. Additional information: Wang and Brush 1996a.

^a Adapted from Table 5.2.1, Helton et al. (1998); figure and equation numbers correspond to figures and equations in that report.

Table 1.1. LHS Variables Used in the BRAGFLO Model (Continued)^a

Variable	Description
<i>WGRMICI</i>	Microbial degradation rate for cellulose under inundated conditions (mol/kg•s). Used in BRAGFLO. Defines R_{mi} in Eq. (4.2.51) for regions 23, 24 in Fig. 4.2.1. Distribution: Uniform. Range: 3.17×10^{-10} to 9.51×10^{-9} mol/kg•s. Mean, median: 4.92×10^{-9} mol/kg•s, 4.92×10^{-9} mol/kg•s. Data base identifier: 657 (WAS_AREA, GRATMICI), 2128 (REPOSIT, GRATMICI). Variable 3 in LHS. Additional information: Wang and Brush 1996a.
<i>WMICDFLG</i>	Pointer variable for microbial degradation of cellulose. Used in BRAGFLO. Distribution: Discrete, with 50% 0, 25% 1, 25% 2. $WMICDFLG = 0, 1, 2$ implies no microbial degradation of cellulose, microbial degradation of only cellulose, microbial degradation of cellulose, plastic and rubber. Data base identifier: 2823 (WAS_AREA, PROBDEG), 2824 (REPOSIT, PROBDEG). Variable 2 in LHS. Additional information: Tierney 1996a.
<i>WRBRNSAT</i>	Residual brine saturation in waste (dimensionless). Used in BRAGFLO. Defines S_{br} in Eqs. (4.2.13) - (4.2.14) for use in regions 23, 24 in Fig. 4.2.1. Also used in BRAGFLO_DB; see Sect. 4.7.4. Distribution: Uniform. Range: 0 to 0.552. Mean, median: 0.276, 0.276. Data base identifiers: 670 (WAS_AREA, SAT_RBRN), 2741 (REPOSIT, SAT_RBRN). Variable 7 in LHS. Additional information: Vaughn 1996a.
<i>WRGSSAT</i>	Residual gas saturation in waste (dimensionless). Used in BRAGFLO. Defines S_{qr} in Eq. (4.2.14) for use in regions 23, 24 in Fig. 4.2.1. Also used in BRAGFLO_DB; see Sect. 4.7.4. Distribution: Uniform. Range: 0 to 0.15. Mean, median: 0.075, 0.075. Data base identifiers: 671 (WAS_AREA, SAT_RGAS), 2137 (REPOSIT, SAT_RGAS). Variable 6 in LHS. Additional information: Solutions Engineering 1995.

^a Adapted from Table 5.2.1, Helton et al. (1998); figure and equation numbers correspond to figures and equations in that report.

2. Mathematical Model of Disturbed Rock Zone

This section briefly describes the modeling assumptions for the DRZ with respect to void volume and permeability and the assumptions for fluid flow that were numerically implemented by BRAGFLO. A brief background on the mechanical processes that caused the development of the DRZ is given below.

The WIPP repository is excavated within laterally continuous halites and polyhalites. The halite is interbedded with thin layers of clay and anhydrite. The removal of halite to create the waste region creates pressure nonequilibrium between the newly created open surfaces (near atmospheric pressure) and the host rock. The visco-elastic nature of halite, coupled with this newly created stress-strain field, causes the halite within the vicinity of the excavated face to deform as it closes the excavated room. This process is commonly called creep closure. The creep closure process is enough to initiate grain boundary separation and create microfractures within a few meters of the excavation. Some of these microfractures grow in size and form macrofractures, and in some cases, the excavated face of the host rock exfoliates along these larger fracture lines. When this happens, the exfoliated rock is not connected to the host rock and becomes part of the room rubble. Once disengaged from the host rock, the detached material will no longer transmit fluids from the enhanced fracture network that penetrates into the host rock. With time, the visco-elastic nature of the rock will cause the surrounding rock to close in on the excavated void. As this happens, microfractures will close or 'heal' as the excavated room closes and pressures rise to that of lithostatic. Given the processes described above, the volume of the DRZ will also be reduced as the room shrinks in size.

In the creation of a DRZ, several host rock properties are changed due to the process of creep closure. These are 1) increased void volumes due to halite dilation and 2) enhanced fluid permeability via larger and more connected voids, along grain boundaries. (A more detailed discussion of the DRZ numerical conceptualization can be found in the 1996 WIPP PA Salado Flow analysis document [Bean et al., 1996].)

Because the DRZ lies above and below the excavated area (see Figure 1.3), its void volume and permeability can affect brine and gas flow between the waste disposal areas and other areas of

the repository. Of interest is the level of realism implemented in the PA's DRZ numerical model with respect to effective DRZ permeabilities and void volumes and how the DRZ numerical model couples with the model used to derive void volume and permeability for the waste regions.

For the 1996 PA, the void volume of the DRZ is a function of a) halite porosity (five years after closure, a sampled parameter), b) DRZ compressibility, and c) changes in the initial value for DRZ porosity given its functional relationship with compressibility and pressure.¹ DRZ permeability is a function of a) absolute permeabilities,² b) *actual* brine or gas saturations, and c) residual brine and gas saturations. The model used by BRAGFLO for waste panel volumes is the product of a separate set of calculations that take into account the visco-elastic nature of the host rock and the waste material. This is incorporated in BRAGFLO by use of a look-up table.

The following section will demonstrate that:

- While *absolute* (i.e., formation or nonadjusted) DRZ permeability is approximately two orders of magnitude less than *absolute* waste panel permeability, DRZ *effective* permeability can be greater than waste panel permeability given the extent of brine or gas saturations within the two regions.
- Even though initial DRZ void volumes are much smaller than the waste disposal regions, toward the later half of the modeled period there are many realizations where DRZ void volumes are much greater than those of the waste disposal region.

Due to the preceding modeling assumptions implemented by the 1996 PA, the DRZ can become a gas or brine pathway that significantly promotes or 'short circuits' fluid flow between the upper and lower waste panels.

¹ Pressure fluctuations from processes active within the waste regions and the repository affect the void volume of the DRZ in a similar fashion as the model for the waste region itself, but to a different degree, as the two regions use two different numerical models.

² Formation permeability values given 100% brine saturation.

The organization of this section is as follows:

- First, a brief description is given as to how the BRAGFLO model determines DRZ volumes, the relationship between DRZ volumes and waste panel volumes, and how these volumes change with respect to time and location.
- Second, the functional relationship between *effective* permeabilities, gas and brine saturations, and other sampled parameters is briefly described.
- Third, gas saturations within the DRZ and the upper and lower waste panel are briefly compared. (Details of gas saturations are provided in Section 3.)
- Fourth, a short analysis is presented of the range in *effective* permeabilities between the DRZ and the two modeled waste regions at various times within the modeled period.
- Finally, a brief description is given of the mathematical model employed by BRAGFLO used to derive *effective* permeabilities.

2.1 Numerical Implementation of the DRZ Pore Volumes

In the BRAGFLO model, the DRZ volume is a function of the adjoining Salado halite porosity given by:

$$\Phi_{o_{DRZ}} = \Phi_{o_{halite}} + .0029 \quad (2-1)$$

where

$$\Phi_{o_{halite}} = \text{halite porosity at the initial time (a sampled variable) at reference pressure } p_0$$

This porosity value represents the region after the five-year waste panel emplacement period. The formation compressibility affects DRZ porosity by:

$$\Phi_{DRZ} = \Phi_{o_{DRZ}} \exp[C_f (p - p_0)] \quad (2-2)$$

where

$$C_f = \text{DRZ rock compressibility of the material.}$$

The value of rock compressibility is converted to pore compressibility by dividing bulk compressibility by $\Phi_{o\text{DRZ}}$ (assigned value of $7.41 \times 10^{-10} \text{ Pa}^{-1}$).

For this study, DRZ void volumes above and below the waste panels were compared. Figure 2.1 shows hairplots³ illustrating the variations in DRZ void volumes for an E1 intrusion for different realizations with time. Labels defining these areas are given below:

- PVL_UWPS = DRZ volumes (m^3) above the lower waste panel, south of the borehole,
- PVL_UWPN = DRZ volumes (m^3) above the lower waste panel, north of the borehole,
- PVL_UROR = DRZ volumes (m^3) above the upper waste panels,
- PVL_LWPS = DRZ volumes (m^3) below the lower waste panel, south of the borehole,
- PVL_LWPN = DRZ volumes (m^3) below the lower waste panel, north of the borehole,
- PVL_LROR = DRZ volumes (m^3) below the upper waste panels.

The set of boxplots⁴ given in Figure 2.2 shows the DRZ void volumes taken at 999, 1500, and 10,000 years. For comparison, plots of waste panel volumes taken at the same time are provided below the DRZ plots. The waste panel void volumes rapidly decrease soon after repository closure, experience a slight increase between 1000 and 1200 years, then fluctuate between declining and increasing values from 1200 to 10,000 years (see Helton et al., 1998, Section 8.3). Volumes for the majority of simulations stabilize around 6000 years.

³ Hairplots illustrate results for the entire suite of 100 simulations, which are overlaid on one plot.

⁴ Boxplots present results in graphical form as the mean, median, 25th and 75th quantile groups, as well as outliers within a population set. Boxplots are presented from data taken at significant times within the modeled period.

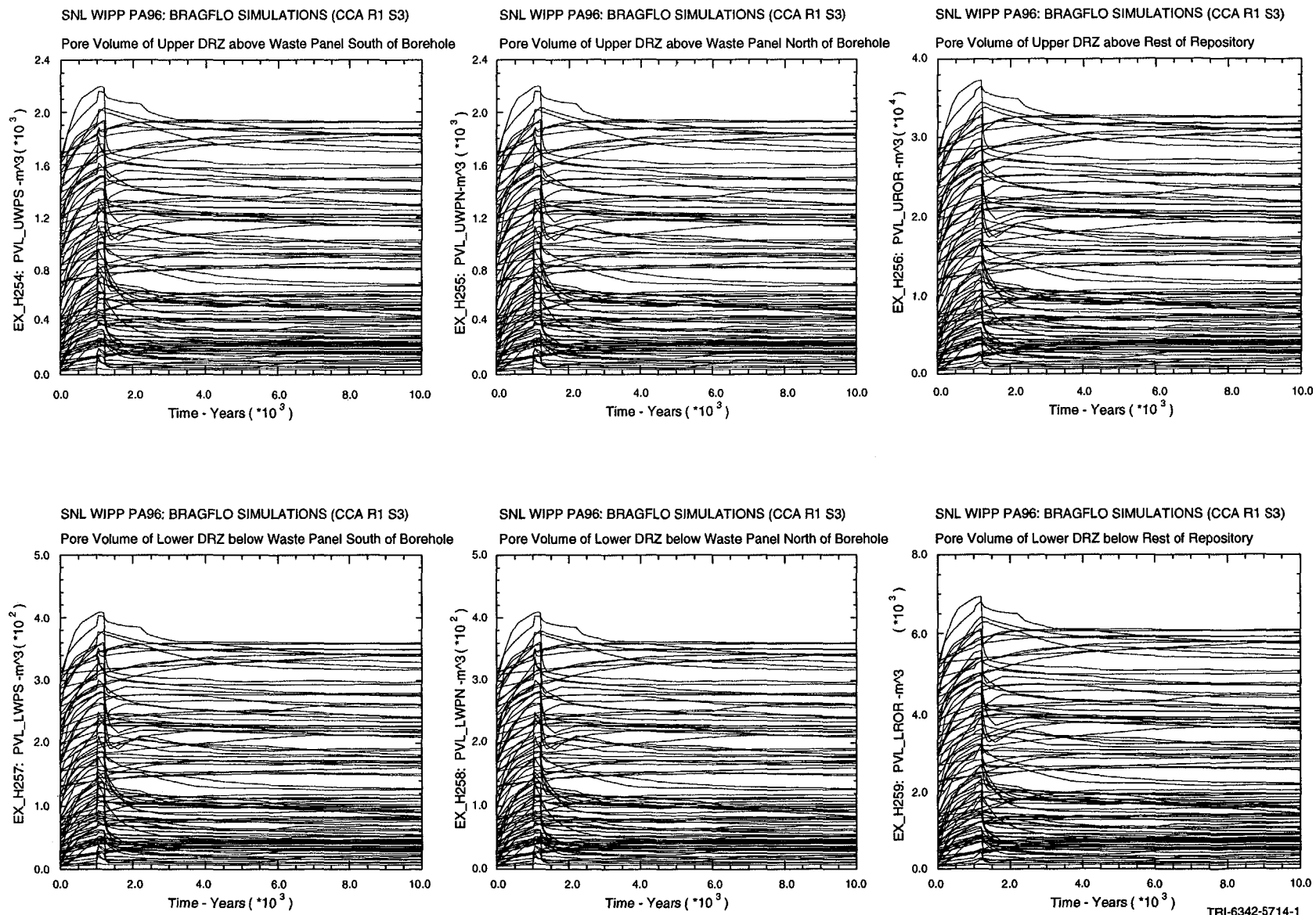


FIGURE 2.1. VOID VOLUMES OF THE DRZ as a function of time for an E1 intrusion (individual curves represent different realizations of problem parameters)

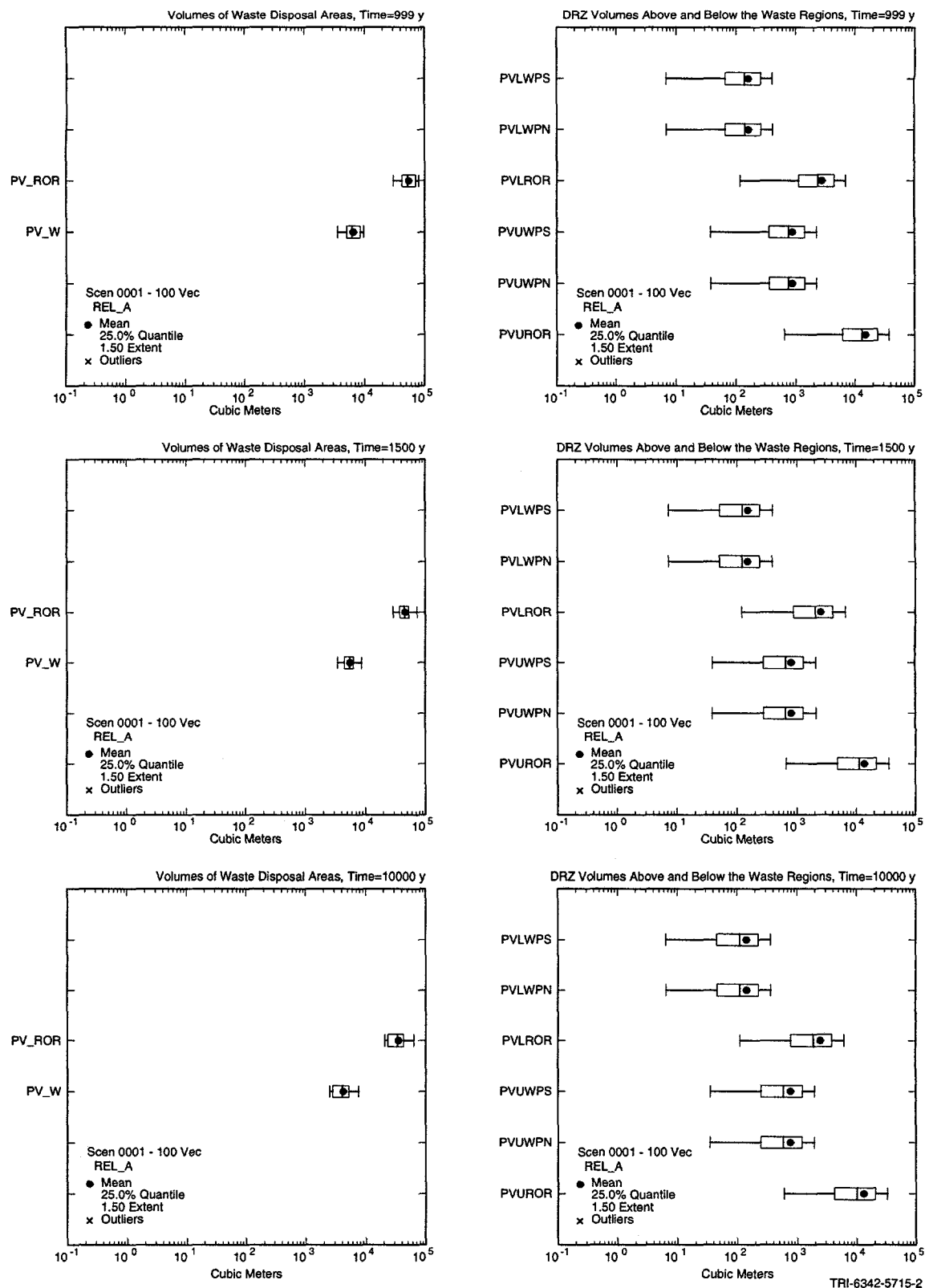


FIGURE 2.2. BOXPLOTS FOR CHANGES IN waste panel (left column) and DRZ void volume (right column) at 999, 1500, and 10,000 years

It is evident from the hairplots in Figure 2.1 that all DRZ volumes are proportional to one another and appear to change in unison. General trends observed for DRZ volume changes are 1) a gradual increase in void volumes is seen soon after repository closure, 2) voids slightly increase at the time of intrusion (1000 years), 3) volumes reach near maximum levels value during the 200-year period when the lower borehole is connected only to the lower Castile reservoir (and minimum connection exists between the Salado and the upper units), 4) DRZ voids rapidly decline when the upper borehole plug degrades at 1200 years, and 5) DRZ volumes are reduced to relatively constant values soon after 2200 years, when the lower portion of the borehole closes.

All DRZ volume changes above and below the waste panels are directly proportional to one another (see Figure 2.3). Because of this relationship, changes in DRZ volumes with respect to other processes and properties are given only for the DRZ above the upper waste panel (PVL.UROR).

All DRZ regions do not behave as isolated zones, but respond to repository processes in unison and to the same extent. This behavior is not unique to the DRZ. The lower and upper waste panel volumes do not behave as isolated units but respond in unison to repository processes as illustrated in Figure 2.4. The plots given in Figure 2.4 show the relationship between void volumes of the lower and upper waste panels at 999 and 10,000 years. Examining these figures, it is seen that the volumes of the two waste panels are also directly proportional to one another.

Waste panel volumes are a function of initial room porosity and pressure changes, somewhat similar to DRZ volumes, but the mathematical formulation of waste panel volumes is dependent on a different conceptual model. This model is numerically formulated with a code called SANTOS.⁵ Because the two numerical models differ, coupling the DRZ and the waste panel volume changes in BRAGFLO may not capture the creep closure conceptual model described at the beginning of this section. Consequently, the void volumes of the waste panels and the DRZ change at quite different rates and to a different extent; this is illustrated in Figure 2.5.

⁵ Details are described in the BRAGFLO analysis package (Bean et al., 1996).

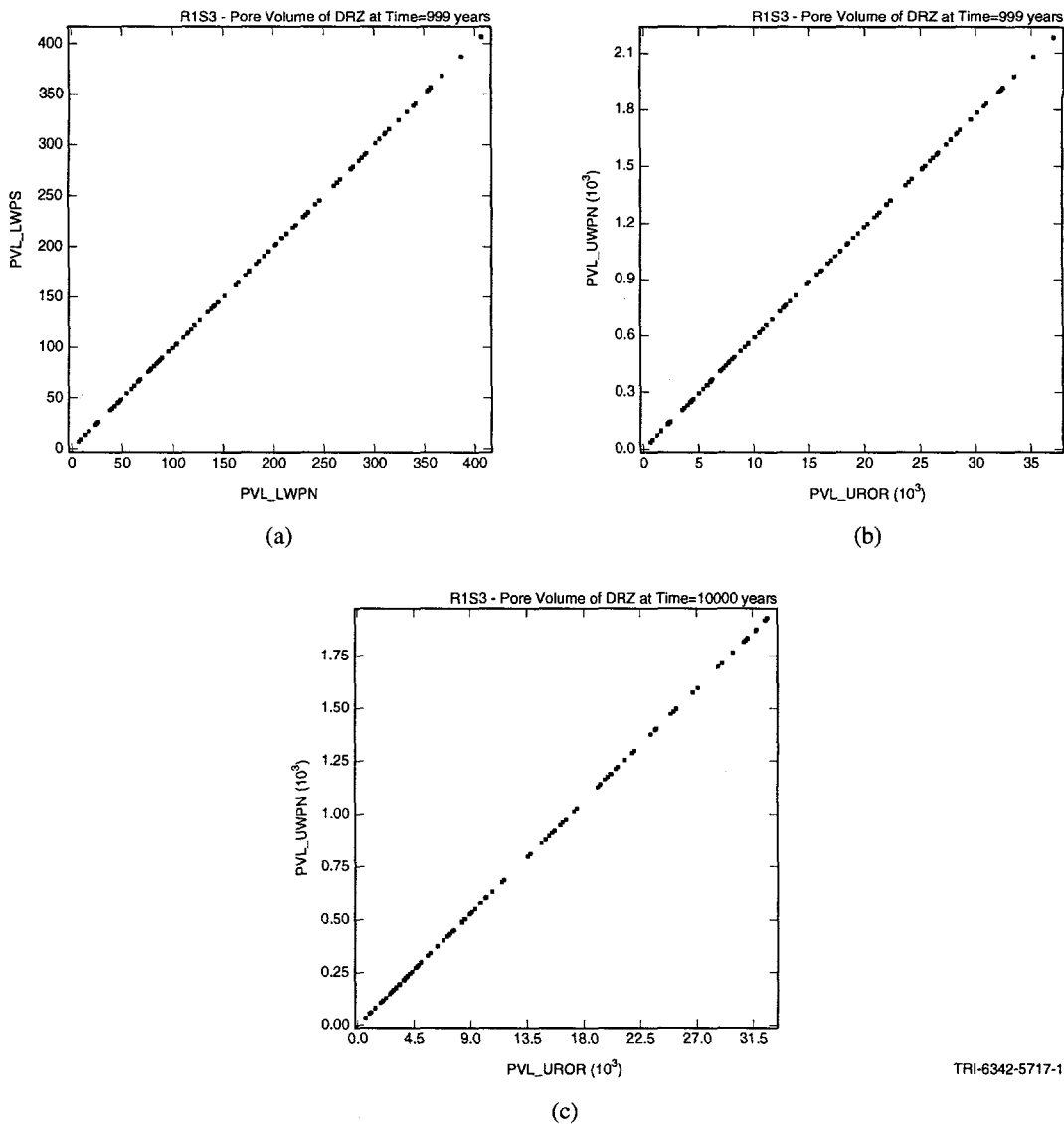


FIGURE 2.3. SCATTERPLOTS FOR (a) DRZ void volumes below the south side of the lower waste panel versus DRZ void volumes below the north side of the lower waste panel at 999; (b) DRZ void volumes above north side of lower waste panel with respect to DRZ void volume above upper waste panel at 999 years; and (c) DRZ void volumes above the north side of the lower waste panel with respect to DRZ void volumes above the upper waste panel at 10,000 years

Interestingly, at 10,000 years there are simulations in which the DRZ void volumes are actually larger than those of the waste disposal regions (see Figure 2.5).

The right plot of Figure 2.5 shows that at 10,000 years there are realizations with relatively large DRZ void volumes associated with relatively small upper waste panel volumes. When adding

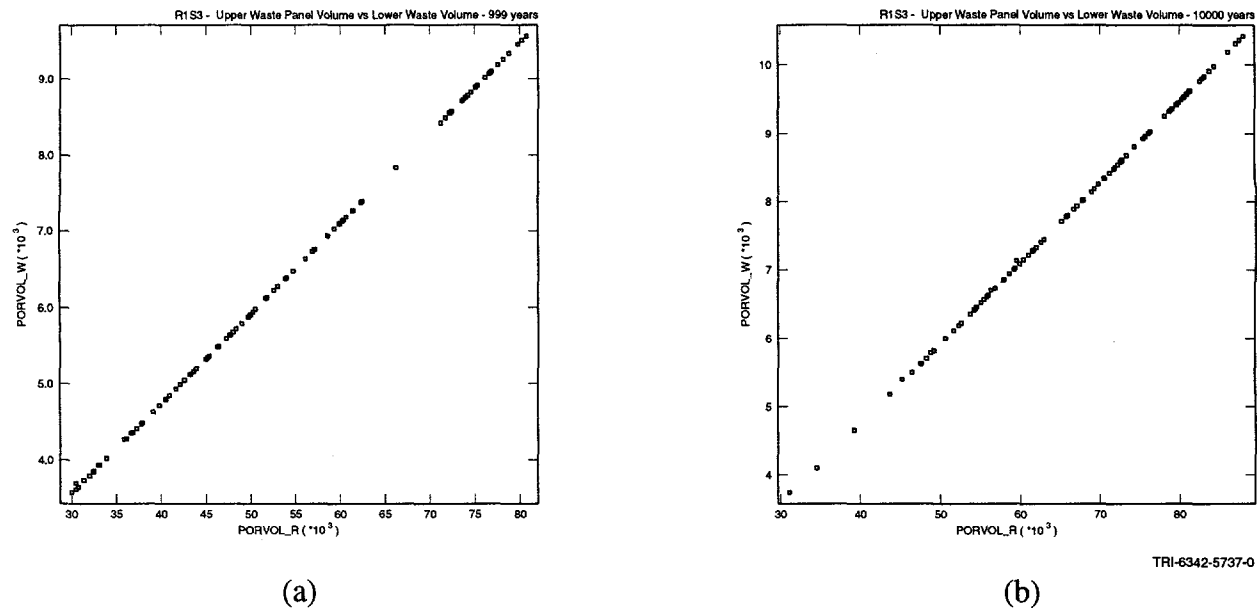


FIGURE 2.4. VOLUME OF LOWER WASTE PANELS versus upper waste panels (PORVOL_W vs PORVOL_R) (a) at 999 and (b) 10,000 years. The two plots show the lower and upper waste panels are proportional to one another

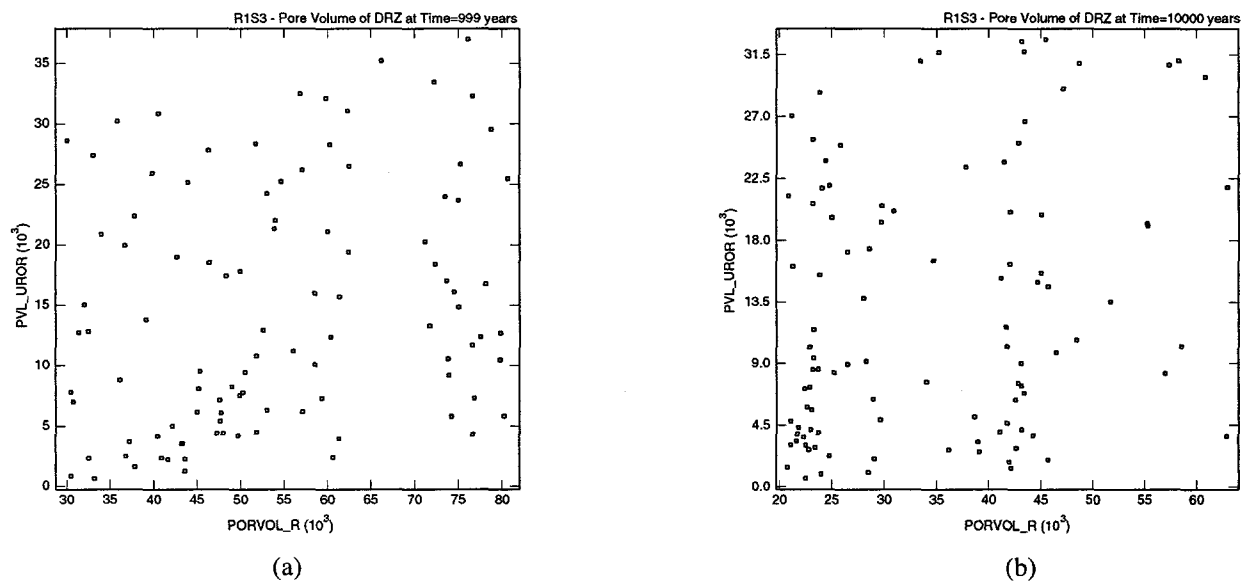


FIGURE 2.5. UDRZ VOID VOLUME ABOVE THE UPPER WASTE PANELS WITH RESPECT TO upper waste panel void volumes (PVL_UOR and PORVOL_R, respectively) at (a) 999 and (b) 10,000 years (top two plots)

the DRZ volume below the waste panel, this difference is enhanced. Conversely, multiple realizations have relatively small DRZ void volumes coupled with relatively large upper waste panel volumes.

Given this analysis, the following questions are asked:

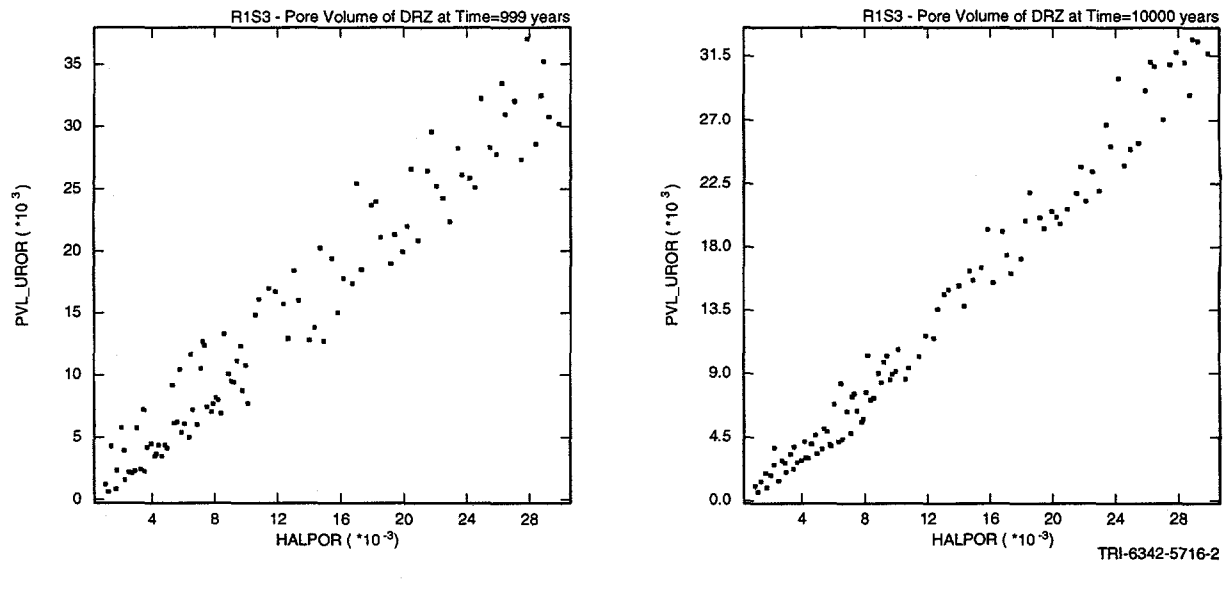
- What are the dominant variables and processes that impact DRZ volumes, and
- How strongly does the relationship between halite porosity and DRZ volume persist throughout the modeled period?

The answers to these questions are evident in Figures 2.6 and 2.7. Figure 2.6 is a set of scatterplots showing a strong correlation of halite porosity with UDRZ void volumes located above the upper waste panel at 999 and 10,000 years. It should be noted that only modest changes in DRZ void volumes occur for all realizations between 999 and 10,000 years. SRRC analysis shows the sensitivity of DRZ void volumes is dominated by halite porosity alone. This is illustrated in Figure 2.7, which is the SRRC plot for the DRZ void above the upper waste panel (PVL_UOR) with respect to HALPOR.

By comparison, the sensitivity analysis reported in Helton et al. (1998) shows that panel room volumes are influenced by those parameters affecting repository pressures (i.e., microbial degradation, gas generation, etc.).

The following questions come to mind:

- Is there an inconsistency in the model results as to what impacts volume changes between the DRZ and disposal room models, and
- Is it realistic to have DRZ volumes larger than waste panel volumes given current knowledge of the visco-plastic response of the Salado halite to the WIPP excavation?



(a)

(b)

FIGURE 2.6. DRZ VOID VOLUMES (m³) ABOVE the upper waste panel (PVL_UROR) at (a) 999 and (b) 10,000 years with respect to halite porosity (HALPOR)

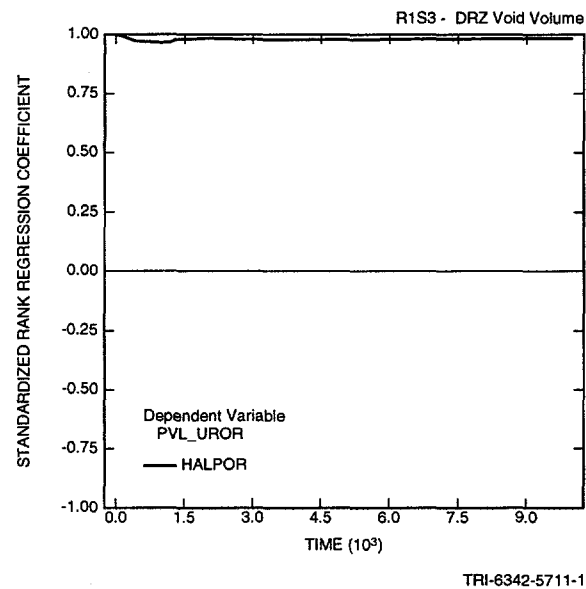


FIGURE 2.7. SRRC RESULTS SHOWING HALPOR is the most influential LHS parameter affecting UDRZ void volumes above the upper waste panel (PVL_UROR)

2.2 *Derivation of Effective Brine and Gas Permeabilities for Disturbed Rock Zone, Panel Closures, and Waste Disposal Area*

As described in the BRAGFLO analysis report (Bean et al., 1996), two-phase flow is modeled throughout the numerical grid, including the repository, the DRZ, and surrounding vicinity (including regions such as the marker beds). For two-phase flow calculations, a permeability for brine and gas must be derived when the porous medium is not fully saturated with one or the other fluid; this permeability is called *effective* permeability. To determine an *effective* permeability, BRAGFLO uses a relative permeability, which is the ratio of the *effective* permeability (permeability at less than 100% saturation) with respect to absolute permeability (permeability at 100% saturation). The relative permeability of a porous media is defined as

$$k_{rl} = \frac{k_l}{k}, \quad (2-3)$$

where

k_n = relative permeability of the formation to phase l

k_l = effective permeability of the formation to phase l

k = absolute permeability of formation

2.2.1 How Fluid Saturation Impacts Effective Permeability

The effective or relative permeability with respect to a fluid phase depends on the saturation of that phase. For fluids within a phase to remain mobile, a continuous flow path for that phase must be maintained in the porous media. As the phase saturation decreases, the ability for that phase to transport fluid decreases. There is a saturation at which continuity of the flow path breaks down and advective transport within the phase is no longer possible. The maximum saturation at which this occurs is called the residual saturation for that phase. The effective permeability for a phase as seen from Equation 2.3 is the product of the formation permeability and the phase relative permeability. Therefore, the dependence of effective permeability on saturation is equivalent to the dependency of relative permeability on saturation.

As described in Section 2.3, the Brooks-Corey model represents relative brine saturation as a function of effective brine saturation by

$$S_e = \frac{S_b - S_{br}}{1 - S_{br}} \quad (2-4)$$

This empirical equation guarantees that the effective saturation is zero at residual brine saturation and has value one when brine saturation is one. Figure 2.8 shows a plot of this equation for residual brine saturations 0.0 and 0.55. As demonstrated in Figure 2.8, when residual brine saturation is relatively high, this causes effective brine saturation to become relatively low.

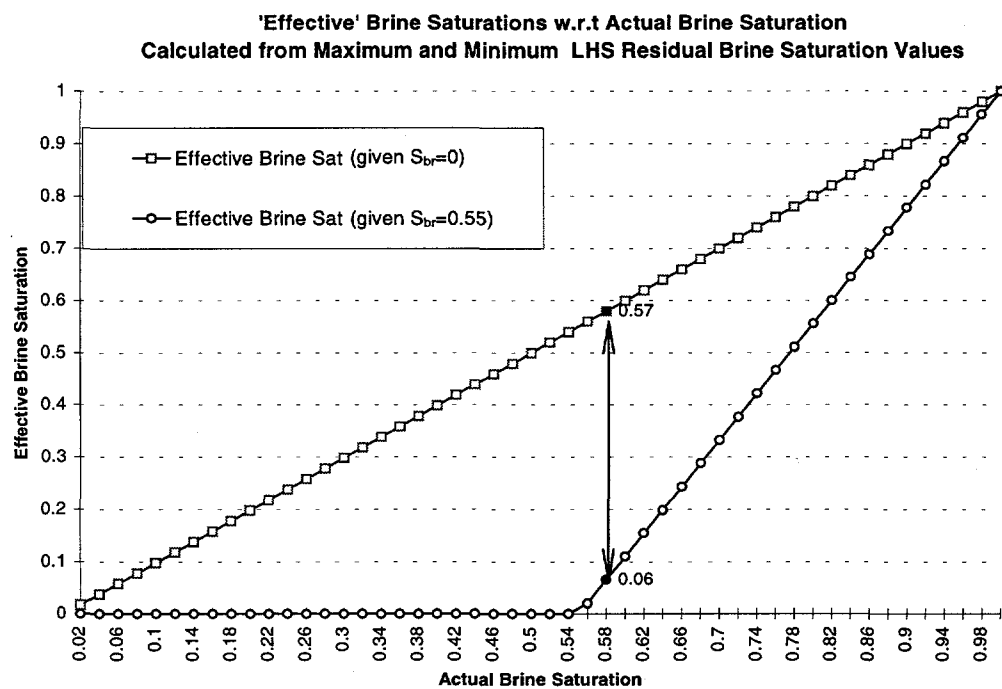


FIGURE 2.8. BOUNDING VALUES FOR EFFECTIVE brine saturations assigned to the waste disposal area

Several empirical models have been developed to derive relative permeabilities in terms of saturation; the Brooks-Corey model is used by BRAGFLO. (A brief description of the Brooks-Corey mathematical model used by BRAGFLO for the 1996 PA to determine relative permeabilities is provided at the end of this section.) Input parameters for the DRZ, waste panels, and panel closures required for the relative permeability model are residual saturations, pore size distribution, and absolute permeability. These values, together with formation permeability, are listed in Table 2-1.

Table 2.1. Input Parameters Affecting Permeability in the DRZ, Panel Closures, and Waste Disposal Area

Parameter	DRZ	Panel Closures	Waste Disposal Area
Pore size distribution (λ)	0.7	0.94	2.89
Residual brine saturation (S_{br})	0.0	0.2	sampled range (0.0 - .55)
Residual gas saturation (S_{gs})	0.0	0.2	sampled range (0.0 - .15)
Absolute permeability (k_{abs} , m^2)	1.0×10^{-15}	1.0×10^{-15}	$\sim 1.70215 \times 10^{-13}$

2.2.2 DRZ and the Waste Panel Effective Permeabilities

For the waste disposal area, while absolute permeabilities are higher than in the DRZ, given the wide range in sampled brine and gas residual saturations, effective permeabilities (a function of relative and absolute permeability) can vary over several orders of magnitude and go below that of the panel closures and the DRZ. Figure 2.9 illustrates the bounding values for effective brine and gas permeabilities derived for the waste disposal area, again using the maximum and minimum assigned residual brine saturations. One can see that a large value for brine saturation can still translate to a very low effective brine saturation and permeability, given a high assigned sample value for residual brine saturation.

Given that the interface between the DRZ/waste disposal area has a large surface area, the DRZ pathway for fluid flow to and from the waste disposal areas can become significant if brine or gas saturations appreciably differ between the DRZ and adjoining waste areas. BRAGFLO results for the E1 scenario indicate the brine saturation for the upper waste panel is generally much less than that for the lower waste panel, the LDRZ, and the UDRZ to the south of the panel closures (see Table 2.2). As indicated by the values for brine saturation in Table 2.2, the lower waste panel has the highest brine saturation and the upper waste panel has the lowest. In the majority of cases after intrusion, brine saturations in the DRZ below both waste panels and above the upper waste panel are higher than the upper waste panel itself.

**Bounding Values for 'Effective' Gas and Brine Permeabilities in the Waste Disposal Areas
Calculated from Minimum and Maximum LHS Residual Brine and Gas Saturations**

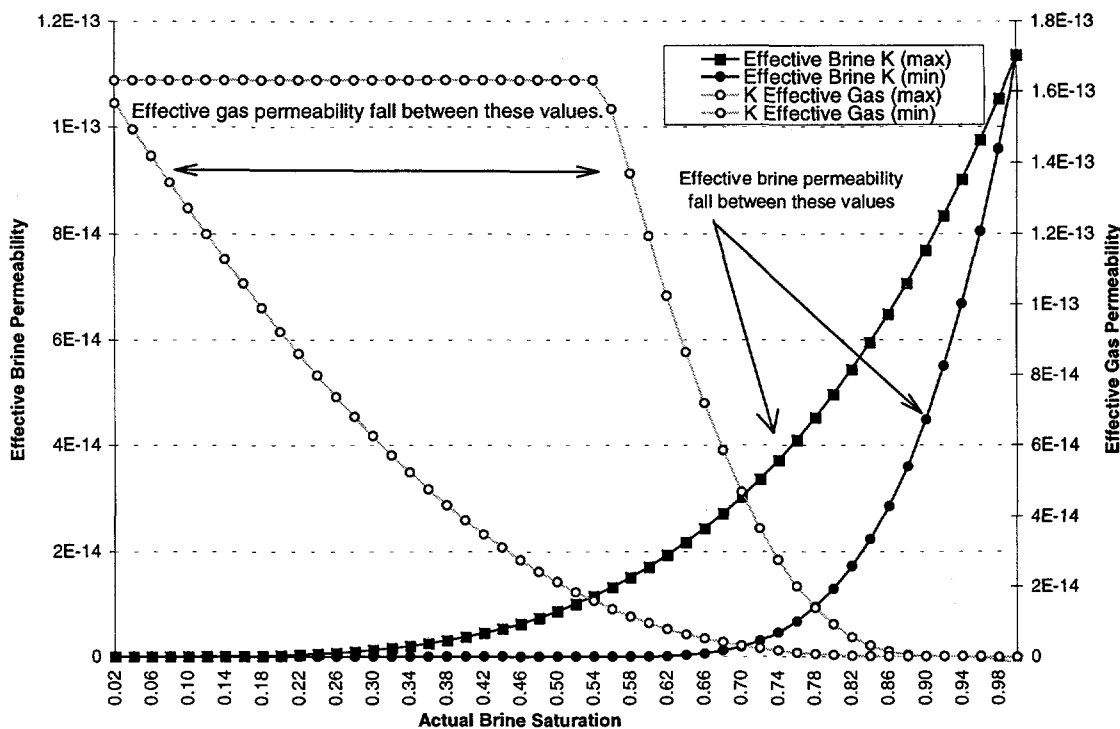


FIGURE 2.9. BOUNDING EFFECTIVE BRINE AND gas permeabilities assigned to the waste disposal area using the functional relationship between effective permeability and residual brine and gas saturations.

Consequently, it is possible for effective brine permeabilities of the upper waste panel to fall below those of the DRZ, especially for realizations with very high sampled residual brine saturations.

The bars in Figure 2.10 show the effective brine permeabilities for each simulation using absolute brine saturations of ~ 0.20 and 0.30^6 and their respective LHS residual brine saturation values.

The shaded area of the plot shows the range of effective brine permeabilities for the DRZ area above and below the lower waste panel and below the upper waste panel, given the mean values

⁶ Brine saturation values falling within the mean and median for the upper waste panel that are most likely to occur in the upper waste panel between 1000 and 10,000 years.

Table 2.2. Mean, Median, Minimum, and Maximum Brine Saturations Calculated from 300 LHS Elements for the Lower and Upper Waste Panel, the DRZ Above and Below the Upper Waste Panel, and the DRZ Below the Lower Waste Panel

	WAS_SATB	REP_SATB	SATBUWPN	SATBUROR	SATBLROR
1,000 years					
Mean	0.768	0.276	0.137	0.121	0.724
Median	0.882	0.187	0.123	0.123	0.719
Minimum	0.003	0.000	0.029	0.029	0.194
Maximum	0.986	0.961	0.957	0.262	~1.000
	WAS_SATB	REP_SATB	SATBUWPN	SATBUROR	SATBLROR
10,000 years					
Mean	0.873	0.261	0.485	0.138	0.807
Median	0.912	0.194	0.651	0.112	0.818
Minimum	0.171	~0.000	0.082	0.072	0.340
Maximum	0.996	0.978	0.978	0.613	0.999

* WAS_SATB = brine saturation lower waste panel
 REP_SATB = brine saturation upper waste panel
 SATBUWPN = brine saturation upper DRZ (above north side of lower waste panel)
 SATBUROR = DRZ brine saturation, above upper waste panel
 SATBLROR = DRZ brine saturation, below upper waste panel.

seen for DRZ brine saturations (i.e., brine saturations between ~0.60 to ~0.87). Note that more than 50% of the realizations have upper waste panel effective permeabilities less than DRZ permeabilities. As this figure illustrates, even though absolute permeabilities in the DRZ are two orders of magnitude lower than the waste panel, given the degree of brine saturation in the DRZ, it is very likely that effective brine permeability in the DRZ be higher than those for the waste regions. Consequently, the effective permeability and the volume of DRZ can facilitate or inhibit fluid flow between the waste disposal areas and the borehole. Details of fluid flow within these areas are discussed in Sections 4, 5, and 6.

Given the preceding analysis, the following questions arise:

- Is it realistic to have a constant permeability (absolute) assigned to the DRZ given the volume variation (a function of halite porosity) of the DRZ, and

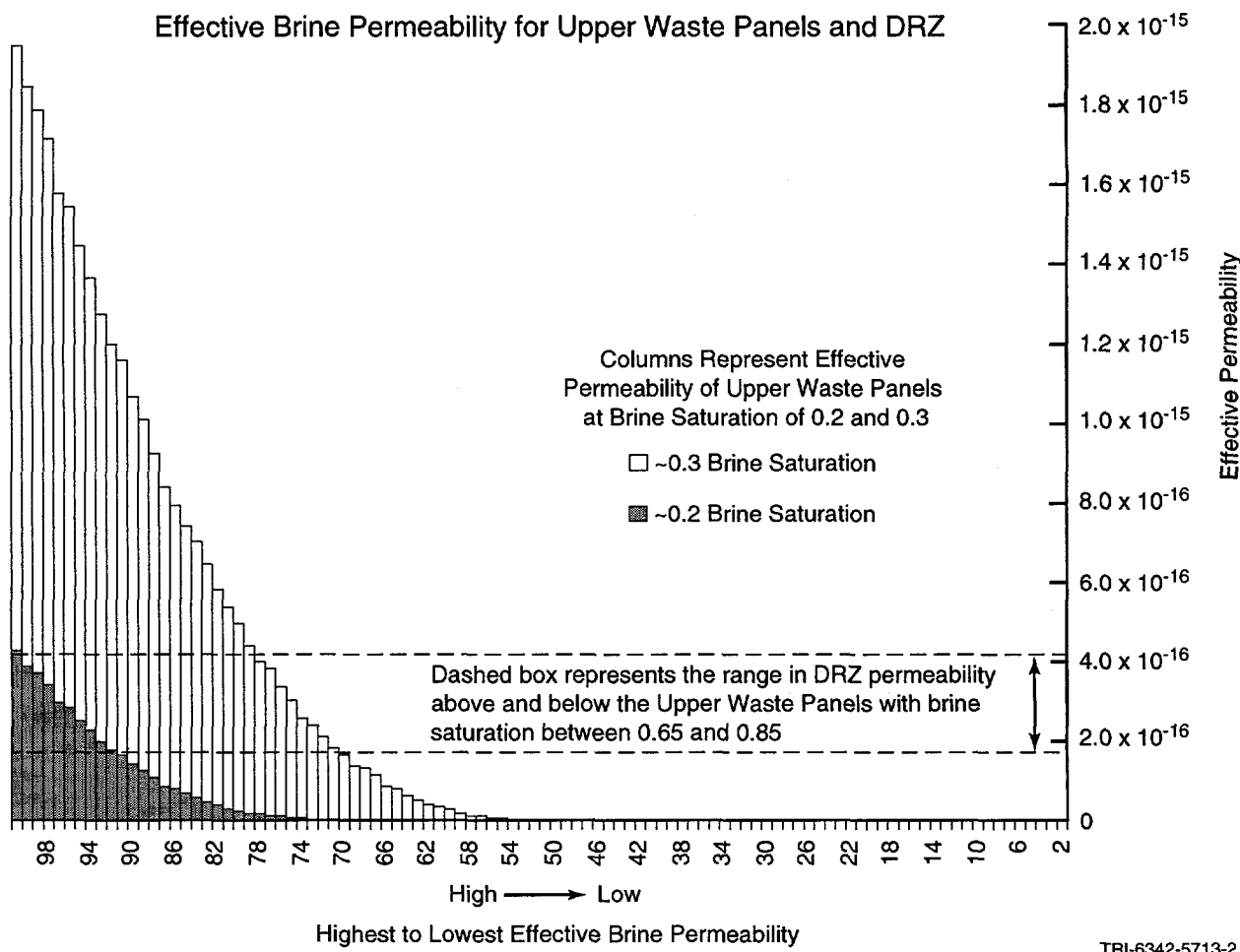


FIGURE 2.10. RANKED EFFECTIVE BRINE PERMEABILITIES for the upper waste panel at absolute brine saturations of ~0.20 to 0.30. The shaded box on the plot represents the range for effective brine permeability in the DRZ for brine saturations ranging between 0.6 and 0.87, which represent median values for DRZ brine saturation above the north side of the lower waste panel and below the upper waste panels. The plots illustrate there are over 54 simulations (within a 100 simulation set) that will have DRZ permeability greater than upper waste panel permeability.

- How does a constant and relatively high value for DRZ permeability affect repository performance with respect to fluid movement between panels?

2.3 Mathematical Model Used to Derive Effective Permeability

The following is a brief review of the mathematics employed in the Brooks-Corey model.

Details are given in the BRAGFLO analysis package.

For the DRZ, the panel closures, and the waste disposal area, BRAGFLO employs a modified Brooks-Corey model, which is defined below:

$$k_{rb} = S_e^{(2+3\lambda)/\lambda} \quad (2-5)$$

$$k_{rg} = (1 - S_e)^2 (1 - S_e^{(2+\lambda)/\lambda}) \quad (2-6)$$

where

k_{rb} = relative permeability to the brine phase

S_e = effective saturation

λ = pore size distribution constant

k_{rg} = relative permeability to the gas phase.

Effective saturation for brine is defined as

$$S_e = \frac{S_b - S_{br}}{1 - S_{br}}, \quad (2-7)$$

where

S_b = actual brine saturation

S_{br} = residual brine saturation.

Effective saturation for gas is defined as

$$S_e = \frac{S_b - S_{br}}{1 - S_{gr} - S_{br}}. \quad (2-8)$$

where

S_{gr} = residual gas saturation.

As a reminder to the reader, residual saturation is the point where a fluid is no longer continuous within the pore space, and consequently flow of that fluid ceases.

Intentionally Left Blank

3. Gas Saturation in the Waste Disposal Areas and Adjoining DRZ

As discussed in Section 2, effective permeabilities are partially functions of saturation. Given this functionality, when the fluid saturation levels in the DRZ significantly differ between regions or change with time from those of the adjoining waste disposal areas, a highly heterogeneous and ‘transient’ permeability field is created between the waste disposal areas and the DRZ.

Therefore, the variation in fluid saturation within the DRZ can cause a heterogeneous *effective* ‘permeability field’ unique to each realization, which in turn can create preferential brine and gas flow paths between the upper and lower waste panels, and in the event of an intrusion, the borehole. The purpose and organization of this section is to 1) compare gas saturation between the waste disposal areas and adjoining DRZ, 2) discuss trends and general patterns for gas saturation within the waste disposal areas and the DRZ, 3) determine the potential impacts of DRZ fluid flow on repository performance, and 4) discuss those variables that control DRZ saturation.

For brevity, only gas saturation (as opposed to brine saturation) is discussed in this section. In the BRAGFLO model, brine saturation is a function of gas saturation (i.e., brine saturation = 1 – gas saturation). A detailed description of brine saturation within the waste panels is provided in Chapter 8.3 of Helton et al. (1998).

Table 3.1 defines the variables names for gas saturation within the waste panels and adjoining DRZ (which are illustrated in Figure 3.1.1).

Table 3.1 Dependent Variables Defining Gas Saturations in the Waste Panels and Adjoining DRZ (note variable names shown on boxplots are abbreviated and given in parenthesis)

Variable	Description
WAS_SATG (W_SATG)	Lower waste panel gas saturation
REP_SATG (R_SATG)	Upper waste panel gas saturation
SATGUWPN (SGUWPN)	UDRZ gas saturation, above north side of lower waste panel
SATGUWPS (SGUWPS)	UDRZ gas saturation, above south side of lower waste panel
SATGUROR (SGUROR)	UDRZ gas saturation, above upper waste panel
SATGLWPN (SGLWPN)	LDRZ gas saturation, below north lower waste panel
SATGLWPS (SGLWPS)	LDRZ gas saturation, below south lower waste panel
SATGLROR (SGLROR)	LDRZ gas saturation, below upper waste panel

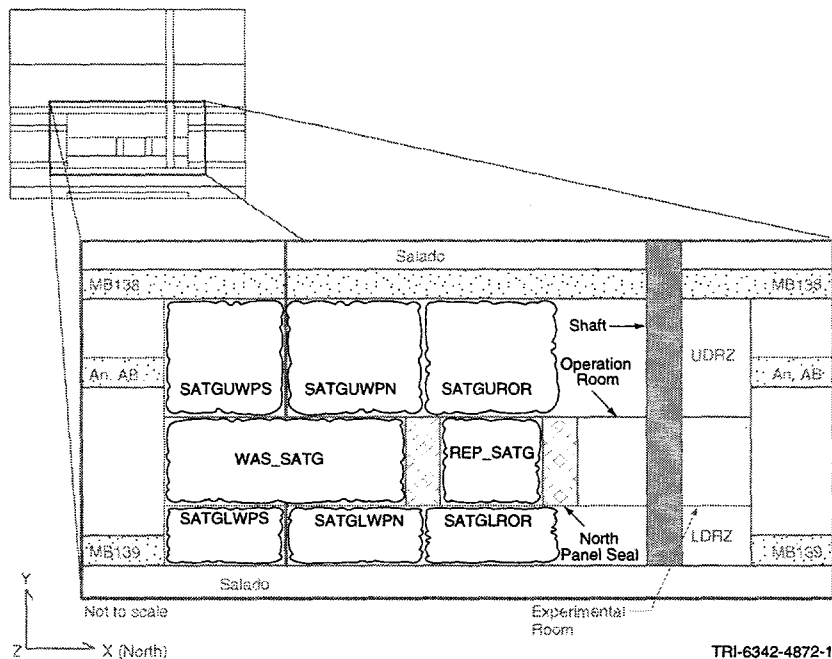


FIGURE 3.1.1. REGIONS OF DISPOSAL SYSTEM for which gas saturations were evaluated

3.1 Comparison of Gas Saturation for the Waste Disposal Areas and Adjoining DRZ

This section provides boxplots for gas saturation in the DRZ and waste disposal areas at 999, 1500, 5500, and 10,000 years, and hairplots that show variations in gas saturation in the waste panels and their adjoining DRZ over time. The box plots present the mean, median, 25th, and

75th quantiles and outliers for gas saturations. The boxplots in Figures 3.1.2 and 3.1.3 show that, prior to intrusion,

- At 999 years in the UDRZ region above all waste panels, the majority of realizations have gas saturation well above the 0.90 level.
- In the LDRZ below the upper waste panels, a wide range in gas saturation occurs. This spread ranges from 0.8 to well below 0.1. Gas saturation in the LDRZ below the lower waste panel is much less than in the LDRZ directly up-dip. There are multiple realizations with gas saturation in the LDRZ lying below the lower waste panel that are above the 0.2 level.
- In the waste disposal areas, gas saturation is relatively high, with the upper waste panel having the highest value, with less spread and fewer outliers.

For times after intrusion:

- At 1500, 5500, and 10,000 years, gas saturation in the UDRZ above the lower waste panels remains fairly significant (above 0.20 levels). Mean UDRZ gas saturation levels above the south and north halves of the lower (intruded) waste panel fall between ~0.3 and 0.5, with the values for the south half being slightly lower than the values for the north.
- At 1500, 5500, and 10,000 years, the highest gas saturation occurs in the UDRZ above the upper waste panel for the majority of realizations, with a mean value above ~0.8. Gas saturations within this area of the UDRZ fluctuate less between realizations.
- LDRZ gas saturation below the lower waste panel dramatically drops between 999 and 10,000 years. Mean values at 1500 and 10,000 yr are well below 0.09.

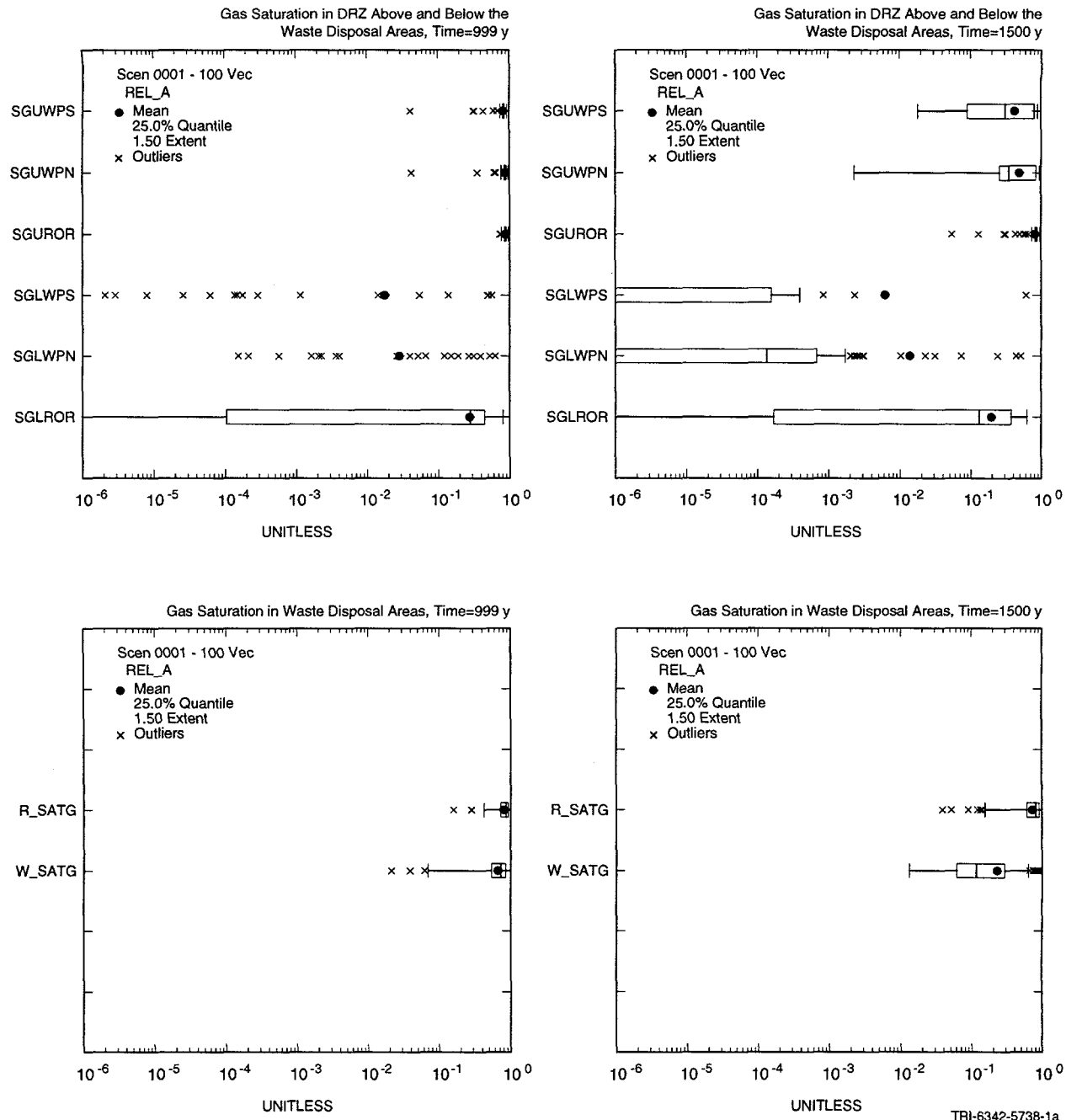


FIGURE 3.1.2. BOXPLOTS FOR GAS SATURATION levels (unitless) taken at 999 and 1500 years in the DRZ (top row) and within the lower and upper waste panels (bottom row)

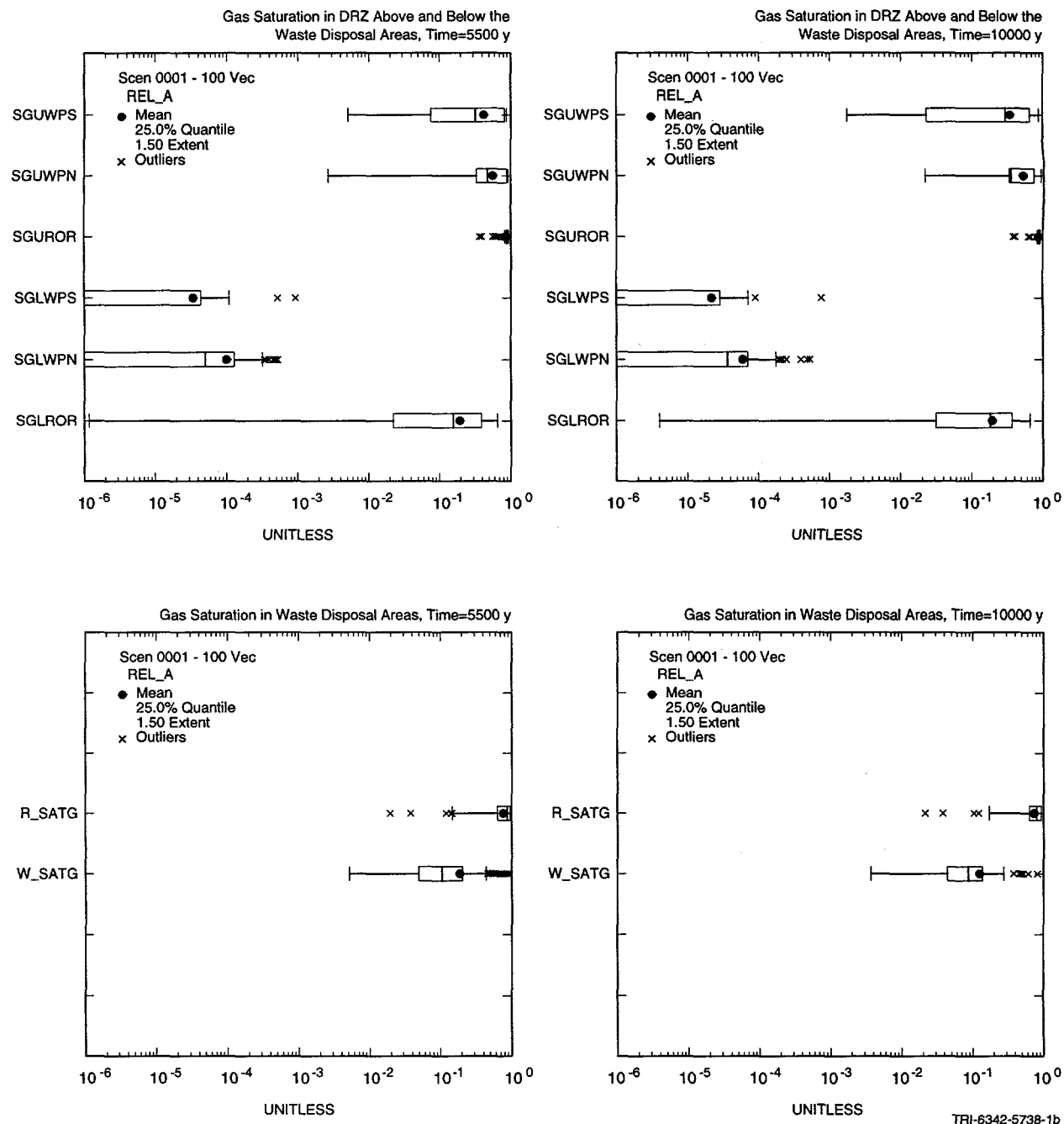


FIGURE 3.1.3. BOXPLOTS FOR GAS SATURATION levels (unitless) taken at 5500 and 10,000 years in the DRZ (top row) and within the lower and upper waste panels (bottom row)

- Gas saturations within the upper and lower waste panel are dramatically different from those at 999 years. The upper waste panel remains dominantly gas saturated, with a mean value well above 0.8, similar to that seen prior to intrusion.
- The lower waste panel has a dramatic reduction in gas saturation after 999 years, with mean values falling from 0.3 to below 0.1 between 1500 and 10,000 years.

When comparing boxplots for the DRZ and the waste disposal areas, it should be noted that:

- All DRZ areas experience a decrease in gas saturation levels as a result of the intrusion event. The decline in degree of gas saturation is most marked in the down-dip regions of the DRZ.
- Mean values for gas saturation in the waste disposal areas are higher than mean values for gas saturation in the LDRZ lying directly below these areas; the most pronounced difference is seen between the upper waste panel and the LDRZ just below this area.
- UDRZ gas saturations above the upper waste panel have less spread and remain the highest levels throughout the modeled period.
- A large variation exists between realizations for UDRZ gas saturation lying directly above the lower waste panel. Of interest is the increasing spread, from 1500 to 10,000 years, for UDRZ gas saturation in the area just south of the borehole. In contrast, in the UDRZ just north of the borehole the spread for UDRZ gas saturation constricts, with the bulk of realizations showing an overall decline in UDRZ gas saturation.

3.1.1 Summary of Gas Saturation in the Lower (WAS_SATG) and Upper (REP_SATG) Waste Panels

Figure 3.1.4 gives hairplots for gas saturations in both the lower and upper waste panels. For the first 100 years after repository closure, gas saturations of the upper and lower waste panels are similar. Differences in saturations between the two regions begin to appear around 500 years, and are primarily due to the 1-degree slope of the repository; the lower waste panel tends to be less gas saturated than to the upper waste panels as brine drainage accumulates in this down-dip area. The upper waste panels tend to become more gas saturated as gas produced early on migrates and is stored in the up-dip location of the excavated area. After intrusion, a dramatic difference is seen in gas saturation between the lower (intruded) and upper (unintruded) waste panels. For most realizations, soon after intrusion, gas saturation for the lower waste panels dramatically decreases to minimum levels; in the upper waste panels gas saturations remain well above ~0.8 (i.e., ~80% of the void volume is gas filled).

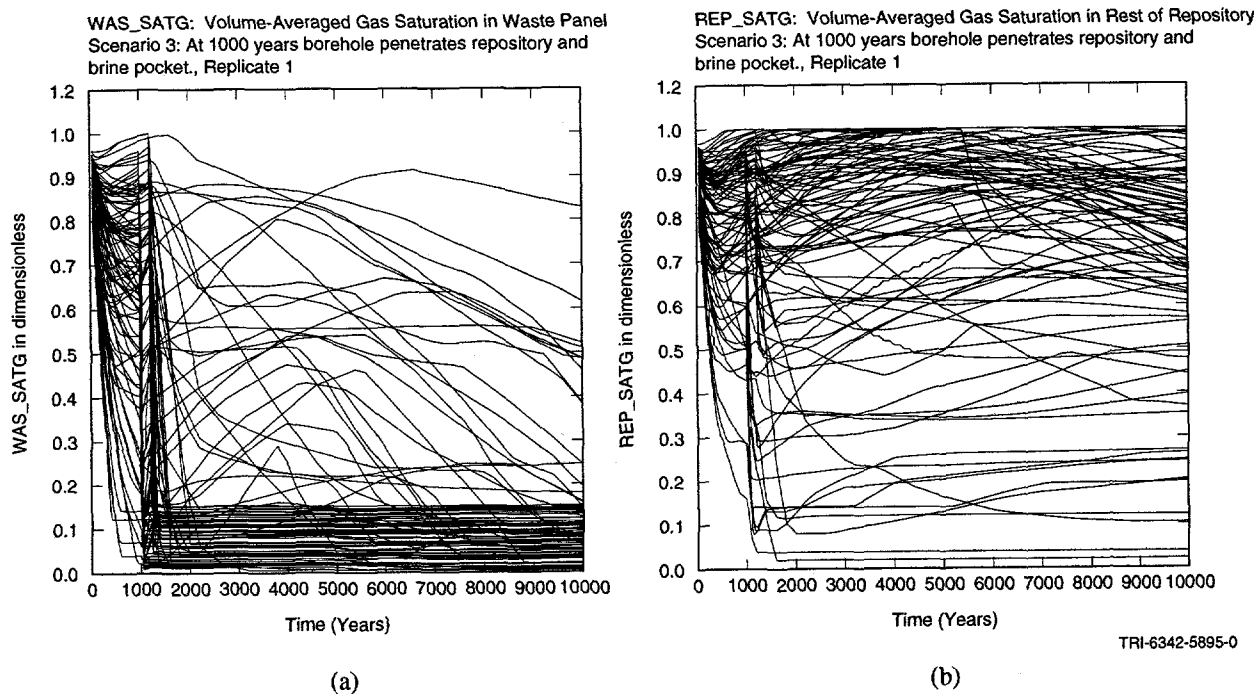


FIGURE 3.1.4. GAS SATURATION HAIRPLOTS FOR (a) lower and (b) upper waste panels

3.1.2 Summary of Gas Saturation in the DRZ

Figure 3.1.5 gives hairplots for gas saturations in all modeled regions of the DRZ. The upper left and middle plots show gas saturations for the area above the south and north side of the lower waste panel, respectively (divided by the borehole). The upper right plot gives the gas saturations for the UDRZ above the upper waste panel. The lower left and middle plots show gas saturations for the LDRZ below the south and north sides of the lower waste panel, respectively; the lower right plot shows gas saturations for the area below the upper waste panel.

Note the marked reduction in gas saturation that all DRZ regions experience between intrusion (1000 years) and borehole degradation (1200 years). Of additional interest are the four distinct levels for gas saturation (seen in Figure 3.1.5) that most realizations tend to cluster around in the UDRZ above the southern half of the lower waste panel (south of the borehole). The number of ‘cluster zones’ seems to diminish moving up-dip.

A brief overview of gas saturation within the UDRZ and LDRZ is given in the next two sections.

3.1.2.1 *UDRZ Gas Saturation*

The top row in Figure 3.1.5 shows the variation with time for UDRZ gas saturation. For the majority of realizations, UDRZ gas saturations above the upper and lower waste panels steadily increase from ~0.0 to values well above ~0.7 within the first hundred years after repository closure. This increase is due to brine drainage out of the DRZ to the waste panel below and the migration into the DRZ of gas from microbial gas production and, to a lesser extent, iron corrosion. The increase soon subsides, and thereafter, gas saturations decline to values below ~0.4. Gas saturations in the UDRZ above the upper waste panel stay above 0.8 for the majority of simulations from ~200 to 999 years. After intrusion, the similarity between saturations in the UDRZ above the two waste regions tends to diminish. Generally, gas saturation increases moving up-dip (south to north).

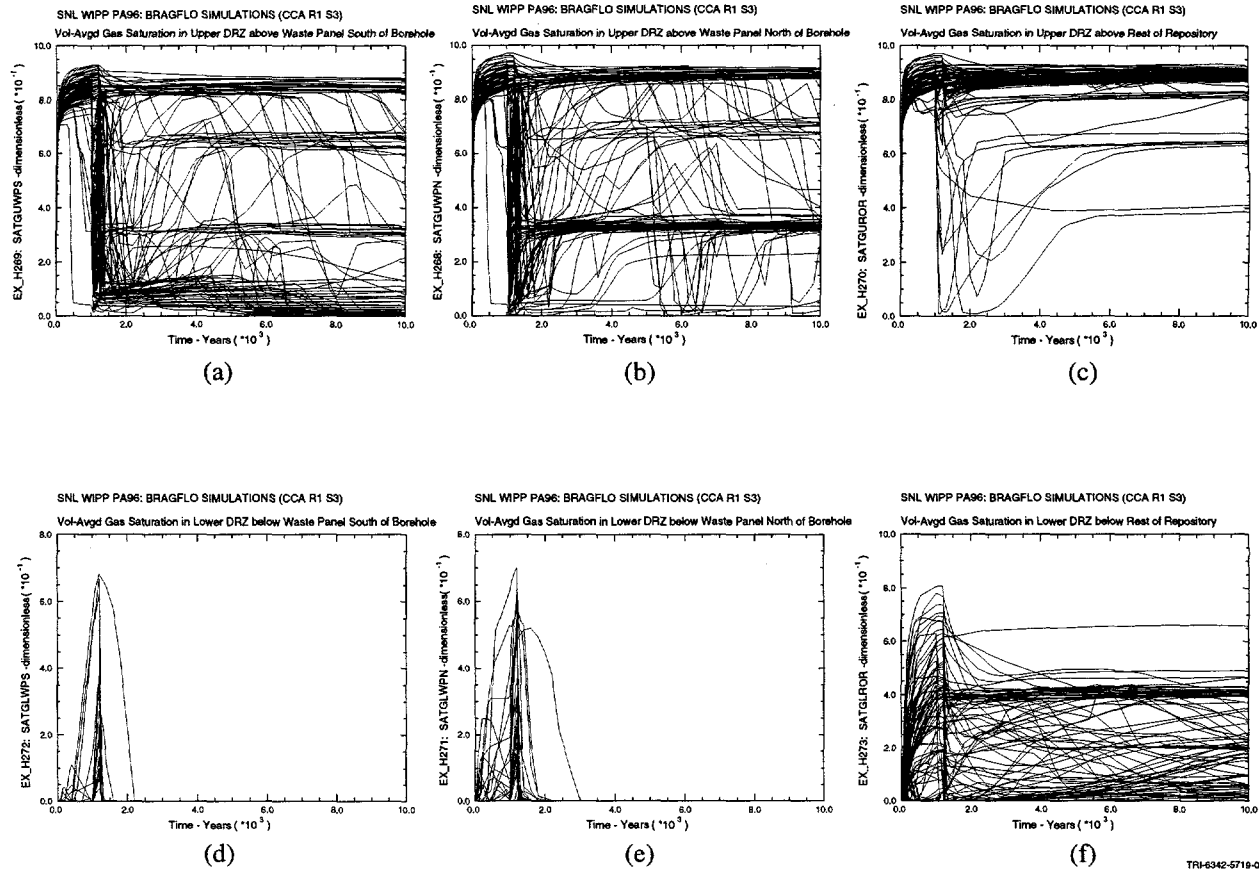


FIGURE 3.1.5. UDRZ GAS SATURATION LEVELS above the (a) south and (b) north side of the lower waste panel, and (c) above the upper waste panel. LDRZ gas saturation levels below the (d) south and (e) north side of the lower waste panel, and (f) below the upper waste panel

After intrusion and upper borehole degradation, UDRZ saturation levels above the lower waste panel cluster into several distinct regions. Of interest is the reduction in the number of cluster ‘zones’ just north and south of the area divided by the borehole. There are four distinct zones in the south half, and only two distinct zones due north. For the UDRZ region south of the borehole, gas saturation levels for most realizations cluster around four levels, ~0.15, 0.3, 0.6, and 0.85, with a larger population appearing to hover around the ~0.15 and 0.85 level. Interestingly, some realizations seem to have UDRZ gas saturation levels that migrate among all four levels from the time of upper borehole degradation to the end of the modeled period. The reason for the two additional gas saturation levels that appear in the area south of the borehole, but not seen to the north, is the tendency for an entrapped gas ‘bubble’ to form in the area just south of the borehole. This ‘bubble’ persists and tends to form for realizations that have medium values for borehole permeability and relatively high values for halite porosity.

Gas saturation tends to settle in fewer clusters in the UDRZ just north of the borehole (still above the intruded waste panel). In this area, gas saturation tends to cluster around the 0.8 and 0.3 levels. As in the UDRZ due south, multiple realizations experience a fluctuation in saturation levels that migrate from one saturation level to another.

Prior to intrusion, UDRZ gas saturation above the upper waste panel does not vary much between realizations. Gas saturation remains well above 0.85 for the majority of realizations. After intrusion, UDRZ gas saturation here only slightly decreases; most realizations have gas saturations that cluster around 0.85. Between 1200 and 4000 years, a few realizations have gas saturations that drop dramatically below 0.8. However, these levels begin to rise, and around ~4000 years eventually settle at ~0.8.

3.1.2.2 LDRZ Gas Saturation

The bottom row in Figure 3.1.5 shows the variation over time for LDRZ gas saturation. Similar to the UDRZ, gas saturation in the LDRZ increases moving up-dip. For many realizations, LDRZ gas saturation below the lower waste panel reaches to values well above 0.3 prior to intrusion. Gas saturation is reduced to near 0.0 (approaching near complete brine saturation) between 1200 and 2200 years, coincident with the time that the lower borehole experiences creep closure.

In the area below the upper waste panel, a wide range exists in gas saturation values prior to intrusion. Approximately one fourth of the realizations have saturations well above the mean value of ~0.3, with a few climbing to values above the 0.8 level. At the time of upper borehole degradation (1200 years), gas saturation in the LDRZ is reduced to relatively low levels for many realizations, then increases again midway through the modeled period. Numerous realizations have saturations that cluster around the 0.4 level and remain there from the time of upper borehole degradation to the end of the modeled period.

3.2 Effects of Gas Saturation On Fluid Flow Between Waste Regions

Because the DRZ has no capillary pressure for gas or brine to overcome *and* a value of zero for residual gas and brine saturation, and because these material properties are coupled with a ‘slab’ geometry, the DRZ serves like a continuous seepage face joining all the repository. This seepage face transmits fluid between the down-dip and the up-dip regions of the repository. The condition that enhances fluid flow is the degree of fluid saturation. Consequently, any hindrance to flow provided by the panel closures is effectively negated by the adjoining DRZ above and below the waste panels. The DRZ effectively allows (or transmits) the more dynamic processes that occur in the lower waste panel (i.e., the intrusion event) to propagate up-dip to the upper waste panel, effectively short circuiting any hindrance to fluid flow between the two waste regions provided by the panel closures.

Because the upper waste panel is less brine saturated than the LDRZ, the LDRZ becomes a brine ‘line’ source. Because the upper waste panel is less gas saturated than the UDRZ, the UDRZ becomes a gas ‘line’ sink. The two conditions, in effect for most realizations, keep the upper waste panel dynamically linked to the more active and transient processes occurring in the lower waste panel connected to the borehole. This condition affects repository performance in the following ways.

- A single intrusion event into a single waste panel will immediately reduce gas saturations throughout the entire repository, most markedly in the lower waste panel. Because the UDRZ is continuous and has high DRZ *effective* gas permeability, gas is easily transmitted toward the borehole via the UDRZ from all waste disposal areas, which lowers repository pressure. Lower gas saturation promotes brine drainage from the adjoining anhydrites, and because the LDRZ is more brine saturated, more drainage will come from the lower southern anhydrites (i.e., south MB 139). Once the lower waste panel is brine filled, excess brine will flow up-dip, via the LDRZ, toward the upper waste panel. From the LDRZ, brine flows up through the upper waste panel floor where it can be used for iron corrosion. Gas from corrosion flows out the upper waste panel ceiling to the UDRZ. From the UDRZ, given the borehole connection, this gas will flow down-dip toward the borehole.

- In effect, the DRZ configuration and degree of saturation promotes a counterclockwise circular fluid path between the up-dip and down-dip regions of the repository. Eventually, gas evacuation will lower pressures throughout the entire repository until they are equilibrated to that of the overlying units via the borehole connection. After this equilibration is achieved, minimal pressure differences will exist between each panel because of the DRZ ‘manifold’ that connects waste regions. Consequently, when a second intrusion into another waste panel occurs, its impact on overall repository performance will be far less than that of the first.

3.3 *Variables Affecting Gas Saturation in the Waste Panels and Adjoining DRZ*

3.3.1 *Variables Influencing Lower (WAS_SATG) and Upper (REP_SATG) Waste Panel Gas Saturation Levels*

3.3.1.1 *Variables Influencing Lower Waste Panel Gas Saturation (WAS_SATG) Levels*

Standardized rank regression coefficients (SRRCs) for variables influencing gas saturation in the lower waste panel are given in Figure 3.3.1a. This figure indicates that, prior to intrusion, WAS_SATG is inversely correlated with HALPOR (halite porosity) and positively correlated with microbial degradation (controlled by the WMICDFLG ‘switch’). Low values for HALPOR mean less brine will drain into the waste panel, keeping the panel more gas than brine filled. High values for microbial degradation mean microbial generated gas will fill up the waste room, increase pressures, and inhibit brine drainage from both the DRZ and the anhydrites.

After intrusion, WAS_SATG is inversely correlated with borehole permeability (BHPRM) and positively correlated with residual gas saturation (WRGSSAT). Low BHPRM values mean brine is impeded from entering into the repository and gas is impeded from flowing out (keeping repository pressures at relatively higher levels). Thus, gas is more likely to remain in the waste regions early in the modeled period rather than later. Gas will flow out of the waste region only when gas saturation levels are above the assigned residual gas saturation values (WRGSSAT).

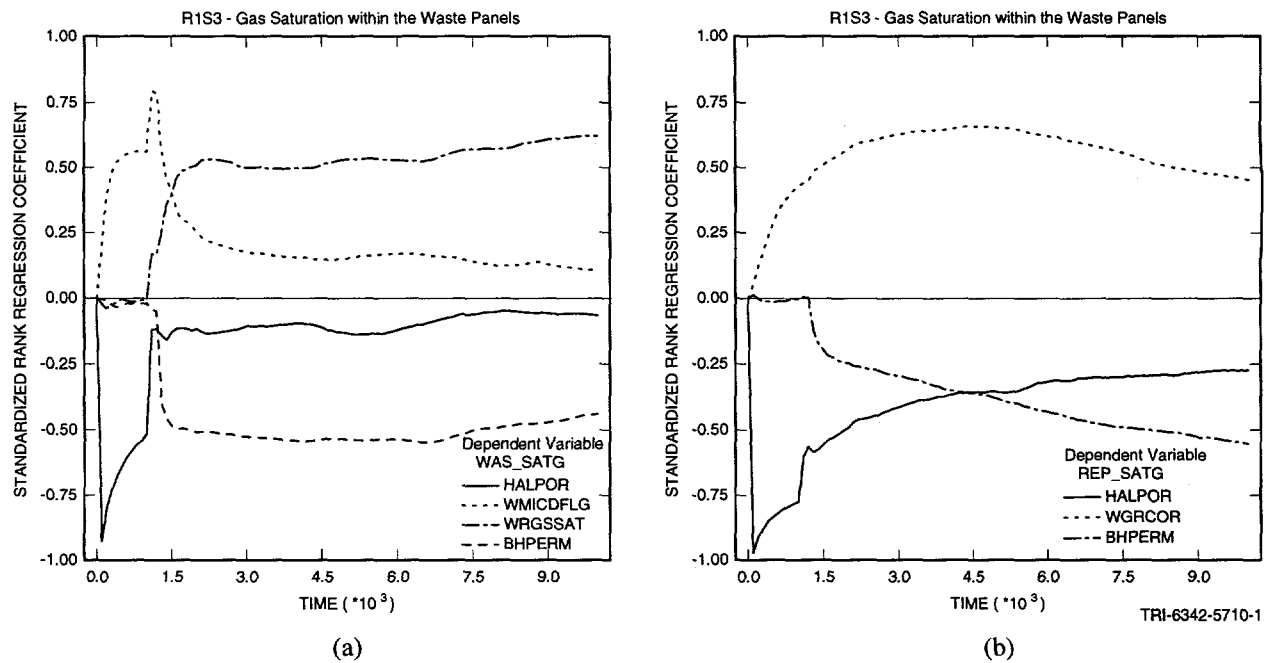


FIGURE 3.3.1. STANDARDIZED RANK REGRESSION COEFFICIENT (SRRC) results showing most influential independent variables for gas saturations in (a) lower and (b) upper waste panels

Consequently, those realizations with high values for WRGSSAT will have higher gas saturation levels.

3.3.1.2 *Variables Influencing Upper Waste Panel Gas Saturation (REP_SATG) Levels*

SRRCs for variables most influencing gas saturation in the upper waste panels are given in Figure 3.3.1b. This figure indicates that, prior to intrusion, the single variable of significant influence on REP_SATG is halite porosity (HALPOR). HALPOR influences REP_SATG for the same reason this variable influences WAS_SATG.

After intrusion, iron corrosion rates (WGRCOR) and borehole permeability (BHPRM) influence REP_SATG. BHPRM influences REP_SATG for the same reason it influences WAS_SATG. WGRCOR shows up as influencing REP_SATG for less obvious reasons. The upper waste panel is an important storage site for gas later in the modeled period, especially for realizations with small DRZ volumes and low borehole permeabilities. As a reminder, the dominant gas-producing mechanism after intrusion is iron corrosion. As gas is produced in all waste regions, but more extensively in the lower waste panel, it migrates upward through the ceiling of the

waste disposal areas to the UDRZ. Gas will tend to move into the up-dip regions of the repository, especially for those realizations with high values for iron corrosion and with low values for BHPRM. As DRZ storage capacity reaches maximum values, some gas migrates back down through the upper waste panel ceiling, thus keeping gas saturation in the upper waste panel relatively high due to the influx of gas produced in the lower waste panel.

3.3.2 Variables Influencing DRZ Gas Saturation Levels

3.3.2.1 *UDRZ Gas Saturation Levels Above the Lower Waste Panel (South and North Sides - SATGUWPS and SATGUWPN, respectively) and Above the Upper Waste Panels (SATGUROR)*

The plots in Figure 3.3.2 show that, prior to intrusion, halite porosity (HALPOR) and microbial degradation (WMICDFLG > 0) most influence gas saturation in the UDRZ above all waste panels.

Microbial degradation is important because it is the dominant gas-producing process early in the modeled period. The correlation between WMICDFLG and UDRZ gas saturations increases in strength between the time of intrusion and upper borehole degradation. Upon upper borehole degradation, decreased pressure results in brine from the lower brine reservoir displacing resident gas upward to the UDRZ; those realizations with microbial degradation will have more gas to be displaced upward (as indicated in the correlation ‘spike’ at 1000 years). The inverse correlation with HALPOR is due to the functional relationship that halite porosity plays in DRZ volumes. Those realizations with low HALPOR values will have smaller DRZ void volumes and have smaller gas storage capacities. This limited DRZ storage will ‘fill up’ more rapidly for realizations with gas generation from microbial degradation.

Because the south side of the UDRZ adjoins south MB 138, any brine drainage from south MB138 will drain into the south UDRZ. This brine competes with gas for DRZ void volume, hence the inverse correlation with anhydrite permeability (ANHPRM) and SATGUWPS. Brine

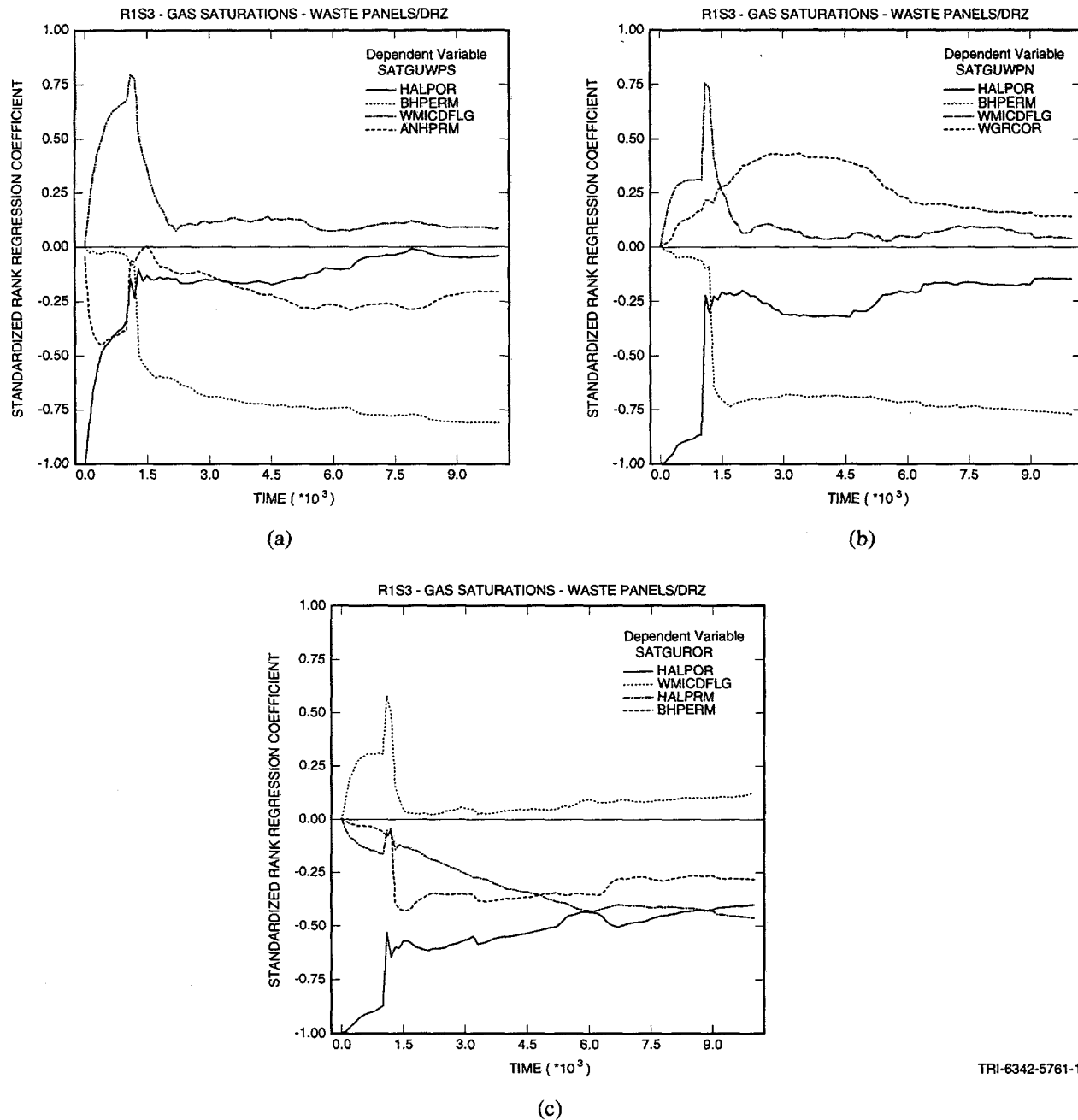


FIGURE 3.3.2. STANDARDIZED RANK REGRESSION COEFFICIENT (SRRC) results showing most influential independent variables for gas saturations above lower waste panel for area (a) south of borehole, (b) north of borehole, and (c) above the upper waste panel

drainage from the anhydrites to the DRZ is at the DRZ/anhydrite interface (more specifically, from south MB 138 and Anhydrite AB). Because the area north of the borehole does not contact an anhydrite layer, no correlation is seen between anhydrite permeability and DRZ gas saturation just north of the borehole (SATGUWPN or SATGUROR).

Halite permeability above the DRZ will facilitate the transmission of brine from the overlying units to the DRZ and brine that drains from the undisturbed halite will displace resident DRZ gas. Therefore, a very weak inverse correlation is seen between SATGUROR and halite permeability (HALPRM).

3.3.2.2 *Gas Saturation in LDRZ Below South and North Sides of the Waste Panel (SATGLWPS and SATGLWPN) and Below the Upper Waste Panel (SATGLROR)*

Figure 3.3.3 illustrates SRRC for the most influential variables controlling gas saturation in the LDRZ.

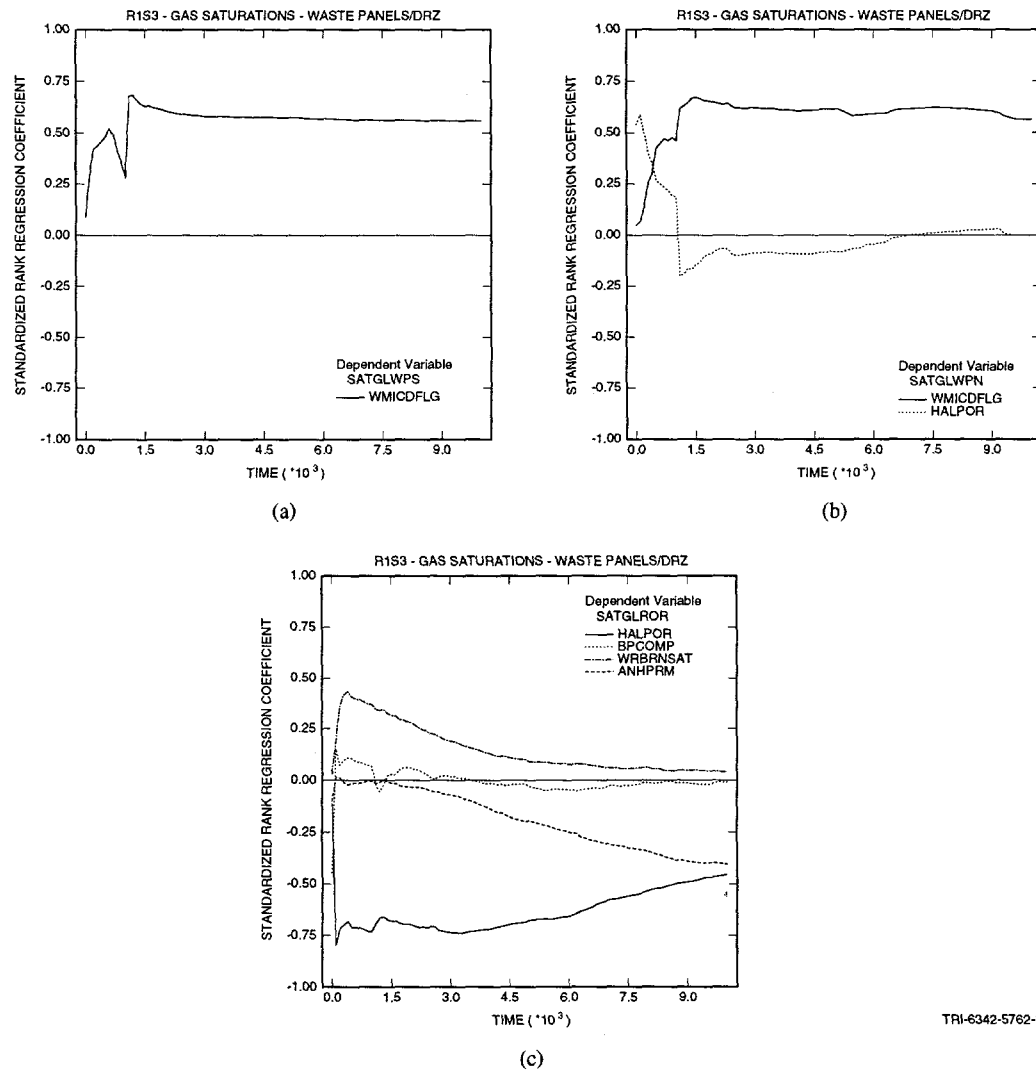


FIGURE 3.3.3. STANDARDIZED RANK REGRESSION COEFFICIENT results showing most influential independent variables for gas saturations below the lower waste panel for area (a) south of borehole, (b) north of borehole, and (c) below the upper waste panel

In general, parameters that control LDRZ gas saturation levels below all waste panels prior to intrusion also appear to dominate after the intrusion. Note that there is no connection to the lower brine reservoir prior to 1000 years. Therefore, the brief correlation at ~100 years between brine reservoir compressibility (BPCOMP) and LDRZ gas saturation below the upper waste panel is an anomaly.

Prior to intrusion, LDRZ gas saturation levels below the south and north halves of the lower waste panel (SATGLWPS and SATGLWPN) are positively correlated with microbial degradation (WMICDFLG > 0) and halite porosity (HALPOR). Those realizations with microbial degradation and large volumes of brine drainage will have relatively large volumes of gas produced. Gas storage space will be limited as gas migrates up-dip. Consequently, some of this gas will be displaced to the LDRZ.

Gas saturation in the LDRZ below the upper waste panel, SATGLROR, is negatively correlated with halite porosity, HALPOR, before and several thousands of years after intrusion. Low values for HALPOR equate to smaller DRZ volumes for gas storage. Gas storage space will become more limited in the more up-dip region of the repository, as this is the end point of the gas migration route prior to intrusion. Thus, the degree of gas saturation in the LDRZ below the upper waste panel is controlled more by available gas storage space, rather than gas production processes.

Residual brine saturation, WRBRNSAT, controls the amount of brine that is retained in the waste regions prior to draining to the LDRZ. High values for WRBRNSAT mean less brine goes to the LDRZ; consequently, a weak positive correlation exists between WRBRNSAT and SATGLROR within the first 100 years of closure. The negative correlation between SATGLROR and anhydrite permeability, ANHPRM, becomes significant at ~6000 years. Coupling this negative correlation with that for HALPOR and SATGLROR implies those realizations with high ANHPRM values and relatively lower DRZ void volumes will have enough brine from anhydrite drainage at ~6000 years to fill up the LDRZ voids.

Intentionally Left Blank

4. Brine and Gas Flow in the UDRZ

Vertical and lateral brine and gas flow within and between the UDRZ and regions of the waste disposal area are discussed in this section. Three flow boundaries were evaluated for vertical flow and two for lateral flow. For vertical flow, these boundaries were between the UDRZ and 1) the lower waste panel, 2) the top of the panel closure separating the two modeled waste disposal regions, and 3) the upper waste panel. Lateral flow (parallel to the ceiling of the waste panels) was calculated within the UDRZ through the two vertical sections above the north and south boundary of the panel closure. These boundaries within the UDRZ were selected to determine the extent to which the panel closures may serve as a source or sink between the UDRZ and the two waste disposal areas. (A more detailed evaluation of flow within the panel closures between the two waste disposal areas is discussed in Section 5.) Figure 4.1.1 depicts those regions and boundaries where UDRZ flow was evaluated.

The organization of Section 4 is as follows. Section 4.1 presents the variables defining vertical flow crossing the highlighted boundaries between the UDRZ and each delineated zone. Following these definitions, hairplots — results for the entire suite of 100 simulations overlaid

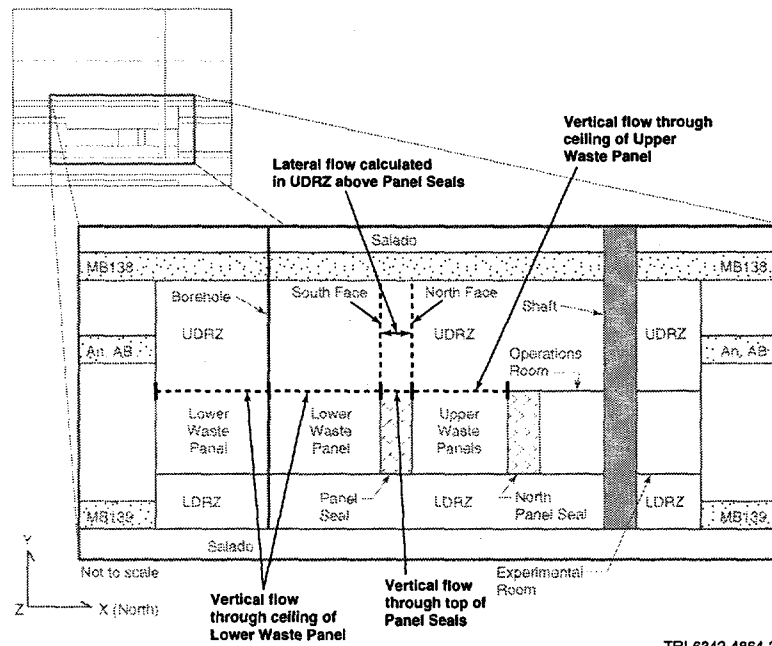


FIGURE 4.1.1. LOCATIONS IN UDRZ AT which lateral and vertical brine and gas flow were assessed

on one plot —are presented for each defined variable. These hairplots illustrate the variation in behaviors that may occur for a single variable from simulation to simulation, given the unique combination of sampled variables assigned to each simulation. Hairplots are referred to throughout each subsection. Using the same format, descriptions of the variables defining lateral fluid flow in the UDRZ are then presented.

To better understand the trends and overall behavior of each variable throughout the modeled period, boxplots for each variable will be presented at the end of Section 4.1. As a reminder, boxplots present in graphical form the mean, median, 25th and 75th quantile groups of a variable over the 100 simulations, as well as outliers within a population set. Boxplots are presented for results at four significant times within the modeled period. These are as follows:

- 999 years, just prior to intrusion,
- 1500 years, 300 years after the upper borehole plug degrades,
- 5500 years, midway through the modeled period,¹ and
- 10,000 years, the end of the modeled period.

Section 4.2 gives a brief overview of UDRZ brine and gas flow throughout the modeled period. Scatterplots are presented to illustrate the relationship between flow in the UDRZ and other processes inside the waste disposal area. Section 4.3 will present the dependent variables most affecting flow in the UDRZ. Section 4.4 provides a pictorial representation of the written summary for brine and gas flow given in Section 4.2.

¹ Prior examination of several dependent variables within the suite of simulations revealed several processes had stabilized soon after 5000 years. Therefore, it was decided to choose values for dependent variables at 5500 years rather than 5000 years.

4.1 Variables Used to Define Flow

4.1.1 Vertical Flow Between UDRZ Waste Disposal Area and the Panel Closures

Vertical brine and gas flow between the UDRZ and the lower waste panel was subdivided between the area residing north and south of the borehole (as depicted in Figure 4.1.1). Table 4.1 lists variable names defining vertical flow from the UDRZ into the top of the lower waste panel. Figures 4.1.2 through 4.1.5 are hairplots graphically depicting this vertical brine and gas flow (cumulative).

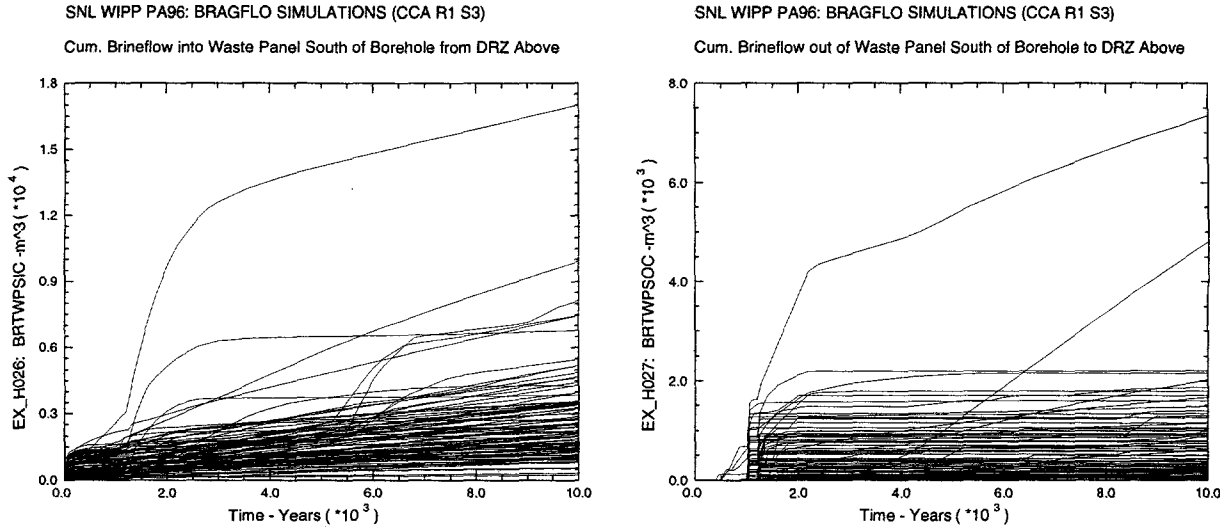
Table 4.2 defines variable names for vertical brine and gas flow between the UDRZ and the top of the panel closures; the corresponding hairplots are presented in Figures 4.1.6 and 4.1.7.

Table 4.1. Dependent Variables for Vertical Brine and Gas Flow Through the Ceiling of the Lower Waste Panel South and North of Borehole (note variable names shown on boxplots are abbreviated and given in parenthesis)

Variable	Definition
South of Borehole	
BRTWPSIC (BRTWSIC)	Cumulative brine flow (m^3) into the top of the lower waste panel from UDRZ
BRTWPSOC (BRTWSOC)	Cumulative brine flow (m^3) out of the top of the lower waste panel into UDRZ
GSTWPSIC (GSTWSIC)	Cumulative gas flow (m^3) into the top of the lower waste panel from UDRZ
GSTWPSOC (GSTWSOC)	Cumulative gas flow (m^3) out of the top of the lower waste panel into UDRZ
North of Borehole	
BRTWPNC (BRTWNIC)	Cumulative brine flow (m^3) into the top of the lower waste panel from UDRZ
BRTWPNC (BRTWNOC)	Cumulative brine flow (m^3) out of the top of the lower waste panel into UDRZ
GSTWPNC (GSTWNIC)	Cumulative gas flow (m^3) into the top of the lower waste panel from UDRZ
GSTWPNC (GSTWNOC)	Cumulative gas flow (m^3) out of the top of the lower waste panel into UDRZ

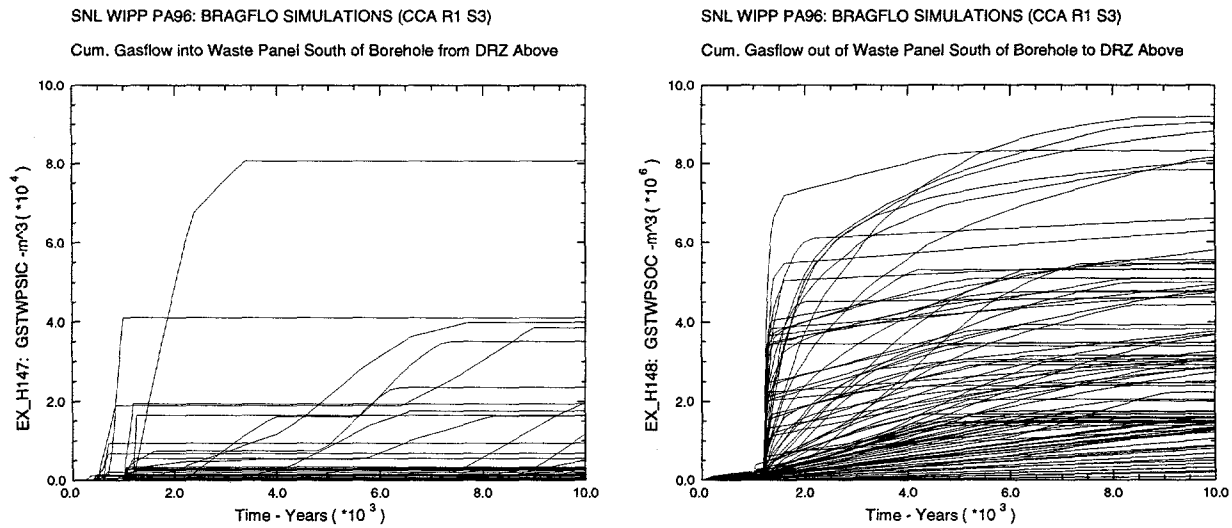
Table 4.2. Dependent Variables for Vertical Brine and Gas Flow Into and Out of Top of Panel Closures

Variable	Definition
BRNDTPSC	Cumulative brine flow (m^3) down into the top of the panel closure from UDRZ
BRNUTPSC	Cumulative brine flow (m^3) up out of the top of the panel closure into UDRZ
GASDTPSC	Cumulative gas flow (m^3) down into the top of the panel closure from UDRZ
GASUTPSC	Cumulative gas flow (m^3) up out of the top of the panel closure into UDRZ



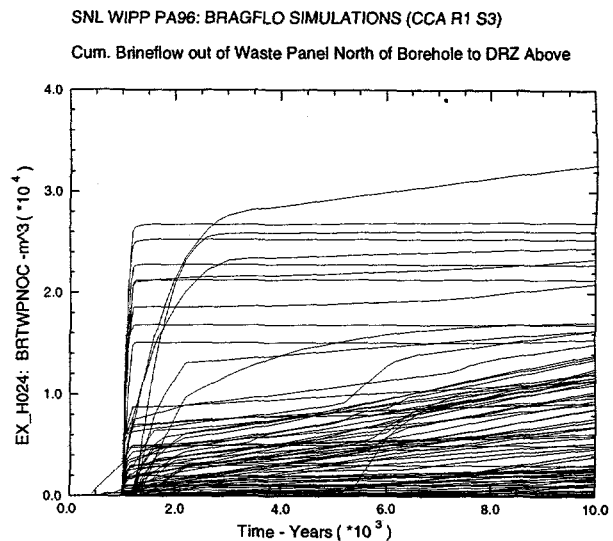
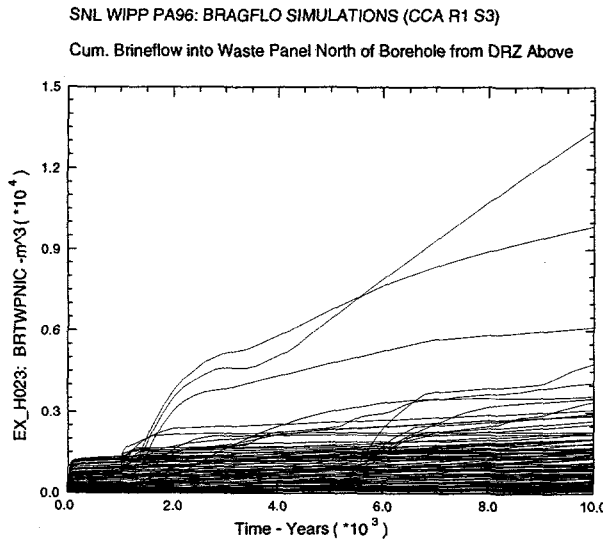
TRI-6342-5609-0

FIGURE 4.1.2. HAIRPLOTS FOR CUMULATIVE VERTICAL brine flow (m^3) between the UDRZ and the south half of the lower waste panel ceiling



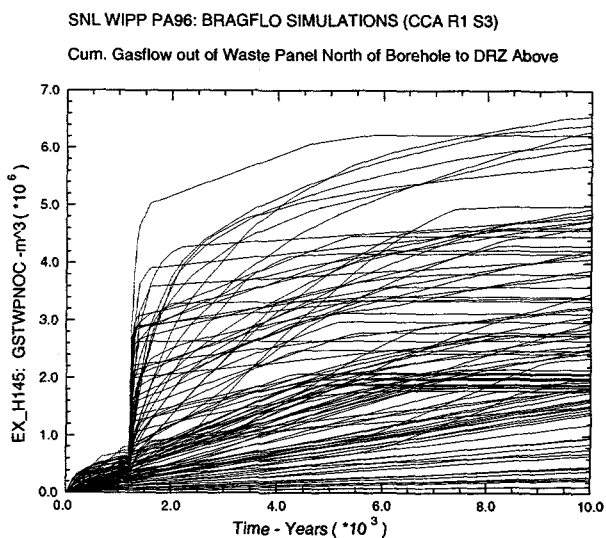
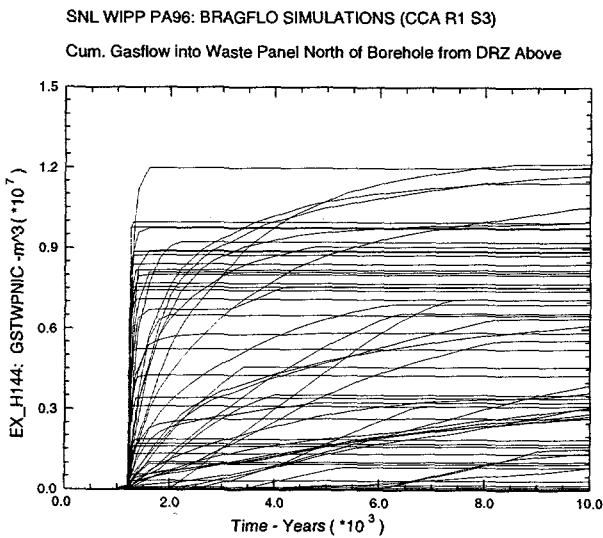
TRI-6342-5610-0

FIGURE 4.1.3. HAIRPLOTS FOR CUMULATIVE VERTICAL gas flow (m^3) between the UDRZ and the south half of the lower waste panel ceiling



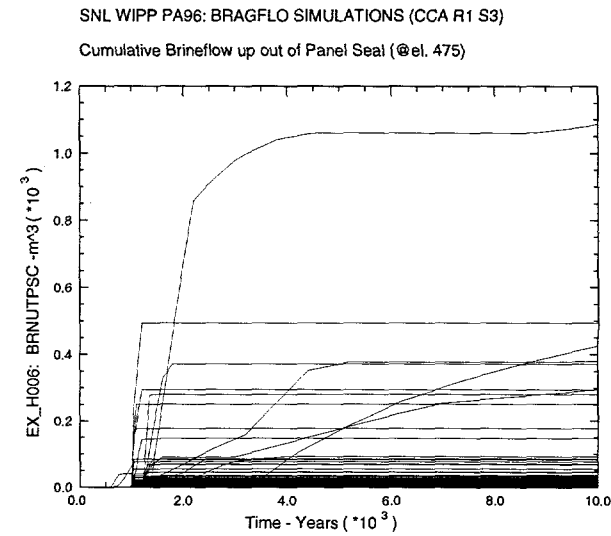
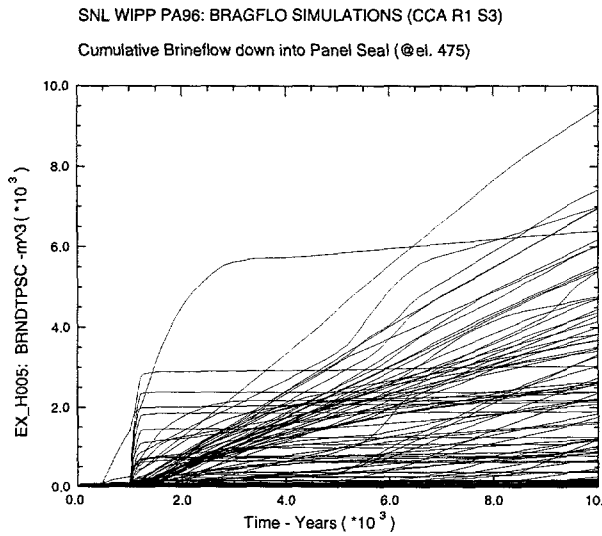
TRI-6342-5611-0

FIGURE 4.1.4. HAIRPLOTS FOR CUMULATIVE VERTICAL brine flow (m^3) between the UDRZ and the north half of the lower waste panel ceiling



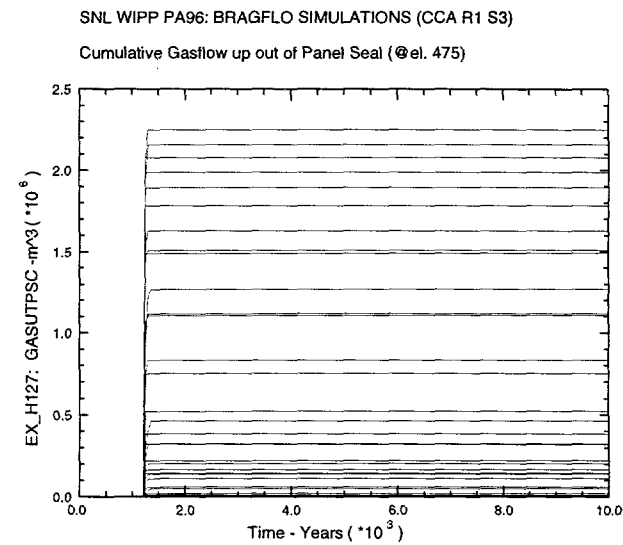
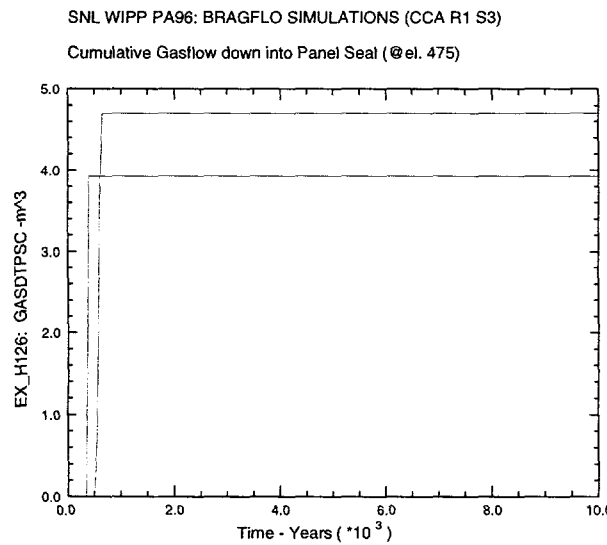
TRI-6342-5612-0

FIGURE 4.1.5. HAIRPLOTS FOR CUMULATIVE VERTICAL gas flow (m^3) between the UDRZ and the north half of the lower waste panel ceiling



TRI-6342-5613-0

FIGURE 4.1.6. HAIRPLOTS FOR CUMULATIVE VERTICAL brine flow (m^3) between the UDRZ and the top of the panel closure



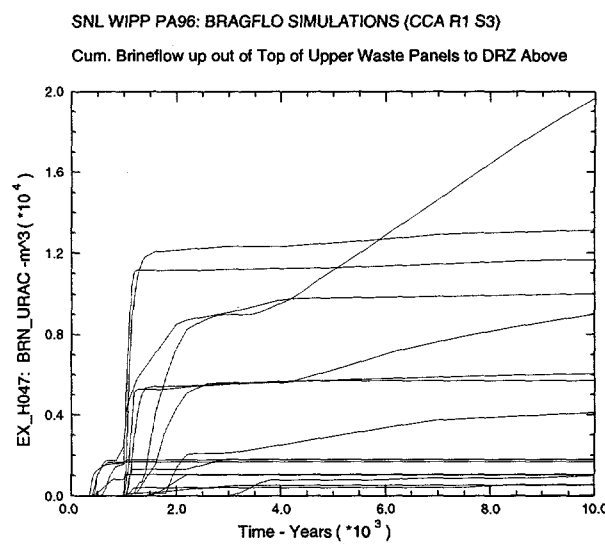
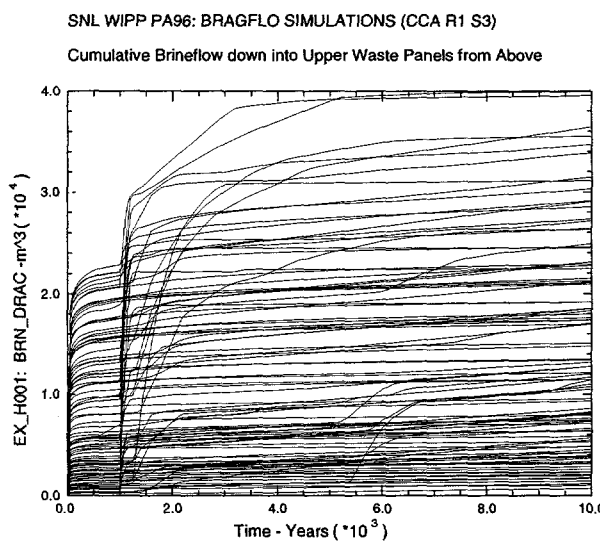
TRI-6342-5614-0

FIGURE 4.1.7. HAIRPLOTS FOR CUMULATIVE VERTICAL gas flow (m^3) between the UDRZ and the top of the panel closure

Table 4.3 defines the variables for vertical brine and gas flow between the UDRZ and the ceiling of the upper waste panels (see also Figure 4.1.1). Figures 4.1.8 and 4.1.9 are hairplots for these cumulative gas and brine flows.

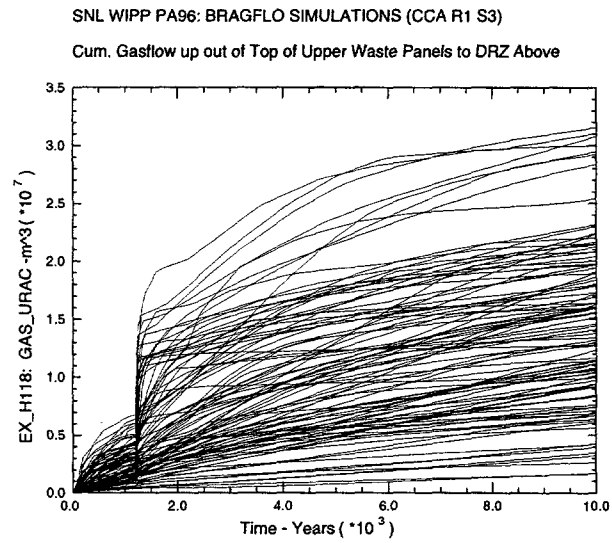
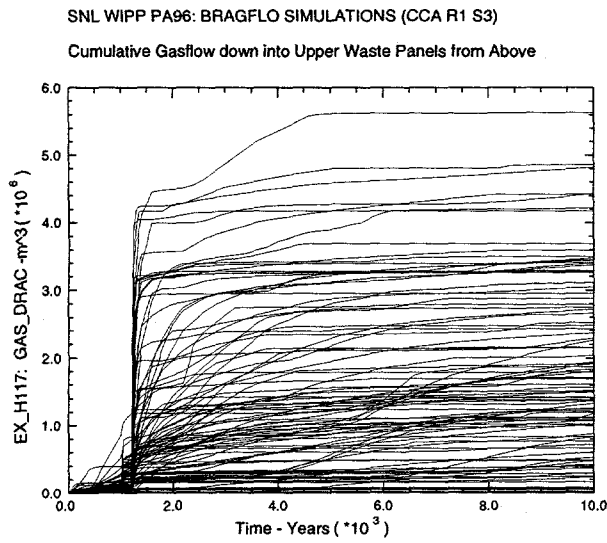
Table 4.3. Dependent Variables for Vertical Brine and Gas Flow Into and Out of Upper Waste Panel Closures (variable names shown on boxplots are abbreviated and given in parenthesis)

Variable	Definition
BRN_DRAC (BRNDRAC)	Cumulative brine flow (m^3) down through the ceiling of the upper waste panels from UDRZ
BRN_URAC (BRNURAC)	Cumulative brine flow (m^3) up through the ceiling of the upper waste panels into the UDRZ
GAS_DRAC (GASDRAC)	Cumulative gas flow (m^3) down through the ceiling of the upper waste panels from UDRZ
GAS_URAC (GASURAC)	Cumulative gas flow (m^3) up through the ceiling of upper waste panels into the UDRZ



TRI-6342-5615-0

FIGURE 4.1.8. HAIRPLOTS FOR CUMULATIVE VERTICAL brine flow (m^3) crossing between ceiling of upper waste panel and UDRZ



TRI-6342-5616-0

FIGURE 4.1.9. HAIRPLOTS FOR CUMULATIVE VERTICAL gas flow (m^3) crossing between ceiling of upper waste panel and UDRZ

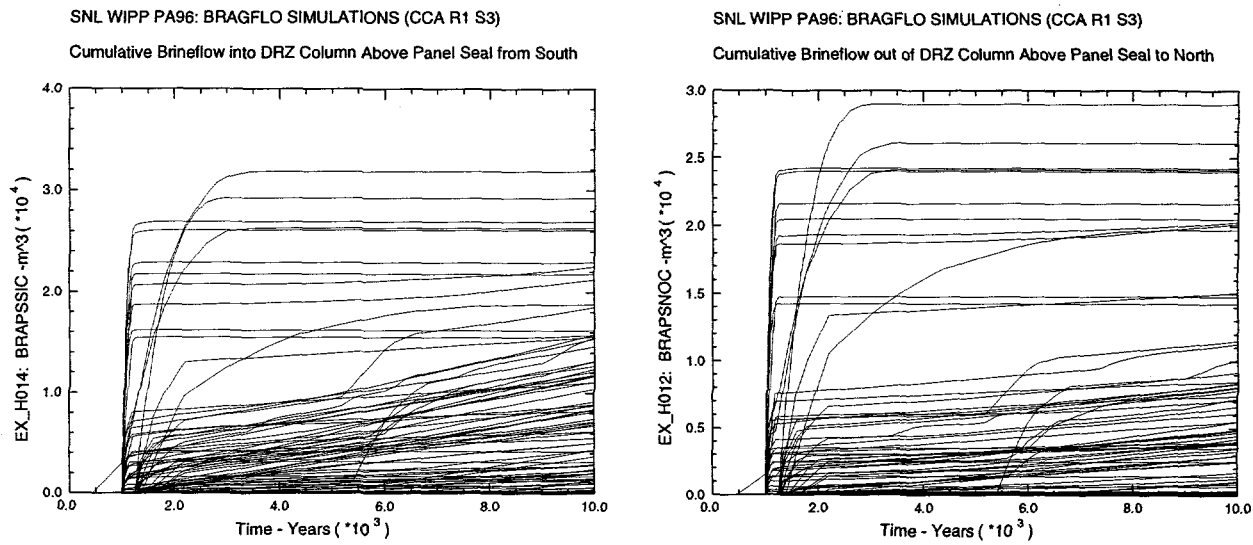
4.1.2 Lateral Gas and Brine Flow in UDRZ Above the Panel Closures

Variable names for lateral north and south flow within the UDRZ, just above the panel closures, are given in Table 4.4 (see also Figure 4.1.1). Figures 4.1.10 through 4.1.13 are hairplots that illustrate cumulative gas and brine flow crossing these regions.

Boxplots for vertical brine and gas flow are depicted in Figures 4.1.14 through 4.1.17. Boxplots for lateral gas flow are depicted in Figures 4.1.18 and 4.1.19.

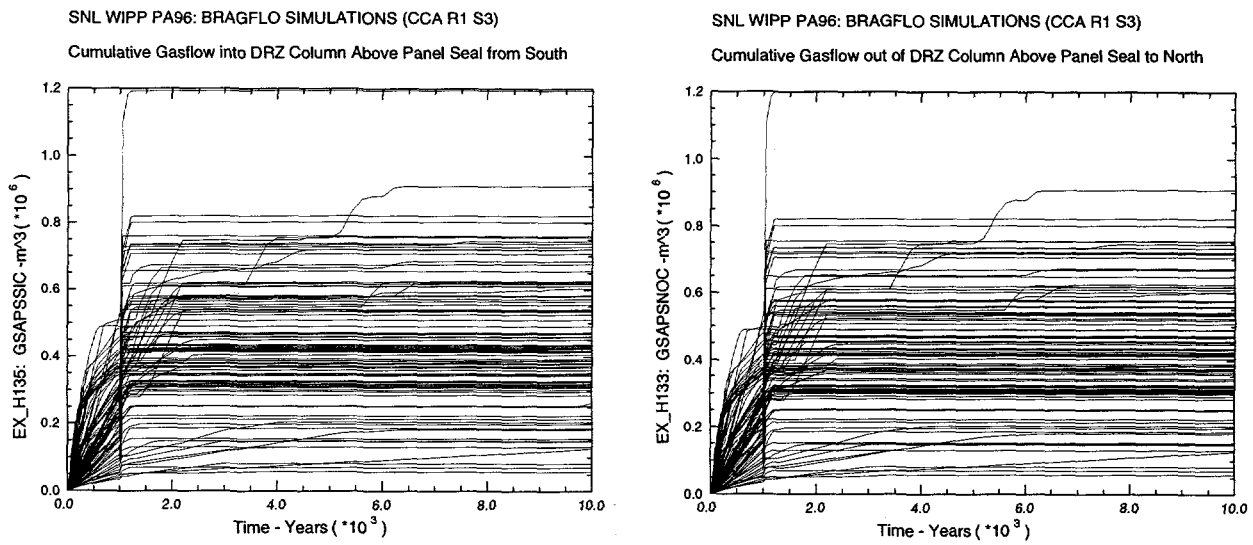
Table 4.4. Dependent Variables for Lateral Brine and Gas Flow Within UDRZ Above South and North Panel Closures

Variable	Definition
North-Flowing Brine	
BRAPSSIC	Lateral cumulative brine (m^3) flowing north within UDRZ crossing the boundary just above the south side of the panel closures
BRAPSNOC	Lateral cumulative brine (m^3) flowing north within UDRZ crossing the boundary just north of the panel closures
GSAPSSIC	Lateral cumulative gas (m^3) flowing north within UDRZ crossing the boundary just above the south side of the panel closures
GSAPSNO	Lateral cumulative gas (m^3) flowing north within UDRZ crossing the boundary just north of the panel closures
South-Flowing Brine	
BRAPSNIC	Lateral cumulative brine (m^3) flowing south within UDRZ crossing the boundary just north of the panel closures
BRAPSSOC	Lateral cumulative brine (m^3) flowing south within UDRZ crossing the boundary just above the south side of the panel closures
GSAPSNIC	Lateral cumulative gas (m^3) flowing south within UDRZ crossing the boundary just north of the panel closures
GSAPSSOC	Lateral cumulative gas (m^3) flowing south within UDRZ crossing the boundary just above the south side of the panel closures



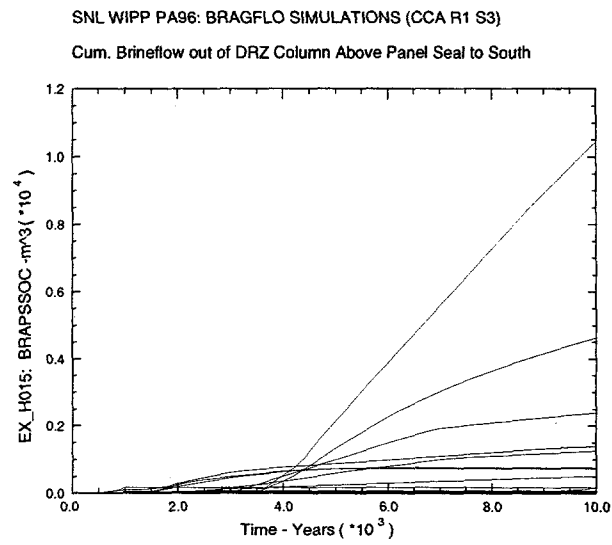
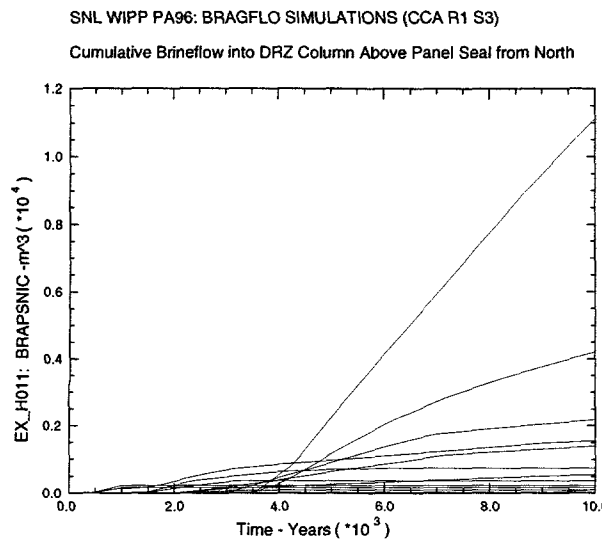
TRI-6342-5617-0

FIGURE 4.1.10. HAIRPLOTS FOR CUMULATIVE LATERAL BRINE flow (m^3) within the UDRZ above the panel closure going in a northerly direction



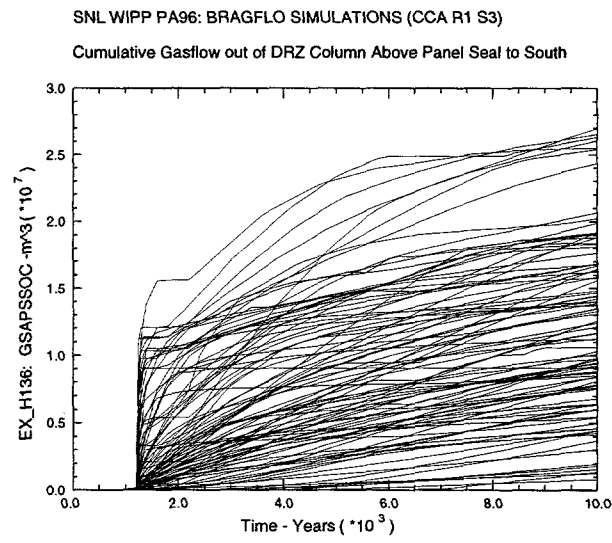
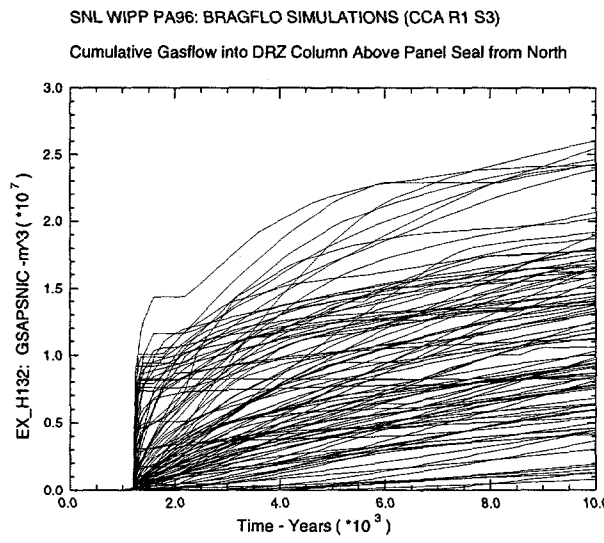
TRI-6342-5618-0

FIGURE 4.1.11. HAIRPLOTS FOR CUMULATIVE LATERAL GAS flow (m^3) within the UDRZ above the panel closure going in a northerly direction



TRI-6342-5619-0

FIGURE 4.1.12. HAIRPLOTS FOR CUMULATIVE LATERAL BRINE flow (m^3) within the UDRZ above the panel closure going in a southerly direction



TRI-6342-5620-0

FIGURE 4.1.13. HAIRPLOTS FOR CUMULATIVE LATERAL GAS flow (m^3) within the UDRZ above the panel closure going in a southerly direction

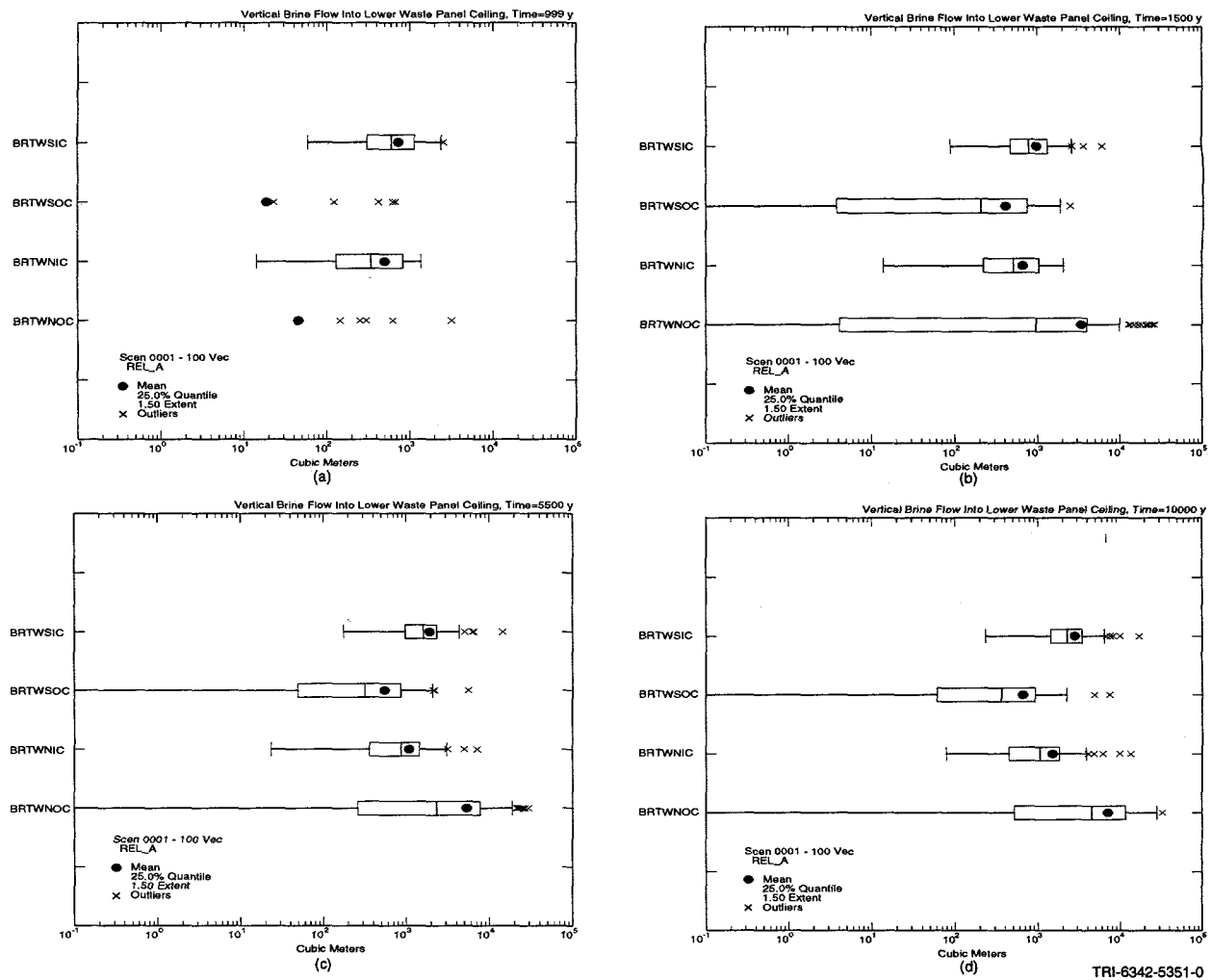


FIGURE 4.1.14. BOXPLOTS FOR VERTICAL BRINE flow through the lower waste panel ceiling at (a) 999 years, (b) 1500 years, (c) 5500 years, and (d) 10,000 years

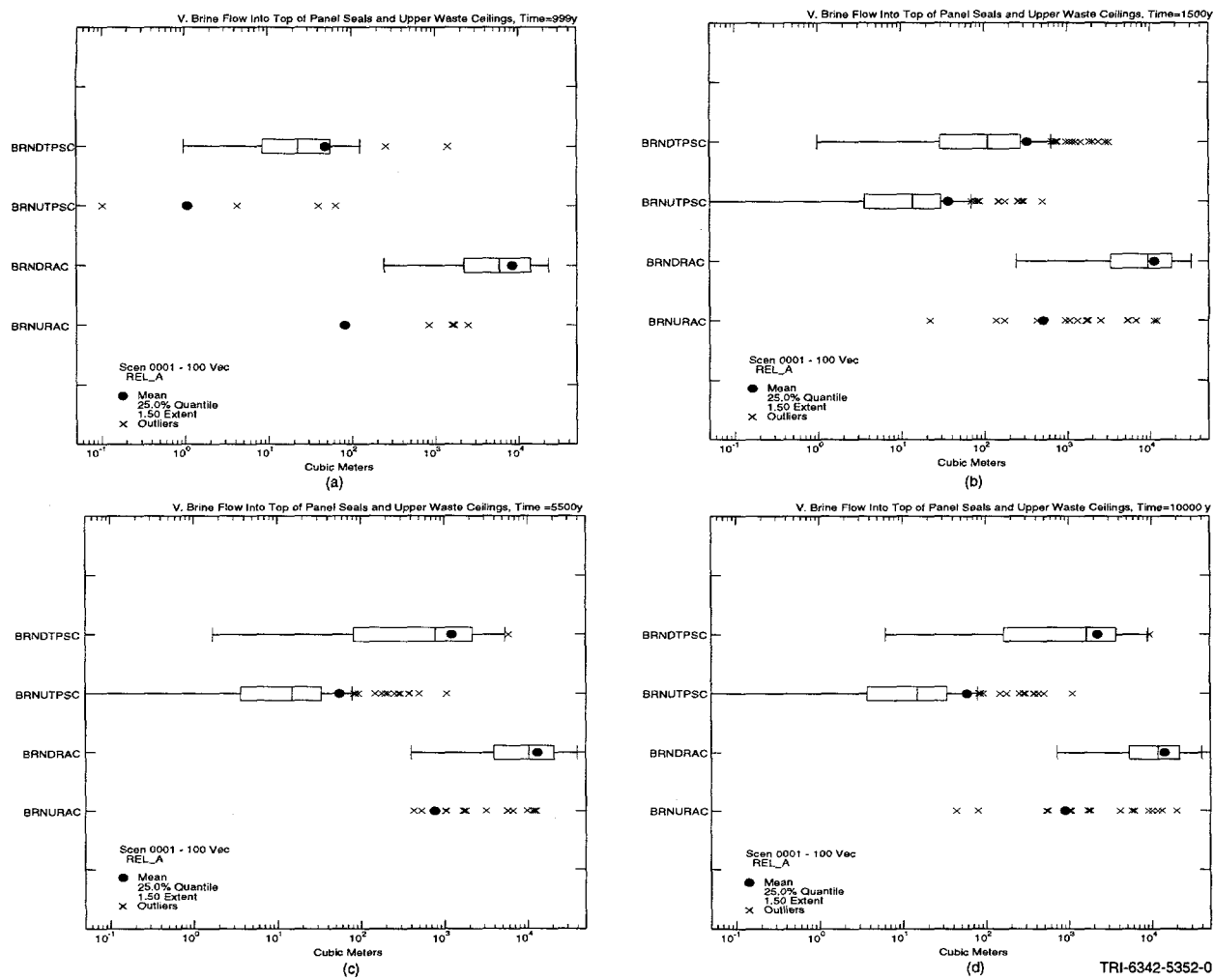


FIGURE 4.1.15. BOXPLOTS FOR VERTICAL BRINE flow through the top of panel closures and upper waste ceilings for (a) 999 years, (b) 1500 years, (c) 5500 years, and (d) 10,000 years

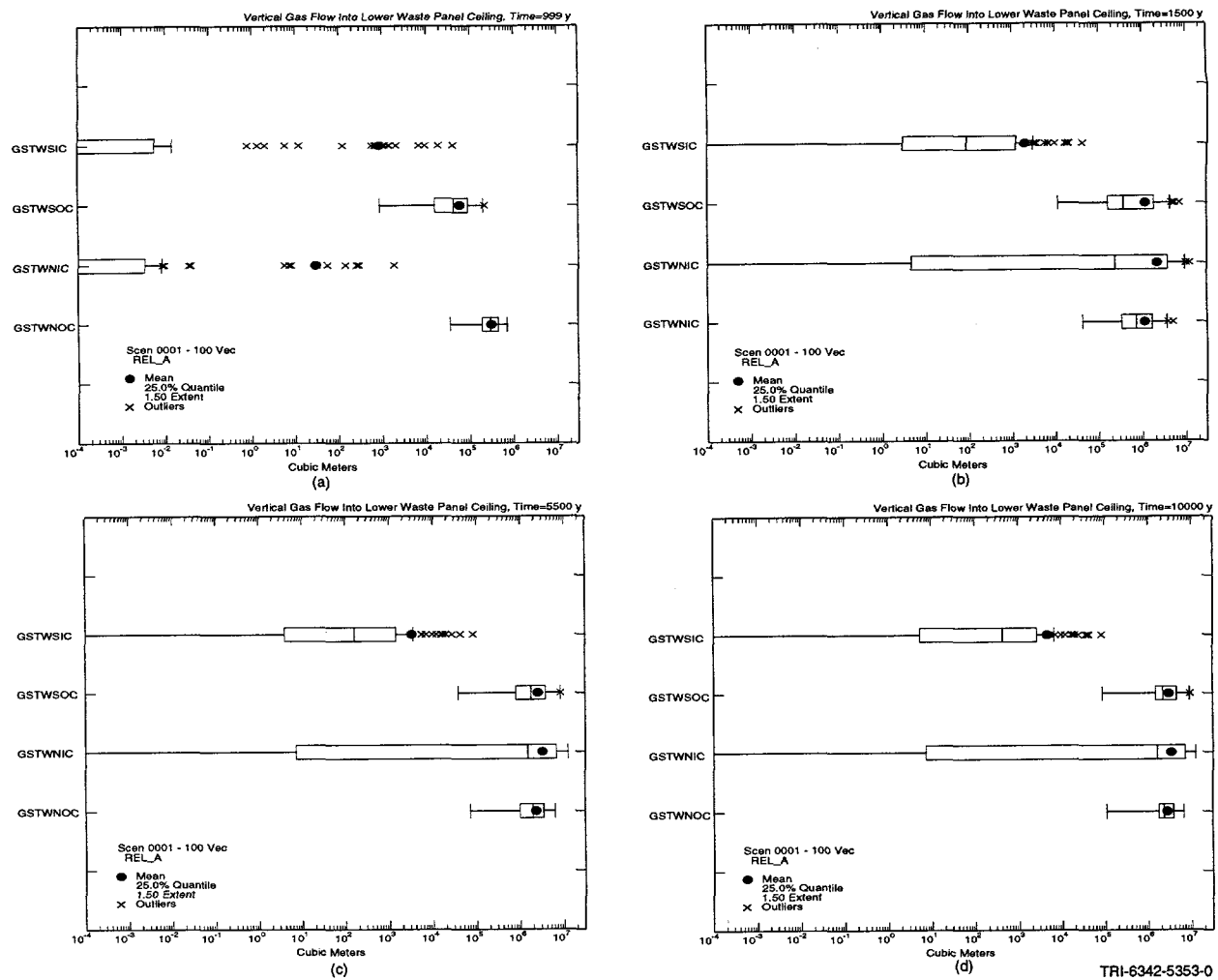


FIGURE 4.1.16. BOXPLOTS FOR VERTICAL GAS flow through the lower waste panel ceiling for (a) 999 years, (b) 1500 years, (c) 5500 years, and (d) 10,000 years

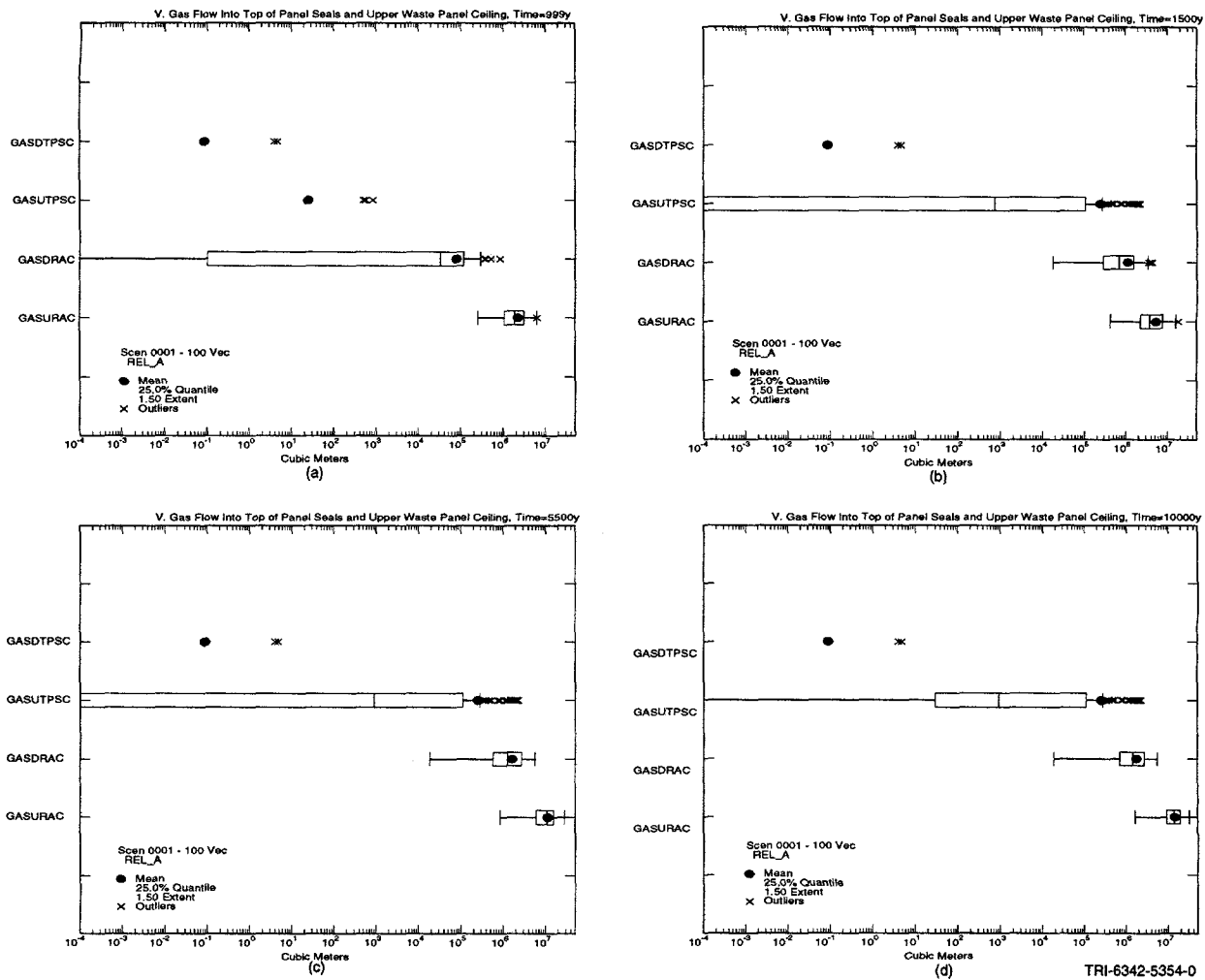


FIGURE 4.1.17. BOXPLOTS FOR VERTICAL GAS flow through the top of panel closures and upper waste panel ceilings for (a) 999 years, (b) 1500 years, (c) 5500 years, and (d) 10,000 years

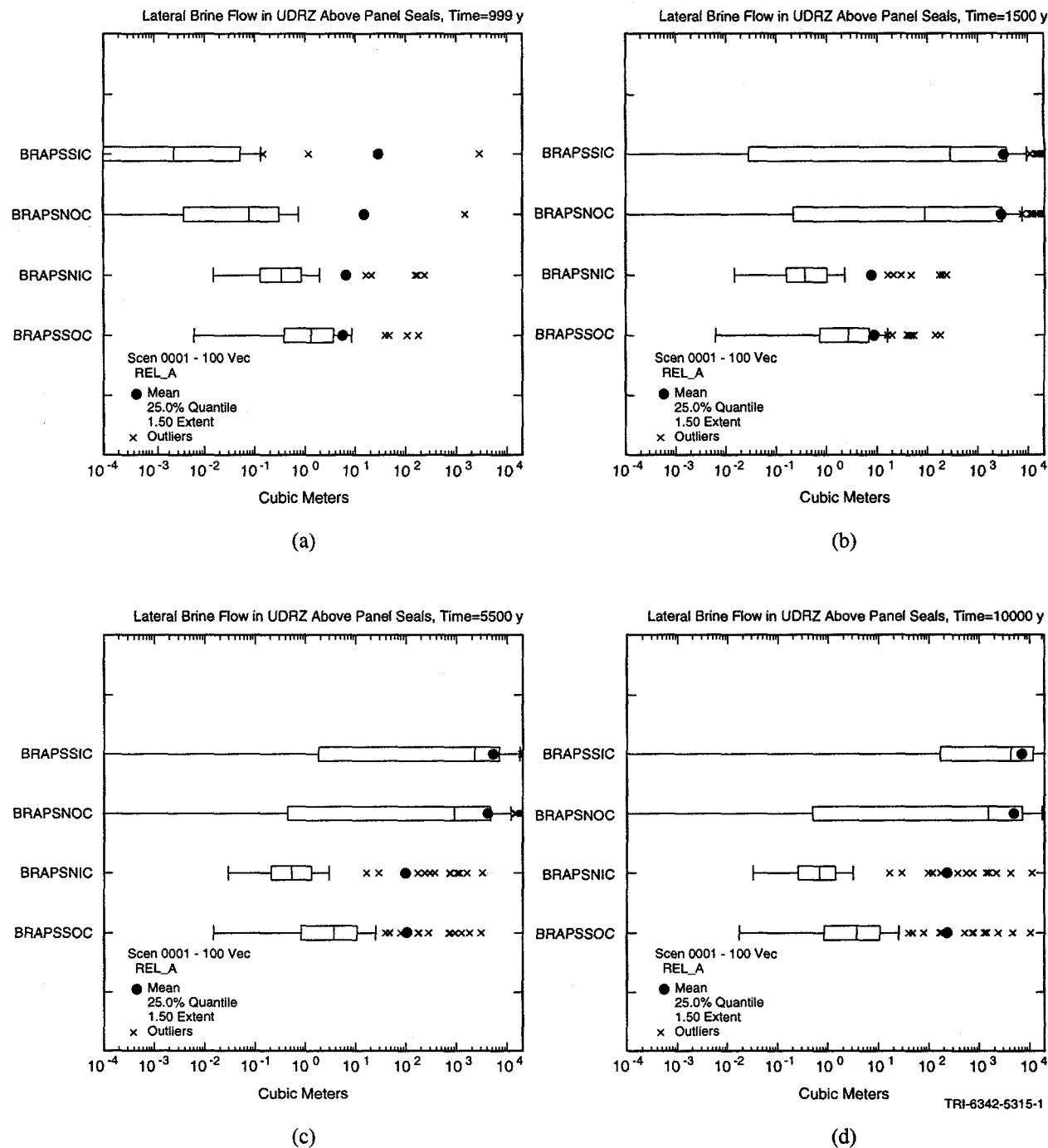


FIGURE 4.1.18. BOXPLOTS FOR LATERAL BRINE flow in the UDRZ passing the area above the panel closures at (a) 999 years, (b) 1500 years, (c) 5500 years, and (d) 10,000 years

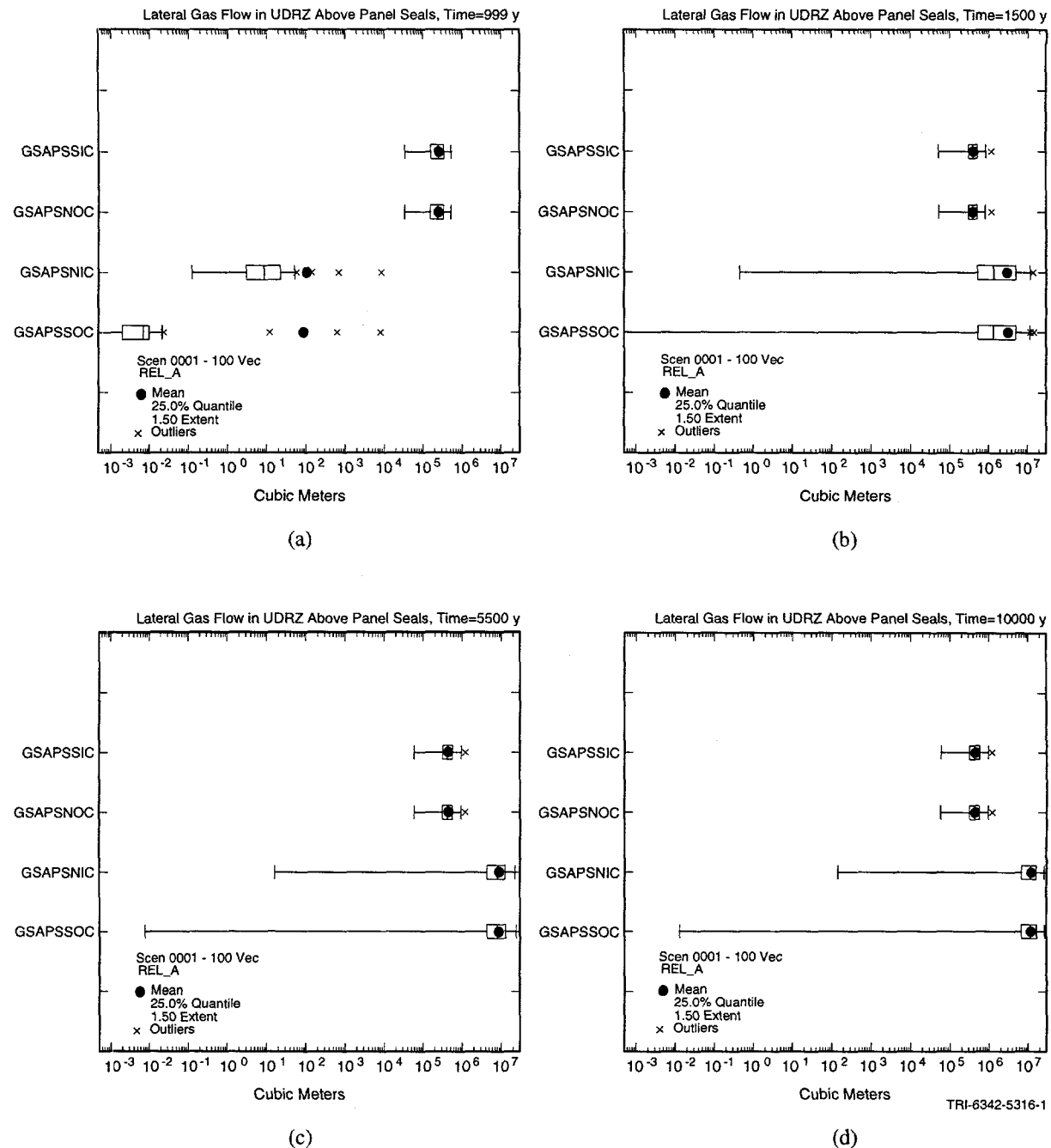


FIGURE 4.1.19. BOXPLOTS FOR LATERAL GAS flow in the UDRZ passing the area above the panel closures at (a) 999 years, (b) 1500 years, (c) 5500 years, and (d) 10,000 years

4.2 Overview of Brine and Gas Flow in the UDRZ

4.2.1 Flow Prior to Time of Intrusion

4.2.1.1 Brine Flow

Prior to intrusion, the primary brine flow direction in the UDRZ is downward, limited to times soon after repository closure, and primarily caused by drainage from the DRZ drainage down to the waste region and secondarily from anhydrite drainage. After the first hundred years of the modeled period, gas flow upwards to the UDRZ impedes downward-flowing brine. Newly-generated gas reduces brine permeabilities in the UDRZ and increases repository pressures, thus lowering the pressure potential that drives brine drainage.

The hairplots in Figures 4.1.10 and 4.1.12 and the boxplots in Figure 4.1.16 show that lateral brine flow in the UDRZ before intrusion is minimal and what little occurs is in a southerly direction. The extent of lateral-flowing brine is affected by gas generation processes within the waste regions. South-flowing brine occurs for those realizations that have relatively low volumes of gas generated and relatively large halite porosities. For these realizations, relatively large UDRZ brine-filled pore voids (a function of halite porosity) drain into the lower portion of the upper waste panels. This drainage is minimally impeded by gas flow upward, and collects at the *south end* of the upper waste panel(s) lying just north of the panel closures. This area approaches near 100% brine saturation, causing brine to overflow through the ceiling of the upper waste panel into the UDRZ, initiating lateral brine flow to the south.

Boxplots for vertical brine drainage at 999 years (prior to intrusion) (Figure 4.1.14), show the majority of brine that drains from the UDRZ passes through the upper waste panel ceiling and is due to the much larger UDRZ surface area abutting the upper waste panel compared to the lower panel.

4.2.1.2 Gas Flow

Prior to intrusion, gas produced in all waste disposal areas predominantly flows upward to the UDRZ. Once in the UDRZ, its flow path is deflected northward by the less permeable undisturbed halite and heads toward the northern (i.e., up-dip) part of the repository. From the

lower waste panel, gas migrates upward to the UDRZ, then heads north, crossing the area above the panel closures. Gas generation early in the modeled period is primarily from microbial degradation of cellulose, rubbers and plastics (half of the sampled set) with only a minor contribution from iron corrosion. Because the down-dip (later the intruded) waste panel is more brine saturated than the up-dip (later the unintruded) waste panels, it has more brine reserves for iron corrosion; thus, a relatively larger portion of gas is produced in the lower waste panel via iron corrosion compared to the upper waste panels.

More gas flows out the north side of the lower waste panel compared to the south side (see boxplots in Figure 4.1.15). This is partially due to the location of the panel relative to dip, making the south half in the down-dip direction more brine saturated compared to the north. The one degree dip of the repository makes the upward gas flow path less than perpendicular to the ceiling; the dip effectively deflects the gas flow path towards the north. Additionally, the differences in the gas-saturation between the south and north halves produce a preferential gas flow path through the north half of the lower waste panel, enhancing the already diagonal gas flow path trajectory. Because the panel closures are more brine- than gas-saturated, they serve as a low permeability gas barrier, deflecting the diagonal gas flow path upward to the UDRZ.

A portion of gas that flows north in the UDRZ eventually passes through the concrete shaft to the experimental rooms, terminating in the operations and experimental rooms. Because gas generation increases repository pressures, a direct relationship is seen between repository pressures and north-flowing gas in the UDRZ and gas flow through the concrete shaft prior to intrusion (see Figure 4.2.6b in Section 4.2.3).

4.2.2 Flow After Time of Intrusion

4.2.2.1 Brine

At 1000 years, the time of repository intrusion, an upward and northward brine pulse is introduced in the UDRZ for the majority of simulations. The pulse is caused by a pressure differential between the lower Castile brine reservoir and the repository producing a pressure

wave² within the repository. The pressure wave propagates up through the borehole. Where Castile compressibilities are high, the pressure wave introduces Castile brine into the lower waste panel and some brine is displaced upward into the UDRZ. For these realizations, the pressure wave displaces a portion of resident brine (brine already in the excavated area prior to intrusion) into the UDRZ. This brine flows laterally up-dip toward the upper waste panels (see the hairplots given in Figure 4.1.10). Brine crosses the area in the UDRZ just above the panel closures while compressing resident UDRZ gas. This gas forms a semi-impermeable gas wedge above the panel closures that deflects brine downward through the top of the panel closures and the south side of the upper waste panel ceiling.

For many realizations, the north-flowing brine pulse lasts only a few hundred years and ceases soon after upper borehole degradation. For others, brine flow up-dip continues to the end of the modeled period and is affected by gas flow patterns and gas saturations within the UDRZ and borehole permeability. The extent of this 'up-dip' brine flow is primarily affected by the ease with which gas is evacuated out the repository and replenishing brine is introduced in the UDRZ from upper units via the borehole, and secondarily by the volume of brine not used for iron corrosion in the lower waste panels. Any excess brine flows through the lower waste panel ceiling into the UDRZ. The ease with which brine flows northward through the UDRZ is affected by resident gas produced in the waste panels and stored in the UDRZ; this results in relatively high gas pressures and saturations inhibiting incoming brine. High gas saturations also mean this area has low-effective brine and high-effective gas permeabilities, two combinations that impede lateral brine flow. Realizations with little gas production have more north-flowing brine in the UDRZ compared to realizations with maximal gas generation (i.e., microbial degradation of cellulose and/or rubber and plastics, and/or high iron corrosion rates) from the time of intrusion to the end of the modeled period.

The ease with which gas is evacuated out of the UDRZ, a function of borehole permeability, affects the extent to which replenishing brine enters the area (discussed in Section 4.3). Consequently, a correlation is observed between north-flowing brine and borehole permeability.

² BRAGFLO does not numerically model a 'wave function.' The term 'pressure wave' describes the advancing pressure gradient that propagates outward from a focal point.

This correlation strength increases with time. For realizations with relatively low borehole permeabilities, the UDRZ regions across all the excavated area remain close to 100% gas saturated throughout the modeled period. For realizations with medium to high borehole permeabilities, the UDRZ gas saturation levels spatially vary as gas is vented out the repository. The southern (down-dip) portion of the UDRZ is the first to reach relatively high brine saturation levels. Once these levels are reached, brine drainage from the ‘south’ Anhydrite AB (which had ceased when the UDRZ was more gas saturated and of high pressure) begins again to flow into the UDRZ. The borehole may still be venting gas upward when the ‘south’ UDRZ becomes brine saturated. Consequently, the UDRZ just up-dip from the borehole becomes less brine permeable. This situation promotes incoming brine that enters the UDRZ via the borehole and/or the south Anhydrite AB, to flow downward through the south ceiling of the lower waste panel rather than the north half.

Gas flow in the borehole decreases when iron corrosion in the lower waste panel is near depletion and coincides with repository pressures approaching that of the overlying units (i.e., hydrostatic pressures). Once hydrostatic pressures are reached, brine flow increases down the borehole from units above the Salado. From the UDRZ, a portion of this brine is partitioned into the lower waste panel and the remainder flows laterally up-dip toward the upper waste panel. Brine flowing up-dip is deflected downward into the top of the panel closures and through the ceiling of the upper waste panel lying just north of the panel closures, provided the brine/gas interface is north of the panel closures. This UDRZ deflection point is the interface between a high brine-saturation zone adjoining a high gas-saturation zone. This brine/gas interface slowly moves up-dip, as more and more gas is vented out the repository, terminating above the area just north of the panel closures. Figure 4.2.11 in Section 4.2.3 illustrates the gas-saturation wedge, which serves as this brine deflection point.

Boxplots (Figure 4.1.14) show the increase in vertical brine drainage through the lower panel ceiling that occurs between 1500 and 5500 years. During this time frame, drainage through the upper waste panel ceiling (Figure 4.1.15) remains at about the same level as prior to intrusion.

After intrusion, few realizations have brine flow in the southerly direction. Those that do have relatively small volumes of gas are generated. If there are small volumes of gas generated, repository pressures will be relatively lower, *and* the UDRZ is then more likely to have higher brine saturations and effective permeabilities. These conditions facilitate brine drainage from north MB 138 and Anhydrite AB. This drainage is then allowed to 'gravity flow' down-dip, southward, through the UDRZ.

4.2.2.2 Gas Flow

Upon intrusion, a pressure wave is transmitted up-dip within the repository caused by the pressure differential between the repository and underlying units via the borehole. For most realizations, this pressure pulse briefly compresses resident gas upward, out of the lower waste panel, and northward through the UDRZ. From the UDRZ, gas is pushed back down through the upper waste panel ceiling and through the concrete shaft. When the upper borehole plug degrades, the pressure gradient reverses; gas flow direction switches from a northerly to a southerly direction.

Parameters that most affect gas flow are (1) borehole permeabilities (which impact the ease with which the pressure gradients between units above and below are transmitted to the repository), (2) the extent of gas produced prior to intrusion (a function of microbial degradation), (3) the extent and rate in which gas is generated after intrusion, and (4) replenishment of brine into the areas where gas is generated. The extent to which 'new' gas is generated, in turn affecting gas flow in the UDRZ, is most affected in the lower panel by iron corrosion rates and in the upper waste panel by the availability of replenishing brine that comes in contact with the iron drums.

Gas flow towards the borehole is initiated when the upper borehole degrades at 1200 years. This gas flow is impeded in realizations that have relatively small DRZ volumes, lower borehole permeabilities, and a component of UDRZ north-flowing brine that is countercurrent to the south-flowing gas. Consequently, gas 'backs up' in the UDRZ within the vicinity of the panel closures and the area lying due north of the closures. This condition keeps the north side of the UDRZ highly gas-saturated, especially for realizations with relatively low borehole permeabilities, preventing replenishing brine from entering the UDRZ and those regions below.

Once south-flowing gas passes through the UDRZ above the panel closures, it will eventually exit the borehole.

When repository pressures are reduced to levels between 6 and 8 MPa, gas flow that exits through the borehole declines, and in some cases, ceases. Once this occurs, replenishing brine drains into the repository via the borehole and/or anhydrite drainage. A portion of the brine that enters the UDRZ flows into the lower waste panel. Some UDRZ brine flows up-dip towards the upper waste panel, thus restricting UDRZ south-flowing gas.

Gas production via microbial degradation is completed by ~1000 years. Gas production via iron corrosion nears completion in the lower waste panel toward the later half of the modeled period for a large majority of realizations because iron, required for gas generation, is close to being completely corroded. Concurrently, gas flow out the lower waste panel ceiling ceases or dramatically declines. For the upper waste panel, no realizations become iron depleted. Therefore, gas production continues in the upper waste panel long after it has ceased in the lower waste panel *if* brine contacts uncorroded iron. For many realizations, gas flow is intermittent through the ceiling of the upper waste panel to the UDRZ. This intermittent gas flow is tied to brine availability: i.e., as brine supplies are used up through the corrosion processes, gas production ceases and will not continue until replenishing brine levels within the waste area rise up-dip to elevations where uncorroded iron resides. Therefore, for the later half of the modeled period, realizations with borehole permeabilities in the middle to upper percentile group will have intermittent lateral gas flow heading toward the borehole. Realizations with lower borehole permeabilities will have less intermittent gas flow.

The following section provides scatterplots pictorially illustrating the relationship between gas and brine flow just described and those independent variables that influence this flow.

4.2.3 Scatterplots

Plots (Figures 4.2.1 through 4.2.14) illustrating brine and gas flow in UDRZ are provided in this section.

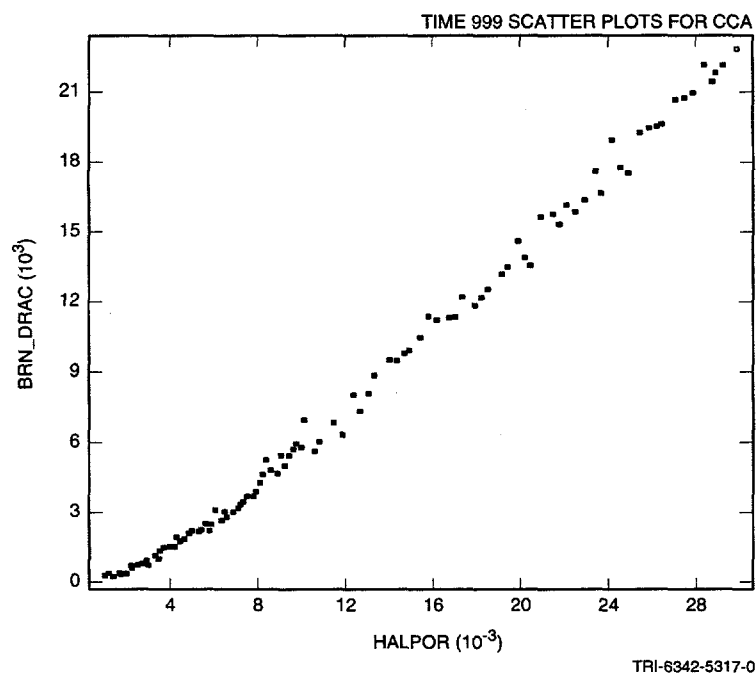
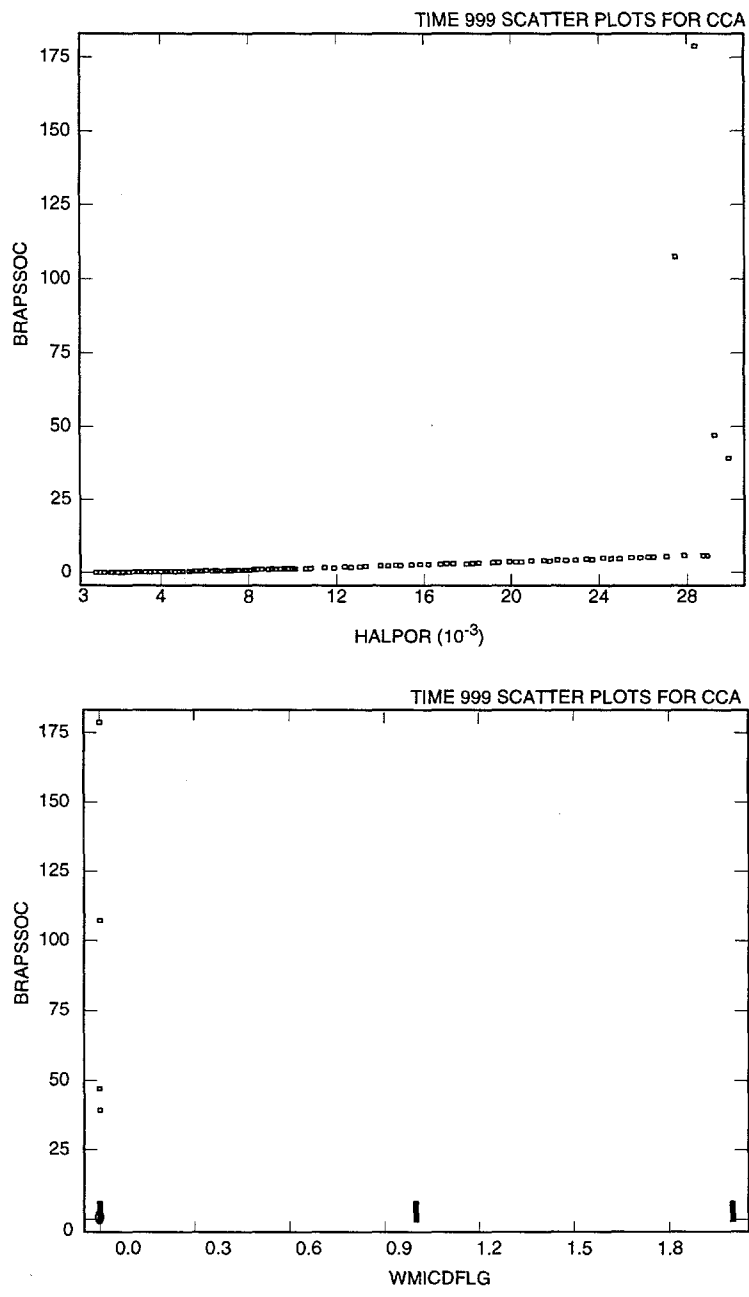
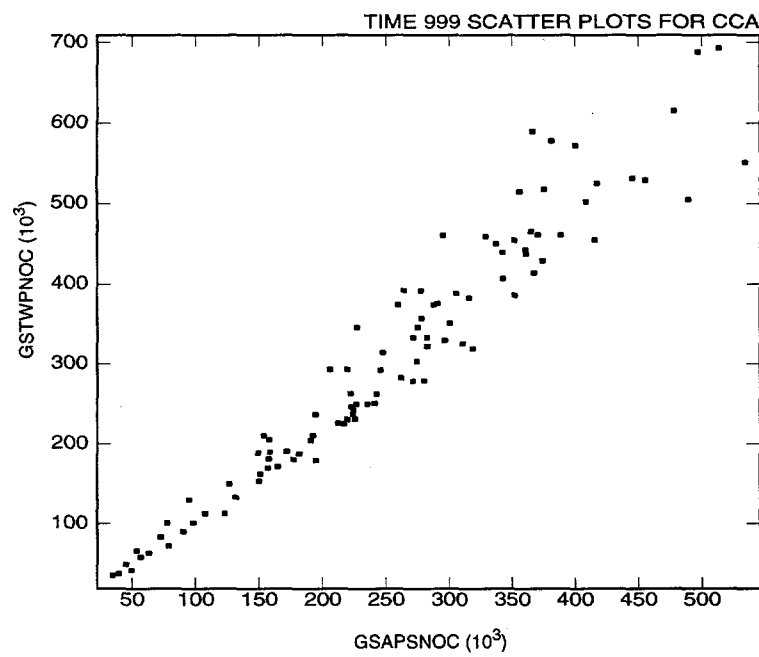


FIGURE 4.2.1. SCATTERPLOTS TAKEN AT 999 YEARS, for cumulative vertical brine drainage (m^3) from the UDRZ downward through the ceiling of the upper waste panels, BRN_DRAC, with respect to halite porosity, HALPOR. This plot illustrates the direct relationship between brine drainage downward through the UDRZ to the upper waste panel and halite porosity. Realizations with relatively large values for HALPOR will have a greater DRZ volume from which brine drains



TRI-6342-5318-0

FIGURE 4.2.2. SCATTERPLOTS TAKEN AT 999 YEARS for south-flowing brine in the UDRZ passing above the closures with respect to halite porosity, HALPOR, and microbial degradation, WMICDFLG. The above two plots show south-flowing brine in the UDRZ, BRAPSSOC, while minimal at 999 years, is enhanced for realizations approaching maximum halite porosity values (HALPOR) and those with no microbial degradation (WMICDFLG) = 0



TRI-6342-5319-0

FIGURES 4.2.3. SCATTERPLOTS, TAKEN AT 999 YEARS, for gas flow out the ceiling of the north half of the lower waste panel, GSTWPNOc, with respect to north-flowing gas in the UDRZ passing above the panel closures, GSAPSNOC. The above scatterplot shows that as gas flows out the north half of the lower waste panel ceiling, its flow path is deflected northward in the UDRZ, passing above the panel closures. This plot implies that a significant volume of gas that exits the ceiling of the north side of the lower waste panel (and to a lesser extent the south side, not shown) flows up-dip through UDRZ toward the north regions of the repository

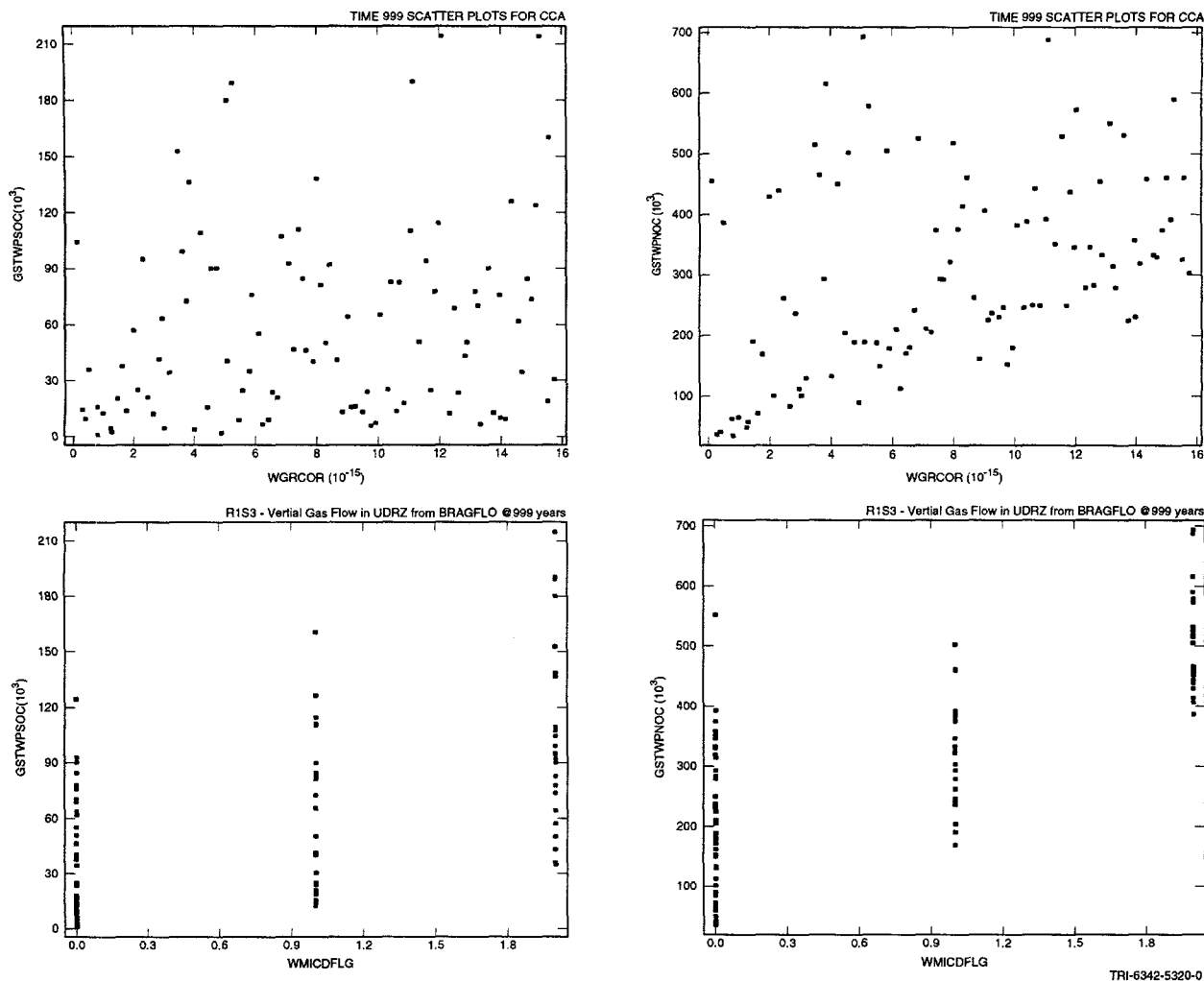
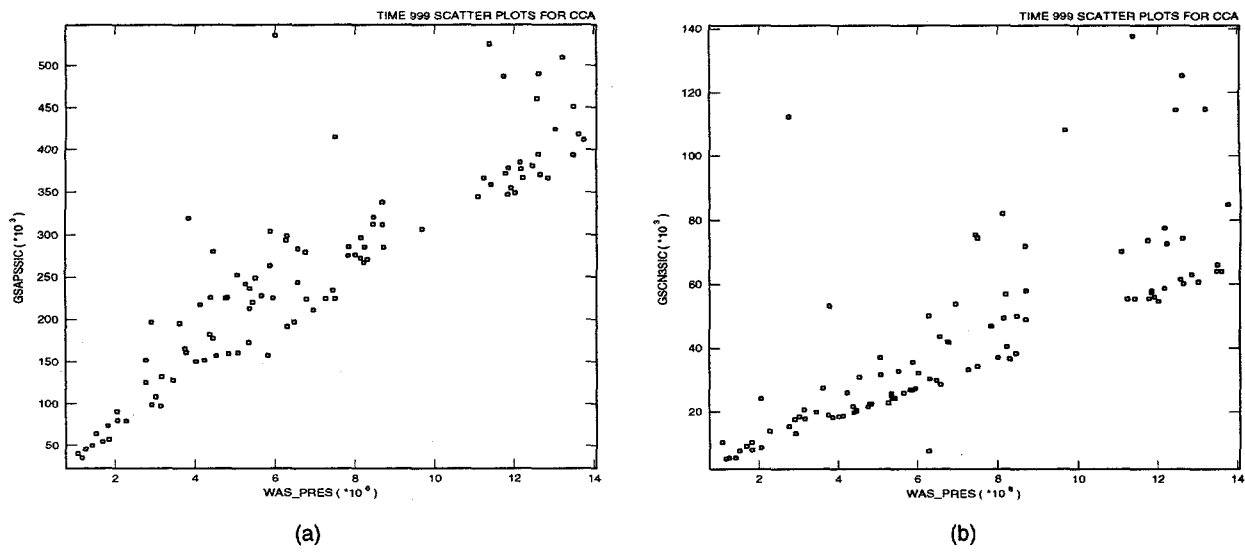
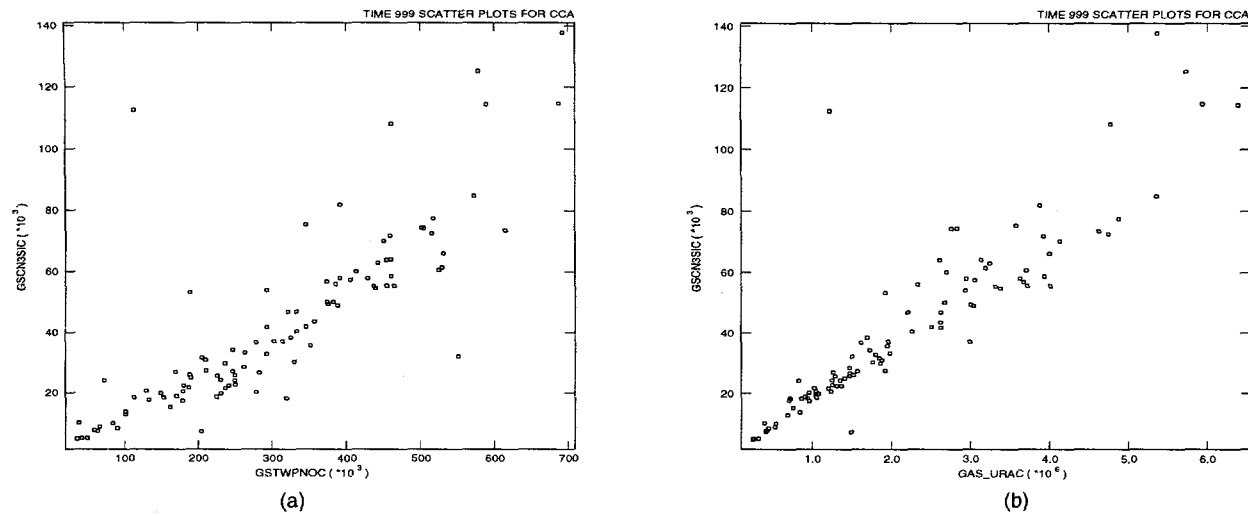


FIGURE 4.2.4. SCATTERPLOTS, TAKEN AT 999 YEARS, for gas flow (m^3) out the north and south ceilings (GSTWPSOC and GSTWPNC, respectively) of the lower waste panel with respect to gas generation processes, i.e., iron corrosion, WRGCOR, and microbial degradation, WMICDFLG. These scatterplots illustrate the differences between gas flow out the upper and lower halves of the lower waste panel ceiling (GSTWPSOC and GSTWPNC, respectively) and show which gas generation processes most impact gas flow through the ceiling. Note that gas flow is greater for GSTWPNC compared to GSTWPSOC and a stronger correlation strength exists between GSTWPNC and microbial degradation (when WMICDFLG > 0) and iron corrosion (WRGCOR) as compared to GSTWPSOC. More gas flows out the upper half of the waste panel ceiling, GSTWPNC, because gas migrates diagonally up-dip from the south to the north, with a preferred path through the less brine-saturated north half. All gas flowing diagonally is deflected upward at the panel closure to the UDRZ. Hence, gas flow out the north ceiling of the lower waste panel represents gas generation processes in effect for both halves of the lower waste panel. This translates into a stronger relationship between WRGCOR and WMICDFLG for gas flow out the north ceiling compared to the south



TRI-6342-5368-0

FIGURES 4.2.5. SCATTERPLOTS, TAKEN AT 999 YEARS, showing the relationship between north-flowing gas (m^3) in the UDRZ passing above the panel closures, GSAPSSIC, and gas passing from the UDRZ through the south side of the concrete shaft, GSCN3SIC, with the lower waste panel pressures (Pa). The above two plots illustrate the relationship between repository pressure and north-flowing gas. Realizations with higher pressures tend to have more gas that flows northward in the UDRZ. This north-flowing gas in the UDRZ passes above the panel closures and through the south side of the concrete shaft



TRI-6342-5367-0

FIGURES 4.2.6. SCATTERPLOTS, TAKEN AT 999 YEARS, showing the relationship between gas flow (m^3) from the UDRZ through the south side of the concrete shaft, GSCN3SIC, with respect to flow into the UDRZ from the ceiling of the north half of the lower waste panel, GSTWPNC, and from the ceiling of the upper lower waste panels, GAS_URAC. This north flowing gas in the UDRZ passes above the panel closures and through the south side of the concrete shaft. Gas flow into the south side of the concrete shaft (GSCN3SIC) coincides with gas flow out the ceiling of the north half of the lower waste panel, (GSTWPNC) and the ceiling of the upper waste panel (GAS_URAC). The two plots imply a large portion of gas that flows out the ceiling of the waste disposal areas is deflected northward and passes or pushes resident UDRZ gas through the concrete shaft

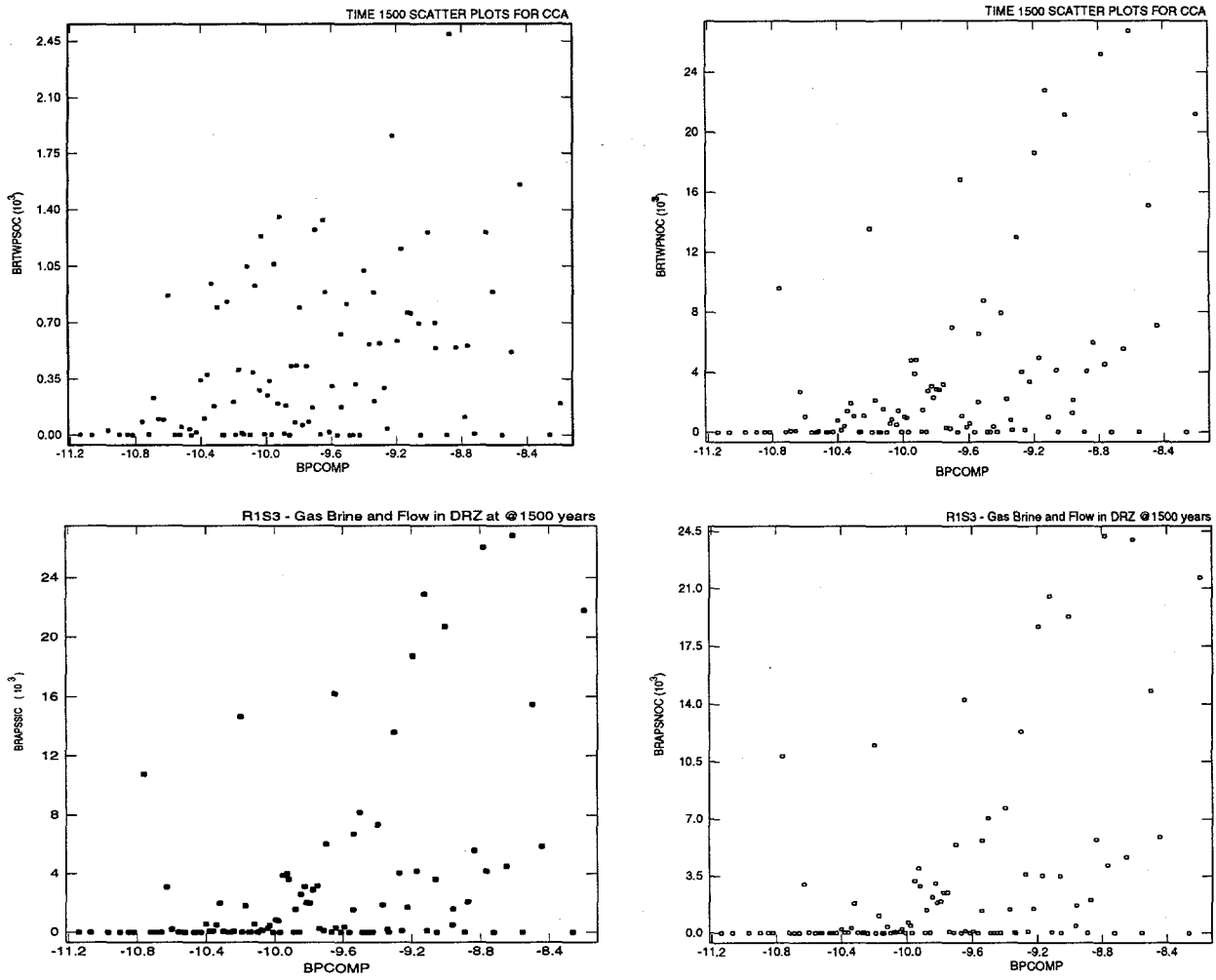
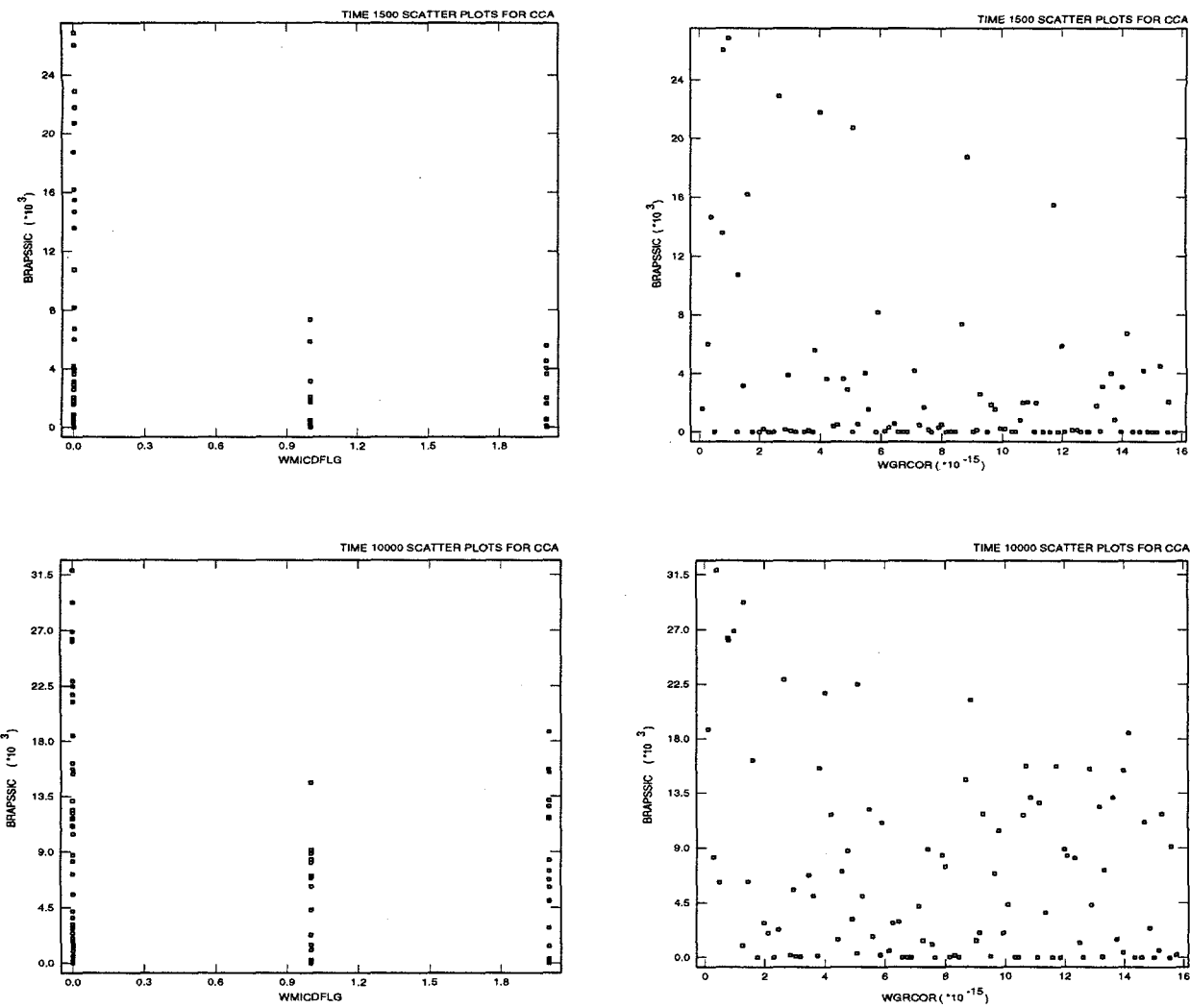


FIGURE 4.2.7. SCATTERPLOTS, TAKEN AT 1500 YEARS, showing the relationship between brine flow (m^3) out the north and south halves of the lower waste panel into the UDRZ (BRTPWSOC and BRTWPNC, respectively), and north flowing brine passing above the panel closures (BRAPSSIC and BRAPSNC) with respect to brine reservoir compressibility, BPCOMP. The above scatterplots show that realizations assigned higher reservoir compressibilities will have more brine that is partitioned into and flows northward in the UDRZ. More brine flows through the north ceiling of the lower waste panel than through the south half. This is because the area above the north ceiling is filled with a more compressible fluid, i.e., gas. Therefore, the pressure wave of the intrusion event can compress more resident fluid above the north half of the lower waste panel compared to the south. Greater compression here allows more brine to enter through the north ceiling. Comparing BRAPSSIC and BRAPSNC, more brine flows out the area north of the panel closures than enters from the south side. This is because the panel closures serve as a source of brine, which flows out the top of the closures into the UDRZ at the time of intrusion. Those realizations with optimal gas generation from microbial degradation, WMICDFLG > 0, and iron corrosion, WGRCOR, will have larger gas volumes generated within the waste disposal areas. These relatively larger quantities of gas will flow up into the UDRZ and approach maximal compressibilities, gas pressures and saturations, rendering the UDRZ less brine-permeable and requiring higher gradients for brine to flow through the UDRZ.



TRI-6342-5322-0

FIGURE 4.2.8. SCATTERPLOTS, TAKEN AT 1500 YEARS and 10,000 years, showing the relationship between north-flowing brine (m^3) in UDRZ above the panel closures with respect to parameters controlling gas generation from microbial degradation (WMICDFLG) and iron corrosion (WRGCOR). Those realizations with low gas production (no microbial degradation; WMICDFLG = 0) and low iron corrosion rates will have more north-flowing brine at 1500 years and 10,000 years

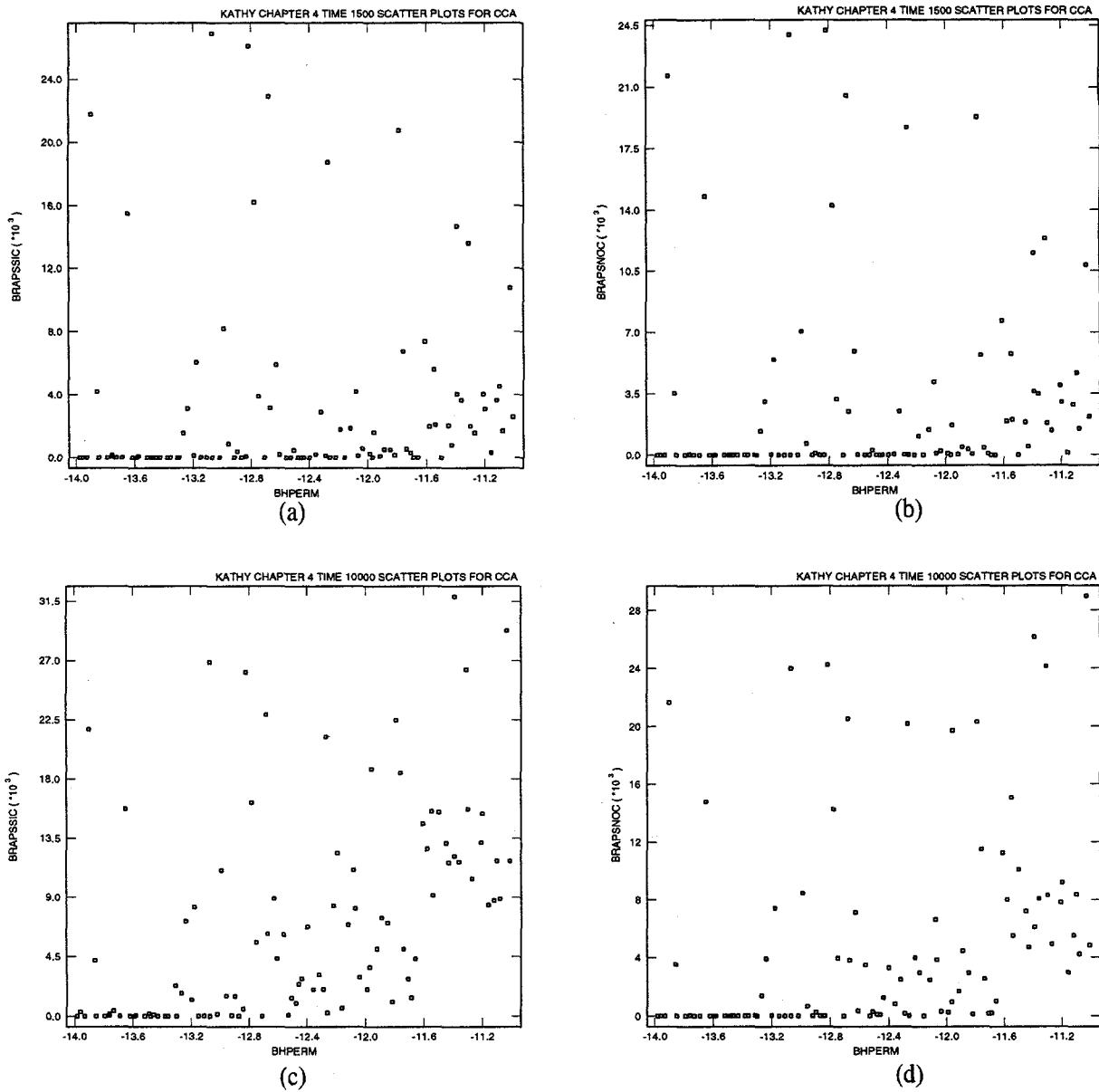


FIGURE 4.2.9. SCATTERPLOTS, TAKEN AT 1500 (a and b) and 10,000 (b and c) years, showing the relationship between north-flowing brine (m^3) in the UDRZ passing above the panel closures with respect to borehole permeabilities, BHPRM, and brine flow from the UDRZ down through panel closures (BRNDTPSC). Realizations with higher borehole permeabilities tend to have more north-flowing brine than those assigned lower values. Comparing the difference between brine volume in BRAPSSIC and BRAPSNO at 1500 and 10,000 years (b) illustrates the role the panel closures themselves play as a brine source or sink within the UDRZ. At the time of intrusion brine is introduced into the UDRZ through the ceiling of the lower waste panels and top of the panel closures (discussed in Section 5), then is deflected up-dip through the UDRZ. Consequently more brine flows out the north face, BRAPSNO, than enters from the south, BRAPSSIC. The difference is the amount that flows out the top of the closures

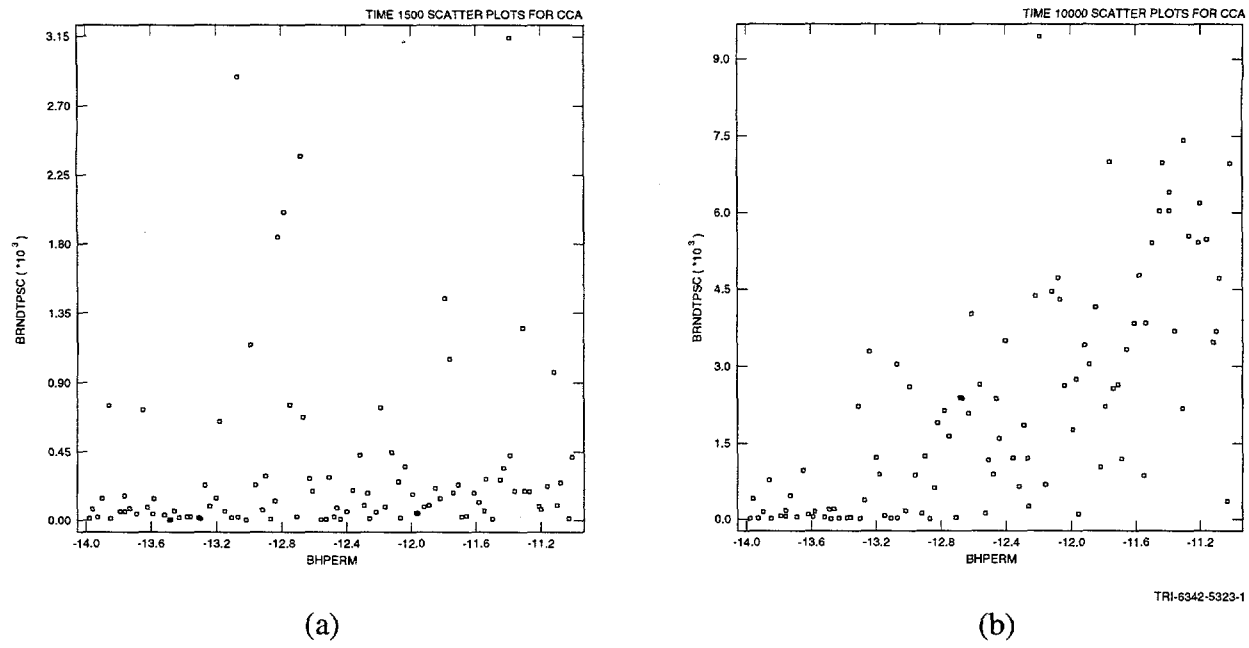
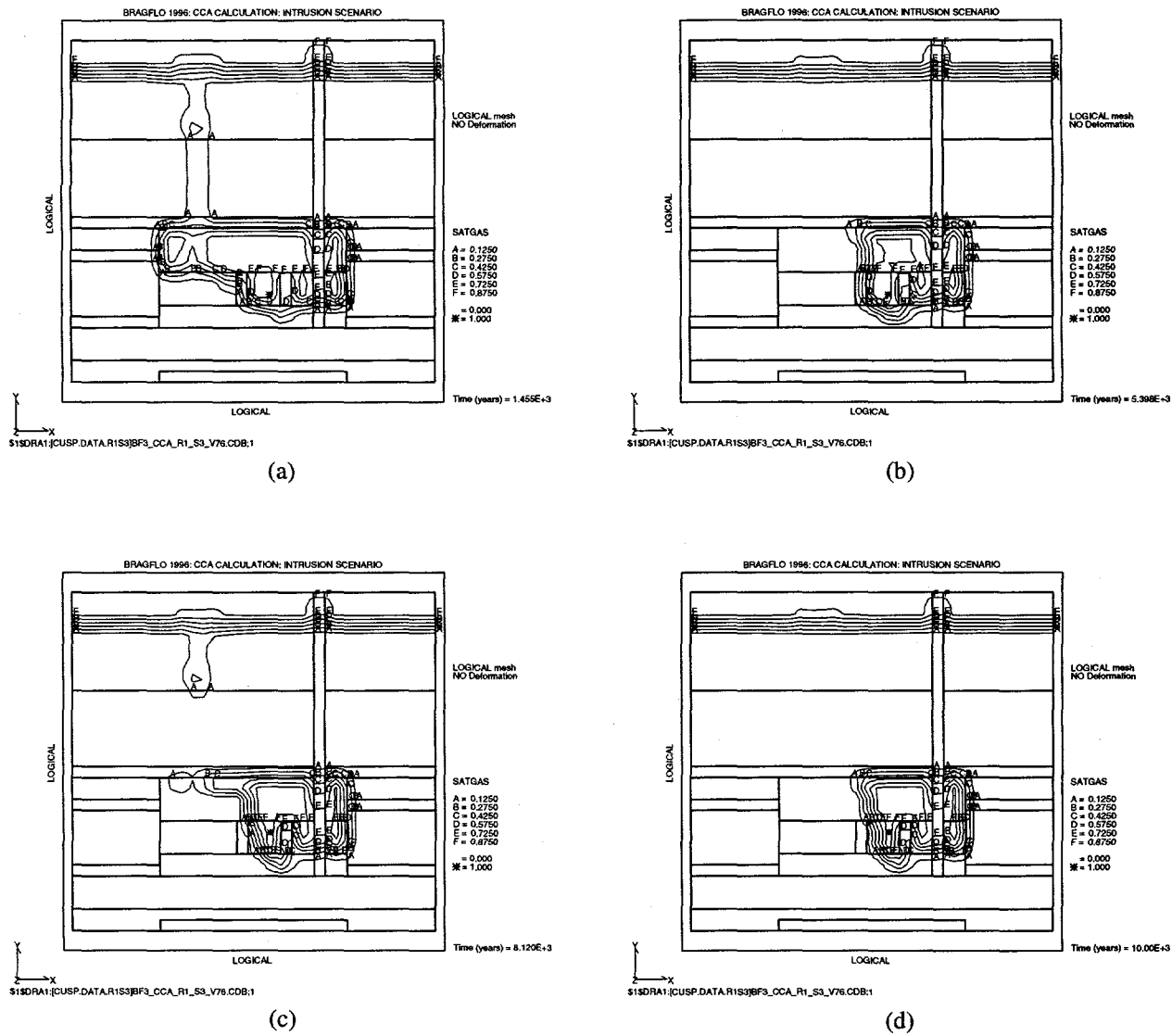
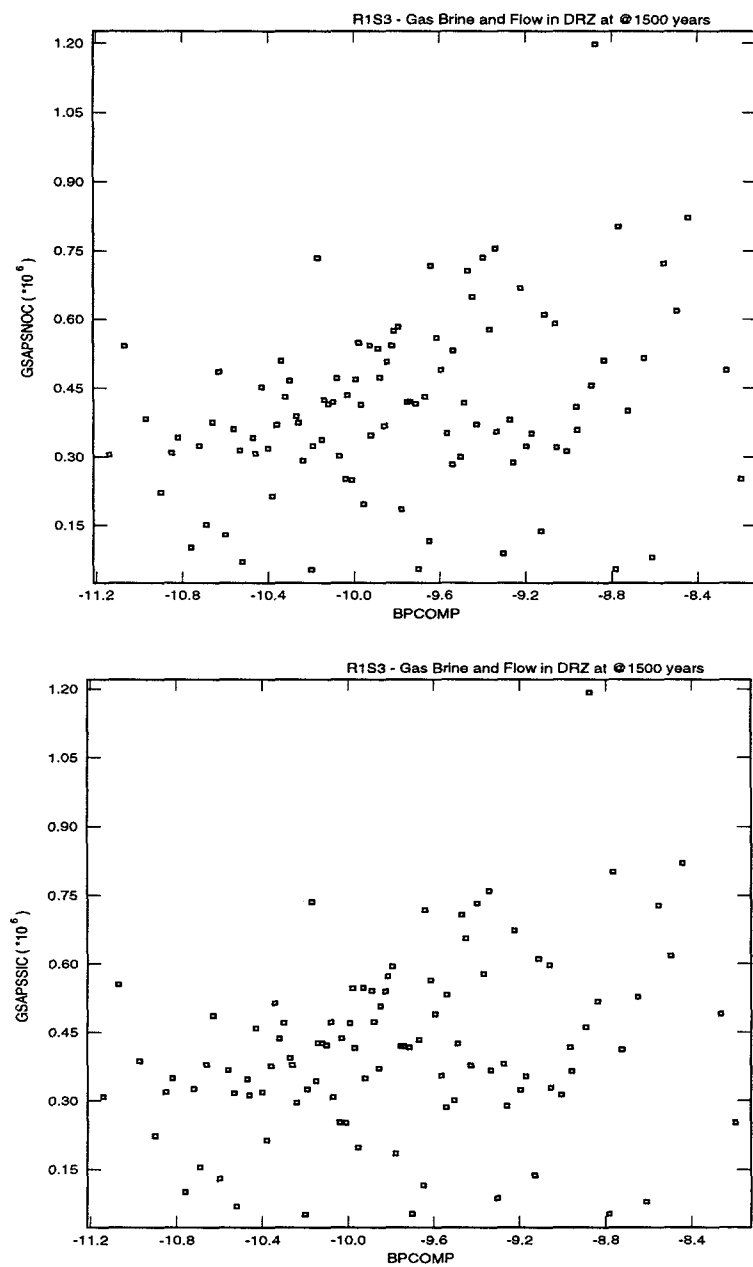


FIGURE 4.2.10. SCATTERPLOTS TAKEN AT 1500 and 10,000 years (a and b) showing the relationship between brine (m^3) flow down through the top of the panel closures (BRNDTPSC) with respect to borehole permeability (BHPRM). Soon after the borehole plugs degrade, the role of the panel closures switches from source to sink. Brine moves up-dip in the UDRZ as it is introduced into the UDRZ via the borehole or as brine 'overflow' from the lower waste panel ceiling. Brine is deflected downward at the brine/gas interface resident in the UDRZ within the vicinity above the panel closures. Some brine flows downward through the top of the panel closures, and the remainder moves up-dip and is deflected downward through the upper waste panels ceilings. Note the increase in correlation between UDRZ north-flowing brine and brine flow down the top of the panel closures with BHPRM between 1500 and 10,000 years. This increase is because of the increasing importance that the borehole plays in facilitating gas out of the repository, and more specifically at the UDRZ, which allows brine flow to enter



TRI-6342-4886-0

FIGURE 4.2.11. GAS SATURATION CONTOUR PLOTS taken at (a) ~1400, (b) 5400, (c) 8100, and (d) 10,000 years for realization 76 (R1S3). The four gas saturation plots show the changing position of the 'gas lens' (i.e., brine/gas saturation interface) that deflects incoming brine flow in the UDRZ downward through the panel closures or through the southern portion of the upper waste panel ceiling. Note the gas bubble that forms by 8100 years in the south side of the UDRZ is not seen at 10,000 years. (Figure 4.1.1 identifies the borehole, the shaft seal, and other features of the modeled area.)



TRI-6342-5355-0

FIGURES 4.2.12. SCATTERPLOTS, TAKEN AT 1500 YEARS, showing the relationship between north flowing gas (m^3) in the UDRZ passing above the panel closures with respect to brine reservoir compressibilities (BPCOMP). The above scatterplots show realizations with high reservoir compressibility will have more gas displaced northward in the UDRZ above the panel closures. (Note: GSAPSSIC is equivalent to GSAPSNO, indicating the panel closure contributes minimal to no gas to the UDRZ)

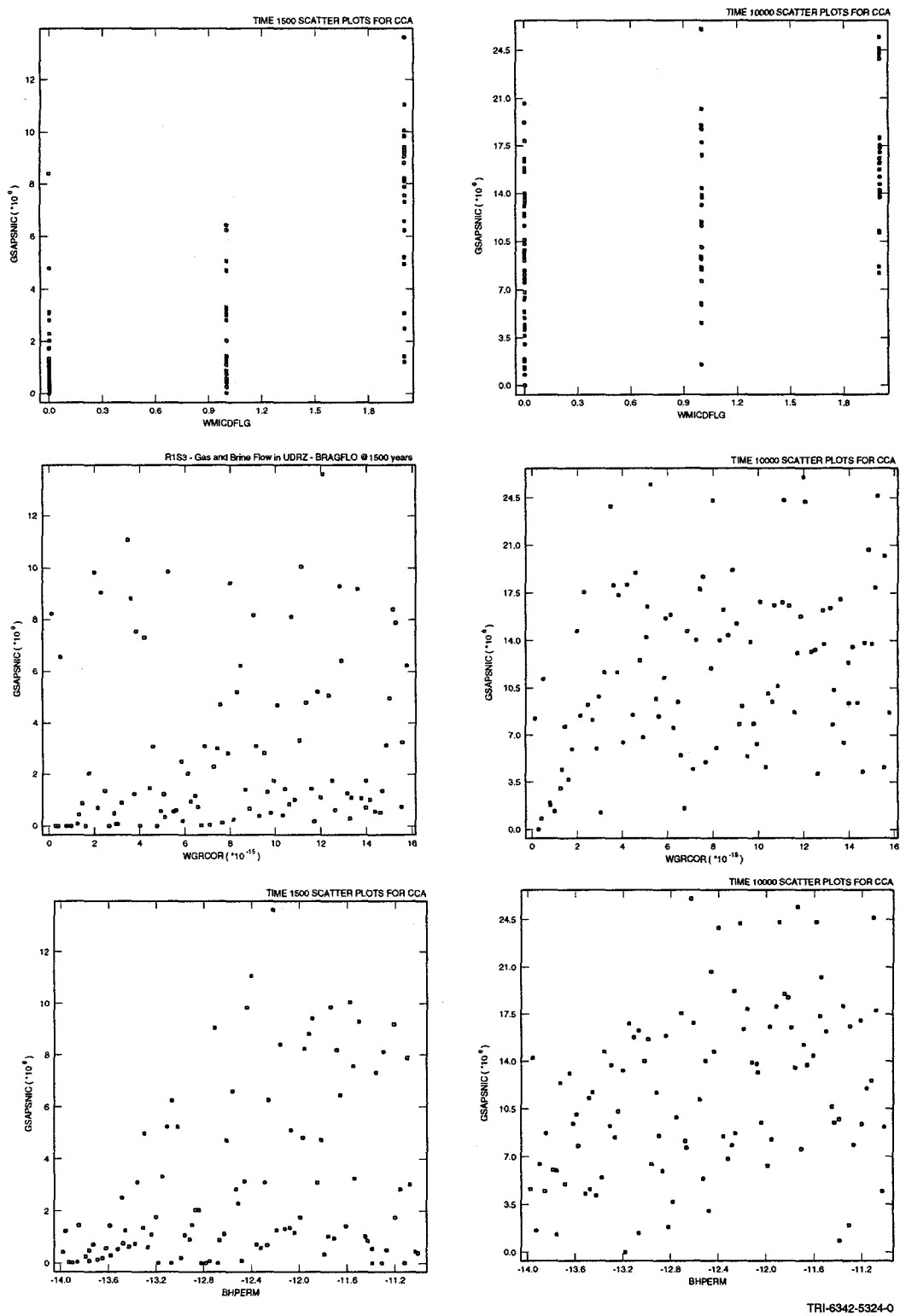
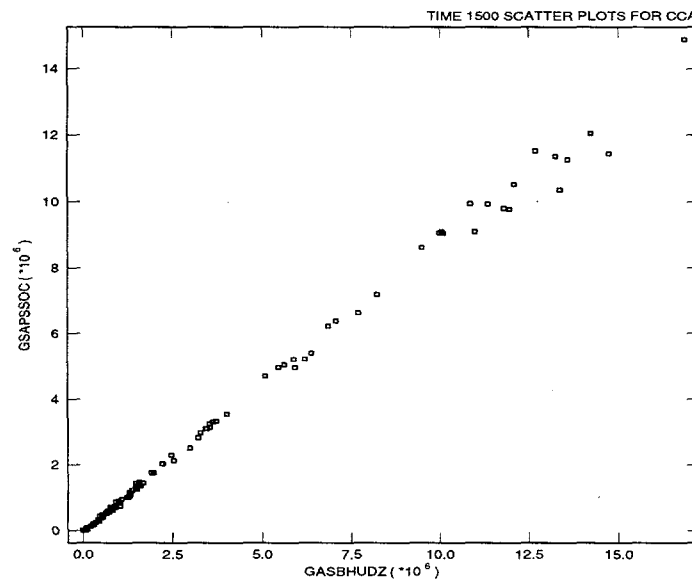
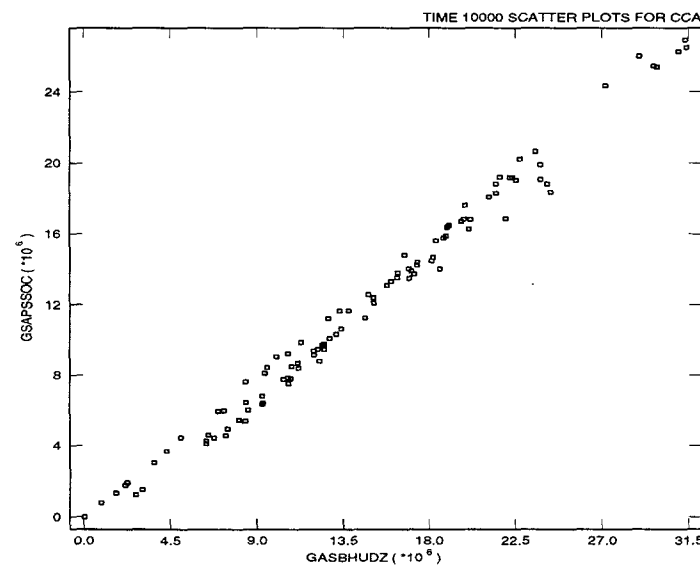


FIGURE 4.2.13. SOUTH-FLOWING GAS (m^3) IN the UDRZ (shown only as GSAPSNIC) at 1500 (left) and 10,000 (right) with respect to microbial degradation flag ($WMICDFLG > 0$), iron corrosion rates $WGRCOR$, and borehole permeability $BHPRM$. Higher gas volumes flow southward for those realizations with high borehole permeabilities, $BHPRM$. Note the increase in correlation for south-flowing gas and $BHPRM$ between 1500 and 10,000 years and the decrease in correlation with $WMICDFLG$



(a)



TRI-6342-5325-0

(b)

FIGURE 4.2.14. SOUTH-FLOWING GAS (m^3) IN the UDRZ taken at (a) 1500 and (b) 10,000 years. The two plots show the majority of gas that flows out the repository via the borehole/UDRZ interface at the top of the UDRZ (GASBHUDZ) at 1500 and 10,000 years has also passed through the UDRZ above the panel closures (GSAPSSOC). The plots illustrate the UDRZ is a significant pathway for gas evacuation out the entire repository via the borehole

4.2.4 Overlay Plots

The flow scenarios described above are depicted in the following overlay plots (Figures 4.2.15 and 4.2.16). These figures illustrate the relationship between UDRZ brine and gas flow direction for realizations assigned relatively high and low borehole permeabilities. Flow is plotted with respect to 1) flow in the borehole, 2) pressures in the lower and upper waste panel, 3) saturation within the lower and upper waste panels, and 4) the extent of iron being corroded. The flow patterns seen for Realization 27 are representative of simulations assigned high values for borehole permeability. Realization 4 represents simulations assigned low borehole permeability values.

Section 7 presents more overlay plots depicting flow between the various regions of the excavated area, including the UDRZ, relative to borehole flow and iron corrosion.

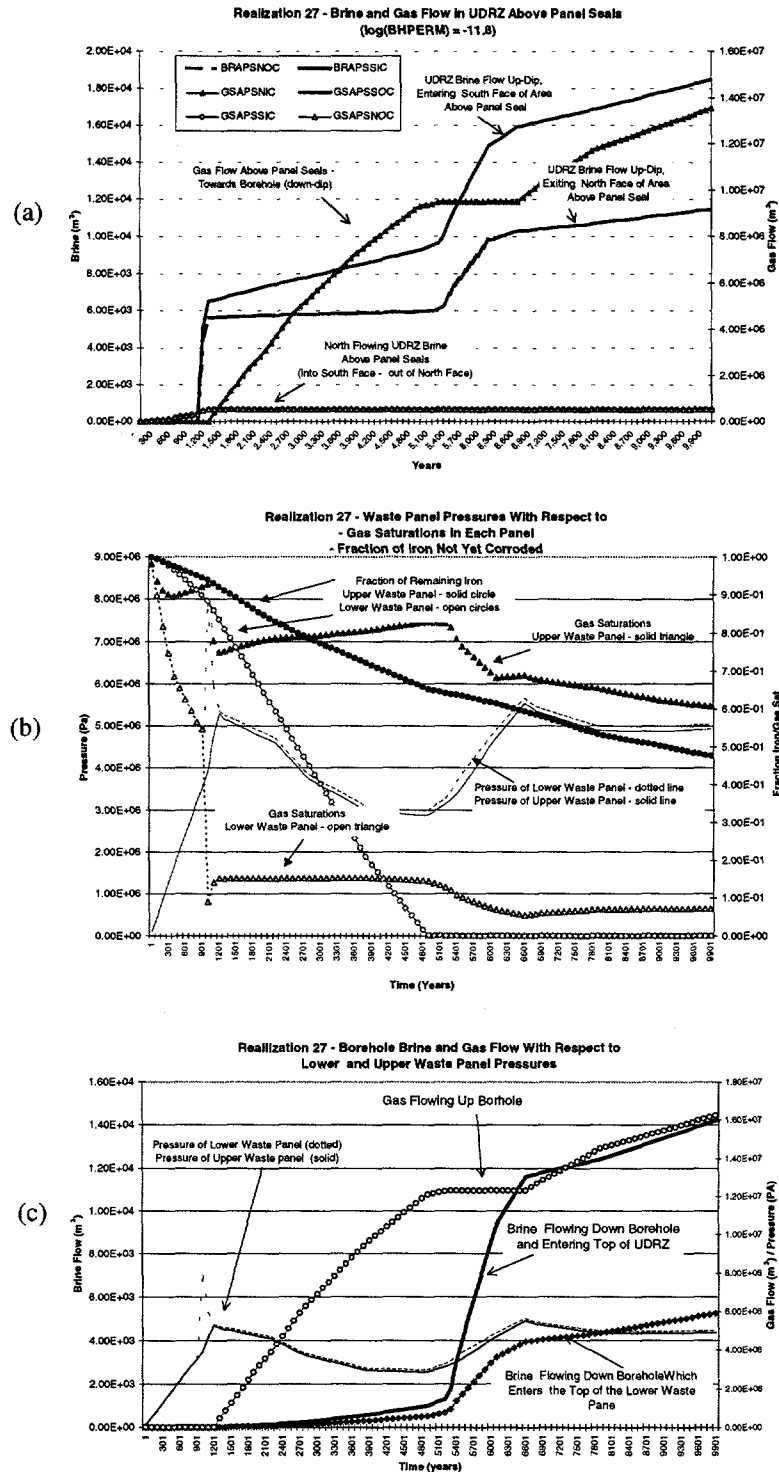


FIGURE 4.2.15. OVERLAY PLOTS FOR REALIZATION 27, representative of realizations assigned high BHPRM values. These plots illustrate changes in brine and gas flow direction (a) in the UDRZ with respect to 1) repository pressure and saturation, 2) the extent of uncorroded iron (b), and 3) borehole flow (c). Note: The switch between gas and brine flow in the UDRZ (a) coincides with the switch between gas and brine flow within the borehole (c). Brine flow down the borehole (c) coincides with iron in the lower waste panel being completely consumed

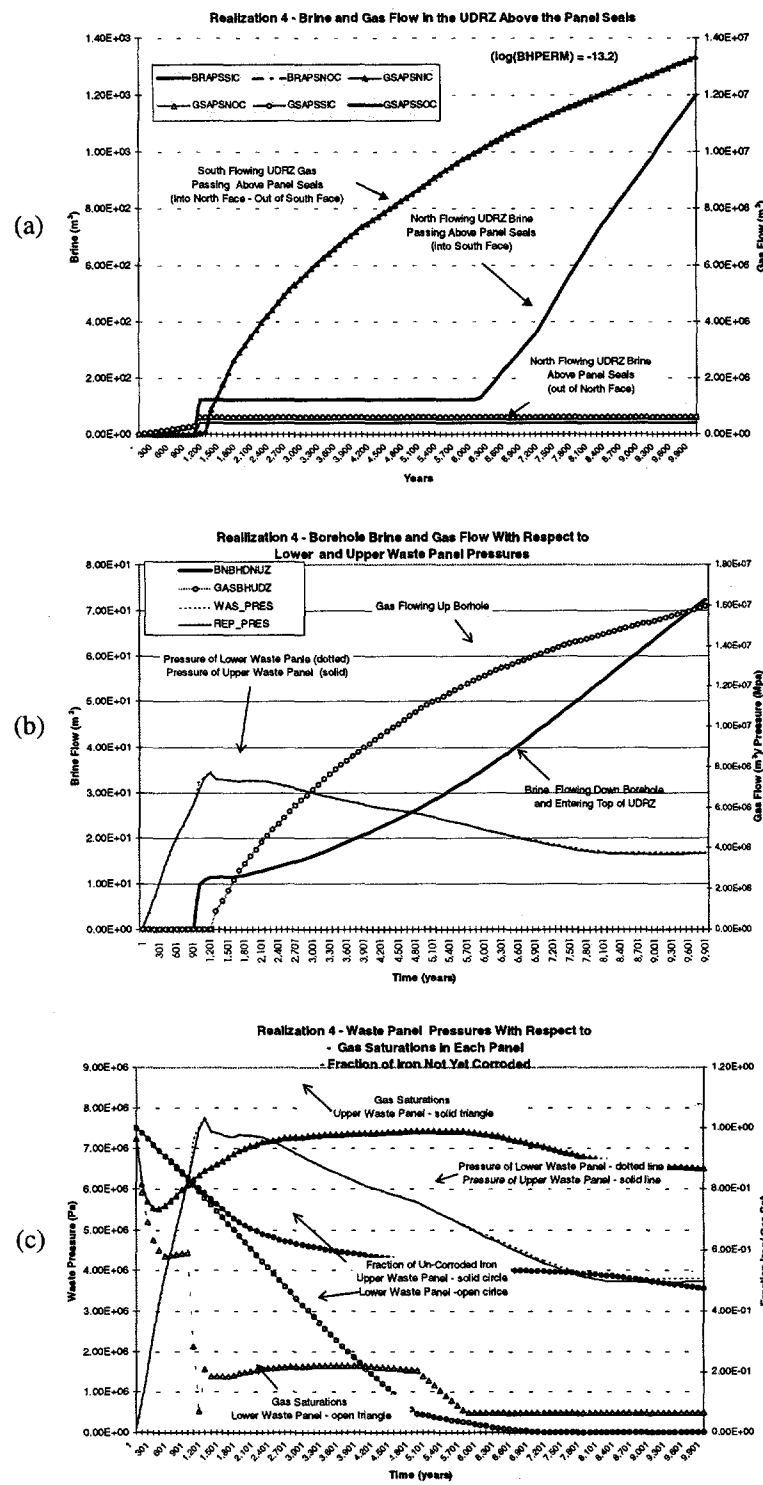


FIGURE 4.2.16. OVERLAY PLOTS FOR REALIZATION 4, representative of realizations assigned low BHPRM values. These plots illustrate changes in brine and gas flow direction in the UDRZ with respect to 1) repository pressure and saturations, 2) the extent of iron uncorroded, and 3) borehole flow. Note: The interrelationship between iron becoming depleted in the lower waste panel (c) coincides with an increase in UDRZ brine flow around 6000 years (a). Plots (a) and (b) show gas flow out the boreholes; (b) is at the same rate as lateral south-flowing gas in the UDRZ

4.3 Parameters Affecting Brine and Gas Flow in the UDRZ

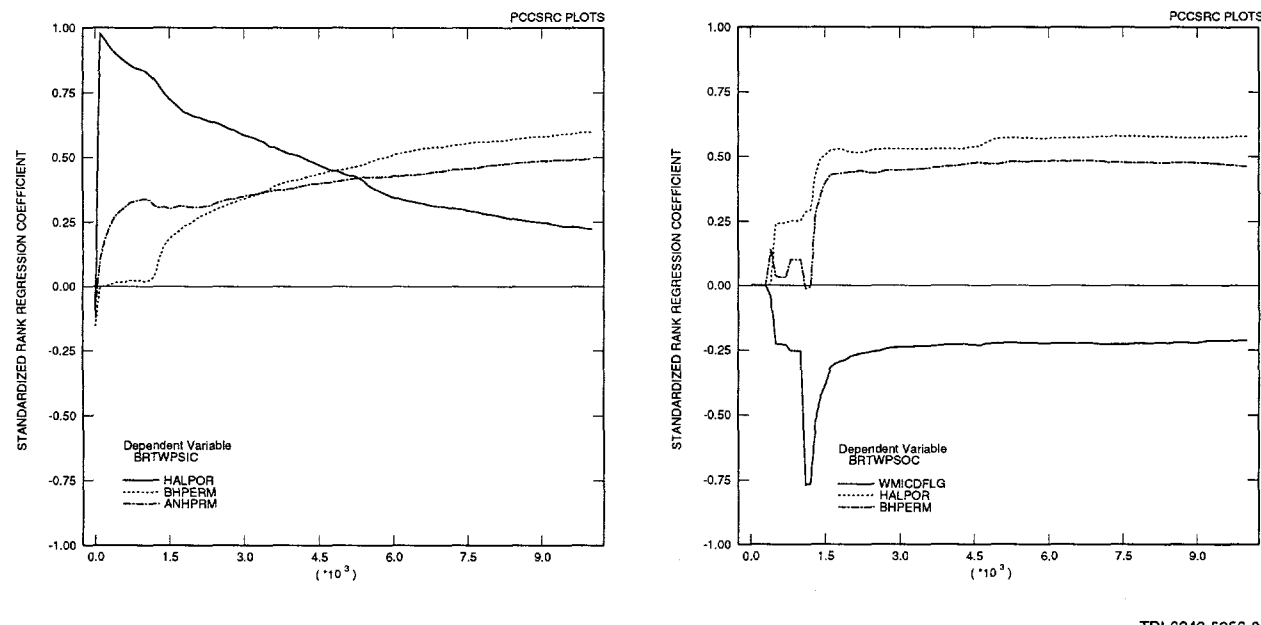
This section presents plots of SRRCs between the sampled independent variables and those dependent variables that define gas and brine flow in the UDRZ region over the 10,000-year modeled period.

4.3.1 Brine Flow

4.3.1.1 Vertical Brine Flow Into the Lower Waste Panel

Vertical Brine Flow Between the South Side of the Lower Waste Panel and UDRZ

Figure 4.3.1 illustrates the most influential parameters controlling vertical brine flow between the south portion of the lower waste panel and the UDRZ.



TRI-6342-5356-0

FIGURE 4.3.1. STANDARDIZED RANK REGRESSION COEFFICIENT (SRRC) results showing the most influential independent variables for vertical brine flow (m^3) between south portion of lower waste panel and UDRZ

Downward Flow (BRTWPSIC). Prior to intrusion, SRRC analysis shows that vertical brine flow from the UDRZ into the south half of the lower waste panel, BRTWPSIC, is most influenced by HALPOR. After intrusion, a strong correlation appears between BRTWPSIC and the LHS parameters ANHPRM and BHPRM. The correlation strength between BRTWPSIC and these independent variables gradually increases through the end of the modeled period. HALPOR is

the most influential variable affecting BRTWPSIC because it determines the amount of fluid-filled UDRZ volumes that drain brine downward into the waste disposal area.

Once repository pressures are lowered and gas has been evacuated out the south side of the UDRZ, brine will tend to flow out the marker beds. The ease of drainage out of the marker bed is directly a function of ANHPRM. Because the south half of the upper waste panel abuts the south face of Anhydrite AB, drainage from this marker bed will flow directly through the south half of the lower waste panel ceiling, hence the strong correlation with ANHPRM.

The correlation strength increases for BHPRM because this parameter affects changes in repository pressure *and* facilitates the ease with which gas is evacuated out of the UDRZ, allowing brine to enter. These ‘dynamic processes’ promote brine drainage from the south lying anhydrites *and*, eventually, brine flow down the borehole, some entering through the south waste panel ceiling.

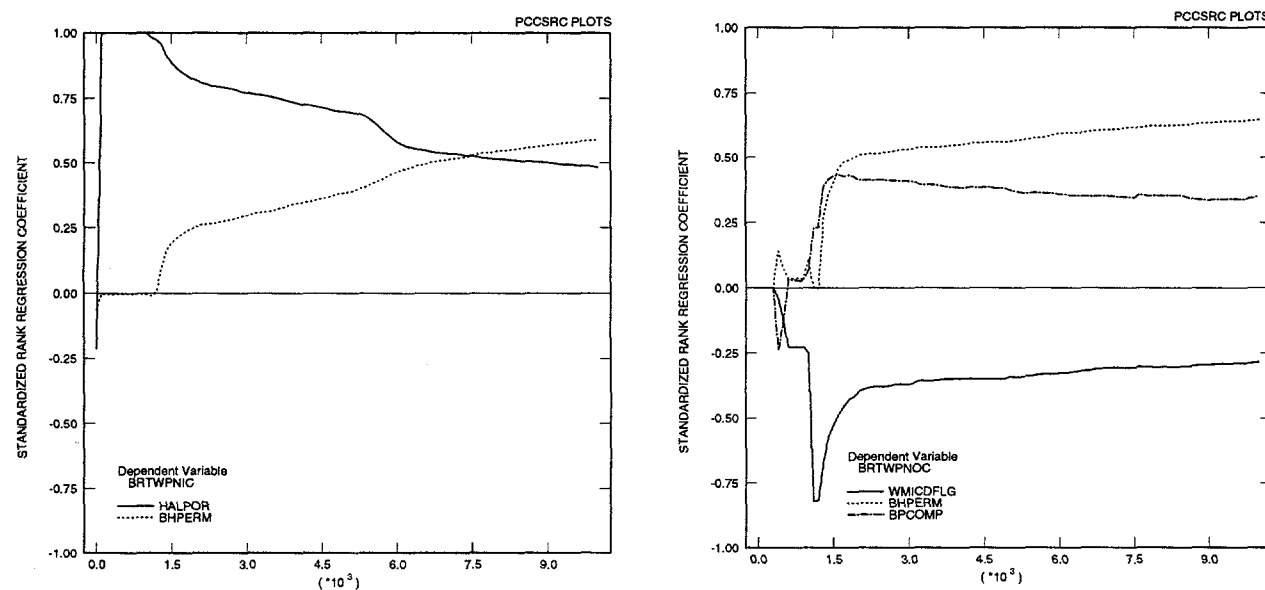
Upward Flow (BRTWPSOC). Brine flow out the south half of the lower waste panel ceiling to the UDRZ occurs briefly between the time of intrusion and again during the time of borehole degradation (see hairplots in Figure 4.1.1 and the boxplots in Figure 4.1.14). This pulse of *upward* flowing brine is inversely correlated with microbial degradation, WMICDFLG > 0, coincident with the time of borehole degradation. For those realizations where WMICDFLG is partially or fully in effect, gas saturations will be high within the disposal areas. These realizations will have relatively higher repository pressures. High gas pressures inhibit brine flow from the brine reservoir to the repository. This condition impedes the displacement of brine into the UDRZ at the time of the intrusion pressure wave.

The strong negative correlation between BRTWPSOC and WMICDFLG decreases soon after the upper borehole plug degrades, and is replaced by an increase in correlation strength for the LHS parameters BHPRM and HALPOR. The positive correlation with BHPRM and HALPOR results from these two parameters impacting the volume of incoming brine that is displaced upward during the pressure pulse of the intrusion and borehole degradation events. Large HALPOR values mean more brine has accumulated in the south regions of the repository; this brine is

displaced upward through the waste panel ceiling during the two pressure pulses. Larger BHPRM values mean the pressure gradient between the repository and/or the upper and lower units is more easily transmitted via the borehole. This pressure transmission enables more resident brine to be displaced and/or more gas to be evacuated out of the UDRZ, allowing replenishing brine to enter.

Vertical Brine Flow in Lower Waste Panel North of Borehole

Figure 4.3.2 illustrates the most influential parameters controlling vertical brine flow north of the borehole.



TRI-6342-5357-0

FIGURE 4.3.2. STANDARDIZED RANK REGRESSION COEFFICIENT (SRRC) results showing the most influential independent variables for vertical brine flow between north portion of lower waste panel and UDRZ

Downward Flow (BRTWPNC). Prior to and after intrusion, the parameters that most influence downward-flowing brine from the UDRZ to the lower waste panel residing north of the borehole (BRTWPNC) are similar to those for BRTWPSIC, except that the parameter ANHPRM is absent. Anhydrite drainage does not significantly affect flow into the north side of the lower waste panel because 1) the positioning of the north half of the lower waste panel is up-dip from the south anhydrites, and 2) the positioning of the borehole. The borehole's ongoing flow

processes and assigned material properties serve as barriers to brine crossing from the southern to the northern half of the lower waste panel.

Upward Flow. Prior to intrusion, brine partitioned upward into the UDRZ, BRTWPNC, is minimal to nonexistent. Therefore, no further discussion is provided.

After intrusion, parameters controlling BRTWPNC are similar as that for BRTPWSOC—i.e., positively correlated with BHPRM and negatively correlated with WMICDFLG. However, no correlation exists with HALPOR, and a strong correlation with BPCOMP shows up that is not seen for BRTPWSOC. The positive correlation with BPCOMP is due to this variable affecting the amount of Castile brine that is released upward through the borehole into the lower waste panel (given the appropriate pressure gradient). Incoming brine enters both halves of the lower waste panel, but because the two halves will have significantly different gas/brine saturations, their ‘compression potentials’ will be very different. Because the UDRZ above the north half of the waste panel is filled with a more compressible gas, the pressure wave of the intrusion can more easily introduce Castile brine through the north ceiling.

Vertical Brine Flow Between Top of Panel Closures and UDRZ

Figure 4.3.3 illustrates the most influential parameters controlling vertical brine flow between the top of the waste panel closures and the UDRZ (BRNDTPSC and BRNUTPSC).

Downward Flow (BRNDTPSC). Prior to intrusion, HALPOR is the most important parameter affecting downward vertical brine through the top of the panel closures from the UDRZ, for the same reasons as described previously for BRTWPSIC and BRTWPNC.

At the time of intrusion, realizations with high pressures and gas saturations in the UDRZ, a function of WMICDFLG, will have less brine displaced down through the top of the panel closures during the pressure wave of the intrusion event. Hence, the BRNDTPSC is negatively correlated with WMICDFLG for the period between the intrusion event and borehole degradation.

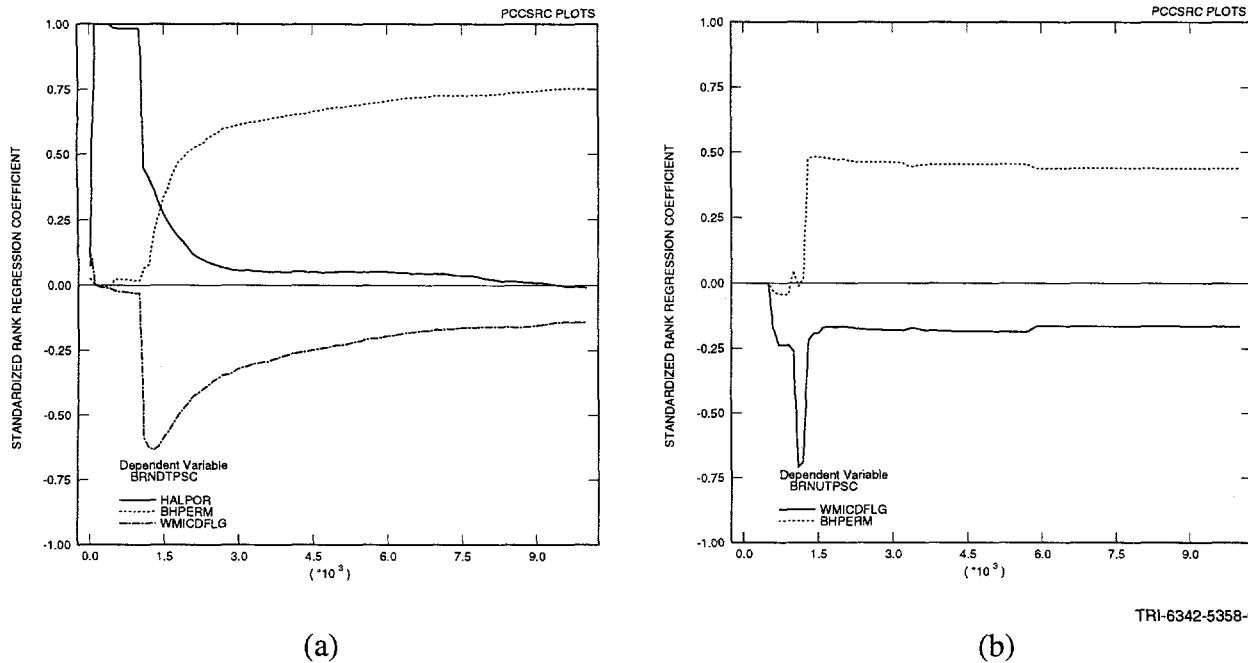


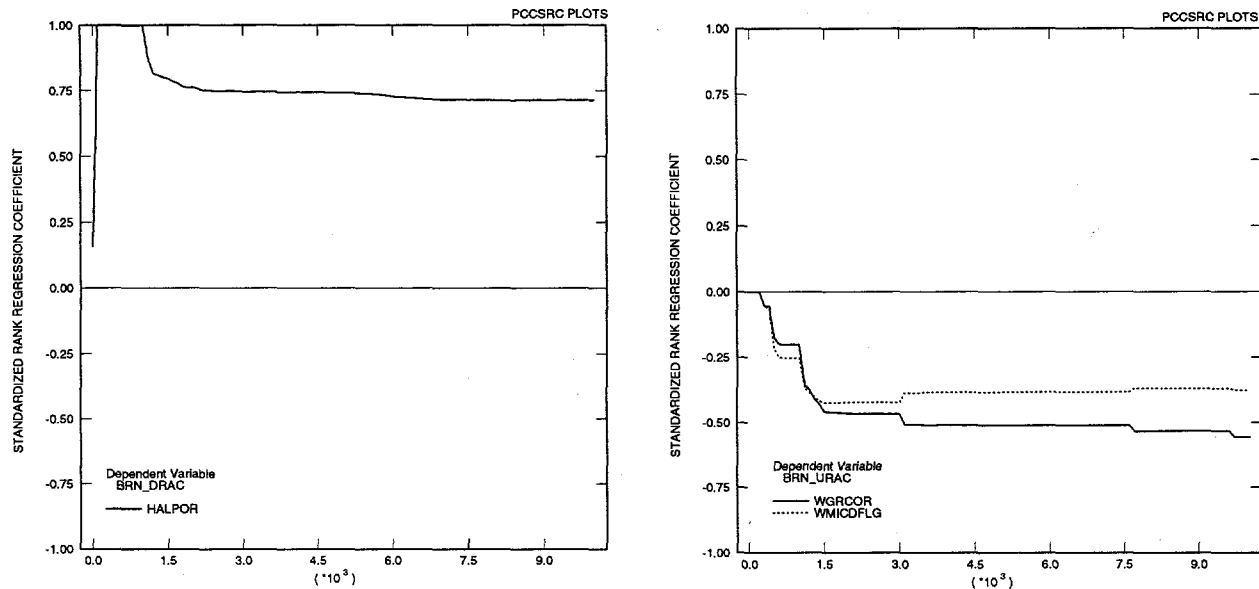
FIGURE 4.3.3. STANDARDIZED RANK REGRESSION COEFFICIENT (SRRC) results showing the most influential independent variables for vertical brine flow (a) into top of waste panel closures from UDRZ and (b) out top of waste panel closures to UDRZ

The parameter BHPRM replaces WMICDFLG as influencing BRNDTPSC soon after ~1200 years, when the upper borehole plug degrades. BHPRM gains in correlation strength from 1500 to 10,000 years because of the multiple functions that the borehole plays in depressurizing the repository, evacuating gas out the UDRZ and enabling replenishing brine to enter the UDRZ region above the panel closures.

Upward Flow (BRNUTPSC). Upward flowing brine exiting the top of the panel closures (BRNUTPSC) is negatively correlated with WMICDFLG and positively correlated with BHPRM for the same reasons that these parameters influence upward brine flow through the two halves of the lower waste panel—i.e., the high gas pressures created by microbial degradation create more resistance for brine moving into the UDRZ during the pressure wave of the intrusion event.

Vertical Brine Flow into the Ceiling of the Upper Waste Panel

Figure 4.3.4 illustrates the most influential parameters controlling vertical brine through the ceiling of the upper waste panel.



TRI-6342-5359-0

FIGURE 4.3.4. STANDARDIZED RANK REGRESSION COEFFICIENT (SRRC) results showing the most influential independent variables for vertical brine flow between upper waste panel and UDRZ

Downward Flow (BRN_DRAC). Downward-flowing brine into the ceiling of the upper waste panel (BRN_DRAC) before and after intrusion is primarily a function of HALPOR. HALPOR is important for several reasons:

- The volume of brine that drains into the ceiling of the fluid-filled upper waste panel is a function of DRZ pore volumes, and HALPOR is the primary variable that determines UDRZ pore volumes.
- Large UDRZ pore volumes affect the ease with which gas can be evacuated out of the UDRZ, allowing replenishing brine to enter this area.

Upward Flow. Brine flow upward, through the ceiling of the upper waste panel (BRN.URAC), before and after intrusion, occurs for only a few simulations (see boxplots in Figure 4.1.14) and

ceases for all but three simulations soon after the closure of the lower borehole plug at 2200 years (see Figure 4.1.8). An inverse correlation exists between BRN.URAC and the parameters WMICDFLG and WGRCOR. Simulations that do have an upward flow of brine have minimum gas generation from either microbial degradation (WMICDFLG = 0, or 1) or iron corrosion (WGRCOR). Consequently, the UDRZ and upper waste panels will have higher brine saturations and lower repository pressures. The two conditions favor brine to up-well from the south side of the upper waste panel to the UDRZ.

* **4.3.1.2 Lateral Brine Flow In the UDRZ Crossing the Area Above the Panel Closures**

South-Flowing Brine

Figure 4.3.5 illustrates the most influential parameters controlling the lateral south-flowing brine within the UDRZ that passes above the panel closures (BRAPSNIC and BRAPSSOC).

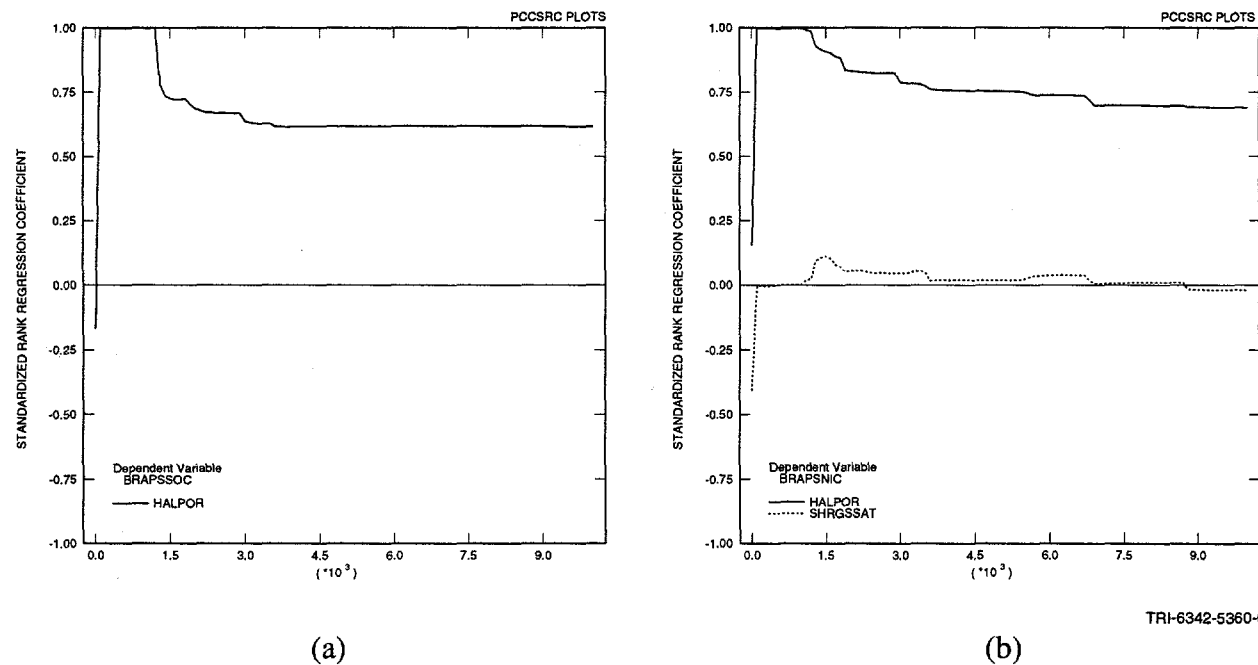


FIGURE 4.3.5. STANDARDIZED RANK REGRESSION COEFFICIENT (SRRC) results showing the most influential independent variables for lateral south-flowing brine in UDRZ (a) south and (b) north of panel closures

Prior to intrusion, south-flowing brine in the UDRZ is minimal (less than $\sim 100 \text{ m}^3$) and occurs for only a few simulations (see boxplots in Figure 4.1.16). After intrusion, the number of simulations with south-flowing brine remains about the same as that prior to intrusion. A strong

correlation exists between south-flowing brine and HALPOR before and after intrusion, for the same reasons given for BRN_DRAC.

North-Flowing Brine Above Panel Closures (BRAPSSIC and BRAPSNOC)

Figure 4.3.6 illustrates the most influential parameters controlling lateral north-flowing brine above the panel closures (BRAPSSIC and BRAPSNOC) within the UDRZ.

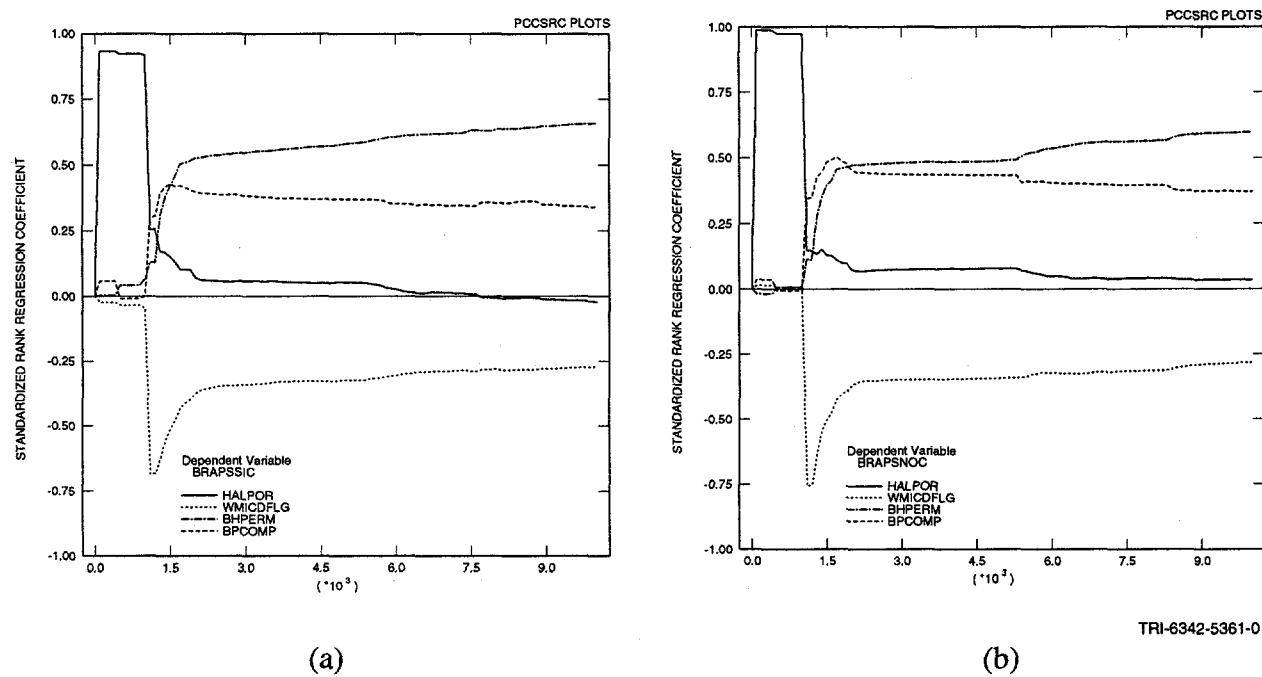


FIGURE 4.3.6. STANDARDIZED RANK REGRESSION COEFFICIENT (SRRC) results showing the most influential independent variables for vertical brine flow (m^3) between south portion of lower waste panel and UDRZ

Prior to intrusion, northward (up-dip) brine flow does not occur in the UDRZ. Thus, the correlation strength between north-flowing brine and HALPOR is due to numerical noise and is disregarded.

After intrusion, brine flow northward above the panel is initiated (see Figure 4.1.1). The uncertainty for brine flow northward is inversely correlated with WMICDFLG between 1000 and 1200 years. After 1200 years, north-flowing brine is positively correlated with the BPCOMP and BHPRM after the upper borehole plug degrades.

Those realizations with biodegradation of cellulose and/or rubber and plastics ($WMICDFLG > 0$, 50% of the sampled set) have relatively higher gas saturations and pressures in the UDRZ. High gas saturations reduce effective brine permeabilities. These two conditions impede incoming brine from flowing up-dip above the panel closures once in the UDRZ. The strong inverse correlation with $WMICDFLG$ dramatically declines once the upper borehole plug degrades, enabling gas to be evacuated out the repository via the borehole and reducing UDRZ gas saturations and pressures.

Greater $BPCOMP$ values enhance the likelihood that brine fills up the lower waste panel, or is displaced up into the UDRZ. During the pressure wave of the intrusion event, some brine flows up-dip once in the UDRZ. When the upper borehole plug degrades, a second pressure wave occurs within the repository, promoting additional brine displacement into the UDRZ, some sourced from the Castile reservoir. Consequently, a brief increase in $BPCOMP$ correlation strength is seen for up-dip brine flow between 1200 and 1500 years. Concurrently, $BHPRM$ rapidly increases in correlation strength.

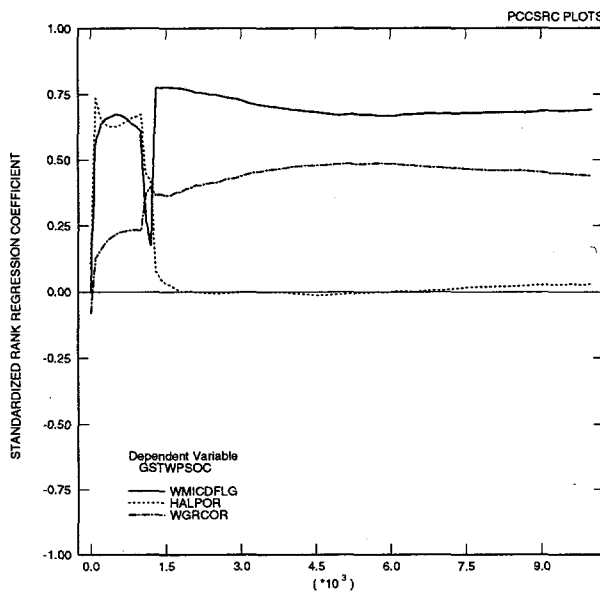
$BHPRM$ becomes the dominant parameter for north-flowing brine from 1200 years to the end of the modeled period. Realizations with high $BHPRM$ values have relatively rapid gas evacuation out of the UDRZ and excavated areas, and, in turn, reduce repository pressures. Once pressures are reduced, brine is allowed to enter the UDRZ either from anhydrite drainage or down the borehole. Some of this brine is diverted from a vertical to a lateral up-dip (northerly) flow direction in the UDRZ.

4.3.2 Gas Flow

4.3.2.1 *Vertical Gas Flow Between the Lower Waste Panel and UDRZ*

Vertical Gas Flow Between South Portion of the Lower Waste Panel and UDRZ

Figure 4.3.7 illustrates the most influential parameters controlling vertical gas flow between the south portion of the lower waste panel and the UDRZ.



TRI-6342-5362-0

FIGURE 4.3.7. STANDARDIZED RANK REGRESSION COEFFICIENT (SRRC) results showing the most influential independent variables for vertical gas flow out of south portion of lower waste panel

Downward Flow (GSTWPSIC). GSTWPSIC occurs for only a few realizations during the time of intrusion and lower borehole closure (see boxplots in Figure 4.1.16 and hairplots in Figure 4.1.3). No single variable was found to significantly affect gas flow downward from the UDRZ through the ceiling of the south lower waste panel (GSTWPSIC). Consequently, discussion will be given only for gas flow upward through the waste panel ceiling.

Upward Flow (GSTWPSOC). Prior to intrusion, gas flow out the south half of the lower waste panel ceiling (GSTWPSOC) is influenced by WMICDFLG and HALPOR. Both parameters impact gas production within the waste disposal areas. Biodegradation (WMICDFLG > 0) is the dominant gas generation independent variable for the first 1000 years, and is not limited by the availability of brine, but rather by the quick degradation of plastics and cellulosics in the waste disposal area. Because biodegradation of cellulose and/or rubber and plastics (WMICDFLG > 0) is assigned to 50% of the realizations, it dominates the uncertainty within the sampled set for GSTWPSOC. Prior to intrusion, brine supplies for iron corrosion tend to be limited; therefore, gas generation from corrosion is affected by those parameters affecting brine supplies rather than corrosion rates. Because UDRZ brine drainage is the primary brine source to the waste areas

prior to intrusion, and because the volume of brine drained is a function of halite porosity, a positive correlation is seen between GSTWPSOC and HALPOR.

After intrusion, a large volume of brine is introduced into the excavated area via the borehole from either the lower or upper non-Salado units, and tends to accumulate in the south region of the lower waste panel. At this time, gas production from iron corrosion changes from being brine-limited to corrosion-rate limited; thus, post-intrusion gas rising up to the UDRZ tends to be influenced by iron corrosion rates, WGRCOR. Because the cumulative gas volumes created by iron corrosion do not exceed that from biodegradation (when WMICDFLG > 0) until well after the intrusion event, WGRCOR does not dominate the uncertainty for GSTWPOC until midway through the modeled period.

Vertical Gas Flow Between North Portion of the Lower Waste Panel and UDRZ

Figure 4.3.8 illustrates the most influential parameters controlling vertical gas flow between the north portion of the lower waste panel and the UDRZ.

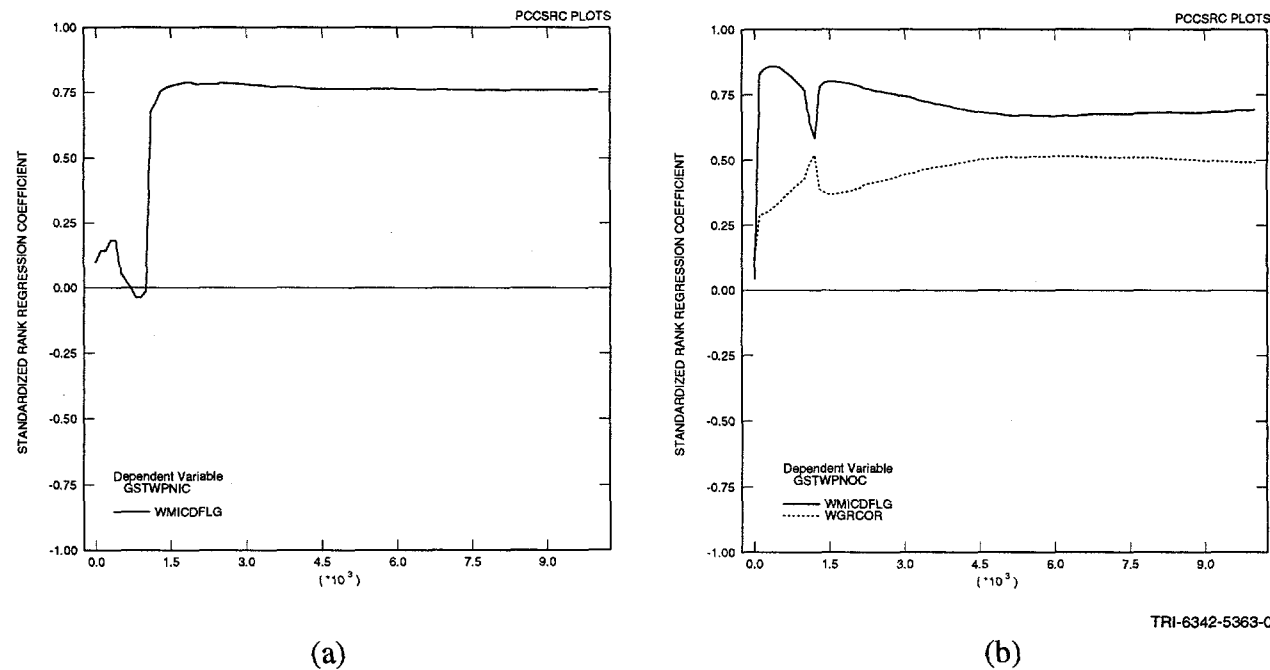


FIGURE 4.3.8. STANDARDIZED RANK REGRESSION COEFFICIENT (SRRC) results showing the most influential independent variables for vertical gas flow (a) into and (b) out of north portion of lower waste panel

Downward Flow (GSTWPNIC). Prior to intrusion, no gas flows downward from the UDRZ to the lower waste panel (GSTWPNIC). Therefore, no further discussion is presented.

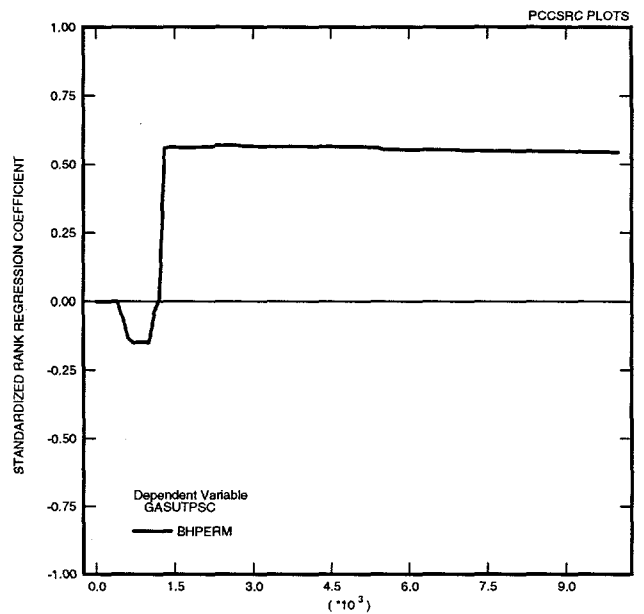
When the upper borehole plug degrades, a pulse of gas is pushed from the UDRZ down through the north half of the lower waste panel. Plug degradation produces a pressure gradient between the up-dip and down-dip regions of the repository, promoting a surge of gas towards the borehole. Due to model configuration, the borehole serves as a bottleneck, creating a localized high pressure zone as gas is constricted within the smaller confines of the UDRZ as it approaches the borehole. The constricted flow causes gas to be forced down through the north waste panel ceiling prior to exiting the borehole. This situation is more likely to occur for realizations with high gas production early on, hence the strong correlation strength with WMICDFLG.

Upward Flow (GSTWPNOC). Prior to and after intrusion, upward gas flow through the northern half of the lower waste panel ceiling into the UDRZ—GSTWPNOC—is enhanced for those realizations assigned gas generation from WMICDFLG, for reasons similar to those described for GSTWPSOC.

Soon after intrusion, in both halves of the lower waste panel, plentiful brine supplies exist for iron corrosion for the majority of realizations. Gas generation from iron corrosion becomes corrosion-rate limited, rather than brine-limited. Consequently, the correlation strength between WGRCOR and GSTWPSOC increases. The correlation strength for WGRCOR plateaus at ~5500 years and decreases slightly thereafter, because the number of simulations producing gas via iron corrosion decreases as iron inventories become depleted.

Vertical Gas Flow In and Out of the Panel Closures

This section describes vertical gas flow out of the panel closures, GASUTPSC, as depicted in Figure 4.3.9.



TRI-6342-5768-0

FIGURE 4.3.9. STANDARDIZED RANK REGRESSION COEFFICIENT (SRRC) results showing the most influential independent variable on upward-flowing gas out of the panel closure

A brief pulse of gas is pushed out the top of the panel closures when the upper borehole degrades. This pulse is positively correlated with BHPRM. Those realizations with high values for BHPRM will have a better connection between the repository and the upper units, causing a larger 'pressure pulse' to displace gas through the panel closures.

Effectively no gas flows down through the top of the panel closures.

4.3.2.2 Vertical Gas Flow Between the Upper Waste Panel and UDRZ

Figure 4.3.10 illustrates the most influential parameters controlling vertical gas flow between the upper waste panel and the UDRZ.

Downward Flow (GAS_DRAC)

Prior to intrusion, gas flow down into the ceiling of the upper waste panel, GAS_DRAC, is negatively correlated with HALPOR because this parameter affects the size of DRZ volumes where gas is stored as it flows upward from the waste

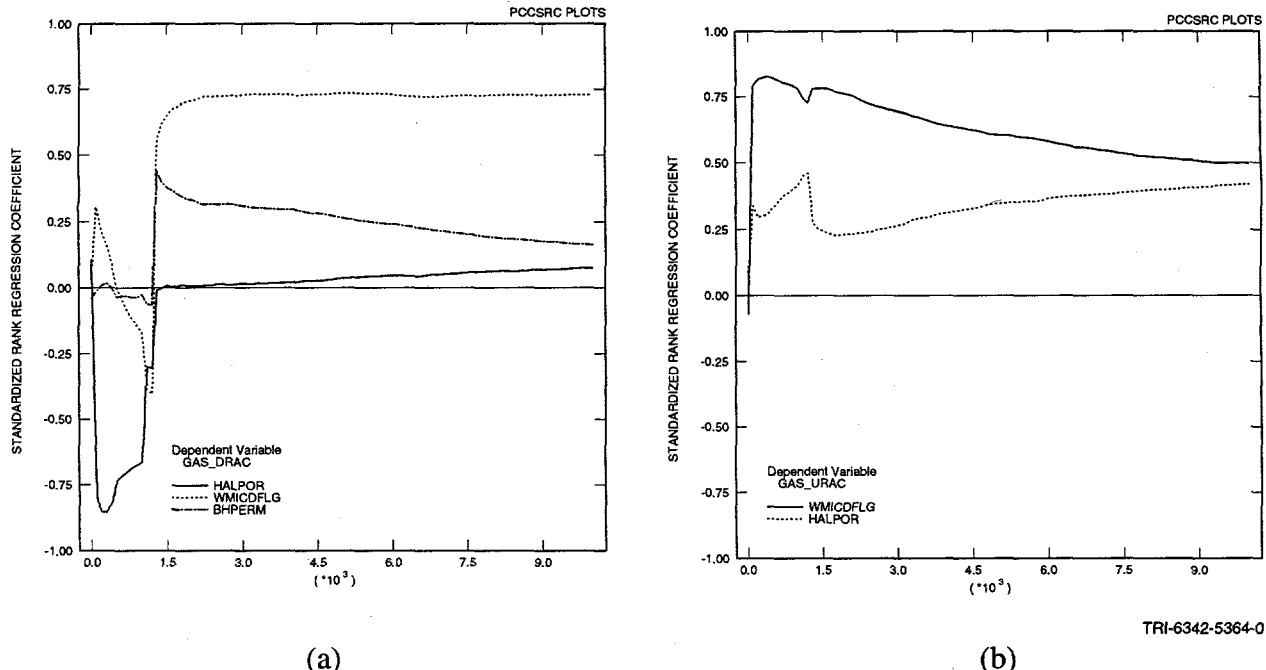


FIGURE 4.3.10. STANDARDIZED RANK REGRESSION COEFFICIENT (SRRC) results showing the most influential independent variables on controlling vertical gas flow (a) down to upper waste panel from DRZ and (b) up into UDRZ from upper waste panel

regions. As discussed in Section 3, low HALPOR values mean smaller UDRZ volumes, and smaller UDRZ volumes mean less gas storage space. The UDRZ reaches its maximum gas storage capacity earlier for those realizations with smaller DRZ volumes. Once this DRZ gas storage capacity is maximized, newly-generated gas flowing up-dip in the UDRZ introduced from the south will be deflected downward from the UDRZ through the upper waste panel ceiling to the more compressible upper waste panel where it is stored.

After intrusion, an increase in GAS_DRAC is seen for many realizations, which lasts between ~1000 and 3000 years (see hairplot in Figure 4.1.9 and boxplots in Figure 4.1.16). A strong correlation begins to appear at this time between GAS_DRAC and WMICDFLG and BHPRM. WMICDFLG determines the extent of this downward flow from the UDRZ for the same reasons as given for GSTWPNC, discussed previously. In short, simulations with microbial degradation will be more gas pressurized and, consequently, are more likely to have gas back up through the upper waste panel ceiling as it flows toward the borehole. High values for BHPRM mean the pressure wave between the repository and the upper and lower units, created at the time of

intrusion, can be more easily transmitted within the repository. This pressure pulse compresses and moves resident UDRZ gas back down through the ceiling of the upper waste panel within the time frame of the intrusion event (at 1000 years) to lower borehole closure (at 2200 years). Because creation of the pressure wave is partially a function of BHPRM, a spike is seen in the correlation strength for this parameter and GAS_DRAC.

Upward Flow (GAS.URAC)

Gas flow out of the ceiling of the upper waste panel (GAS.URAC) is strongly correlated with microbial degradation ($WMICDFLG > 0$), the dominant gas-production mechanism early in the simulation, for reasons similar to those given for GASTWPNO. After intrusion, an increase in correlation strength is seen for HALPOR, which is not seen in GSTWPNO or GSTPWSOC.

HALPOR affects the uncertainty for GAS.URAC for the following reasons:

- HALPOR determines the amount of UDRZ volumes draining brine into the excavated area early in the modeled period. Some of this brine is stored in the experimental and operations rooms and the LDRZ. As the repository gas pressure increases, brine stored in the experimental and operation rooms is impeded from flowing down-dip toward the upper waste panel. When repository gas pressures are reduced after intrusion, much of the brine stored in the LDRZ and in the operations and experimental rooms flows into the upper waste panel, where it is used for gas production via iron corrosion. Consequently, the extent of DRZ brine drainage early on positively affects the amount of gas exiting the upper waste panel ceiling later in the modeled period due to its delayed release.
- Large values for HALPOR mean there is more room for replenishing brine to pass through the UDRZ while gas is being evacuated. Some of this brine is used for gas production while later rises up through the upper waste panel ceiling.

4.3.2.3 Lateral Gas Flow In the UDRZ Crossing the Area Above the Panel Closures

North-Flowing Gas

Figure 4.3.11 illustrates the most influential parameters controlling lateral, north-flowing gas above the panel closures within the UDRZ.

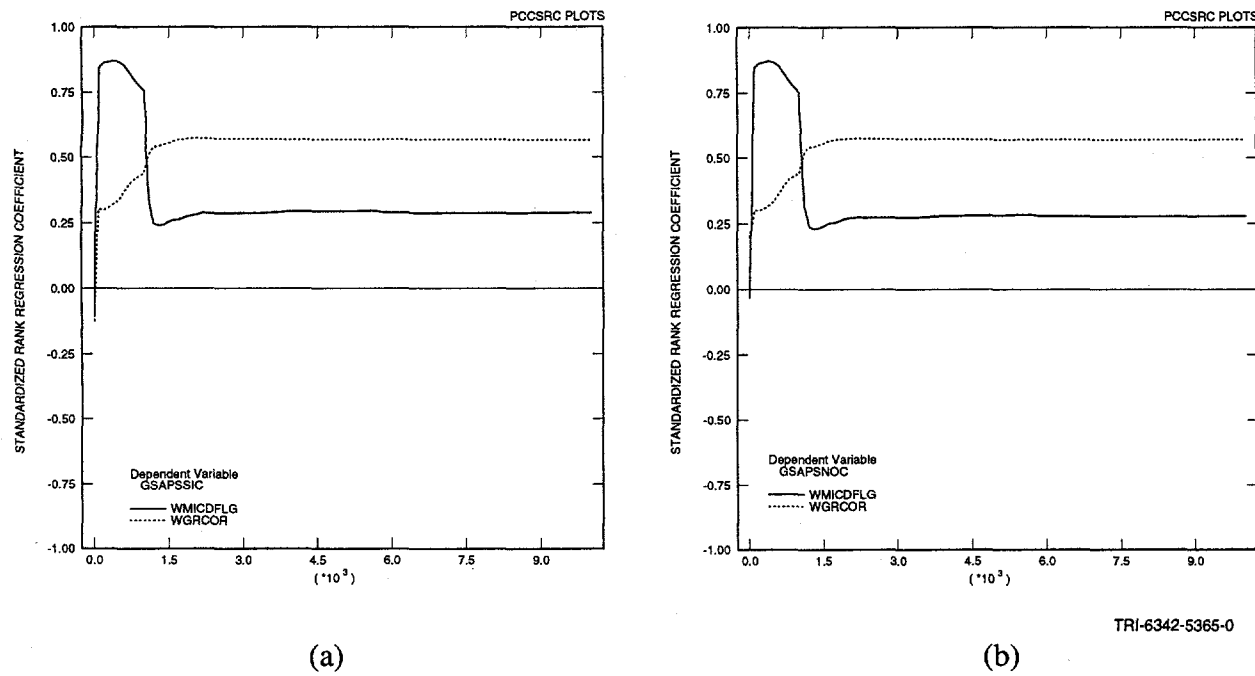


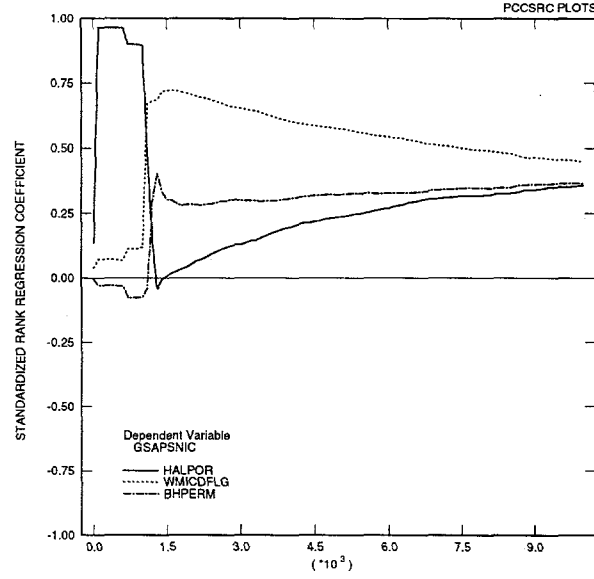
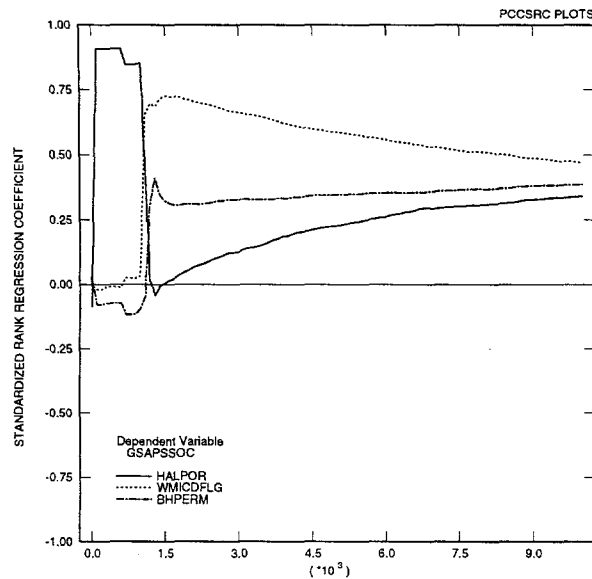
FIGURE 4.3.11. STANDARDIZED RANK REGRESSION COEFFICIENT (SRRC) results showing the most influential independent variables for lateral, north-flowing gas within UDRZ above the (a) south and (b) north side of panel closures (GSAPSSIC and GSAPSNC, respectively)

Prior to intrusion, the lateral flow of gas in the UDRZ is principally to the north. The uncertainty for north-flowing gas is dominated by biodegradation because it is the dominant gas-generation process for the first 1000 years of the modeled period. Gas generated by corrosion is brine-limited, thus it does not come into play as a dominant gas-generating process affecting north-flowing gas until a limited time just after the intrusion event, when replenishing brine enters the waste regions and is then used for gas production via iron corrosion.

After intrusion, the number of realizations with north-flowing gas is greatly reduced because the dominant gas flow direction is southward.

South-Flowing Gas (GSAPSSOC and GSAPSNC)

Figure 4.3.12 illustrates the most influential parameters controlling lateral, south-flowing gas above the panel closures within the UDRZ.



TRI-6342-5366-0

FIGURE 4.3.12. STANDARDIZED RANK REGRESSION COEFFICIENT (SRRC) results showing the most influential independent variables for controlling lateral, south-flowing gas above panel closures within the UDRZ (GSAPSSOC and GSAPSNIC)

Prior to upper borehole degradation, minimum to no gas flows south above the panel closures, GSAPSSOC and GSAPSNIC; thus the positive correlation with halite porosity early in the simulation period is spurious.

At the time of upper borehole degradation, south-flowing gas is initiated. Flow in this direction is strongly correlated with WMICDFLG.

WMICDFLG is strongly correlated with south-flowing gas for several reasons. Simulations with gas produced from microbial degradation early in the modeled period have relatively higher volumes of gas, which tend to create higher repository pressures. Higher repository pressures tend to create a significant pressure potential between the repository and upper units. At the time of upper borehole degradation, this relatively large pressure potential between the upper and lower units and the repository is transmitted through the borehole, creating a pressure wave between the up-dip and down-dip regions of the repository toward the borehole. The pressure wave carries gas with it. High BHPRM values mean less impedance for gas evacuation out of the repository, the majority of which is funneled through the UDRZ, reducing repository

pressures. Once pressures are reduced, replenishing brine from anhydrite drainage or drainage from units above or below the repository is more likely to occur. This brine can be used for additional gas generation via iron corrosion if it contacts uncorroded drums.

Intentionally Left Blank

5. Brine and Gas Flow between the Upper and Lower Panels via Panel Closures

This section describes lateral brine and gas flow across the panel closures.¹ Two flow boundaries were evaluated for lateral flow across the panel closures—the south face of the closure abutting the lower waste panel and the north face of the panel closure abutting the upper waste panels. Figure 5.1.1 depicts those boundaries of the panel closures where flow was evaluated. Vertical flow between the DRZ and the top and bottom of the panel closures is described in Sections 4 and 6, respectively.

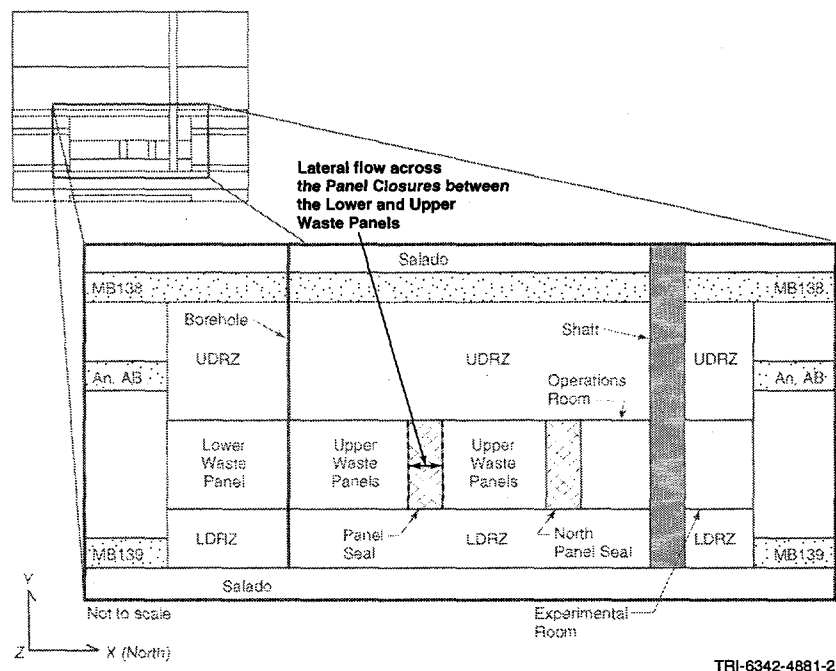


FIGURE 5.1.1. REGIONS OF DISPOSAL SYSTEMS for which lateral flow across panel closures was assessed

The organization of Section 5 is as follows. Section 5.1 presents those variables defining lateral flow through the panel closures. Following these definitions, hairplots—results for the entire suite of simulations overlaid on one plot—are presented for each defined variable. These hairplots illustrate the variation in behaviors that may occur for a single variable from simulation

¹ Throughout this report, the term 'panel closures' is used in text; in some illustrations, the term 'panel's' is used instead.

to simulation, given the unique combination of sampled variables assigned to each simulation, and are referred to throughout each subsection.

To facilitate a better understanding of trends and the overall behavior of each dependent variable throughout the modeled period, boxplots for each dependent variable are presented at the end of Section 5.1. Boxplots graphically present the mean, median, 25th and 75th quantile groups, as well as outliers within a population set. Boxplots are presented for data at four significant times within the modeled period. These are as follows:

- 999 years, just prior to intrusion,
- 1500 years, 300 years after the upper borehole plug degrades,
- 5500 years, midway through the modeled period,² and
- 10,000 years, the end of the modeled period.

Section 5.2 gives a brief overview of brine and gas flow through the closures during the modeled period. Scatterplots are presented to illustrate the relationship between flow through the closures and sampled parameters. Section 5.3 presents the variables most affecting panel closure flow.

5.1 Variables Used to Define Flow

Variables defining lateral brine and gas flow within the panel closure between the upper and lower waste panels are given in Table 5.1. Table 5.2 lists variables for gas flow between the same regions. Figures 5.1.2 through 5.1.5 are hairplots for cumulative brine and gas crossing the north and south faces of the panel closure.

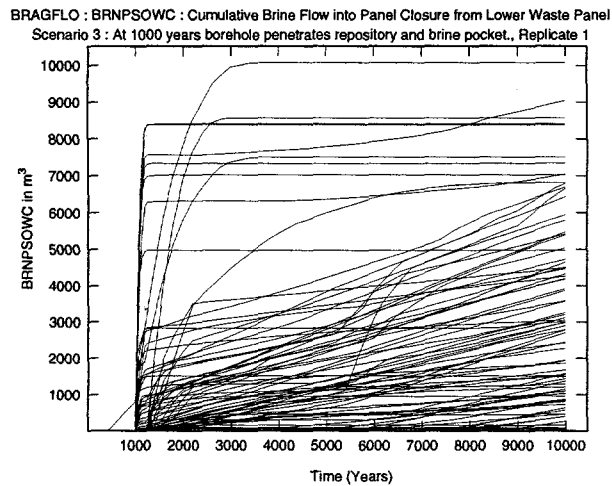
² Prior examination of several variables within the suite of simulations revealed several processes had settled soon after 5000 years. Therefore, values were chosen for variables at 5500 years rather than 5000 years.

Table 5.1. Dependent Variables for Cumulative Brine Flow (m³) Between the Upper and Lower Waste Panels Via Panel Closures. (Note, variable names shown on boxplots are abbreviated and given in parenthesis.)

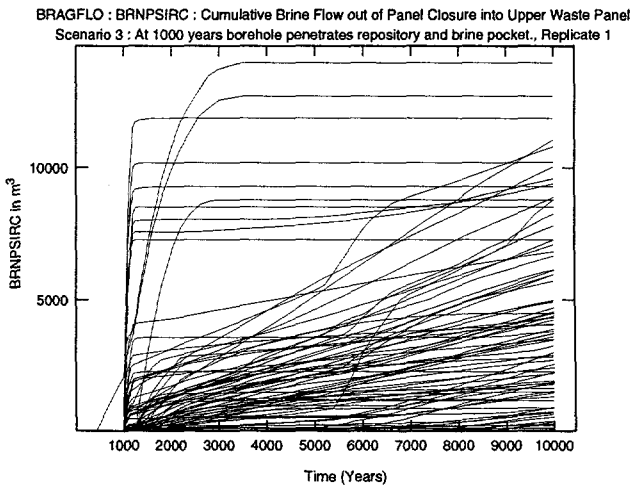
Variable	Definition
South-Flowing Brine	
BRNPSIWC (BPSIWC)	Cumulative brine flow (m ³) out of panel closures into the lower waste panel (i.e., flow out of the south face of the panel closure)
BRNPSORC (BPSORC)	Cumulative brine flow (m ³) into panel closures from the upper waste panel (i.e., flow into the north face of the panel closure)
North-Flowing Brine	
BRNPSIRC (BPSIRC)	Cumulative brine flow (m ³) out of panel closures into the upper waste panel (i.e., flow crossing out of north face of the panel closure)
BRNPSOWC (BPSOWC)	Cumulative brine flow (m ³) into panel closures from the lower waste panel (i.e., flow into the south face of the panel closure)

Table 5.2. Dependent Variables for Cumulative Gas Flow (m³) Between the Upper and Lower Waste Panels Via Panel Closures

Variable	Definition
South-Flowing Gas	
GASPSIWC (GPSIWC)	Cumulative gas flow (m ³) out of panel closures into the lower waste panel (i.e., flow out of the south face of the panel closure)
GASPSORC (GPSORS)	Cumulative gas flow (m ³) into panel closures from the upper waste panel (i.e., flow into the north face of the panel closure)
North-Flowing Gas	
GASPSIRC (GPSIRC)	Cumulative gas flow (m ³) out of panel closures into the upper waste panel (i.e., flow out of the north face of the panel closure)
GASPSOWC (GPSOWC)	Cumulative gas flow (m ³) into panel closures from the lower waste panel (i.e., flow into the south face of the panel closure)



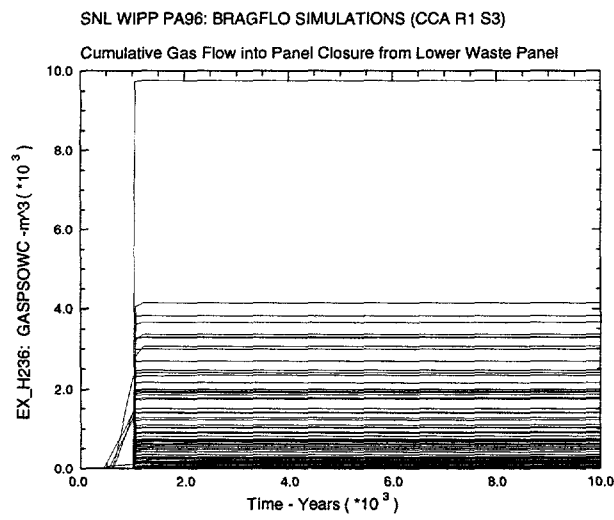
(a)



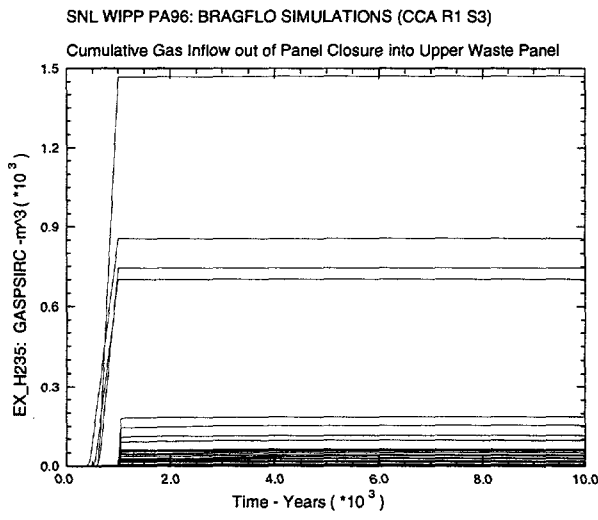
(b)

TRI-6342-5685-0

FIGURE 5.1.2. CUMULATIVE BRINE FLOW (m^3) ACROSS panel closures (a) out of the lower waste panel and (b) into the upper waste panel



(a)

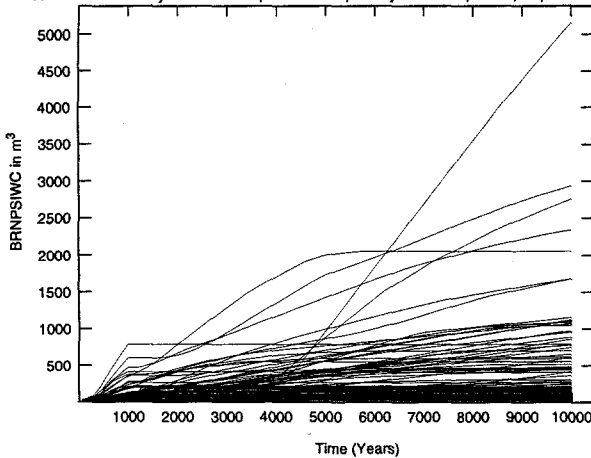


(b)

TRI-6342-5631-0

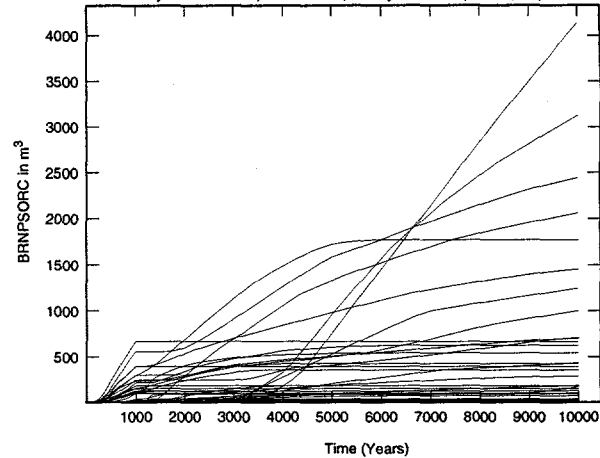
FIGURE 5.1.3. CUMULATIVE GAS FLOW (m^3) ACROSS panel closures (a) out of the lower waste panel and (b) into the upper waste panel

BRAGFLO : BRNPSIWC : Cumulative Brine Flow out of Closure into Lower Waste Panel Scenario 3 : At 1000 years borehole penetrates repository and brine pocket., Replicate 1



(a)

BRAGFLO : BRNPSORC : Cumulative Brine Flow into Panel Closure out of Upper Waste Panel Scenario 3 : At 1000 years borehole penetrates repository and brine pocket., Replicate 1



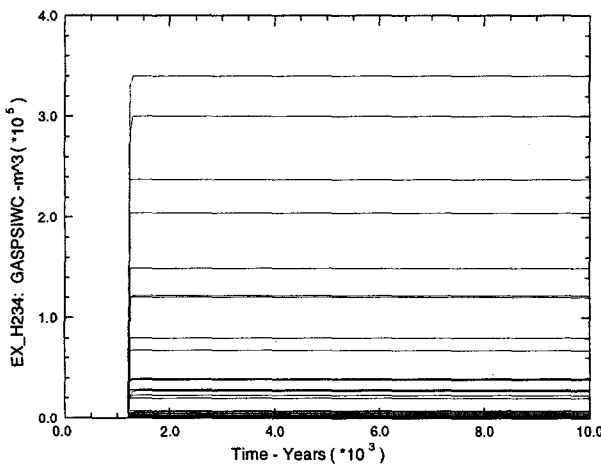
TRI-6342-5686-0

(b)

FIGURE 5.1.4. CUMULATIVE BRINE FLOW (m³) ACROSS panel closures (a) into the lower waste panel and (b) out of the upper waste panel

SNL WIPP PA96: BRAGFLO SIMULATIONS (CCA R1 S3)

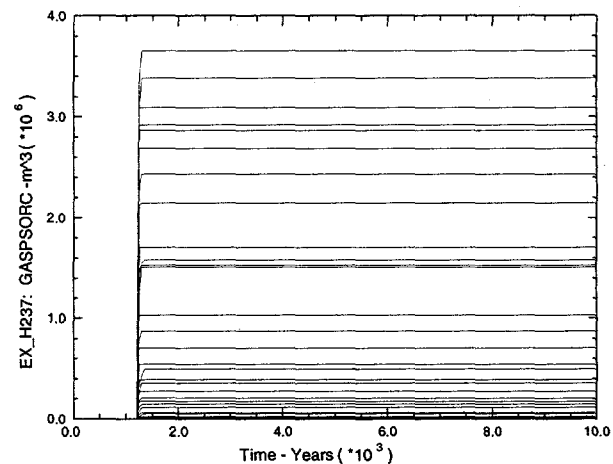
Cumulative Gas Inflow out of Panel Closure into Lower Waste Panel



(a)

SNL WIPP PA96: BRAGFLO SIMULATIONS (CCA R1 S3)

Cumulative Gas Flow into Panel Closure from the Upper Waste Panel



(b)

TRI-6342-5632-0

FIGURE 5.1.5. CUMULATIVE GAS FLOW (m³) ACROSS panel closures (a) into the lower waste panel and (b) out of the upper waste panel

Boxplots for cumulative brine flow across the panel closures are depicted in Figure 5.1.6 and boxplots for cumulative gas flow across the panel closures appear in Figure 5.1.7.

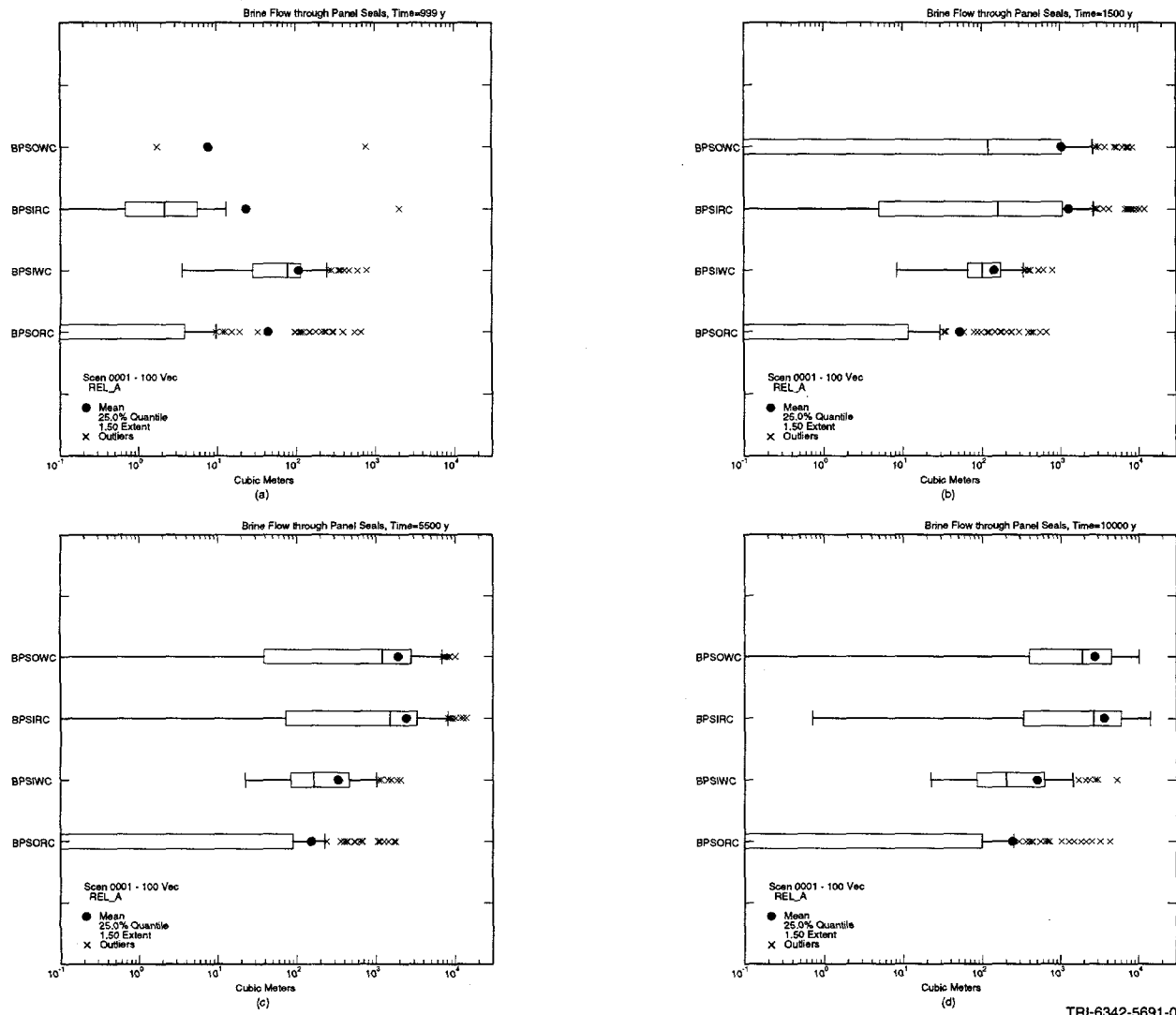
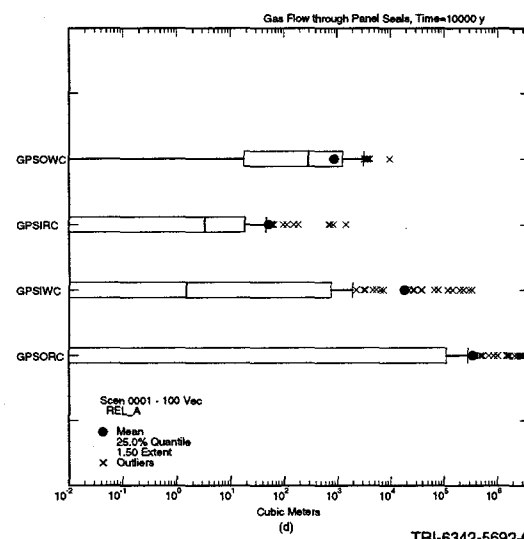
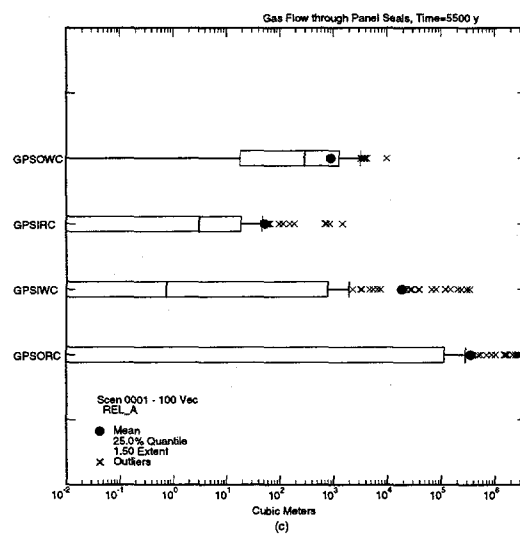
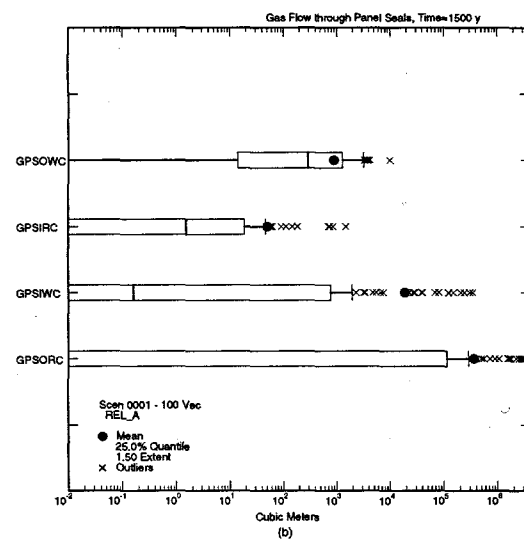
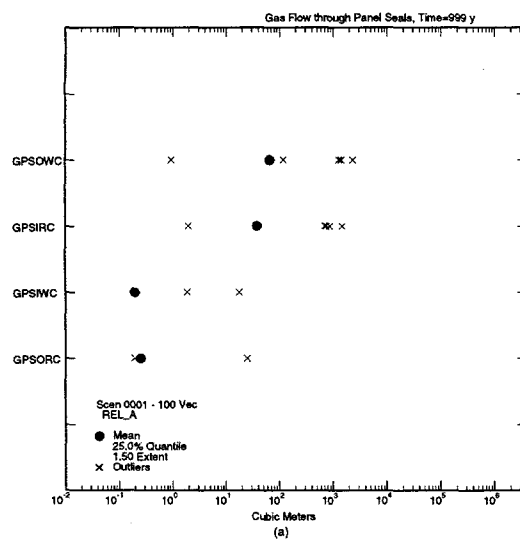


FIGURE 5.1.6. BOXPLOTS FOR BRINE ACROSS panel closures. Boxplots show flow taken at (a) 999, (b) 1500, (c) 5500, and (d) 10,000 years

TRI-6342-5691-0



TRI-6342-5692-0

FIGURE 5.1.7. BOXPLOTS OF GAS ACROSS panel closures. Boxplots show flow taken at (a) 999, (b) 1500, (c) 5500, and (d) 10,000 years

5.2 General Summary of Lateral Flow Across the Panel Closures

The panel closures can potentially serve as a seepage face, transmitting brine or gas to and from the waste disposal areas and between the UDRZ and the LDRZ, thus affecting repository performance. Therefore, the efficiency of the closures and the extent to which they transmit fluid between the regions is of interest. This section briefly describes *lateral* brine and gas flow between the upper and lower waste disposal areas via the panel closures. Vertical fluid flow in and out of the closures' tops and bottoms is described in the sections pertaining to flow in the UDRZ and the LDRZ (Sections 4 and 6).

5.2.1 Brine Flow

5.2.1.1 Prior to Intrusion

Less than 1000 m³ of brine flows laterally through the panel closures prior to intrusion. For realizations that do have brine flow, the dominant lateral brine flow direction is southward, from the upper to the lower waste panel, and is driven by gravitational gradient. Overall, more brine drains out of the closure's south face to the lower waste panel than enters from the north face. The extra contribution of brine that exits the south face is due to vertical brine flow into the top and bottom of the closures via the UDRZ and the LDRZ, respectively, which is then deflected southward within the panel closures.

Lateral brine flow through the closures is affected by DRZ volumes, *effective* brine permeabilities within the waste disposal regions, and gas saturations within the lower waste panel and/or the upper waste panels, which are functions of HALPOR, WRBRNSAT, and WMICDFLG, respectively (see Figure 5.2.2 in Section 5.2.2). For vectors with halite porosities in the upper 50th percentile group, the potential for brine to flow from the upper waste panel to the lower waste panel increases. However, those realizations with large halite porosities may not contribute to flow crossing the panel closure if they have high assigned values for residual brine saturations (WRBRNSAT, an LHS parameter) coupled with large volumes of gas generated via microbial degradation (a function of the WMICDFLG switch). Realizations that are assigned

halite porosities in the upper 50th percentile *and* have little or no gas generation from microbial decay will have relatively larger volumes of brine flowing through the panel closures. For realizations with halite porosities in the lower 50th percentile, brine is not passed from the upper to the lower waste panels via the panels closures.

Only one realization, which was assigned the highest anhydrite permeability, exhibited any brine flow through the closures from the lower waste panel to the upper waste panels.

5.2.1.2 After Intrusion

Lateral brine flow through the closures increases dramatically after intrusion. The direction (either to the north or to the south) and volumes of brine crossing the panel closures is strongly dependent on borehole permeabilities, the amount of brine flow from the brine reservoir, iron corrosion rates, and the time frame in which iron in the lower waste panel is completely corroded—functions of BHPRM, BPCOMP, and WGRCOR.

For realizations with relatively high borehole permeabilities, gas is readily evacuated out the lower waste panel, enabling replenishing brine to enter. These conditions cause the lower waste panel to become more brine-saturated than the upper waste panel, enabling iron corrosion in this area to become rate- rather than brine-limited. As a result, excess brine accumulates in this down-dip region. This excess brine creates a pressure gradient between the two waste regions which promotes the passage of brine from the lower to the upper waste panel via the closures.

For realizations with low borehole permeabilities, the repository generally maintains higher gas saturation levels and pressure. Combined, these conditions inhibit brine drainage into the repository from the anhydrites or down the borehole. High gas saturation and pressures maintain the same brine flow direction as that prior to intrusion, but with more brine draining out the south face of the panel closure than into the north side. The brine source into the closures comes from brine that drains by gravity from the north portion of the LDRZ southward, accumulates in the south portion of the LDRZ under the lower waste panel, and then backs up through the bottom of the panel closures. Brine continues to flow out the panel closures' south face until most of the

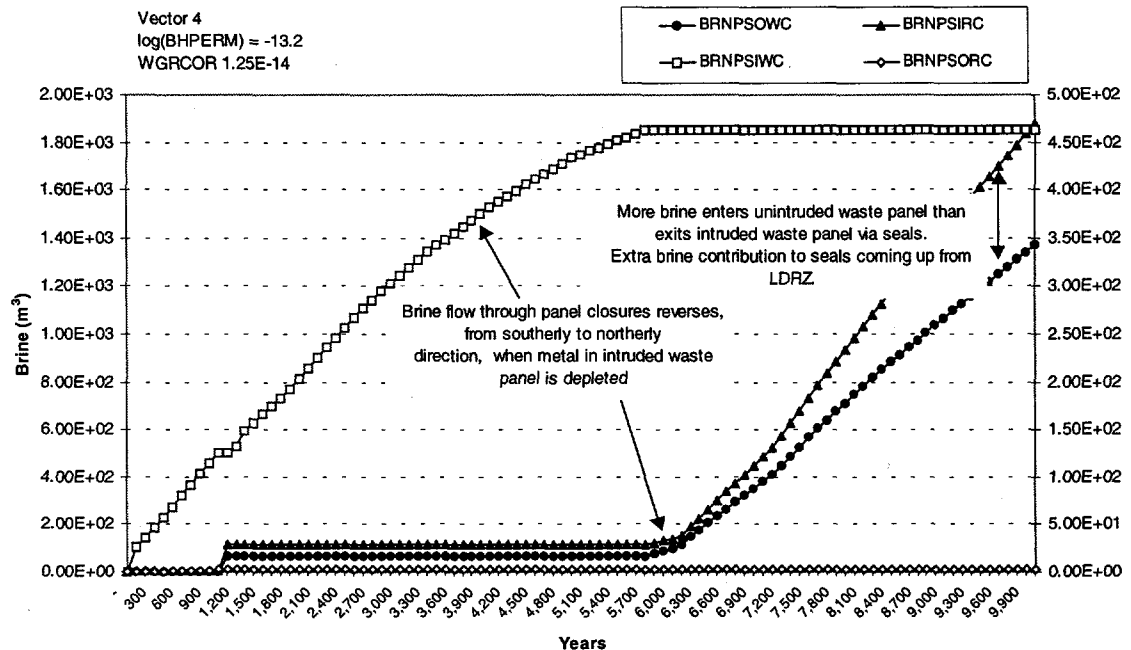
iron is corroded in the lower waste panel. Once iron in the lower waste panel is corroded, brine begins to accumulate in the lower waste panel, gradients are then reversed between the two waste disposal regions, and lateral flow direction in the panel closures reverses from a down-dip to an up-dip direction.

Figure 5.2.1 shows overlay plots illustrating flow through the panel closures for two realizations assigned low and high borehole permeabilities (Realizations 4 and 50, respectively). The change in flow direction that occurs for Realization 4 around 5000 years should be noted.³

Scatterplots that illustrate the gas and brine flow patterns just described, *and* their correlation with those sampled variables, follow the overlay plots.

³ Section 7 includes additional overlay plots illustrating several processes dominant in the repository and how these processes affect brine (and gas) flow between waste and non-waste regions of the repository.

R1S3 - Brine Flow Through Panel Closures



R1S3 - Brine Flow Through Panel Closures

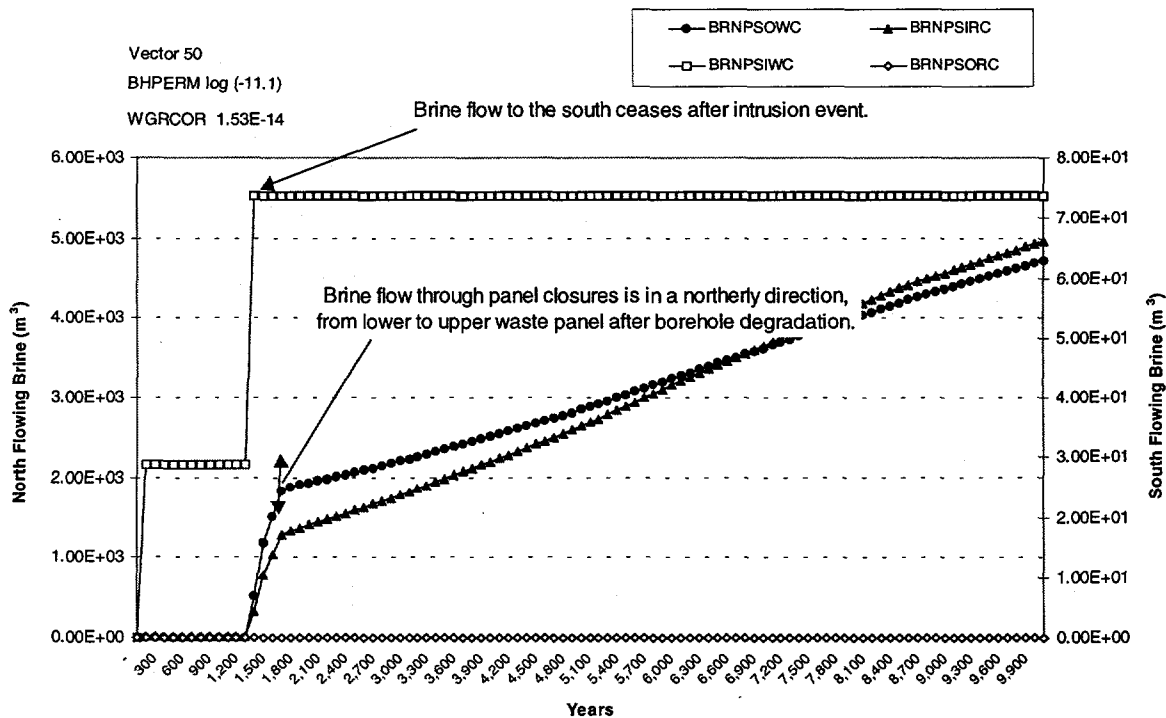


FIGURE 5.2.1. OVERLAY PLOTS SHOWING RELATIONSHIP between brine flow direction through panel closures with respect to borehole permeabilities and time of intrusion. The upper frame is representative of a realization assigned a low borehole permeability; the lower frame represents a high borehole permeability

5.2.2 Gas Flow

For the majority of realizations, two gas pulses pass between the lower and upper waste panels via the panel closures. The first pulse of gas occurs at the time of intrusion (1000 years) due to the pressure pulse within the repository when the borehole connects the Castile reservoir (usually of high pressure) to the repository. The second gas pulse occurs at 1200 years, when the upper borehole plug degrades. Realizations with reservoir pressures greater than the repository will have a pressure pulse transmitted through the repository, which carries Castile brine upward to the lower waste panel. This brine-induced pressure pulse displaces resident gas from the lower to the upper waste panel via the panel closures.

When the upper borehole plugs degrade at 1200 years, repository pressures are quickly reduced for realizations with high gas pressures produced from microbial degradation and high borehole permeabilities. This pressure reduction causes a second pressure pulse to pass through the repository, but in the opposite direction from the first. A gas pulse enters the north side of the panel closures and exits the south side (from the upper to the lower waste panel via the panel closures). Immediately after the second gas pulse, a large influx of brine displaces any gas in the panel closures. Brine primarily enters the closures from the LDRZ and the lower waste panel. Because capillary pressure is modeled in the panel closures, and the closures have a relatively high residual gas saturation of 0.2 (a non-sampled parameter), gas does not displace brine in the panel closures after the 1200 year pulse. The following scatterplots (Figure 5.2.2) illustrate the relationship between gas and brine flow through the panel closures just described and the independent variables influential to this flow.

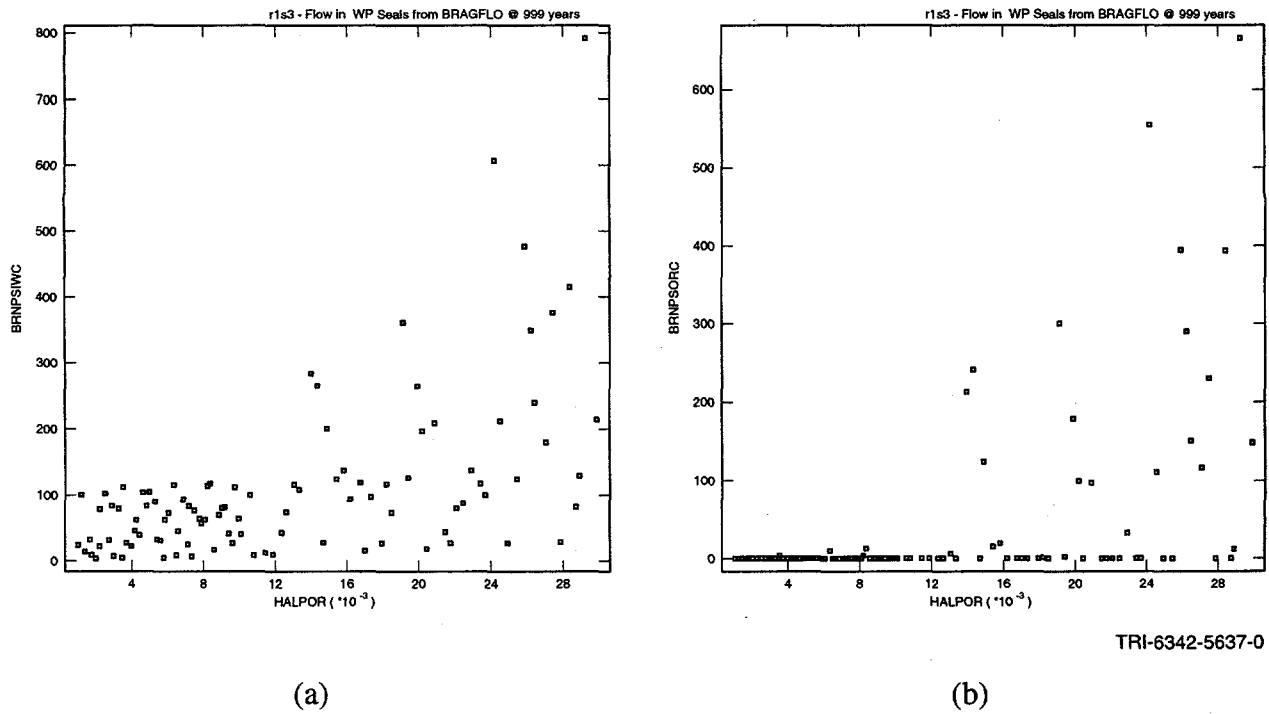


FIGURE 5.2.2. SCATTERPLOTS OF BRINE FLOW just prior to intrusion (999 years) (a) into lower waste panel via the south panel closure face and (b) out of the upper waste panel through the north panel closure face with respect to halite porosities for flowing brine. Note: The plot indicates that more brine flows through the panel closures in realizations with high halite porosities. The right plot (b) for BNPSORC vs HALPOR shows that brine flow crosses the panel closures from the upper waste panels toward the lower waste panel for realizations with halite porosities $\geq 1.4 \times 10^{-3}$; for realizations with halite porosities $< 1.4 \times 10^{-3}$, no brine flows from the upper waste panels via the panel closures. The left plot (a) shows small amounts of brine exit the panel closures south face to the lower waste panel without passing through the upper waste panel

Figure 5.2.3 shows that realizations with high residual brine saturations have limited brine flow laterally crossing the panel closure face.

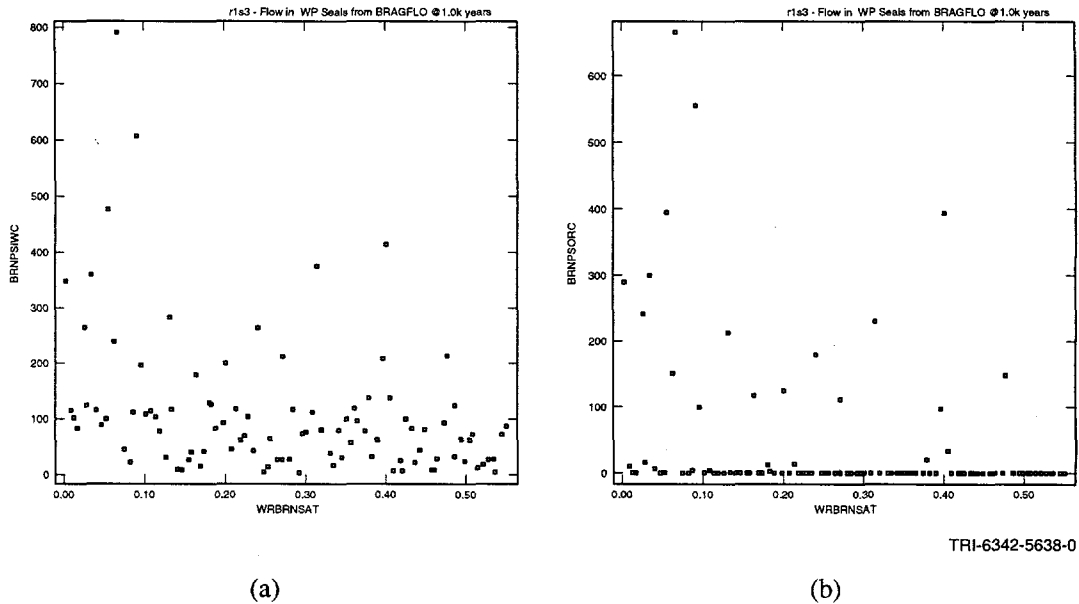


FIGURE 5.2.3. SCATTERPLOTS OF BRINE FLOW through panel closures just prior to intrusion (1000 years) with respect to residual brine saturations assigned to waste disposal area for brine flowing (a) into the upper waste panel via the south panel closure face and (b) out of the upper waste panel through the north panel closure face. The plot indicates that more brine flows through the panel closures in realizations with low residual brine saturation

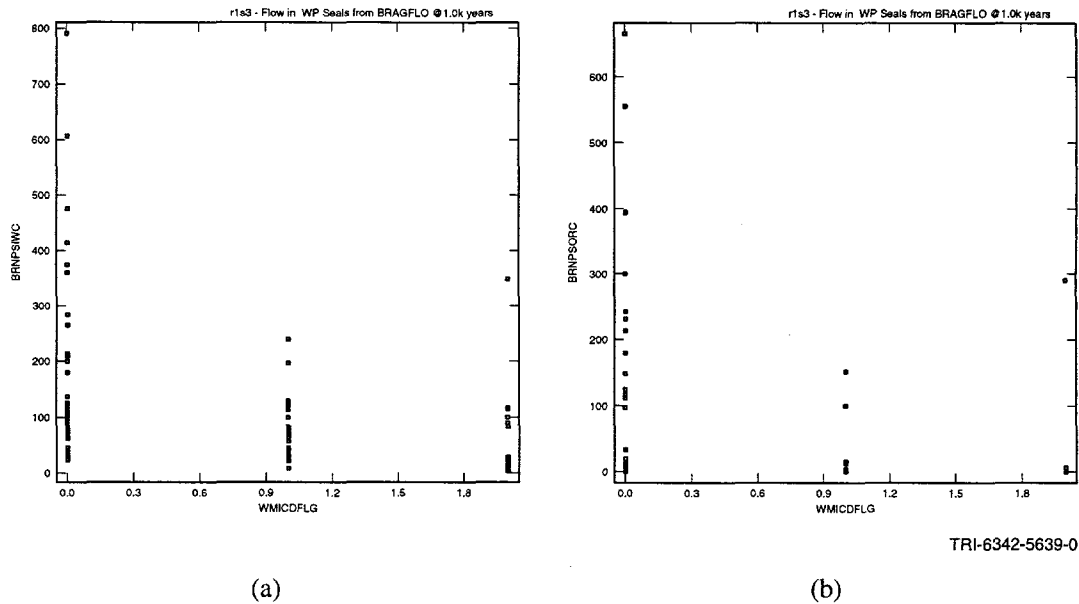


FIGURE 5.2.4. SCATTERPLOTS OF BRINE FLOW through panel closures just prior to intrusion (1000 years) with respect to microbial degradation for brine flowing (a) into the lower waste panel via the south panel closure face and (b) out of the upper waste panel through the north panel closure face. The plot indicates that more brine flows through the panel closures in realizations with low microbial degradation

The following scatterplots taken at 10,000 years (Figure 5.2.5) show (a) the strong positive relationship between brine flow entering the south side of the panel closures from the lower waste panel and Castile reservoir compressibility, (b) a negative correlation seen with microbial degradation, and (c) noncorrosion rates. For comparison, scatterplots are provided for brine that enters the upper waste panel via the closure face with respect to the same independent variables ((d) reservoir pressures, (e) microbial degradation and iron, and (f) corrosion rates). Note that more brine enters the upper waste panel than exits the lower waste panel via the closures. The extra contribution of brine enters the closure tops and bottoms via the DRZ.

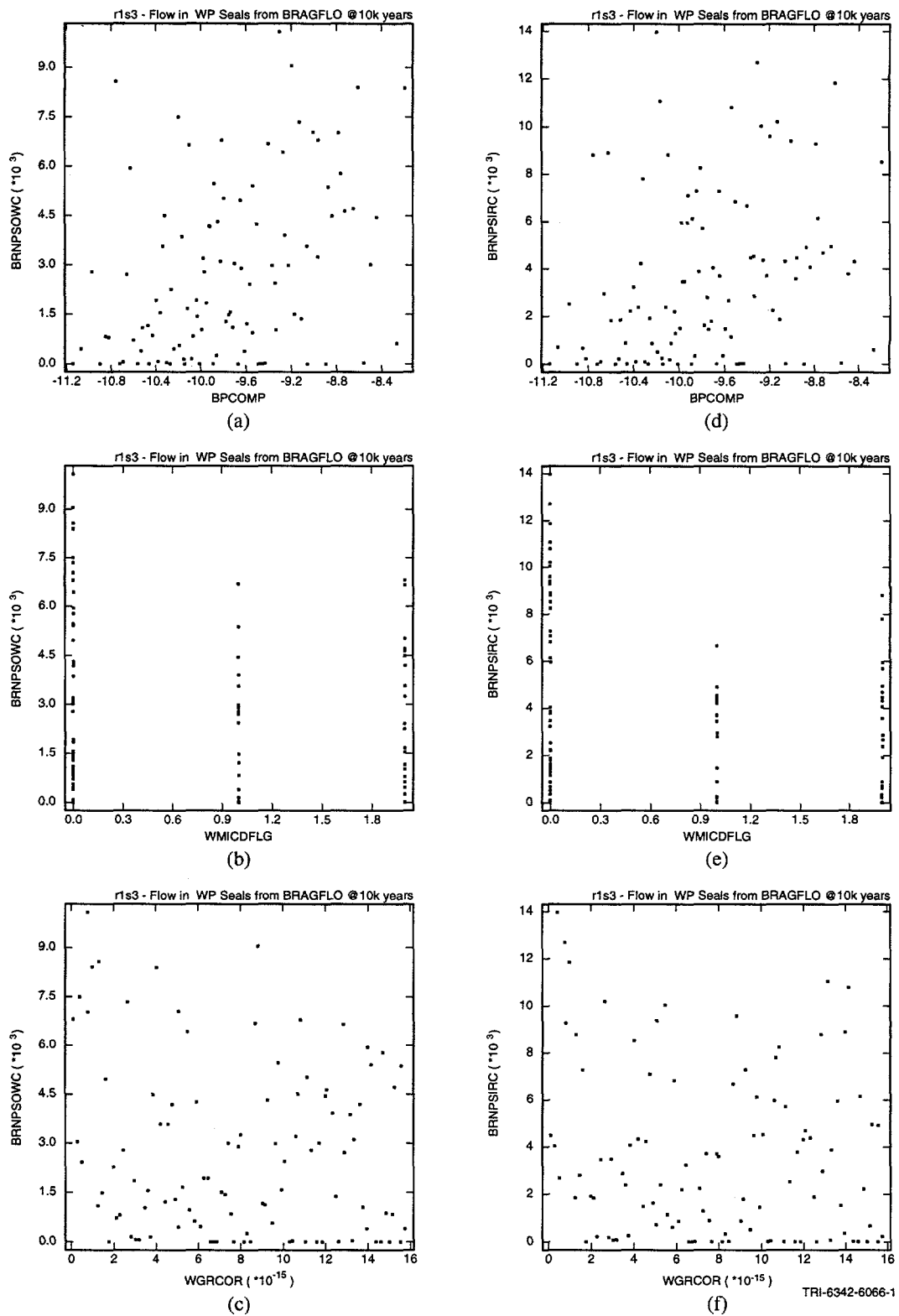


FIGURE 5.2.5. SCATTERPLOTS FOR BRINE ENTERING the south face (a,b,c) of the panel closure (BRNPSOWC) and exiting the panel closure north face (d,e,f) (BRNPSIRC) with respect to BPCOMP, WMICDFLG, and WGRCOR

The scatterplots given in Figure 5.2.6 show flow direction through the panel closure is strongly correlated with borehole permeability.

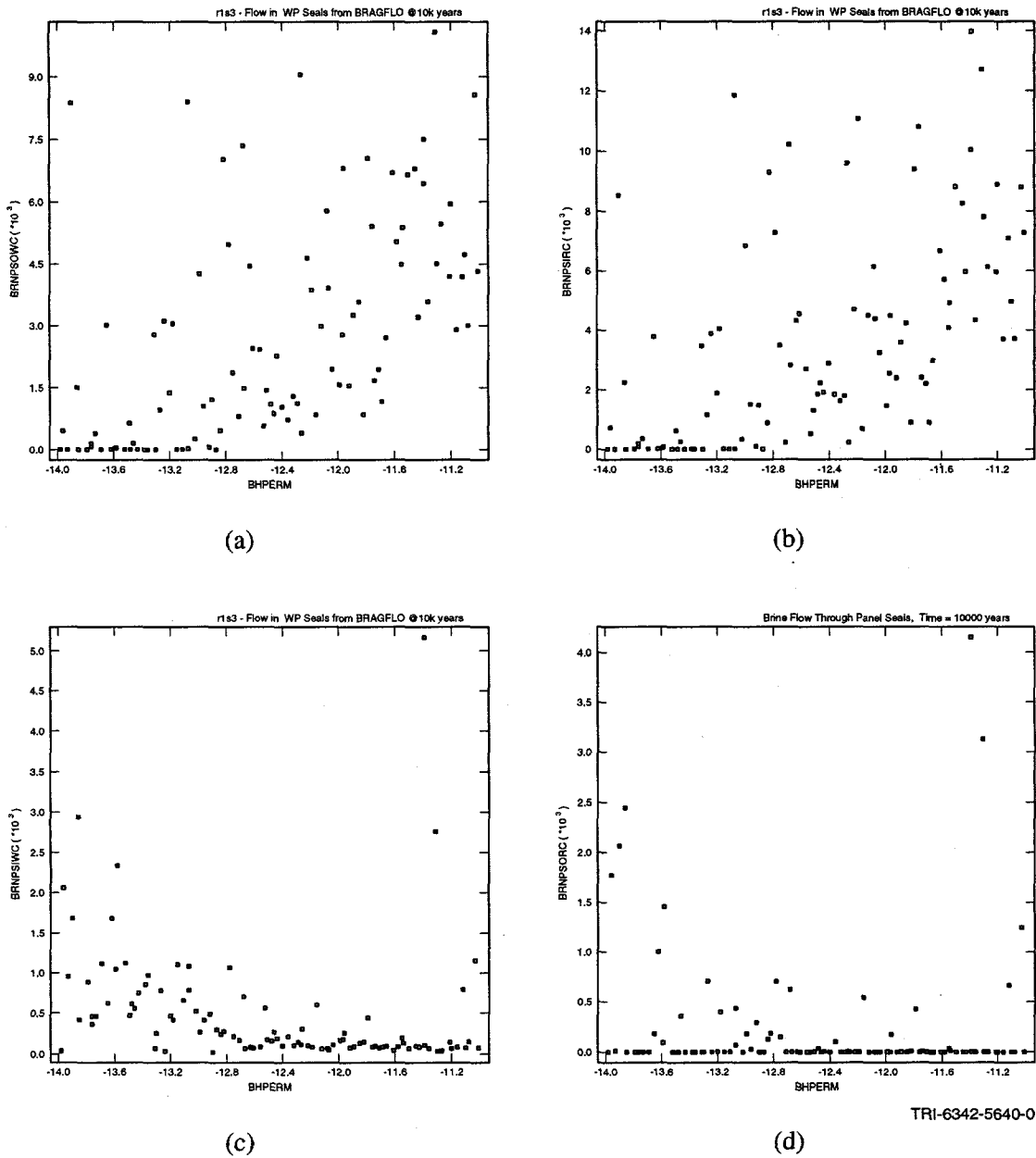


FIGURE 5.2.6. SCATTERPLOTS OF BRINE FLOW through panel closures at 10,000 years with respect to borehole permeabilities (BHPRM given on these plots as BHPERM) for brine flowing (a) into the lower waste panel via the south panel closure face, (b) out of the upper waste panel through the north panel closure face, (c) into the upper waste panel via the south panel closure face, and (d) out of the upper waste panel through the north panel closure face. These plots illustrate the dominant flow direction through the panel closures for those realizations assigned high borehole permeability. Up-dip will be from the lower waste panel to the upper waste panel. Conversely, realizations assigned lower borehole permeabilities will have brine flow through the panel closures in a down-dip direction. Note the difference in the volume of brine that enters and exits the closure north and south face. The extra contribution is due to brine that passes up through the closures' top or bottoms via the DRZ.

5.3 Parameters Affecting Lateral Flow Across the Panel Closures

5.3.1 Brine Flow

5.3.1.1 South-Flowing Brine: Flow out of the Upper Waste Panels and Flow into the Lower Waste Panels (BRNPSORC, BRNPSIWC)

Figure 5.3.1 illustrates the independent variables that most affect lateral south-flowing brine within the panel closures using SRRC analysis.

For the first few hundred years after repository closure, brine flow out of the upper waste panels via the panel closures is positively correlated with HALPOR and negatively correlated with parameters that influence effective brine saturations within the waste panels, i.e., WRBRNSAT and WMICDFLG. Realizations with higher assigned values for residual brine saturation (WRBRNSAT) will have lower *effective* brine permeabilities within the waste disposal area.

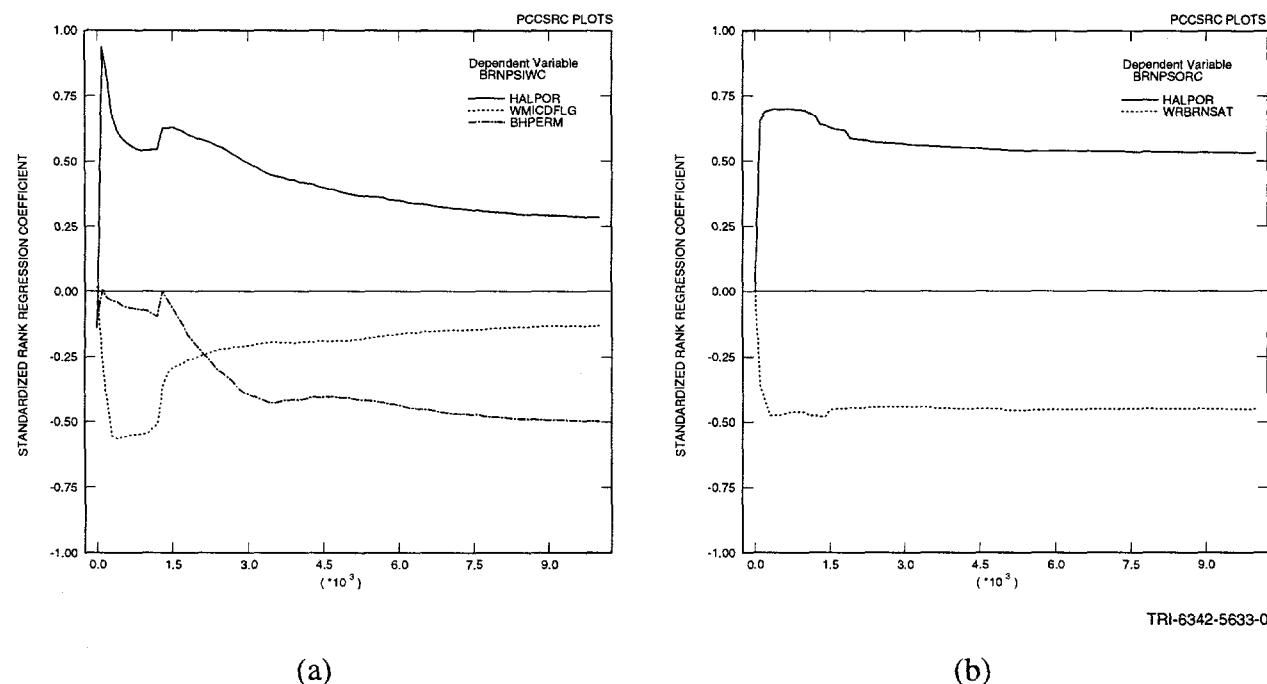


FIGURE 5.3.1. STANDARDIZED RANK REGRESSION COEFFICIENT (SRRC) results showing the most influential independent variables for south-flowing brine (a) into the lower waste panel and (b) out of the upper waste panel

These lower brine permeabilities create more resistance to brine flowing laterally within the upper waste panel toward the panel closures. Consequently, less brine will actually enter the closures. Additionally, when assigned values for WRBRNSAT are high, brine flow will cease altogether at a higher values of 'absolute' brine saturation. Realizations with WMICDFLG > 0 (50% of the sampled set) will have high gas saturations rendering lower effective brine permeabilities; hence, residual brine saturation is more likely to be reached. After intrusion, south-flowing brine through the panel closures ceases for most realizations. For the few realizations with a component of south-flowing brine, low borehole permeability, with low residual brine saturation, and high halite porosities seem to be the determining factors.

5.3.1.2 *North-Flowing Brine: Flow out of the Lower Waste Panels and Flow into the Upper Waste Panels (BRNPSIRC, BRNPSOWC).*

Figures 5.3.2 through 5.3.4 illustrate the independent variables that most affect lateral north-flowing brine within the panel closures from SRRC analysis.

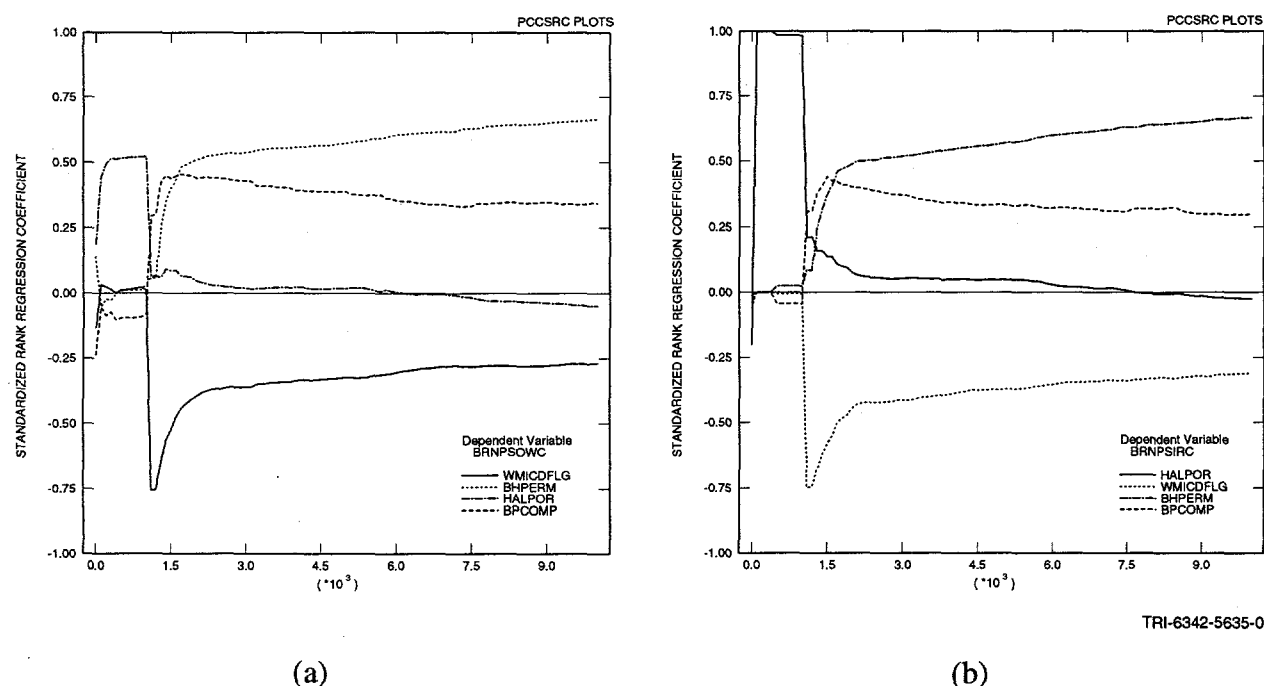


FIGURE 5.3.2. STANDARDIZED RANK REGRESSION COEFFICIENT (SRRC) results showing the most influential independent variables for north-flowing brine (a) out of the lower waste panel and (b) into the upper waste panel

Prior to intrusion north-flowing brine through the panel closures is practically zero, so it is not discussed further. After intrusion, a positive correlation exists between north-flowing brine and parameters BHPRM and BPCOMP, and negative correlations appear between the north-flowing brine and parameters WMICDFLG and WGRCOR. Large quantities of gas produced via microbial degradation or iron corrosion will render the repository more gas saturated and of higher pressures. Consequently, gas will take longer to evacuate the repository, and repository pressures will be lowered at a slower rate before brine can flow into the excavated areas.

Additionally, high values for WGRCOR mean more brine is 'consumed' via iron corrosion. More brine consumed via corrosion reduces the accumulation of excess brine that would flow through the panel closures.

High brine volumes in the lower waste panel mean this area will have relatively high pressures (due to a higher density of brine) and will result in an 'oversupply' of brine in this area. High brine volumes and high pressures promote brine flow through the south face of the panel closures toward the upper waste panel. Both high BHPRM and high BPCOMP promote relatively large amounts of brine to enter the lower waste panel, which, in turn, promotes brine flow up-dip through the south face of the panel closures. The more compressible the Castile formation, the more of its brine will be released through the borehole into the lower waste panel, some transmitted through the closures. BHPRM increases in correlation strength with north-flowing brine between 1200 to 10,000 years and replaces the negative correlation with microbial degradation and halite porosities. This increase in correlation strength is because at 1200 years, the upper borehole plug degrades, causing gas to be evacuated out of the repository, and reducing repository pressures; the extent of this evacuation is a function of BHPRM. Once repository pressures are reduced, brine is more likely to flow into the lower waste panel via anhydrite or borehole drainage, creating a brine oversupply in the lower waste panel, some of which would flow through the panel closures.

5.3.2 Gas Flow

5.3.2.1 *South-Flowing Gas out of the Upper Waste Panels and into the Lower Waste Panels (GASPSORC, GASPSIWC)*

Figure 5.3.3 illustrates the independent variables that most affect lateral south-flowing gas within the panel closures using SRRC analysis.

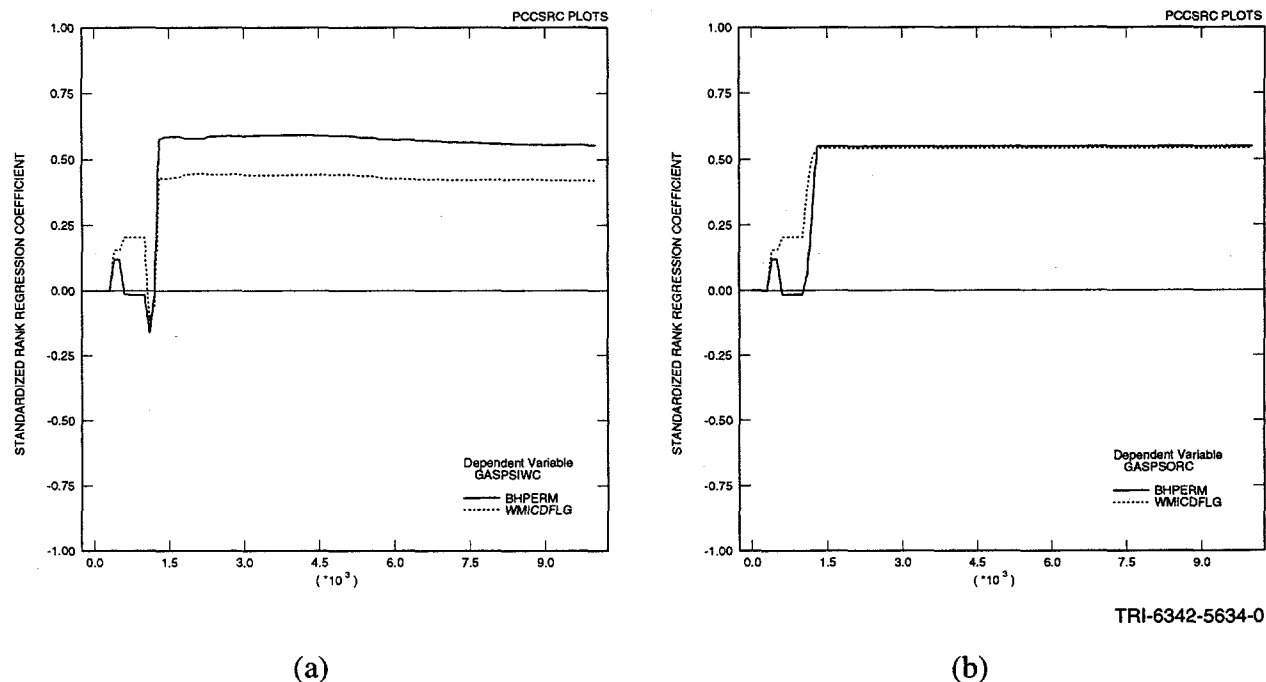


FIGURE 5.3.3. STANDARDIZED RANK REGRESSION COEFFICIENT (SRRC) results showing the most influential independent variables for south-flowing gas (a) into the lower waste panel and (b) out of the upper waste panels

Gas flow in the southerly direction is positively correlated with microbial degradation (a function of WMICDFLG), which is the major gas-producing mechanism at the time of intrusion, and BHPRM, which controls gas flowing out of the repository, toward the borehole. South-flowing gas through the panel closures occurs briefly, as a pulse, when the borehole degrades; this causes a pressure differential, i.e., gradient, between the up- and down-dip portions of the repository. The pressure differential creates a 'gas pulse' from the up-dip regions of the repository towards the borehole. This relatively high pressure gradient is able to overcome capillary threshold pressures assigned to the panel closures, displacing resident brine. The flow carries gas that is 'pushed' through the north face of the panel closures and out the south face.

After the gas pressure wave subsides, a brine pulse follows, originating from the LDRZ. After this brine pulse, the closures remain brine-saturated through the rest of the modeled period. Gas pressures and saturation levels are too low within the DRZ or waste regions to overcome the threshold pressure necessary to displace resident brine. Consequently, gas flow through the closures ceases after ~1500 years.

5.3.2.2 *North-Flowing Gas out of the Lower Waste Panel and into the Upper Waste Panel (GASPSOWC, GASPSIRC)*

Figure 5.3.4 illustrates the independent variables most affecting north flowing gas out of the lower waste panel into the panel closure south face using SRRC analysis.

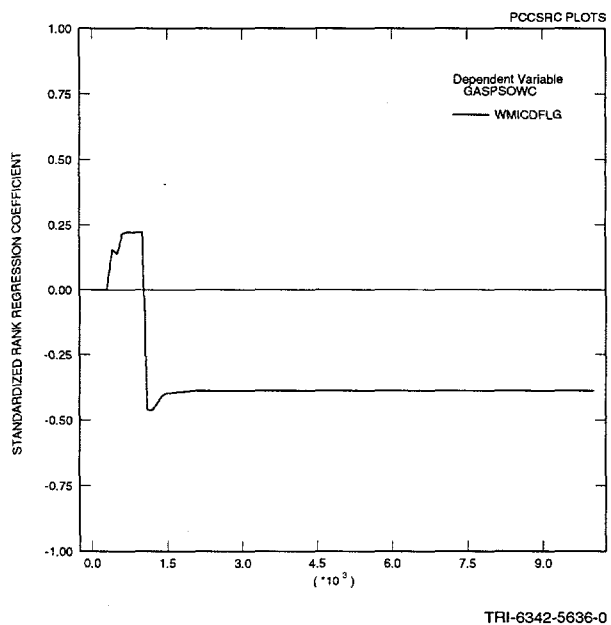


FIGURE 5.3.4. STANDARDIZED RANK REGRESSION COEFFICIENT (SRRC) results showing the most influential independent variable for north-flowing gas out of the lower waste panel

The pulse of north flowing gas from the lower waste panel through the panel closures at 1000 years is positively correlated with WMICDFLG. Those realizations with microbial degradation will have higher gas saturations and higher repository pressures. In combination, these conditions mean the pressure wave will push more gas from the lower to the upper waste panel at the time of intrusion.

No correlation is seen between the sampled parameters and gas flow out of the north face of the panel closures into the upper waste panel.

Intentionally Left Blank

6. Brine and Gas Flow in Lower Disturbed Rock Zone

Vertical and lateral brine and gas flow within and between the LDRZ and regions of the waste disposal area are discussed in this section. Figure 6.1.1 depicts the regions and boundaries where LDRZ flow was evaluated. Three flow boundaries were evaluated for vertical flow and two for lateral flow. For vertical flow, these boundaries were between the LDRZ and the lower waste panel, the bottom of the panel closure separating the two modeled waste regions, and the upper waste panel. Lateral flow was calculated within the LDRZ (parallel to the floor of the waste panels) in the region just below the panel closures. This region was selected in order to determine the extent to which the panel closures may serve as a source or sink between the LDRZ and the two waste disposal areas. (A more detailed evaluation of flow within the panel closures between the two waste disposal areas is discussed in Section 5.)

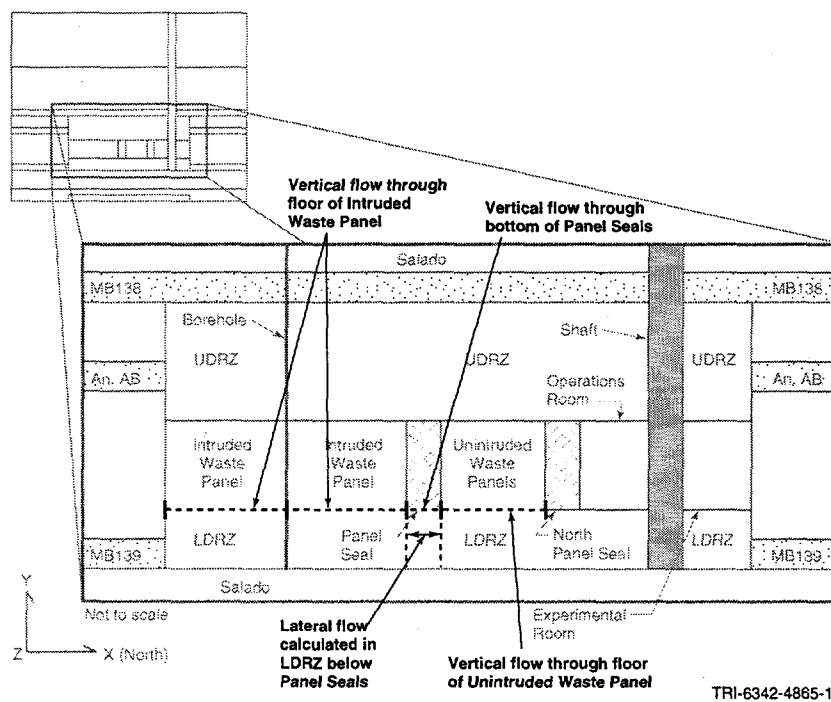


FIGURE 6.1.1. LOCATIONS IN LDRZ AT which lateral and vertical brine and gas flow were assessed

The organization of Section 6 is as follows. Section 6.1 presents those dependent variables defining vertical flow crossing the highlighted boundaries. Following these definitions, hairplots, results for the entire suite of simulations overlaid on one plot, will be presented for each defined dependent variable. These hairplots illustrate the variation in behaviors that may occur for a single dependent variable within the suite of realizations. These plots will be referenced throughout each subsection.

Boxplots for each dependent variable will be presented at the end of Section 6.1. Boxplots present in graphical form values for the mean, median, 25th, and 75th quantiles and outliers within a population. In this way, trends and overall behaviors of each dependent variable throughout the modeled period can be better understood. For this report, boxplot data was taken at four significant times within the modeled period:

- 999 years, just prior to intrusion,
- 1500 years, 300 years after the upper borehole plug degrades,
- 5500 years, approximately midway through the modeled period¹, and
- 10,000 years, the end of the modeled period.

These boxplots will also be referenced throughout Section 6.

Section 6.2 gives a brief overview of LDRZ brine and gas flow throughout the modeled period. Scatterplots to illustrate the relationship between flow in the LDRZ and other processes inside the waste disposal area are presented at the end of this section. Section 6.3 gives the dependent variables most affecting flow in the LDRZ.

¹ Prior examination of several dependent variables within the suite of simulations revealed several processes had settled soon after 5000 years. Therefore, values for dependent variables at 5500, rather than 5000, years were chosen.

6.1 *Variables Used to Define Flow*

6.1.1 **Vertical Flow**

Vertical flow of brine and gas into and out of the lower waste panel north and south of the borehole was also assessed. The dependent variables listed in Table 6.1 relate to vertical flow into the bottom of the lower waste panel. Hairplots defining flow in and out of these regions over the modeled period are given in Figures 6.1.2 through 6.1.5.

Table 6.1. Dependent Variables for Vertical Brine and Gas Flow Into/Out of Lower Waste Panel.
(Note, variable names given on the boxplots are in parenthesis)

Variable	Definition
South of Borehole	
BRBWPSIC (B_BWSI)	Cumulative brine flow (m^3) into bottom of lower waste panel floor south of borehole from LDRZ
BRBWPSOC (B_BWSO)	Cumulative brine flow (m^3) out of bottom of lower waste panel floor south of borehole into LDRZ
GSBWPSIC (G_BWSI)	Cumulative gas flow (m^3) into bottom of lower waste panel floor south of borehole from LDRZ
GSBWPSOC (G_BWSO)	Cumulative gas flow (m^3) out of bottom of lower waste panel floor south of borehole into LDRZ
North of Borehole	
BRBWPNIC (B_BWNI)	Cumulative brine flow (m^3) into bottom of lower waste panel floor north of borehole from LDRZ
BRBWPNOC (B_BWNO)	Cumulative brine flow (m^3) out of bottom of lower waste panel floor north of borehole into LDRZ
GSBWPNIC (G_BWNI)	Cumulative gas flow (m^3) into bottom of lower waste panel floor north of borehole from LDRZ
GSBWPNOC (G_BWNO)	Cumulative gas flow (m^3) out of bottom of lower waste panel floor north of borehole into LDRZ

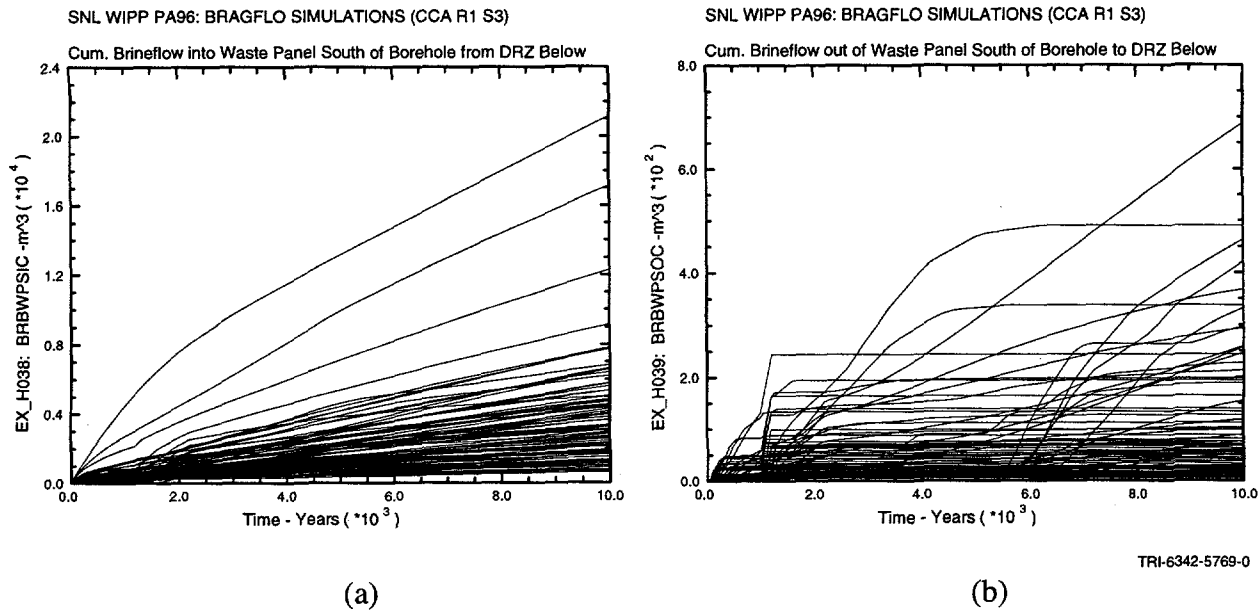


FIGURE 6.1.2. VERTICAL BRINE FLOW (m³) (a) into and (b) out of floor of lower waste panel south of borehole

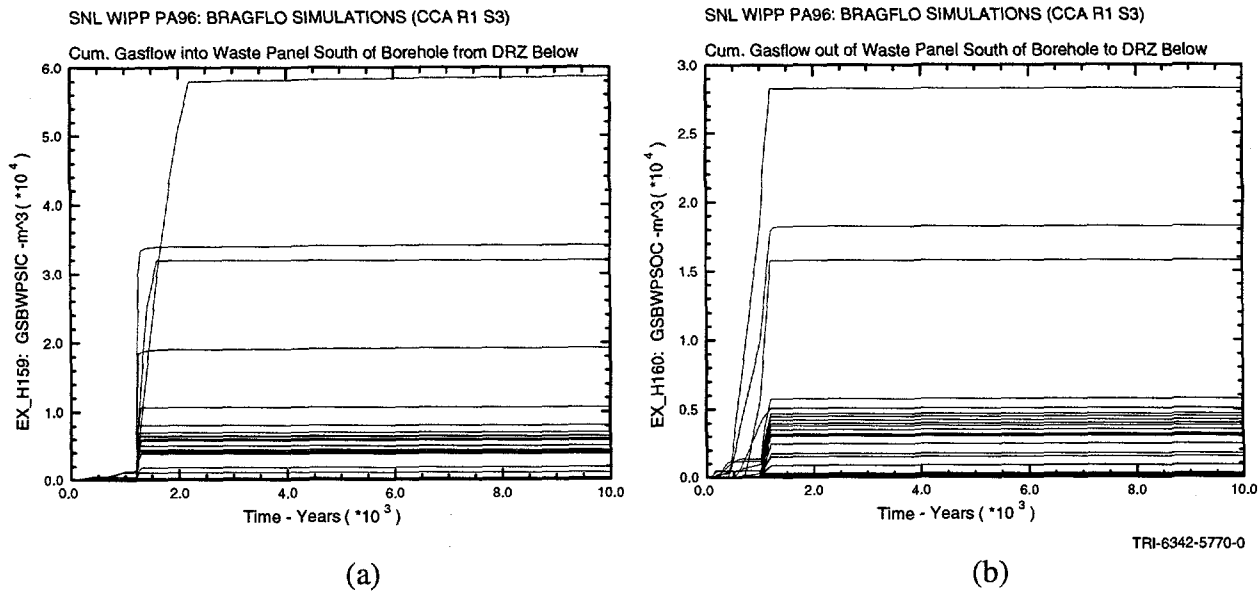


FIGURE 6.1.3. VERTICAL GAS FLOW (m³) (a) into and (b) out of floor of lower waste panel south of borehole

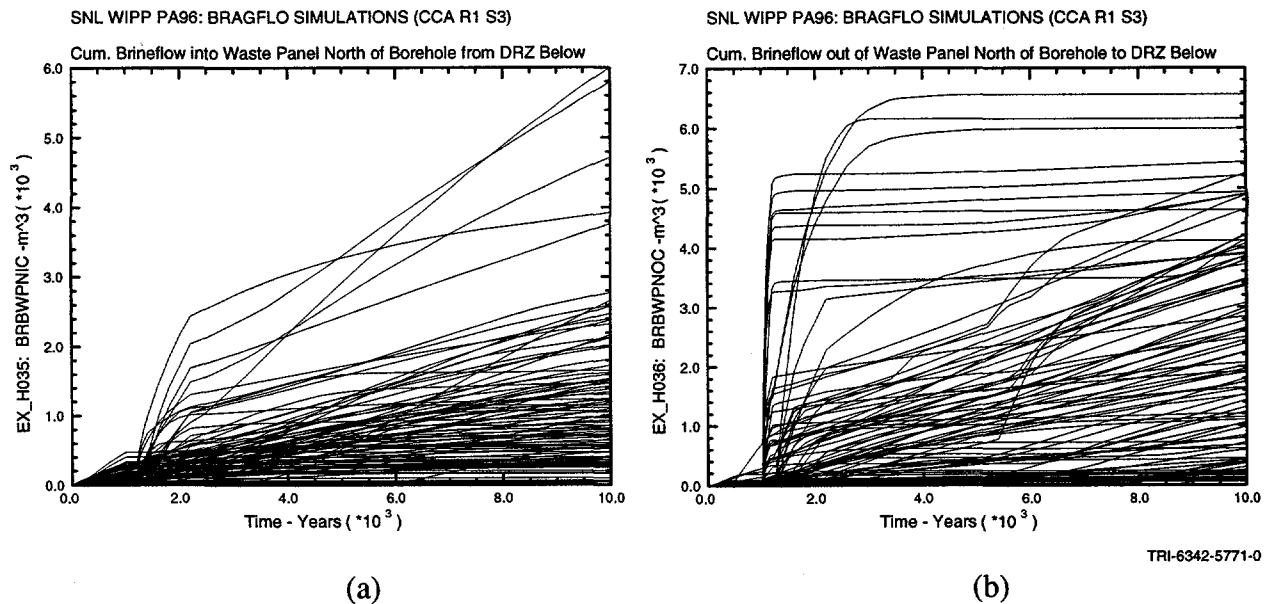


FIGURE 6.1.4. VERTICAL BRINE FLOW (m³) (a) into and (b) out of floor of lower waste panel north of borehole

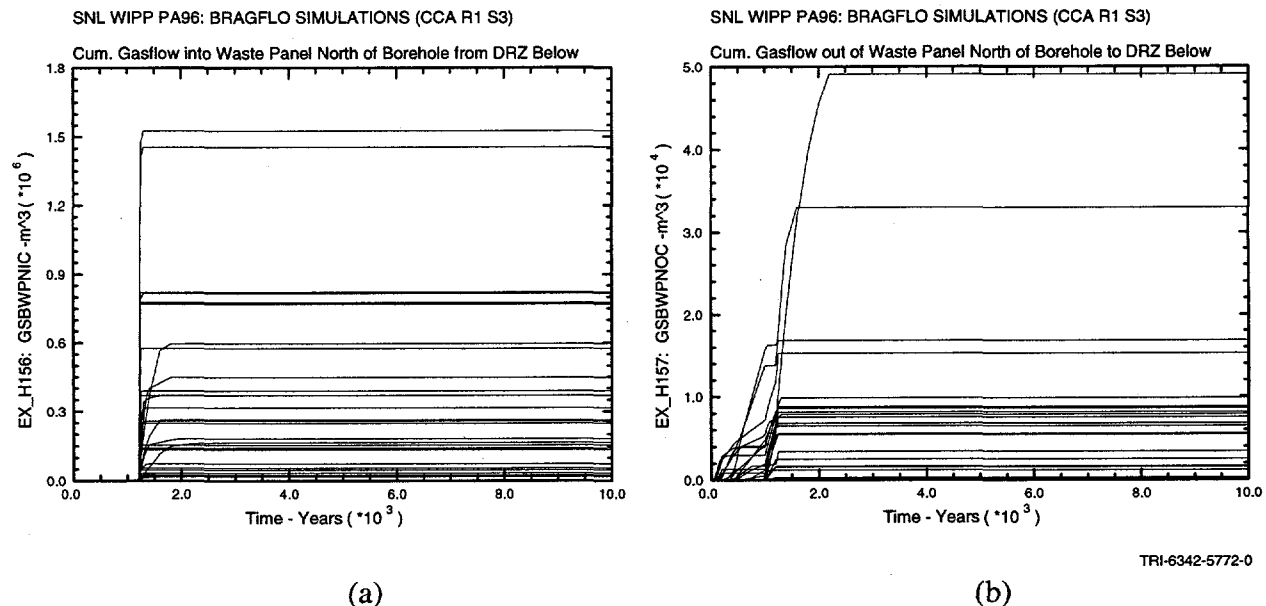


FIGURE 6.1.5. VERTICAL GAS FLOW (m³) (a) into and (b) out of the floor of lower waste panel north of borehole

Vertical flow into and out of the bottom of the upper waste panel and into and out of the bottom of the panel closures is defined by the dependent variables listed in Table 6.2. Hairplots defining flow in and out of these regions over the modeled period are given in Figures 6.1.6 and 6.1.9.

Table 6.2. Dependent Variables for Vertical Brine and Gas Flow Into/Out of Upper Waste Panel and Panel Closures (note variable names shown on boxplots are abbreviated and given in parenthesis)

Variable	Definition
Panel Closures	
BRNUBPSC (BRUBPS)	Cumulative brine flow (m^3) into bottom of panel closures from LDRZ
BRNDBPSC (BRDBPS)	Cumulative brine flow (m^3) out of the bottom of panel closures into LDRZ
GASUBPSC (GSUBPS)	Cumulative gas flow (m^3) into bottom of panel closures from LDRZ
GASDBPSC (GSDBPS)	Cumulative gas flow (m^3) out of bottom of panel closures into LDRZ
Upper Waste Panel	
BRN_URBC (B_UBBC)	Cumulative brine flow (m^3) through upper waste panel floor from LDRZ
BRN_DRBC (B_DRBC)	Cumulative brine flow (m^3) down into the LDRZ from the upper waste panel floor
GAS_URBC (G_URBC)	Cumulative gas flow (m^3) through upper waste panel floor from LDRZ
GAS_DRBC (G_DRBC)	Cumulative gas flow (m^3) down into LDRZ from upper waste panel floor

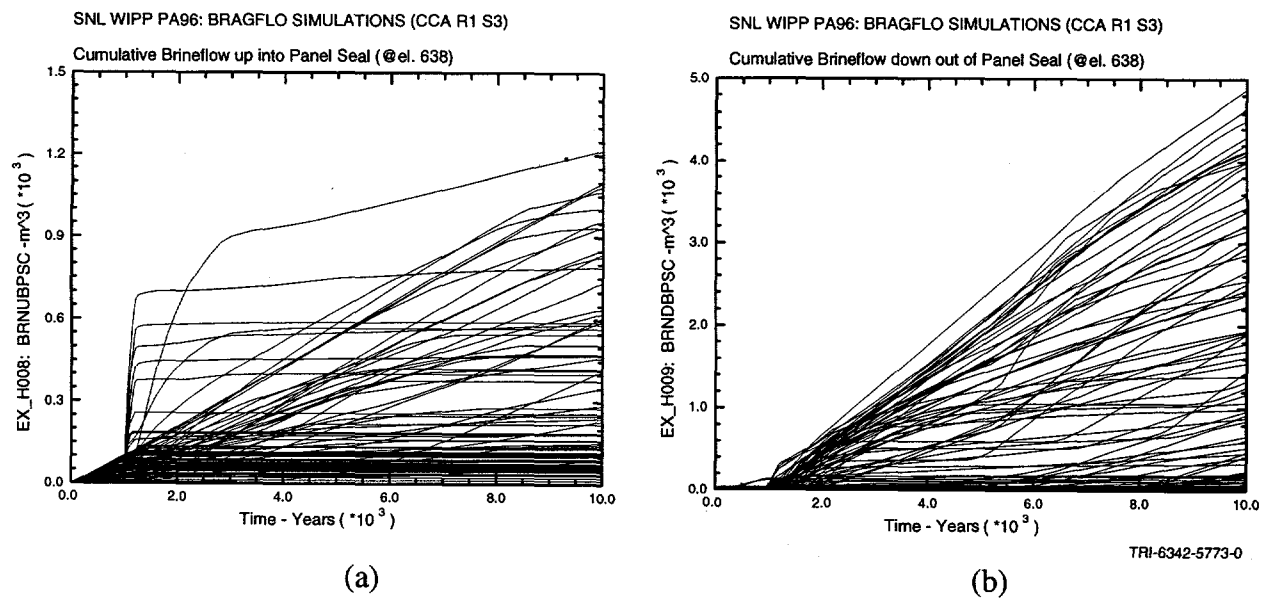


FIGURE 6.1.6. VERTICAL BRINE FLOW (m^3) (a) into and (b) out of bottom of panel closures

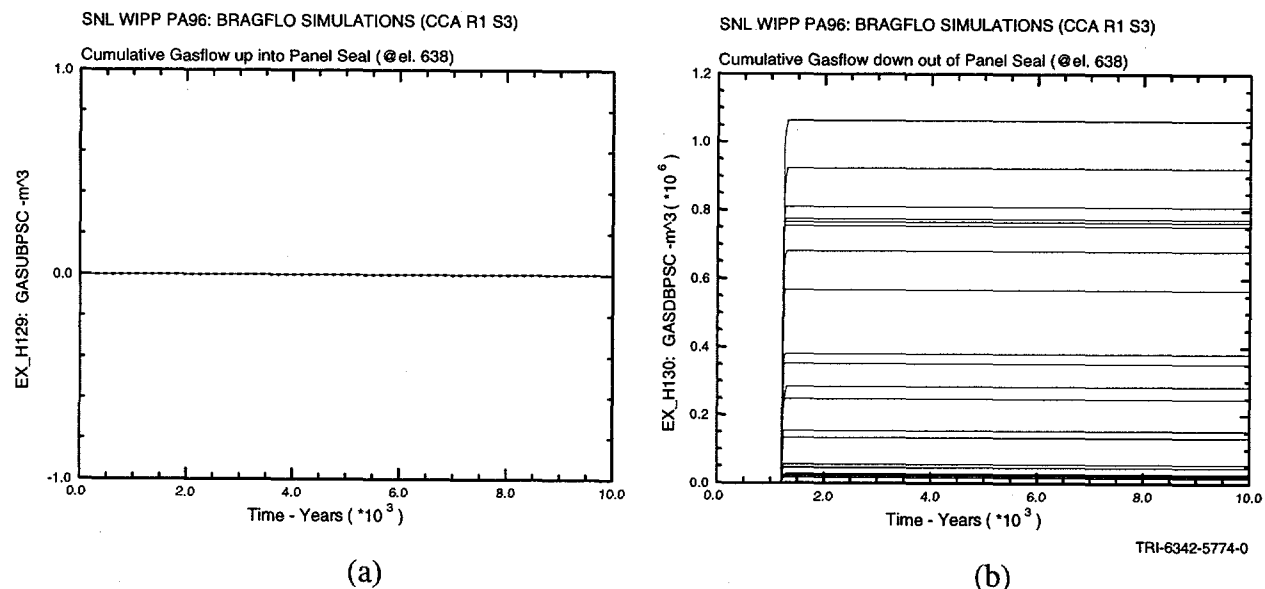


FIGURE 6.1.7. VERTICAL GAS FLOW (m^3) (a) into and (b) out of bottom of panel closures

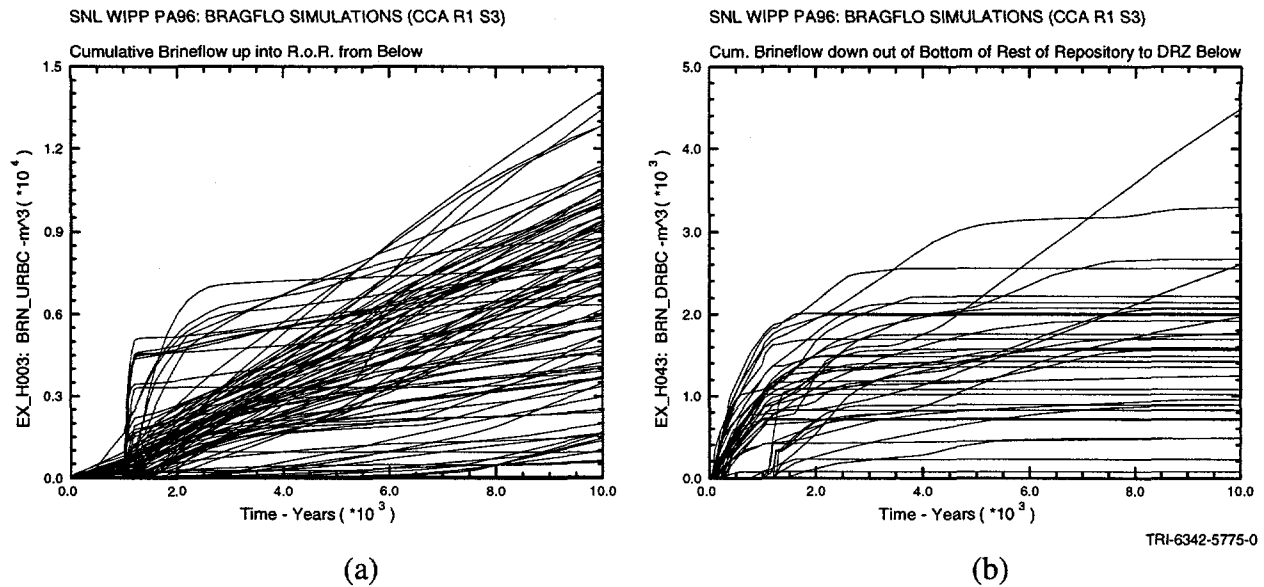


FIGURE 6.1.8. VERTICAL BRINE FLOW (m³) (a) into and (b) out of upper waste panel floor

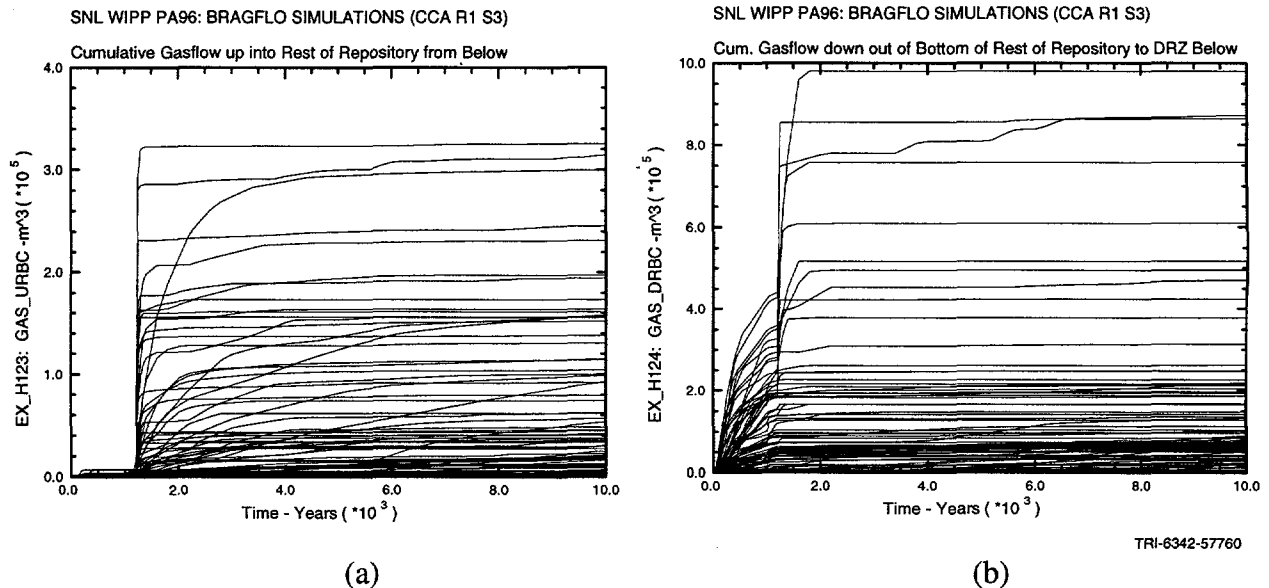


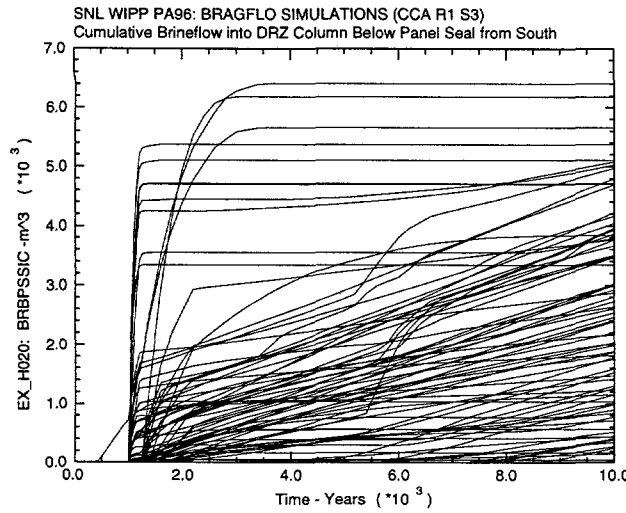
FIGURE 6.1.9. VERTICAL GAS FLOW (m³) (a) into and (b) out of upper waste panel floor

6.1.2 Lateral Flow

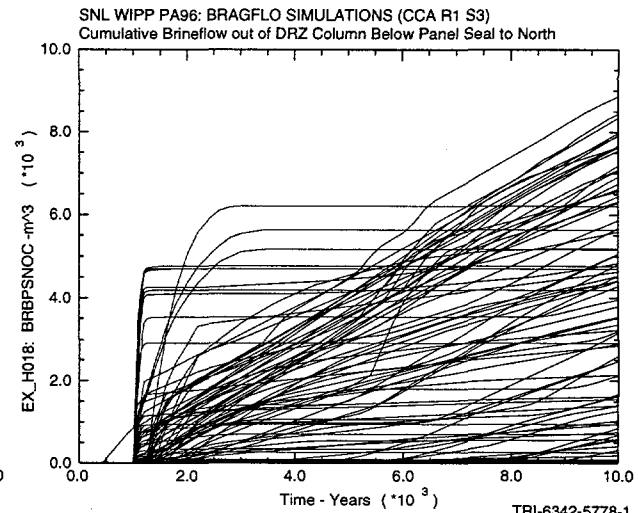
Lateral flowing fluid within the LDRZ in the region just below the panel closures is defined by the variables listed in Table 6.3. Hairplots defining flow in and out of these regions over the modeled period are given in Figures 6.1.10 through 6.1.13. Boxplots for vertical brine and gas flow through the floor of the upper and lower waste panel are presented in Figures 6.1.14 through 6.1.17. Boxplots for lateral brine and gas flow in the LDRZ crossing the area under the panel closures are presented in Figures 6.1.18 and 6.1.19.

Table 6.3. Dependent Variables for Lateral Brine and Gas Flow Below Panel Closures (note variable names shown on boxplots are abbreviated and given in parenthesis)

Variable	Definition
North Flowing	
BRBPSSIC (BBPSSI)	Cumulative brine flow (m^3) north in LDRZ, crossing boundary just below south side of panel closures
BRBPSNOC (BBPSNO)	Cumulative brine flow (m^3) flow north in LDRZ, crossing boundary just below north side of panel closures
GSBPSSIC (GBPSSI)	Cumulative gas flow (m^3) flow north in LDRZ, crossing boundary just below south side of panel closures
GSBPSNOC (GBPSNO)	Cumulative gas flow (m^3) flow north in LDRZ, crossing boundary just below north side of panel closures
South Flowing	
BRBPSNIC (BBPSNI)	Cumulative brine flow (m^3) flow south in LDRZ, crossing boundary just below north side of panel closures
BRBPSSOC (BBPSSO)	Cumulative brine flow (m^3) flow south in LDRZ, crossing boundary just below south side of panel closures
GSBPSNIC (GBPSNI)	Cumulative gas flow (m^3) flow south in LDRZ, crossing boundary just below north side of panel closures
GSBPSSOC (GBPSSO)	Cumulative gas flow (m^3) flow south in LDRZ, crossing boundary just below south side of panel closures

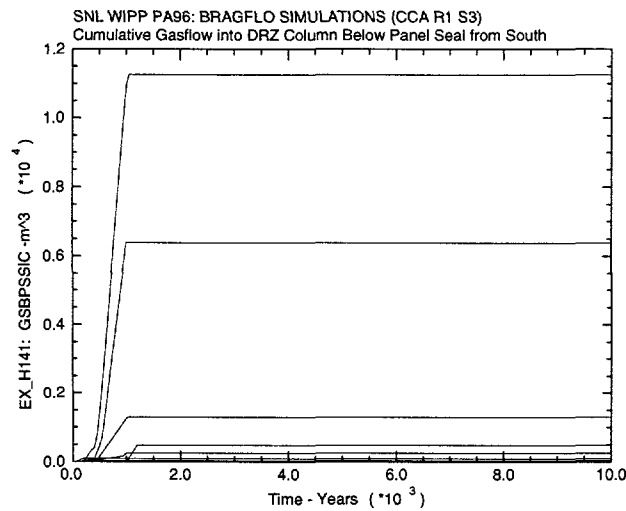


(a)

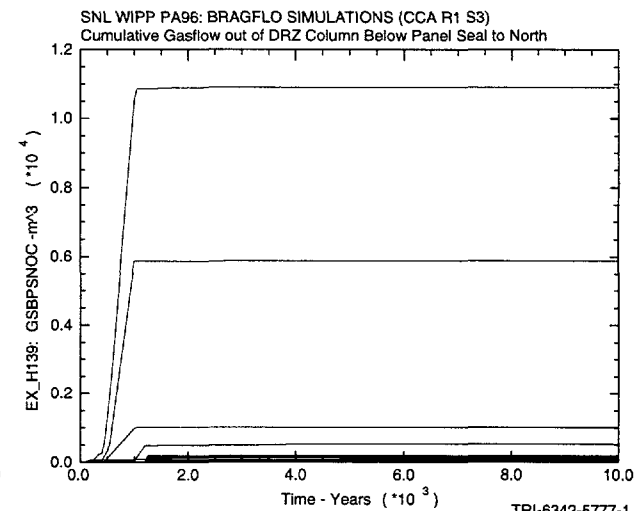


(b)

FIGURE 6.1.10. LATERAL NORTH-FLOWING BRINE (m^3) in the LDRZ flowing in the area (a) south and (b) north of the panel closures

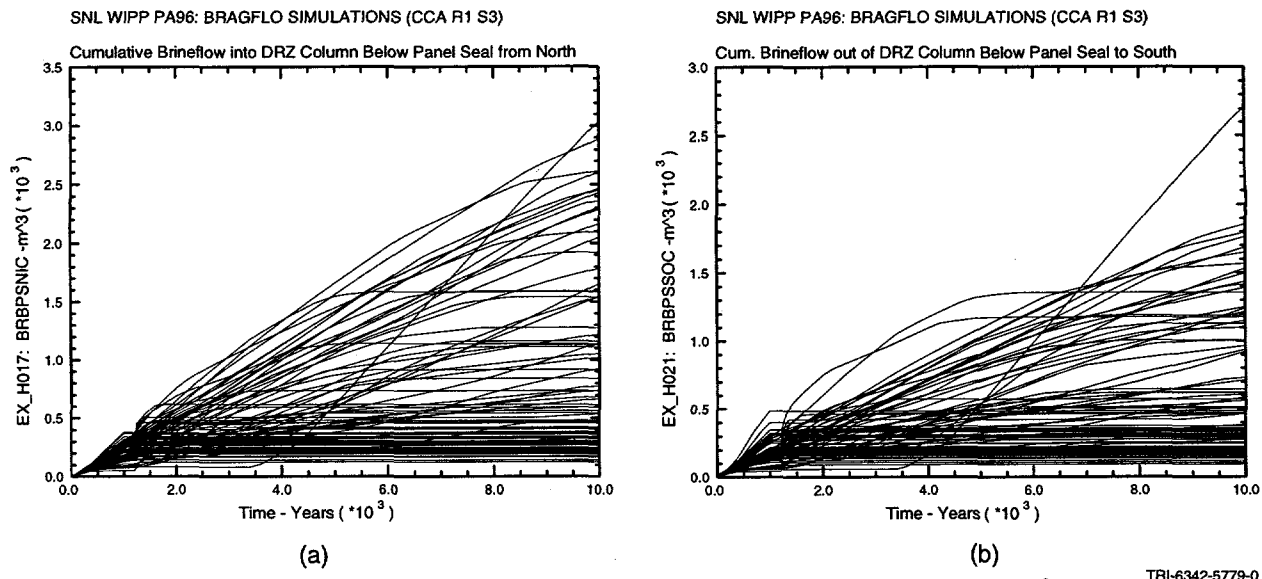


(a)



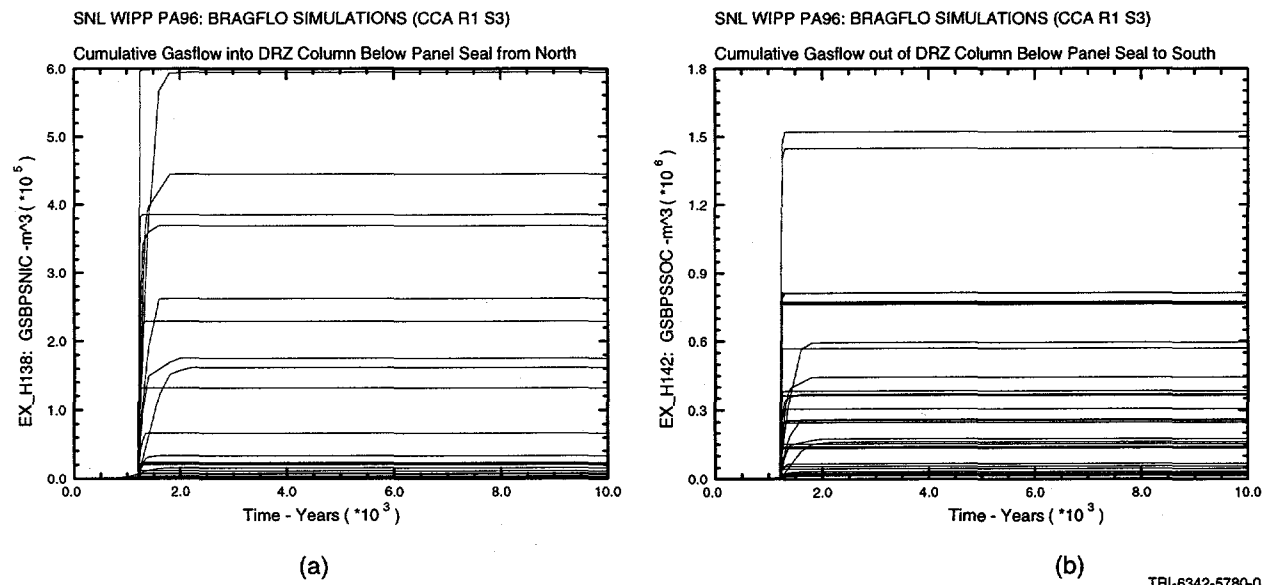
(b)

FIGURE 6.1.11. LATERAL NORTH-FLOWING GAS (m^3) in the LDRZ below (a) south side of panel closures and (b) north side of panel closures



TRI-6342-5779-0

FIGURE 6.1.12. LATERAL SOUTH-FLOWING BRINE (m³) in the LDRZ below (a) north side of panel closures and (b) south side of panel closures



TRI-6342-5780-0

FIGURE 6.1.13. LATERAL SOUTH-FLOWING GAS (m³) in the LDRZ below (a) north side of panel closures and (b) south side of panel closures

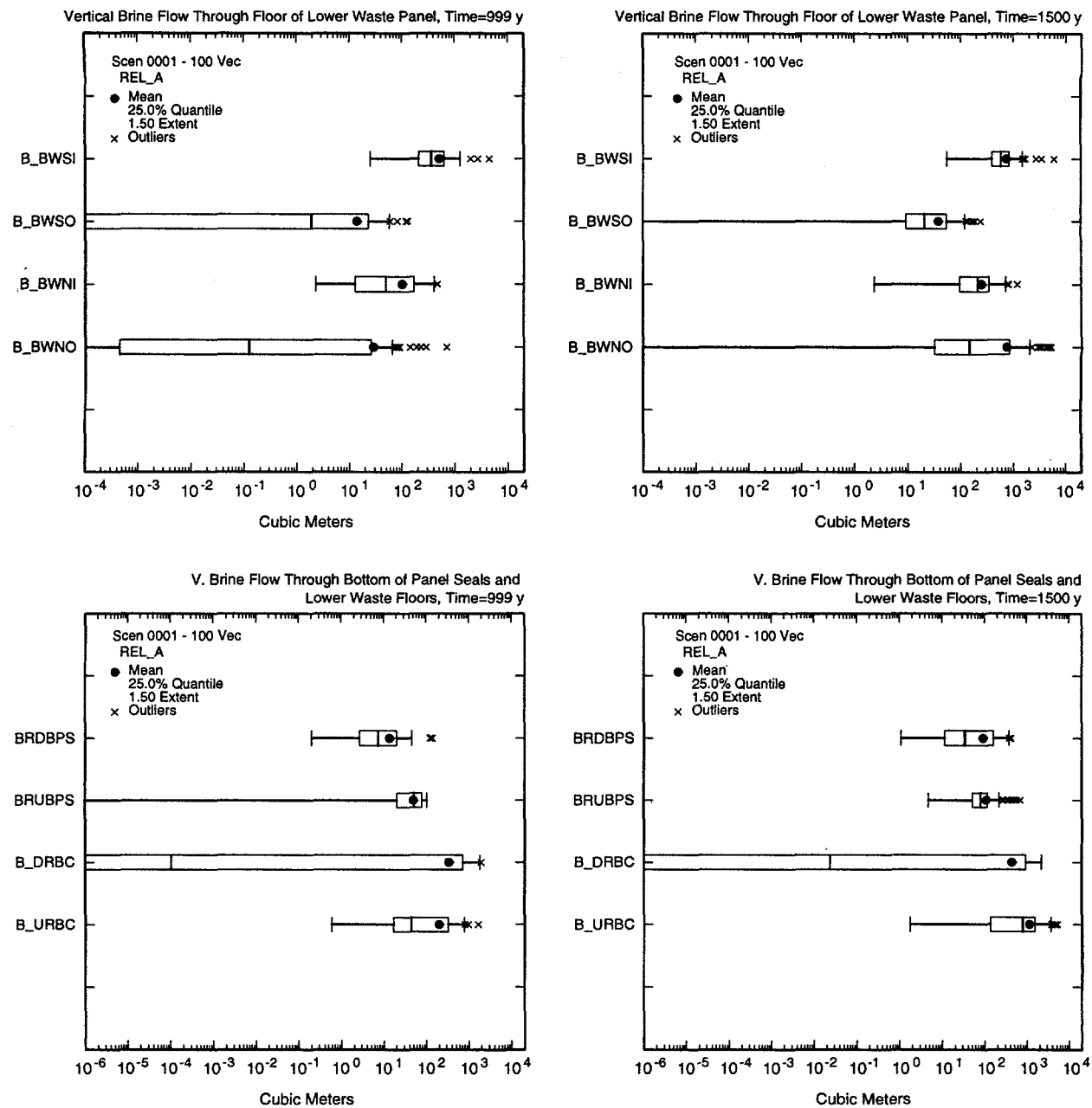
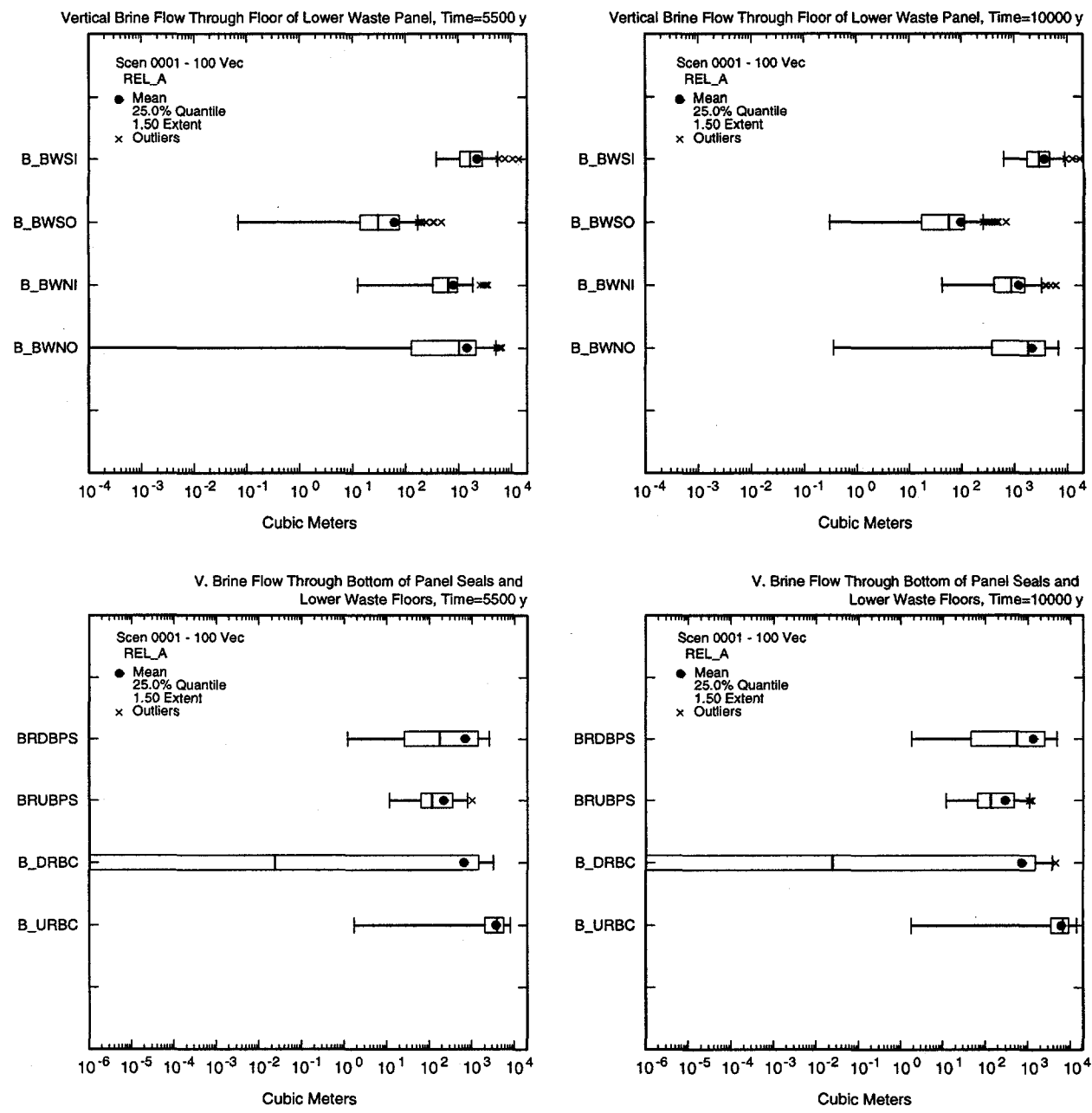
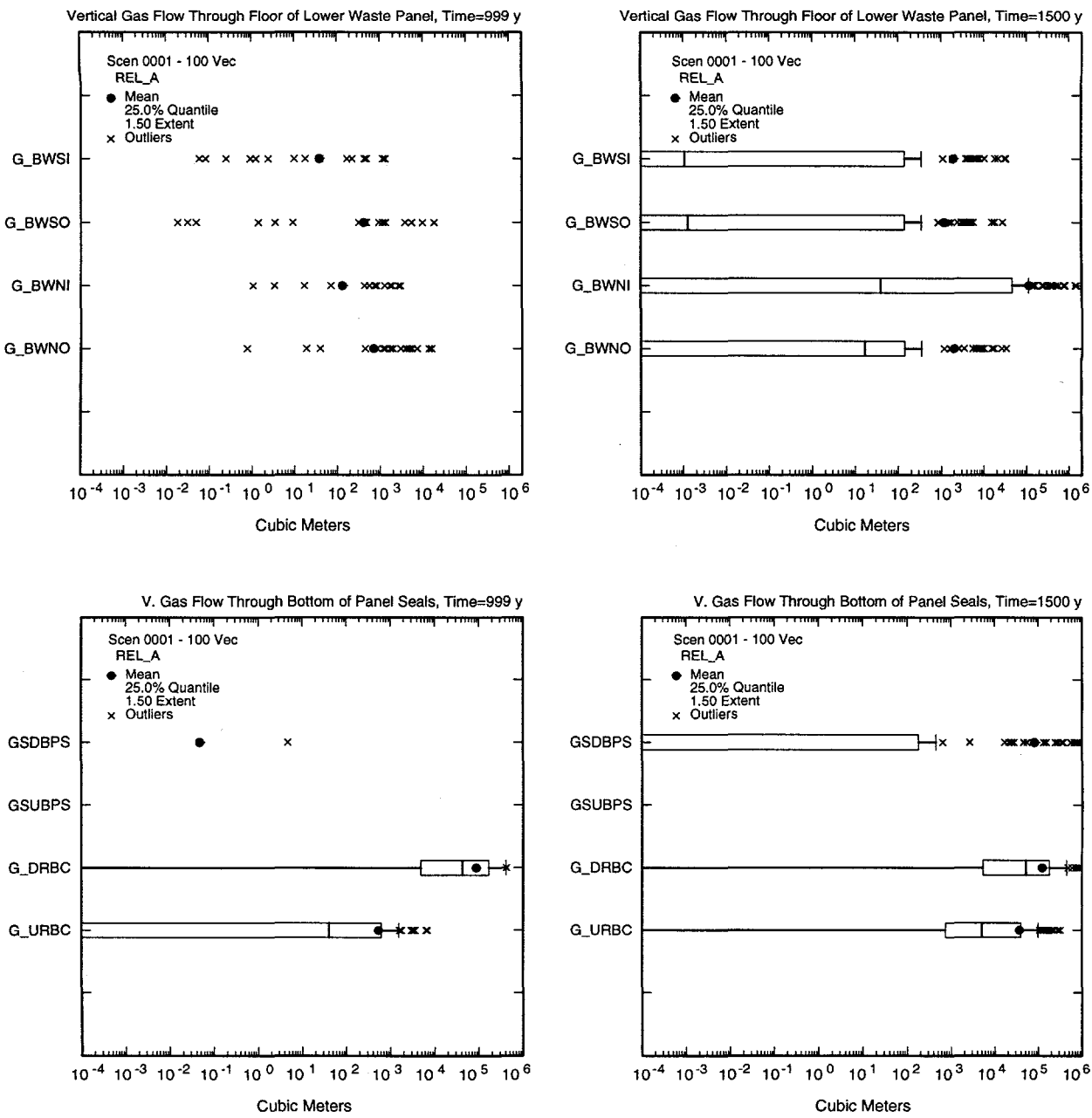


FIGURE 6.1.14. BOXPLOTS FOR VERTICAL BRINE flow through south and north halves of lower waste panel floor (top plots); and through the bottom of the panel closures and floor of the upper waste panel. Boxplots show flow at 999 and 1500 years



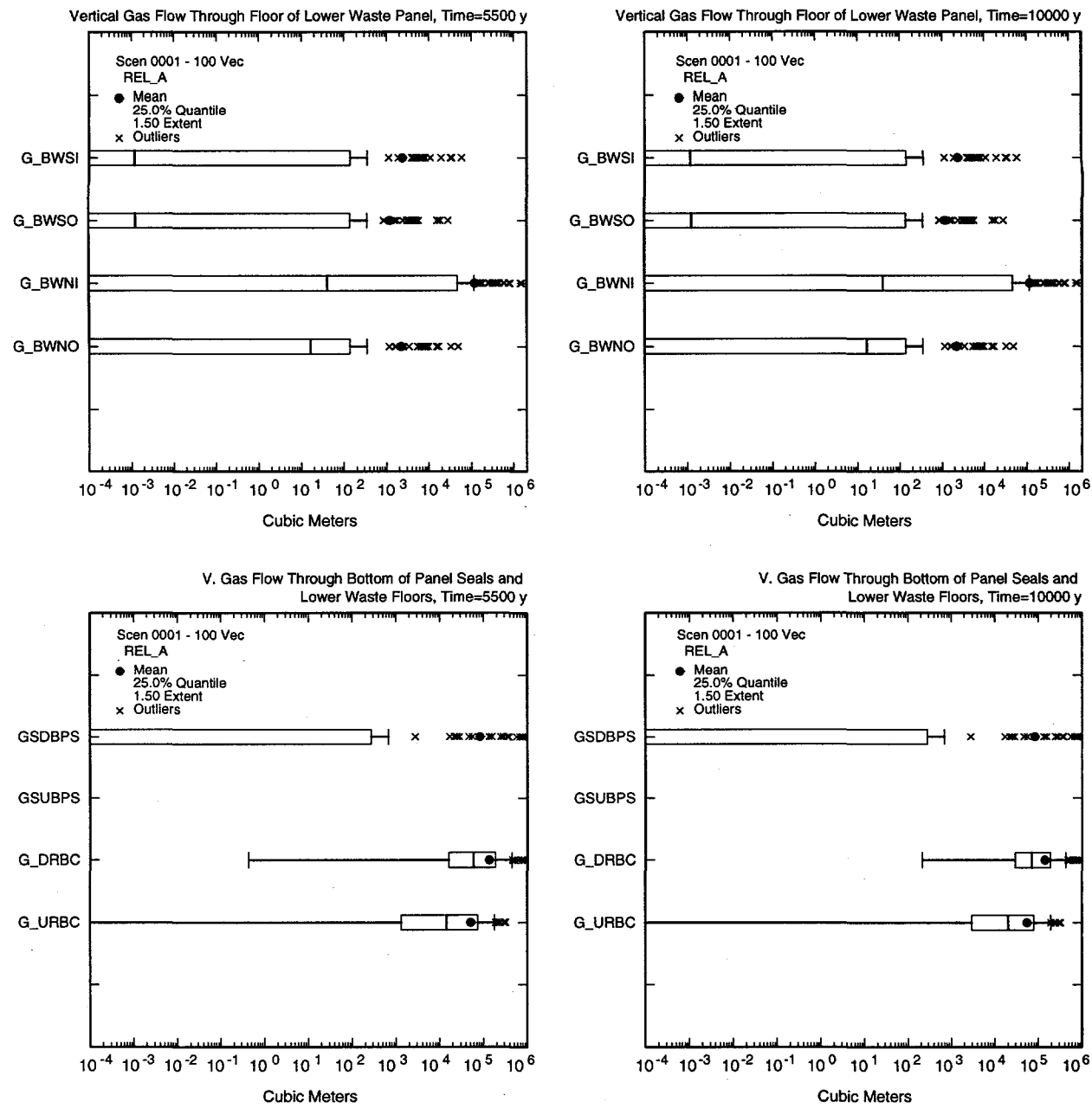
TRI-6342-5781-1b

FIGURE 6.1.15. BOXPLOTS FOR VERTICAL BRINE flow through south and north halves of lower waste panel floor (top plots); and through the bottom of the panel closures and floor of the upper waste panel. Boxplots show flow at 5500 and 10,000 years



TRI-6342-5782-1a

FIGURE 6.1.16. BOXPLOTS FOR VERTICAL GAS flow through the south and north halves of the lower waste panel (top plots); and through the bottom of the panel closures and floor of the upper waste panel. Boxplots show flow at 999 and 1500 years



TRI-6342-5782-1b

FIGURE 6.1.17. BOXPLOTS FOR VERTICAL GAS flow through the south and north halves of the lower waste panel (top plots); and through the bottom of the panel closures and floor of the upper waste panel. Boxplots show flow at 5500 and 10,000 years

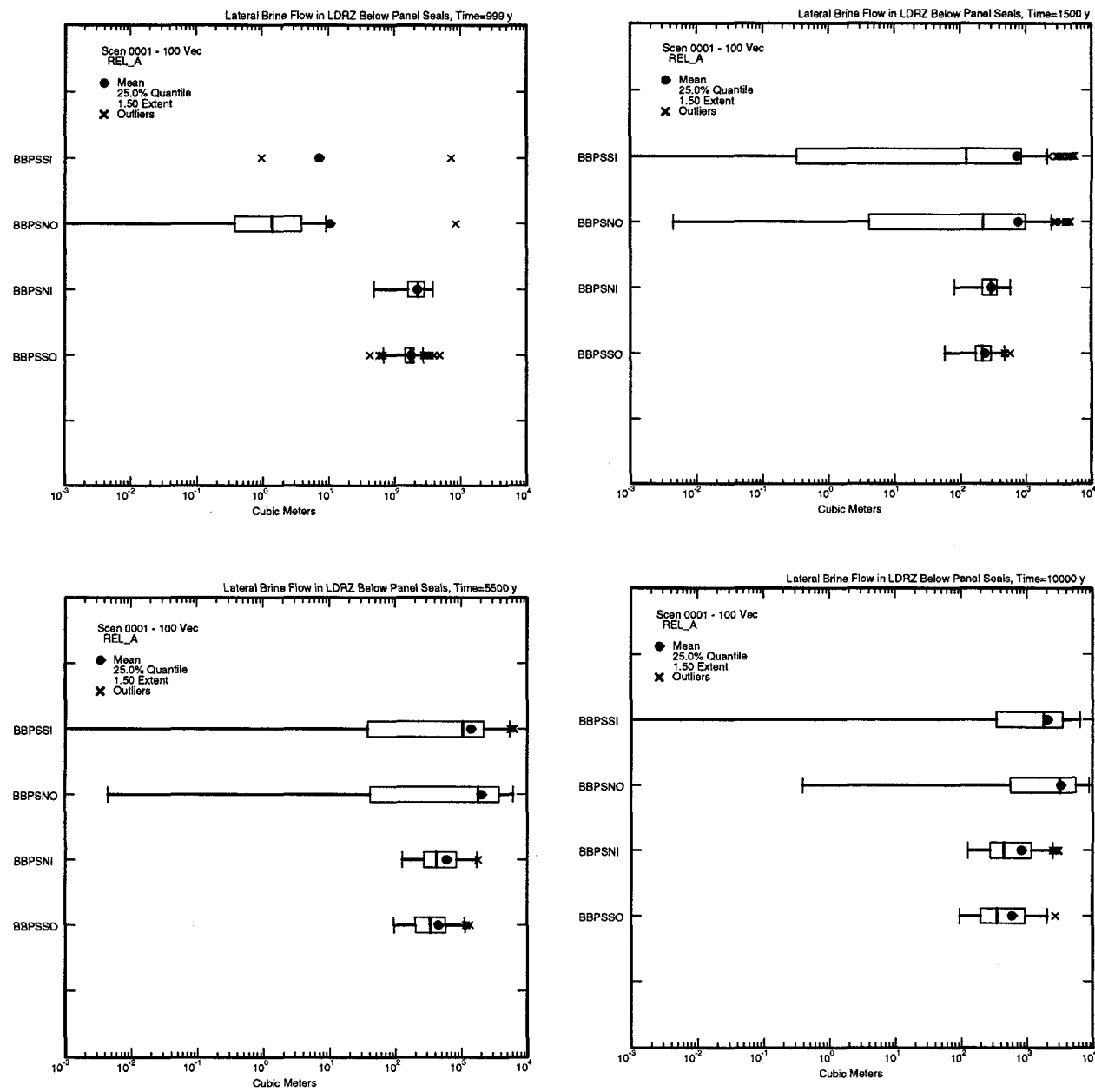
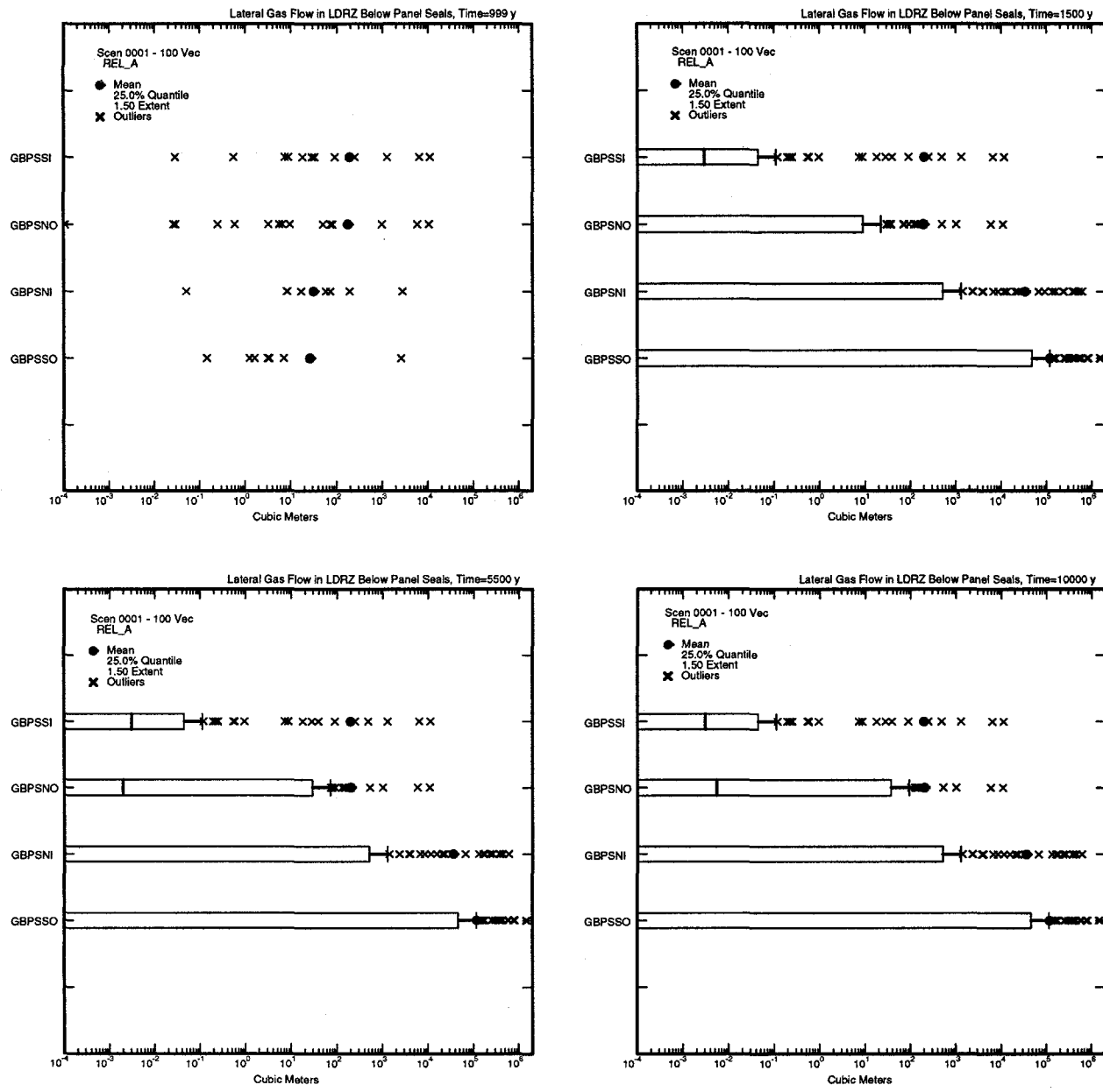


FIGURE 6.1.18. BOXPLOTS FOR LATERAL BRINE flow in LDRZ crossing the area under the panel closures. Boxplots show flow taken at 999, 1500, 5500, and 10,000 years

TRI-6342-5783-0



TRI-6342-5784-0

FIGURE 6.1.19. BOXPLOTS FOR LATERAL GAS flow in LDRZ crossing the area under the panel closures. Boxplots show flow taken at 999, 1500, 5500, and 10,000 years

6.2 Summary of Brine Flow in LDRZ

6.2.1 Flow Prior to Time of Intrusion

Brine Flow

For the first few hundred years after repository closure, repository pressures are much lower than in the host rock. This creates pressure gradients between the two DRZ regions, which promote *vertical* brine flow downward from the UDRZ, through the excavated areas, toward the LDRZ. In the lower waste panel, vertical downward drainage into the LDRZ lasts only a few hundred years; for the upper waste panels, downward brine flow continues up until the time of intrusion, long after downward flow has ceased in the lower waste panel (compare Figures 6.1.2 and 6.1.4, left side, with Figure 6.1.8, left side). Generally, lateral brine flow is predominantly southward prior to intrusion; north-flowing brine is nonexistent in all but one realization, which had the highest assigned value for anhydrite permeability (see hairplots given in Figures 6.1.10 and 6.1.12).

As brine vertically drains into the LDRZ, its flow direction is deflected laterally southward at the interface of the less permeable undisturbed halitic host rock. From here, brine that drained through the excavated region joins south-flowing brine drained from the anhydrite layers (notably direct brine drainage from 'north' MB 139).

For those realizations with low DRZ volumes (a function of halite porosity), as south-flowing brine passes under the panel closures, some preferentially flows upward through the closure bottom and is then deflected down-dip (southward) into the lower waste panel.

Drainage into the LDRZ from the panel closures is predominantly downward for the majority of realizations (see boxplots in Figure 6.1.14). Realizations with high assigned values for halite porosity will have more brine flow downward through the panel closures to the LDRZ, and is enhanced for realizations with no gas production from microbial degradation.

As brine flows through the LDRZ voids,² it moves upward through the waste panel floors. Because the south half of the lower waste panel is down-dip *and* abuts south MB 139, the total volume of brine that moves upward through the lower waste panel 'south' floor is far greater than the volume of the north side of the lower waste panel, ranging from 2 to 10 times greater (see Figure 6.2.1 and boxplots for brine flow taken at 999 years in Figure 6.1.14).

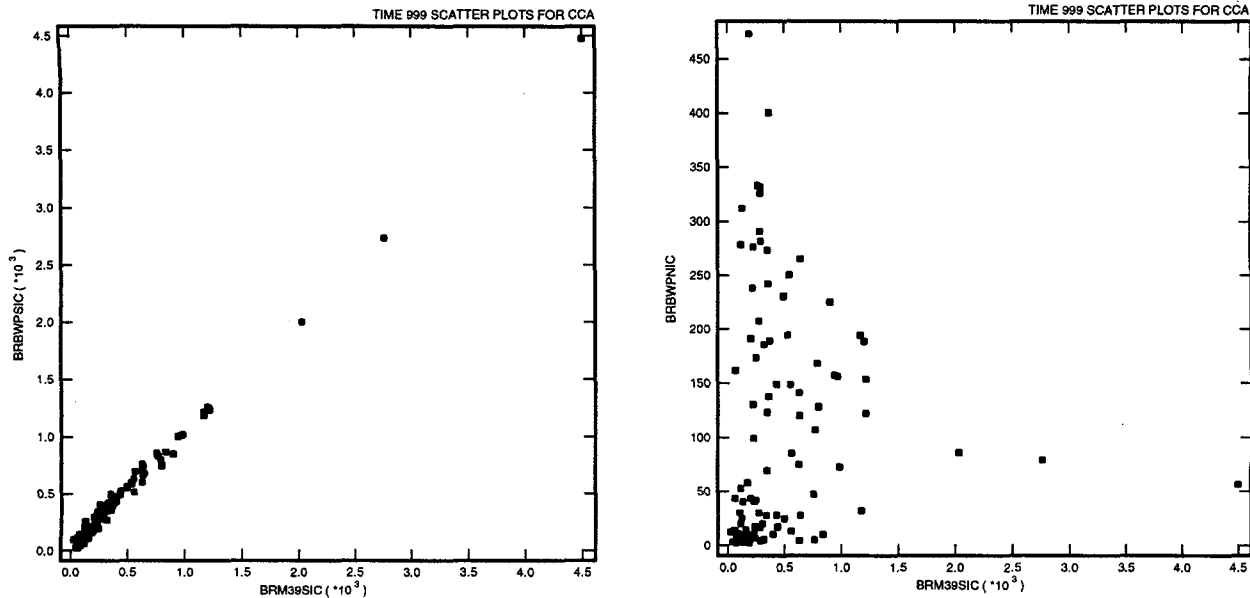
Those realizations that have relatively large volumes of gas generated (predominantly from microbial degradation) and high assigned values for waste residual brine saturation will have lower effective brine permeabilities within the waste regions. Consequently, these realizations will have less brine drainage from the waste panels downward into the LDRZ (despite large volumes of brine draining into the waste panels from the UDRZ) (see Figure 6.2.2), less south-flowing brine, and less brine that 'backs up' within the LDRZ, which then re-enters upward through the waste region floors later in the modeled period. Additionally, realizations with microbial gas generation tend to have higher repository pressures. As repository pressures increase, the pressure gradient between the repository and host rock decreases. The decline in this gradient inhibits brine drainage from the adjoining host rock. Consequently, an inverse relationship is seen between brine seepage back up from LDRZ to the waste panels and repository pressure (see Figure 6.2.3).

Gas Flow

The hairplots given in Figures 6.1.7, 6.1.9, 6.1.11, and 6.1.13 and the boxplots given in Figure 6.1.15 show the gas flow in the LDRZ is predominantly downward, and occurs mainly from the upper waste panels. Some realizations do have gas entering the LDRZ from the lower waste panel.

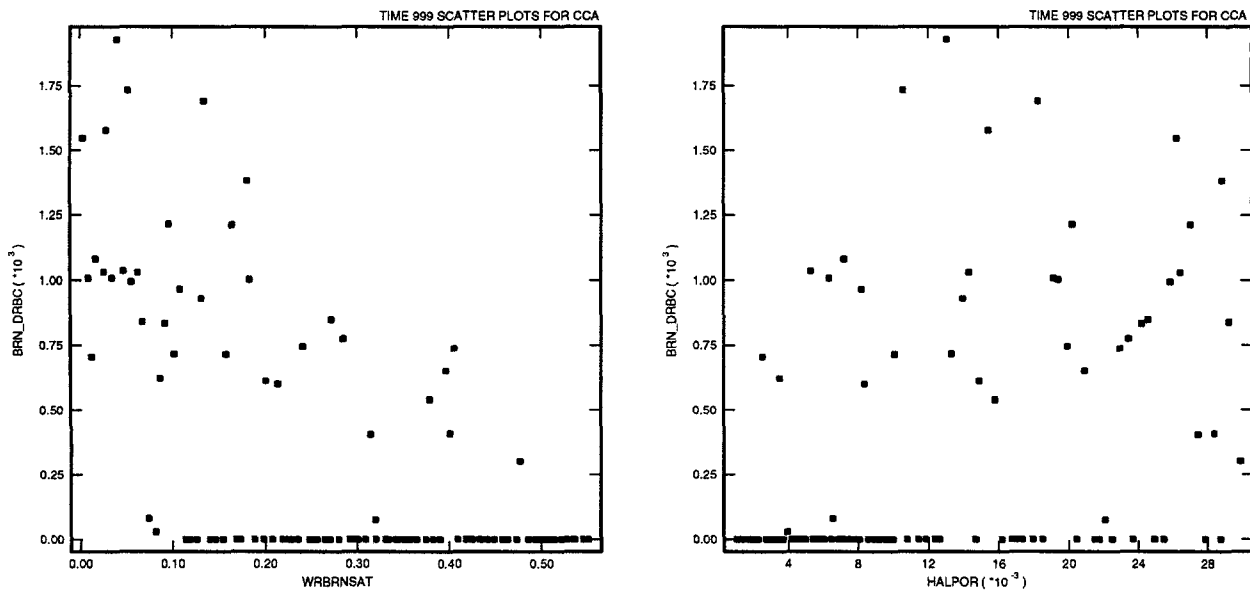
As the gas produced accumulates in the excavated areas, gas pressures increase, for many realizations, to values greater than those in the LDRZ. For these realizations, gas is pushed downward into the LDRZ through the waste region floors and, for some realizations, moves northward (up-dip) towards the most northern portions of the repository (see Figure 6.2.4). This

² As discussed in Section 3, DRZ void volumes increase after repository closure due to an increase in pressure.



TRI-6342-5798-0

FIGURE 6.2.1. SCATTERPLOTS FOR BRINE FLOW at 999 years out of MB 139 lying south of the repository to the LDRZ (BRM39SIC) and flow upward through the south floor and north floor of the lower waste panel, BRBWPNC and BRBWPNC, respectively. These plots show brine flow from south MB 139 predominantly flows up through the south waste panel floor rather than the north floor



TRI-6342-5799-0

FIGURE 6.2.2. SCATTERPLOTS FOR BRINE DRAINAGE from the upper waste panel floor to the LDRZ (BRN_DRBC) at 999 years, with respect to residual brine saturation (WRBRNSAT) and halite porosity (HALPOR). The above plots show that more brine flows out the waste panel floor for those realizations assigned low values for WRBRNSAT; brine flow to the LDRZ from the upper waste panel is less sensitive to HALPOR values

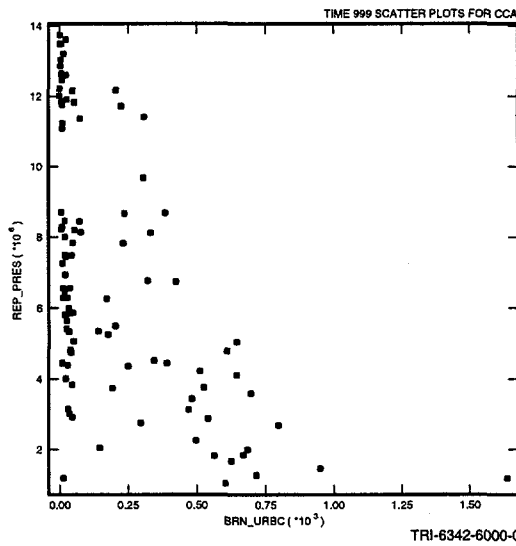


FIGURE 6.2.3. SCATTERPLOTS FOR UPWARD BRINE flow from the LDRZ through the upper waste panel floor (BRN_URBC) with respect to upper waste panel pressure (REP_PRES) at 999 years. The above plot shows realization with low repository pressure tend to have more brine flow from the LDRZ through the lower waste panel floor

is most likely to occur for those realizations with gas generated from microbial degradation and relatively small DRZ volumes (a function of halite porosities) coupled with medium to high iron corrosion rates. Lateral-flowing gas in a southerly direction is nonexistent prior to intrusion.

More gas flows through the floor of the up-dip waste panel than through the down-dip waste panel because less brine accumulates in the up-dip location of the repository. In gravity segregation, the less dense fluid (gas) will flow up-dip, with the denser fluid (water) flowing down-dip. Also the up-dip waste panel has a larger floor surface, and so the relative size and location of the up-dip waste panel means that more void volume is available for gas storage as it migrates up-dip in the UDRZ from the lower waste panel.

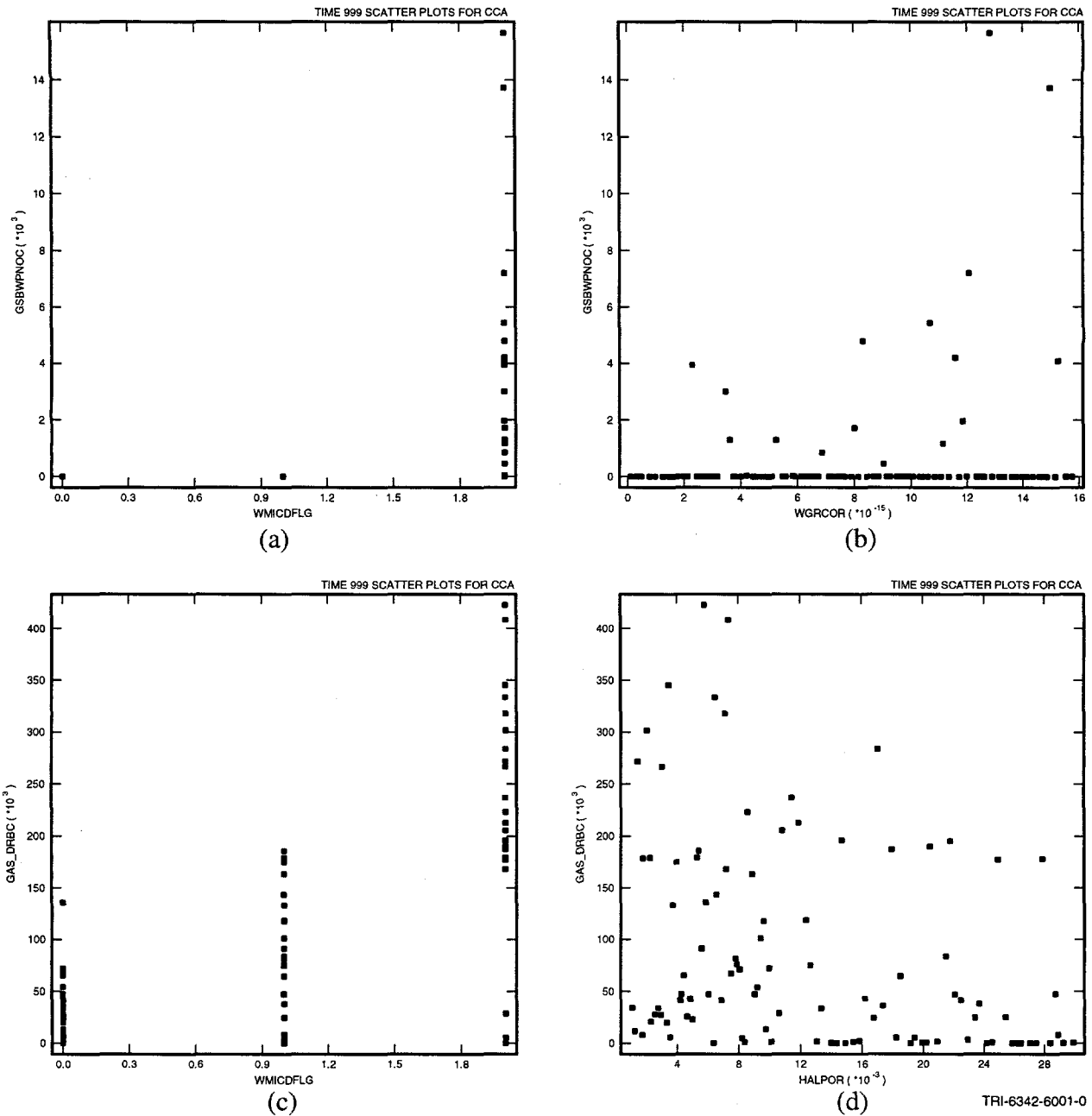


FIGURE 6.2.4. SCATTERPLOTS FOR GAS FLOW downward to the LDRZ from the floor of the north half of the lower waste panel (GSBWPNOC) with respect to iron corrosion rates (WGRCOR) and microbial degradation (WMICDFLG > 0); gas flow into the floor of the upper waste panels (GAS_DRBC), with respect to halite porosity (HALPOR). The top two plots show that realizations with gas generation from microbial degradation and high iron corrosion rates will have more gas flowing into the LDRZ. The bottom plots show those realizations with gas generated from microbial degradation coupled with low values for HALPOR will tend to have gas flow down from the upper waste panels to the LDRZ

6.2.2 Flow After Intrusion

For the majority of realizations at the time of repository intrusion, 1000 years, an upward and northward brine pulse is introduced in the LDRZ. The pulse is caused by a pressure differential between the lower Castile brine reservoir and the repository, creating a pressure pulse propagating up through the borehole, which pushes brine through the LDRZ. For cases where Castile compressibilities are high, the pressure pulse introduces Castile brine into the LDRZ with some flowing upward through the north and south floors of the lower waste panel. A portion of this brine flows up-dip in the LDRZ passing below the panel closures; some is partitioned upward through the bottom of the closures; and the remainder flows north passing under and up through the floor of the upper waste panel. For many realizations, the brine surge lasts only a few hundred years between intrusion and upper borehole degradation.

For the few realizations with brine reservoir pressures lower than repository pressures, a pulse of brine flows downward through the waste panel floors and out the bottom of the panel closure to the LDRZ, heading towards the borehole.

When the upper borehole plug degrades at 1200 years, a pathway is created between the units above and below the repository. This pathway creates another pressure pulse, which propagates a second brine surge through the LDRZ. At this time, both lateral and vertical brine flow direction in the LDRZ and panel closures become most dependent on borehole permeability values, rather than repository or the lower reservoir properties and conditions. For the drainage through the panel closures, realizations assigned relatively high values for borehole permeability will generally have downward flowing brine out of the panel closure bottoms to the LDRZ; conversely, realizations with low borehole permeabilities will have more upward flow direction from the LDRZ through the closure bottoms. Brine that flows downward from the panel closures to the LDRZ will tend to flow in the LDRZ up-dip towards the upper waste panel. From the LDRZ, brine moves upward through the floor of the upper waste panel (see Figure 6.2.5).

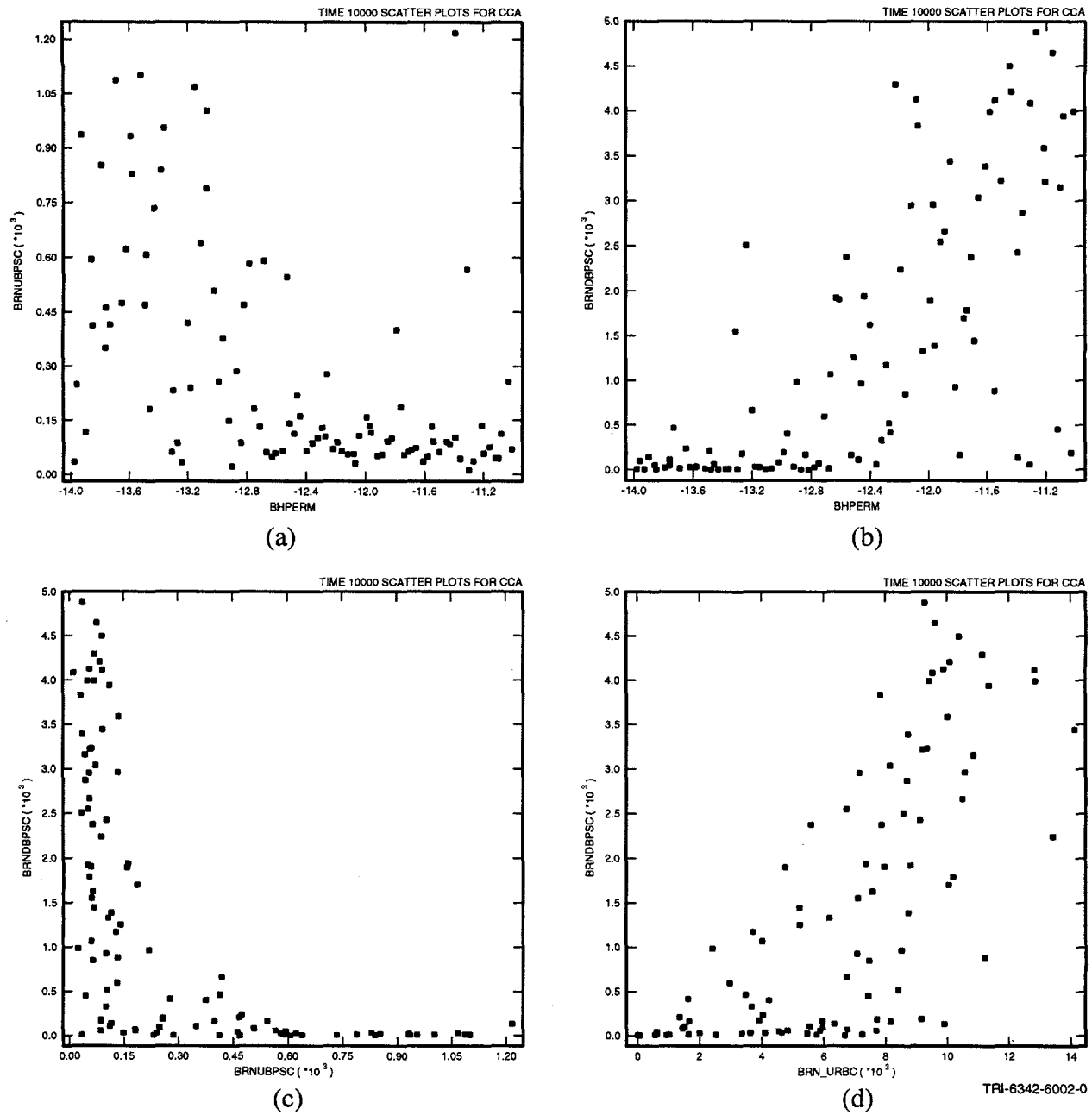


FIGURE 6.2.5. SCATTERPLOTS SHOWING THE RELATIONSHIP between upward (BRNUBPSC) and downward (BRNDBPSC) brine flow from the bottom of the panel closures to the LDRZ and borehole permeability (BHPRM); brine flow upward through the floor of the upper waste panel (BRN_URBC) with respect to flow through the bottom of the panel closures; and the relationship between upward and downward brine flow in the panel closures (BRNDBPSC versus BRNUBPSC) and the floor of the upper waste panel (BRNDBPSC versus BRN_URBC). The plot (a) shows that realizations with low BHPRM tend to have brine flow from the LDRZ upward through the bottom of the panel closures. Conversely, those realizations with high BHPRM values will have brine flowing out the bottom of the panel closure to the LDRZ (plot b). The plots (c) show those realizations with significant volumes of upward brine flow will have minimum brine flow downward, and vice versa for downward flow. The plot (d) illustrates the strong relationship between brine flow from the panel closures downward to the LDRZ and flow upward through the upper waste panel floor. The implication is that brine that passes down through the panel closures will flow up-dip and be partitioned through the upper waste panel floor

Soon after the intrusion event, lateral flow in the LDRZ is closely associated with brine reservoir compressibility and borehole permeability. The realizations with high reservoir compressibilities and high borehole permeabilities will have a significant component of brine flowing in the up-dip direction. Over time, the correlations between reservoir compressibility and brine flow through the DRZ becomes less prominent (see Figure 6.2.6) while the correlation with borehole permeability increases (see Figure 6.2.7). For realizations with borehole permeabilities greater than 10^{-13} m^2 , the upper borehole plug degradation results in LDRZ brine flow reversing from a southerly direction, dominant prior to intrusion, to a northerly direction. Brine flow in the LDRZ is also significantly affected by gas saturation in the UDRZ, specifically the south UDRZ. Once the south UDRZ is 'degassed,' brine will again drain from MB 138 lying south of the UDRZ and Anhydrite AB. This brine will flow through the south half of the upper waste panel ceiling to the UDRZ, contributing to brine accumulations in the lower waste panel. If brine supplies are greater than needed for iron corrosion, brine will begin to drain out the north side of the lower waste panel floor to the LDRZ. Generally, the primary *vertical* flow direction through the

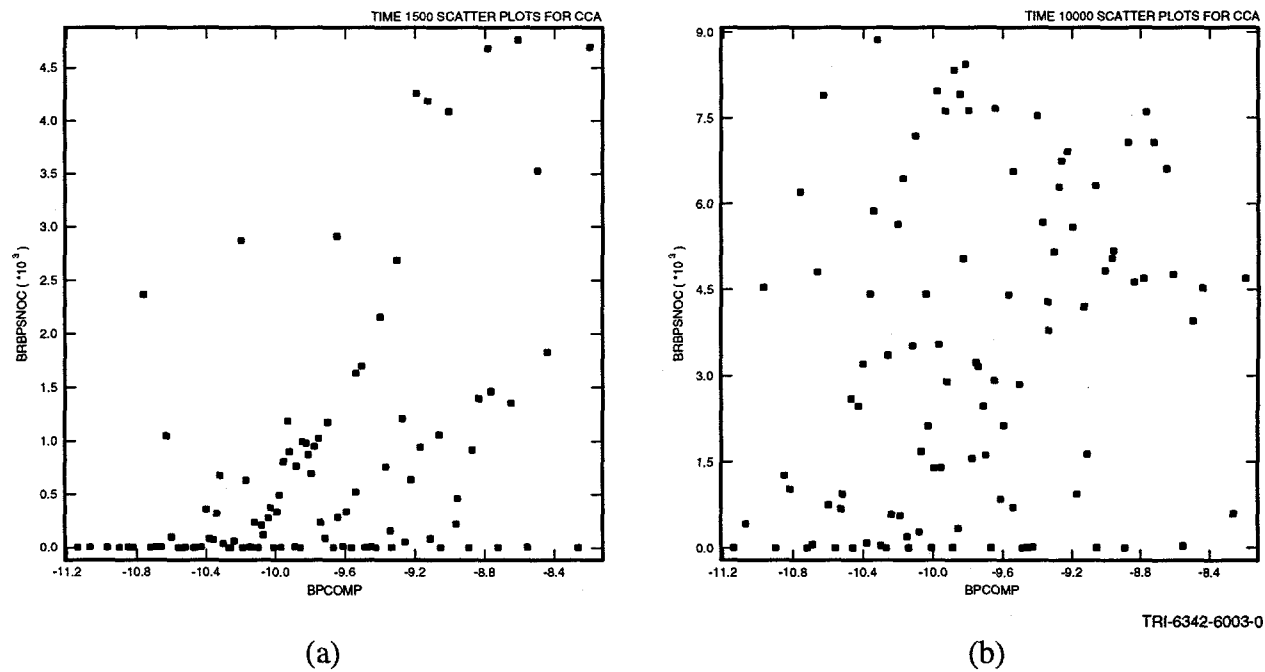


FIGURE 6.2.6. SCATTERPLOTS ILLUSTRATING THE RELATIONSHIP between brine flow passing below the closures in the LDRZ in the up-dip direction (BRBPSNOC) and brine reservoir compressibilities (BPCOMP) at 1500 years (a) and 10,000 years (b). The two plots show those realizations with relatively high values for BPCOMP will have more brine that flows northward (up-dip) in the LDRZ area just below the panel closures. The correlation is relatively stronger at 1500 years

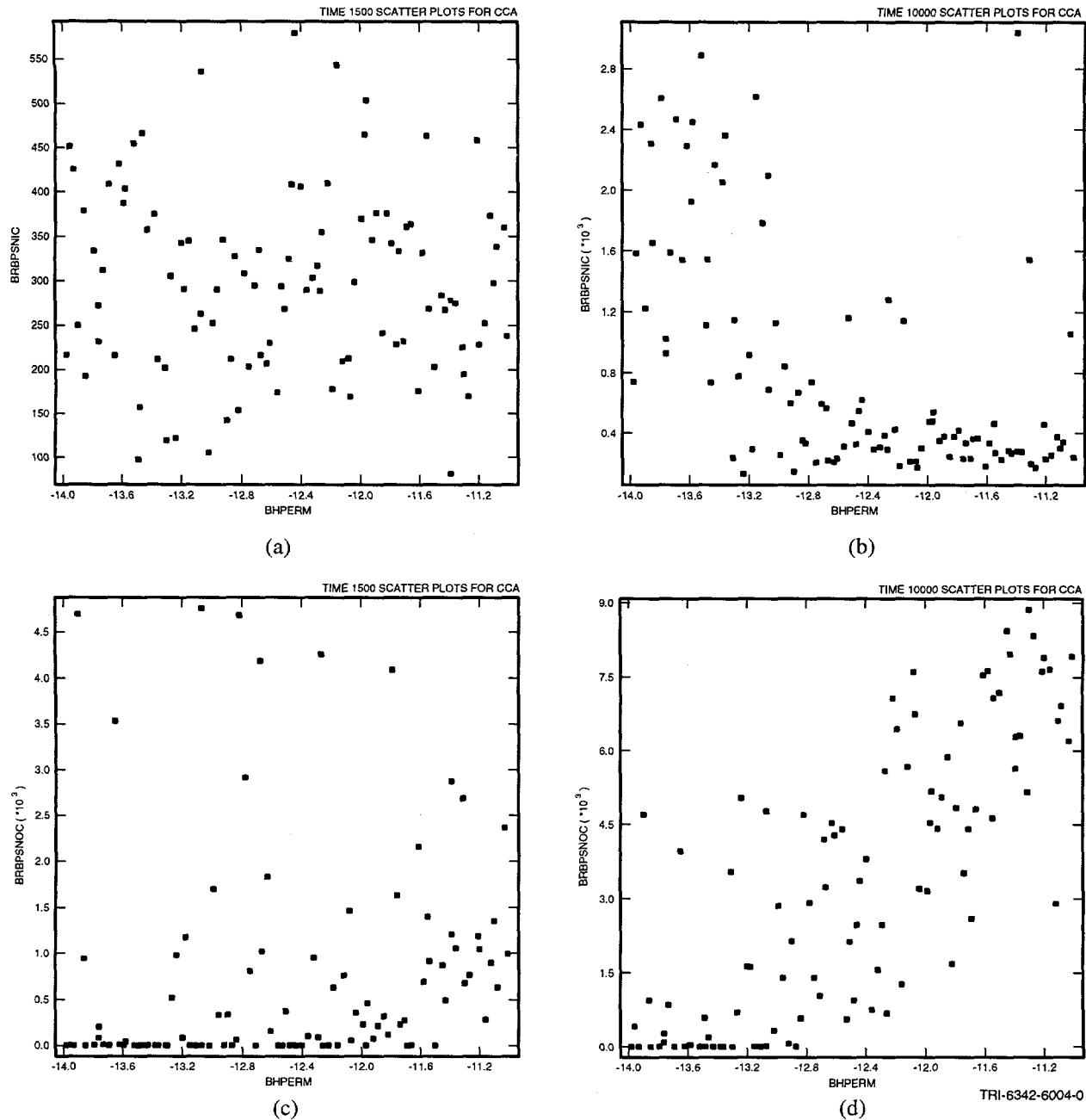
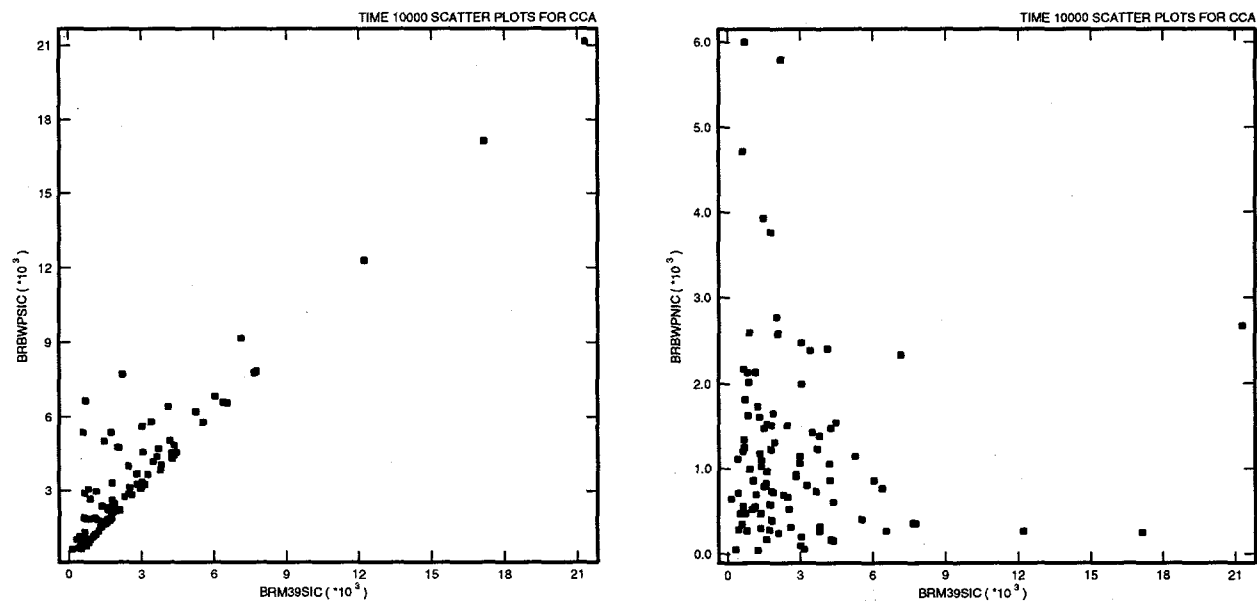


FIGURE 6.2.7. SCATTERPLOTS ILLUSTRATING THE RELATIONSHIP between south (BRBPSNIC) and north flowing brine (BRPBSNOC) passing below the panel closures and borehole permeability (BHPRM) at 1500 (plots a and b) and 10,000 (plots c and d) years. The plots (a) and (b) show the increase in correlation strength between south flowing brine in the LDRZ (BRBPSNIC) and BHPRM between 1500 (top left) and 10,000 years (top right). The bottom two plots show realizations with high values for BHPRM tend to have LDRZ brine flow in the up-dip direction (i.e., to the north). Additionally, the plots (c) and (d) show the correlation between north flowing brine (BRPBSNOC) and BHPRM also increases in strength between 1500 and 10,000 years

northern half of the lower waste panel floor is downward, and upward through the southern half. Two to ten times more brine drains downward through northern half of the lower waste panel floor than downward drainage through the southern half, because less brine 'up-welling' occurs from the LDRZ to the waste panel north side compared to the south. Most of *south* MB 139 drainage moves upward through the south lower waste panel floor rather than flowing through the 'north' lower waste panel floor (see Figure 6.2.8). The cause of the predominant upward flow direction through the south waste panel floor is the combination of it being in close proximity to south MB 139 and the south half being located down-dip relative to the north. Large quantities of brine collect in the most southern portion of the LDRZ, creating localized pressure gradients that promote upward flow between the LDRZ and the south panel floor.

The steady influx of brine upward through the south half of the lower waste panel floor (combined with brine introduced through the south waste panel ceiling) *and* the relatively low-permeable boundary of the undisturbed halite south of the waste panel creates relatively lower gradients between the borehole and the area south of the borehole, compared to the area north of



TRI-6342-6005-0

FIGURE 6.2.8. SCATTERPLOTS ILLUSTRATING THE RELATIONSHIP between brine draining from the south side of MB 139 (BRMB39SIC) and brine flow from the LDRZ up through floor of the southern and northern halves of the lower waste panels (BRBWPSC and BRBWPNC, respectively) at 10,000 years. These plots show the majority of brine that drains from the south side of MB 139 flows up through the south side of the lower waste panel floor as opposed to the north half

the borehole. This condition causes more brine to flow out the north half of the borehole compared to the south, resulting in more brine introduced into the north half of the lower waste panel via the borehole compared to the south. A portion of this newly introduced brine flowing into the northern half of the lower waste panel (not needed for iron corrosion) will flow down through its floor to the LDRZ, then flow up-dip in the LDRZ, joining brine that drains from the panel closure. (Note: brine entering from the UDRZ or the north half of the lower waste panel, passing through the panel closures, will preferentially drain downward through the panel closure to the LDRZ, rather than flow out the north face of the panel closure to the upper waste panel.) As the brine flows up-dip, it is deflected upward into the upper waste panel (see Figure 6.2.9) as it approaches a zone of high gas saturation in the LDRZ, or converges with LDRZ brine flowing in the down-dip direction. The latter is brine draining from north MB 139, north Anhydrites AB, or 'stored' brine draining from the operation and experimental rooms.

Lateral flow direction in the LDRZ is closely associated with assigned values for borehole permeability. Realizations with relatively high borehole permeability will have brine flow in an up-dip direction, while those with low borehole permeability will have brine flow in a down-dip direction (see Figure 6.2.6).

For realizations assigned relatively low borehole permeability (less than 10^{-13} m^2 , gas flowing out the repository via the borehole meets more resistance. Consequently, gas flow in the borehole, if at all, continues for a longer period of time, and repository pressures do not decline as rapidly after upper borehole degradation. (For those realizations with no microbial degradation and relatively high corrosion rates combined with low borehole permeabilities, repository pressures may actually increase.) Relatively high gas saturations within the borehole and the UDRZ, coupled with high gas pressures, inhibit brine drainage from Anhydrites AB and MB 138 and brine drainage down the borehole. Replenishing brine to be used in iron corrosion is more dependent on brine sources that flow into the LDRZ from the northern or southern MB 139, or brine drained earlier in the modeled period and stored in the operational and experimental rooms rather than that introduced via the borehole. Consequently, LDRZ brine flowing below the panel closure remains in a southerly direction until most iron in the lower panel is corroded; once

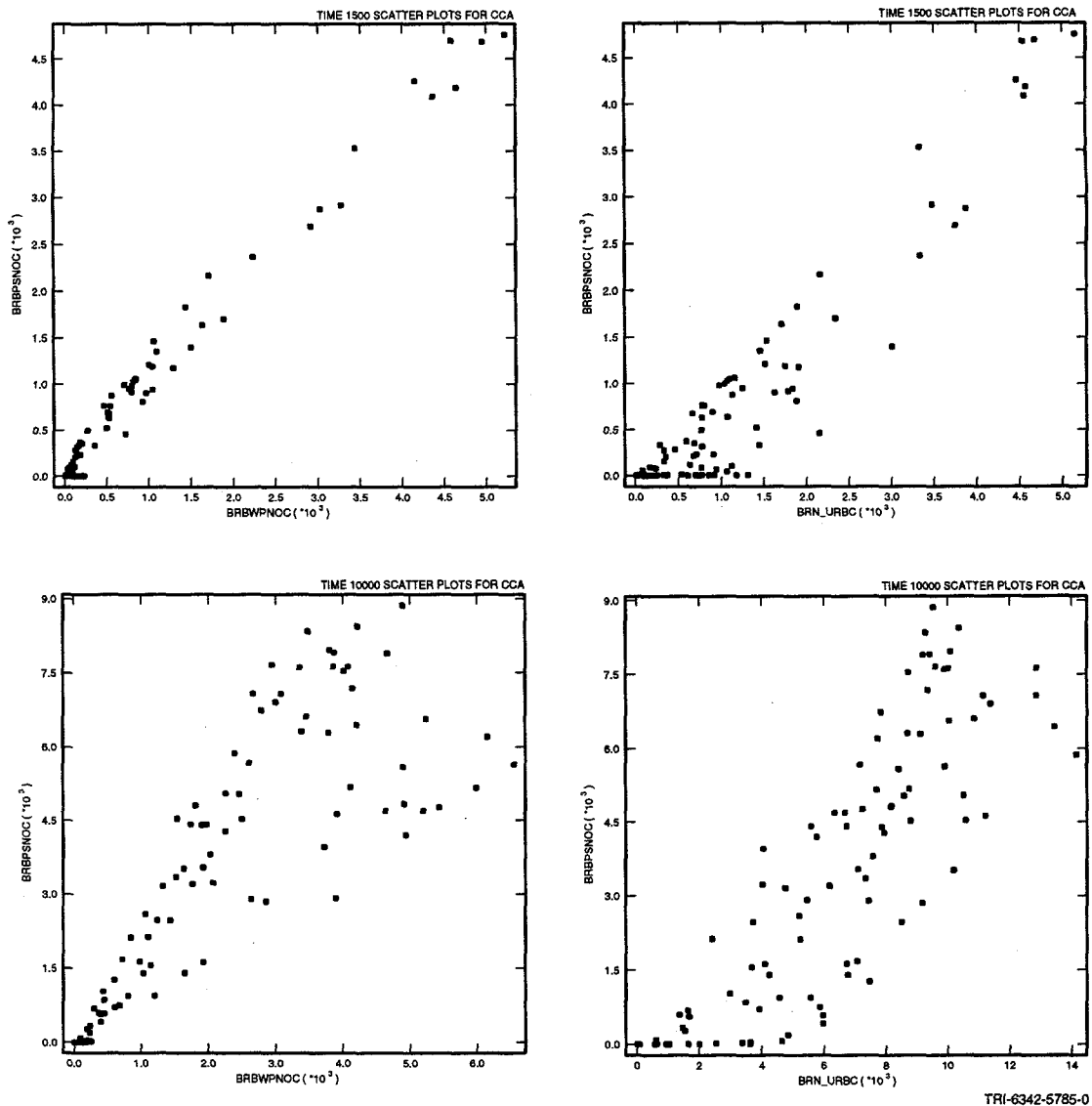


FIGURE 6.2.9. SCATTERPLOTS, TAKEN AT 1500 and 10,000 years, showing the relationship between brine drainage out the 'north half' of the lower waste panel floor (BRBWPNC), north flowing brine in the LDRZ below the panel closures (BRBPSNOC), and brine flow upward, through the floor of the upper waste panel (BRN_URBC). The top left plot shows at 1500 years, a large portion of brine that drains out the 'north half' of the lower waste panel floor to the LDRZ (BRBWPNC) will flow up-dip, passing under the panel closures (BRBPSNOC) and heading towards the upper waste panel. The top right plot shows a large portion of brine that passes under the panel closures (BRBPSNOC) will seep through the floor of the upper waste panel (BRN_URBC). The bottom right plot shows that the strong relationship seen at 1500 years between BRBWPNC and BRBPSNOC has weakened at 10,000 years. The bottom left plot shows that, for many realizations, more brine flows up-dip in the LDRZ passing under the panel closures (BRBPSNOC) than drains out the 'north side' of the lower panel floor (BRBWPNC). The extra contribution of brine to the LDRZ flowing in an up-dip direction is from brine drainage out the bottom of the panel closures. The bottom right plot shows significantly more brine seeps up through the upper waste panel floor (BRN_URBC) than flows up-dip in the LDRZ below the panel closures BRBPSNOC at 10,000 years. The extra contribution of brine as BRN_URBC is from brine drainage to the LDRZ from the 'north' anhydrites and experimental and operational rooms. This brine, once in the LDRZ, flows down-dip passing under the upper waste panel where some seeps up through the lower waste panel floor. Note: Because the primary flow direction through the 'south' lower waste panel floor is up-ward, drainage from this side of the lower waste panel does not significantly contribute to up-dip LDRZ brine flow

corrosion is near completion, LDRZ flow direction reverses and flows up-dip rather than down-dip.

Less gas can be evacuated out the repository for realizations with low borehole permeability. Consequently, gas saturations and pressures within the upper waste panel tend to remain high and remain elevated for longer periods of time within the modeled period. This situation inhibits brine from passing from the LDRZ upward through the floors of the upper waste panels as it drains down-dip from the far northern portion of the LDRZ. However, as brine passes under the brine-saturated panel closures, some brine passes up through the bottom of the closures where it flows down-dip into the north half of the lower waste panel. Because the north half of the lower waste panel is more gas-saturated than the closures, its effective brine permeability will be lower than the panel closures. This condition promotes the entry of more brine through the panel closures' bottom than through the north half of the lower waste panel floor.

Brine accumulates in the LDRZ below the south side of the lower waste panel. Here, pressure gradients and brine permeabilities promote brine flow up into the bottom of the lower waste panel, where some brine, if not all, is used for iron corrosion.

Given limited brine supplies, realizations assigned medium to high iron corrosion rates will have an undersupply of brine contacting iron for corrosion. These realizations will have limited downward brine drainage out the north and south floor of the lower waste panel during the entire modeled period. For realizations with high corrosion rates and abundant brine supplies (from high volumes of anhydrite drainage and/or large volumes of early DRZ brine drainage 'stored' and then released later in the modeled period), iron in the lower waste panel becomes completely corroded in the later half of the modeled period. When this happens, south-flowing brine will accumulate in the south LDRZ and the south half of the lower waste panel, eventually building up enough hydrostatic pressure to produce a brine 'mound' within the lower waste panel. The formation of this mound promotes a reverse in brine flow direction up-dip to the northern half of the lower waste panel. Any brine accumulation in the northern portion of the lower waste panel seeps downward through the north waste panel floor to the LDRZ. Once brine oversupplies are

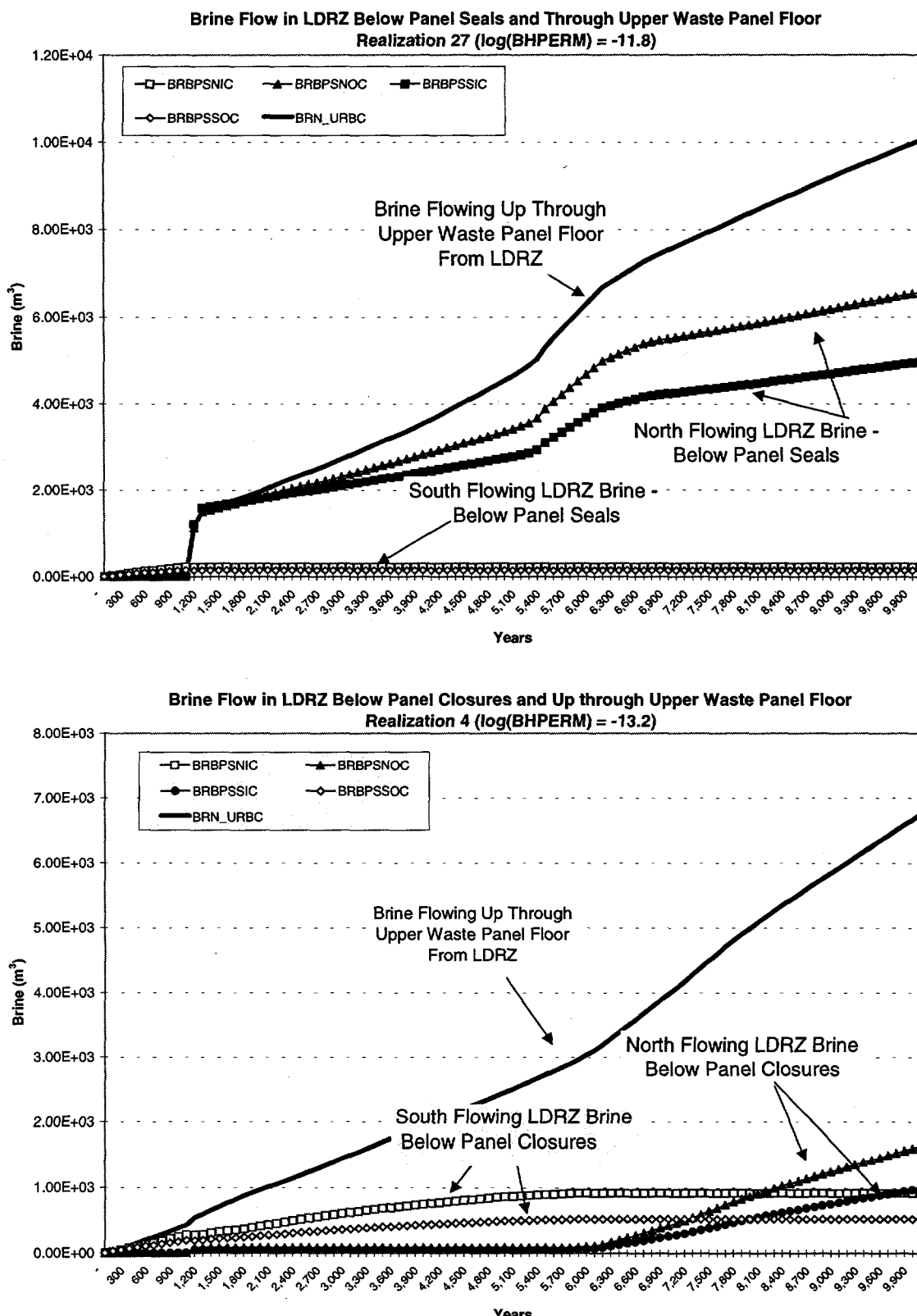


FIGURE 6.2.10. OVERLAY PLOTS ILLUSTRATING CHANGES in brine flow direction and rates representative for realizations assigned high and low borehole permeabilities

created in the lower waste panel (i.e., more brine enters the waste panel than is needed for corrosion and brine saturation approach), brine flow direction soon reverses from a southerly to a northerly direction in the LDRZ.

The flow scenarios described above are depicted in Figure 6.2.10. The two plots illustrate the relationship between LDRZ brine flow direction within the various regions of the LDRZ for realizations assigned relatively high (Realization 27) and low (Realization 4) borehole permeability. The plots show a reversal in brine flow direction, which occurs for Realization 27 soon after upper borehole degradation (1200 years). For Realization 4, LDRZ brine flow reverses flow direction in the LDRZ, from south flowing (down-dip) to a northerly direction (up-dip) between 5400 and 6000 years only after all iron in the lower waste panel is completely corroded. Section 7 presents more overlay plots describing flow between the various regions of the excavated area relative to borehole flow and iron corrosion.

6.3 Parameters Affecting Vertical and Lateral Flow in the LDRZ

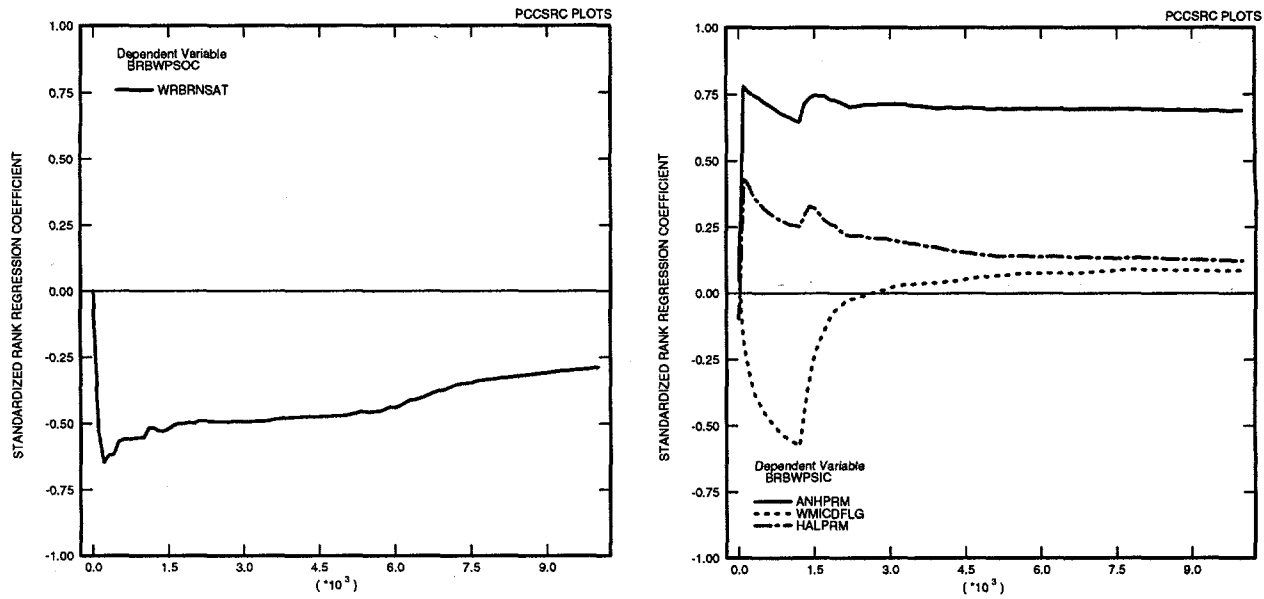
The independent variables most affecting the dependent variables for vertical and lateral flow within the LDRZ defined in Section 6.1 were assessed using SRRC analysis. SRRC plots were generated and analyzed for the most significant LHS independent variables that affect LDRZ brine and gas flow time. Those variables most affecting each dependent variable defining flow within each region are discussed below.

6.3.1 Vertical Flow Between LDRZ and Lower Waste Panel Floor

6.3.1.1 Vertical Brine Flow Between LDRZ and the Lower Waste Panel

Brine Flow Between the LDRZ and the South Half of the Lower Waste Panel

Figure 6.3.1 depicts those parameters most affecting downward (BRBWPSOC - right) and upward (BRBWPSIC - left) brine flow from the floor of the south half of the lower waste panel.



TRI-6342-5786-0

FIGURE 6.3.1. STANDARDIZED RANK REGRESSION COEFFICIENT (SRRC) results showing the most influential independent variables for downward, BRBWPNC (left), and upward, BRBWPNC (right), brine flow from the LDRZ to south half of the lower waste panel

Downward Brine Flow

Brine flow downward through the 'south' lower waste panel floor primarily occurs early in the modeled period when the lower waste panel is more gas- than brine-saturated and of relatively low pressure. Drainage out the south waste panel floor is from brine that collects in the lower waste panel due to UDRZ and anhydrite brine drainage. Residual brine saturation values (WRBRNSAT) appear as the singlemost important parameter affecting flow from the south waste panel to the LDRZ because it is one of several parameters that determine the effective brine permeability within the waste panel. An inverse correlation exists between WRBRNSAT and BRBWPSC. High values of WRBRNSAT mean the effective brine permeability within the waste region will be lower and, consequently, less brine will drain from the waste region to the LDRZ. Additionally, once residual brine saturation is reached, all brine flow will cease.

Upward Brine Flow

Brine flow *into* the south side of the lower waste panel floor (BRBWPSC) is strongly influenced by ANHPRM throughout the entire modeled period, partially because of the close proximity of

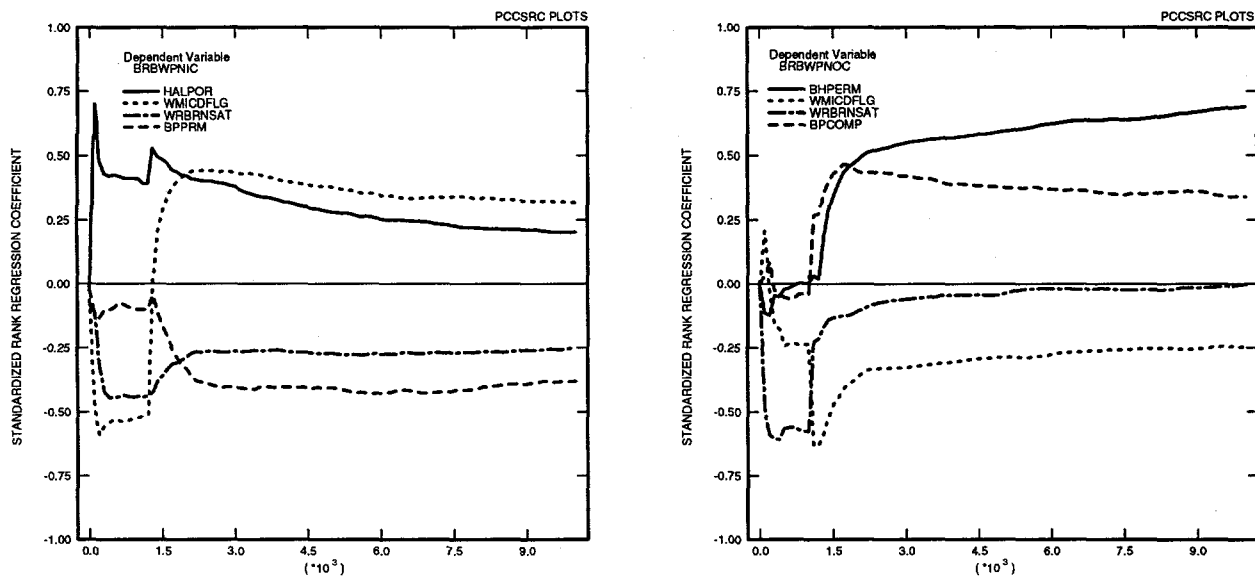
the south side of the waste panel to the ‘south’ MB 139. A large majority of south MB 139 drainage that flows into the LDRZ moves upward, through the south floor of the lower waste panel (see Figure 6.2.8). The ease with which brine drains from MB 139 is a function of ANHPRM, hence the strong positive correlation between ANHPRM and BRBWPSIC. A weak correlation is seen between halite permeability and this flow (HALPRM and BRBWPSIC). Those realizations with high values for HALPRM will tend to replenish the anhydrite layers with brine as brine drains from the anhydrites to the LDRZ. A higher HALPRM value means more ‘halite’ brine drains to the anhydrites, which drain to the LDRZ. More anhydrite drainage to the LDRZ makes brine more likely to up-well from the LDRZ through the lower waste panel floor, hence the positive correlation between HALPRM and BRBWPSIC.

A negative correlation is seen between WMICDFLG and BRBWPSIC prior to intrusion, with the negative correlation dramatically increasing in strength after the time of intrusion. Those realizations with no gas generated from microbial degradation will tend to have relatively lower pressures and higher gradients between the two regions promoting brine drainage from the non-excavated to the excavated areas. Consequently, more brine will tend to accumulate in the LDRZ and up-well through the lower waste panel floor. The pressure gradient that promotes brine to flow upward from the lower Castile reservoir to the repository is likely to be greater for realizations with no microbial degradation.

Flow Between the LDRZ and the North Half of the Lower Waste Panel

Figure 6.3.2 depicts those parameters most affecting downward (BRBWPNOC) and upward (BRBWPNIC) brine flow from the floor of the north half of the lower waste panel.

Vertical brine flow out of the ‘north’ lower waste panel floor into the LDRZ (BRBWPNOC) prior to intrusion is inversely correlated to WRBRNSAT and WMICDFLG for the same reason as that given for downward flow in the south half (BRBWPSOC).



TRI-6342-5787-0

FIGURE 6.3.2. STANDARDIZED RANK REGRESSION COEFFICIENT (SRRC) results showing the most influential independent variables for downward, BRBWPNC (left), and upward, BRBWPNC (right), brine flow from the LDRZ to lower waste panel

After the intrusion event, brine not needed for corrosion flows out the north lower waste panel floor to the LDRZ. The extent of brine accumulation in the lower waste panel is partially dependent on gas and brine flow within the borehole. High values for borehole permeability, BHPRM, mean more gas will be evacuated out the repository, reducing repository pressures. Reduced repository pressures mean more brine is likely to flow into the lower waste panel, either from the borehole itself or the adjoining 'upper anhydrites' (south MB 139 and south Anhydrite AB), and brine accumulation oversupplies in the waste panels are more likely to occur. This excess brine will drain out the 'north' waste panel floor to the LDRZ.

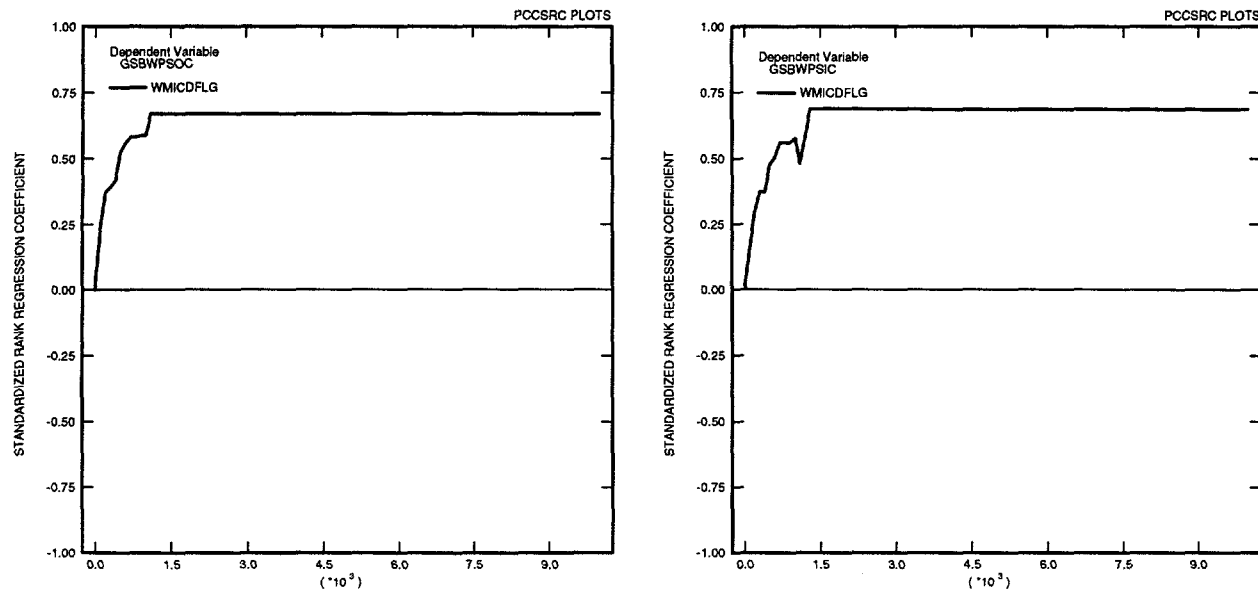
For realizations with low values for BHPRM, brine accumulations in the lower waste panel are less likely to occur.

Brine flow out of the north side of the lower waste panel floor is affected by the amount of brine introduced into the lower waste panel from the brine reservoir that flows back down to the LDRZ. Hence, a positive, but brief, correlation exists between BRBWPNC and BPCOMP.

6.3.1.2 Vertical Gas Flow Between LDRZ and Lower Waste Panel Floor

Gas Flow Between the LDRZ and the South Half of the Lower Waste Panel

Figure 6.3.3 depicts those parameters most affecting gas flow downward (GSBWPSOC) and upward (GSBWPSIC) from the floor of the south half of the lower waste panel.



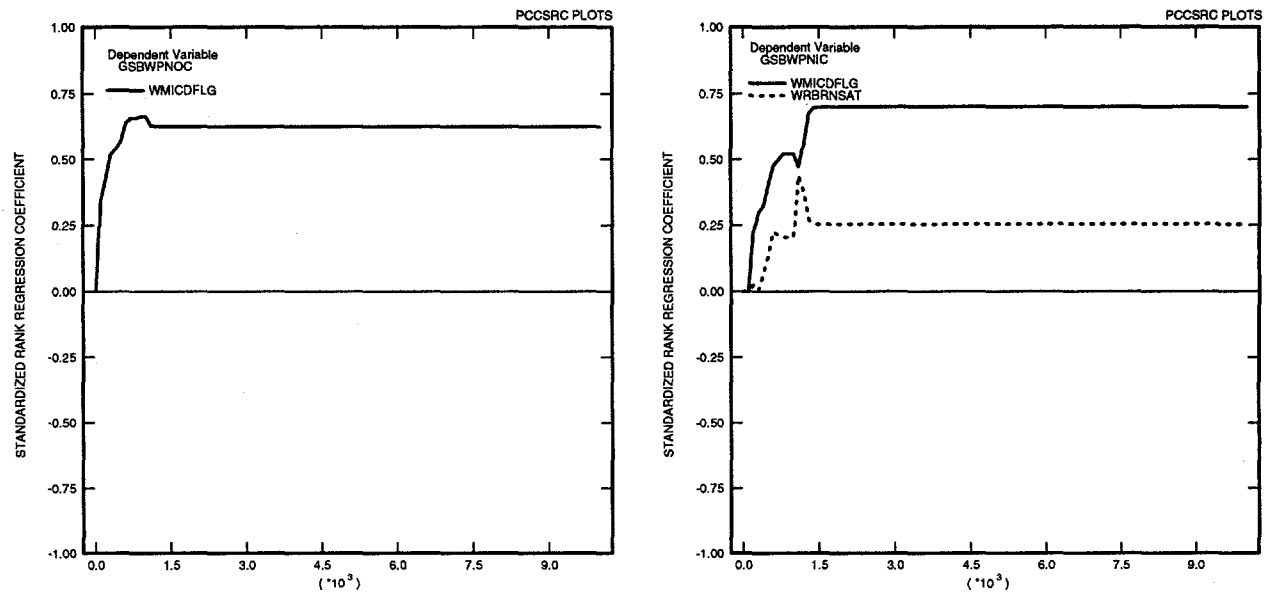
TRI-6342-5788-0

FIGURE 6.3.3. STANDARDIZED RANK REGRESSION COEFFICIENT (SRRC) results showing the most influential independent variable for downward, GSBWPSOC (left), and upward, GSBWPSIC (right), gas flow from the LDRZ to south half of the lower waste panel

Gas flow downward between the LDRZ and the south side of the lower waste (GSBWPSOC) and upward (GSBWPSIC) is dominated by the parameter that dominates gas production early in the modeled period, i.e., microbial degradation (WMICDFLG). Large quantities of gas are more likely to be produced for the realizations in which microbial degradation of cellulose, fiber, or plastics occurs. This condition will produce relatively high waste panel pressures and, as gas pressures rise, gas will eventually move down through the lower waste panel floor, displacing resident LRDZ brine. The pressure pulse, created with the intrusion event, will displace more gas upward from the LDRZ to the waste panel. Hence, a slight increase in the correlation between the two parameters is seen at 1000 years.

Gas Flow Between the LDRZ and the North Half of the Lower Waste Panel

Figure 6.3.4 depicts those parameters most affecting gas flow out of (GSBWPNOC) and into (GSBWPNIC) the north side of the lower waste panel floor.



TRI-6342-5789-0

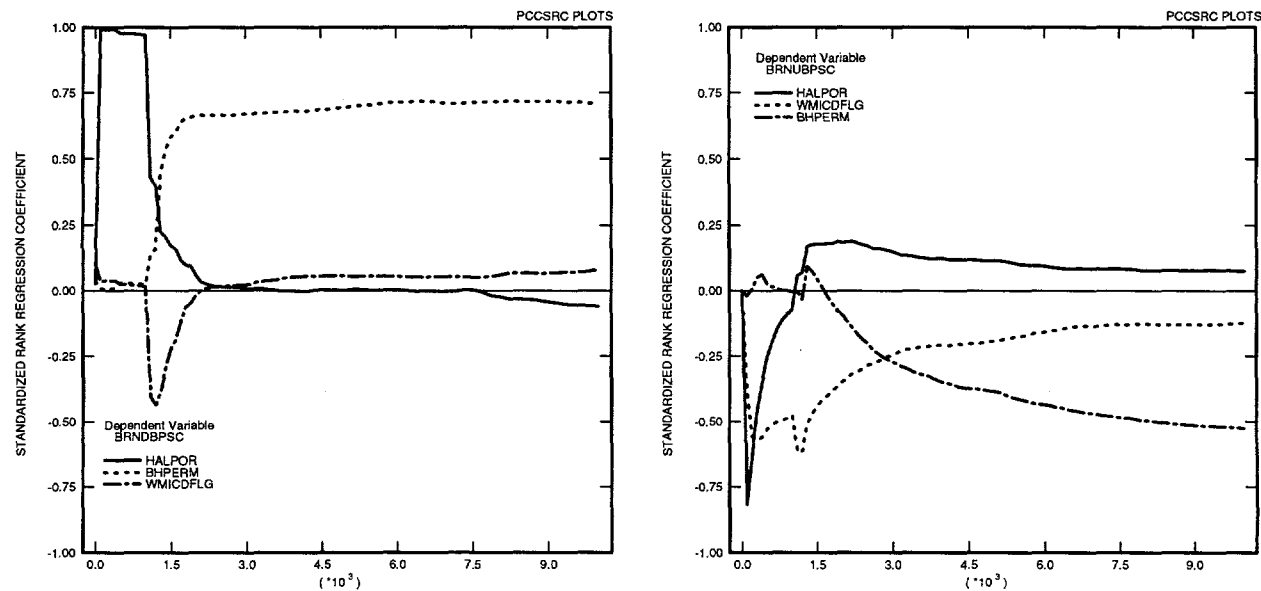
FIGURE 6.3.4. STANDARDIZED RANK REGRESSION COEFFICIENT (SRRC) results showing the most influential independent variables for downward, GSBWPNOC (left), and upward, GSBWPNIC (right), gas flow from the LDRZ to north half of the lower waste panel

6.3.2 Vertical Flow Between Panel Closures and LDRZ

Prior to intrusion, GSBWPNOC and GSBWPNIC are both positively correlated with microbial degradation ($WMICDFLG > 0$) for the same reason as for gas flow through the south half of the lower waste panel, described above. The positive, but brief, correlation between GSBWPNIC and WRBRNSAT soon after the upper borehole degrades is due to the role that WRBRNSAT plays in determining effective brine and gas permeability; a high value for WRBRNSAT equates to low values for effective brine permeability, which inhibits brine flow and promotes gas flow. Therefore, the ease with which gas flows between the LDRZ and the waste region is enhanced for simulations assigned high WRBRNSAT.

6.3.2.1 Brine Flow Between Panel Closures and LDRZ

Figure 6.3.5 depicts those parameters most affecting brine flow out of (BRNDBPSC) and into (BRNUBPSC) the bottom of the panel closures.



TRI-6342-5797-0

FIGURE 6.3.5. STANDARDIZED RANK REGRESSION COEFFICIENT (SRRC) results showing the most influential independent variables for downward, BRNDPSC (left), and upward, BRNUPSC (right), brine flow between the LDRZ and the panel closures

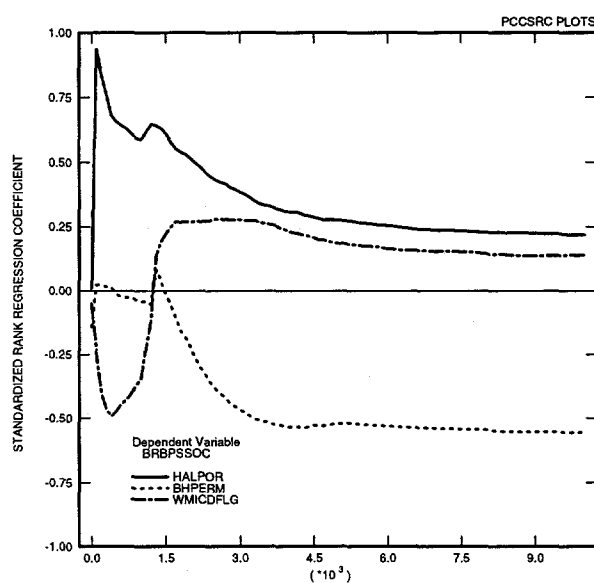
Parameters most affecting downward brine flow out of the bottom of the panel closure, BRNDBPSC, are HALPOR prior to intrusion, and BHPRM after intrusion. Downward brine flow, BRNDBPSC, is positively correlated to BHPRM for the same reason as downward brine flow on the north side of the waste panel.

Conversely, parameters such as BHPRM and HALPOR, which are positively correlated to downward flow within the panel closure, are negatively correlated to upward panel closure flow, BRNUBPSC, with the exception of WMICDFLG. The closures experience a brief pulse of gas at the time of borehole degradation; the magnitude of the gas pulse is a function of the amount of gas produced. More gas is produced for the simulations assigned microbial degradation, WMICDFLG > 0. This gas pulse impedes brine flow down through the closures; hence, an inverse correlation exists between BRNDBPSC, BRNUBPSC, and WMICDFLG at the time of borehole

degradation. WMICDFLG controls the extent and magnitude of a gas pulse passing through the closures, which impedes all brine flow; consequently, WMICDFLG negatively affects brine flow within panel closures, regardless of direction.

6.3.2.2 *Gas Flow Between Panel Closures and LDRZ*

Figure 6.3.6 depicts those parameters most affecting gas flow down through the bottom of the panel closures (GASDBPSC).



TRI-6342-5790-0

FIGURE 6.3.6. STANDARDIZED RANK REGRESSION COEFFICIENT (SRRC) RESULTS showing the most influential independent variables for downward, GASDBPSC, gas flow between the LDRZ and the panel closures

No gas flows from LDRZ upward through the bottom of the panel closures, GASUBPSC (see Figure 6.1.7). The short pulse of gas that passes down through the panel closures, GASDBPSC, is a direct function of the volume of gas produced and resident within both waste panels just prior to intrusion. Because microbial degradation is the dominant gas-producing process in both waste panels prior to intrusion, it shows up as the most influential parameter affecting gas flow in the panel closures, hence the positive correlation. BHPRM shows up as an influential parameter because it controls depressurization of the repository. High BHPRM means gas is more easily evacuated out the repository via the borehole.

6.3.3 Vertical Flow Between Upper Waste Panels and LDRZ

6.3.3.1 Brine Flow Between the LDRZ and the Upper Waste Panel

Figure 6.3.7 depicts those parameters most affecting brine flow downward (BRN_DRBC) and upward (BRN_URBC) from the floor of the south half of the upper waste panel.

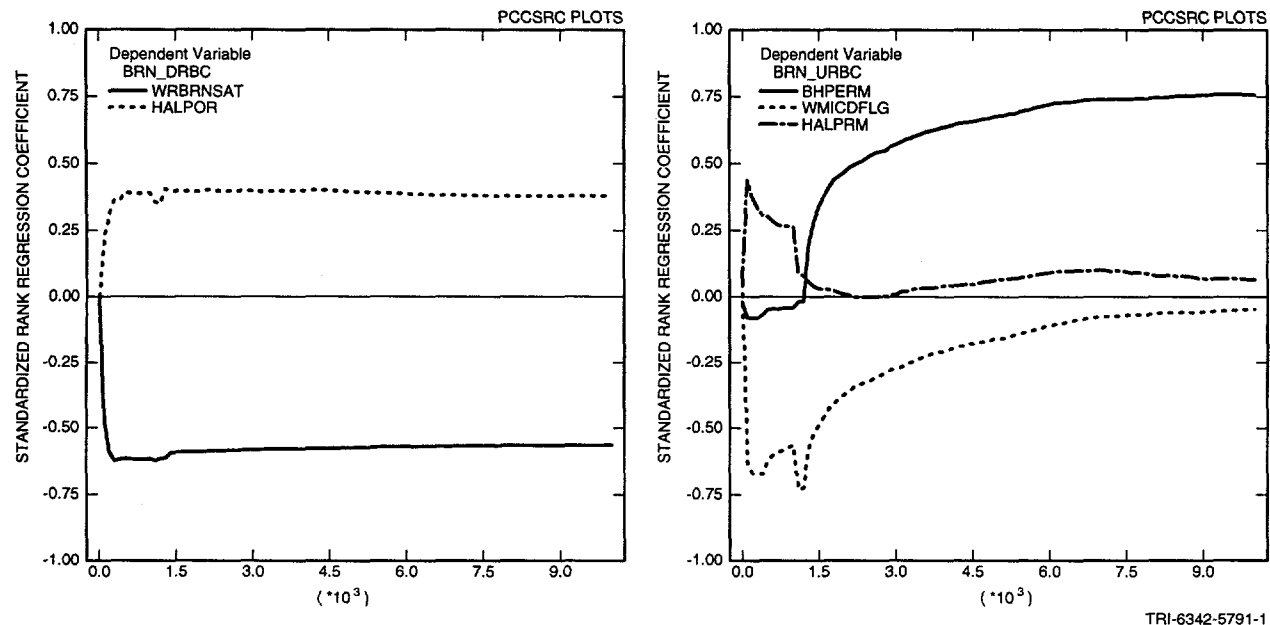


FIGURE 6.3.7. STANDARDIZED RANK REGRESSION COEFFICIENT (SRRC) results showing the most influential independent variables for downward, BRN_DRBC (left), and upward, BRN_URBC (right), brine flow from the LDRZ to upper waste panel

Prior to intrusion, downward brine flow out of the upper waste panel (BRN_DRBC) into the LDRZ is positively correlated with HALPOR (halite porosity) and inversely correlated with WRBRNSAT (residual brine saturation). The major source of LDRZ brine is vertical drainage from the UDRZ to the LDRZ via the excavated regions. Consequently, large HALPOR means that large UDRZ brine volumes exist that drain from the UDRZ to the LDRZ via the excavated areas. WBRNSAT appears as an important parameter affecting flow to the LDRZ because it is one component used to determine effective brine permeabilities within the excavated area. For example, if two simulations have the same 'actual' brine saturation, the simulation with a high WBRNSAT will have a lower effective brine permeability.

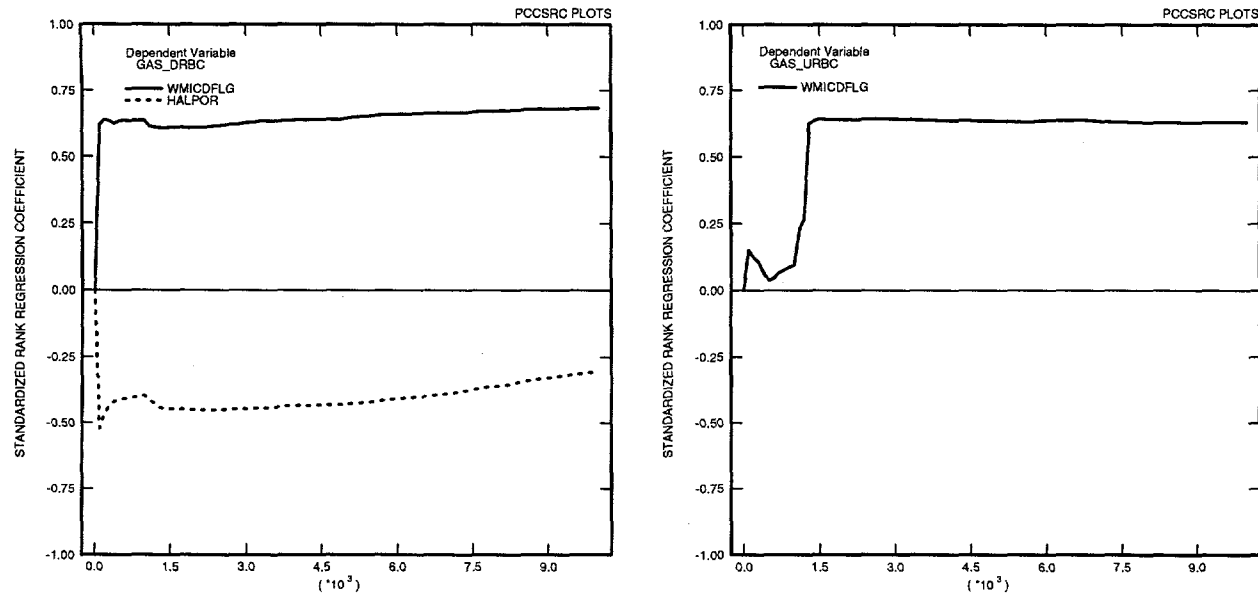
After intrusion, the upper waste panel is primarily gas-saturated, so the small amount of brine that exists within the upper waste panels is consumed by iron corrosion. Thus, little excess brine exists in the upper waste panel to migrate down to the LDRZ. Consequently, brine flow out of the floor of the upper waste panels effectively ceases. Therefore, any correlation with independent parameters determining the uncertainty for downward-flowing brine after intrusion will not be discussed.

Figure 6.3.7 (right) shows that, prior to intrusion, a strong inverse correlation exists between BRN_URBC and microbial degradation flag, WMICDFLG, and a positive correlation exists with halite permeability (HALPRM). WMICDFLG is inversely correlated to BRN_URBC for the same reasons given for BRBWPSIC. Higher halite permeability affects the transmission of brine from the undisturbed halite to the DRZ *and* the all adjoining anhydrites (MB 138, Anhydrite AB, and MB 139). All these sources, lumped together, positively affect the volume of brine that accumulates in the LDRZ, which eventually ‘up-wells’ through the upper panel floors from the LDRZ.

After intrusion, WMICDFLG and HALPRM decline as important parameters affecting BRN_URBC, and BHPRM begins to increase in importance. As discussed in the previous section, BHPRM not only affects the amount of brine introduced into the LDRZ, but also the ease with which gas can be evacuated out of the repository via the UDRZ. Rapid gas evacuation out the repository via the borehole produces strong pressure (and saturation) gradients between the LDRZ and the upper waste panels. These ‘localized’ pressure gradients promote brine flow from the LDRZ up through the waste panel floor.

6.3.3.2 Gas Flow Between the LDRZ and the Upper Waste Panel

Figure 6.3.8 (left) depicts those parameters most affecting gas flow out of (GAS_DRBC) and into (GAS_URBC) the upper waste panel floor via the LDRZ.



TRI-6342-5792-0

FIGURE 6.3.8. STANDARDIZED RANK REGRESSION COEFFICIENT (SRRC) results showing the most influential independent variables for downward, GAS_DRBC (left), and upward, GAS_URBC (right), gas flow from the LDRZ to upper waste panel

Prior to intrusion, GAS_DRBC is negatively correlated with HALPOR and positively correlated with microbial degradation (WMICDFLG > 0). Large volumes of gas are produced when WMICDFLG is in full effect, which in turn produces high repository pressures. Low values for HALPOR mean DRZ gas pressures rise more rapidly, causing a pressure gradient to form between the waste panel and the LDRZ, which promotes gas flow into the LDRZ. Therefore, as more gas is produced, gas storage space becomes limited in the UDRZ and upper waste panel and causes some gas to flow through lower waste panel floor to the LDRZ.

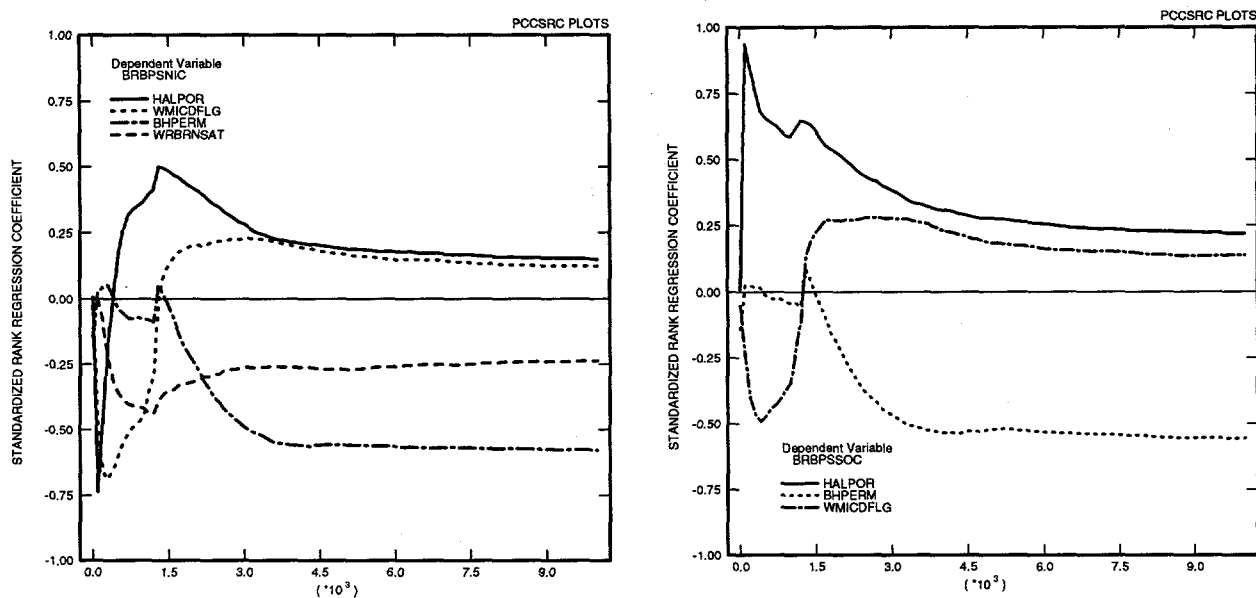
Figure 6.3.8 (right) shows gas flow upward through the panel floor (GAS_URBC) is positively correlated with the biodegradation flag, WMICDFLG. Those realizations with high gas volumes and pressures at the time of intrusion are more likely to have gas flow into the LDRZ from the upper waste panel floors, a function of WMICDFLG > 0 , prior to the time of intrusion. WMICDFLG affects GAS_URBC because approximately the same realizations will then have gas that moves back up from the LDRZ through the waste panel floors and into the upper borehole at the time of intrusion.

6.3.4 Lateral Flow Within the LDRZ

6.3.4.1 Lateral Flow in a Southerly Direction Assessed Below the Panel Closure

Brine Flow

Figure 6.3.9 (right) shows the sampled parameters most affecting south-flowing brine into the north face BRBPSNIC and out the south face BRBPSSOC of the LDRZ below the panel closures.



TRI-6342-5793-0

FIGURE 6.3.9. STANDARDIZED RANK REGRESSION COEFFICIENT (SRRC) RESULTS showing the most influential independent variables for lateral south-flowing brine in the LDRZ passing under the panel closures, into the north face, BRBPSNIC (left), and out the south face, BRBPSSOC (right)

Prior to intrusion, what little brine that flows south in the LDRZ (BRBPSNIC and BRBPSSOC) is inversely correlated with WRBRNSAT and WMICDFLG from the time of repository closure to intrusion. Because a large portion of brine that drains out of the upper waste panel flows southward in the LDRZ, those parameters affecting BRN_DRBC, such as WRBRNSAT and WMICDFLG, also will affect south-flowing brine in the LDRZ, as described in Section 6.3.3. The positive correlation between HALPOR and BRBPSSOC is due to the brine that drains from the panel closures (sourced from the UDRZ) to the LDRZ (see Section 6.3.2). The inverse

correlation between HALPOR and brine flowing into the north face (BRBPSNIC) for the first few hundred years after closure is probably spurious.

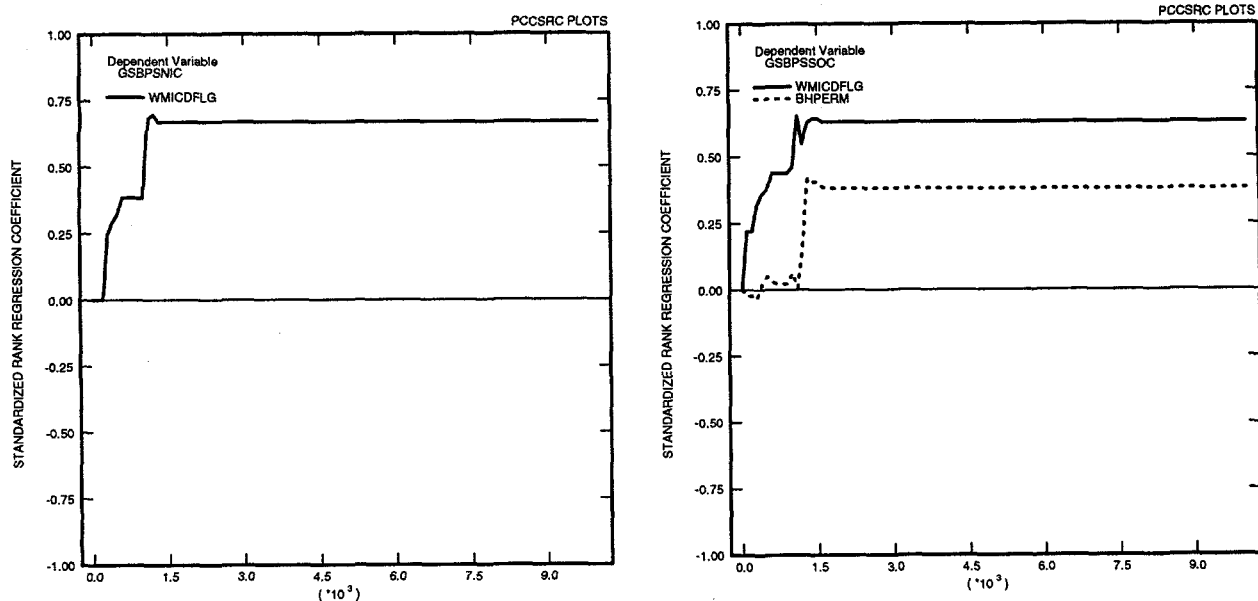
After intrusion, the correlation between both BRBPSNIC and BRBPSSOC and HALPOR is most likely due to UDRZ brine that was drained earlier and had been ‘stored’ in the operations and experimental rooms. This brine flows to the LDRZ from the experimental and operations rooms between repository closure and ~2200 years. The brine drains southward in the LDRZ and, for realizations with low borehole permeabilities, eventually passes below the panel closure.

An inverse correlation exists between south-flowing brine and BHPRM. Realizations with low values for BHPRM will have less brine introduced via the borehole into the excavated and the DRZ regions. For these realizations, a brine mound is *less likely* to be produced in the down-dip regions of the LDRZ. (The brine mound would produce relatively higher pressures in the down-dip regions of the LDRZ as compared to the up-dip regions.) Therefore, the gravitational gradient, which promotes south-flowing brine prior to intrusion, will be the dominant drive mechanism between the down-dip and up-dip regions of the LDRZ.

Gas Flow

Figure 6.3.10 (right) shows the sampled parameters most affecting south-flowing gas into the north face (GSBPSNIC) and out the south face (GSBPSSOC) of the LDRZ area below the panel closures.

South-flowing gas in the LDRZ (which occurs for only a few realizations - see Figure 6.1.19) is correlated with microbial degradation and residual brine saturation (WRBRNSAT). For realizations with large gas volumes generated from microbial degradation ($WMICDFLG > 0$), the repository will most likely have ‘gas’ pressures greater than the Salado or Rustler units. Therefore, soon after upper borehole degradation, a pressure pulse promotes gas flow between the repository and the upper units, and within the repository between the up-dip (and down-dip) regions towards the borehole. This pressure pulse promotes gas flow towards the borehole.



TRI-6342-5794-0

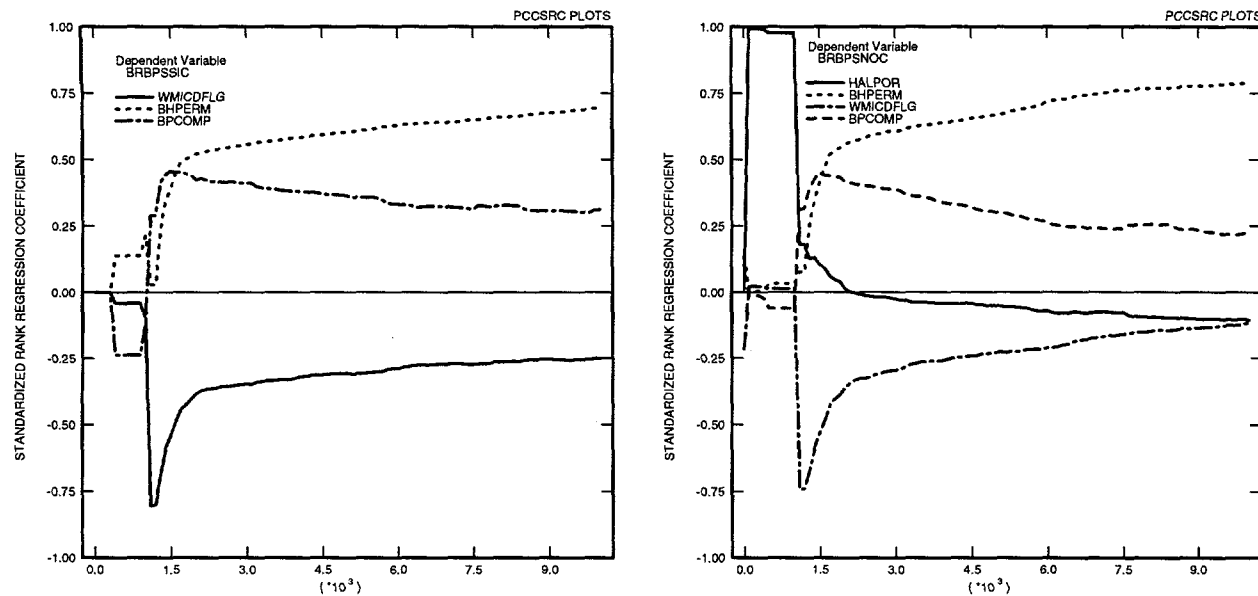
FIGURE 6.3.10. STANDARDIZED RANK REGRESSION COEFFICIENT (SRRC) results showing the most influential independent variables for lateral south-flowing gas in the LDRZ passing under the panel closures into the north face, GSBPSNIC (left), and out the south face, GSBPSSOC (right)

Those realizations with microbial degradation will produce more gas, which migrates to the LDRZ and is carried down-dip towards the borehole during the 'intrusion' pressure pulse. Hence, a positive correlation is seen between WMICDFLG and south-flowing gas.

6.3.4.2 *Lateral Flow in Northern Direction Assessed Below the Panel Closures*

Brine Flow

Figure 6.3.11 (right) shows the sampled parameters most affecting brine flow into the south face (BRBPSSIC) and out the north face (BRBPSNOC) in the LDRZ below the panel closures. Before intrusion, no sampled parameter is correlated with brine flow to the north. After intrusion, the pulse of north-flowing brine that occurs in the LDRZ at the time of borehole intrusion is strongly correlated with the Castile brine reservoir compressibility, BPCOMP. The value of BPCOMP controls the volume of brine that flows up the borehole and is introduced into the LDRZ.



TRI-6342-5795-0

FIGURE 6.3.11. STANDARDIZED RANK REGRESSION COEFFICIENT (SRRC) RESULTS showing the most influential independent variables for lateral north-flowing brine in the LDRZ passing under the panel closures into the south face, BRBSSIC (left), and out the north face, BRBPSNOC (right)

The correlation between BPCOMP and north-flowing brine decreases in value and is overtaken in importance by borehole permeability, BHPRM. BHPRM controls many processes that affect north-flowing brine in the LDRZ. These processes come into play sequentially. High values for BHPRM mean gas is easily evacuated out the excavated and DRZ regions, lowering repository pressures and increasing effective brine permeabilities in the down-dip region. These conditions enhance brine flow into the LDRZ, producing a brine 'mound' in down-dip LDRZ. The mound is likely to produce relatively higher pressures in the down-dip regions (from this newly introduced brine) compared to that in the up-dip regions, thus promoting LDRZ brine to flow up-dip.

Gas Flow

Figure 6.3.12 (right) shows the sampled parameters most affecting north flowing gas into the south face (GSBPSSIC) and out the north face (GSBPSNOC) in the LDRZ below the panel closures.

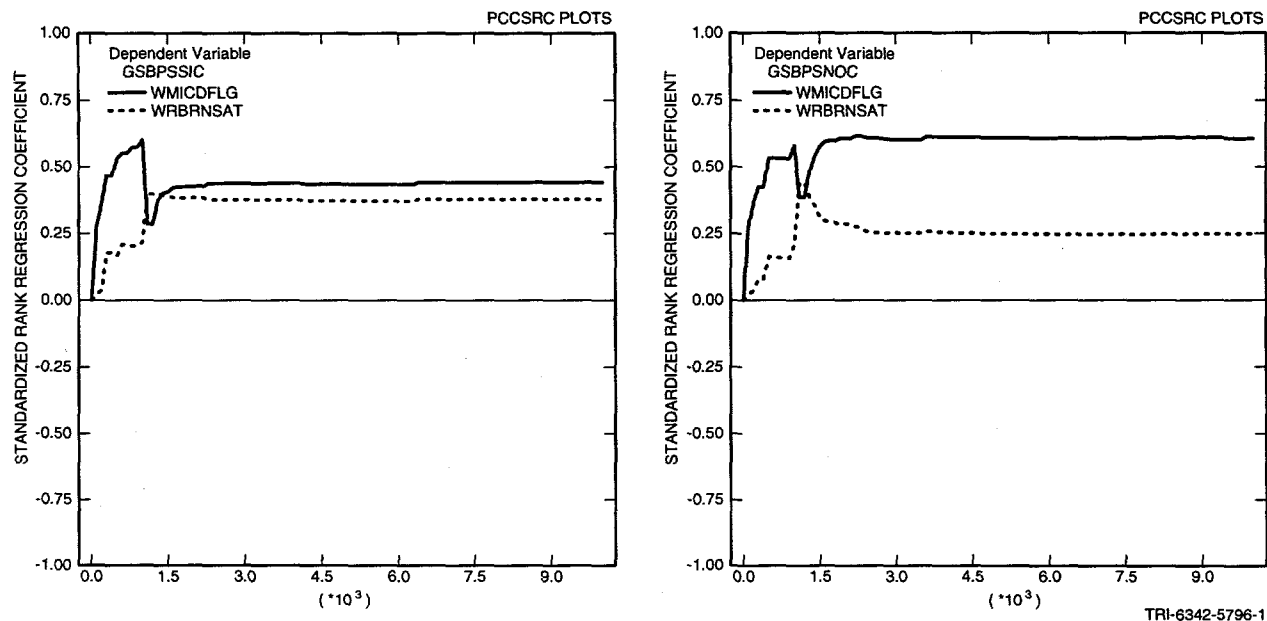


FIGURE 6.3.12. STANDARDIZED RANK REGRESSION COEFFICIENT (SRRC) RESULTS showing the most influential independent variables for lateral south-flowing gas in the LDRZ passing under the panel closures into the north face, GSBPSSIC (left), and out the south face, GSBPSNOC (right)

Only a few realizations have north-flowing gas in the LDRZ prior to intrusion; those that do have significant gas generated from microbial degradation. Gas pressures will tend to be elevated in all available void spaces, causing gas to displace resident brine as gas storage space in the lower waste panel is reduced, the LDRZ being one of many zones for gas storage. Those realizations with higher gas production early on, a function of $WMICDFLG > 0$, will have gas migrate in the LDRZ. Some of this gas will move up-dip in the LDRZ toward the upper regions of the repository. Hence, a positive correlation exists between north-flowing gas and $WMICDFLG > 0$.

A pulse of gas moves up-dip in the LDRZ as a result of the pressure pulse created by the intrusion event. If the lower waste panel is at a residual brine-saturation level, which is most likely at the time of intrusion (1000 years), the response to the pressure pulse from the intrusion

event is to displace gas—not brine—down through the waste panels to the LDRZ. Some of this gas will move up-dip in the LDRZ. The ease with which gas moves, given this pressure pulse, is partially a function of residual brine saturations. For those simulations assigned high residual brine saturation values, WRBRNSAT, gas flow is greater than brine flow. Thus, a correlation exists between WRBRNSAT and north-flowing gas.

7. Discussion of Overlay Plots for Brine and Gas Flow Within Borehole, UDRZ, and LDRZ

As reported in Helton et al. (1998), microbial degradation, borehole permeability, and, to a lesser extent, iron corrosion rates and brine reservoir initial pressure, appear as the more significant sampled variables impacting repository behavior for an E1-type intrusion throughout the modeled period. Therefore, in order to understand how these properties and processes affect repository behavior, overlay plots for gas and brine fluxes crossing boundaries of various modeled regions of the repository are provided in this section. Representative realizations were selected that were assigned either high or low borehole permeabilities, coupled with or without microbial degradation, and assigned either high or low iron corrosion rates. Table 7.1 lists the realizations. Figure 7.1 is a logic diagram depicting the realizations selected and their rank (out of a sample size of 100) within the LHS set of assigned values.

Table 7.1. Representative Realizations Examined

Realization	WMICDFLG	Logarithm of BHPRM (m ²)	Rank BHPRM ^a	WGRCOR (m/s)	Rank WGRCOR ^a	Logarithm of BPCOMP (l/Pa)	Rank BPCOMP ^a	BPINTPRS (Pa)	Rank BPINTPRS ^a
Range/ Distribution	Sample between 0, 1, 2 ^b	-14 to -11 uniform	—	0 to 1.58×10^{-14} uniform	—	-11.3 to -8.0 triangular	—	1.11×10^7 to 1.70×10^7 triangular	—
50	2	-1.11E+01	4	1.43E-14	4	-8.65E+00	7	1.27E+07	75
20	2	-1.39E+01	95	1.16E-14	28	-8.89E+00	13	1.34E+07	51
27	0	-1.24E+01	26	1.42E-14	11	-9.54E+00	36	1.31E+07	61
4	0	-1.32E+01	74	1.25E-13	21	-9.11E+00	19	1.19E+07	94
47	0	-1.38E+01	92	3.03E-14	80	-1.04E+01	81	1.40E+07	36

^a Rank is ordered as 1 = highest sampled value, 100 = lowest sampled value

^b 0 - no microbial degradation

1 - limited microbial degradation of cellulose only

2 - fully activated microbial degradation of cellulose, rubber, and plastics

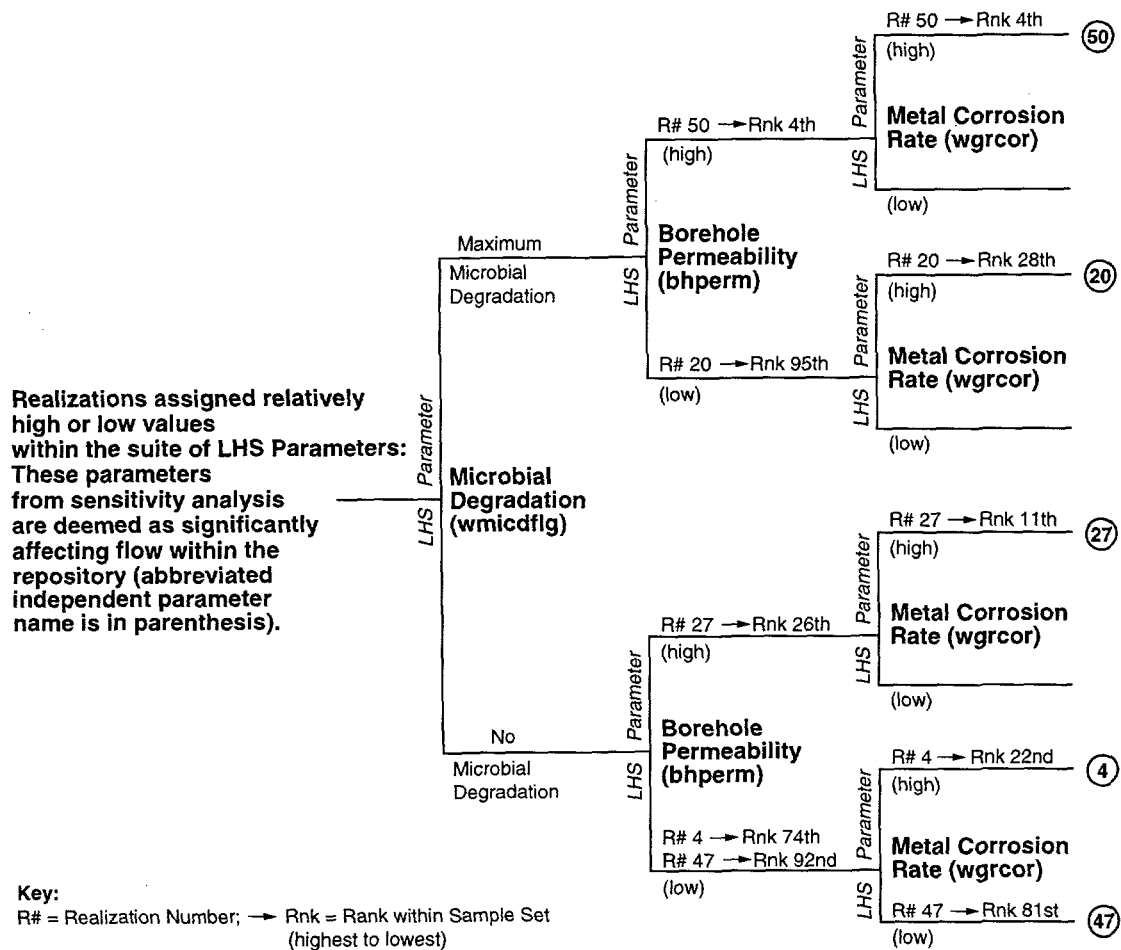


FIGURE 7.1. LOGIC DIAGRAM ILLUSTRATING REALIZATIONS REPRESENTATIVE of sampled parameter combinations that affect general trends in repository performance

Each plot was selected to aid in the understanding of the significant processes and/or fluid flow affecting repository behavior. In total, nine overlay plots are provided for each realization. The regions where flow and processes were assessed and depicted in the overlay plots are illustrated in Figures 7.2, 7.3, and 7.4.

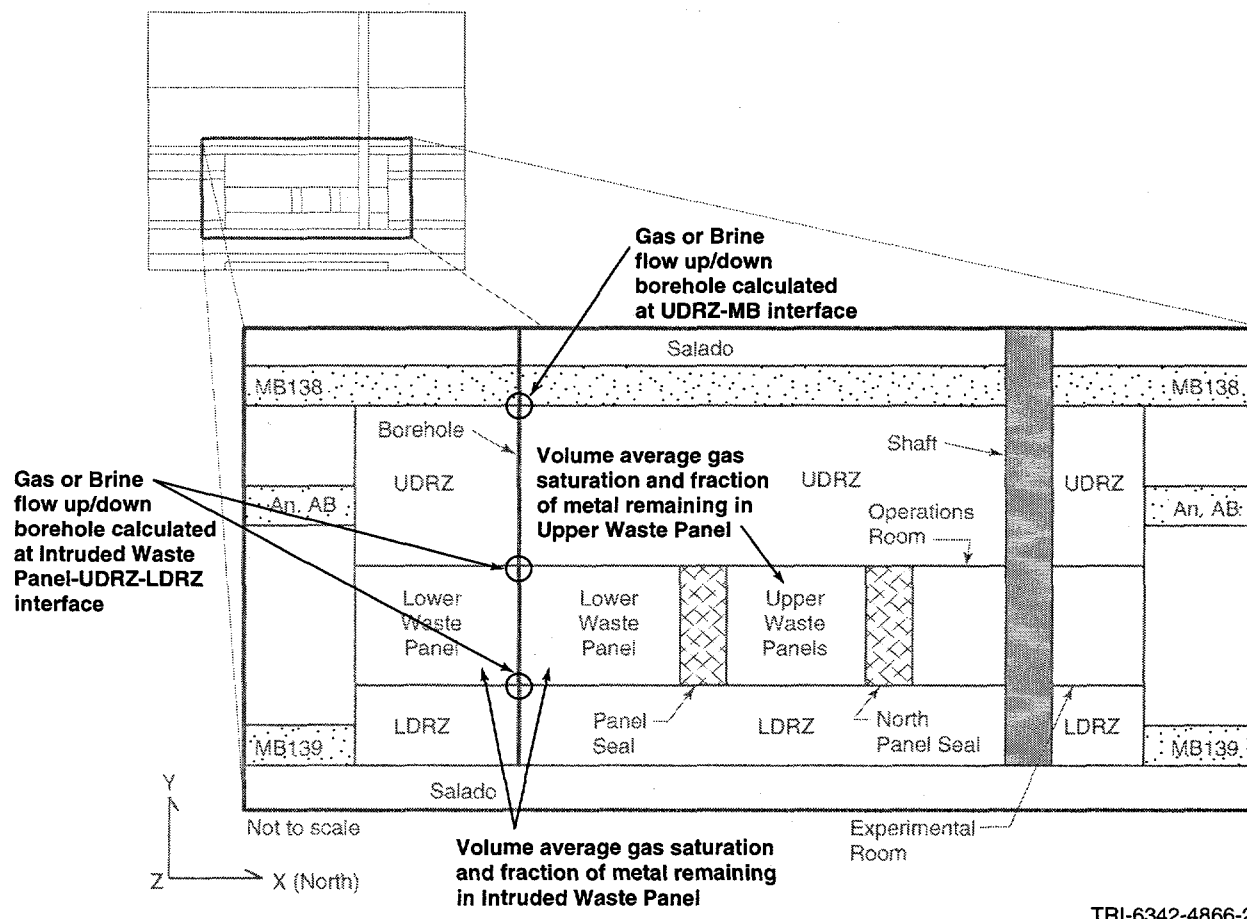
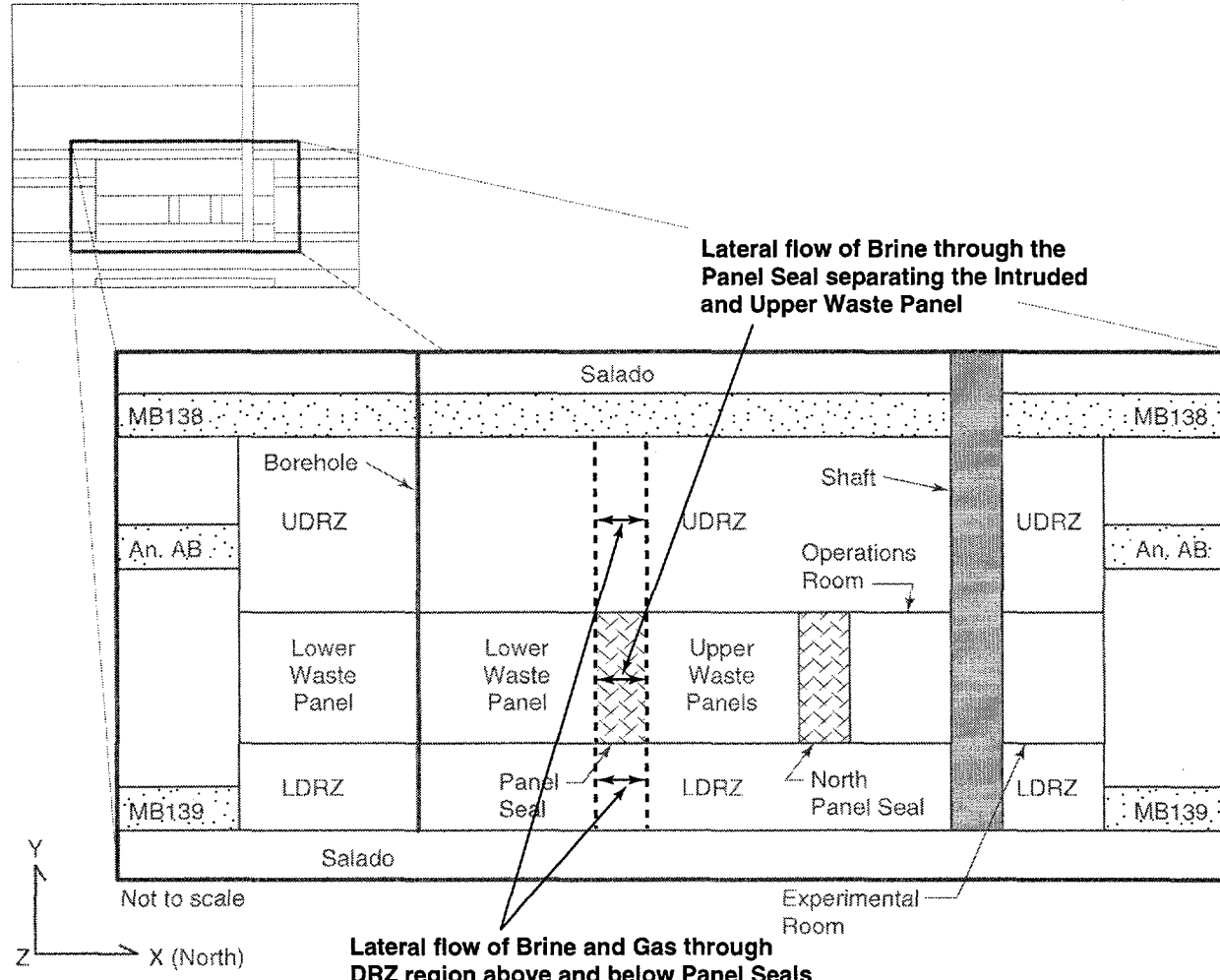


FIGURE 7.2. REGIONS WITHIN MODELED AREA WHERE repository pressures, fraction of iron remaining, brine and gas saturations in lower and upper waste panels, and gas and brine borehole flow were calculated



TRI-6342-4887-2

FIGURE 7.3. REGIONS WITHIN DRZ AND PANEL CLOSURES where lateral brine and gas flow were calculated

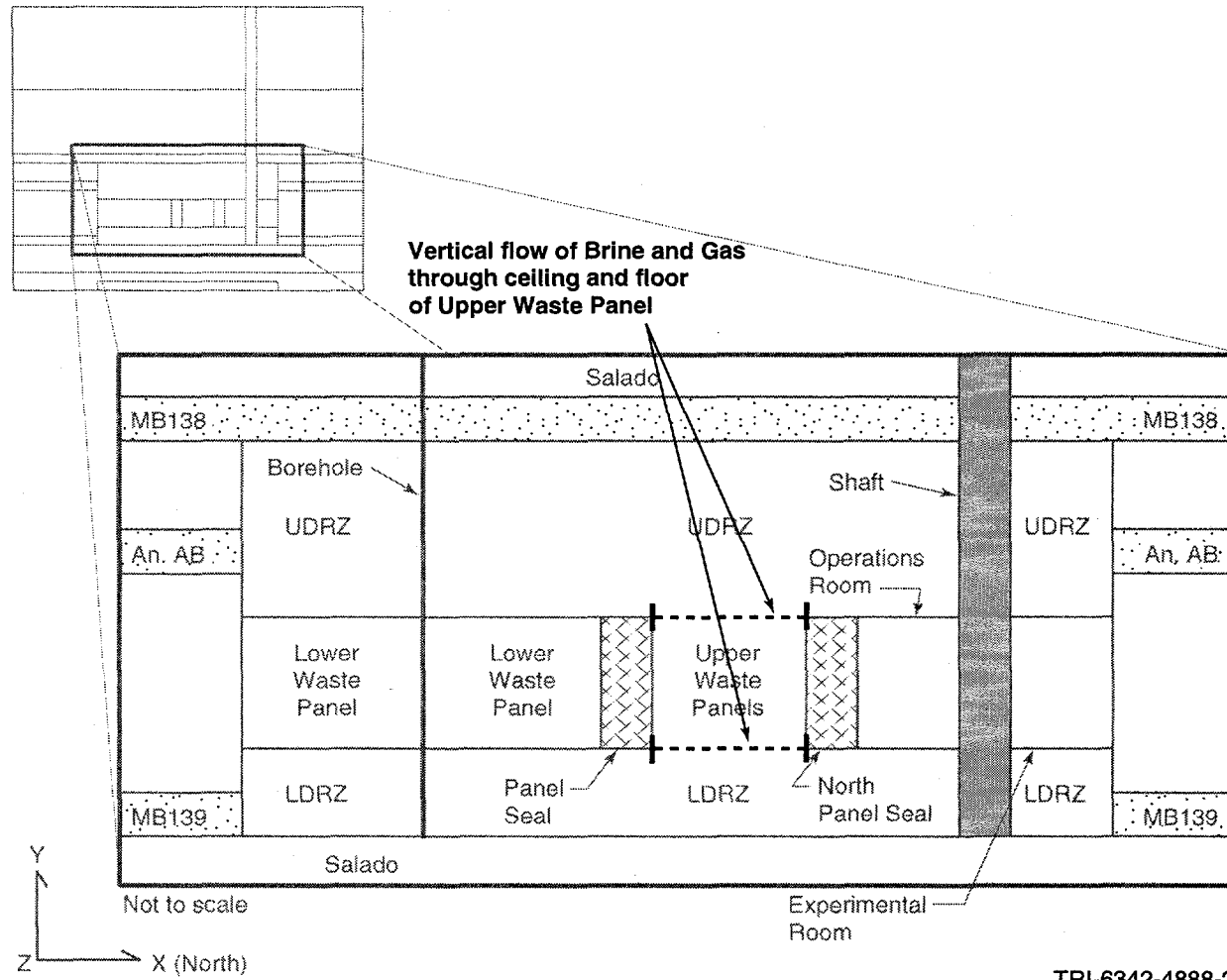


FIGURE 7.4. REGIONS WITHIN THE DRZ/UPPER WASTE panel interface where vertical brine and gas flow were calculated

Table 7.2 describes the dependent variables depicted in the overlay plots.

Table 7.2. Dependent Variables Described in Overlay Plots

Figure 7.x.1 overlay curves - top plot:

Volume Average Repository Pressures, Saturations, and Fraction Iron Remaining

Lower waste panel (WP) pressure	WAS_PRES
Upper waste panel (ROR) pressure	REP_PRES
Lower waste panel gas saturation	WAS_SATG
Upper waste panel gas saturation	REP_SATG
Fraction of uncorroded iron remaining in lower waste panel	FEREM_W
Fraction of uncorroded iron remaining in upper waste panel	FEREM_R

Figure 7.x.1 overlay curves - bottom plot:

Cumulative Gas and Brine Flow Within Borehole

Brine flow up borehole measured at top of lower waste panel (WP)	BRNBHUPC
Brine flow up borehole measured at top of UDRZ	BNBHUDRZ
Brine flow down borehole measured at top of UDRZ	BNBHDNUZ
Brine flow down borehole measured at top of lower waste panel	BRNBHDNC
Gas flow up borehole measured at top of UDRZ (WP)	GASBHUDRZ

Figure 7.x.2 overlay curves

Volume Average Brine Reservoir Pressure Overlaid with Flow in Borehole

Volume average pressure in brine reservoir (Pa)	B_P_PRES
Brine flow up borehole measured at bottom of lower waste panel and upper portion of LDRZ	BRNBHUPP
Brine flow down borehole at top of lower waste panel*	BRNBHDNC

Figures 7.x.3 and 7.x.4:

Cumulative Lateral Flow Within Panel Closures Between the Lower and Upper Waste Panels

Brine flow through panel closure into lower waste panel (WP)	BRNPSIWC
Brine flow through panel closure into upper waste panel (ROR)	BRNPSIRC
Brine flow through panel closure from lower waste panel	BRNPSOWC
Brine flow through panel closure from upper waste panel	BRNPSORC

Figure 7.x.3 overlay curves - top plot:

Cumulative Lateral North- and South-Flowing Brine Within UDRZ

North-flowing UDRZ brine entering south face of region just above panel closure	BRAPSSIC
North-flowing UDRZ brine exiting north face of region just above panel closure	BRAPSNOC
South-flowing UDRZ brine entering north face of region just above panel closure	BRAPSNIC
South-flowing UDRZ brine exiting south face of region just above panel closure	BRAPSSOC

Figure 7.x.3 overlay curves - bottom plot:

Cumulative Lateral North- and South-Flowing Brine Within LDRZ

North-flowing LDRZ brine entering south face of region just above panel closure	BRBPSSIC
North-flowing LDRZ brine exiting north face of region just above panel closure	BRBPSNOC
South-flowing LDRZ brine entering north face of region just above panel closure	BRBPSNIC
South-flowing LDRZ brine exiting south face of region just above panel closure	BRBPSSOC

* For reference, the curve indicating brine flow in the borehole, as measured at the bottom of the waste panel, is overlaid with the curve indicating brine flow measured at the top of the waste panel.

Table 7.2. Dependent Variables Described in Overlay Plots (Continued)

Figure 7.x.4 overlay curves - top plot:

Cumulative Lateral North- and South-Flowing Gas Within UDRZ

North-flowing UDRZ gas entering south face of region just above panel closure	GSAPSSIC
North-flowing UDRZ gas exiting north face of region just above panel closure	GSAPSNC
South-flowing UDRZ gas entering north face of region just above panel closure	GSAPSNC
South-flowing UDRZ gas exiting south face of region just above panel closure	GSAPSSOC

Figure 7.x.4 overlay curves - bottom plot:

Cumulative Lateral North- and South-Flowing Gas Within LDRZ

North-flowing LDRZ gas entering south face of region just above panel closure	GSBPSSIC
North-flowing LDRZ gas exiting north face of region just above panel closure	GSBPSNC
South-flowing LDRZ gas entering north face of region just above panel closure	GSBPSNC
South-flowing LDRZ gas exiting south face of region just above panel closure	GSBPSSOC

Figure 7.x.5 overlay curves - top plot:

Vertical Brine and Gas Flow Through Upper Waste Panel's (ROR) Ceiling

Upflowing brine	BRN.URAC
Downflowing brine	BRN.DRAC
Upflowing gas	GAS.URAC
Downflowing gas	GAS.DRAC

Figure 7.x.5 overlay curves - bottom plot:

Vertical Brine and Gas Flow Through Upper Waste Panel's (ROR) Floor

Upflowing brine	BRN.URBC
Downflowing brine	BRN.DRBC
Upflowing gas	GAS.URBC
Downflowing gas	GAS.DRBC

7.1 Realization 50 - Overlay Plot Summary

High borehole permeability - $10^{-11.1}$ m², rank 4/100

Large halite porosity - 0.0279, rank 6/100

Microbial degradation – 2, degradation of cellulose, rubber, and plastics; corrosion rate - 1.53×10^{-14} m/s, rank 4/100

Brief Summary: Realization 50 represents repository behavior affected by high gas generation prior to intrusion due to fully-activated microbial degradation (i.e., degradation of cellulose, rubber, and plastics) and high iron corrosion rates. Corrosion is enhanced due to plentiful brine supplies provided by UDRZ brine drainage. Consequently, repository pressure prior to intrusion is one of the highest values seen (90th percentile).

After intrusion and upper borehole degradation, relatively high borehole permeability causes gas to be easily evacuated out of the repository and repository pressures quickly decline. Because gas is easily vented out of the repository via the borehole and pressures lowered, brine reenters the repository via the marker beds or the borehole. This brine enables all available iron to become completely corroded in the lower waste panel midway through the modeled period. High gas production combined with high borehole permeability means that flow within the borehole is dominated by gas and does not taper off until all the iron in the lower waste panel is corroded. Once iron in the lower waste panel is corroded, gas flow out the borehole is reduced, allowing more brine to flow down the borehole.

7.1.1 Overlay Plots for Pressures in Lower (WAS_PRES) and Upper (REP_PRES) Waste Panels; Gas Saturation in the Lower (WAS_SATG) and Upper (REP_SATG) Waste Panels; Fraction of Uncorroded Iron in Lower (FEREM_W) and Upper (FEREM_R) Waste Panels (Figure 7.1.1 - top plot)

Note: All dependent variables are defined in title of each section.

Repository pressures dramatically change at 1000, 1200, and ~1700 years

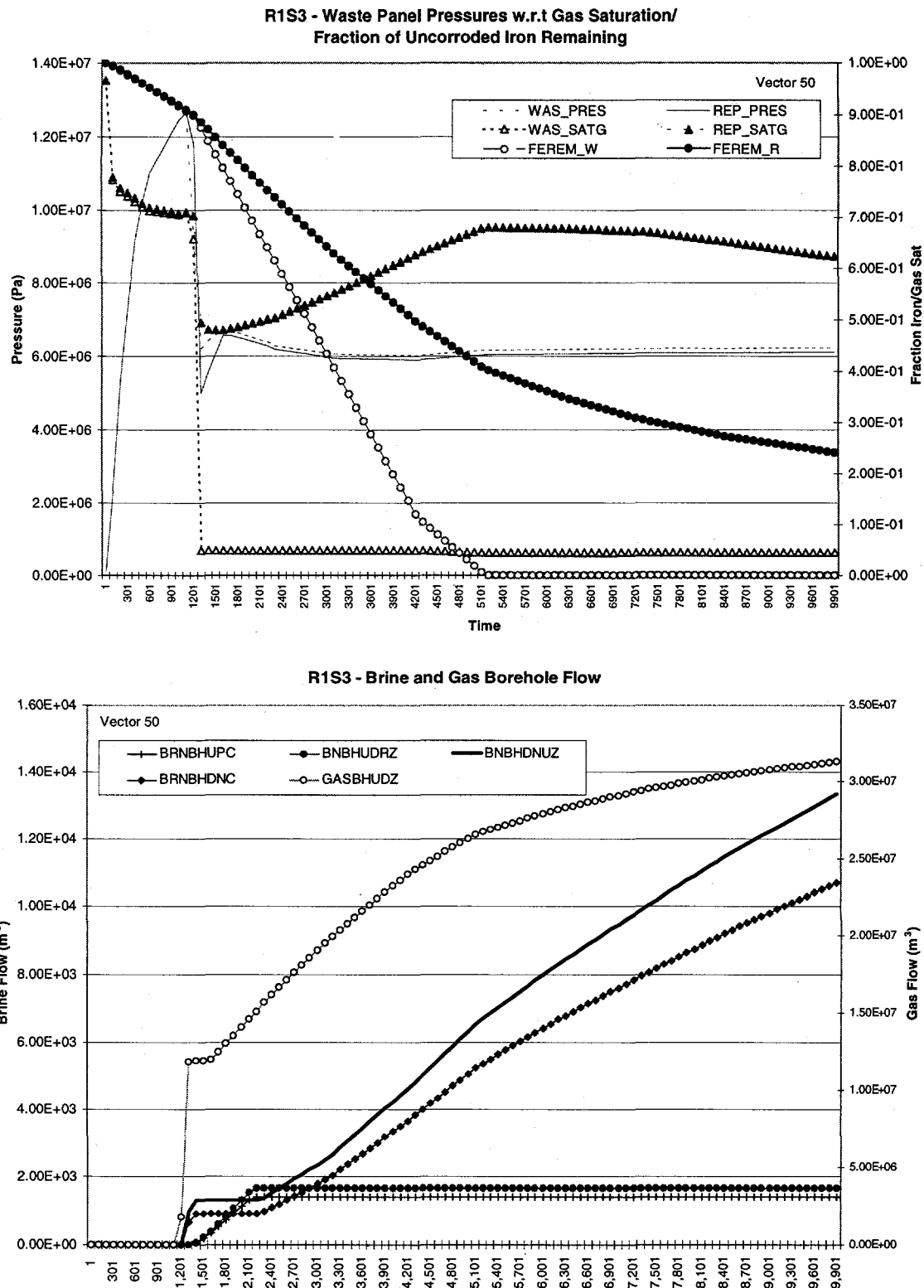


FIGURE 7.1.1. OVERLAY PLOTS FOR REALIZATION 50 depicting pressures, fraction of iron remaining, and gas saturations for lower and upper waste panels (top plot) and cumulative brine and gas flow within borehole at intersection of borehole with the top of lower waste panel and top of the UDRZ (bottom plot)

Repository Pressure for the Lower (WAS_PRES) and Upper (REP_PRES) Waste Panel

Repository pressures for both waste panels at 1000 years, the time of intrusion, are in the 90th percentile group due to the large amounts of gas generated from microbial degradation and relatively high iron corrosion rates. After plug degradation at 1200 years, borehole permeability is high, and so gas quickly evacuates out of the repository causing repository pressures to drop. Coincident with a decline in repository pressures, gas saturation within the lower waste panel (WAS_SATG) drops to residual gas saturation levels so that the lower waste panel has relatively high brine saturation. Rapid pressure changes occur within the repository from the time of intrusion to just after the upper borehole plug degrades (at 1200 years), creating a pressure 'trough' between 1200 and ~1700 years; the pressure difference between the repository and the upper units at this time prevents gas from flowing out the borehole. At ~1700 years, repository pressures go above hydrostatic (6.0 MPa), high enough to initiate gas flow up the borehole (see Figure 7.1.1, bottom plot).

Gas Saturation in Both the Upper (REP_SATG) and Lower Waste Panels (WAS_SATG)

Figure 7.1.1 - top plot

Gas saturation levels change dramatically at 1000, 1200, and ~5000 years

Large halite porosity means large DRZ pore volumes will drain brine into the waste regions early in the modeled period and large quantities of gas will be stored in the UDRZ. Large volumes of DRZ brine drainage mean both the lower and upper waste panels have a plentiful supply of brine for iron corrosion. As gas is produced, it is stored in the UDRZ. At the time of intrusion at 1000 years, pressures in the repository are slightly reduced (~1 to 2 MPa) as gas flows down the borehole towards the Castile reservoir. The reduction in gas saturation for both the lower and upper waste panels is about the same until 1200 years, when the upper borehole plug degrades. At this time, repository pressures dramatically drop, causing incoming brine from the non-Salado units above the repository to enter and fill the lower waste panel via the borehole, reducing gas saturation to near residual levels. After 1200 years, because the lower part of the repository and UDRZ is nearly 100% brine saturated, gas produced in the upper waste panel is prevented from

flowing out the borehole. Little pore space is available to store newly-produced gas. As a result, gas saturation in the upper waste panel increases until ~5000 years, when gas generation in the lower waste panel from iron corrosion ceases. Pressure above the lower waste panel is slightly reduced. This reduction creates a positive pressure gradient between panels and borehole, which promotes gas flow from the upper waste panel to the borehole. At that time, gas can then be evacuated out of the upper waste panel.

Fraction of Iron Uncorroded in Lower (FEREM_W) and Upper (FEREM_R) Waste Panel

The fraction of iron uncorroded in lower waste panel (FEREM_W) and upper waste panel (FEREM_R).

The fraction of iron actively being corroded changes at 1200 and 5000 years

Iron corrosion rates within the lower and upper waste panels are similar because plentiful brine supplies exist in both waste regions from DRZ brine drainage prior to intrusion. At the time of borehole degradation (1200 years), more brine enters the lower waste panel than the upper waste panel due to positioning; thus, the rate of iron corrosion in the lower waste panel increases due to an increase in brine availability. Consequently, iron in the lower waste panel is depleted at ~5000 years. A slight decrease in iron corrosion (iron depletion) rates occurs in the upper waste panel at the same time that iron corrosion in the lower waste panel is complete. This rate again declines at ~5000 years since iron corrosion in the upper waste panel is limited to that region where brine collects at the interface of the panel closures and the lower end of the upper waste panel. Once iron is corroded in this area, the corrosion of iron located up-dip is dependent on the brine pool¹ moving up-dip in the upper waste panel.

7.1.2 Overlay Plots for Flow in Borehole

Figure 7.1.1 - bottom plot

Brine flow rates up borehole measured at the top of the lower waste panel (BRNBHUPC), and top of the UDRZ (BNBHUDRZ);

¹ No actual brine pool exists in the repository; this term refers to a near 100% brine-saturated zone within the porous media.

Brine flow down borehole measured at the top of UDRZ (BNBHDNUZ) and top of the lower waste panel (BRNBHDNC);
Gas flow up borehole measured at the top of UDRZ (GASBHUDZ).

Brine flow in the borehole changes dramatically at 1200, 2200, and ~5000 years.

Brine Flow in the Borehole

No flow in the upper borehole is seen until 1200 years, when the upper borehole plug degrades. At the time of borehole degradation, pressure gradients between the brine reservoir and the repository, and between the repository and the units above the repository, promote brine flow up the borehole (BRNBHUPC, BNBHUDRZ). This upward flow of brine ceases at 2200 years when the lower borehole creep closes and brine in the borehole reverses from an upward to a downward flow direction. Because borehole permeabilities are high, both gas and brine can flow within the borehole concurrently.

A brief pulse (lasting ~100 years) of downward-flowing brine (BNBHDNUZ, BRNBHDNC) occurs at 1200 years when the upper borehole plug degrades from the upper units to the repository. This downward brine flow ceases at ~1300 years, but begins again at 2200 years when the lower borehole permeability is reduced by a factor of 10, which effectively limits flow up the borehole from the lower units. The change in pressure gradient between the repository and the upper units (due to creep closure of the lower borehole) now promotes brine flow down the borehole. Because the lower waste panel is close to full brine saturation (see Figure 7.1.1, top plot), a large portion of incoming brine is deflected at the UDRZ/lower waste panel interface. Some of this brine flows up-dip toward the upper waste panel. When iron in the lower waste panel is depleted by corrosion at ~5000 years, brine consumption ceases. Therefore, at ~5000 years, a larger fraction of replenishing brine coming down the borehole is deflected at the UDRZ and LDRZ toward the upper waste panels (resulting in a decrease in gas saturation within the upper waste panels). This replenishing brine allows the 'brine pool' that has formed in the south portion of the repository to rise. It is only the newly-elevated regions of the brine pool that contact iron which has not been corroded. Brine continues to flow down the borehole through the end of the modeled period.

Gas Flow in the Borehole

A brief pulse of gas (GASBHUDZ) flows up the borehole at 1200 years, the time of borehole plug degradation. At ~1700 years, when repository pressure rises to levels just above hydrostatic (6.0 MPa), gas flow up the borehole continues at a constant flow rate until ~5000 years, when iron in the lower waste panel is consumed. Gas flow decreases at ~5000 years, when the lower waste panel gas generation ceases. Gas generated in the upper waste panel continues to contribute to borehole gas flow through the end of the modeled period.

7.1.3 Overlay Plots for Castile Brine Reservoir Pressures (B_P_PRES) with Respect to Brine Flow Up (BRNBHUPP) and Down (BRNBHDNC) the Borehole

Figure 7.1.2

B_P_PRES (brine reservoir pressure)

BRNBHUPP (brine up borehole measured at the bottom of lower waste panel)

BRNBHDNC (brine down borehole measured at the top of lower waste panel)

A dramatic change in Castile reservoir pressures is seen at 1000, ~1700, and 2200 years.

At the time of intrusion, pressure within the Castile reservoir (B_P_PRES) is only slightly higher than the repository (compare Figure 7.1.2 with Figure 7.1.1, top plot). Thus, a small pressure potential exists between these two regions, promoting brine flow from the Castile upward.

Because the brine reservoir in Realization 50 has such high compressibility (ranked 7th) and high borehole permeability (ranked 4th), a significant volume of brine is released up the borehole (BRNBHUPP) from the Castile to the repository at the time of intrusion.

7.1.4 Overlay Plots for Brine Flow through the Panel Closures to the Upper and Lower Waste Panels

Figures 7.1.3 and 7.1.4 - all plots

North-flowing brine from lower to upper waste panel is defined as BRNPSOWC (brine from the lower waste panel enters the panel closure south face) and BRNPSIRC (brine exits the panel closure north face to the upper waste panel)

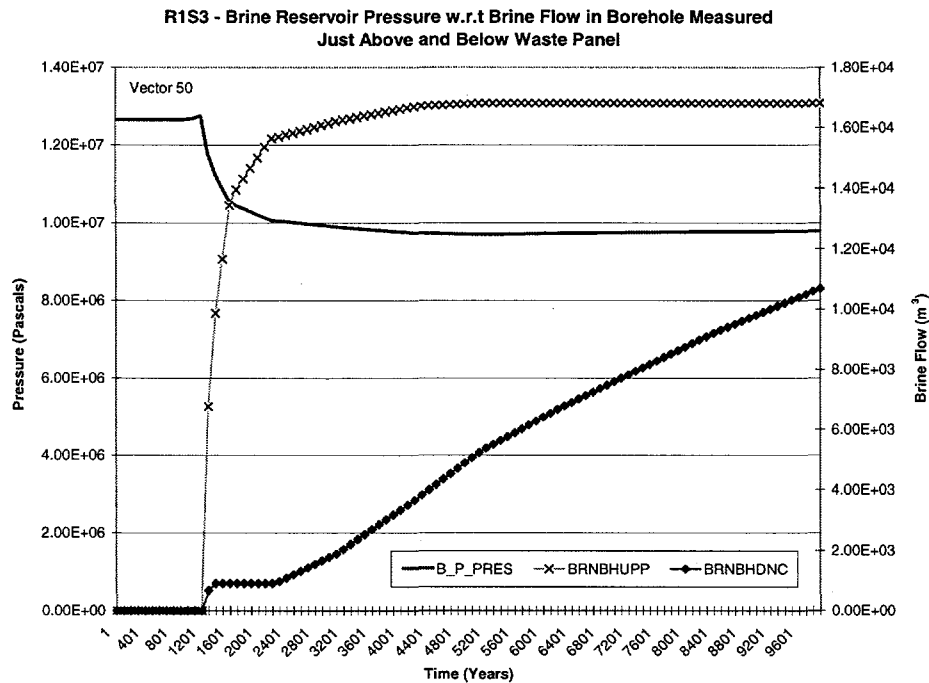


FIGURE 7.1.2. OVERLAY PLOT FOR REALIZATION 50 depicting brine reservoir pressure overlaid with brine flow up and down the borehole measured at the top and bottom of the lower waste panel

South-flowing brine from upper to lower waste panel is defined as BRNPSORC (brine flows through panel closure from upper waste panel) and BRNPSIWC (brine flows through panel closure into lower waste panel)

Brine flow through the panel closures changes at 1200 years

Prior to intrusion, high iron corrosion rates consume large volumes of brine, leaving little brine to migrate between waste regions; therefore, only a small amount of brine flows between the lower and upper waste panels via the panel closures. After the upper borehole plug degrades (at 1200 years), the lower waste panel becomes brine saturated, and gas is easily evacuated out of the repository via the borehole. Because the lower waste panel is brine saturated, any incoming brine not consumed via iron corrosion flows to other portions of the repository. These conditions create a positive pressure gradient between the lower and upper waste panels, promoting some brine flow from the lower waste panel to the upper waste panel via the panel closures.

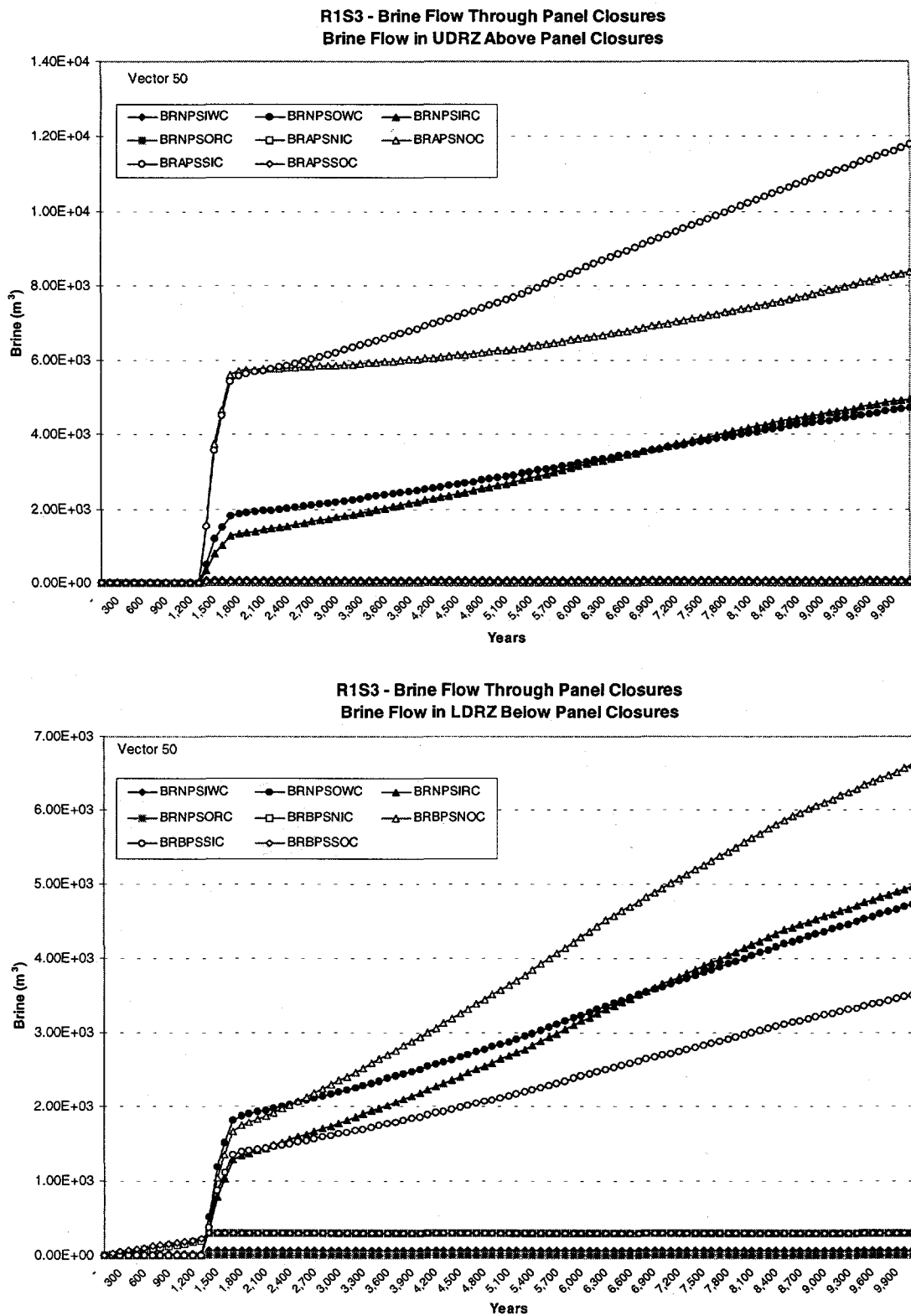


FIGURE 7.1.3. OVERLAY PLOTS FOR REALIZATION 50 depicting brine flow through the panel closures overlaid with lateral brine flow within UDRZ (top plot) and LDRZ (bottom plot), crossing the area just above/below panel closures

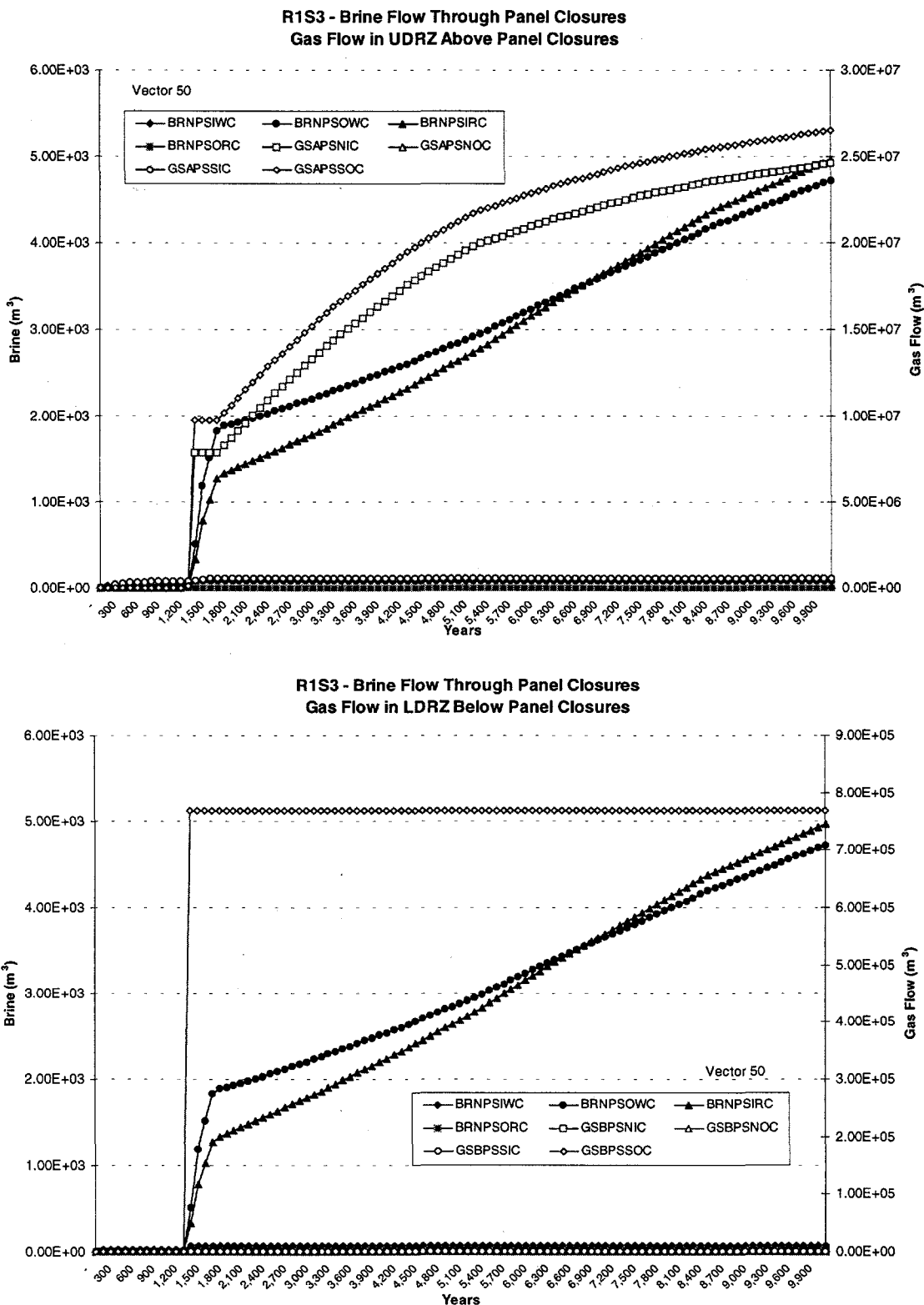


FIGURE 7.1.4. OVERLAY PLOTS FOR REALIZATION 50 depicting brine flow through the panel closures overlaid with lateral gas flow within UDRZ (top plot) and LDRZ (bottom plot), crossing the area just above/below panel closures

7.1.5 Overlay Plots for Lateral Brine Flow in DRZ Above and Below Panel Closures

Lateral Brine Flow in the UDRZ

Figure 7.1.3 - top plot (refer also to Figure 7.3)

North-flowing brine is defined as BRAPSSIC (brine entering south face), and
BRAPSNOC (brine exiting north face)

South-flowing brine is defined as BRAPSSOC (brine exiting south face), and
BRAPSNIC (brine entering north face)

North-flowing brine above the panel closure starts at 1200 years and continues to end of modeled period

Figure 7.1.3, top plot, shows brine flow within the UDRZ overlaid with brine flow through the panel closures. A surge of north-flowing brine (BRAPSSIC, BRAPSNOC) begins at 1200 years when the upper borehole plug degrades, and continues until the end of the modeled period. A portion of that brine drains from the UDRZ down through the panel closures as it flows northward. Evidence of this drainage is seen by smaller volumes of brine leaving the north face of the region above the panel closures (BRAPSNOC) compared to brine volumes entering the south face of that region (BRAPSSIC).

Lateral Brine Flow in the LDRZ

Figure 7.1.3 - bottom plot (refer also to Figure 7.3)

North-flowing brine is defined as BRBPSSIC (brine entering south face), and
BRBPSNOC (brine exiting north face)

South-flowing brine is defined as BRBPSSOC (brine exiting south face), and BRBPSNIC
(brine entering north face)

Changes in brine flow rates and direction in the LDRZ below the panel closures are seen at 1200 and ~1700 years

In the LDRZ, a small amount of brine flows southward below the panel closures (BRBPSSOC, BRBPSNIC) until 1200 years, when the upper borehole plug degrades. At 1200 years, brine flow direction in the LDRZ reverses from down-dip to up-dip. This flow lasts until ~1700 years, when repository pressures rise to just above hydrostatic (see Figure 7.1.1, top plot), then slows

from ~1700 years to the end of the modeled period. A large portion of brine flowing northward in the LDRZ (BRBPSSIC, BRBPSNOC) is from panel closure drainage.

7.1.6 Overlay Plots for Lateral Gas Flow in the DRZ Above and Below the Panel Closures

In Figure 7.1.4, gas flow within the DRZ is compared to brine flow through the panel closures.

Lateral Gas Flow in the UDRZ

Figure 7.1.4 - top plot (refer also to Figure 7.3)

North-flowing gas is defined as GSAPSSIC (gas entering south face) and GSAPSNOc (gas exiting north face)

South-flowing gas is defined as GSAPSSOC (gas exiting south face) and GSAPSNC (gas entering north face)

Gas flow rates and direction in the UDRZ change at 1200; ~1700, and ~5000 years.

Insignificant amounts of gas flow up-dip in the UDRZ (GSAPSSIC, GSAPSNOc) prior to intrusion due to a large DRZ void volume available for gas storage above all waste panels. At the time of borehole plug degradation (1200 years), pressure gradients promote a brief pulse of south-flowing gas within the UDRZ (GSAPSSOC, GSAPSNC) toward the borehole. At this time, a pulse of gas passes through the panel closures up to the DRZ, indicated by differing gas volumes leaving the south side of the region above the panel closures in the UDRZ compared to volumes entering from the north (compare GSAPSSOC to GSAPSNC). This gas pulse ceases in the UDRZ until ~1700 years, when incoming brine from the lower reservoir flows up through the borehole and enters the DRZ. From ~1700 years to 5000 years, UDRZ south-flowing gas continues at a constant rate until all iron in the lower waste panel is completely corroded and it is likely most iron in the lower portion of the upper waste panel is also corroded.

Lateral Gas Flow in the LDRZ

Figure 7.1.4 - bottom plot (refer also to Figure 7.3)

North-flowing gas is defined as GSBPSSIC (gas entering south face) and GSBPSNOc (gas exiting north face)

South-flowing gas is defined as GSBPSSOC (gas exiting south face) and GSBPSNIC (gas entering north face)

Gas flow rates and direction in the LDRZ change at 1200 years

A brief southward pulse of gas (GSBPSSOC, GSBPSNIC) is seen in the LDRZ below the panel closures at 1200 years due to a strong pressure gradient produced between the repository and the upper units when the borehole degrades. This pushes gas in the LDRZ towards the borehole. Immediately after this pulse of gas, no gas flows in the LDRZ.

7.1.7 Overlay Plots for Brine and Gas Flow In/Out the Ceiling and Floor of Upper Waste Panel

Brine Flow Through the Upper Waste Panel Ceiling

Figure 7.1.5 – top plot

BRN_DRAC (downflowing brine) and BRN_URAC (upflowing brine)

Brine flow rates through the upper waste panel ceiling change at 100, 1200, and ~1700 years. For the first ~100 years after decommissioning, significant brine drains from the UDRZ through the ceiling of the upper waste panels (BRN_DRAC). At 1200 years, when the upper borehole closure degrades, repository pressures decline (due to gas evacuation out the borehole), allowing brine to flow up the borehole from the Castile reservoir. A portion of brine is partitioned in UDRZ and flows up-dip, then is deflected downward into the upper waste panel. Later in the modeled period, brine flows down the borehole, then flows into the upper waste panel via the UDRZ and the LDRZ. This flow continues until ~1700 years, when the drop in Castile pressures reduces brine flow upward, and gas flows up the borehole again.

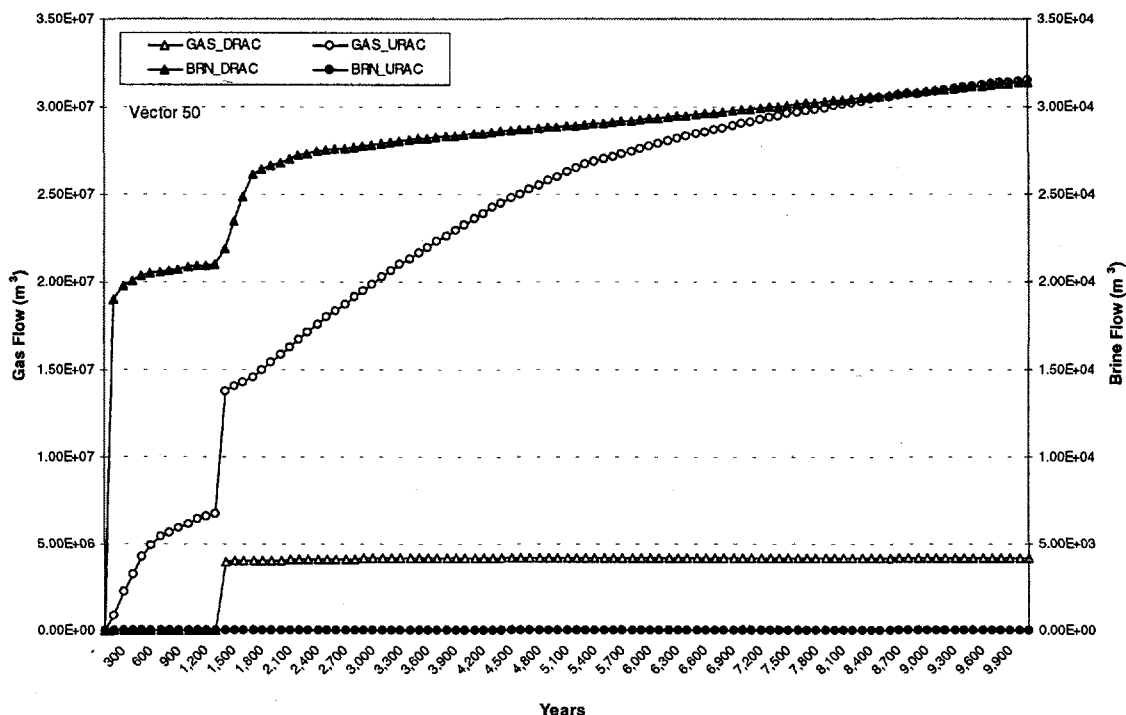
Gas Flow Through the Upper Waste Panel Ceiling

Figure 7.1.5 – top plot

GAS_DRAC (downflowing gas) and GAS_URAC (upflowing gas)

Gas flow rates out the upper waste panel ceiling change at 1200 years

R1S3 - Brine and Gas Flow In and Out the Upper Waste Panel Ceiling



R1S3 - Brine and Gas Flow In and Out the Upper Waste Panel Floor

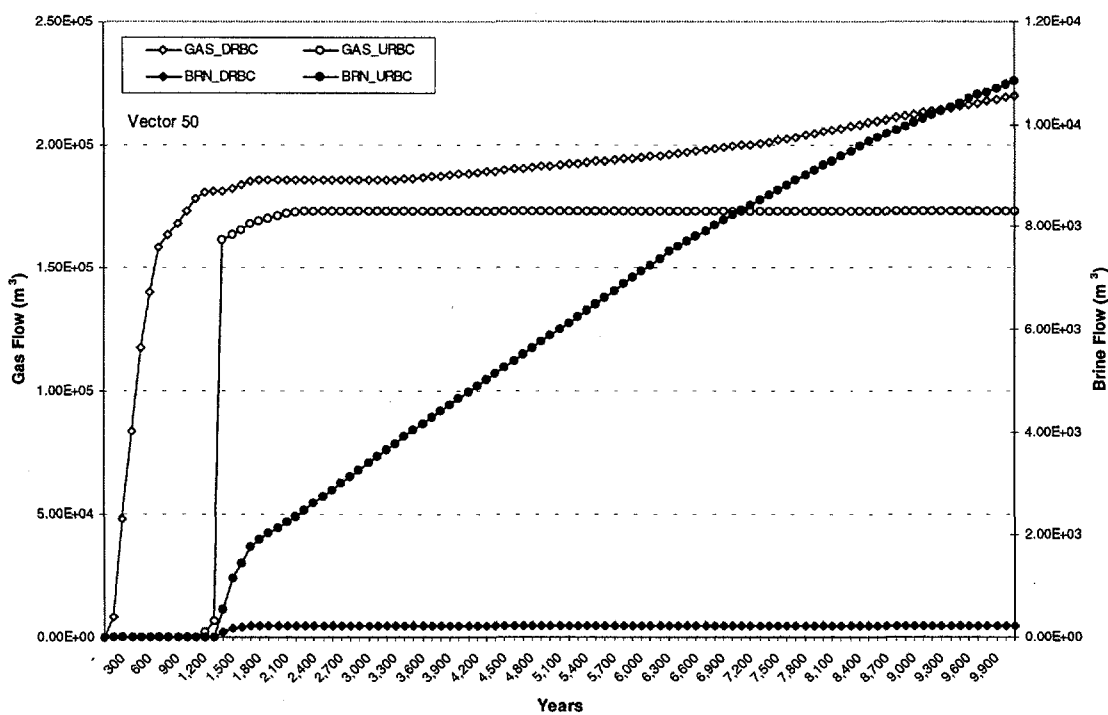


FIGURE 7.1.5. OVERLAY PLOTS FOR REALIZATION 50 depicting vertical brine and gas flow through the ceiling of upper waste panel within the UDRZ (top plot) and LDRZ (bottom plot)

Gas flow out of the upper waste panel ceiling (GAS_URAC) is essentially continuous throughout the modeled period. Gas flow tapers off between ~600 and 1200 years when the repository and the gas within the UDRZ become highly pressurized. (Little gas is released to the marker beds.) Gas flow rates out the ceiling of the upper waste panel increase when the upper borehole plug degrades (1200 years), depressurizing the repository, then decrease at ~5000 years. The decline in the gas flow rate at 5000 years is due to a decrease in gas generated from iron corrosion in the upper waste panel (coincident with complete iron depletion in the lower waste panel).

Brine Flow Through the Upper Waste Panel Floor

Figure 7.1.5 – bottom plot
BRN_DRBC (downflowing gas) and BRN_URBC (upflowing gas)

Brine flow rates through the floor of the upper waste panel change at 1200 and ~1700 years

Brine begins to flow up from the LDRZ through the floor of the upper waste panel (BRN_URBC) at the time of borehole degradation (1200 years) until the end of the modeled period, and serves as a continuous source for the iron corrosion process. This flow is a result of the repository undergoing rapid depressurization caused by gas leaving via the borehole. This evacuation of gas reduces gas saturations and pressures in the upper waste panel and the LDRZ just below the upper waste panel (see Section 7.1.8, gas saturation contour plots at ~1000, ~1200, and ~5000 years), which increases effective brine permeability. Combined, these processes promote brine flow up through the upper waste panel floor. Similar to brine flow down through the upper waste panel ceiling, brine flow rates through the floor are very high between 1200 and ~1700 years. When the brine reservoir pressure declines to levels below that of the repository, at ~1700 years, the pressure potential between the Castile and the repository that promotes brine flow into the LDRZ is diminished; thus, flow through the upper waste panel floor is reduced.

Gas Flow Through the Upper Waste Panel Floor

Figure 7.1.5 – bottom plot

GAS_DRBC (downflowing gas) and GAS_URBC (upflowing gas)

Gas flow rates through the floor of the upper waste panel change at ~600, 1000, and 1200 years

Due to high gas production from microbial degradation and iron corrosion, large volumes of gas are produced that drive gas down through the floor of the upper waste panel into the LDRZ (GAS_DRBC). Gas moves to the LDRZ from the time of repository closure to the time of intrusion. As gas production from microbial degradation ends (at 1000 years) due to the degradation of all cellulosics, less gas moves into the LDRZ. At 1000 years (time of intrusion), gas flow through the upper waste panel floor reverses direction due to the intrusion event, reversing the pressure gradient between the repository and the LDRZ.

7.1.8 Gas Saturation Contour Plots

Figure 7.1.6

SATGAS

Gas saturation contour plots at 1000, ~1212, ~5146, and 10,000 years

The four gas saturation plots (given in Figure 7.1.6) show conditions at 1000 years, just prior to intrusion; at ~1212 years, just after the upper borehole plug degrades; at ~5146 years, when iron in the lower waste panel is close to being completely corroded; and at 10,000 years, the end of the modeled period. A review of all four plots shows that a gas saturation wedge forms in the UDRZ above the upper waste panel closures soon after depletion of steel in the lower waste panel. This wedge persists from ~5146 years until the end of the modeled period. The LDRZ appears to be close to 100% brine saturated soon after the upper borehole plug degrades (1200 years) to the end of the modeled period.

The gas saturation contour plots show that the repository is close to 100% gas saturated at 1000 years, prior to intrusion (Figure 7.1.6a). The plot at 1212 years (Figure 7.1.6b) (taken just after

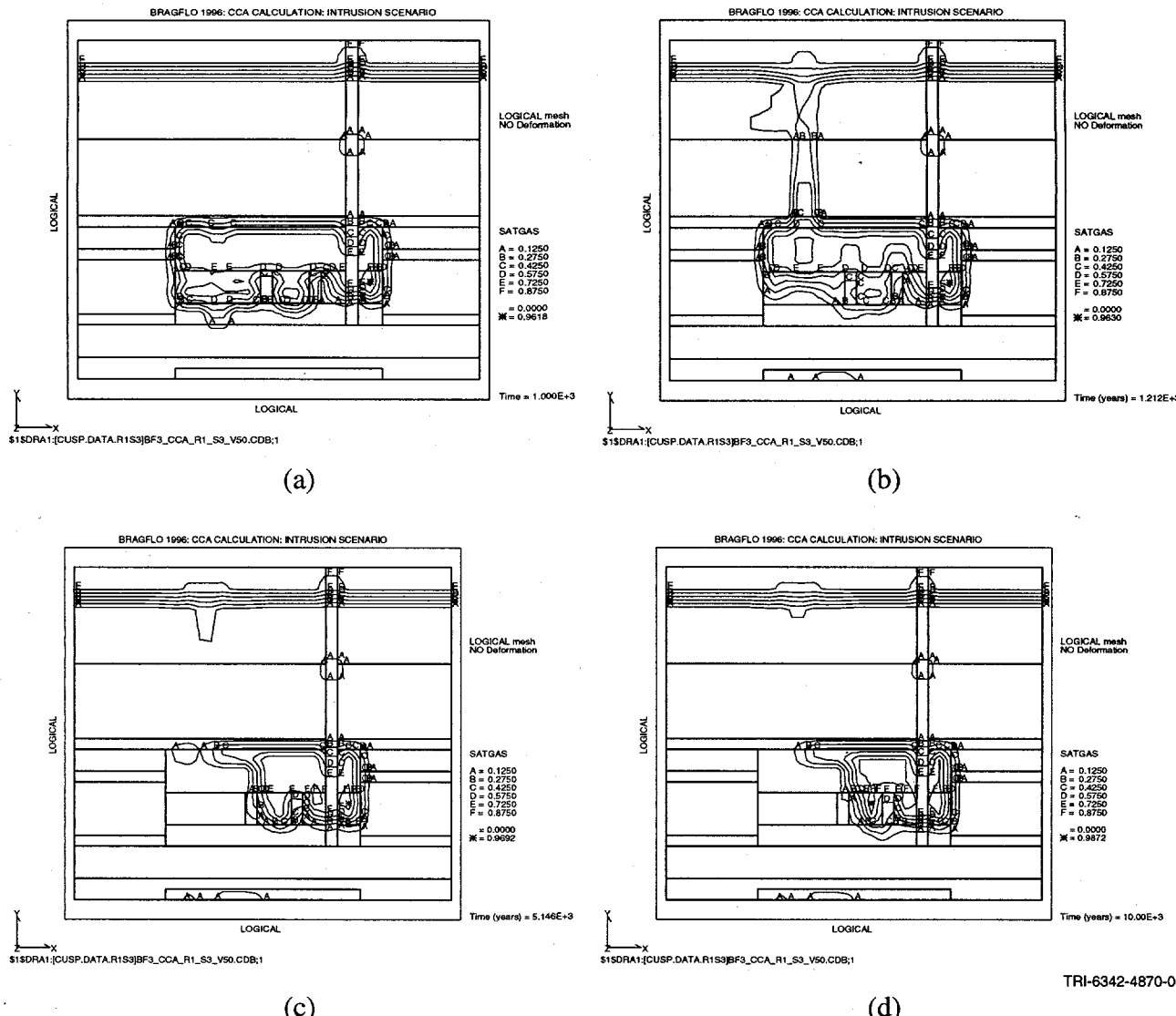


FIGURE 7.1.6. GAS SATURATION CONTOURS FOR REALIZATION 50. (a) 1000 years, just prior to intrusion, (b) 1212 years, (c) ~5100 years, and (d) the end of the modeled period, 10,000 years. Borehole in lower waste panel is not shown; see Figure 7.4 for location of borehole

the upper borehole degrades) indicates that significant gas has evacuated out of the repository via the borehole, enabling replenishing brine to enter through the floor of the lower waste panel.

At ~5146 years (Figure 7.1.6c), the lower waste panel is brine saturated and the upper waste panel remains gas saturated. The UDRZ above the upper waste panel remains gas saturated, along with the upper portion of the UDRZ above the lower waste panel. This level of gas

saturation generates a low effective brine permeability zone in the UDRZ, creating a barrier to lateral brine flow in the UDRZ entering the ceiling of the upper waste panel.

At 10,000 years (Figure 7.1.6d), because the lower waste panel is close to 100% brine saturated (i.e., brine filled), a large portion of brine flowing down the borehole is deflected laterally up-dip in the UDRZ. This brine flows up-dip in the UDRZ and then is deflected downward into the panel closure and through the upper waste panel ceiling (just north of the closure) as a result of the gas bubble that resides in the UDRZ.

7.2 Realization 20 - Overlay Plot Summary

Low borehole permeability - $10^{-13.9} \text{ m}^2$, rank 95/100

Halite porosity - 0.00649, rank 70/100

Microbial degradation -2, degradation of cellulose, rubber, and plastics; corrosion rate - $1.16 \times 10^{-14} \text{ m/s}$, rank 28/100

Brief Summary: Realization 20 is indicative of repository behavior affected by high gas volumes generated early on from microbial degradation, a Castile reservoir at pressures near repository pressure at the time of intrusion, relatively low halite porosity, and low value for borehole permeability. A relatively low value for halite porosity means relatively little brine drains into the waste regions early in the modeled period; a low value for borehole permeability means repository pressures decline at a relatively slower rate after the intrusion event. Pressure declines due to the slow release of repository gas via the borehole. This continuous flow of gas prevents incoming brine from entering the repository via the borehole. Consequently, the lower waste panel remains predominantly gas saturated until ~5000 years, then declines to a ~60% value between 5000 and 10,000 years. The upper waste panels remain nearly 100% gas-saturated throughout the modeled period. The UDRZ remains predominantly gas-saturated throughout the modeled period. UDRZ gas flows up-dip prior to intrusion and down-dip, towards the borehole, after intrusion. The LDRZ is predominantly brine-saturated, and fluid flow of brine in the LDRZ is down-dip throughout the modeled period. Despite the relatively high iron corrosion rate assigned to this realization, because of limited brine supplies early in the modeled period and lack of incoming brine via the borehole after the intrusion event, much less iron is corroded in both waste panels compared to realizations assigned higher borehole permeabilities, higher halite porosities, and lower iron corrosion rates.

7.2.1 Overlay Plots for Pressures in Lower (WAS_PRES) and Upper (REP_PRES) Waste Panels; Gas Saturation in the Lower (WAS_SATG) and Upper (REP_SATG) Waste Panels; Fraction of Uncorroded Iron in Lower (FEREM_W) and Upper (FEREM_R) Waste Panels (Figure 7.2.1 - top plot)

Note: All dependent variables are defined in title of each section.

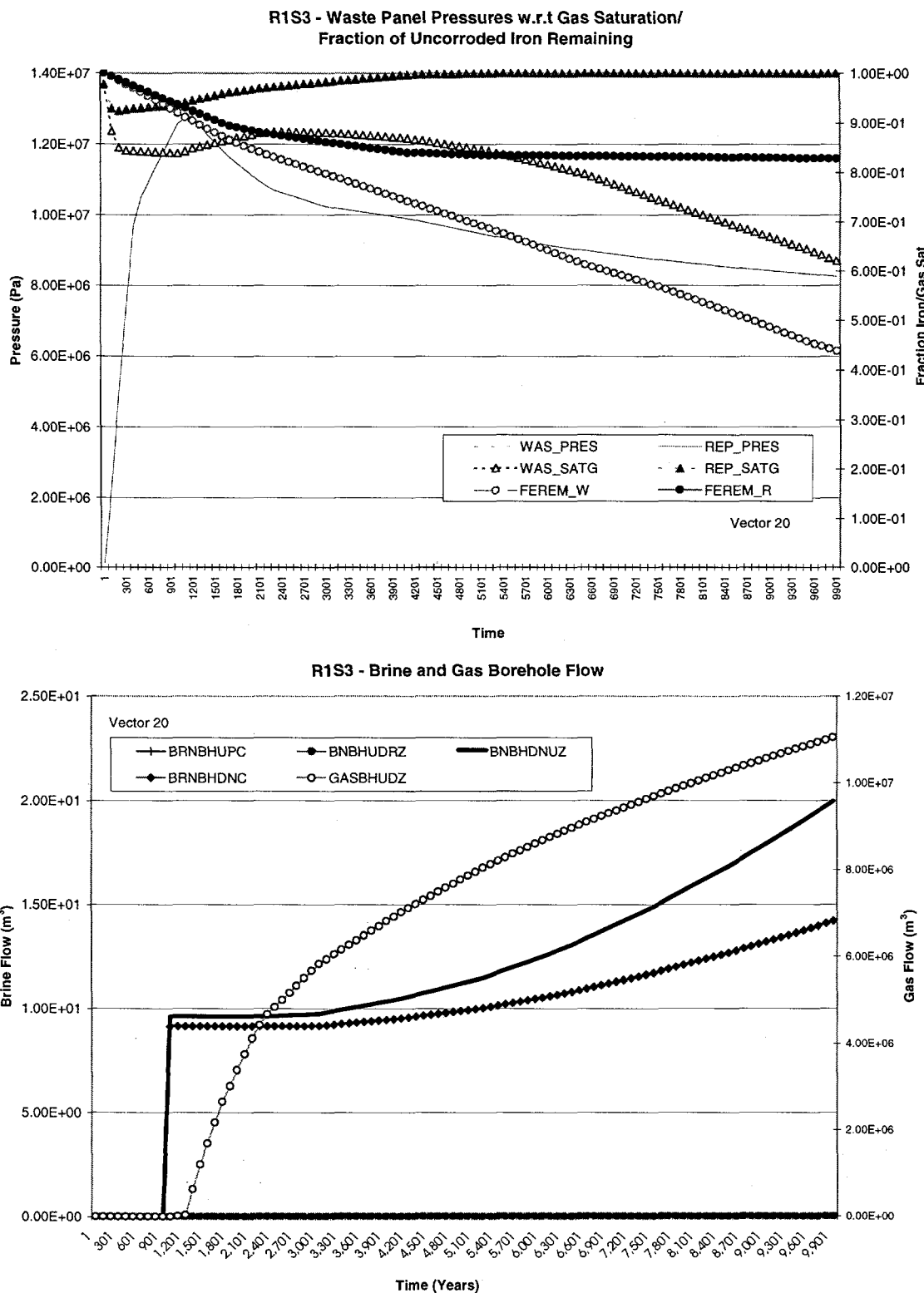


FIGURE 7.2.1. OVERLAY PLOTS FOR REALIZATION 20 depicting pressures, fraction of iron remaining, and gas saturations for lower and upper waste panels (top plot) and cumulative brine and gas flow within borehole at intersection of borehole with top of lower waste panel and top of the UDRZ (bottom plot)

Figure 7.2.1 - top plot

Pressure changes dramatically at 1000, 1200, 2200, and ~1700 years

Repository Pressure for the Lower (WAS_PRES) and Upper (REP_PRES) Waste Panel

Repository pressures (WAS_PRES and REP_PRES) at the time of intrusion are relatively high as a result of high gas production from microbial degradation and, to a lesser extent, high iron corrosion rates. Because this pressure is slightly greater than that of the Castile reservoir, the intrusion event does not create a dramatic change in repository pressures for the 200 years when only the lower borehole is open. The pressure in the Castile slightly increases and stays at this level through 10,000 years. Because of low borehole permeability, when the upper borehole degrades at 1200 years, the repository pressures decline less rapidly than realizations assigned higher borehole permeability. Pressure declines at a slower rate at 2200 years, when the lower borehole closes through creep. The driving force for gas leaving the borehole is now the pressure potential between the repository and upper units, which is not as strong as the potential when the repository was connected to the brine reservoir and the lower borehole had a higher permeability. Because borehole permeability is so low, this new pressure potential cannot as easily promote gas evacuation out the borehole; consequently, repository pressures do not decline as quickly from 2200 years to the end of the modeled period.

Gas Saturation in Both the Upper (REP_SATG) and Lower Waste Panels (WAS_SATG)

Early in the modeled period, brine drains from the UDRZ and the anhydrites and enters the waste regions, which in part reduces gas saturations.² Gas saturation in the lower waste panel (WAS_SATG) reaches a quasi-steady-state level at ~200 years. Gas saturation slightly increases at the time of intrusion, when the pressure pulse of the intrusion introduces a small amount of brine into the lower waste panel from the LDRZ, enough for gas generation via iron corrosion, which increases gas saturation levels, but not enough to flood the region. When the upper borehole degrades at 1200 years, the rate of gas production is greater than the rate of gas evacuation out the borehole because of low borehole permeability. The two conditions cause

repository gas saturation to increase, rather than decrease. Between ~2000 and 4500 years, gas saturations within the repository are at a quasi-plateau point, coincident with the borehole being dominated by gas flow. At ~4000 years, repository pressure declines, due of a cessation of gas production in the upper waste panel. At this lower pressure, more brine can enter via the borehole and lower marker beds (moving through the LDRZ and entering the floor of the lower waste panel). At ~4000 years, the decline in gas saturation rates in the waste panels is in synchrony (see slope of FEREM_W and WAS_SATG curves, Figure 7.2.1) with iron depletion rates. This condition implies that the iron being corroded is in equilibrium with gas evacuation out the borehole and brine consumption via corrosion.

Gas saturation in the upper waste panel (REP_SATG) gradually increases until it reaches nearly 100% gas saturation at ~4000 years. High gas saturations within the upper waste panel keep brine effective permeability very low, inhibiting replenishing brine from entering the upper waste panel. The upper waste panel remains close to 100% gas saturated from ~4000 years to the end of the modeled period, limiting brine entering this region.

Fraction of Iron Uncorroded in Lower (FEREM_W) and Upper (FEREM_R) Waste Panel

Figure 7.2.1 - top plot

FEREM_W (fraction of uncorroded iron remaining in lower waste panel)

Enough replenishing brine is supplied to the lower waste panel to keep iron corrosion constant throughout the modeled period (i.e., the brine in the lower waste panel is never completely consumed). While the corrosion rate for this realization is relatively high, there is enough brine to deplete only half the iron in the lower waste panel by the end of the modeled period.

Figure 7.2.1 - top plot

FEREM_R (fraction of uncorroded iron remaining in upper waste panel)

The fraction of iron actively being corroded changes at ~4000 years

² Waste consolidation also reduces gas saturation levels and concurrently raises gas pressures.

Because gas evacuation out the borehole is limited, a large portion of gas produced in the upper waste panel remains there, rendering the upper waste panel and the UDRZ above it close to 100% gas saturated. Relatively high gas production combined with low borehole permeability keeps repository pressures relatively high and inhibits replenishing brine from entering the upper waste panel via the borehole, the UDRZ, and the LDRZ. At ~4000 years, all brine in the upper waste panel is essentially consumed, so iron depletion ceases.

7.2.2 Overlay Plots for Flow in Borehole

Figure 7.2.1 - bottom plot

Brine flow rates up the borehole measured at the top of the lower waste panel (BRNBHUPC) and top of the UDRZ (BNBHUDRZ);

Brine flow down the borehole measured at the top of the UDRZ (BNBHDNUZ) and top of the lower waste panel (BRNBHDNC);

Gas flow up the borehole measured at the top of the UDRZ (GASBHUZ)

Brine flow rates in the borehole dramatically change at 1000 and 2200 years

Brine Flow in the Borehole

At the time of intrusion, the slightly lower pressure of the brine reservoir allows a small volume of brine to flow ($< 100 \text{ m}^3$) from the repository down the borehole towards the reservoir. The connection between the brine reservoir and the repository maintains a high enough pressure potential to drive gas out of the repository at relatively high flow rates. Gas flow up the borehole impedes brine flow downward. At ~2800 years (soon after the lower borehole has closed through creep), repository pressures have been reduced to levels that enable only a small trickle of brine to flow down the borehole.

Gas Flow in the Borehole

Figure 7.2.1 - bottom plot

GASBHUDZ (gas flow up borehole at top of UDRZ)

Gas flow rates in the borehole dramatically change at 1200 and 2200 years

Low borehole permeabilities coupled with high gas generation from microbial degradation early on cause gas to flow up the borehole (GASBHUDZ) from 1200 years, when the upper borehole plug degrades, to the end of the modeled period. Relatively high gas flow rates exist from 1200 years until 2200 years, while the lower borehole has a ‘good’ connection to the brine reservoir. Gas flow rates decrease at 2200 years when the lower borehole permeability is reduced by a factor of 10, reducing the connection between lower reservoir and repository, which decreases the pressure potential that drives gas up the borehole. At the same time, repository pressures decline at a slower rate and gas saturations within the lower panel partially stabilize until ~4500 years.

7.2.3 Overlay Plots for Castile Brine Reservoir Pressure (B_P_PRES) with Respect to Brine Flow Up (BRNBHUPP) and Down (BRNBHDNC) the Borehole

Figure 7.2.2

B_P_PRES (brine reservoir pressure)

BRNBHUPP (brine up borehole measured at the bottom of lower waste panel)

BRNBHDNC (brine down borehole measured at the top of lower waste panel)

Reservoir pressures dramatically change at 1200 years

Because Castile reservoir pressure (B_P_PRES) is slightly lower than repository pressures, it increases slightly at the time of intrusion when it becomes ‘connected’ to the repository via the borehole. This pressure gradient promotes brine to flow down the borehole (BRNBHDNC) from the repository, albeit a very small volume. A very small flow of brine again flows down the borehole at ~2800 years, soon after the lower borehole creep closes.

Essentially no brine flows up the borehole from the Castile reservoir to the repository or from the repository to the upper units.

**R1S3 - Brine Reservoir Pressure w.r.t Brine Flow in Borehole Measured
Just Above and Below Waste Panel**

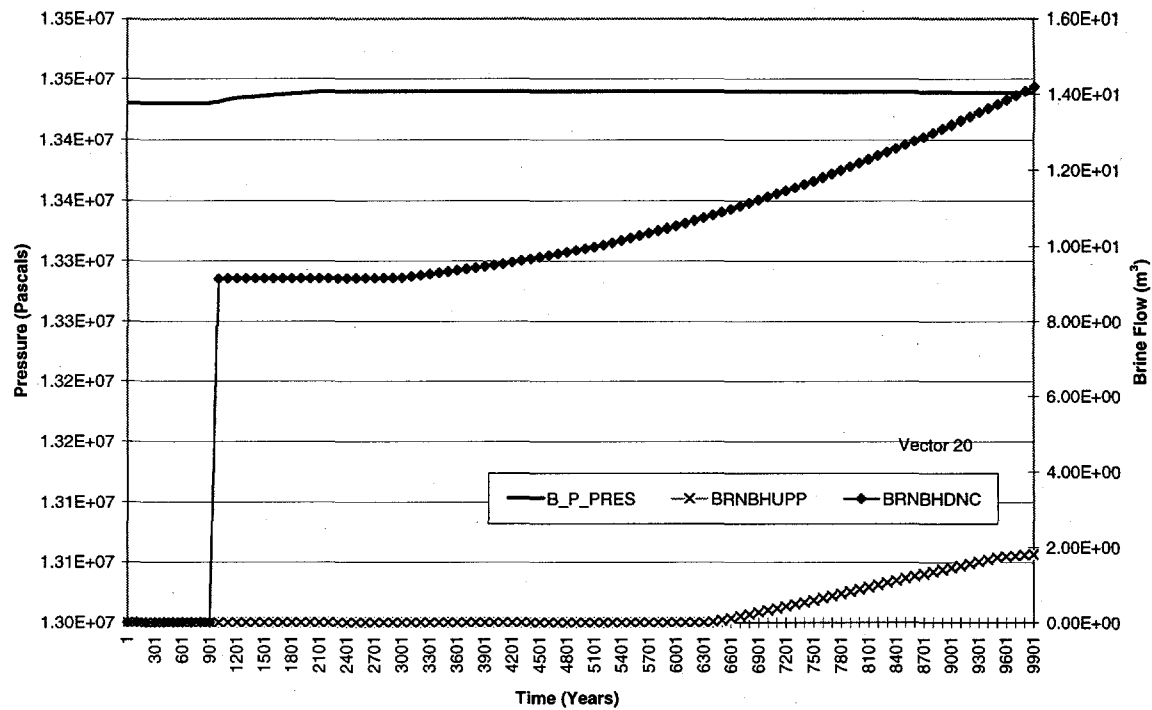


FIGURE 7.2.2. OVERLAY PLOT FOR REALIZATION 20 depicting brine reservoir pressure overlaid with brine flow up and down the borehole measured at the top and bottom of the lower waste panel

7.2.4 Overlay Plots for Brine Flow through the Panel Closures to the Upper and Lower Waste Panels

Figures 7.2.3 and 7.2.4 - all plots

North-flowing brine from lower to upper waste panel is defined as BRNPSOWC (brine from the lower waste panel enters the panel closure south face) and BRNPSIRC (brine exits the panel closure north face to the upper waste panel)

South-flowing brine from upper to lower waste panel is defined as BRNPSORC (brine flows through panel closure from upper waste panel) and BRNPSIWC (brine flows through panel closure into lower waste panel)

Brine flow rates change at 1200 years

Brine flow in the panel closures is predominantly out the closure south face and occurs midway through the modeled period.

Only a small volume of brine (~400 m³ total) flows into the lower waste panel via the closures over the 10,000-year modeled period. This flow is initiated at ~5000 years, coincident with a reduction in gas saturation within the lower waste panel. The brine source (to the panel closures) comes from the LDRZ, as evidenced by a lack of brine flow entering the closures via the upper waste panel (BRNPSORC). Because the upper waste panel is mostly gas saturated, it has very low brine permeability, which inhibits brine from seeping up through the upper waste panel floor as it flows down-dip in the LDRZ. Once south-flowing LDRZ brine encounters the much higher brine-saturated panel closures, it flows upward through the bottom of the closures, then is deflected laterally southward to the lower waste panel.

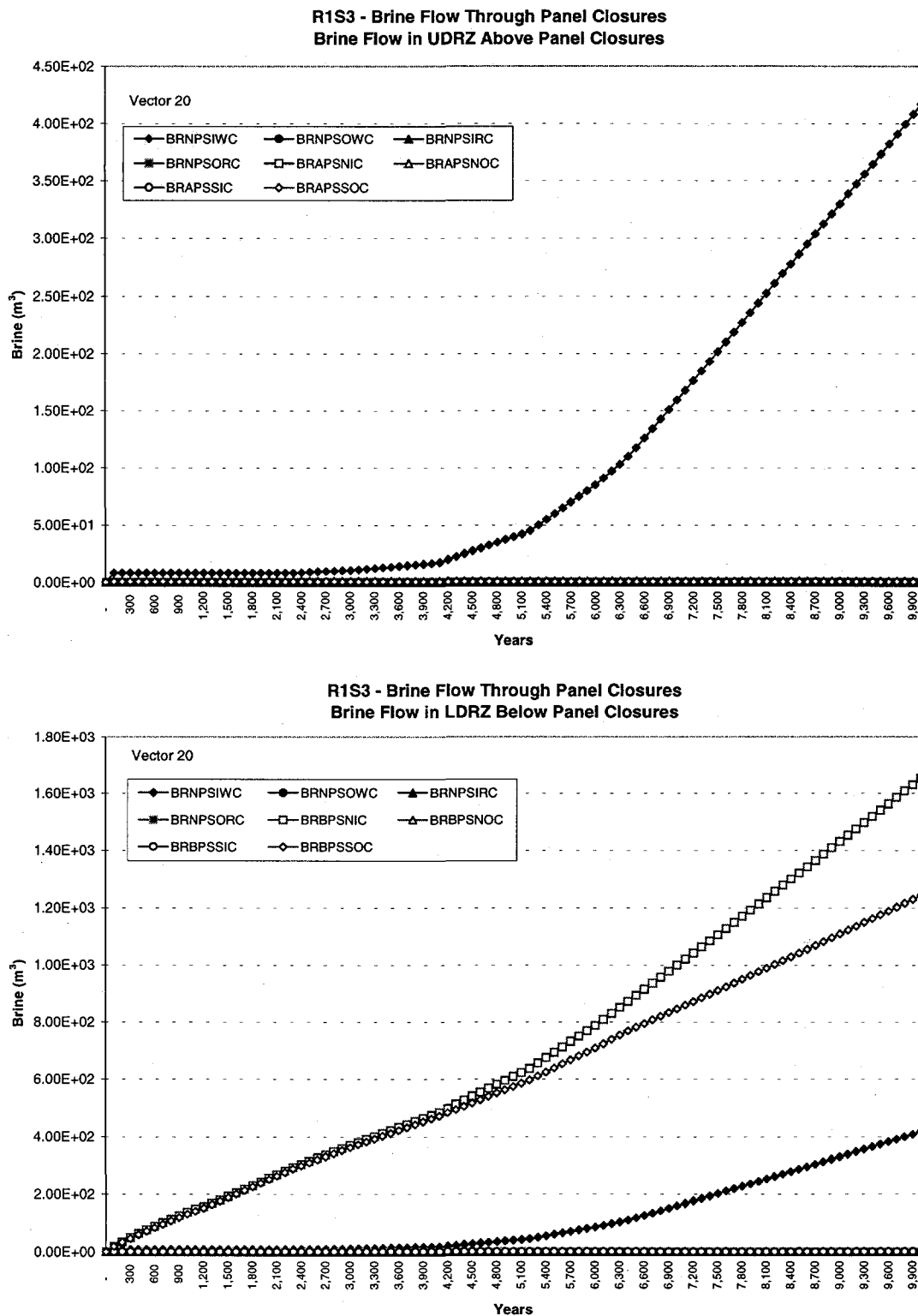


FIGURE 7.2.3. OVERLAY PLOTS FOR REALIZATION 20 depicting brine flow through the panel closures overlaid with lateral brine flow within UDRZ (top plot) and LDRZ (bottom plot), crossing the area just above/below panel closures

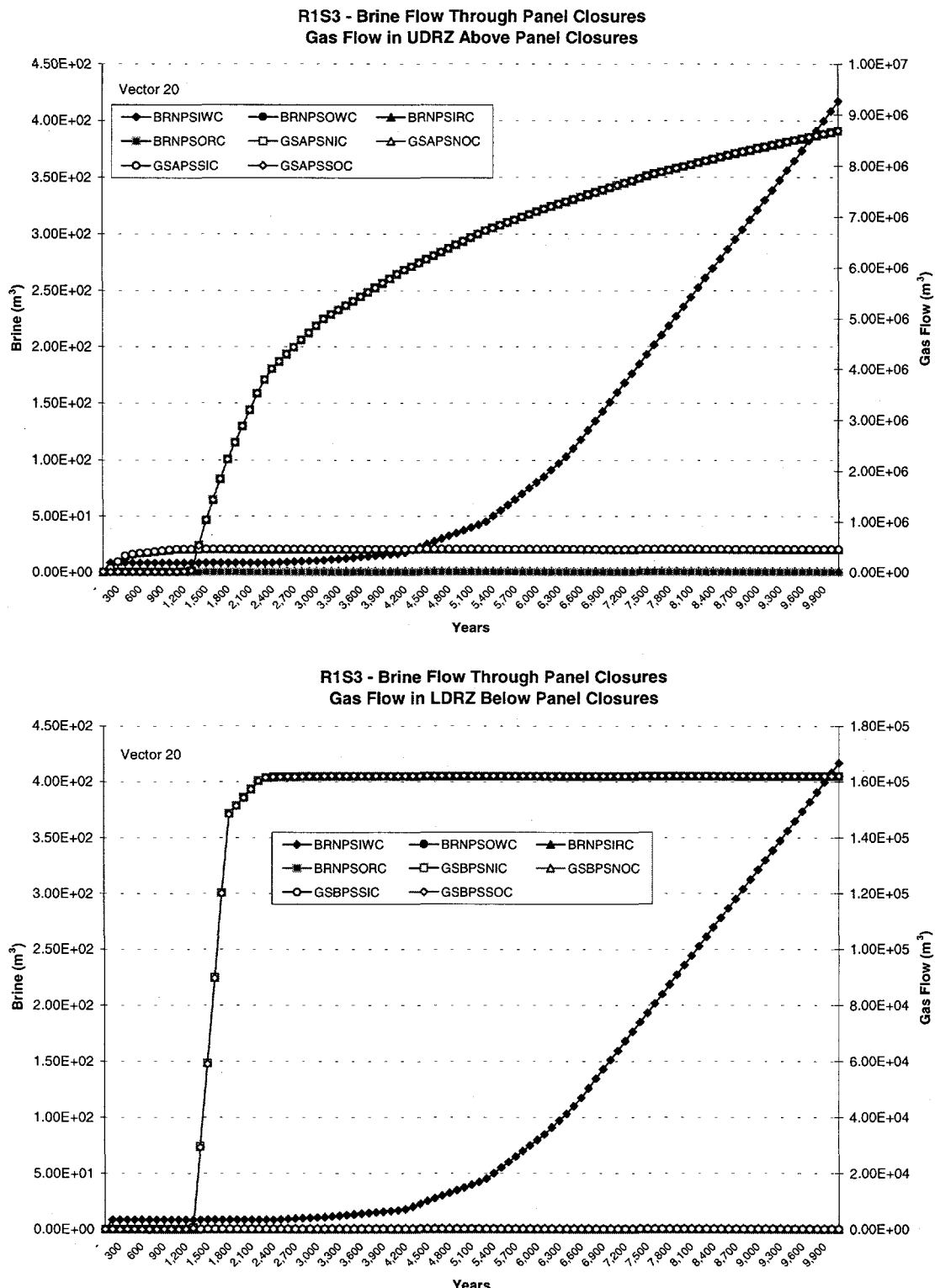


FIGURE 7.2.4. OVERLAY PLOTS FOR REALIZATION 20 depicting brine flow through the panel closures overlaid with lateral gas flow within UDRZ (top plot) and LDRZ (bottom plot), crossing the area just above/below panel closures

7.2.5 Overlay Plots for Lateral Brine Flow in DRZ Above and Below Panel Closures

Lateral Brine Flow in the UDRZ

Figure 7.2.3 (refer also to Figure 7.3)

North-flowing brine is defined as BRAPSSIC (brine entering south face) and BRAPSNOC (brine exiting north face)

South-flowing brine is defined as BRAPSSOC (brine exiting south face) and BRAPSNIC (brine entering north face)

Note: Brine flow through the panel closures is also provided on these plots.

Because the UDRZ is predominantly gas-saturated and gas is the dominant fluid in the borehole, minimal brine enters the UDRZ via the borehole or anhydrite drainage. Consequently, no brine is able to enter the UDRZ region above the panel closures. Therefore, no brine is seen flowing in UDRZ above the panel closures (BRAPSSOC, BRAPSNIC or BRAPSSIC, BRAPSNOC).

Lateral Brine Flow in the LDRZ

Refer to Figure 7.3

North-flowing brine is defined as BRBPSSIC(brine entering south face) and BRBPSNOC (brine exiting north face)

South-flowing brine is defined as BRBPSSOC (brine exiting south face) and BRBPSNIC (brine entering north face)

Below the panel closures, brine flows southward throughout the modeled period (BRBPSSOC, BRBPSNIC). As brine passes below the closures, some brine moves into the closures themselves (as evidenced by the differential between BRBPSSOC, BRBPSNIC). An increase in the brine flow rate occurs ~5000 years (seen in inflection point), coincident with an increase in brine flowing out the south face of the panel closure into the upper waste panel at the same time with repository pressures approach hydrostatic pressure.

7.2.6 Overlay Plots for Lateral Gas Flow in the DRZ Above and Below the Panel Closures

Lateral Gas Flow in the UDRZ

Figure 7.2.4 - top plot (refer also to Figure 7.3)

North-flowing gas is defined as GSAPSSIC (gas entering south face) and GSAPSNOC (gas exiting north face)

South-flowing gas is defined as GSAPSSOC (gas exiting south face) and GSAPSNIC (gas entering north face)

Gas flow in the UDRZ is northward (GSAPSSIC and GSAPSNOC) from the time of repository closure until the upper borehole degrades. Gas reverses flow direction from north to south (GSAPSNIC and GSAPSSOC) at 1200 years, when the upper borehole plug degrades. The borehole connection creates a pressure potential between the highly-pressurized repository and the lower pressures of the upper units. This gradient promotes gas to flow towards the borehole, from the up-dip to the down-dip regions of the repository. The primary pathway is through the UDRZ.

Lateral Gas Flow in the LDRZ

Figure 7.2.4 - bottom plot (refer also to Figure 7.3)

North-flowing gas is defined as GSBPSSIC (gas entering south face) and GSBPSNOC (gas exiting north face)

South-flowing gas is defined as GSBPSSOC (gas exiting south face) and GSBPSNIC (gas entering north face)

A portion of gas that earlier had been pushed down through the floor of the upper waste panel to the LDRZ responds to the depressurization of the repository by moving laterally southward in the LDRZ (GSBPSSOC and GSBPSNIC) from 1200 to ~2400 years.

7.2.7 Overlay Plots for Brine and Gas Flow In/Out the Ceiling and Floor of Upper Waste Panel

Brine Flow Through the Upper Waste Panel Ceiling

Figure 7.2.5 – top plot

BRN_DRAC (downflowing brine) and BRN_URAC (upflowing brine)

Brine flow through the ceiling of the upper waste panel (BRN_DRAC) occurs within the first 300 years of repository closure, due to anhydrite and UDRZ drainage. After 300 years, no brine flows downward through the ceiling of the upper waste panel due to a combination of conditions: 1) after intrusion a low borehole permeability means it takes longer for gas to evacuate out the repository, which inhibits brine from flowing down the borehole, and 2) this keeps the repository pressure relatively high, which also inhibits drainage from the upper anhydrites.

Gas Flow Through the Upper Waste Panel Ceiling

Figure 7.2.5 – top plot

GAS_DRAC (downflowing gas) and GAS_URAC (upflowing gas)

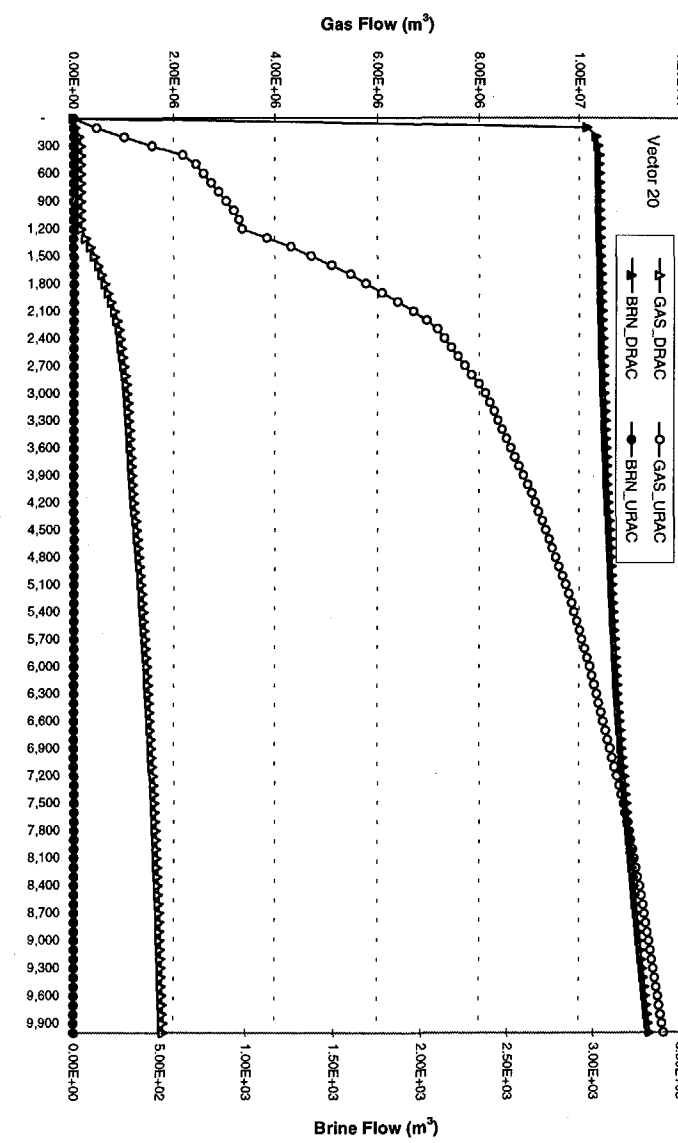
A continuous flow of gas rises upward through the ceiling of the upper waste panel (GAS_URAC) to the UDRZ throughout the modeled period. A slight increase in flow rates occurs at 1200 years when the borehole degrades. Gas flows down into the upper waste panel ceiling (GAS_DRAC) between 1200 and 2200 years as gas stored in the repository accumulates and is restricted from evacuating out the borehole due to low borehole permeability. Thus, gas backs up within the UDRZ as it flows towards the borehole and reenters the upper waste panel via the ceiling from 1200 and 7200 years. Gas flow down through the upper waste panel ceiling is reduced when repository pressure is reduced.

Brine Flow Through the Upper Waste Panel Floor

Figure 7.2.5 – bottom plot

BRN_DRBC (downflowing brine) and BRN_URBC (upflowing brine)

R1S3 - Brine and Gas Flow In and Out the Upper Waste Panel Ceiling



R1S3 - Brine and Gas Flow In and Out the Upper Waste Panel Floor

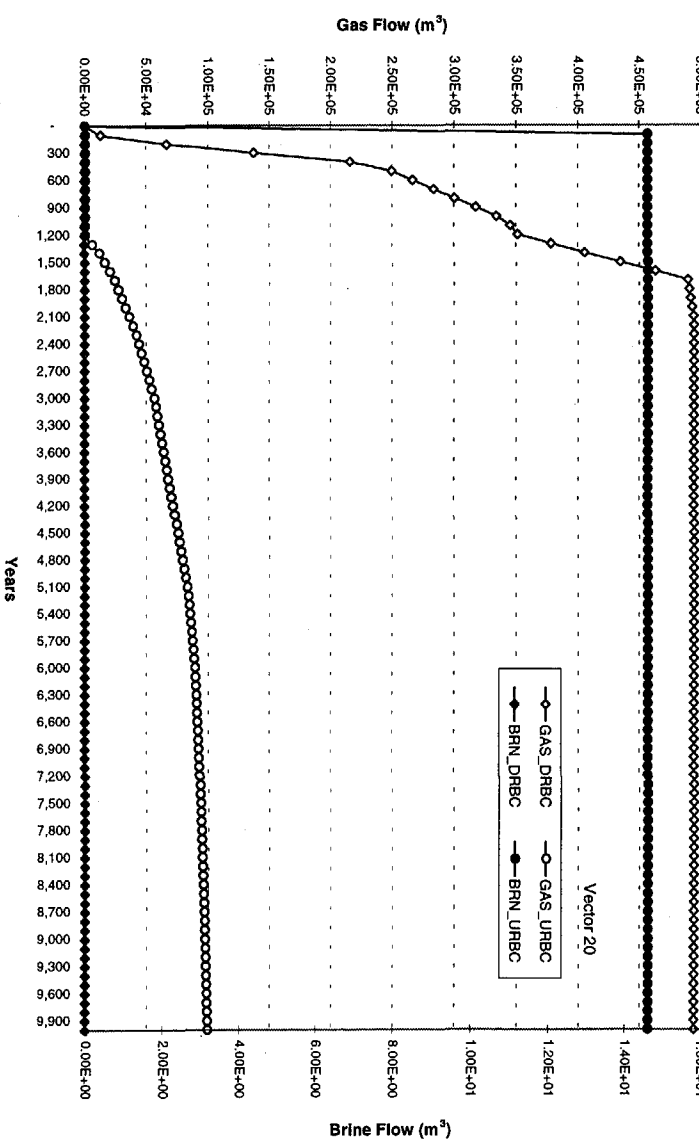


FIGURE 7.2.5. OVERLAY PLOTS FOR REALIZATION 20 depicting vertical brine and gas flow through the ceiling of upper waste panel within the UDRZ (top plot) and LDRZ (bottom plot).

Little brine flows between the LDRZ and the upper waste panel. The small volume of brine that flows from the LDRZ upward, through the upper waste panel floor (BRN_URBC), is a result of the relatively small LDRZ pore volume which more readily 'fill up' from anhydrite brine drainage. A small portion of that drainage overflows into the upper waste panel floor early in the modeled period (prior to ~200 years). Because halite porosity is so low and iron corrosion rates are relatively high, what little brine that drains from the UDRZ to the waste panel is consumed via iron corrosion. Consequently, no excess brine is available to drain from the upper waste panel down to the LDRZ (BRN_DRBC).

Gas Flow Through the Upper Waste Panel Floor

Figure 7.2.5 – bottom plot
GAS_DRBC (downflowing gas) and GAS_URBC (upflowing gas)

Gas flow rates change at 1200 and ~5000 years

Gas flows down through the upper waste panel floor to the LDRZ (GAS_DRBC) early in the modeled period as a result of high gas production from microbial degradation; the two conditions create relatively high repository pressures and limited storage for gas. Limited UDRZ storage capacity causes storage in the upper waste panel and the UDRZ to reach maximum levels. Once reached, gas is pushed down into the LDRZ through the upper waste panel floor.

Gas flow reverses direction at the time of intrusion (1000 years). Gas that flowed into the LDRZ from the upper waste panel and was stored in the LDRZ prior to intrusion now flows from the LDRZ upward through the upper waste panel (GAS_URBC) floor. Flow rates slow down and cease at ~7800 years, soon after repository pressures approach hydrostatic.

7.2.8 Gas Saturation Contour Plots

Figure 7.2.6
SATGAS

Gas saturation contour plots at 1000, ~2289, ~6004, and 10,000 years

The four gas saturation plots show conditions at 1000 years, just prior to intrusion; at ~2289 years, soon after the lower borehole plug constricts; at ~6004 years, soon after brine begins to flow from the panel closures to the lower waste panel; and at 10,000 years, the end of the modeled period.

Comparing the last three plots in Figure 7.2.6 with the contour plot taken at 1000 years, one can see gas flow rates up the borehole are so limited for Realization 20 that a large majority of the excavated area remains between 70% to 100% gas saturated. This high gas saturation is maintained throughout most of the modeled period.

Enough gas flows out the borehole that repository pressures are reduced. This allows brine to drain from MB 139 (especially the south side of MB 139) and collect at the south portion of the LDRZ, as evidenced by LDRZ gas saturation levels being reduced at 2289 years from those seen at 1000 years.

At ~6000 to 10,000 years, both waste regions are above 70% gas saturated. The region below the upper waste panel has a relatively high gas saturation: this impedes brine flowing up from the LDRZ to the upper waste panel floor.

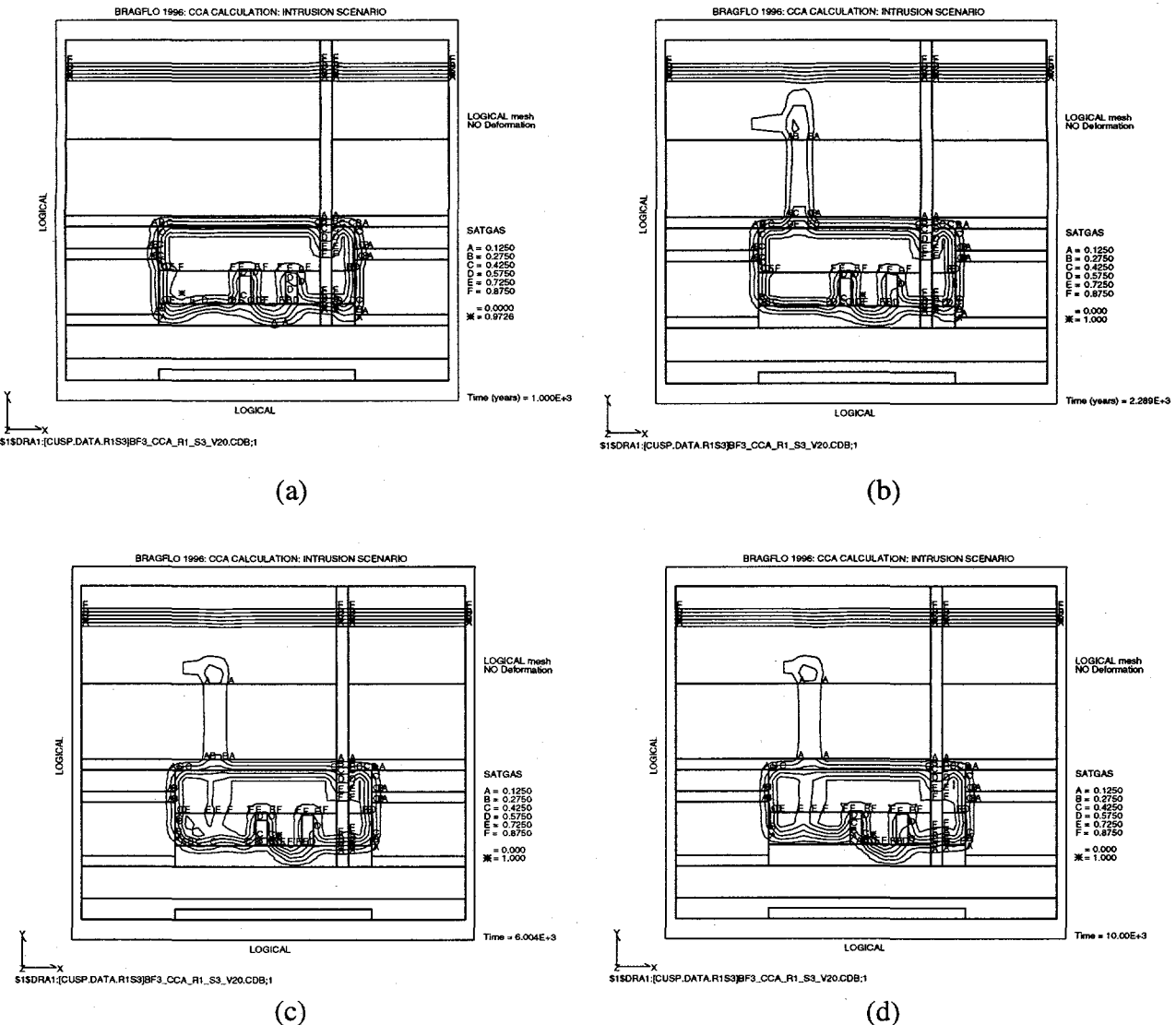


FIGURE 7.2.6. GAS SATURATION CONTOURS FOR REALIZATION 20. (a) 1000 years, just prior to intrusion, (b) ~2289 years, (c) ~6004 years, and (d) the end of the modeled period, 10,000 years. Borehole in lower waste panel is not shown; see Figure 7.4 for location of borehole.

7.3 *Realization 27 - Overlay Plot Summary*

High borehole permeability - $10^{-11.8}$ m², rank 26/100

Halite porosity - .00293, rank 90/100

Microbial degradation – 0, no microbial degradation; corrosion rate - 1.42×10^{-14} m/s, rank 11/100

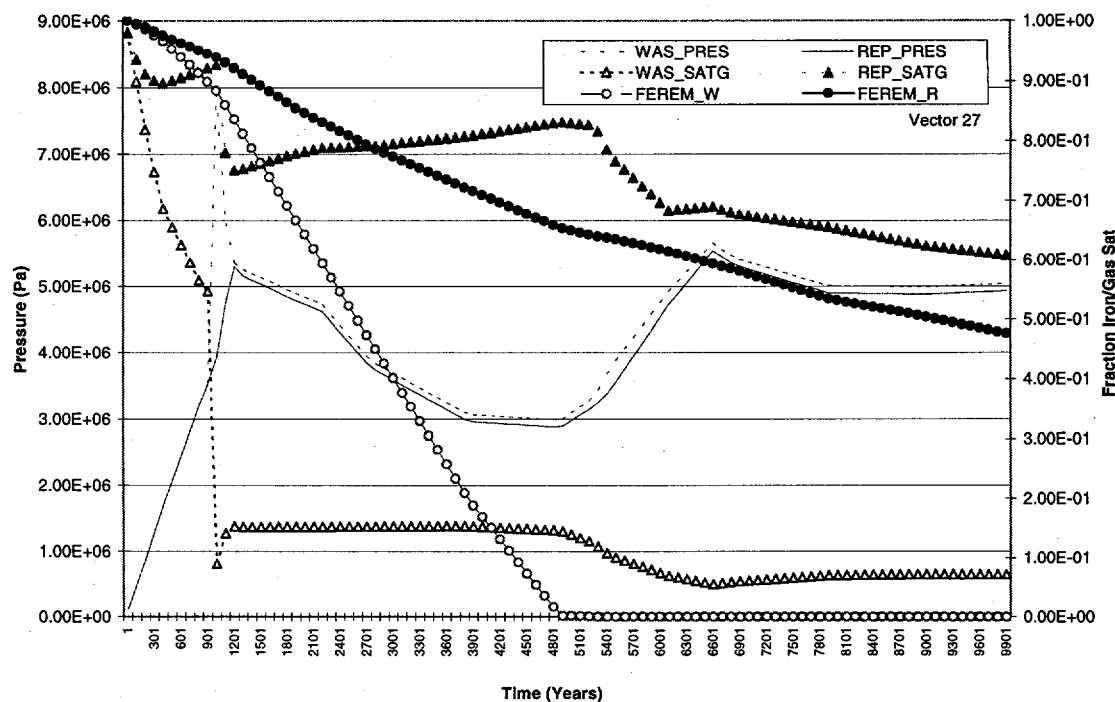
Brief Summary: Realization 27 is representative of repository behavior affected by relatively low gas generation prior to intrusion and high gas generation after intrusion, coupled with relatively high borehole permeability. High borehole permeability evacuates gas out of the repository with ease, causing repository pressures to steadily decline from the intrusion event until ~5000 years. Relatively low gas production prior to intrusion is the result of no microbial degradation in this realization coupled with a small amount of brine needed to supply the relatively high iron corrosion rates. While iron corrosion rates are high, corrosion is limited by the relatively low brine volumes drained from the UDRZ, as a result of a low value for halite porosity. The three conditions mean, prior to intrusion, the repository has relatively low gas production, resulting in relatively low repository pressures. Because of the relatively high value assigned for borehole permeability, gas that is generated early in the modeled period is easily vented out of the borehole at the time of intrusion. After gas has been vented, brine drainage resumes into the waste area, either through the borehole or marker bed drainage, allowing more gas production via the corrosion process. Low halite porosity means not only limited brine drains into the excavated area early in the modeled period, but a smaller DRZ void space for storage exists for brine and gas to be stored and moved between the gas production and non-production areas.

7.3.1 Overlay Plots for Pressure in Lower (WAS_PRES) and Upper (REP_PRES) Waste Panels; Gas Saturation in the Lower (WAS_SATG) and Upper (REP_SATG) Waste Panels; Fraction of Uncorroded Iron in the Lower (FEREM_W) and Upper (FEREM_R) Waste Panels

Figure 7.3.1 - top plot
WAS_PRES, REP_PRES

Pressures dramatically change at 1000, 1200, ~5000, and ~6000 years

**R1S3 - Waste Panel Pressures w.r.t Gas Saturation/
Fraction of Uncorroded Iron Remaining**



R1S3 - Brine and Gas Borehole Flow

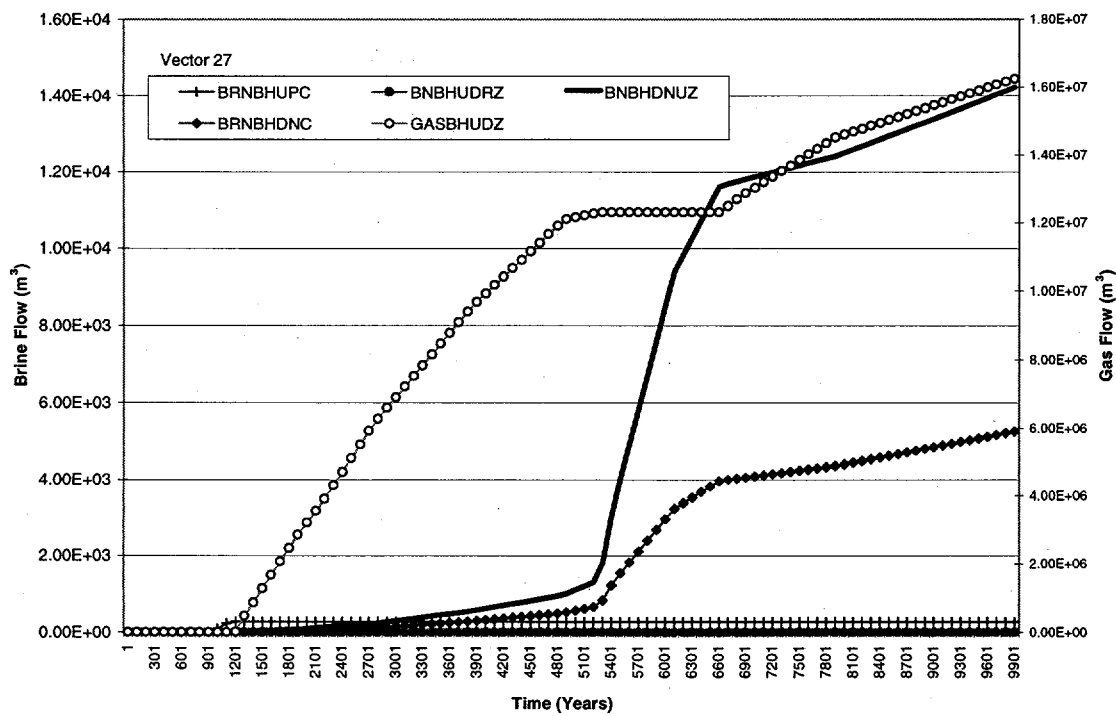


FIGURE 7.3.1. OVERLAY PLOTS FOR REALIZATION 27 depicting pressures, fraction of iron remaining, and gas saturations for lower and upper waste panels (top plot) and cumulative brine and gas flow within borehole at intersection of borehole with top of lower waste panel and top of the UDRZ (bottom plot)

Repository Pressure for the Lower (WAS_PRES) and Upper (REP_PRES) Waste Panel

Repository pressure at the time of intrusion is relatively low (in the bottom 10th percentile) due to the absence of microbial degradation and brine-limited iron corrosion. The intrusion event (1000 years) causes a sharp spike in the lower waste panel pressure curve as incoming brine from the Castile reservoir moves up the borehole and fills the lower waste panel. This spike is not as dramatic for the upper waste panel, and is partially due to the limited communication between the lower and upper waste panels, caused by relatively small DRZ pore volumes between the areas. The brine-filled lower waste panel has a relatively higher pressure (WAS_PRES) than the upper waste panel (REP_PRES) for the remainder of the modeled period, promoting flow up-dip. This pressure gradient promotes up-dip brine flow in the LDRZ and between the panels themselves. At 1200 years, when the upper borehole degrades, any gas generated early in the modeled period easily exits the lower waste panel, because borehole permeabilities are relatively high, thus lowering repository pressures. Repository pressures continue to decrease until all iron in the lower waste panel is depleted from corrosion at ~4800 years. Pressures start to increase again when brine begins to flow down the borehole. This incoming brine flows first into the lower waste panel, and then eventually up-dip to the upper waste panels. Brine flow in the borehole inhibits gas evacuation out the repository. Consequently, pressures increase until ~6600 years, when they approach hydrostatic. Brine flow down the borehole ceases when the repository pressures increase to hydrostatic. Gas flow then begins to flow up the borehole, again causing pressures to decline.

Gas Saturation in Both the Upper (REP_SATG) and Lower (WAS_SATG) Waste Panels

Figure 7.3.1 - top plot
WAS_SATG, REP_SATG

Gas saturation dramatically changes at ~300, 1000, ~5100, and ~6600 years

Gas saturation in the upper waste panel (REP_SATG) changes at ~300, ~1000, ~5100, and 6600 years. Gas saturation in the lower waste panel (WAS_SATG) slowly declines from 0 to ~1000 years, plateaus at 1000 years, and slightly declines between 5000 and 6000 years.

Prior to intrusion, incoming brine from the marker beds, and to a lesser extent halite drainage, pools in the south portion of the excavated area, while newly-generated gas produced in the waste panels rises to the UDRZ, moving up-dip toward the north portion of the repository. As a result, within ~300 years after repository closure, gas saturation in the lower waste panel decreases while gas saturation increases in the upper waste panel (REP_SATG). This trend is enhanced after intrusion, as incoming Castile brine is introduced into the lower waste panel via the borehole and rapidly fills the lower waste panel. Castile brine does not move into the upper waste panel until the upper borehole plugs degrade (1200 years), releasing gas pressure and moving gas to the area above the up-dip portion of the UDRZ and out the borehole. Gas evacuation lowers pressure in the upper waste panel, allowing brine to enter the upper waste panel from the panel closures, the LDRZ, and to a lesser extent, the UDRZ. This influx of brine into the upper waste panel briefly reduces gas saturations there, which then begin to rise as the incoming brine is consumed in the iron corrosion process, producing gas as a byproduct. This gas is not as easily evacuated out of the upper waste panel, because higher gas production within the lower waste panel via iron corrosion is dominating the gas that flows up the borehole. This causes gas saturations within the upper waste panel to increase until the lower waste panel iron is depleted. At the time of iron depletion in the lower waste panel, upward gas flow out the borehole subsides, and downward brine flow from upper units increases from ~5200 to 6600 years. This extra brine travels to the upper waste panel, rapidly reducing overall gas saturations. From ~5000 years on, gas saturation in the upper waste panel begins to decrease, as gas can now be evacuated out the upper waste panel via the borehole, and incoming brine moves up-dip via the LDRZ and the lower waste panel to the upper waste panel.

Fraction of Iron Uncorroded in Lower (FEREM_W) and Upper (FEREM_R) Waste Panel

Figure 7.3.1 - top plot

The fraction of iron remaining in the lower waste panel (FEREM_W) is reduced at a fairly constant rate from the time of repository closure until all iron is consumed at ~5000 years. The amount of iron being corroded slightly increases in the lower waste panel after intrusion due to abundant brine supplies. In the upper waste panel, the fraction of iron consumed via corrosion

(FEREM_R) remains fairly constant throughout the modeled period; a slight perturbation in iron corrosion occurs between 5000 and 6000 years. Prior to intrusion, iron corrosion within the lower and upper waste panels is brine-limited due to little brine drainage from the UDRZ. After intrusion, iron corrosion increases within the lower waste panel due to increased brine supplies, increased anhydrite drainage, and the introduction of Castile brine, which is needed for iron corrosion. This results in complete iron depletion in the lower waste panel by approximately ~4900 years. Because the upper waste panel is primarily gas saturated, iron corrosion in this area is brine-limited rather than corrosion rate-limited. Therefore, the iron depletion in the upper waste panel, while fairly constant throughout the modeled period, is at a lower rate than in the lower waste panel. This constant depletion rate is in equilibrium with incoming brine accumulating in lower portions of the upper waste panel. Brine saturation decreases as corrosion consumes brine. Brine saturation begins to rise at ~5000 years, when iron corrosion in the lower waste panel is complete. This extra brine must contact uncorroded iron in the upper waste panel. Consequently, the amount of iron depletion in the upper waste panel remains brine-limited and thus is maintained fairly close to the same rate as that seen prior to intrusion.

7.3.2 Overlay Plots for Flow in Borehole

Figure 7.3.1 - bottom plot

Brine flow rates up the borehole measured at the top of lower waste panel (BRNBHUPC), top of UDRZ (BNBHUDRZ);

Brine flow down borehole to bottom of UDRZ (BNBHDNUZ), top of lower waste panel (BRNBHDNC)

Brine flow rates in the borehole dramatically change at 1200, ~5000, and ~6700 years

Gas is the dominant fluid in the borehole, flowing upward between 1200 and ~5000 years. Flow subsides between ~5000 to 6700 years, then resumes from 6700 to 10,000 years. The dominant flow direction for brine in the borehole is downward. Brine flow rates are fairly low from 1000 to ~5000 years, increase between ~5000 to ~6000 years, then decline at ~6700 years. At the time of borehole closure degradation (1200 years), repository pressure is high enough that upward-flowing gas becomes the dominant borehole fluid. Because iron corrosion rates are relatively high and plentiful brine supplies exist, large quantities of gas are produced. This gas flow

continues to move up the borehole, limiting any downward-flowing brine (BNBHDNUZ, BRNBHDNZ), until all iron in the lower waste panel is depleted (~5100 years). The cessation of gas production within the lower waste panel minimizes gas flow up the borehole and allows replenishing brine to flow down the borehole from the upper units. An increase in brine flow down the borehole begins at ~5100 years and flows until the repository pressures increase to hydrostatic pressures (~6.0 MPa) at ~6700 years. Because the lower waste panel has no iron left for corrosion and is close to brine saturated (see Figure 7.1.1, top plot), the lower waste panel fills up, causing a large portion of incoming brine to be deflected at the UDRZ/lower waste panel interface. This brine flows up-dip toward the upper waste panel. Some brine drains through the panel closure where it enters the upper waste panel via the panel closure north face; some continues to flow up-dip through the UDRZ, where it enters through the upper waste panel ceiling.

7.3.3 Overlay Plots for Castile Brine Reservoir Pressure (B_P_PRES) with Respect to Brine Flow Up (BRNBHUPP) and Down (BRNBHDNC) the Borehole

Figure 7.3.2

B_P_PRES (brine reservoir pressure)

BRNBHUPP (brine up borehole measured at the bottom of the lower waste panel)

BRNBHDNC (brine down borehole measured at the top of the lower waste panel)

Reservoir pressure dramatically changes at 1000 and ~5200 years

Brine reservoir pressure (B_P_PRES) is reduced at 1000 years. A pulse of Castile brine is introduced into the lower waste panel via the borehole (BRNBHUPP) at 1000 years. Brine flows down the borehole from the upper formations, entering the lower waste panel (BRNBHDNC) between 5100 to ~6300 years, coincident with a slight increase in Castile reservoir pressures.

At the time of intrusion, repository pressures (see Figure 7.3.1, top plot) are much lower than reservoir pressures (B_P_PRES). This pressure differential, when combined with high brine reservoir compressibilities and high borehole permeability, means that significant volumes of brine (within the 90th percentile) flow up the borehole to the lower portion of the repository (BRNBHUPP). Brine reservoir pressures (B_P_PRES) are significantly reduced as large

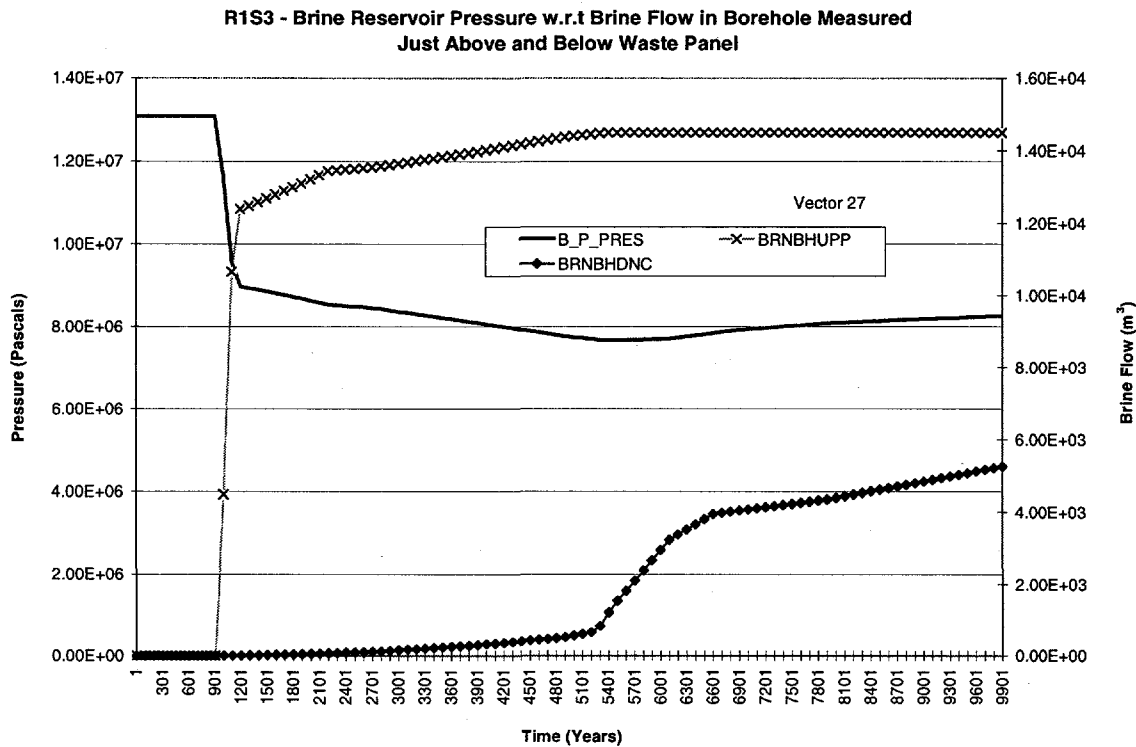


FIGURE 7.3.2. OVERLAY PLOT FOR REALIZATION 27 depicting brine reservoir pressure overlaid with brine flow up and down the borehole measured at the top and bottom of the lower waste panel

volumes of brine flow up to the repository. Brine flow up the borehole tapers off after the lower borehole permeability is reduced by a factor of 10 (at 2200 years). Brine flow upward from the lower reservoir continues until repository pressures approach ~ 3.0 MPa. Brine flow upward from the reservoir ceases when iron within the lower waste panel is completely corroded (reducing gas production in the lower waste panel), coincident with a tapering off of gas flow out the borehole. At ~ 5200 years, repository pressures are ~ 3.0 MPa, well below the pressure of the upper units. At this pressure, pressure gradients promote brine to flow down the borehole (BRBNHDNC) from the upper units, causing an increase in repository pressure and Castile reservoir pressures. The pressure potential between the repository and the reservoir brine no longer promotes brine flow out of the reservoir, but rather into the reservoir (from the repository and upper units). The increase in reservoir pressure plateaus at ~ 6400 years, when flow down the borehole from the upper units declines.

7.3.4 Overlay Plots for Brine Flow through the Panel Closures to the Upper and Lower Waste Panels

Figures 7.3.3 and 7.3.4 - all plots

North-flowing brine from lower to upper waste panel is defined as BRNPSOWC (brine from the lower waste panel enters the panel closure south face) and BRNPSIRC (brine exits the panel closure north face to the upper waste panel)

South-flowing brine from upper to lower waste panel is defined as BRNPSORC (brine flows through panel closure from upper waste panel) and BRNPSIWC (brine flows through panel closure into lower waste panel)

Brine flow rates change at 1000, 5100, and 6100 years

After intrusion, excess brine supplies exist in the lower waste panel* and, simultaneously, the lower waste panel has a higher pressure relative to the upper waste panel from 1000 to 10,000 years. These two conditions create a pressure potential that promotes brine flow from the lower to the upper waste panel via the panel closures. Between ~5000 and ~6200 years, an extra brine surge passes through the closures coincident with brine flow down the borehole from the upper units. Comparing brine volumes that flow through the panel closure's north and south faces, it is seen that the amount of brine that enters the lower waste panel (south face, BRNPSIWC) is less than the amount that exits the upper waste panel (north face, BRNPSORC). The extra contribution of brine that passes out the panel closure south face to the lower waste panel is from the DRZ.

7.3.5 Overlay Plots for Lateral Brine Flow in DRZ Above and Below Panel Closures

Lateral Brine Flow in the UDRZ

Figure 7.3.3 - top plot (refer also to Figure 7.3)

North-flowing brine is defined as BRAPSSIC (brine entering south face) and BRAPSNOC (brine exiting north face)

South-flowing brine is defined as BRAPSSOC (brine exiting south face) and BRAPSNIC (brine entering north face)

North flowing brine above the panel closure starts at 1200 years and continues to end of modeled period

* Iron corrosion does not consume all available brine.

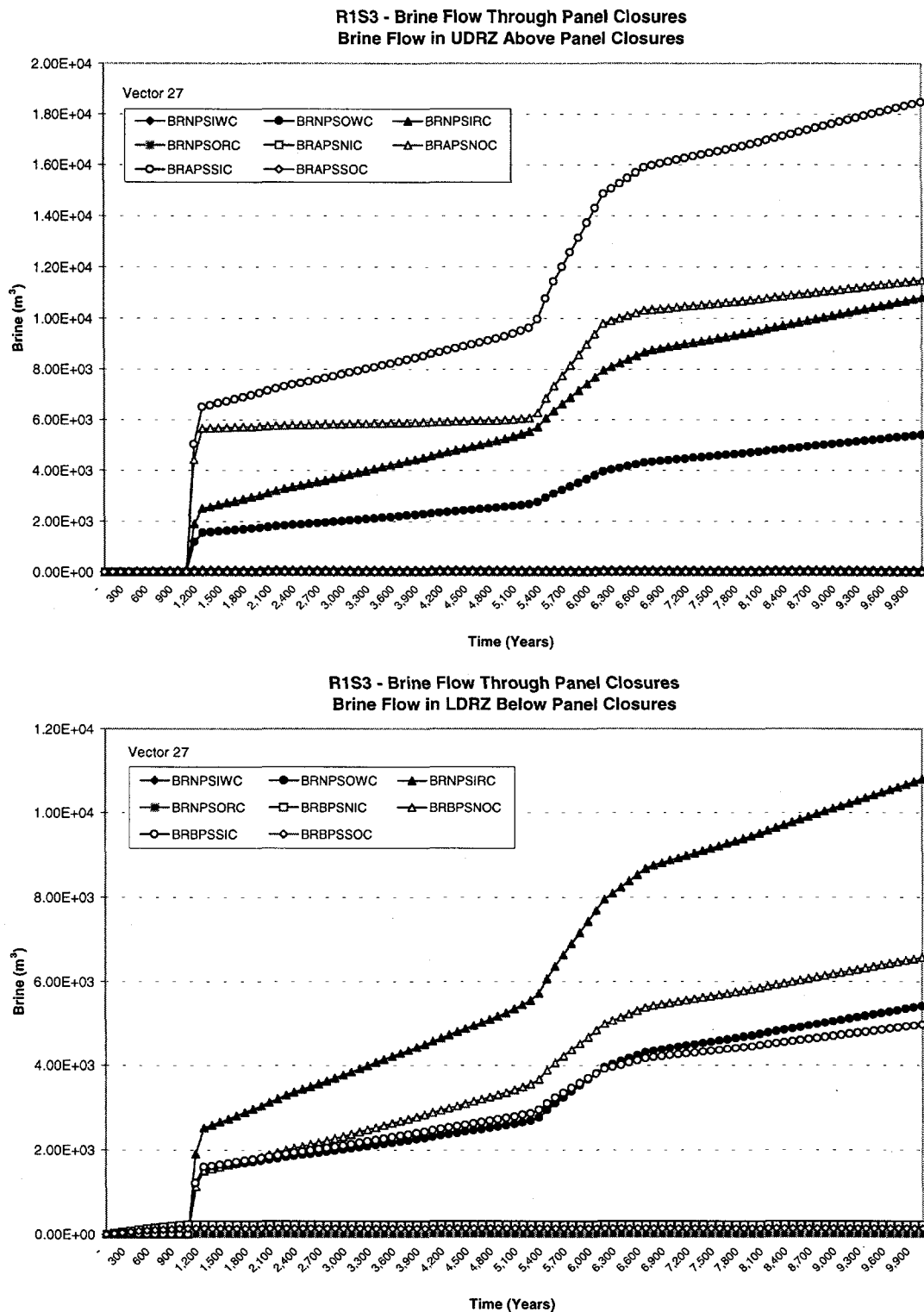
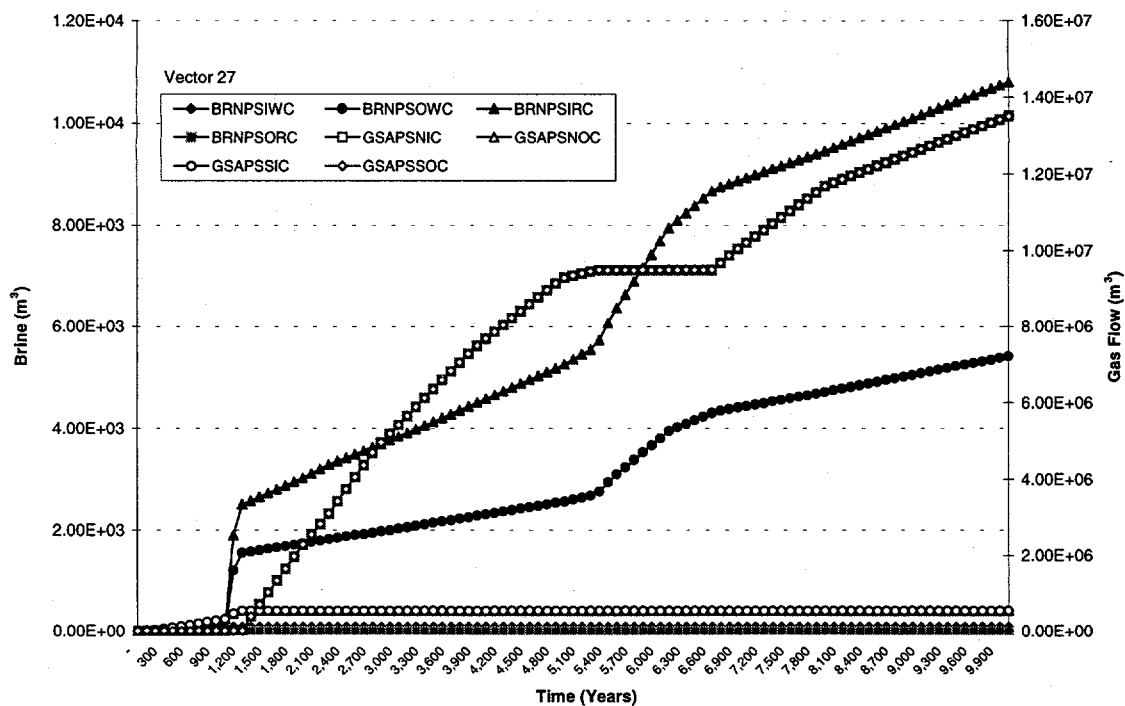


FIGURE 7.3.3. OVERLAY PLOTS FOR REALIZATION 27 depicting brine flow through the panel closures overlaid with lateral brine flow within UDRZ (top plot) and LDRZ (bottom plot), crossing the area just above/below panel closures

R1S3 - Brine Flow Through Panel Closures
Gas Flow in UDRZ Above Panel Closures



R1S3 - Brine Flow Through Closures
Gas Flow in LDRZ Below Panel Closures

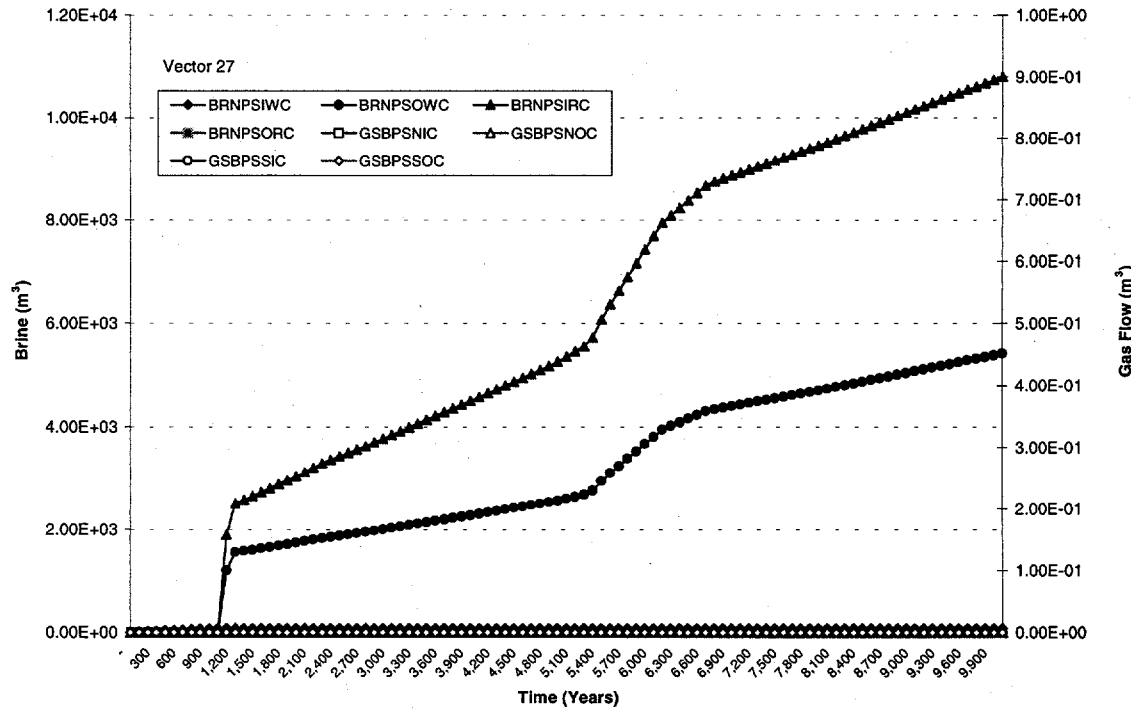


FIGURE 7.3.4. OVERLAY PLOTS FOR REALIZATION 27 depicting brine flow through the panel closures overlaid with lateral gas flow within UDRZ (top plot) and LDRZ (bottom plot), crossing the area just above/below panel closures

Brine flow rates change at 1000, ~5100, and ~6100 years

A pulse of north-flowing brine above the panel closures (BRAPSSIC, BRAPSNOC) is initiated in the UDRZ at 1000 years, the time of intrusion. The sources of brine, between 1000 and ~5000 years, are from brine anhydrite drainage or Castile brine oversupplies stored in the lower waste panel, since minimum brine flows down the borehole prior to ~5000 years. Because the UDRZ above the upper waste panel is primarily gas saturated, this north-flowing brine is deflected downward into the panel closures until ~5000 years, when brine flow down the borehole increases. This extra brine increases repository pressures, which compress resident gas in the UDRZ, moving the gas saturation zone up-dip, allowing UDRZ brine to flow past the region above the panel closure and enter the 'south' ceiling of the upper waste panel.

Lateral Brine Flow in the LDRZ

Figure 7.3.3 - bottom plot (refer also to Figure 7.3)

North-flowing brine is defined as BRBPSSIC(brine entering south face) and BRBPSNOC (brine exiting north face)

South-flowing brine is defined as BRBPSSOC (brine exiting south face) and BRBPSNIC (brine entering north face)

Brine flow rates change dramatically at 1000, 1200, ~5100, and ~6100 years

Prior to intrusion, a small volume of brine flows south in the LDRZ (BRBPSSOC, BRBPSNIC). Little brine drainage from the UDRZ coupled with high iron corrosion rates means less brine in the upper waste panel, and thus little brine drains to the LDRZ. Therefore, LDRZ lateral brine flow to the south is limited to north MB 139 drainage. At the time of intrusion, brine flow direction reverses from south to north, as brine from the Castile reservoir is introduced into the lower waste panel, creating excess brine. This brine pulse initiates a steady up-dip flow of brine (BRBPSSIC, BRBPSNOC), which increases between ~5000 to 6000 years, when down-flowing brine enters the excavated area via the borehole from the upper units. This extra brine is not used for iron corrosion, since all the iron in the lower waste panel is corroded by 5000 years. Consequently, brine not consumed by corrosion flows out the floor of the lower waste panel to the LDRZ, then up-dip toward the upper waste panel.

7.3.6 Overlay Plots for Lateral Gas Flow in the DRZ Above and Below the Panel Closures

Lateral Gas Flow in the UDRZ

Figure 7.3.4 - all plots (refer also to Figure 7.3)

North-flowing brine is defined as BRBPSSIC(brine entering south face) and BRBPSNOC (brine exiting north face)

South-flowing brine is defined as BRBPSSOC (brine exiting south face) and BRBPSNIC (brine entering north face)

Gas flow rates change at 1000, 1200, ~5100, and ~6100 years

Prior to intrusion, a small volume of gas flows laterally up-dip in the UDRZ (GSAPSSIC, GSAPSNOC), crosses the area above the panel closures, and continues to flow northward. This flow direction reverses from north to south at 1200 years, the time of upper borehole degradation. Gas is impeded from flowing southward from ~5000 to 6200 years, when incoming brine flows down the borehole and is deflected northward in the UDRZ. Gas flow southward recommences when incoming brine from down the borehole subsides.

Lateral Gas Flow in the LDRZ

Figure 7.3.4 - bottom plot (refer also to Figure 7.3)

North-flowing gas is defined as GSBPSSIC (gas entering south face) and GSBPSNOC (gas exiting north face)

South-flowing gas is defined as GSBPSSOC (gas exiting south face) and GSBPSNIC (gas entering north face)

Little to no lateral gas flows either north or south in the LDRZ.

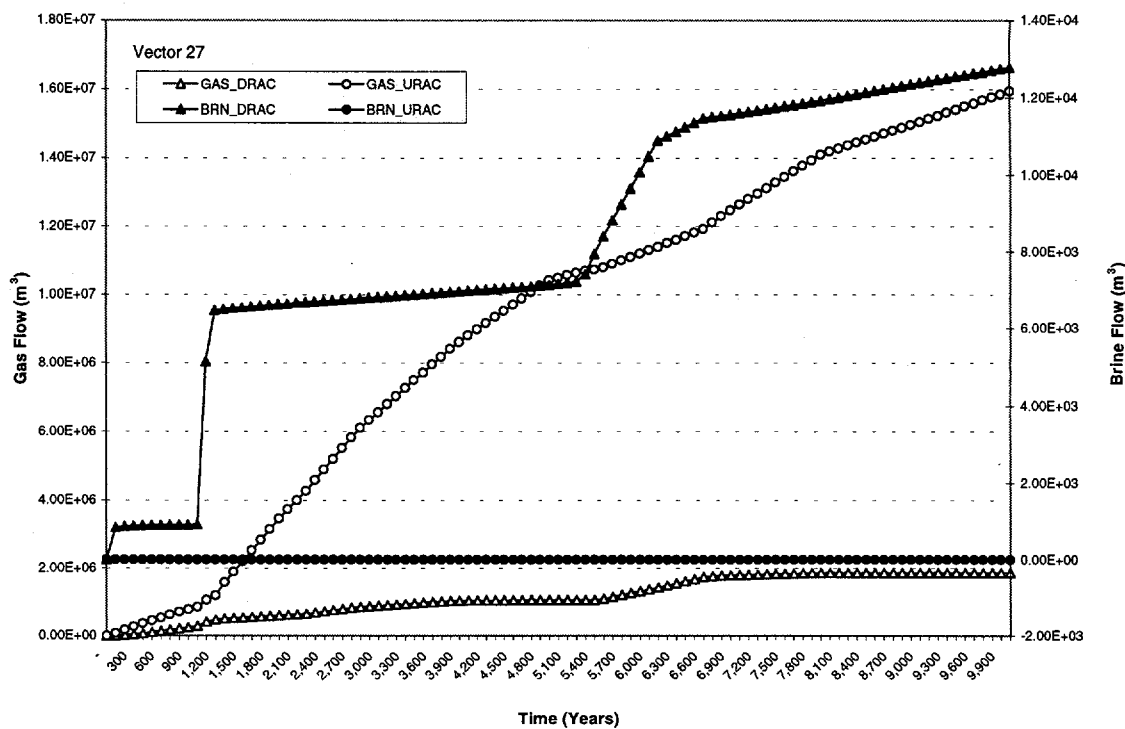
7.3.7 Overlay Plots for Brine and Gas Flow In/Out the Ceiling and Floor of Upper Waste Panel

Brine Flow Through the Upper Waste Panel Ceiling

Figure 7.3.5 – top plot

BRN_DRAC (downflowing brine) and BRN_URAC (upflowing brine)

R1S3 - Brine and Gas Flow In and Out the Upper Waste Panel Ceiling



R1S3 - Brine and Gas Flow In and Out the Upper Waste Panel Floor

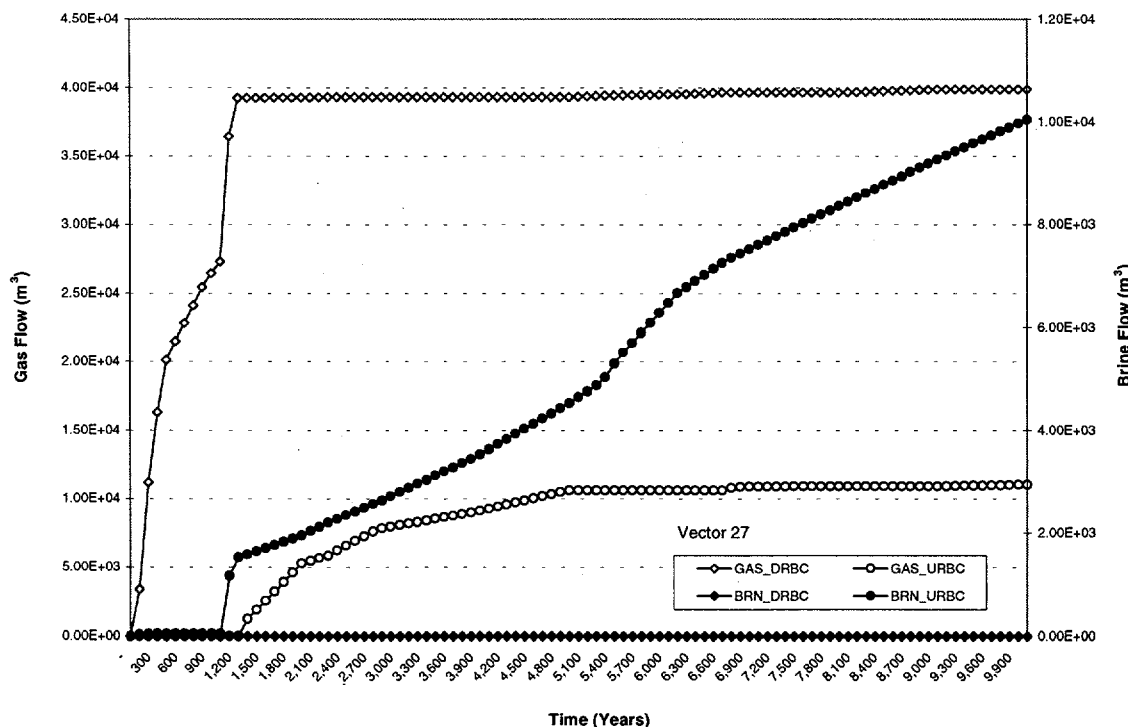


FIGURE 7.3.5. OVERLAY PLOTS FOR REALIZATION 27 depicting vertical brine and gas flow through the ceiling of the upper waste panel within the UDRZ (top plot) and LDRZ (bottom plot)

Because halite porosity is low, a relatively small amount of brine drains from the UDRZ through the upper waste panel (BRN_DRAC) prior to intrusion. After intrusion, two relatively large pulses of brine enter the ceiling of the upper waste panel, each pulse contributing approximately equal amounts of brine. The first pulse occurs between 1000-1200 years, at the time of intrusion, as Castile brine is introduced into the repository via the borehole. Some brine enters the UDRZ and flows up-dip, then back down through the upper waste panel ceiling. The second pulse occurs between ~5000 and 6200 years, when brine flows down the borehole from the upper units.

A large portion of this incoming brine is deflected at the UDRZ/lower waste panel interface, flowing up-dip where it enters the ceiling of the upper waste panel. Because the UDRZ is primarily gas-saturated above the upper waste panel (see gas saturation contour plots, Section 7.3.8), the majority of this brine is deflected downward into the upper waste panel ceiling just north of the panel closures.

Gas Flow Through the Upper Waste Panel Ceiling

Figure 7.3.5 – top plot
GAS_DRAC (downflowing gas) and GAS_URAC (upflowing gas)

A continuous flow of gas exits the ceiling of the upper waste panel (GAS_URAC) throughout the modeled period with significant response changes seen at 1200, 5100, and 6800 years. At 1200 years, gas flow out the ceiling increases when the upper borehole plug degrades, then decreases from ~5200 to 6200 years. The decrease in gas flow rate is due to competition with incoming brine flowing down the borehole, some deflected at the UDRZ and moving up-dip, entering the upper waste panel ceiling. This downward flow of brine hinders gas flow out the upper waste panel ceiling. As brine flow in the borehole subsides at ~6800 years, gas flow rates out of the upper waste panel ceiling increase to about the same rate seen prior to ~5200 years.

Gas flow from the UDRZ down through the upper waste panel ceiling (GAS_DRAC) is partially a function of the DRZ pore volume. Because the UDRZ, for this realization, has such a small pore volume and small (low) compressibility (relative to the waste areas), this area has a relatively small gas storage capacity. Thus, any gas produced that rises to the UDRZ will be

pushed back into the excavated areas as the DRZ reaches its maximum gas storage capacity. A slight increase in gas flow downward through the upper waste panel ceiling occurs between ~5200 and 6200 years, when brine enters the upper waste panel ceiling. This incoming brine displaces resident UDRZ gas, forcing gas back down through the upper waste panel ceiling. When downward brine flow rates through the upper waste panel ceiling decline (~6200 years), downward gas flow also subsides.

Brine Flow Through the Upper Waste Panel Floor

Figure 7.3.5 – bottom plot
BRN_DRBC (downflowing brine) and BRN_URBC (upflowing brine)

Brine flow rates change at 1000, 1200, ~5100, and ~6100 years

A continuous flow of brine enters the upper waste panel floor (BRN_URBC) from the LDRZ between the time of intrusion to the end of the modeled period. This brine flow is initiated as a pulse at 1000 years, when incoming Castile brine enters the excavated area. This pulse is followed by ‘seepage flow.’ An increase in brine flow upward is seen between ~5200 and 6200 years, coincident with increased brine flow down the borehole from units above. This incoming ‘borehole’ brine enters the LDRZ either through drainage out the floor of the lower waste panel or the bottom of the panel closures, moving up-dip where it enters the upper waste panel floor.

Because the upper waste panel has a very low brine saturation, no brine drains out the floor of the upper waste panel to the LDRZ (BRN_DRBC) during the entire modeled period.

Gas Flow Through the Upper Waste Panel Floor

Figure 7.3.5 – bottom plot
GAS_DRBC (downflowing gas) and GAS_URBC (upflowing gas)

Gas flow rates change at 1000 and ~5000 years

Gas flow from the upper waste panel floor to the LDRZ (GAS_DRBC) is partially a function of the DRZ pore volume. Because the DRZ has a relatively small pore volume and very low

compressibility (relative to the waste areas), this area has a small storage capacity for gas. As gas saturation of both the UDRZ and the upper waste panel pore volume reach their optimal value, newly-produced gas will be pushed down through the floor of the upper waste panel to the LDRZ. This downward component of gas flow ceases at the time of upper borehole degradation, because the borehole releases enough gas from the UDRZ and the upper waste panel to eliminate higher gas pressure; prior to intrusion, this high pressure forces gas down to the LDRZ. Gas flow upward from the LDRZ (GAS_URBC) occurs at 1200 years, when the upper borehole plug degrades, the lower waste panel becomes brine-saturated, and the repository closes through creep. A portion of gas that occupied the lower waste panel flows to the LDRZ, moves up-dip, and enters the lower waste panel floor. This upward component of gas flow ceases at ~5000 years.

7.3.8 Gas Saturation Contour Plots

The four gas saturation plots given in Figure 7.3.6 show conditions at (a) ~1226 years, soon after the time of borehole plug degradation; (b) ~4877 years; (c) ~6605 years; and (d) the end of the modeled period, 10,000 years.

The contour plot at ~1226 years (Figure 7.3.6) shows the relatively low gas saturation in the lower waste panel and the south portion of the UDRZ soon after the borehole degrades. This condition is due to rapid gas evacuation out the repository via the borehole due to the relatively high value for borehole permeability that is assigned to this realization.

The plot at 4870 years shows the onset of brine flow down the borehole (that occurs just after iron in the lower waste panel is almost completely corroded). This brine fills the lower waste panel and the south portion of the UDRZ until the two regions are nearly 100% brine saturated. Brine flow enters the upper waste panel via the brine-saturated panel closures, the upper waste panel floor via the LDRZ, and the UDRZ. Lateral up-dip brine flow in the UDRZ is deflected downward into the top of the panel closure or the upper waste panel as the result of the UDRZ gas 'wedge' residing just north of the panel closures. This 'gas wedge' remains in relatively the same location until the end of the modeled period.

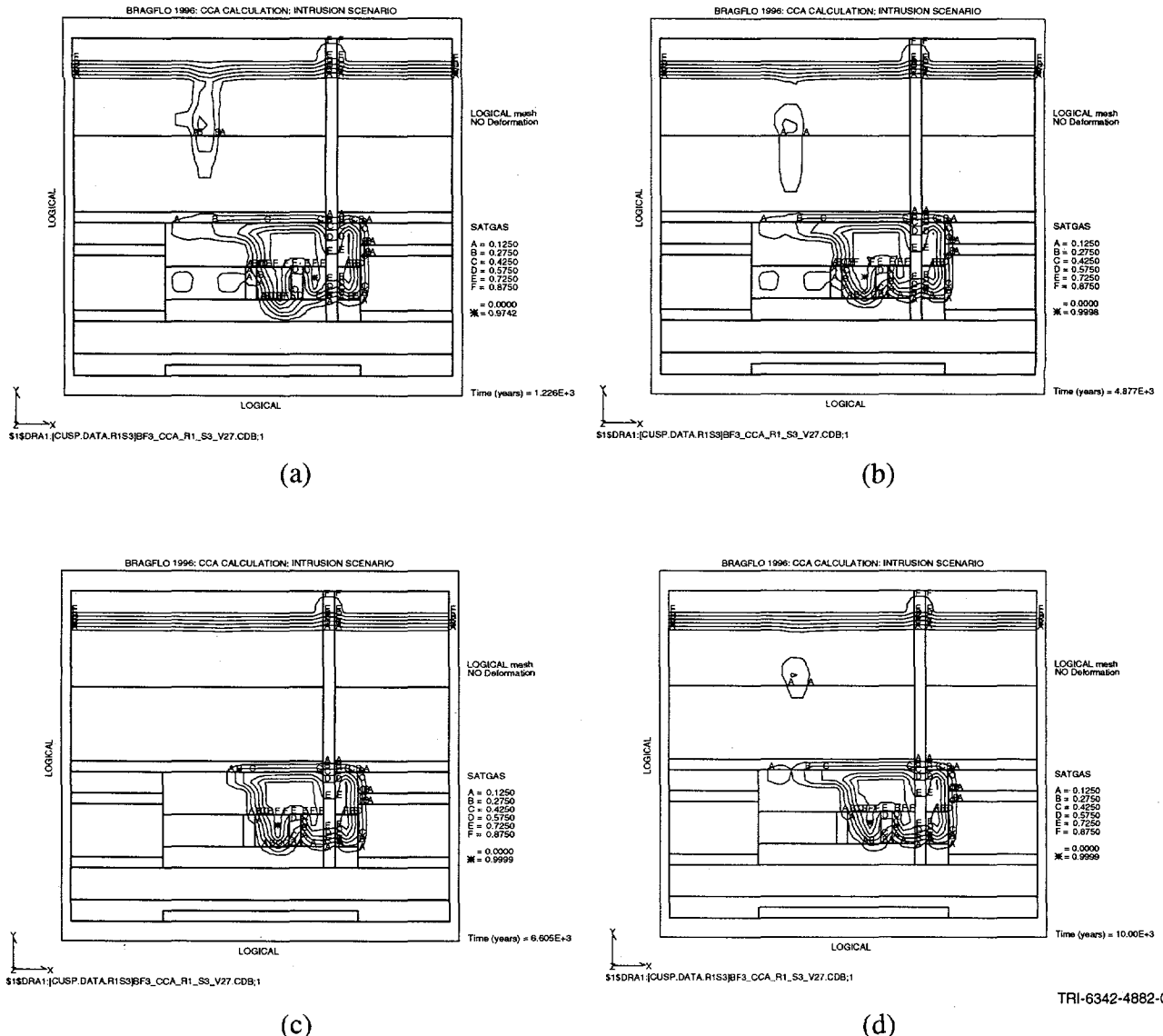


FIGURE 7.3.6. GAS SATURATION CONTOURS FOR REALIZATION 27. (a) 1226 years, the time of borehole degradation, (b) ~4877 years, (c) ~6600 years, and (d) the end of the modeled period, 10,000 years. Borehole in lower waste panel is not shown; see Figure 7.4 for location of borehole.

Because gas was not evacuated out the UDRZ from ~4800 to 6600 years, the contour plot at 10,000 years shows an increase in UDRZ gas saturation above the lower waste panel. Brine flow down the borehole impedes gas from exiting the repository. The buildup of gas produced in the upper waste panel and stored in the upper waste panel and the UDRZ exits the repository from ~6600 to 10,000 years. The gas flow rate out the borehole declines due to the repository having reached near-hydrostatic pressure.

7.4 Realization 4 - Overlay Plot Summary

Low borehole permeability - $10^{-13.2}$ m², rank 74/100

Microbial gas generation - 0, no microbial degradation; rank - bottom third

High corrosion rate - 1.25×10^{-13} m/s, rank 21/100

Large halite porosities - 0.0194, rank 24/100

Brine reservoir intrusion

Pressure - 1.19×10^7 Pa, rank 94/100

Log brine reservoir

Compressibility - $10^{-9.11}$ 1/Pa, rank 19/100

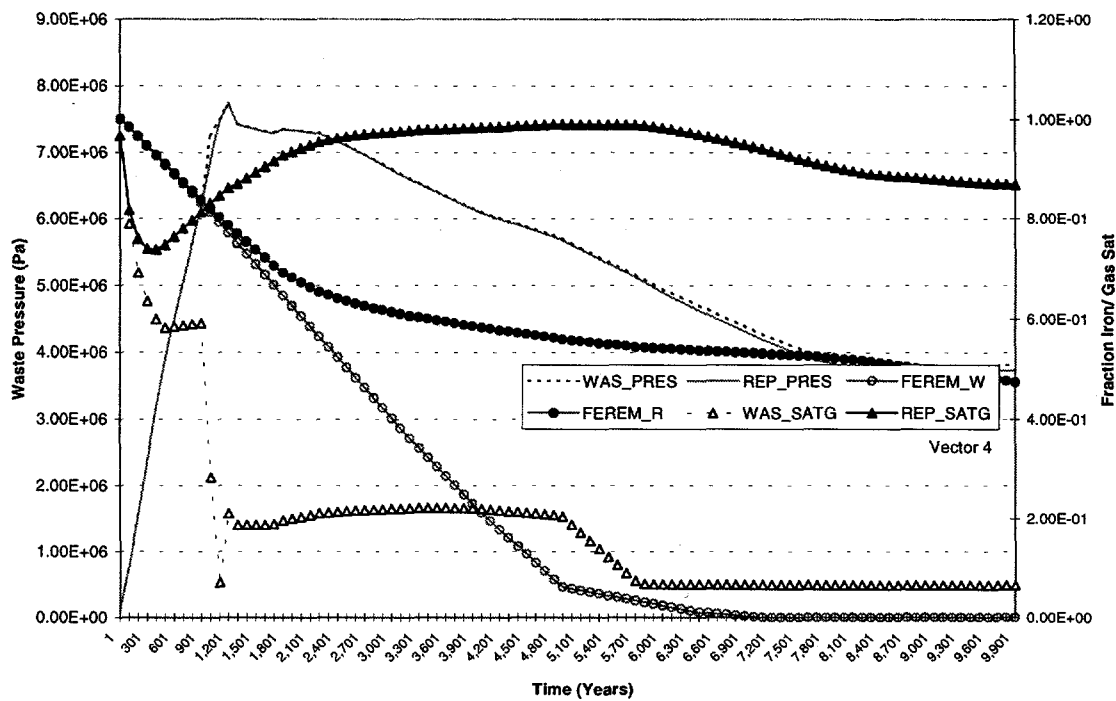
Brief Summary: Realization 4 represents repository behavior affected by medium pressurization prior to intrusion, caused by a lack of gas production via microbial degradation and, because of plentiful brine supplies due to relatively large brine drainage from the UDRZ, a large volume of gas produced via iron corrosion. Median pressure values are used for the set of realizations. Because brine reservoir pressures and borehole permeabilities are among the lowest in the sampled set, the amount of brine contributed to the repository via the intrusion event falls just above the 10th percentile group. The large volumes of brine drained from the DRZ early on coupled with relatively high iron corrosion rates mean that the iron in the lower waste panel is completely corroded midway through the modeled period (~5000 years). Gas evacuation out the repository via the borehole is impeded due to low borehole permeability, which causes a relatively slow decline in repository pressure from the time of intrusion to the end of the modeled period.

7.4.1 Overlay Plots for Pressures in Lower (WAS_PRES) and Upper (REP_PRES) Waste Panels; Gas Saturation in the Lower (WAS_SATG) and Upper (REP_SATG) Waste Panels; Fraction of Uncorroded Iron in Lower (FEREM_W) and Upper (FEREM_R) Waste Panels (Figure 7.4.1 - top plot)

WAS_PRES, REP_PRES

The top plot in Figure 7.4.1 shows the gradual rise in repository pressure is abruptly interrupted at 1000 years, the time of intrusion, and coincides with a decrease in gas saturation in the lower waste panel as brine is introduced into the repository from the lower Castile reservoir. Both top

**R1S3 - Waste Panel Pressures w.r.t Gas Saturation/
Fraction of Uncorroded Iron Remaining**



R1S3 - Brine and Gas Borehole Flow

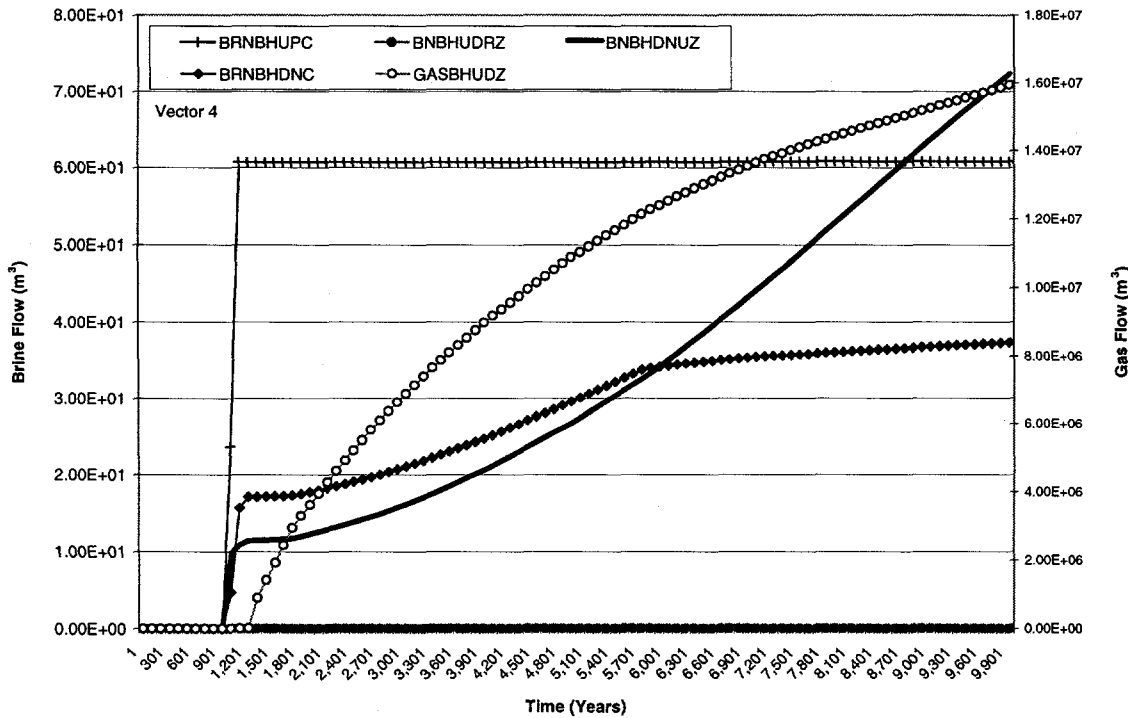


FIGURE 7.4.1. OVERLAY PLOTS FOR REALIZATION 4 depicting pressures, fraction of iron remaining, and gas saturations for lower and upper waste panels (top plot) and cumulative brine and gas flow within borehole at intersection of borehole with top of lower waste panel and top of the UDRZ (bottom plot)

and bottom plots show that at the onset of upper borehole degradation, pressures are slightly reduced as gas is evacuated out the repository via the borehole. The connection to the Castile reservoir causes repository pressure to plateau at relatively high levels between 1200 to 2200 years, when the lower borehole permeability is reduced by a factor of 10. Because upper borehole permeabilities are relatively low, the pressure in both the lower and upper waste panels decreases gradually due to the very slow evacuation of gas out the borehole. Pressures stabilize at ~8000 years when gas production via iron corrosion in the upper waste panel and gas evacuation out the borehole are in relative equilibration.

The bottom plot of Figure 7.4.1 shows that the pulse of brine coming up the borehole (BRNBHUPC), while only a minimal amount, reaches the top of the lower waste panel and coincides with the reduction in lower waste panel saturations. The curve for gas flow out the borehole at the UDRZ interface dominates flow within the borehole.

Gas Saturation in Both the Upper (REP_SATG) and Lower Waste Panels (WAS_SATG)

Figure 7.4.1 - top plot
WAS_SATG, REP_SATG

In the first ~300 years after repository closure, gas saturations in both waste panels decrease. The decrease is due to relatively large volumes of brine that drain from the UDRZ to the waste disposal regions, coupled with the effect of repository creep closure (reducing panel volumes). Because the lower waste panel is lower in elevation than the upper waste panels, brine in the lower waste panel continues to drain from the lower anhydrites through the LDRZ and, to a lesser extent, from the UDRZ through the panel closures. Brine collects within and just below the lower waste panel. Concurrently, gas produced from iron corrosion rises to the UDRZ and moves up-dip, where it is stored in the upper regions of the repository. Some of this gas is stored within the upper waste panel. The combined processes mean that at ~300 years, gas saturation for the upper waste panel (REP_SATG) starts to rise, while gas saturation for the lower waste panel plateaus (WAS_SATG). At the time of upper borehole degradation (1200 years), pressure is released from the repository in the borehole, which allows brine to flow up the borehole from the lower brine reservoir, filling the lower waste panel. This brine is impeded from coming into

the upper waste panel, in part, because gas saturation within the upper waste panel is much higher than in the lower waste panel, rendering the upper waste panel far less brine-permeable than the lower waste panel. Additionally, high iron corrosion rates mean that the majority of brine that enters the lower waste panel is consumed and excess brine is not available to move up into the upper waste panel.

At ~4900 years, the simultaneous decrease in both gas saturation and fraction of iron being corroded in the lower waste panel implies that the lower waste panel is filling up with brine as the amount of iron in the waste panel is reduced, i.e., less of the brine that flows into the lower waste panel is now consumed via corrosion.

A decrease in upper waste panel gas saturation occurs at ~5200 years. The decrease is caused by the onset of a large portion of resident brine in the lower waste panel beginning to collect in the down-dip region of the lower waste panel. This brine is not consumed via iron corrosion because most lower waste panel iron has already been corroded by 5000 years. Brine begins to accumulate down-dip and eventually 'pools' at the edge of the pool moving in the up-dip direction, toward the upper waste panel.

Fraction of Iron Uncorroded in Lower (FEREM_W) and Upper (FEREM_R) Waste Panel

Figure 7.4.1 - top plot

FEREM_W (fraction of iron uncorroded remaining in lower waste panel)

FEREM_R (fraction of iron uncorroded remaining in upper waste panel)

The fraction of iron actively being corroded changes at 1000, ~2000, and ~8100 years

Figure 7.4.1, top plot, shows all iron in the lower waste panel (FEREM_W) is completely corroded at ~6600 years. Iron corrosion (depletion) rates are constant from the time of repository closure until ~5000 years, when the iron depletion rate is dramatically reduced. By 5000 years, most of the iron situated in the down-dip portion of the lower waste panel is corroded, and, therefore, replenishing brine entering the lower waste panel no longer contacts uncorroded iron and must move up-dip before contacting uncorroded iron. This assumption is supported by the simultaneous decrease in both gas saturation and the fraction of iron being corroded in the lower

waste panel, indicating that the waste panel is filling up with brine because less iron is available to consume incoming brine.

Iron depletion in the lower and upper waste panels proceeds at approximately the same rate until 1000 years. Iron depletion in the upper waste panel is dramatically reduced at 1000 years, and is further reduced at ~2000 years. This is caused by a reduction in brine supplies transmitted to the upper waste panel when the lower borehole closes through creep. Iron depletion rates for the upper waste panel do not increase until ~8000 years when brine, now in excess in the lower waste panel, moves up-dip toward the upper waste panel. This brine 'feeds' iron corrosion in the upper waste panel when it contacts uncorroded iron drums. Brine that enters the upper waste panel reaches uncorroded iron in a few thousand years, as seen in the delay of the resumption of iron depletion while gas saturations in the upper waste panel steadily decline.

7.4.2 Overlay Plots for Flow in Borehole

Figure 7.4.1 - Bottom plot

Brine flow rates up borehole measured at the top of the lower waste panel (BRNBHUPC) and top of the UDRZ (BNBHUDRZ);

Brine flow down borehole measured at the top of the UDRZ (BNBHDNUZ) and top of the lower waste panel (BRNBHDNC);

Gas flow up borehole measured at the top of UDRZ (GASBHUDZ).

Brine flow rates change dramatically at 1000 and ~5500 years

Brine Flow in the Borehole

A large pulse of brine flows up the borehole (BRNBHUPC) and enters the lower waste panel from the Castile reservoir at the time of intrusion. This brine flow ceases soon after the intrusion event. At 1200 years, when the upper borehole degrades, gas flows up the borehole (GASBHUDZ) and is the dominant fluid within the borehole from 1200 to 10,000 years; only a very small volume of brine (less than 80 m³ for the entire modeled period) flows down the borehole.

Gas Flow in the Borehole

Gas flow rates change at 1200 and ~5900 years

Gas flow up the borehole is initiated when the upper borehole plugs degrade, at 1200 years. Gas flow rates in the borehole are reduced midway through the modeled period. This is due to a reduction in gas generated within the lower waste panel (since most lower waste panel iron is depleted by then). Because borehole permeabilities are so low, this change in flow rate up the borehole is gradual and occurs between ~4900 and ~6900 years.

7.4.3 Overlay Plots for Castile Brine Reservoir Pressures (B_P_PRES) with Respect to Brine Flow Up (BRNBHUPP) and Down (BRNBHDNC) the Borehole

Figure 7.4.2

B_P_PRES (brine reservoir pressure)

BRNBHUPP (brine up borehole measured at the bottom of lower waste panel)

BRNBHDNC (brine down borehole measured at the top of lower waste panel)

Borehole flow changes at 1200 years

Brine reservoir pressure is reduced at 1000 years, then slightly increases from a low of 11.5 to 13 MPa at 1200 years. Reservoir pressures remain relatively low for the remainder of the modeled period. A brief pulse of brine flows up the borehole from the lower reservoir (BBNBHUPP) at the time of intrusion (1000 years). No brine flows down the borehole from the lower waste panel to the lower reservoir.

Prior to intrusion, brine reservoir pressures (B_P_PRES) are much higher than repository pressures (see Figure 7.4.1). Therefore, a potential exists between the two regions that promote brine flow from the lower reservoir via the borehole to the repository at the time of intrusion (BRNBHUPP). Because the reservoir compressibility is also high (rank 19th), a large volume of brine is able to flow up the borehole (BRNBHUPP) immediately after intrusion, thus rapidly reducing reservoir pressures and decreasing the potential between the two regions. Because upper borehole permeabilities are so low, any flow up or down the borehole between the reservoir and units above the repository is minimized.

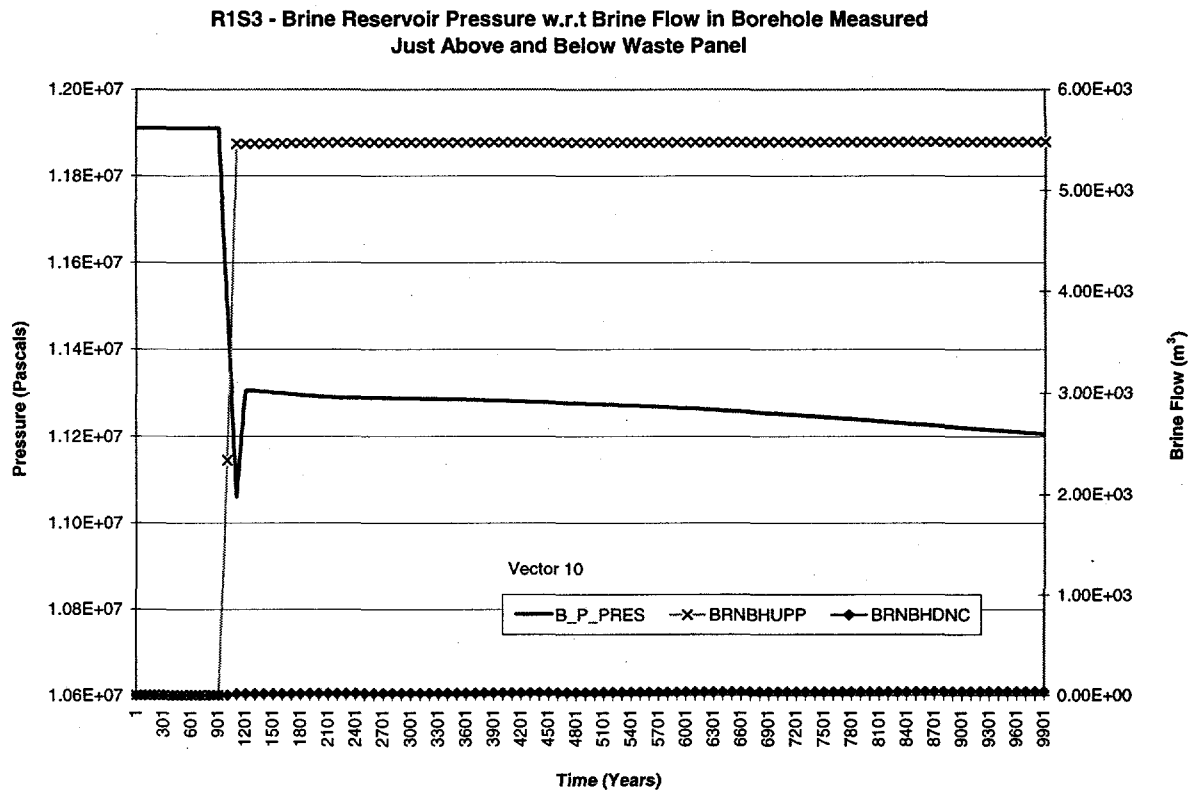


FIGURE 7.4.2. OVERLAY PLOT FOR REALIZATION 4 depicting brine reservoir pressure overlaid with brine flow up and down the borehole measured at the top and bottom of the lower waste panel

7.4.4 Overlay Plots for Brine Flow through the Panel Closures to the Upper and Lower Waste Panels

Figures 7.4.3 and 7.4.4 - all plots

North-flowing brine from lower to upper waste panel is defined as BRNPSOWC (brine from the lower waste panel enters the panel closure south face) and BRNPSIRC (brine exits the panel closure north face to the upper waste panel)

South-flowing brine from upper to lower waste panel is defined as BRNPSORC (brine flows through panel closure from upper waste panel) and BRNPSIWC (brine flows through panel closure into lower waste panel)

Brine flow rate changes at 1200 years

The dominant lateral brine flow direction within the panel closures is out the closure south face and into the lower waste panel. This brine does not pass from the upper waste panel via the closures, but enters the closure bottom or top via the DRZ, then flows down-dip to the lower waste panel.

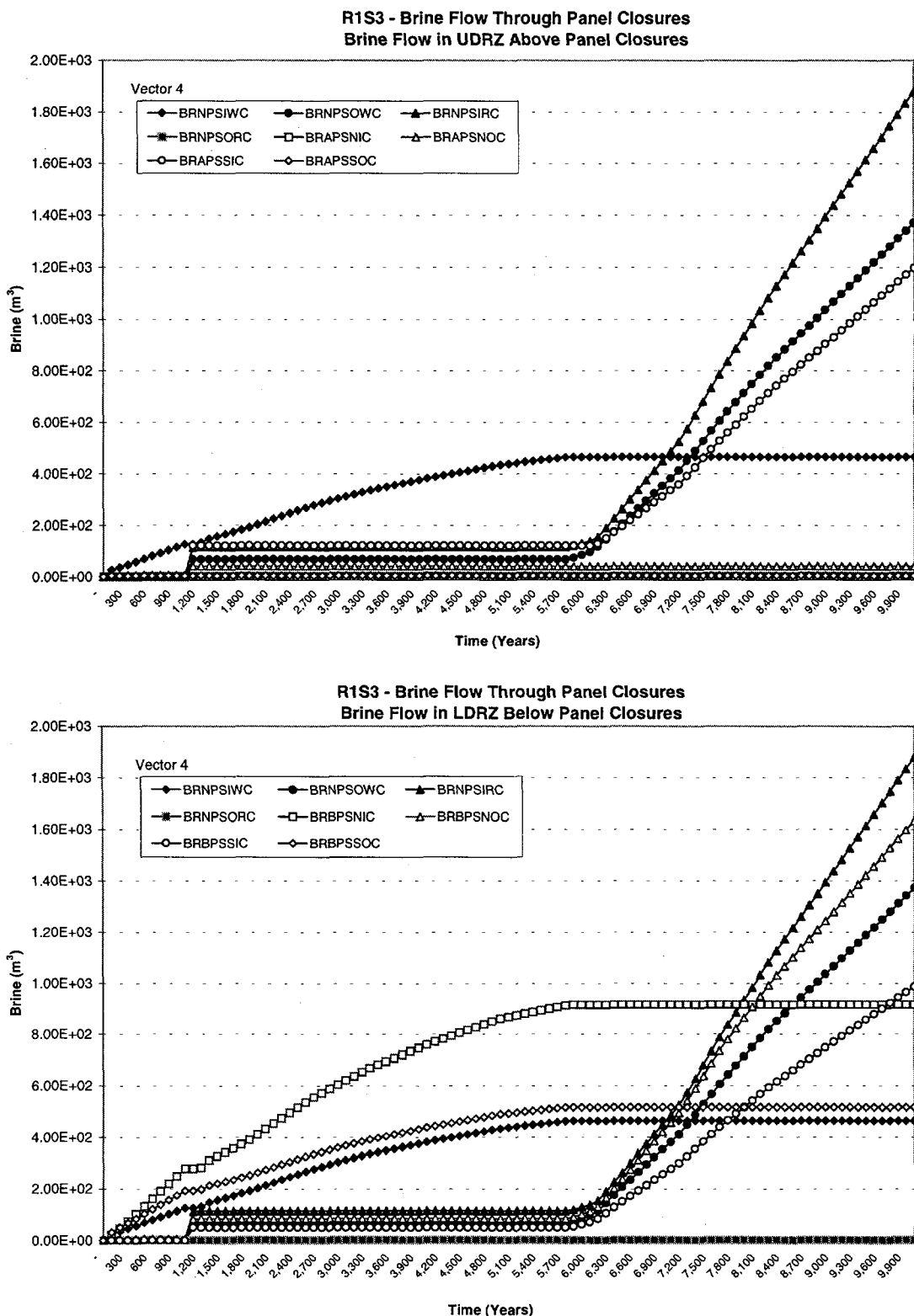


FIGURE 7.4.3. OVERLAY PLOTS FOR REALIZATION 4 depicting brine flow through the panel closures overlaid with lateral brine flow within UDRZ (top plot) and LDRZ (bottom plot), crossing the area just above/below panel closures

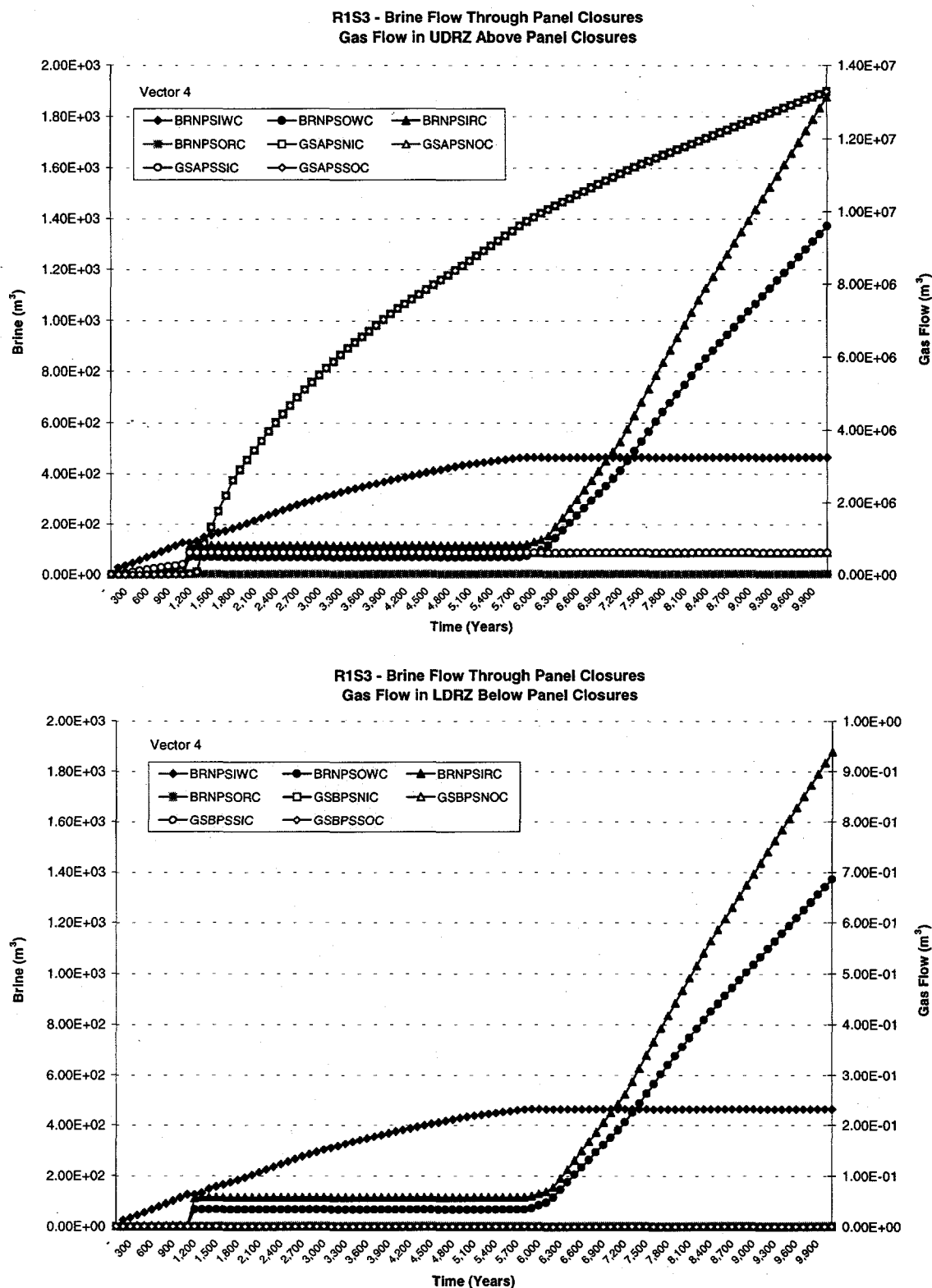


FIGURE 7.4.4. OVERLAY PLOTS FOR REALIZATION 4 depicting brine flow through the panel closures overlaid with lateral gas flow within UDRZ (top plot) and LDRZ (bottom plot), crossing the area just above/below panel closures

Brine flow through the closures reverses direction at ~6000 years, when iron in the lower waste panel is depleted. Brine in the lower waste panel accumulates, filling this region up, then moves up-dip to the upper waste panel, passing through the panel closures. More brine enters the upper waste panel than exits the lower waste panel side (compare BRNPSOWC vs. BRNPSIRC) via the closures; the extra contribution is caused by brine that enters the closure tops and bottoms via the DRZ.

7.4.5 Overlay Plots for Lateral Brine Flow in DRZ Above and Below Panel Closures

Lateral Brine Flow in the UDRZ

Figure 7.4.3 - top plot (refer also to Figure 7.3)

North-flowing brine is defined as BRAPSSIC (brine entering south face) and BRAPSNOC (brine exiting north face)

South-flowing brine is defined as BRAPSSOC (brine exiting south face) and BRAPSNIC (brine entering north face)

Brine flow rates change at 1000, ~5700, and ~6000 years

The top plot in Figure 7.4.3 shows that little brine flows laterally within the UDRZ above the panel closures prior to ~6000 years. At ~6000 years, when most iron within the lower waste panel is depleted and the lower waste panel becomes brine saturated, brine begins to flow north in the UDRZ (BRAPSSIC, BRAPSNOC) towards the upper waste panels, crossing the area above the panel closures. A large portion of brine does not cross the UDRZ area just north of the closures, but instead is deflected downward into the panel closures by the gas wedge in the UDRZ residing above the upper waste panels (see Section 7.4.8, gas saturation contour plots).

Lateral Brine Flow in the LDRZ

Figure 7.4.3 - bottom plot (refer also to Figure 7.3)

North-flowing brine is defined as BRBPSSIC (brine entering south face) and BRBPSNOC (brine exiting north face)

South-flowing brine is defined as BRBPSSOC (brine exiting south face) and BRBPSNIC (brine entering north face)

Brine flow rates change at 1000, ~5700, and ~6000 years

The bottom plot in Figure 7.4.3 shows that brine flow in the LDRZ just below the panel closures, prior to ~6000 years, is in a southerly direction (BRBPSSIC, BRBPSNOC). More brine flow enters the area below the closures from the north than exits to the south, indicating that some brine flows up into the bottom of the panel closures. Flow direction changes from south to north at ~6000 years, when the lower waste panel becomes brine saturated and iron corrosion nears completion, as indicated in Figure 7.4.1 (top plot). Brine accumulates in the lower waste panel, drains to the LDRZ, then moves up-dip toward the upper waste panel. Because more brine exits the north area below the closures than enters from the south (BRBPSSIC versus BRBPSNOC), the extra contribution is probably from brine drainage out the bottom of the panel closures to the LDRZ. From the area below the panel closure, brine moves up-dip toward the upper waste panel.

7.4.6 Overlay Plots for Lateral Gas Flow in the DRZ Above and Below the Panel Closures

Figure 7.4.4 illustrates gas flow within the UDRZ with respect to brine flow through the panel closures.

Lateral Gas Flow in the UDRZ

Figure 7.4.4 - top plot (refer also to Figure 7.3)

North-flowing gas is defined as GSAPSSIC (gas entering south face) and GSAPSNOc
(gas exiting north face)

South-flowing gas is defined as GSAPSSOC (gas exiting south face) and GSAPSNC
(gas entering north face)

Brine flow rates change at 1200 years

The curves for gas flow indicate little gas flows up into the UDRZ via the panel closures. Prior to intrusion, some of the gas generated in the lower waste panel enters the UDRZ, where it moves up-dip (GSAPSSIC, GSAPSNOc) toward the back of the repository. Because the UDRZ pore volume is very large (due to relatively large values for halite porosity), an appreciable amount of gas is stored in the UDRZ just above the lower waste panel. This extra storage limits gas flow that moves up-dip to the north positions of the repository. After borehole degradation at 1200 years, lower pressures within the borehole produce gradients that promote flow from the north

portion of the upper waste panel toward the borehole. Consequently, gas flow in the UDRZ changes direction from north to south.

Lateral Gas Flow in the LDRZ

Figure 7.4.4 - bottom plot (refer also to Figure 7.3)

North-flowing gas is defined as GSBPSSIC (gas entering south face) and GSBPSNOC (gas exiting north face)

South-flowing gas is defined as GSBPSSOC (gas exiting south face) and GSBPSNIC (gas entering north face)

Gas flow rates and direction in the UDRZ change at 1200, 1700, and ~5000 years

Figure 7.4.4 illustrates gas flow within the LDRZ with respect to brine flow through the panel closures. Essentially no lateral gas flow occurs within the LDRZ below the panel closures.

7.4.7 Overlay Plots for Brine and Gas Flow In/Out Ceiling and Floor of Upper Waste Panel

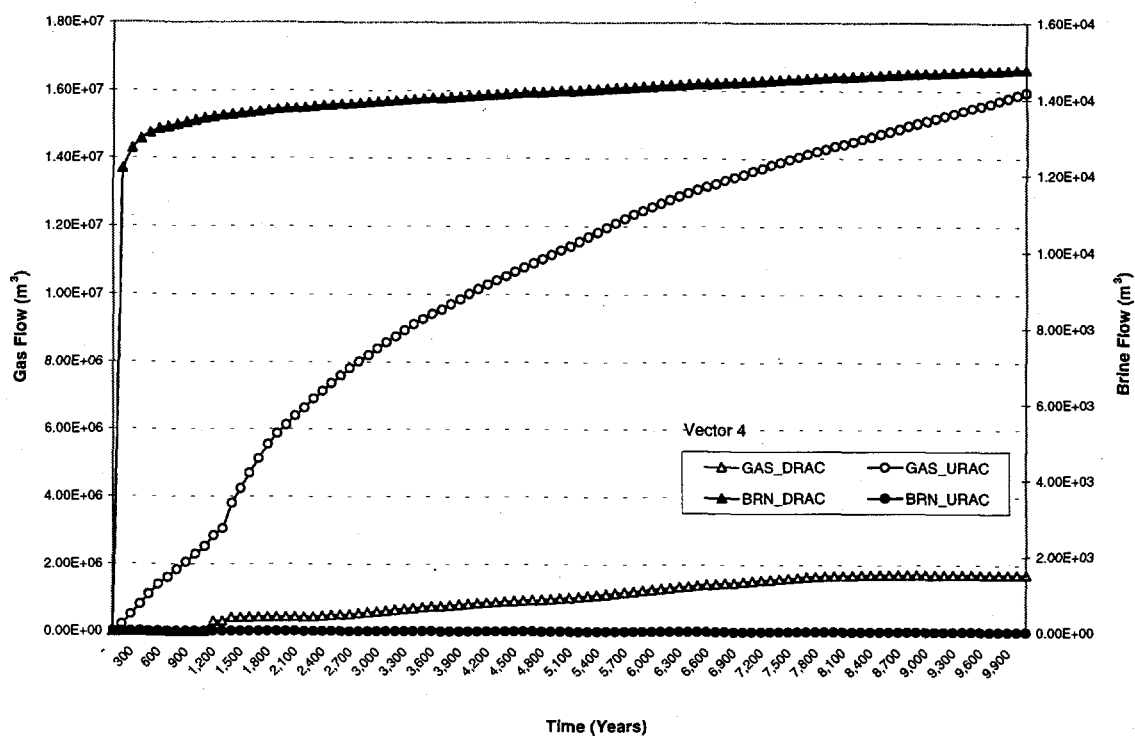
Brine Flow Through the Upper Waste Panel Ceiling

Figure 7.4.5 – top plot

BRN_DRAC (downflowing brine) and BRN_URAC (upflowing brine)

Because halite porosities are relatively high, large volumes of brine drain from the UDRZ through the upper waste panel ceiling (BRN_DRAC) within the first 300 years after repository closure. Very little brine flows from the UDRZ to the upper waste panel after ~500 years. Gas evacuation out the UDRZ is impeded by low borehole permeabilities. This keeps gas saturations at relatively high levels in the UDRZ and upper waste panel, and inhibits brine from entering or exiting through the upper waste panel ceiling. Consequently, no brine flows out the upper waste panel ceiling (BRN_URAC).

R1S3 - Brine and Gas Flow In and Out the Upper Waste Panel Ceiling



R1S3 - Brine and Gas In and Out the Upper Waste Panel Floor

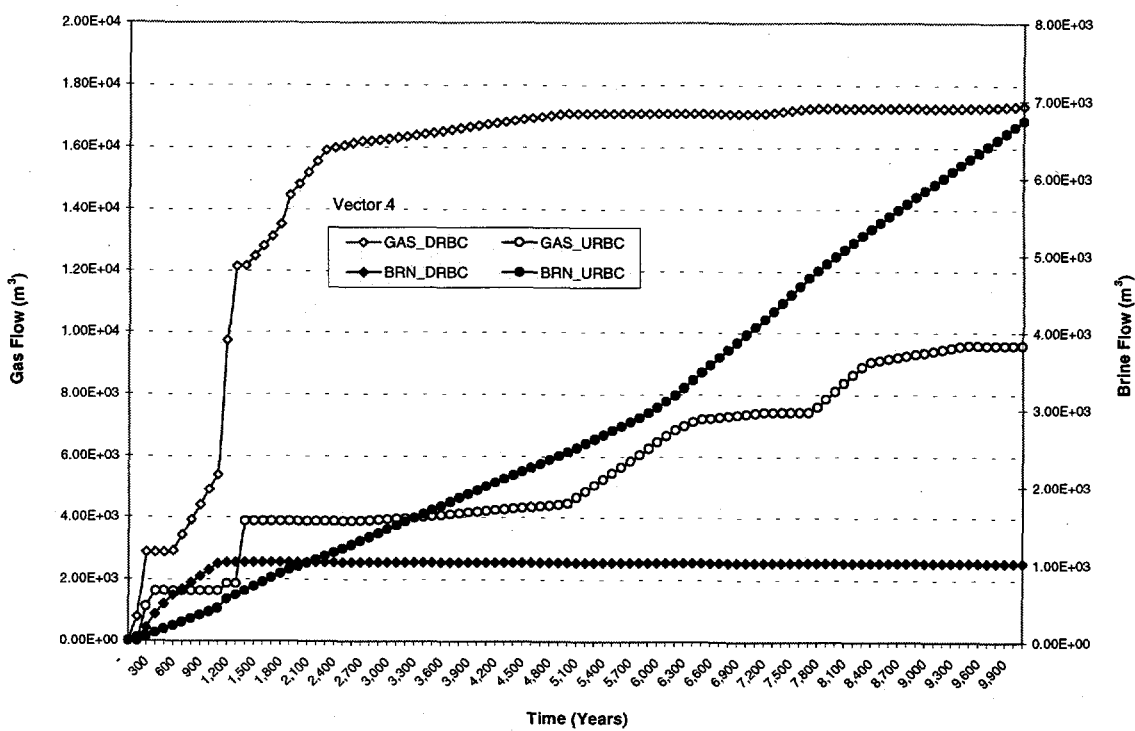


FIGURE 7.4.5. OVERLAY PLOTS FOR REALIZATION 4 depicting vertical brine and gas flow through ceiling of upper waste panel within the UDRZ (top plot) and LDRZ (bottom plot)

Gas Flow Through the Upper Waste Panel Ceiling

Figure 7.4.5 – top plot

GAS_DRAC (downflowing gas) and GAS_URAC (upflowing gas)

A continuous flow of gas exits the ceiling of the upper waste panel (GAS_URAC) throughout the modeled period, with significant inflection points at 1200 years, when the upper borehole plug degrades. Because borehole permeabilities are relatively low, gas is impeded in the UDRZ as it flows from the back of the repository towards the borehole. This causes some gas to flow downward from the UDRZ through the upper waste panel ceiling (GAS_DRAC). This downward flow ceases around ~7500 years as repository pressures plateau.

Brine Flow Through the Upper Waste Panel Floor

Figure 7.4.5 – bottom plot

BRN_DRBC (downflowing brine) and BRN_URBC (upflowing brine)

Brine flow rates change at 1000 and ~6300 years

Brine flows out the floor of the upper waste panel (BRN_DRBC) from the time of repository closure until 1000 years. This brine is from UDRZ drainage that passes through the upper waste panel, is not used in the corrosion process, and continues to flow downward to the LDRZ. Brine flow upward through the upper waste panel floor (BRN_URBC) is continuous throughout the modeled period. Initially, this brine ‘pools’ in the LDRZ from anhydrite and halite drainage, eventually moving in the LDRZ up-dip where it seeps upward into the lower waste panel floor. At ~6000 years, the amount of brine entering the upper waste panel from the LDRZ increases, coincident with iron corrosion in the lower waste panel nearing completion. Brine ceases to be consumed in the lower waste panel via corrosion, causing it to accumulate. This brine drains down from the lower waste panel to the LDRZ and moves up-dip towards the upper waste panel, where some flows upward through the upper waste panel floor.

Gas Flow Through the Upper Waste Panel Floor

Figure 7.4.5 – bottom plot

GAS_DRBC (downflowing gas) and GAS_URBC (upflowing gas)

Gas flow through the upper waste panel floor is punctuated by several upward (GAS_URBC) and downward (GAS_DRBC) pulses.

Gas flow from the LDRZ upward through the upper waste panel floor (GAS_URBC) occurs at several distinct times. The first influx occurs at ~300 years as brine pools in the LDRZ, pushing gas back up through the south end of the upper waste panel floor. The second influx, at 1200 years, is a result of the pressure pulse created when the upper borehole degrades, displacing gas that was stored in the LDRZ to the upper waste panel floor. The third influx occurs at ~5000 years, when iron corrosion in the lower waste panel begins to subside. Brine accumulates in the lower waste panel because iron corrosion here is nearly complete, draining down through the lower waste panel floor to the LDRZ. The increased volume of brine entering the LDRZ from the lower waste panel brine drainage displaces stored LDRZ gas, displacing it upward through the upper waste panel floor. The fourth influx of gas is coincident with the repository pressures declining to a relatively low plateau value of ~4.8 MPa. These lower pressures enable brine to flow from adjoining anhydrites and displace any resident gas up from the LDRZ through the upper waste panel floor.

Gas flow down through the upper waste panel floor is initially due to a combination of high gas production via corrosion and waste panel creep closure. The reduction in panel pore volume displaces gas down through the upper waste panel floor to the LDRZ at the time of intrusion. The pulse of brine that enters the repository from the Castile displaces gas from the upper waste panel down to the LDRZ. When the lower borehole constricts, at 2200 years, the connection to the Castile unit is reduced and gas flow downward ceases.

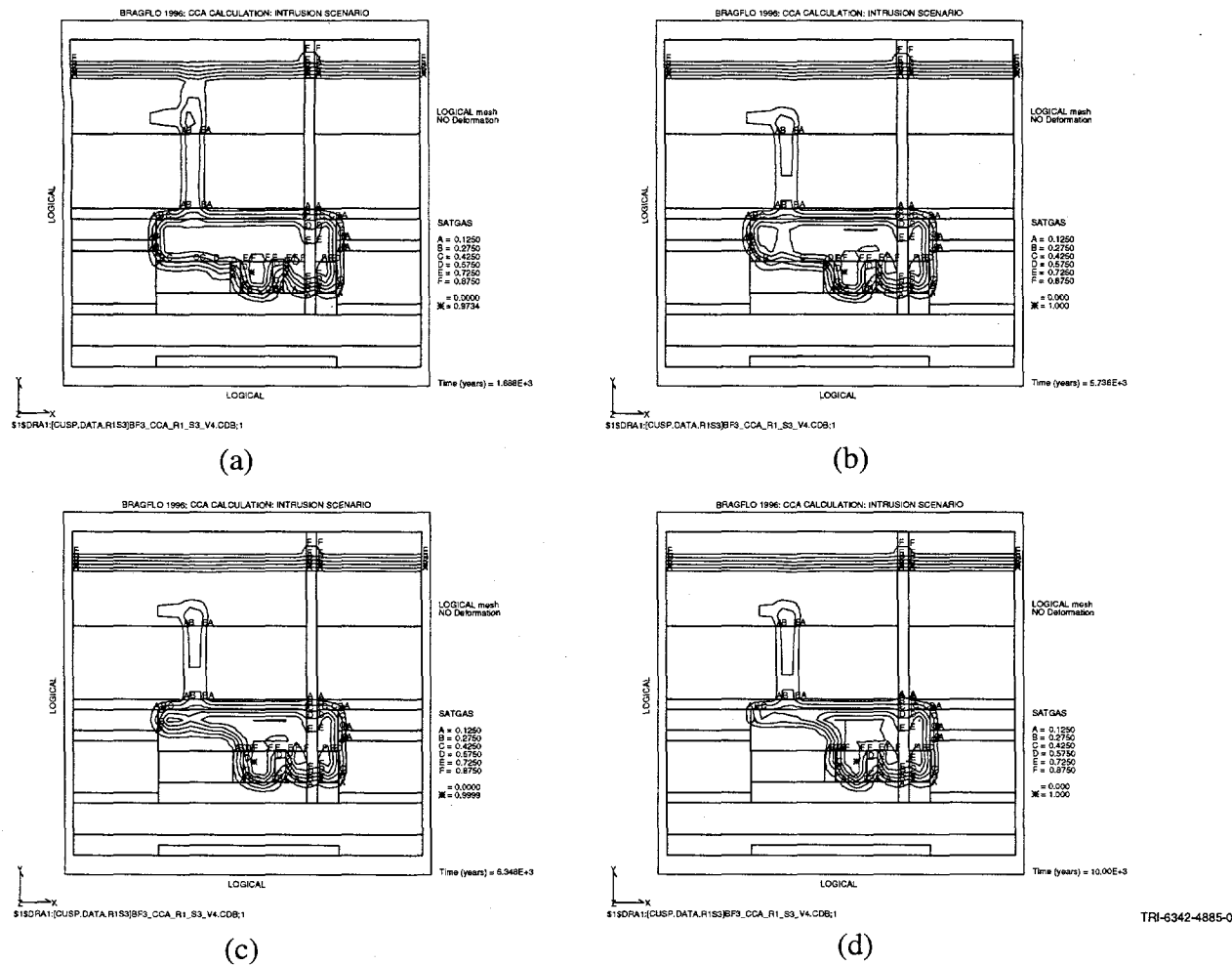


FIGURE 7.4.6. GAS SATURATION CONTOURS FOR REALIZATION 4. (a) ~1680 years, (b) ~5730 years, (c) ~6340 years, and (d) 10,000 years, the end of the modeled period. Borehole in lower waste panel is not shown; see Figure 7.4 for location of borehole.

7.4.8 Gas Saturation Contour Plots

Figure 7.4.6

SATGAS

Gas saturation contour plots at 1000, ~1212, ~5146, and 10,000 years

Gas saturation contours for the BRAGFLO modeled domain (Figure 7.4.6) are provided at:

~1680 years (Figure 7.4.6a), several hundred years after the upper borehole plugs have degraded; ~5730 years (Figure 7.4.6b), when the majority of iron in the lower waste panel is depleted and the panel has started to fill with brine; ~6340 years (Figure 7.4.6c), when all the iron in the lower waste panel is depleted; and 10,000 years (Figure 7.4.7d), the end of the modeled period.

At 1688 years, gas flow out the borehole is slow (due to low borehole permeabilities), causing the UDRZ and the upper waste panels to have relatively high gas saturation levels. The down-dip portion of the LDRZ (below the lower waste panel) is predominantly brine-saturated. Brine, arising primarily from 'south' MB 139, flows up through the south floor of the lower waste panel where it can support iron corrosion.

At 5730 years, gas saturation levels in the lower waste panel are reduced to the assigned LHS value for residual gas saturation (0.0641). Gas continues to flow out the borehole, but at a slower rate; gas that enters the borehole has been stored predominantly in the upper waste panel and the UDRZ. Gas saturations in the up-dip portion of the UDRZ actually increase from those values seen at 1680 years for several reasons.

- Repository pressures have been reduced to levels that are too low to displace gas through the relatively low permeable borehole. Consequently, a portion of gas generated between 1600 and 5700 years backs up in the up-dip portion of the repository.
- Because iron in the lower waste panel is close to being completely corroded, gas generation and brine consumption via the corrosion process subsides, causing brine to accumulate. Excess brine (drained from 'south' MB 139) accumulates and fills up the lower waste panel and some moves up-dip via the LDRZ to the upper waste panel. This increase in brine to the upper waste panel promotes an increase in gas generation via iron corrosion. Gas flows up to the UDRZ where it is stored prior to exiting the repository via the borehole.

The plot at ~6348 years shows a gas saturation wedge starting to form in the UDRZ as replenishing brine begins to fill the lower waste panel, spilling up into the southern portion of the UDRZ. The region of the UDRZ above the upper waste panel has relatively high gas saturation levels. This gas is impeded from exiting the repository via the borehole due to the brine wedge that exists in the UDRZ above the lower waste panel.

At 10,000 years, the repository has gas saturation levels very similar to that seen at 6348 years. UDRZ gas saturations above the upper waste panel have increased as less gas is able to laterally

flow toward the borehole. This condition is partially due to the lower waste panel and the south portion of the UDRZ becoming more brine saturated as excess brine moves up-dip through the UDRZ, somewhat restricting the south-flowing gas toward the borehole.

7.5 *Realization 47 - Overlay Plot Summary*

Low borehole permeability - $10^{-13.8}$ m², rank 92/100

Halite Porosity - 0.00303, rank 88/100

Microbial degradation - 0, no microbial degradation; corrosion rate - 3.03×10^{-15} m/s, rank 81/100

Brief Summary: Realization 47 represents repository behavior affected by very low volumes of gas generated due to the absence of microbial degradation and low iron corrosion rates.

Consequently, the repository pressurizes very slowly prior to intrusion (within the lower 10th percentile). The combination of low repository pressure with low borehole permeabilities means little brine and gas are released through the borehole. Therefore, the repository pressure is minimally affected by the intrusion event and the pressure after intrusion increases at about the same rate as that prior to intrusion. Brine sources for iron corrosion are primarily from halite and anhydrite drainage early in the modeled period and the pulse of brine introduced from the Castile reservoir at the time of intrusion. Because the UDRZ remains highly gas saturated throughout the modeled period (giving this area a very low effective brine permeability), little brine can drain from the south Anhydrite AB or down the borehole, through the UDRZ, then through the waste region ceiling later in the modeled period. After intrusion, brine drains from MB 139 and from the operations and experimental rooms (stored there from early DRZ drainage) to the LDRZ. This replenishing brine is used in iron corrosion in the down-dip waste region and is transmitted to the waste regions via the LDRZ.

7.5.1 **Overlay Plots For Pressures in Lower (WAS_PRES) and Upper (REP_PRES) Waste Panels; Gas Saturation in the Lower (WAS_SATG) and Upper Waste Panels (REP_SATG); Fraction of Uncorroded Iron in Lower (FEREM_W) and Upper (FEREM_R) Waste Panels**

Figure 7.5.1 - top plot

Repository pressures change at 1000, 1200, 2220, and 4000 years

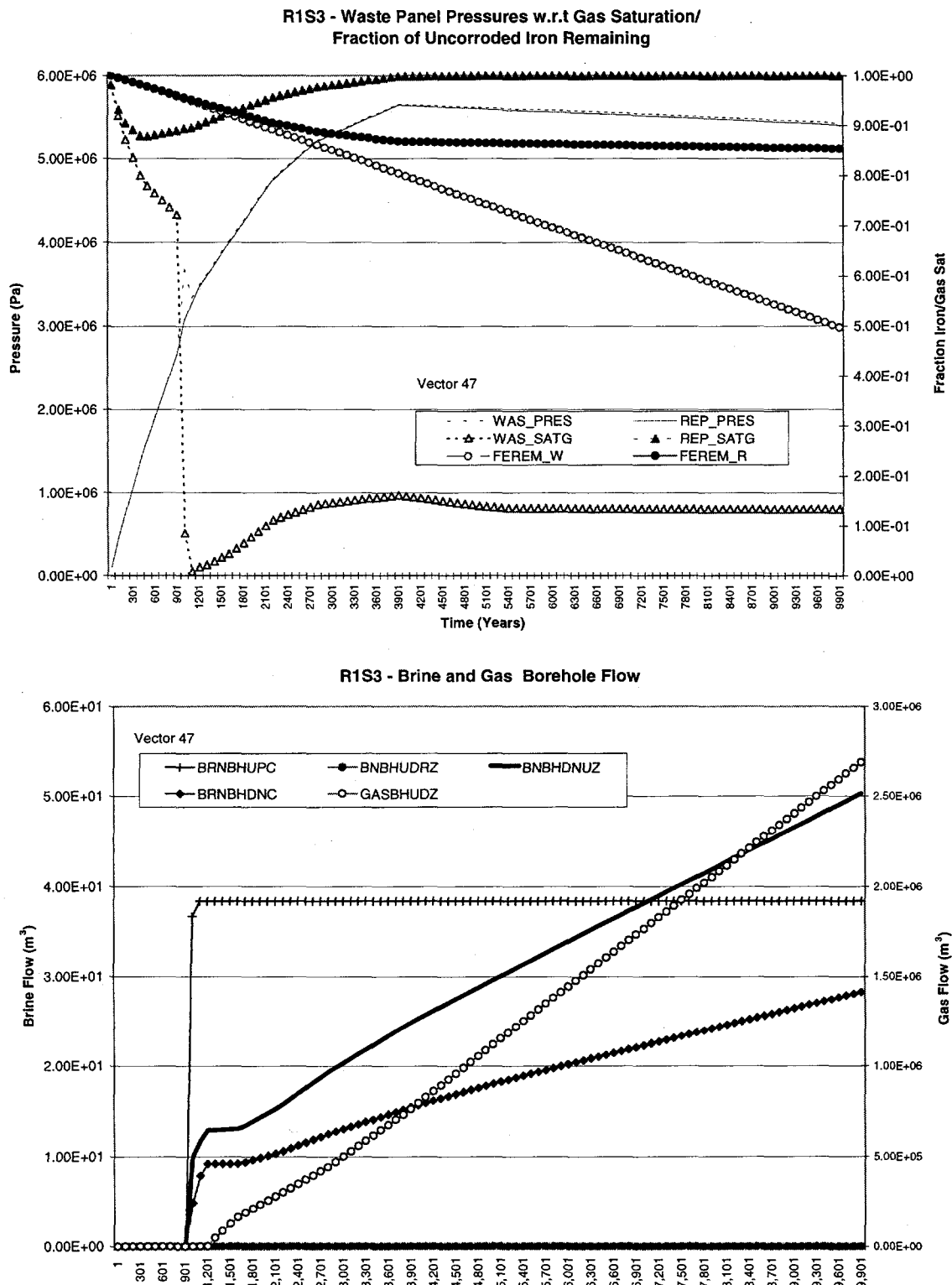


FIGURE 7.5.1. OVERLAY PLOTS FOR REALIZATION 47 depicting pressures, fraction of iron remaining, and gas saturations for lower and upper waste panels (top plot) and cumulative brine and gas flow within borehole at intersection of borehole with top of lower waste panel and top of the UDRZ (bottom plot)

Repository Pressures for the Lower (WAS_PRES) and Upper (REP_PRES) Waste Panel

Repository pressure at the time of intrusion is one of the lowest of the sampled suite (within the 10th percentile group). The low pressure is caused by a lack of gas production from microbial degradation and relatively little gas production from iron corrosion. The low gas production is exacerbated by relatively small amounts of brine drainage from the UDRZ into the waste regions, a function of small DRZ pore volumes, thus making iron corrosion brine-limited. At the time of intrusion, the borehole connects the repository to the relatively highly pressurized brine reservoir, causing a pulse of Castile brine to enter the repository and creating a pressure spike within the lower waste panel. While the brine pulse is limited to the time of intrusion, the borehole connection to the lower Castile serves as a quasi-hydraulic piston, transmitting reservoir pressure up to the repository and, more specifically, the lower waste panel. This flow from the lower non-Salado units briefly increases the repository's pressure. After upper borehole degradation, gas evacuation out the upper borehole partially relieves pressure. Once pressure is released at 1200 years, repository pressures begin to increase at about the same rate as that seen prior to intrusion until ~4000 years. At ~4000 years, repository pressure plateaus at ~5.5 MPa, close to hydrostatic pressure.

Gas Saturation in Both the Upper (REP_SATG) and Lower Waste Panels (WAS_SATG)

Gas saturation changes (Figure 7.5.1 - top plot) are seen at 1000, ~2000, and 4000 years. The most dramatic change is seen in the lower waste panel (WAS_SATG), with gas saturation dramatically dropping at the time of intrusion. Upper waste panel gas saturation (REP_SATG) is between 90% to 100% throughout the modeled period.

The lower waste panel is nearly 70% gas saturated just prior to intrusion, as shown by the saturation curve at 999 years and becomes nearly 100% brine saturated just after intrusion (1000 years) as this region fills with incoming brine from the Castile and the anhydrites. Because borehole permeability is very low, at the time of upper borehole degradation (1200 years), little gas is vented out the repository via the borehole. This keeps the upper waste panel gas saturation at nearly the same level as just prior to intrusion. Gas saturation approaches 100% in the upper

waste panel at ~4000 years. As gas is produced in the upper waste panel, it moves into the DRZ region above and below this panel where it is stored. (The UDRZ from the area above the upper waste panel to the shaft remains close to 100% gas saturated, as illustrated in the gas saturation plots in Section 7.5.8.)

Fraction of Iron Uncorroded in Lower (FEREM_W) and Upper (FEREM_R) Waste Panel

Figure 7.5.1 - top plot

FEREM_W (fraction of iron uncorroded remaining in lower waste panel)

FEREM_R (fraction of iron uncorroded remaining in upper waste panel)

The supply of brine is enough that corrosion remains fairly constant in the lower waste panel during the modeled period. However, corrosion rates are so low that iron is never depleted in the lower waste panel. For the upper waste panel, brine supplies are depleted by ~4000 years. Consequently, iron corrosion appears to cease at ~4000 years, coincident with this area reaching close to 100% gas saturation. This cessation in iron corrosion in the upper waste panel at 4000 years means gas generated in the repository is primarily limited to the lower waste panel. This condition is reflected in the stabilization of repository pressure at ~4000 years and implies equilibrium between gas generated in the lower waste panel and gas flowing up the borehole.

7.5.2 Overlay Plots for Flow in Borehole

Figure 7.5.1 - bottom plot

Brine flow rates up the borehole measured at the top of the lower waste panel

(BRNBHUPC) and top of the UDRZ (BNBHUDRZ)

Brine flow down the borehole measured at the top of the UDRZ (BNBHDNUZ) and top of the lower waste panel (BRNBHDNC)

Gas flow up the borehole measured at the top of the UDRZ (GASBHUZ)

Brine Flow in the Borehole

A small pulse of brine flows down the borehole at 1000 and ~1600 years. Less than 50 m³ of brine enters the repository via the borehole over the entire modeled period. More than 75% of the total volume of brine that enters the repository is due to a very slow trickle flowing down the borehole from ~1600 to 10,000 years.

Gas Flow in the Borehole

Gas slowly exits the repository via the borehole (GASBHUDZ) at the time of upper borehole degradation, 1200 years, and continues to flow up the borehole for the remainder of the modeled period.

7.5.3 Overlay Plots for Castile Brine Reservoir Pressure (B_P_PRES) with Respect to Brine Flow Up (BRNBHUPP) and Down (BRNBHDNC) the Borehole

Figure 7.5.2

B_P_PRES (brine reservoir pressure)

BRNBHUPP (brine up borehole measured at the bottom of lower waste panel)

BRNBHDNC (brine down borehole measured at the top of lower waste panel)

Reservoir pressure changes at 1000 and 1200 years

A rapid reduction in Castile reservoir pressure (B_P_PRES) is seen at 1000 years; at 1200 years, when the upper borehole degrades, reservoir pressures slightly increase. Brine reservoir pressures are much higher than repository pressure (see WAS_PRES and REP_PRES in Figure 7.5.1, top plot), therefore a strong pressure potential exists between the two regions, promoting upward flow of brine to the repository (BRNBHUPP) at the time of intrusion. This potential is enough to overcome relatively low borehole permeability, so that a brine pulse ($\sim 3500 \text{ m}^3$) is released up the borehole to the repository at the time of intrusion. Low brine reservoir compressibility means that the Castile does not recover after the intrusion event. Because borehole permeability is so low, the pressure potential is not sufficient to move brine or gas to the upper units above the Salado via the borehole, at 1200 years, when the upper borehole degrades.

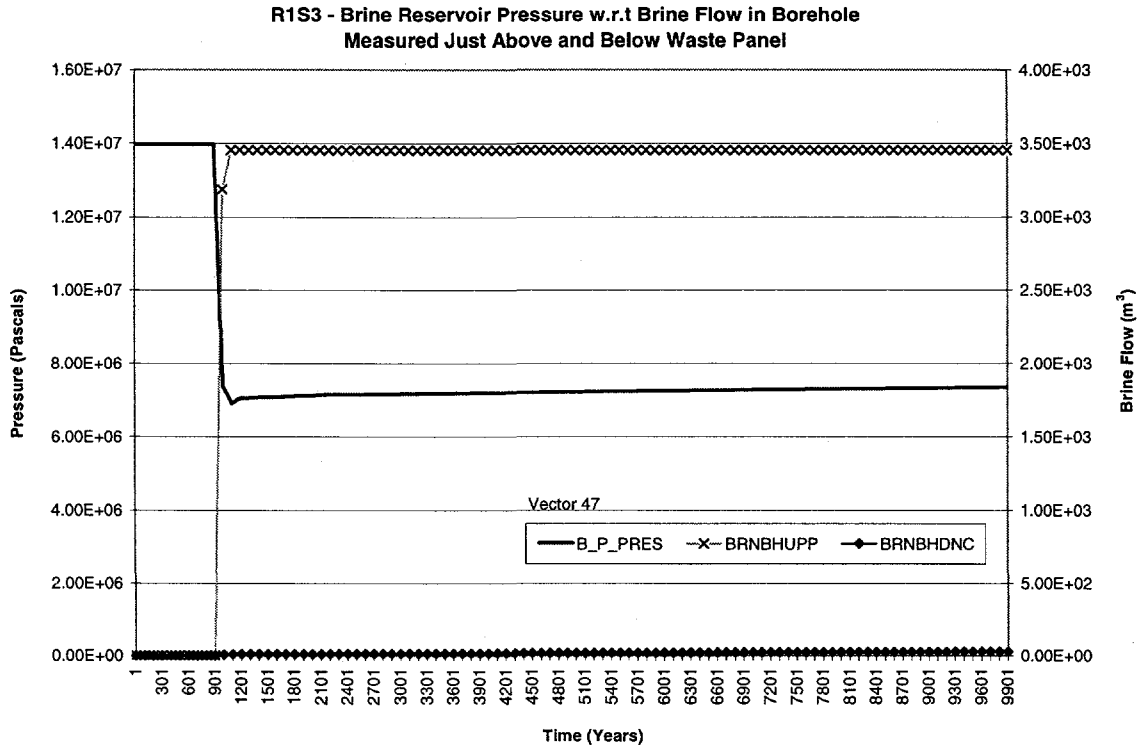


FIGURE 7.5.2. OVERLAY PLOT FOR REALIZATION 47 depicting brine reservoir pressure overlaid with brine flow up and down the borehole measured at the top and bottom of the lower waste panel

7.5.4 Overlay Plots for Brine Flow through the Panel Closures to the Upper and Lower Waste Panels

Figure 7.5.3 and 7.5.4 - all plots

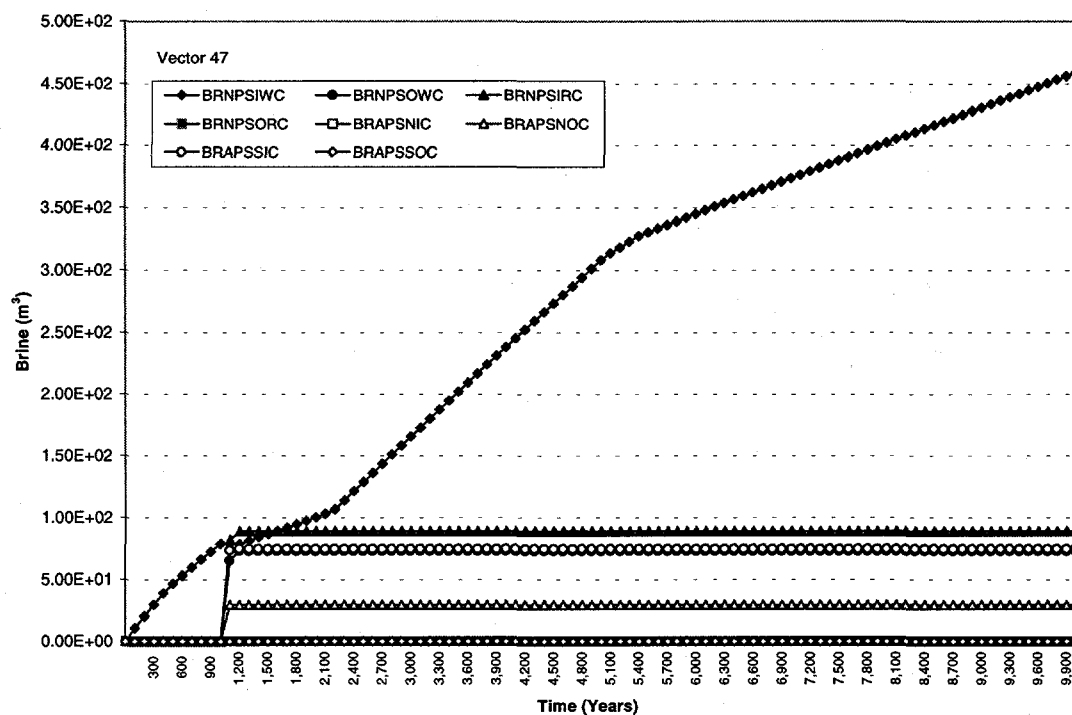
North-flowing brine from lower to upper waste panel is defined as BRNPSOWC (brine from the lower waste panel enters the panel closure south face) and BRNPSIRC (brine exits the panel closure north face to the upper waste panel)

South-flowing brine from upper to lower waste panel is defined as BRNPSORC (brine flows through panel closure from upper waste panel) and BRNPSIWC (brine flows through panel closure into lower waste panel)

Brine flow rates dramatically change at 1200 years

Brine flows from the panel closures to the lower waste panel from the time of repository closure until intrusion, 1000 years, ceases from 1000 to 2200 years, then resumes at 2200 years. Flow rates diminish at 5000 years. No brine flows through the closure's north face from the upper

R1S3 - Brine Flow Through Panel Closures
Brine Flow in UDRZ Above Panel Closures



R1S3 - Brine Flow Through Panel Closures
Brine Flow in LDRZ Below Panel Closures

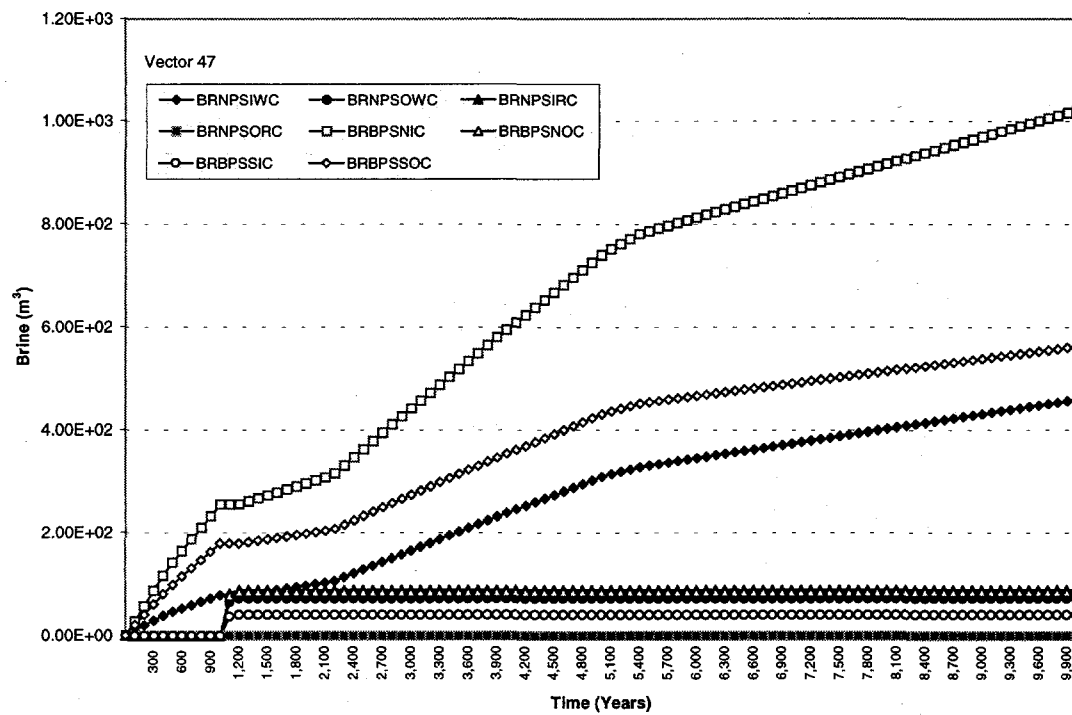


FIGURE 7.5.3. OVERLAY PLOTS FOR REALIZATION 47 depicting brine flow through the panel closures overlaid with lateral brine flow within UDRZ (top plot) and LDRZ (bottom plot), crossing the area just above/below panel closures

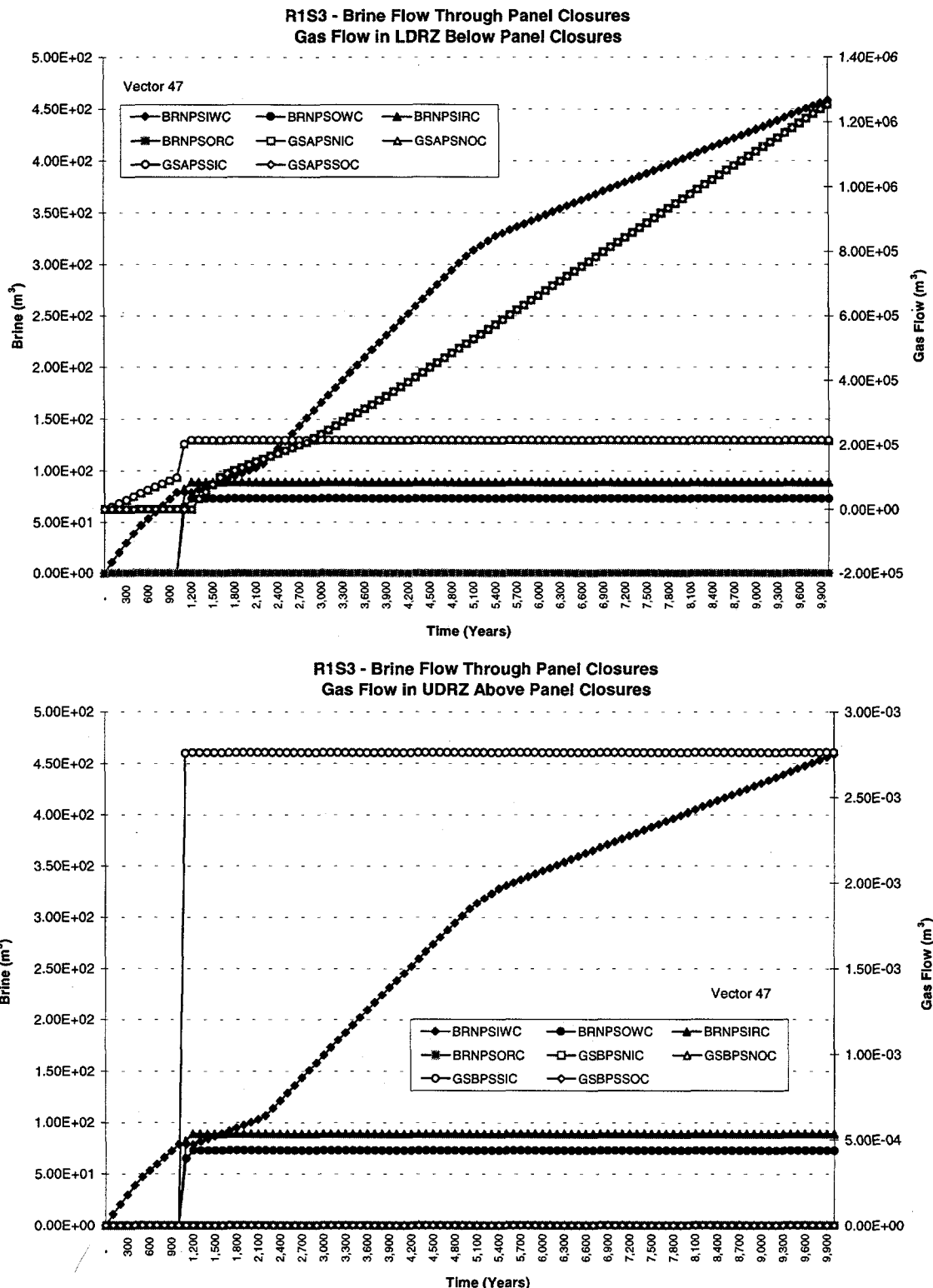


FIGURE 7.5.4. OVERLAY PLOTS FOR REALIZATION 47 depicting brine flow through the panel closures overlaid with lateral gas flow within UDRZ (top plot) and LDRZ (bottom plot), crossing the area just above/below panel closures

waste panel (BRNPSORC). A brief pulse of brine flows from the lower waste panel through the panel closure south face (BRNPSOWC) and out of the north face to the upper waste panel (BRNPSIRC) when the upper borehole plug degrades. Because the DRZ porosity is relatively small, the two waste regions have a relatively small DRZ region connecting them. This causes the two waste panels to behave more like separate units. Therefore, more brine exchange between the waste regions is forced through the panel closures rather than through the DRZ.

Brine flows out the south face of the panel closures into the lower waste panel (BRNPSIWC) throughout the entire model period. Note that the majority of this brine is not associated with brine drainage that collects in the upper waste panels, then drains through the closures. Brine that enters the lower waste panel via the closures is that which flows up through the bottom of the panel closures via the LDRZ and is primarily from MB 139 drainage prior to intrusion and, to a lesser extent, Castile brine that was partitioned into the LDRZ at the time of intrusion. A reduction in brine flow is seen between 1200 and 2200 years, when the repository is well connected to the brine reservoir. The borehole connection to the reservoir serves as a quasi-hydraulic piston, transmitting reservoir pressure (and brine) up to the repository and, more specifically, the lower waste panel. This situation slightly elevates pressure in the lower waste panel relative to the rest of the repository, causing a reverse in the pressure potential between the upper and the lower waste panel, which reduces brine flow rates from the panel closures to the lower waste panel. After the lower borehole permeability is reduced by a factor of 10, the connection between the brine reservoir and the lower waste panel is restricted and flow rates out the south face of the panel closures resume to levels similar to those seen prior to intrusion. At ~5000 years, brine flow out the panel closure is reduced, coincident with a repository pressure plateau at ~5.5 MPa.

7.5.5 Overlay Plots for Lateral Brine Flow in DRZ Above and Below Panel Closures

Lateral Brine Flow in the UDRZ

Figure 7.5.3 - top plot (refer also to Figure 7.3)

North-flowing brine is defined as BRAPSSIC (brine entering south face) and
BRAPSNOC (brine exiting north face)

South-flowing brine is defined as BRAPSSOC (brine exiting south face) and BRAPSNIC (brine entering north face)

North flowing brine above the panel closure starts at 1200 years and continues to end of modeled period

No south-flowing brine is seen in the UDRZ above the panel closures. A brief pulse of brine flows through the UDRZ, due to the pressure pulse of the intrusion event at 1000 years. Little brine flow occurs in the UDRZ after the intrusion event because low borehole permeability impedes gas evacuation out the repository and keeps the UDRZ and borehole gas-saturated. This high gas saturation restricts brine flow down the borehole and the anhydrites from draining into the UDRZ.

Lateral Brine Flow in the LDRZ

Figure 7.5.3 - bottom plot (refer also to Figure 7.3)

North-flowing brine is defined as BRBPSSIC(brine entering south face) and BRBPSNOC (brine exiting north face)

South-flowing brine is defined as BRBPSSOC (brine exiting south face) and BRBPSNIC (brine entering north face)

Brine flow rates change at 1000, 2200, and ~5000 years

The dominant flow direction below the panel closures is southward (BRBPSSOC, BRBPSNIC) (down-dip) throughout the modeled period. Because borehole permeabilities are so low, incoming brine to the lower and upper waste panels from non-Salado sources above and below the repository is limited. Therefore, brine supplies to the LDRZ are limited to MB 139 brine drainage and, to a lesser extent, Anhydrite AB, MB 138, and UDRZ brine stored in the experimental and operations rooms from 'early' brine drainage and then released later in the modeled period. Because the upper waste panel is primarily gas-saturated and the lower waste panel is brine-saturated, as brine flows down-dip, more brine will flow up into the panel closures than is deflected into the lower waste panel rather than flow through the floor of the upper waste panel.

7.5.6 Overlay Plots for Lateral Gas Flow in DRZ Above and Below the Panel Closures

Figure 7.5.4 compares gas flow within the UDRZ to brine flow through the panel closures.

Lateral Gas Flow in the UDRZ

Figure 7.5.4 - top plot (refer also to Figure 7.3)

North-flowing gas is defined as GSAPSSIC (gas entering south face) and GSAPSNOC (gas exiting north face)

South-flowing gas is defined as GSAPSSOC (gas exiting south face) and GSAPSNIC (gas entering north face)

Gas flow rates and direction in the UDRZ change at 1200, 1700, and ~5000 years

Prior to intrusion, gas generated in the lower waste panel flows up to the UDRZ. Because this realization is assigned a low halite porosity, gas saturation approaches nearly 100% early on in the UDRZ. As a result, relative to other realizations, large volumes of gas move up-dip (GSAPSSIC, GSAPSNOC) via the UDRZ towards the northern regions of the repository, where gas is stored. This flow direction ceases at 1200 years, when the upper borehole plug degrades and the pressure potential in the UDRZ just above the lower and upper waste panels reverses. From 1200 years to the end of the modeled period, gas flow in the UDRZ above the panel closures is from north to south (GSAPSSOC, GSAPSNIC) as gas is slowly evacuated out the repository via the borehole.

Lateral Gas Flow in the LDRZ

Figure 7.5.4 - bottom plot (refer also to Figure 7.3)

North-flowing gas is defined as GSBPSSIC (gas entering south face), and GSBPSNOC (gas exiting north face)

South-flowing gas is defined as GSBPSSOC (gas exiting south face), and GSBPSNIC (gas entering north face)

The pressure pulse caused by the intrusion event (1000 years) causes a brief northward pulse of gas to flow in the LDRZ below the panel closures.

7.5.7 Overlay Plots for Brine and Gas Flow In/Out the Ceiling and Floor of Upper Waste Panel

Brine Flow through the Upper Waste Panel Ceiling

Figure 7.5.5 – top plot

BRN_DRAC (downflowing brine) and BRN_URAC (upflowing brine)

Brine flow rates dramatically change at ~300 years

Most of the brine enters the ceiling of the upper waste panel (BRN_DRAC) via the UDRZ early in the modeled period from DRZ drainage. Brine drainage still continues after 300 years, but flow rates are dramatically reduced from 300 to 10,000 years. No brine flows out the ceiling of the upper waste panel (BRN_URAC) to the UDRZ for the entire modeled period.

Gas Flow Through the Upper Waste Panel Ceiling

Figure 7.5.5 – top plot

GAS_DRAC (downflowing gas) and GAS_URAC (upflowing gas)

A continuous flow of gas enters the UDRZ via the ceiling of the upper waste panel (GAS_URAC) throughout the modeled period. The rate of gas flow declines at ~4000 years, coincident with a near cessation of iron corrosion in the upper waste panel and a decrease in repository pressures.

Brine Flow Through the Upper Waste Panel Floor

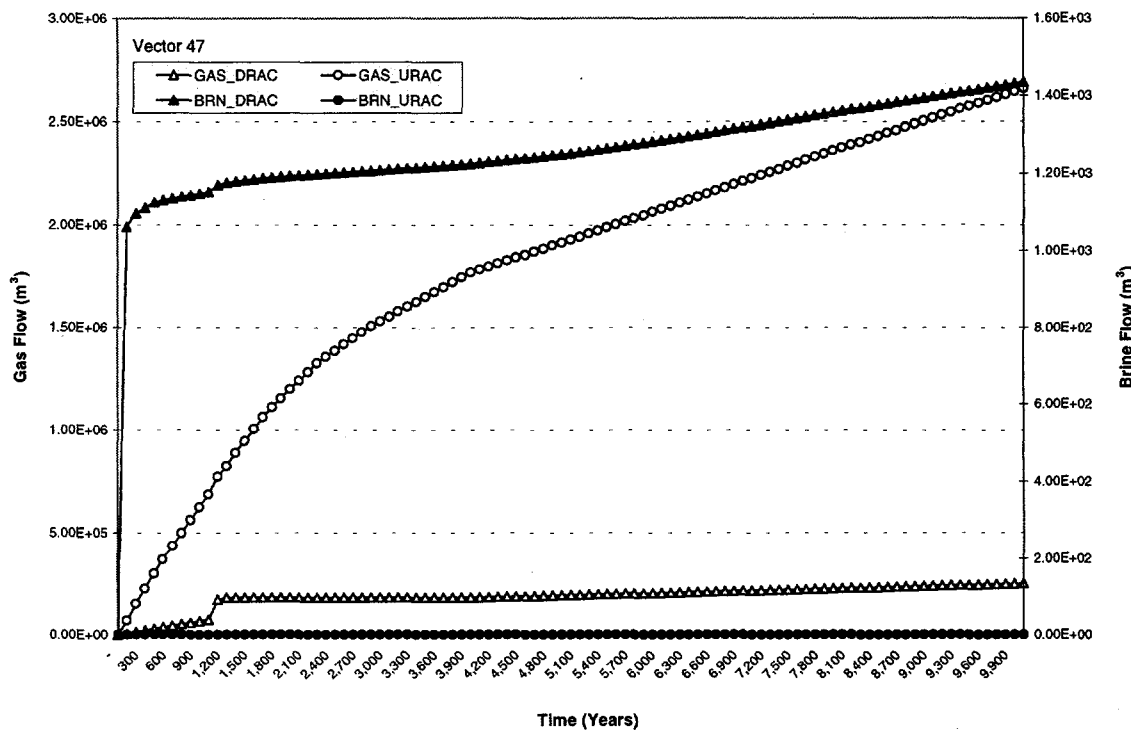
Figure 7.5.5 – bottom plot

BRN_DRBC (downflowing brine) and BRN_URBC (upflowing brine)

Brine flow rates dramatically change at ~300, 1000, 2200, and ~5000 years

The upper waste panel has relatively little brine supplied from UDRZ drainage, borehole flow, and/or anhydrite drainage. Consequently, no brine accumulates there and brine flow out the floor of the upper waste panel (BRN_DRBC) is practically nonexistent before and after the intrusion event.

R1S3 - Brine and Gas Flow In and Out the Upper Waste Panel Ceiling



R1S3 - Brine and Gas Flow In and out the Upper Waste Panel Floor

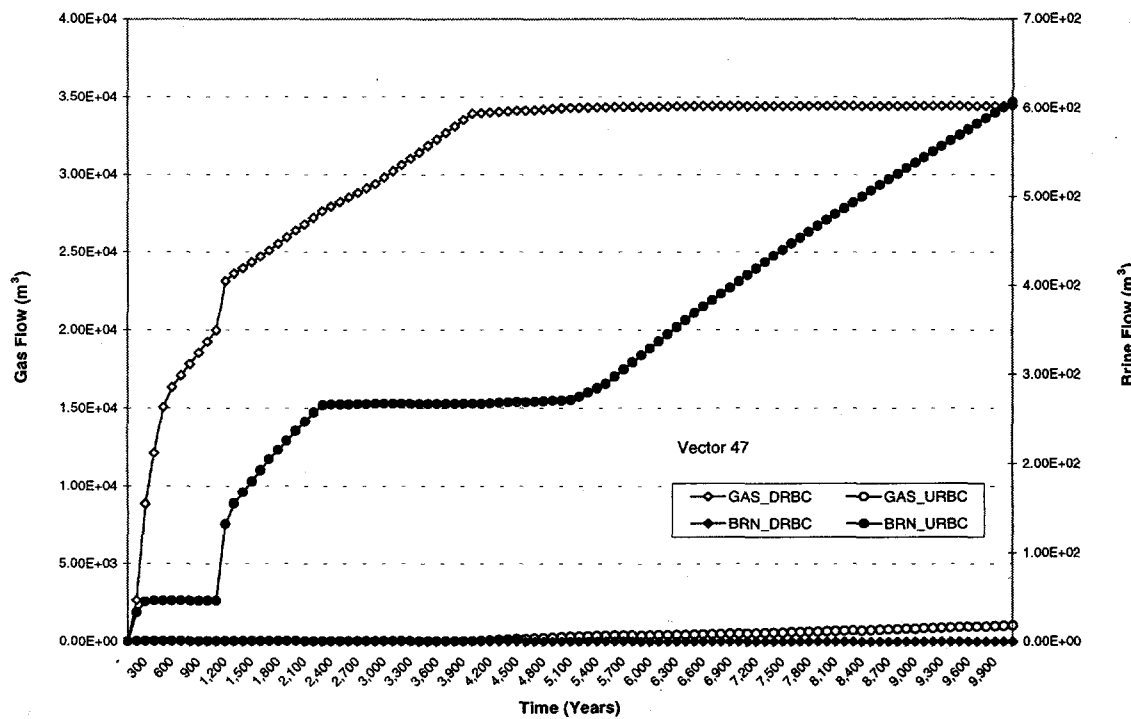


FIGURE 7.5.5. OVERLAY PLOTS FOR REALIZATION 47 depicting vertical brine and gas flow through the ceiling of the upper waste panel within the UDRZ (top plot) and LDRZ (bottom plot)

Brine flow upward from the LDRZ into the upper waste panel floor occurs at three distinct times and is partially a function of limited LDRZ pore volume (due to this realization's relatively low halite porosities, rank 88/100).³ The first flow influx is seen soon after repository closure. Brine from both sides of MB 139 drains to the LDRZ and collects in the south portion of the LDRZ, creating a brine 'pool' there. (Brine saturation becomes relatively high.) As the pool grows in size, its north edge moves up-dip to the area below the upper waste panel. From the LDRZ, brine seeps upward through the upper waste panel floor. This brine seepage upward subsides around 300 years for several reasons. The pool shrinks in size as the LDRZ pore volume increases. The increase in pressure reduces the gradient that promotes brine drainage out the marker beds. Coincidentally, the upper waste panel iron corrosion begins to consume brine faster than replenishing brine (supplying brine to the upper waste panel) accumulates in the LDRZ brine pool.

The second influx of brine seepage through the upper waste panel floor occurs at the time of intrusion (1000 years), when the connection to the reservoir introduces additional brine to the LDRZ, again increasing the size of the brine pool in the LDRZ. The pool's north edge moves up-dip to the area below the upper waste panel. Pressure gradients and brine saturation in the LDRZ are high enough to promote brine flow from the LDRZ through the upper waste panel floor between 1000 and 2200 years, when the connection to the reservoir is enhanced via an open borehole. Flow ceases when the lower borehole permeability is reduced by a factor of 10 at 2200 years. The third influx occurs at ~5000 years and continues to the end of the modeled period, coincident with repository pressures leveling at ~5.5 MPa. At the same time, the lower waste panel gas saturation has also plateaued (see WAS_SATG in Figure 7.5.1 top panel), indicating brine fluxes in and out the floor of the lower waste panel to the LDRZ are in equilibrium. These conditions imply south (and, to a lesser extent, north) MB 139 brine drainage that has accumulated in the southern portion of the LDRZ. The pool again increases in size, with the north edge moving up-dip to the area below the upper waste panel, causing brine to seep through the upper waste panel floor.

³ The dominant lateral LDRZ flow direction below the panel closures after intrusion is down-dip. Therefore, flow upward into the floor of the upper waste panel comes from brine that collects directly below the lower waste panel.

Gas Flow Through the Upper Waste Panel Floor

Figure 7.5.5 – bottom plot

GAS_DRBC (downflowing gas) and GAS_URBC (upflowing gas)

Because relatively little gas is evacuated out of the borehole (due to low borehole permeability), and the DRZ volume for this realization is relatively small, gas saturation of the UDRZ and the upper waste panel reaches relatively high values and high pressures. This condition causes gas to move down through the upper waste panel floor to the LDRZ. After intrusion, more gas is produced in the lower waste panel as a result of brine entering through the south floor. As more gas is produced via iron corrosion (much faster than it can be evacuated out of the repository), gas flows from the lower to the upper waste panel via the UDRZ. This causes the upper waste panel to become nearly 100% gas-saturated (see gas saturation contour plots in Section 7.5.8, from ~2200 to 10,000 years). This gas eventually moves into the LDRZ via the upper waste panel floor (GAS_DRBC). When all existing upper waste panel brine is consumed via corrosion (see the gas saturation curve in Figure 7.5.1, top plot), gas production in the upper waste panel via corrosion effectively ceases at 4000 years. This coincides with an effective cessation of gas flow downward through the upper waste panel floor and a reduction in repository pressure (see Figure 7.5.1, top plot).

7.5.8 Gas Saturation Contour Plots

Figure 7.5.6 depicts the gas saturation contours at 1000 years, just prior to intrusion; ~2212 years; ~3896 years; and the end of the modeled period, 10,000 years. Realization 47 has low halite porosity, and thus a small DRZ pore volume for gas and brine storage. Consequently, at 1000 years, prior to intrusion, the upper waste panels, operations room, and experimental room have received little DRZ brine drainage, keeping these regions at nearly 100% gas saturation. Because borehole permeability is one of the lowest in the sample set, relatively little gas is evacuated out the repository via the borehole. This condition causes the UDRZ to have relatively high gas saturations north and south of the borehole throughout the modeled period, impeding brine flow into the repository via the borehole or anhydrite drainage. Gas saturation in the LDRZ

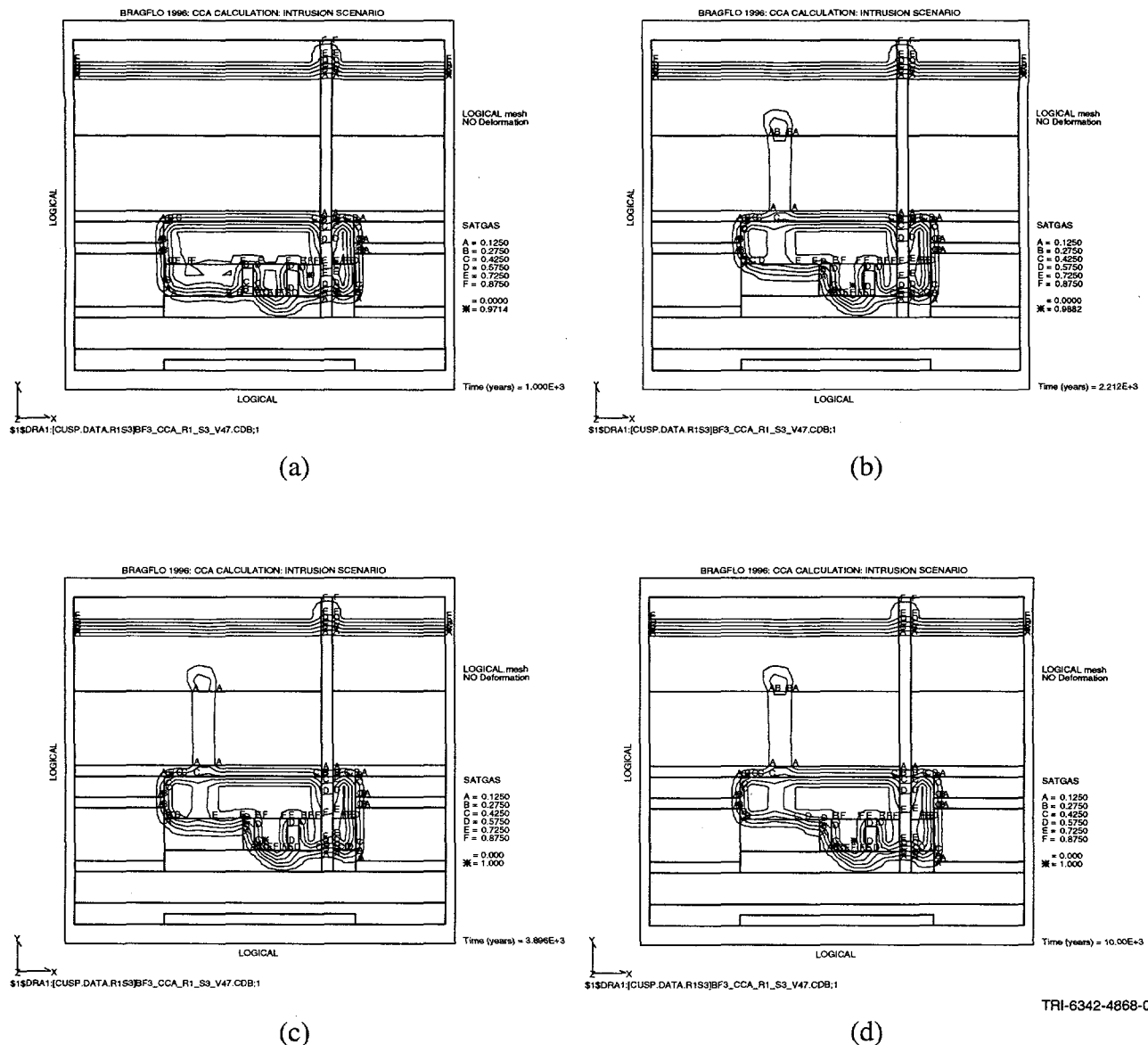


FIGURE 7.5.6. GAS SATURATION CONTOURS FOR REALIZATION 47. (a) 1000 years, just prior to intrusion, (b) ~2212 years, (c) ~3986 years, and (d) the end of the modeled period, 10000 years. Borehole in lower waste panel is not shown; see Figure 7.4 for location of borehole.

just below the upper waste panel also remains well above ~0.2 along the length of the upper waste panel.

The influx of brine from the Castile reservoir at 1000 years to the lower waste panel reduces gas saturation from 1000 years to the end of the modeled period. The contour plot taken at 2212 years is indicative of this condition.

Because the DRZ pore volumes provide very little storage space in the UDRZ, as gas is generated early in the modeled period, some gas moves down into the LDRZ (also see Figure 7.5.5, bottom plot), creating relatively high gas saturations in the LDRZ below the upper waste panel. Thus, any brine flow from the borehole or south MB 139 to the LDRZ, then upward to the waste regions, is restricted to the lower waste panel and that portion of the upper waste panel lying just north of the panel closures. At ~2212, ~3896, and 10,000 years, brine slowly fills the lower waste panel, primarily due to south MB 139 drainage.

Intentionally Left Blank

References

Bean, J.E., M.E. Lord, D.A. McArthur, R.J. MacKinnon, J.D. Miller, and J.D. Schreiber. 1996. "Analysis Package for the Salado Flow Calculations (Task 1) of the Performance Assessment Analysis Supporting the Compliance Certification Application (CCA)." Analysis Package. Albuquerque, NM: Sandia National Laboratories. Sandia WIPP Central Files WPO # 40514.

Christian-Frear, T.L. 1996a. "Salado Halite Rock Compressibility from Room Q Analysis." Records Packages. Albuquerque, NM: Sandia National Laboratories. Sandia WIPP Central Files WPO # 30598, WPO # 31220.

Christian-Frear, T.L. 1996b. "Salado Halite Permeability from Room Q Analysis." Records Package. Albuquerque, NM: Sandia National Laboratories. Sandia WIPP Central Files WPO # 30721.

Davies, P., and R. Beauheim. 1996. "Changes to the Parameter Records Package and Form # 464 for Far-Field Permeability of Salado Halites." Memo to M. Tierney, March 7, 1996. Albuquerque, NM: Sandia National Laboratories. Sandia WIPP Central Files WPO # 36772.

DOE (U.S. Department of Energy). 1996. *Title 40 CFR Part 191 Compliance Certification Application for the Waste Isolation Pilot Plant*. DOE/CAO-1996-2184. Carlsbad, NM: United States Department of Energy, Waste Isolation Pilot Plant, Carlsbad Area Office. Vols. I-XXI.

Domski, P. 1996a. "Salado: Halite Permeability." Records Package. Albuquerque, NM: Sandia National Laboratories. Sandia WIPP Central Files WPO # 31218.

Domski, P. 1996b. "Salado: Halite Pressure." Records Package. Albuquerque, NM: Sandia National Laboratories. Sandia WIPP Central Files WPO # 31221.

Freeze, G.F. 1996a. "Non-Salado: Castile Brine Reservoir Rock Compressibility." Records Package. Albuquerque, NM: Sandia National Laboratories. Sandia WIPP Central Files WPO # 31084.

Freeze, G.F. 1996b. "Non-Salado: Castile Brine Reservoir Permeability." Records Package. Albuquerque, NM: Sandia National Laboratories. Sandia WIPP Central Files WPO # 31070.

Freeze, G., and K. Larson. 1996. "Initial Pressure in the Castile Brine Reservoir," *Title 40 CFR Part 191 Compliance Certification Application for the Waste Isolation Pilot Plant*. DOE/CAO-1996-2184. Carlsbad, NM: United States Department of Energy, Waste Isolation Pilot Plant, Carlsbad Area Office. Vol. X, Appendix MASS, Attachment 18-1, 1 p. (Memo to M. Tierney, March 20, 1996. Sandia WIPP Central Files WPO # 37148.)

Helton, J.C. 1993. "Uncertainty and Sensitivity Analysis Techniques for Use in Performance Assessment for Radioactive Waste Disposal," *Reliability Engineering and System Safety*. Vol. 42, no. 2-3, 327-367.

Helton, J.C., D.R. Anderson, M.G. Marietta, and R.P. Rechard. 1997. "Performance Assessment for the Waste Isolation Pilot Plant: From Regulation to Calculation for 40 CFR 191.13," *Operations Research*. Vol. 45, no. 2, 157-177.

Helton, J.C., J.E. Bean, J.W. Berglund, F.J. Davis, K. Economy, J.W. Garner, J.D. Johnson, R.J. MacKinnon, J. Miller, D.G. O'Brien, J.L. Ramsey, J.D. Schreiber, A. Shinta, L.N. Smith, D.M. Stoelzel, C. Stockman, and P. Vaughn. 1998. *Uncertainty and Sensitivity Analysis Results Obtained in the 1996 Performance Assessment for the Waste Isolation Pilot Plant*. SAND98-0365. Albuquerque, NM: Sandia National Laboratories.

Howarth, S.M. 1996. "Salado Halite Porosity." Records Package. Albuquerque, NM: Sandia National Laboratories. Sandia WIPP Central Files WPO # 30601.

Howarth, S.M., and T. Christian-Frear. 1997. *Porosity, Single-Phase Permeability, and Capillary Pressure Data from Preliminary Laboratory Experiments on Selected Samples from Marker Bed 139 at the Waste Isolation Pilot Plant*. SAND94-0472/1/2/3. Albuquerque, NM: Sandia National Laboratories. Vols. 1-3.

Hurtado, L.D. 1996. "Correction of Lambda Distribution." Memo to M. Tierney, February 12, 1996. Albuquerque, NM: Sandia National Laboratories. Sandia WIPP Central Files WPO # 32287.

Iman, R.L., M.J. Shortencarier, and J.D. Johnson. 1985. *A FORTRAN 77 Program and User's Guide for the Calculation of Partial Correlation and Standardized Regression Coefficients*. NUREG/CR-4122, SAND85-0044. Albuquerque, NM: Sandia National Laboratories.

Kelley, V., T. Jones, and J. Ogintz. 1996a. "WIPP Seal System Parameters for Performance Assessment BRAGFLO Compliance Calculations." Memo to L.D. Hurtado, Sandia National Laboratories, January 15, 1996. Austin, TX: Intera Inc. Sandia WIPP Central Files WPO # 30995.

Kelley, V.A., T.L. Jones, and J.B. Ogintz. 1996b. "WIPP Shaft Seal System Parameters Documentation to Support Performance Assessment BRAGFLO Compliance Calculations." Memo to L.D. Hurtado, Sandia National Laboratories, March 22, 1996. Austin, TX: Intera Inc. Sandia WIPP Central Files WPO # 40258.

Knowles, M.K., D. Borns, J. Fredrich, D. Holcomb, R. Price, D. Zeuch, T. Dale, and R.S. Van Pelt. 1998. "Testing the Disturbed Zone Around a Rigid Inclusion in Salt," *The Mechanical Behavior of Salt, Proceedings of the Fourth Conference, Montreal, Quebec, Canada, June 17-18, 1996*. Eds. M. Aubertin and H.R. Hardy, Jr. SAND95-1151C. Clausthal-Zellerfeld, Germany: TTP Trans Tech Publications. 175-188.

Larson, K. 1997. "Tracing the Source: The 32,000 m³ Reservoir Volume Used in Determination of GRIDFLO Parameter Probabilities." Albuquerque, NM: Sandia National Laboratories. Sandia WIPP Central Files WPO # 44401 attachment.

Mayer, G., F. Jacobs, and F.H. Wittmann. 1992. "Experimental Determination and Numerical Simulation of the Permeability of Cementitious Materials," *Nuclear Engineering and Design*. Vol. 138, no. 2, 171-177.

O'Brien, D.G. 1995. "Critical Gas Saturation Recommendations for WIPP." WIPP Letter Report to D.M. Stoelzel, November 15, 1995. Littleton, CO: Solutions Engineering. Sandia WIPP Central Files WPO # 38769.

Popielak, R.S., R.L. Beauheim, S.R. Black, W.E. Coons, C.T. Ellingson, and R.L. Olsen. 1983. *Brine Reservoirs in the Castile Formation, Waste Isolation Pilot Plant (WIPP) Project, Southeastern New Mexico*. TME 3153. Albuquerque, NM: U.S. Department of Energy, Waste Isolation Pilot Plant.

Powers, D.W., J.M. Sigda, and R.M. Holt. 1996. "Probability of Intercepting a Pressurized Brine Reservoir Under the WIPP," *Title 40 CFR Part 191 Compliance Certification Application for the Waste Isolation Pilot Plant*. DOE/CAO-1996-2184. Carlsbad, NM: United States Department of Energy, Waste Isolation Pilot Plant, Carlsbad Area Office. Vol. X, Appendix MASS, Attachment 18-6. (Final report also available in Sandia WIPP Central Files WPO # 40199.)

Repository Isolation Systems Department. 1996. *Waste Isolation Pilot Plant Shaft Sealing System Compliance Submittal Design Report*. SAND96-1326/1-2. Albuquerque, NM: Sandia National Laboratories. Vols. 1-2.

Saulnier, G.J., Jr., P.S. Domske, J.B. Palmer, R.M. Roberts, W.A. Stensrud, and A.L. Jensen. 1991. *WIPP Salado Hydrology Program Data Report #1*. SAND90-7000. Albuquerque, NM: Sandia National Laboratories.

Stensrud, W.A., T.F. Dale, P.S. Domske, J.B. Palmer, R.M. Roberts, M.D. Fort, G.J. Saulnier, Jr., and A.L. Jensen. 1992. *Waste Isolation Pilot Plant Salado Hydrology Program Data Report #2*. SAND92-7072. Albuquerque, NM: Sandia National Laboratories.

Swift, P.N., K.W. Larson, and R.L. Beauheim. 1996. "Treatment of Castile Brine Reservoir in the 1996 CCA Performance Assessment." Memo to L.E. Shephard and M.S.Y. Chu, October 3,

1996. Albuquerque, NM: Sandia National Laboratories. Sandia WIPP Central Files WPO # 41885.

Thompson, T.W., W.E. Coons, J.L. Krumhansl, and F.D. Hansen. 1996. "Inadvertent Intrusion Borehole Permeability, Final Draft." May 20, 1996. Albuquerque, NM: Sandia National Laboratories. Sandia WIPP Central Files WPO # 41131.

Thompson, T.W., W.E. Coons, J.L. Krumhansl, and F.D. Hansen. 1996. "Inadvertent Intrusion Borehole Permeability," *Title 40 CFR Part 191 Compliance Certification Application for the Waste Isolation Pilot Plant*. DOE/CAO-1996-2184. Carlsbad, NM: United States Department of Energy, Waste Isolation Pilot Plant, Carlsbad Area Office. Vol. X, Appendix MASS, Attachment 16-3. (Final report dated July 8, 1996.)

Tierney, M.S. 1996. "Reasons for Choice of the PROBDEG Parameter (id nos: 2824 and 2823) on February 22, 1996." Memo to file, March 29, 1996. Albuquerque, NM: Sandia National Laboratories. Sandia WIPP Central Files WPO # 34881.

Vaughn, P. 1996a. "WAS_AREA and REPOSIT SAT_RBRN Distribution." Memo with attachments to M. Tierney, February 13, 1996. Albuquerque, NM: Sandia National Laboratories. Sandia WIPP Central Files WPO # 34902.

Vaughn, P., and D. McArthur. 1996. "CUMPROB Parameter Definition and Usage." Memo to M. Tierney, May 20, 1996. Albuquerque, NM: Sandia National Laboratories. Sandia WIPP Central Files WPO # 37542.

Wang, Y., and L. Brush. 1996a. "Estimates of Gas-Generation Parameters for the Long-Term WIPP Performance Assessment," *Title 40 CFR Part 191 Compliance Certification Application for the Waste Isolation Pilot Plant*. DOE/CAO-1996-2184. Carlsbad, NM: United States Department of Energy, Waste Isolation Pilot Plant, Carlsbad Area Office. Vol. X, Appendix MASS, Attachment 8-2. (Memo to M. Tierney, January 26, 1996. Sandia WIPP Central Files WPO # 35162.)

Wang, Y., and L. Brush. 1996b. "Modify the Stoichiometric Factor y in BRAGFLO to Include the Effect of MgO Added to WIPP Repository as Backfill," *Title 40 CFR Part 191 Compliance Certification Application for the Waste Isolation Pilot Plant*. DOE/CAO-1996-2184. Carlsbad, NM: United States Department of Energy, Waste Isolation Pilot Plant, Carlsbad Area Office. Vol. X, Appendix MASS, Attachment 8-2. (Memo to Martin Tierney, February 23, 1996. Sandia WIPP Central Files WPO # 22286.)

WIPP PA (Performance Assessment). 1992-1993. *Preliminary Performance Assessment for the Waste Isolation Pilot Plant, December 1992*. SAND92-0700/1-5. Albuquerque, NM: Sandia National Laboratories. Vols. 1-5.

WIPP Distribution
SAND99-1043

Federal Agencies

US Department of Energy (4)
Office of Civilian Radioactive Waste Mgmt.
Attn: Deputy Director, RW-2
Acting Director, RW-10
Office of Human Resources & Admin.
Director, RW-30
Office of Program Mgmt. & Integ.
Director, RW-40
Office of Waste Accept., Stor., & Tran.
Forrestal Building
Washington, DC 20585

US Department of Energy
Yucca Mountain Site Characterization Office
Attn: Project Director
P. O. Box 30307
Las Vegas, NV 89036-0307

US Department of Energy
Research & Waste Management Division
Attn: Director
P.O. Box E
Oak Ridge, TN 37831

US Department of Energy (6)
Carlsbad Area Office
Attn: I. Triay
G. T. Basabilvazo
D. Galbraith
M. McFadden
J. A. Mewhinney
Mailroom
P.O. Box 3090
Carlsbad, NM 88221-3090

US Department of Energy
Office of Environmental Restoration and
Waste Management
Attn: M. Frei, EM-30
Forrestal Building
Washington, DC 20585-0002

US Department of Energy (3)
Office of Environmental Restoration and
Waste Management
Attn: J. Juri, EM-34, Trevion II
Washington, DC 20585-0002

US Department of Energy
Office of Environmental Restoration and
Waste Management
Attn: S. Schneider, EM-342, Trevion II
Washington, DC 20585-0002

US Department of Energy (2)
Office of Environment, Safety & Health
Attn: C. Borgstrom, EH-25
R. Pelletier, EH-231
Washington, DC 20585

US Department of Energy (2)
Idaho Operations Office
Fuel Processing & Waste Mgmt. Division
785 DOE Place
Idaho Falls, ID 83402

US Environmental Protection Agency (2)
Radiation Protection Programs
Attn: M. Oge
ANR-460
Washington, DC 20460

Timothy M. Barry
Chief, Science – Policy, Planning and
Evaluation
PM 223X I.S. EPA
Washington, DC 20460

Norman A. Eisenberg
U.S. Nuclear Regulatory Commission
Office of Nuclear Material Safety and
Safeguards
Division of Waste Management
Washington, D.C. 20555

Boards

Defense Nuclear Facilities Safety Board
Attn: D. Winters
625 Indiana Ave. NW, Suite 700
Washington, DC 20004

Nuclear Waste Technical Review Board (2)
Attn: Chairman
J. L. Cohen
2300 Clarendon Blvd. Ste 1300
Arlington, VA 22201-3367

State Agencies

Attorney General of New Mexico
P.O. Drawer 1508
Santa Fe, NM 87504-1508

Environmental Evaluation Group (3)
Attn: Library
7007 Wyoming NE
Suite F-2
Albuquerque, NM 87109

NM Environment Department (3)
Secretary of the Environment
1190 St. Francis Drive
Santa Fe, NM 87503-0968

NM Bureau of Mines & Mineral Resources
Socorro, NM 87801

Westinghouse Electric Corporation (5)

Attn: Library
J. Epstein
J. Lee
R. Kehrman
S. J. Patchet
P.O. Box 2078
Carlsbad, NM 88221

S. Cohen & Associates
Attn: Bill Thurber
1355 Beverly Road
McLean, VA 22101

T. William Thompson
Golder Associates, Inc.
44 Union Blvd. Suite 300
Lakewood, CO 80228

Michael B. Gross
Michael Gross Enterprises
21 Tradewind Passage
Corte Madera, CA 94925

Laboratories/Corporations

Battelle Pacific Northwest Laboratories
Battelle Blvd.
Richland, WA 99352

Dr. Pamela Doctor
Battelle Northwest
P.O. Box 999
Richland, WA 99352

Los Alamos National Laboratory
Attn: B. Erdal, INC-12
P.O. Box 1663
Los Alamos, NM 87544

M. D. McKay
F600
Los Alamos National Laboratory
Los Alamos, NM 87545

Tech Reps. Inc. (3)
Attn: J. Chapman (1)
Loretta Robledo (2)
5000 Marble NE, Suite 222
Albuquerque, NM 87110

National Academy of Sciences WIPP Panel

Tom Kiess (15)
Staff Study Director
GF456
2101 Constitution Ave.
Washington, DC 20418

Universities

University of New Mexico
Geology Department
Attn: Library
141 Northrop Hall
Albuquerque, NM 87131

University of Washington
College of Ocean & Fishery Sciences
Attn: G. R. Heath
583 Henderson Hall, HN-15
Seattle, WA 98195

Libraries

Thomas Brannigan Library
Attn: D. Dresp
106 W. Hadley St.
Las Cruces, NM 88001

Government Publications Department
Zimmerman Library
University of New Mexico
Albuquerque, NM 87131

New Mexico Junior College
Pannell Library
Attn: R. Hill
Lovington Highway
Hobbs, NM 88240

New Mexico State Library
Attn: N. McCallan
325 Don Gaspar
Santa Fe, NM 87503

New Mexico Tech
Martin Speere Memorial Library
Campus Street
Socorro, NM 87810

WIPP Information Center
Attn: Y. Acosta
4021 National Parks Highway
Carlsbad, NM 88220

Foreign Addresses

Atomic Energy of Canada, Ltd. (2)
Whiteshell Laboratories
Attn: B. Goodwin
T. Andres
Pinawa, Manitoba, CANADA R0E 1L0

Dr. Arnold Bonne
Acting Head of the Waste Technology Section
Division of Nuclear Fuel Cycle and Waste
Management
International Atomic Energy Agency
P.O. Box 100
A-1400 Vienna
AUSTRIA

Claudio Pescatori
AERI/NEA/OECD
LeSeine St. Germain
12 Boulevard des iles
92130 Issy-les-Moulineaux
FRANCE

Francois Chenevier (2)
ANDRA
Parc de la Croix Blanche
1-7 rue Jean Monnet
92298 Chatenay-Malabry Cedex
FRANCE

Claude Sombret
Centre d'Etudes Nucleaires de la Vallee Rhone
CEN/VALRHO
S.D.H.A. B.P. 171
30205 Bagnols-Sur-Ceze
FRANCE

Commissariat a L'Energie Atomique
Attn: D. Alexandre
Centre d'Etudes de Cadarache
13108 Saint Paul Lez Durance Cedex
FRANCE

Ghislain de Marsily
Univeristy Pierre et Marie Curie
Laboratoire de Geologie Applique
4, Place Jussieu
T.26-5e etage
75252 Paris Cedex 05
FRANCE

Bundesanstalt fur Geowissenschaften und
Rohstoffe
Attn: M. Langer
Postfach 510 153
D-30631 Hannover
GERMANY

Bundesministerium fur Forschung und
Technologie
Postfach 200 706
5300 Bonn 2
GERMANY

Gesellschaft fur Anlagen und Reaktorsicherheit
(GRS)
Attn: B. Baltes
Schwertnergasse 1
D-50667 Cologne
GERMANY

European Commission (3)

Attn: Francesca Campolongo
Karen Chan

Stefano Tarantola

JRC Isprs, ISIS
I-21020 Ispra
ITALY

David Rios Insua
University Rey Juan Carlos
ESCET-URJC, C. Humanes 63
E-28936 Mostoles
SPAIN

Shingo Tashiro
Japan Atomic Energy Research Institute
Tokai-Mura, Ibaraki-Ken, 319-11
JAPAN

Toshimitsu Homma
Nuclear Power Engineering Corporation
3-17-1 Toranomon Minato-Ku
Tokyo 1015
JAPAN

Netherlands Energy Research Foundation ECN
Attn: J. Prij
3 Westerduinweg
P.O. Box 1
1755 ZG Petten
THE NETHERLANDS

Willem Van Groenendaal
Tilburg University
P.O. Box 90153
NL - 5000 Le Tilburg
THE NETHERLANDS

Svensk Karnbransleforsorjning AB
Attn: F. Karlsson
Project KBS (Karnbranslesakerhet)
Box 5864
S-102 48 Stockholm
SWEDEN

Nationale Genossenschaft fur die Lagerung
Radioaktiver Abfalle (2)
Attn: S. Vomvoris
P. Zuidema
Hardstrasse 73
CH-5430 Wettingen
SWITZERLAND

AEA Technology
Attn: J. H. Rees
D5W/29 Culham Laboratory
Abington, Oxfordshire OX14 3DB
UNITED KINGDOM

AEA Technology
Attn: W. R. Rodwell
044/A31 Winfrith Technical Centre
Dorchester, Dorset DT2 8DH
UNITED KINGDOM

Daniel A. Galson
Galson Science Ltd.
35, Market Place
Oakham
Leicestershire LE15 6DT
UNITED KINGDOM

AEA Technology
Attn: J. E. Tinson
B4244 Harwell Laboratory
Didcot, Oxfordshire OX11 ORA
UNITED KINGDOM

Other

Dennis Powers
Star Route Box 87
Anthony, TX 79821

R. L. Iman
1065 Tramway Lane NE
Albuquerque, NM 87122

Internal

MS	Org.	
0701	6100	P. B. Davies
0737	6831	E. J. Nowak
1127	6215	J. R. Tillerson
0737	6833	E. H. Ahrens
0779	6849	D. R. Anderson
0779	6848	H. N. Jow

0771	6800	M. Chu
0733	6832	J. T. Holmes
1395	6821	M. Marietta
0771	6000	W. D. Weart
0773	6821	G. K. Froehlich
1395	6810	F. D. Hansen
0779	6848	K. W. Larson
1395	6800	S. Y Pickering
1395	6821	B. L. Baker
1395	6821	M. K. Knowles
1395	6821	M-A. Martell
1399	6850	P. E. Sanchez
1395	6821	Y. Wang
0733	6832	L. H. Brush
0733	6832	H. W. Papenguth
0733	6832	A. C. Peterson
0733	6832	M. D. Siegel
0779	6849	J. E. Bean
0779	6849	F. J. Davis
0779	6849	L. J. Dotson
0779	6849	K. M. Economy (5)
0779	6849	J. C. Helton (5)
0779	6848	J. D. Johnson
0779	6821	J. D. Miller
0779	6848	H. C. Ogden
0779	6849	M. J. Shortencarier
0779	6849	J. D. Schreiber
0779	6821	M. S. Tierney
0779	6821	M. E. Fewell
1395	6821	J. W. Garner
0779	6849	T. Hadgu
0779	6849	M. E. Lord
0779	6849	J. L. Ramsey
0779	6849	R. P. Rechard
0779	6849	D. Rudeen
0779	6849	A. Schenker
0779	6849	A. H. Treadway
1395	6821	P. Vaughn (5)
0779	6849	J. A. Jones
1146	6849	J. H. Saloio
0735	6115	A. R. Lappin
1395	6810	N. Z. Elkins
1395	6860	R. D. Waters
0731	6811	K. Hart (2)
0731	6811	NWM Library (20)
9018	8940-2	Central Technical Files
0899	4916	Technical Library (2)
0612	4912	Review and Approval Desk, For DOE/OSTI